Sources and processes controlling the occurrence of legacy POPs and organic contaminants of emerging concern in European air

Dissertation for the degree of Philosophiae Doctor

By

Helene Lunder Halvorsen

Department of Chemistry

Faculty of Mathematics and Natural Sciences

University of Oslo

2023

Series of dissertations submitted to the
Faculty of Mathematics and Natural Sciences, University of Oslo
No. 2669

ISSN 1501-7710

Det er i motbakke det går oppover!

Acknowledgements

My first thanks go to my inspiring teachers during the first 12 years at school. You motivated me to study chemistry so I could end up at NILU. After working with PAHs and quality assurance for some years, I was ready for new challenges and to have the ability to participate more in research projects. When I returned from maternal leave with Mariell, I took the opportunity to become Kine's successor, with Knut as a supervisor, despite watching the endless work on finishing her PhD; "Vil du virkelig dette?!" (quote Kine)

"Jada!", I was optimistic, blue eyed and blond haired, ready to finish the project in 3 years. Hay no problema! However, it has been one long hike up to the top of this mountain. No wonder why they call it a "dannelsesreise"! I have been lost, I have done all the mistakes that are possible to make, I have wanted to quit and give up many times, but I have risen, I have solved many issues, I have learned to focus on things only I can control, I have learned to manage my time better, and I have learned to "write, write, write". There are no shortcuts in the "dannelsesreise", but now finally, more than 7 years later, after reaching many small peaks, I finally see the goal! My eyes are still blue, but the blond hair is more greyish.

the appreciated collaboration, but also for the once-in-a-life experience at Svalbard and all the other small and large things we have shared.

Thank you to my other co-authors, Alexey Gusev and Victor Shatalow at MSC-East, and my colleague, Sabine Eckhardt, for contributions in the modelling part and valuable feedback. I also have numerous volunteers within the EMEP programme to thank for their valuable assistance collecting the air samples. Thank you to Ingjerd and Maja for driving for endless hours and handling the mosquitos in the Norwegian woods, and to Christine and David for assistance in the field.

At MILK, I would especially like to thank Anders and Aasmund for all moral support, Faith for teaching me in the laboratory, Berit and Maja for helping me preparing the samplers, and Maja (again) and Alexander for sharing student frustration. A huge thanks also to my Murphy-friend (Kine), for always making my day better, both inside and outside NILU! You help me put life in general into perspective and I could not have managed this without all the "head-ventilating" trips we have had, with or without skis.

To my mamma (Ina), thank you for always encouraging me to be a scientist! (For your information, I now also have a degree in how to adjust to ever-changing plans 😵) Thanks also to my family for always being there, and to all of my friends for filling the time I have had spare with good company and lots of fun!

This thesis could not have been completed without my favorite man, Christian; Thank you for your understanding and patience, feeding me, and for being a safe embrace when things have been rough.

Mariell and Melvin, you remind me what is important in life and help me "reset" from day to day. I have been studying as long as both of you can remember and I know you are ready for me to finish.

Finally, I have. And I am more than ready for "Livet etter"!

Table of content

List of abbreviations

AAS	-	Active air sampling
aBFRs	-	Alternative brominated flame retardants
DCM	-	Dichloromethane
DDE	-	Dichlorodiphenyldichloroethylene
DDT	-	Dichlorodiphenyltrichloroethane
DP	-	Dechlorane Plus
DRCs	-	Dechlorane related compounds
EMEP	-	European Monitoring and Evaluation Programme
FLEXPART	-	FLEXible PARTicle dispersion model
GAPS	-	Global Atmospheric Passive Sampling
GC/MS	-	Gas chromatography mass spectrometry
GFF	-	Glass fiber filter
GLEMOS	-	Global EMEP Multi-media Modeling System
HCB	-	Hexachlorobenzene
HCHs	-	Hexachlorocyclohexanes
K_{OA}	-	octanol-air equilibrium partitioning coefficient
LRAT	-	Long-range atmospheric transport
LRATP	-	Long range atmospheric transport potential
MDL	-	Method detection limit
MONET	-	MOitoring NETwork
MS	-	Mass spectrometer
NEM	-	Nested Exposure Model
OCECs	-	Organic contaminants of emerging concern
OCPs	-	Organochlorine pesticides
OPFR	-	Organophosphorus Flame Retardants
PAS	-	Passive air sampler
PCBs	-	Polychlorinated biphenyls
PBDE	-	Polybrominated diphenyl ethers
PeCB	-	Pentachlorobenzene

POPs	-	Persistent organic pollutants
POG	-	Polymer-coated glass
PRC	-	Performance reference compounds
PUF	-	Polyurethane foam
PUF-PAS	-	Polyurethane foam-based passive air sampler
RRF	-	Relative Response Factor
SPMD	-	Semipermeable membrane devices
SIP	-	Sorbent-impregnated polyurethane foam disk
SPE	-	Solid-phase extraction
UNEP	-	United Nations Global Environment Programme

List of papers

Paper I:

Lunder Halvorsen, H.; Bohlin-Nizzetto, P.; Eckhardt, S.; Gusev, A.; Krogseth, I. S.; Moeckel, C.; Shatalov, V.; Skogeng, L. P.; Breivik, K. Main sources controlling atmospheric burdens of persistent organic pollutants on a national scale. *Ecotoxicology and Environmental Safety,* 2021, 217, 112172.

Paper II:

Lunder Halvorsen, H.; Bohlin-Nizzetto, P.; Eckhardt, S.; Gusev, A.; Moeckel, C.; Shatalov, V.; Skogeng, L. P.; Breivik, K. Spatial variability and temporal changes of POPs in European background air. *Atmospheric Environment*, 2023, 299, 119658.

Paper III:

Skogeng, L. P.; Lunder Halvorsen, H.; Breivik, K.; Eckhardt, S.; Herzke, D.; Moeckel, C.; Krogseth, I. S. Spatial distribution of dechlorane plus and dechlorane related compounds in European background air. *Frontiers in Environmental Science,* 10, 1083011, 2023.

Paper IV:

Lunder Halvorsen, H.; Bohlin-Nizzetto, Moeckel, C.; Breivik, K. Spatial distribution of PCB-11 in background air across Europe. Manuscript in preparation.

Summary

Regulated persistent organic pollutants (POPs) are a group of chemicals that may cause harmful health and environmental effects, largely due to their toxicity and bioaccumulating properties. POPs are persistent and many are semi-volatile substances, capable of undergoing long-range environmental transport (LRT) to regions far away from their sources to remote regions like the Arctic. To replace some of the regulated POPs, alternative chemicals have been introduced to the market (e.g. alternative flame retardants). Many of these chemicals have physical-chemical properties similar to POPs and may fulfill hazard criteria which define POPs, such as potential for LRT. The focus of this thesis is on the occurrence and long-range atmospheric transport (LRAT) of both legacy POPs and a group of alternative chemicals which may be classified as organic contaminants of emerging concern (OCECs).

International regulations have contributed to reduce the emissions of POPs into the environment, but most POPs are still present in the atmosphere, both in source and remote regions. This may be due to continued primary emissions and the persistence of secondary emissions. The latter is particularly relevant for semi-volatile POPs which can be re-emitted from previously contaminated surface media. More knowledge of the relative importance of primary and secondary emission sources is thus needed for chemical management strategies aiming to protect environmental and human health from POPs and POP-like chemicals. We hypothesize that the concentrations of POPs in the air over Europe may be a) spatially variable, b) variable for different POPs (both on a group level and for individual compounds), c) likely to have decreased over time in response to primary emission reductions, and d) increasingly influenced by secondary emissions. The aim of this thesis was to use high spatial resolution measurements in concert with mechanistic modelling, to gain new insights into the main sources controlling atmospheric burdens of POPs and OCECs across Europe, with an emphasis on LRAT to Norway and the Arctic.

Selected POPs and OCECs in passive air samples from Norway and Europe were analyzed with gas chromatography in combination with mass spectrometry (GC-MS). At the regional level, 101 background sites in 33 European countries were included, utilizing the network of background monitoring sites under the European Monitoring and Evaluation Programme (EMEP). At the national scale, 45 background sites, 2 remote sites and 10 urban sites in Norway were included. By combining data from these two campaigns, it was possible to assess whether local sources or long-range atmospheric transport mainly control the

atmospheric concentrations of studied chemicals in the more remote parts of Europe. Population density data and three different atmospheric transport models were also applied to help identify primary vs. secondary emissions, and transboundary vs. national emissions, across the study region. Results were compared to a similar study from 2006 to assess how the atmospheric burdens of POPs have changed over a decade.

The results show that the chlorobenzenes and hexachlorocyclohexanes (HCHs) dominate the atmospheric background concentrations of POPs across Europe. The concentrations of PCB-11 exceeded the individual concentrations of the other PCBs (polychlorinated biphenyls) at most sites and strongly suggest significant primary emissions of PCB-11. Also, the OCEC, dechlorane plus, was found to be ubiquitous. The highest concentrations of most targeted POPs and dechlorane plus were mainly observed in densely populated regions in Europe. The lowest concentrations occurred in the more remote regions (Norway and the Arctic) and were mainly attributed to LRAT. In contrast, the concentrations of hexachlorobenzene (HCB) increased with latitude. This may be explained by enhanced secondary emissions in northern regions and/or a stronger influence of LRAT from global source regions. HCB was furthermore the only POP with higher concentrations in 2016 than in 2006.

The highest spatial variability among the POPs was found for the DDTs (dichlorodiphenyltrichloroethane) and PCBs. A possible larger influence of emissions on their atmospheric burdens was indicated in the southern part of Europe than the northern part. Despite this, model predictions of PCB-153 and the isomeric ratios for the DDTs, suggested that secondary emissions are generally more important than primary emissions across Europe as a whole.

This thesis highlights the advantages of combining high spatial resolution observations with mechanistic modelling approaches. This combined approach is an important supplement to ongoing long-term monitoring efforts and offers new knowledge that cannot be inferred from measurements alone, and can be used by policy makers to assess potential opportunities for further emission reductions of legacy POPs. In future monitoring efforts we recommend including PCB-11 and dechlorane plus along with other POPs. We also recommend considering both complementary sampling strategies and alternative sampling strategies when targeting the most volatile POPs and particle-associated chemicals. Further development of emission inventories for a wider range of chemicals of interest and concern will be required to model their source-receptor relationships.

Norsk sammendrag

Persistente organiske miljøgifter (POP-er) er en gruppe kjemikalier som har blitt regulert på global skala på grunn av risiko for helse- og miljøskadelige effekter. POP-er har til felles at de er giftige, bioakkumulerende og persistente. Mange av disse forbindelsene er semi-flyktige forbindelser. Kombinasjonen av disse egenskapene medfører at POP-er er i stand til å transporteres via luft over lange avstander, fra kildeområder til mer avsidesliggende områder, som for eksempel Arktis. For å erstatte noen av de regulerte POP-ene, har alternative forbindelser blitt introdusert på markedet (f.eks. alternative flammehemmere). Mange av disse har fysikalske egenskaper som ligner POP-ene, og kan dermed oppfylle ett eller flere av farekriteriene som definerer en POP, slik som potensiale for langtransport. Fokuset i denne avhandlingen er på forekomst og atmosfærisk langtransport (LRAT) av både POP-er og ikke-regulerte organiske forbindelser av økende miljørelevans (OCEC).

Internasjonale reguleringer har bidratt til å redusere utslipp av POP-er, men på grunn av lang levetid i miljøet finnes de fortsatt i atmosfæren, både i kilderegioner og i mer avsidesliggende regioner. Dette kan skyldes at primære utslipp fortsatt finnes og vedvarende sekundære utslipp. Sistnevnte type utslipp er spesielt relevant for semi-flyktige forbindelser, som kan fordampe fra tidligere forurensede reservoarer. Mer kunnskap om den relative betydningen av primære og sekundære utslippskilder er derfor nødvendig informasjon for relevante kjemikaliehåndteringsstrategier som tar sikte på å beskytte mennesker og miljø fra POP-er og POP-lignende kjemikalier. Sentrale hypoteser for denne avhandlingen er at konsentrasjonene av POP-er i europeisk luft er a) romlig variable, b) varierer for ulike POP-er (både på gruppenivå og for individuelle forbindelser), c) har sunket over tid på grunn av reduserte primære utslipp, og d) i økende grad påvirkes av sekundære utslipp. Målet med avhandlingen var å bruke målinger med høy romlig oppløsning kombinert med mekanistiske modeller, for å få ny innsikt om hovedkildene som kontrollerer de atmosfæriske konsentrasjonene av POP-er og OCEC-er over hele Europa, med spesiell vekt på LRAT til Norge og Arktis.

Passive luftprøver fra Norge og Europa ble analysert for utvalgte POP-er og OCEC-er ved bruk av gasskromatografi i kombinasjon med massespektrometri (GC-MS). I avhandlingen er data fra 101 antatte bakgrunnsstasjoner i 33 europeiske land kombinert med data fra 47 bakgrunnsstasjoner i Norge, inkludert to stasjoner på Svalbard, for å vurdere om luftkonsentrasjonene av POP-er i de mer avsidesliggende delene av Europa hovedsakelig påvirkes av lokale kilder eller LRAT. Bakgrunnsnivåene ble videre sammenliknet med data fra mer bynære stasjoner. Befolkningstetthet og tre ulike modeller for atmosfæriske transport

ble brukt for å nærmere belyse primære vs. sekundære utslipp samt LRAT vs. nasjonale utslipp i Europa. Resultatene ble sammenlignet med en tilsvarende studie fra 2006 for å vurdere om luftkonsentrasjonene av POP-er har endret seg i løpet av et tiår.

Resultatene viser at klorbenzen-ene og heksaklorsykloheksan (HCH) dominerer bakgrunnsbelastningen av POP-er i luft over hele Europa. I tillegg ble det funnet høyere konsentrasjoner av PCB-11 enn for hver av de andre PCB-ene (polyklorerte bifenyler) på de fleste steder, noe som indikerer betydelige primærutslipp av PCB-11. Dekloran pluss, som er av økende miljørelevans, ble også funnet i betydelige konsentrasjoner over hele Europa. For de fleste POP-er, samt dekloran pluss, ble høyest konsentrasjoner observert i de tettest befolkede områdene. De laveste konsentrasjonene forekom i de mer avsidesliggende områdene (Norge og Arktis), og ble i hovedsak tilskrevet LRAT. I motsetning til andre POP-er, økte konsentrasjonene av heksaklorbenzen (HCB) med breddegrad, noe som kan forklares med økte sekundære utslipp i nord og/eller økt påvirkning av LRAT fra globale kilderegioner. Samtidig var konsentrasjonene av HCB høyere i 2016 enn i 2006.

Størst romlig variabilitet ble funnet for DDT-ene (diklordifenyltrikloretan) og PCB-ene, og det var indikasjoner på at luftkonsentrasjonene i den sørlige delen av Europa er mer påvirket av primære kilder, enn den nordlige delen. Til tross for dette antydet modelldata for PCB-153 og isomerforhold for DDT-ene at sekundære utslipp generelt er viktigere enn primære utslipp over hele Europa.

Denne avhandlingen fremhever at kombinasjonen av observasjoner med høy romlig oppløsning og mekanistiske modeller, er et viktig supplement til eksisterende overvåkning. Denne tilnærmingen gir ny kunnskap som er vanskelig å utlede på basis av observasjoner alene, og gir viktig informasjon for at beslutningstakere skal kunne vurdere ytterligere utslippsreduserende tiltak. Ut ifra resultatene i avhandlingen anbefales det å inkludere PCB-11 og dekloran pluss, i tillegg til andre POP-er i fremtidige overvåkingsprogrammer. Det anbefales også å vurdere både komplementære og alternative prøvetakingsmetoder for de mest flyktige POP-ene, og for partikkelbundne forbindelser. Videre utvikling av utslippsestimater for flere forbindelser med økende miljørelevans vil være nødvendig når kilde-reseptorforhold for disse skal vurderes.

1. Introduction

1.1. Properties of POPs

Persistent organic pollutants (POPs) are a group of organic chemicals, consisting of typically halogenated aromatic or aliphatic compounds. These include organochlorine pesticides (OCPs), halogenated industrial chemicals and unintentionally byproducts that are formed during various combustion and manufacturing processes. POPs usually possess semi-volatile properties and are characterized to be persistent (P), bioaccumulative (B), toxic (T), and with long-range environmental transport potential (LRTP) (Jones 1999). As a result, they have been recognized as a serious, global threat to human health and the environment. Polychlorinated biphenyls (PCBs) and dichlorodiphenyltrichloroethanes (DDTs) are examples of traditional semi-volatile POPs. Per- and polyfluoroalkyl substances (PFAS) are examples of less volatile and more water-soluble POPs that have gained more recent attention.

Public attention and concerns related to possible harmful effects of POPs on the environment and human health grew in the 1960s, and was triggered by for example Rachel Carson, raising the issue of chlorinated insecticides in the book "Silent spring" (Carson, 1962). Analytical developments had enabled detection of these chemicals in trace amounts (Gohlke & McLafferty, 1993). In the light of this, DDTs were analyzed in samples from the Swedish environment by Sören Jensen. During the analyses he also discovered large quantities of PCBs (Jensen, 1972). Both compound classes had been synthesized for many years already, and despite known health-related issue among workers at their factories, it was important contributions like Carson's book and Jensen's findings that initiated increased focus on the environmental effects of these compounds.

An accident in western Japan in 1968 (Aoki, 2001), where rice oil was contaminated with PCBs, demonstrated the severe consequences of human exposure to PCBs. About 2000 people were poisoned and suffered in the acute phase from symptoms like chloracne ("Yusho disease"), while endocrine disrupting effects were observed in the long-term. Children born several years after the accident showed serious health effects as a consequence of exposure to PCBs when in the womb.

These historical examples demonstrated that while PCBs were valued for their chemical stability as e.g. electrical insulators and DDTs represented a cost-effective insecticide, their

hazardous properties were increasingly recognized as a potential threat to human and environmental health.

1.1.1. *Persistent, bioaccumulating and toxic (PBT)*

In spite of being classified as persistent, POPs can degrade in environmental media such as air, water, soils and sediments through abiotic processes like photooxidation, photolysis and hydrolysis, and through biodegradation by microorganisms (Boethling et al., 2009). However, their high persistence make them degrade slowly, which is reflected in their long half-lives (e.g. >2 months in water and >6 months in soil/sediments (UNEP, 2020)). Partitioning to other media and mode of entry are processes that may further prolong the overall environmental persistence of POPs (Webster et al., 1998). Partitioning and degradation processes associated with POPs are often temperature dependent and the persistence in cold environments like the Arctic may be enhanced relative to temperate regions (Wania & Mackay, 1993; Wong et al., 2021).

Once chemicals are released, they may enter an organism through ingestion, dermal contact or respiration. The chemical properties of POPs favor uptake and retention in organisms, especially in fatty tissues. The ability of POPs to bioaccumulate in an organism is related to their high persistence and partitioning behavior (Campfens & Mackay, 1997; Kidd et al., 1998). This also results in high potential to concentrate as they move through the food chain (e.g. biomagnification), putting top-predators like polar bears and killer whales at elevated risk (Letcher et al., 2009; Schlingermann et al., 2020), but also humans (McLachlan et al., 2011). In organisms (both humans and wildlife), POPs may cause adverse effects like endocrine disruption, reproductive and immune dysfunction, neurobehavioral and developmental disorders, and/or cancer (Buha Djordjevic et al., 2020; Letcher et al., 2010; Maleky & Sarafpur, 2001; Ross et al., 1995; UNEP, 2020; Weihe et al., 2016). However, a hazardous chemical may not pose any risk unless it is actually released to the environment in large enough quantities (Mackay et al., 2001).

1.1.2. *Long-range atmospheric transport potential (LRATP)*

Since the 1970's, POPs like DDTs and PCBs have been known to be present in remote regions like the Arctic (Clausen & Berg, 1975), and long-range transport (LRT) was suggested to occur (Ottar, 1981). The potential to undergo LRT describes the ability of a chemical to travel by e.g. air and ocean currents.

Physical-chemical properties such as vapor pressure and water solubility influence the environmental fate of chemicals (Wania & Mackay, 1993). The semi-volatile POPs targeted in this thesis generally have low water solubility and the ability to volatilize from surface media. Because of this, they have a large transport potential in air (i.e. half-life >2 days (UNEP, 2020)), which also is the fastest transport route to remote areas such as the Arctic.

In the atmosphere, POPs exist either as gases and/or in condensed form sorbed to atmospheric aerosol particles (Wania & Mackay, 1996). The octanol-air partition coefficient (K_{OA}) is often used to describe gas-particle partitioning of POPs in the atmosphere, which is a function of temperature. Because of their high persistency and long lifetime (i.e. half-life more than 2 days in air (UNEP, 2020)), they may be transported long distances with air masses. As temperature falls, there is a tendency for chemicals present in gas phase in the atmosphere to "condense" onto land, water or particles (Wania & Mackay, 1993). Due to differences in K_{OA}, compounds may "condense" at different air temperatures. This means that the more volatile and persistent POPs (log K_{OA} 6-8) have high mobility and the potential to be transported over long distances before being deposited (Beyer et al., 2003; Wania & Mackay, 1996). Re-emissions into the atmosphere may occur after deposition, and they may be transported through a series of evaporation and deposition steps, a process also called "grasshopping" (Gouin et al., 2004; Wania, 2003). Warm temperatures in tropical and subtropical regions favor evaporation, while cold temperatures at higher/lower latitudes favor deposition from the atmosphere. On the other hand, less volatile POPs (log K_{OA} 8-10) tend to increasingly partition onto particles and remain closer to the region of their emission because of rapid dry/wet particle deposition (Beyer et al., 2003; Wania & Mackay, 1993, 1996). However, findings of involatile and thereby mainly particle-associated POPs (log K_{OA}>12) in snow and ice in the Arctic suggest that long-range particle transport also occurs (Hermanson et al., 2010; Meyer et al., 2012). The LRATP of POPs is not only dependent on the loss due to dry deposition, but also on wet deposition dependent on the water solubility of the POPs. Degradative loss processes in air due to e.g. OH-radical reactions (Anderson & Hites, 1996; Mackay et al., 2001) may also affect the LRATP of POPs. Overall, LRATP of POPs is limited by atmospheric reaction and net atmospheric deposition. The relative significance of these two processes vary for different POPs.

1.2. Regulations

To protect human health and the environment from POPs, regulations have been introduced aiming to eliminate or restrict their production, use and emissions. During the 1980's, national

measures in many European countries (e.g. Norway) were implemented to reduce the production and use of some POPs (Breivik et al., 1999; Breivik et al., 2002a; Pacyna et al., 2003). Later, in 1998, the Geneva Convention on Long-Range Transboundary Air Pollution (CLRTAP) established the Aarhus protocol on POPs in Europe (UNECE, 1998), which entered into force in 2003. Building on the CLRTAP Aarhus protocol, a global treaty on POPs was established in 2001, i.e. the Stockholm Convention (UNEP, 2020). The Stockholm Convention entered into force in 2004. By 2023, 29 countries within Europe have signed the Aarhus protocol, while the Stockholm Convention has been signed by 152 countries globally. Both Conventions are continually revised and chemicals fulfilling the four hazard criteria of POPs (i.e. P, B, T and LRTP), and assessed to represent a risk to environmental and human health, have been added to the list of regulated POPs. While 16 and 12 chemicals / chemical groups were initially regulated under the Aarhus protocol and the Stockholm Convention respectively, a total of 25 and 28 chemicals and chemical groups are regulated under these two agreements by 2023, respectively. The increasing number of POPs that have been regulated illustrates the importance of collecting data on OCEC to inform possible new regulations.

1.3. Air monitoring

Air rapidly responds to changes in emissions and is therefore among the core media in the Global Monitoring plan, used to evaluate the effectiveness of the Stockholm Convention (UNEP, 2013). POPs in air are commonly sampled using active sampling techniques. However, these samplers are driven by pumps and require electricity and trained personnel, and the operation of active air samplers (AAS) are therefore associated with high cost. Passive air samplers (PAS), on the other hand, are simple and cost-efficient, and thereby enables air sampling at multiple locations simultaneously.

Within Europe, a monitoring program was established to examine suspected long-range transport of air pollutants in 1972 (Ottar, 1976). While this program initially focused on acidic precipitation, the network of monitoring sites was later continued in the European Monitoring and Evaluation Programme (EMEP) under CLRTAP, in which active air monitoring of POPs were included from 1999 (Tørseth et al., 2012). Monitoring in the Norwegian Arctic already started in 1991 (Bohlin-Nizzetto et al., 2017). In 2020, 12 background air monitoring sites (including three monitoring stations in Norway) reported concentrations of POPs to EMEP. While this monitoring program is based on a limited network of AAS optimized to assess time trends at the individual sites, both temporal and spatial trends in Europe are further assessed in two PAS networks; Global Atmospheric Passive Sampling network (GAPS) (Pozo et al., 2006;

Schuster et al., 2021a) and the Monitoring Network (MONET) (Holoubek et al., 2011; Kalina et al., 2019). These AAS and PAS monitoring efforts, together with other smaller networks and case-studies, enable regular evaluation of the effectiveness of the Stockholm Convention under the Global Monitoring Plan. A few case-studies (Gioia et al., 2007; Halse et al., 2011; Jaward et al., 2004) have further assessed the spatial trends in Europe, but except Halse et al. (2011) (n=86), the number of background sampling sites has been limited (<46). There are also a limited number of studies focusing on background concentrations of POPs on national level, e.g. Czech Republic, Spain and Chile (Kalina et al., 2018; Munoz-Arnanz et al., 2016; Pozo et al., 2004).

1.4. Targeted compounds

Most legacy POPs were intentionally produced as i) industrial chemicals used in many different applications and often as additives in products, or ii) OCPs commonly used in agriculture and therefore applied directly in the environment. Some POPs are not deliberately produced, but may form or be released inadvertently during combustion, or form as byproducts in manufacturing processes.

Table A1 provides detailed information, including log K_{OA} and the year of regulation for the individual compounds and compound groups examined in this thesis. The sources and emissions of the studied compounds are described below.

1.4.1. Legacy POPs

PCBs

From 1930 to 1993, a total of 1.3 million tons of PCBs were estimated to have been intentionally produced as technical mixtures (e.g. Aroclors), with the highest production in the 1960s and 1970s (Breivik et al., 2007; Li et al., 2023). The intentionally produced PCBs (I-PCBs) have been extensively used in industry as heat exchange fluids, as additives in building materials and in electrical products. For this reason, emissions of I-PCBs are assumed to be linked to population density. Emissions of I-PCBs have been reported to be widespread in central parts of Europe (Breivik et al., 2002b). While the I-PCBs are no longer produced, they remain in products which are still in use (e.g. old electric equipment) and waste products. Primary emissions are therefore still continuing, e.g. because of burning of waste (Breivik et al., 2016; Li & Wania, 2018).

The PCB group consists of 209 congeners with varying numbers (1-10) and positions of chlorine substituents. A group of seven PCBs (28, 52, 101, 118, 138, 153 and 180) have been

used as indicator for the technical mixtures (e.g. Megson et al., 2019). Some PCBs have a coplanar structure and are found to have dioxins-like properties (Van den Berg et al., 1998).

Unintentional emissions of PCBs (U-PCBs) also exists, with PCB-11 being the most dominant PCB congener detected in air (Mastin et al., 2022). PCB-11 is mainly associated with the manufacturing of the pigment diarylide yellow (Hu & Hornbuckle, 2010), but may also form in combustion and thermic processes (Vorkamp, 2016). With reduced emissions of I-PCBs, the relative contribution of unintentional emissions of PCB-11 is likely to increase.

HCB and PeCB

Hexachlorobenzene (HCB) and pentachlorobenzene (PeCB) have previously been used e.g. as fungicides, and 155 000 tons of HCB have been produced with the largest production in the 1980s (Li et al., 2023). HCB is known to have been extensively used within Europe (Barber et al., 2005). Despite production and use of HCB and PeCB have ceased, unintentional primary emissions of both PeCB and HCB may still be ongoing (Bailey, 2001; Bailey et al., 2009).

HCHs

Hexachlorohexanes (HCHs) were intentionally produced OCPs, that were used extensively as insecticides within Europe (Breivik et al., 1999). The global usage of technical HCH (55-80% α-HCH, 5-14% β-HCH, 8–15% γ-HCH) and Lindane (>99% γ-HCH) have been estimated to be 10 million tons (1948-1997) and 720 000 tons (1970-1993) respectively (Li & Macdonald, 2005). Notably, γ-HCH has the highest insecticidal activity of the isomers.

Until an EU ban in 1979, the major source of HCHs within Europe was technical HCH. Former Soviet Union, France, Germany and Spain are the countries reported to have experienced the highest technical HCH use (Li & Macdonald, 2005). From 1979, most European countries were using Lindane only. However, the use of technical HCH continued in some countries in former Soviet Union and eastern Europe (Breivik et al., 1999). Large stockpiles of HCHs have later been reported to be a significant source in many European countries (Vijgen et al., 2019).

DDTs and metabolites

DDT is an insecticide to control insect-transmitted human diseases, such as malaria, and as agricultural pest control. From 1940 to 2000, 4.5 million tons of DDTs were estimated to be produced (Li & Macdonald, 2005), with the highest production in the 1950s and 1960s (Li et al., 2023). Within Europe, the former Soviet Union has experienced the highest overall DDT use, while the agricultural use in Italy and Hungary has been reported to be significant.

Technical DDT is composed of a mixture of isomers, with 80% *p,p'*-DDT and 20% *o,p'*-DDT (Li & Macdonald, 2005). Some DDTs also exist as impurities in the miticide Dicofol (46% *o,p'*-DDT, 7% *p,p'*-DDT and 18% *o,p'*-DDE) (Qiu et al., 2005). Furthermore, degradation of DDT leads to the metabolites DDE (dichlorodiphenyldichloroethylene) and DDD (dichlorodiphenyldichloroethane) (Ricking & Schwarzbauer, 2012).

Aldrin and metabolites

Aldrin, dieldrin and endrin were insecticides used to kill e.g. termites. They have been produced in amounts of 233 000 tons of Aldrin, 26 000 tons of dieldrin and 57 000 tons of endrin globally, with the highest production in the 1960s and 1970s (Li et al., 2023). Aldrin may degrade to dieldrin (Gannon & Bigger, 1958). Furthermore, isodrin and endrin are isomers of aldrin and dieldrin, respectively, and isodrin and endrin were also byproducts in the production of aldrin and dieldrin.

Chlordanes and heptachlor

Technical chlordane was used as an insecticide in agriculture and in control of termites, and 180 000 tons have been produced globally, with the highest production in the 1970s (Li et al., 2023). The insecticide consists mainly of cis- and trans-chlordane (11% and 13% respectively (Bidleman et al., 2002)), which may be degraded to oxychlordane. Technical chlordane also contains heptachlor and trans-nonachlor in appreciable amounts (5% of each), while chlordane and cis-nonachlor (Sovocool et al., 1977) have been detected in relatively low amounts. Technical heptachlor has also been used and was produced in 45 000 tons, peaking in the 1960s (Li et al., 2023). Heptachlor may degrade to heptachlor epoxide (exo/endo).

Endosulfans

Technical endosulfan was used as insecticide and 622 000 tons have been produced globally, with the highest production in the 2000s (Li et al., 2023). Technical endosulfan consists of 60-70% of endosulfan I (α-isomer) and 30-40% endosulfan II (β-isomer) (Weber et al., 2010). Endosulfan sulfate is a degradation product of endosulfan.

1.4.2. Organic contaminants of emerging concern (OCECs)

Due to the continued demand for chemicals with similar functions as the POPs, some of the legacy POPs are being replaced with alternative compounds. These organic contaminants of emerging concern (OCECs) may exhibit similar physical-chemical properties to the POPs, and thus potentially fulfill some or all of the POP hazard criteria.

Alternative flame retardants are one group of OCECs, used for replacing the regulated PBDEs (polybrominated diphenyl ethers) in fulfilling fire safety standards in e.g. electronics (Vorkamp & Riget, 2014). Dechloranes are examples of alternative chlorinated flame retardants. Organophosphate flame retardants (OPFRs) and alternative brominated flame retardants (aBFRs) are other replacements for PBDEs.

PBDEs, alternative flame retardants and chlorinated paraffins were originally targeted in the analysis. However, results are only presented for dechloranes, due to high influence of co-extracted substances (section 3.4-3.5) and high background concentrations for the other chemicals.

Dechloranes

Of the known dechloranes, dechlorane plus (DP) has been identified as a potential new POP. It was proposed for listing under the Stockholm Convention in 2018 (UNEP, 2019) and was recently recommended for listing (UNEP, 2023). Technical DP has been used in industrial polymers in electronics and building materials as a replacement for the chlorinated flame retardant Mirex (Table A1) and the brominated flame retardant decabromodiphenyl ether (regulated since 2017 under the Stockholm Convention). The production volume of DP is highly uncertain, with estimated global production volume varying between 750 and 6000 tonnes annually in 2020 (Hansen et al., 2020). Technical DP consists of 20-40% of the syn-isomer and 60-80% of the anti-isomer (Wang et al., 2010).

Other dechlorane related compounds (DRCs), i.e. dechlorane-601 (Dec-601), dechlorane-602 (Dec-602), dechlorane-603 (Dec-603) and dechlorane-604 (Dec-604) have also been used as alternative flame retardants, but the knowledge of production and use is limited (Sverko et al., 2011).

1.5. Main sources

While primary emissions of POPs (described in section 1.4) historically have dominated the atmospheric burdens of POPs, POPs also have the potential to be re-emitted from surface media contaminated in the past (Jones, 1994; Ma et al., 2011; Wania & Mackay, 1996). These so-called secondary emissions are likely to increase with increasing global temperatures (Ma et al., 2011; Nizzetto et al., 2010). Furthermore, as the primary emissions decrease, the relative importance of secondary emissions is assumed to increase. It is therefore questioned whether further reductions in primary emissions in Europe will influence the overall concentrations in

air, and more knowledge of the relative importance of primary and secondary emission sources is therefore needed.

The relative contribution of primary and secondary emission within Europe is hypothesized to vary i) spatially, due to differences in historical production and use from country to country, and ii) for different POPs (both on a group level and for individual compounds). Furthermore, the emissons of some POPs are assumed to be linked to population density (e.g. PCBs), while the emissions of others also may be related to rural areas (e.g. OCPs). Nonetheless, the atmospheric burdens of POPs in central parts of Europe are likely to be more affected by local sources, than the more remote regions, such as Norway and the Arctic.

Contrary, long-range atmospheric transport (LRAT) is assumed to largely influence the atmospheric concentrations in remote regions (Halse et al., 2011; Hung et al., 2016; Jaward et al., 2004; Meijer et al., 2003). However, the concentrations in the remote regions may not always be attributed to LRAT only (e.g. Norway (Halse et al., 2012) and the Arctic (Hung et al., 2022)), and a better understanding of the influence of national emissions vs. transboundary emissions is important in order to inform policy-makers whether further reductions in atmospheric concentrations are more efficiently achieved through national control measures or through international collaboration.

2. Objectives

The main objective of this thesis was to assess the main sources (primary emissions, secondary emissions, LRAT and national emissions) controlling the occurrence of selected POPs and OCECs in European background air, with special emphasis on Norway and the Arctic.

The sub-objectives were to:

Objective I (Paper I)

Improve the understanding of the occurrence and spatial patterns of POPs in background air on a national scale (Norway) and compare background concentrations with measurements from an area expected to be more influenced by local emissions.

Objective II (Paper II)

Improve the understanding of the occurrence and spatial patterns of POPs in background air across Europe.

Objective III (Paper III)

Improve the understanding of the occurrence and spatial patterns of the emerging contaminant dechlorane plus and dechlorane related compounds in European background air.

Objective IV (Paper IV)

Improve the understanding of the occurrence and spatial patterns of the unintentionally produced PCB-11 in European background air.

3. Methods

3.1. Theory

3.1.1. Air sampling

Air sampling is traditionally performed using AAS, with a pump that draws air through a sampling medium (Bidleman & Olney, 1974). Under EMEP, air samples are collected with AAS equipped with a glass fiber filter (GFF) to capture particle-associated chemicals in sequence with two polyurethane foam plugs (PUF) to capture gas-phase chemicals (EMEP, 2001). High-volume bulk samples are collected under controlled flow with high temporal resolution, typically 24-48 hours per week. This provides known sample volumes and short-term concentrations (Melymuk et al., 2014), which in combination with atmospheric transport models offers possibilities to study specific LRAT episodes (e.g. (Eckhardt et al., 2007)).

Air sampling using PAS is a complementary and more cost-efficient strategy than using AAS. A major benefit with PAS in the context of this thesis, is that this method may be particularly useful to help expand the spatial coverage of air measurements (Jaward et al., 2004; Shoeib & Harner, 2002). In this thesis, PAS was therefore the chosen method to obtain a comprehensive dataset for evaluation of spatial patterns across Europe and Norway. With PAS, chemicals are accumulated to the sampling media mainly through diffusion. To obtain consistent uptake and reduce the influence of environmental factors, the sampling medium is deployed inside a sampler housing protecting it from wind, precipitation and light, yet allowing a free flow of air around the sampling media. Several types of PAS have been developed over the last decades, with different designs and sampling media (sorbents), e.g. polymer-coated glass (POG) (Harner et al., 2003), semipermeable membrane devices (SPMD) (Petty et al., 1993), sorbent-impregnated polyurethane foam disk (SIP) (Shoeib et al., 2008) and XAD-2 resin-based PAS (Wania et al., 2003), and with different uptake capacities (Melymuk et al., 2014). The polyurethane foam-based PAS (PUF-PAS, Figure 1) developed by Shoeib & Harner (2002) is well characterized and has been extensively used in PAS monitoring for sampling semi-volatile organic contaminants like POPs (Holoubek et al., 2011; Pozo et al., 2006). The use of PUF-PAS in this thesis also assured consistency in the comparison of results against data from the European PAS campaign conducted in 2006 (Halse et al., 2011), GAPS (Schuster et al., 2021a), and MONET (Kalina et al., 2019).

The sampling with PUF-PAS is based on diffusive uptake of gas-phase chemicals from air to a PUF disk (i.e. the sampling sorbent), which is deployed inside two steel bowls (Figure 1)

(Jaward et al., 2004). Due to lower sampling rate (typically in the range 3-4 m^3/day (Wania & Shunthirasingham, 2020)) than the flow of an AAS, deployment for weeks to months (typically 12 weeks) is necessary for the PUF disks in order to collect detectable amounts (Kalina et al., 2019; Schuster et al., 2021a). This means that the PUF-PAS provides long-term time-averaged concentrations. Since the exact sampled air volume is not known with PUF-PAS, only semi-quantitative concentrations are derived from an estimated uptake rate (section 3.3) (Melymuk et al., 2014; Wania & Shunthirasingham, 2020).

The uptake of particle-associated compounds with log K_{OA}>12 (like dechloranes, **Paper III**) by the PUF-PAS, is associated with larger uncertainties than the uptake of gas-phase compounds. Fine aerosols (i.e. particles <1µm) may behave similarly to gases and become consistently trapped inside the PUF disk (Chaemfa et al., 2009). Coarser particles may also be deposited on the PUF, but the sampling efficiency of particle-associated compounds has been shown to be lower compared to gas-phase compounds for PAS with the MONET design (Bohlin et al., 2014; Kalina et al., 2017; Markovic et al., 2015), which is applied in this work. One reason for this may be that the freely-hanging MONET-sampler housing (diameter 30 (upper bowl) and 24 cm (lower bowl)) filters out coarser particles (Klanova et al., 2008). In contrast, the PUF-PAS used within GAPS (diameter 24.5 and 19.5 cm) is placed in a fixed position (Harner et al. 2006) and has shown to have higher efficiency of particle collection than the MONET sampler (Chaemfa et al. 2009, Markovic et al. 2015). The PUF-disks used within GAPS also have lower density (0.021 g/cm^3) than the PUF-disks in this study (0.027 g m^{-3}) which may be another reason for the higher sampling efficiency with the GAPS sampler.
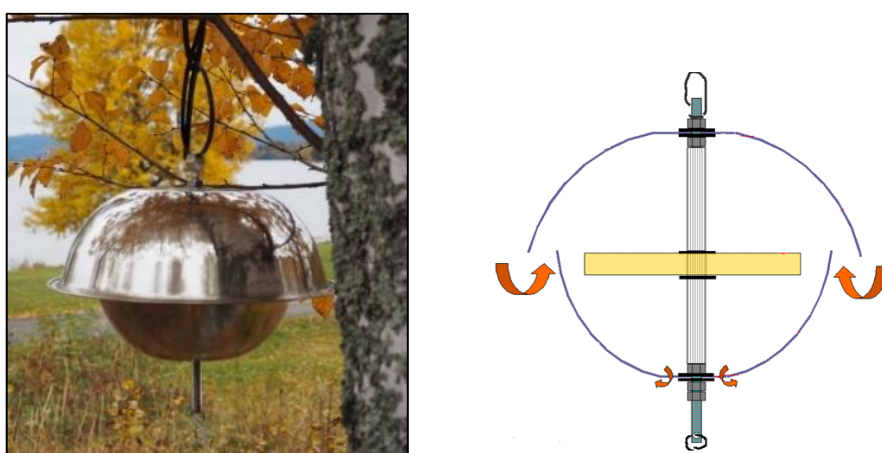
Figure 1. Illustration of the polyurethane foam-based passive air sampler (PUF-PAS) with the MONET design (Bohlin et al., 2014; Markovic et al., 2015), which is applied in this work.

The PUF is porous with high capacity for organic chemicals. Consequently, chemicals in air may penetrate and accumulate in the PUF. The diffusion of a gas-phase chemical from air to the PUF is described as a three-step process (Figure 2) from i) ambient air to the air inside the sampling chamber, ii) air inside the sampling chamber to the air-side boundary layer of the PUF-air interface, and iii) the air-side boundary layer to the sampler-side boundary layer, and further into the PUF (Bartkow et al., 2005). By using the Whitman two-film approach (Whitman, 1923), the concentration in the air-side boundary layer is assumed to equal the concentration in the sampler-side boundary layer. The overall flux (F, Eq. 1) from ambient air and into the PUF can be described by Fick's first law, which is a function of the overall mass transfer coefficient (k) (or velocity of the chemical across the PUF-air interface, m/day), the surface area of the PUF (A_{PUF}, m^2), the difference between the concentration in air (C_{air}, pg/m^3) and the concentration in the PUF (C_{PUF}, pg/m^3), and the PUF-air partition coefficient ($K_{PUF-air}$, dimensionless);

$$F = kA_{PUF}(C_{air} - C_{PUF}/K_{PUF-air}) \qquad\qquad (Eq.\ 1)$$
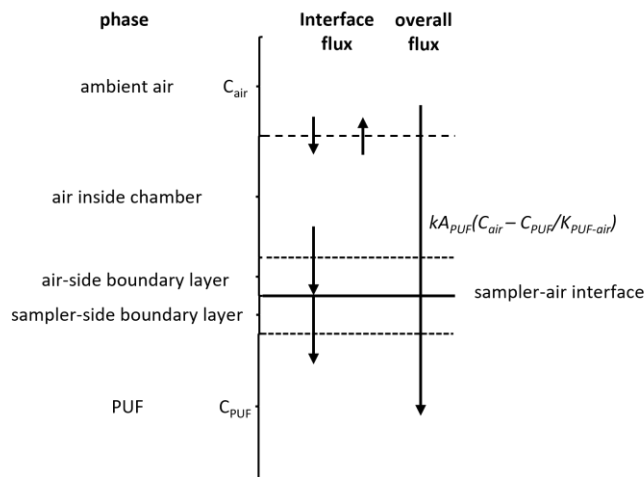
Figure 2. The three-step diffusion process of a chemical from air to the sampling chamber (Bartkow et al., 2005)

The accumulation of a chemical in the gas-phase is the difference between the rate of uptake (k_u) and the rate of elimination (k_e) (Eq. 2). Considering that the uptake is air-side controlled and the overall and air-side mass coefficients k and k_{air} are equal, the relation to the net flux (i.e difference between uptake and elimination flux) is the following (Bartkow et al., 2005; Shoeib & Harner, 2002);

$$V_{PUF}\left(\frac{dC_{PUF}}{dt}\right) = k_u C_{air} - k_e C_{PUF} = (k_{air} A_{PUF})C_{air} - \left(k_{air} \frac{A_{PUF}}{K_{PUF-air}V_{PUF}}\right)C_{PUF} \qquad (Eq.\ 2)$$

When Eq. 2 is solved and accounted for that $K_{PUF\text{-}air} = C_{PUF}/C_{air} = V_{air}/V_{PUF}$, an expression for the air volume of a chemical sampled with the PUF-PAS (V_{PUF}) as a function of time (t) is generated (Eq. 3) (Harner et al., 2004). An illustrative figure of this uptake curve is given in Figure 3.

$$V_{air} = K_{PUF-air}V_{PUF}\left[1 - e^{-\left(\frac{k_{air}A_{PUF}}{K_{PUF-air}V_{PUF}}\right)t}\right] \qquad (Eq.\ 3)$$
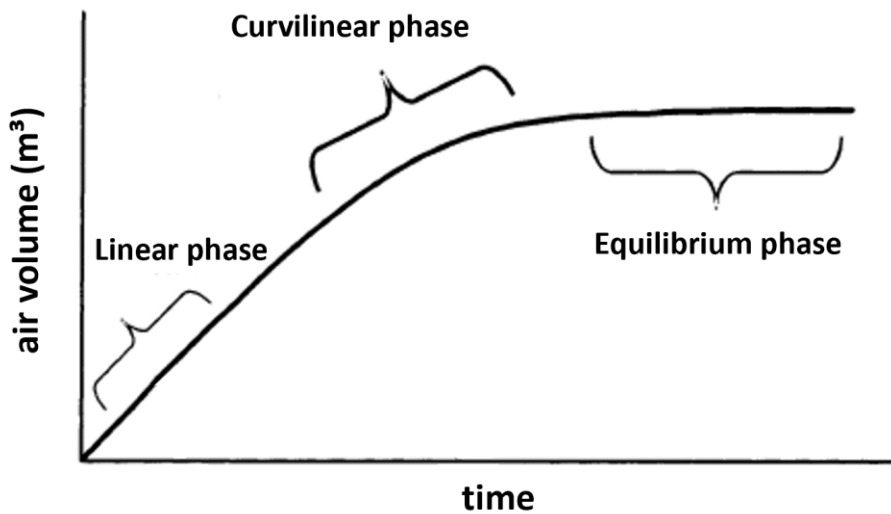
Figure 3. Illustrative uptake curve of a chemical sampled with PUF-PAS, showing three phases of uptake (Harner, 2017; Shoeib & Harner, 2002).

The chemicals accumulate in the PUF-PAS through a linear, curvilinear and equilibrium phase (Figure 3) (Shoeib & Harner, 2002). Initially, C$_{PUF}$ is small and hence the elimination rate (k_e) in Eq. 2 is negligible. This generates a linear function. The concentration of chemicals in the PUF (C$_{PUF}$) increases with increasing sampling time, and the elimination rate (k_e) becomes larger. Consequently, the uptake is reduced and enters the curvilinear phase. Finally, when equilibrium is established between the air and PUF, there is no net uptake (i.e. uptake = elimination rate) and C$_{PUF}$ becomes constant.

The PUF-PAS used in this thesis are designed as kinetic samplers, to ideally be operated in the linear phase for the full deployment length. Consequently, the slope equal to $k_{air}A_{PUF}C_{air}$, with $k_{air}A_{PUF}$ representing the rate of uptake or sampling rate (SR, m^3/day). The uptake rate can be estimated from calibration studies against AAS, or by the use of performance reference compounds (PRCs) (section 3.1.2).

3.1.2. Estimating sampled air volumes with PUF-PAS

The sampled air volume (V_{air}, Eq. 3) is essential in the calculation of air concentrations per m³ (C_{air}, section 3.6). A template based on Eq. 3 (Harner, 2017) is considered to be the most frequent method for estimating the air volume of a gas-phase chemical sampled with the PUF-PAS. This method has also been applied in this thesis.

The sampling rate is an important input to the Harner-template. In **Paper I**, **II** and **IV**, PRCs were used to obtain site-specific sampling rates and account for environmental conditions like wind speed at the sampling sites (section 3.1.3) (Bartkow et al., 2006; Moeckel et al., 2009). The PRCs are a range of compounds that cannot be found in the environment but cover a range of volatilities (e.g. from PCB-1 to PCB-198, **paper I**, **II** and **IV**). They will therefore volatilize into the atmosphere at different rates during the deployment period (t), and the loss of PRCs ($\frac{C}{C_0}$) are used to calculated SR (Moeckel et al., 2009);

$$SR = \frac{-\ln\left(\frac{C}{C_0}\right)K_{PUF-air}\rho_{PUF}V_{PUF}}{t} \qquad (Eq.~4)$$

In Eq. 4, C_0 and C are the concentrations of PRCs at the beginning and the end of the deployment period, respectively, and ρ_{PUF} is the density (g/m³) of the PUF.

The PRCs experiencing losses between 40% and 80% (relative to PCB-198, (Moeckel et al., 2009)) were used to calculate an average site-specific SR which was applied to all compounds (i.e. not compound-specific R (Bohlin et al., 2014)). For sites with none- or only one PRC fulfilling the required loss, the sampling rates were instead estimated from wind speeds at the given sites (Tuduri et al., 2006). Average wind speeds at each site during the exposure period were retrieved from the ERA Interim database from European Centre for Medium-Range Weather Forecasts (ECMWF).

PRCs are not applicable for predominantly particle-associated compounds (e.g. dechloranes). Instead, a generic SR (2.3 m³/day (Drage et al., 2016)) was used in **Paper III**. While the sampling rate accounts for the lower uptake efficiency of particles with the MONET sampler (54%), compared to the GAPS sampler (92%) (Markovic et al., 2015), a constant sampling rate does not account for sampling conditions such as temperature and wind speed at a given sampling sites. However, the predominantly particle-bound dechloranes are less affected by changes in temperature than more volatile compounds (Bohlin-Nizzetto et al., 2020).

Data on PUF characteristics (A_{PUF}, V_{PUF} and ρ_{PUF}) and the $K_{PUF\text{-}air}$ for each compound are needed when calculating the air volume sampled (Eq. 3). $K_{PUF\text{-}air}$ is a thermodynamic parameter and describes the maximum uptake capacity of the PUF. $K_{PUF\text{-}air}$ is highly correlated to the *log* K_{OA} (Table A1) for each compound (Eq. 5) (Shoeib & Harner, 2002);

$$log\,K_{PUF-air} = (0.6366\,logK_{OA} - 3.1774) \qquad (Eq.\ 5)$$

3.1.3. Uncertainties with PUF-PAS

The uptake of compounds in gas-phase to the PUF is influenced by the meteorological conditions at a given site (Klanova et al., 2008). Though the PUF is sheltered, it has been shown that high wind (>4 m/s) may result in an increased SR due to reduced thickness of the air boundary layer (Figure 2) (Huckins et al., 2002; Tuduri et al., 2006). The use of PRCs account for variations in sampling rates caused by differences in wind speed. The use of the Harner-template also compensates for the differences in temperature from site to site. The ambient air temperatures and wind speeds were not measured at each site but based on data from ECMWF and averaged over the sampling period. Beyond the compensation of wind speed and temperature, comparison with AAS data may further control and/or evaluate the sampling artifacts associated with PUF-PAS. Overall, PUF-PAS is regarded to be a useful sampling method for comparing spatial variability, despite its semi-quantitative nature.

To minimize the uncertainties related to sampling with PUF-PAS, sampling in the linear phase is preferable. However, the elimination rate in Eq. 2 is dependent on $K_{PUF\text{-}air}$ or K_{OA} (Eq. 5) which varies over many orders of magnitude for the targeted compounds in this thesis (Table A1). Hence, the length of the linear phase may vary widely and some of the more volatile compounds may therefore enter the curvilinear or equilibrium phase during the sampling period. Furthermore, the uptake capacity for different compounds will be different at different deployment temperatures. For gas phase compounds, the amount adsorbed to the PUF is generally higher at lower temperatures than at high temperatures due to a longer linear-phase (Klanova et al., 2008). For more volatile compounds with log K_{OA}<8 (e.g. HCB and PCB-11, Table A1, **Paper I/ II** and **IV**), the curvilinear or equilibrium phase may be reached during the deployment period (even at low temperatures) (Figure 3) (Francisco et al., 2017). As the rate of uptake is decreasing during the sampling period, the amount taken up by the sampler is lower compared to less volatile compounds (e.g. PCB-153, Table A1) still in the linear phase. Eq. 3 used for calculating air volumes in the Harner template, accounts for the elimination rate, and consequently, a lower volume is estimated for volatile compounds.

It is worth noting that Eq. 2-3 assumes that i) the air-side controls the uptake and ii) the concentration in air (C_{air}) stays constant during the deployment period. The resistance within the PUF is inversely related to K_{OA}, and hence is assumed to be negligible for the POPs given their large K_{OA}, with air-side controlled uptake as a result. However, Zhang et al. (2011) showed that also the sample-side has impact on the uptake due to a decreasing rate while the chemicals penetrate into the PUF, i.e. chemicals mainly accumulate in the outer layer. This also has an impact on the use of PRCs which presupposes that the distribution of sampled chemicals and PRCs within the PUF is similar. Furthermore, if sampling is conducted during the curvilinear phase, the rate of uptake is gradually decreasing and may lead to larger impact of the air sampled in the beginning of the period. If equilibrium is reached there is also the possibility of formation of new equilibriums due to a change in concentration. Consequently, the PUF-PAS does not provide a true time-averaged concentration if overreaching the linear phase (Wania & Shunthirasingham, 2020).

3.2. Sampling strategy

The first study (**Paper I**) utilized data from a passive air sampling campaign in Norway with 47 sampling sites, including two remote sites on Spitsbergen (Figure 4). As far as possible, background sites included in previous studies were selected. Ten urban sites around the city of Oslo were additionally included, to compare and evaluate the assumed background concentrations with concentrations from an urban area expected to be influenced by local emissions.

The campaign in Norway was coordinated with a European campaign (**Paper II-IV**). Passive air samples were collected at 101 sampling sites across 33 countries along a European-Arctic transect (35 °N to 82 °N, 52°W to 48 °E, Figure 5). With a few exceptions (Capo Granitola and Monte Curcio in Italy, and four sites in Russia), the sampling sites were existing background monitoring stations reporting various inorganic and organic compounds in air to EMEP (Tørseth et al., 2012), in order to obtain a dataset representing the assumed background concentrations at each site.

The sampling period in both campaigns was coordinated in time to facilitate comparison of results, covering three months in the period from June to October 2016.
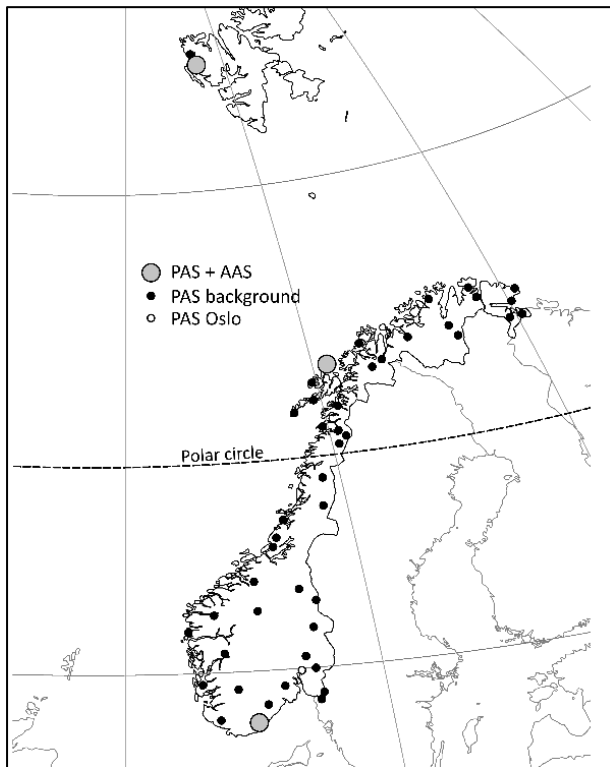
Figure 4. The spatial coverage of background sites monitoring POPs with PAS (black/grey) in this study along with the spatial coverage of sites in the Norwegian national monitoring program sampling POPs using AAS (grey) (Bohlin-Nizzetto et al., 2017). Ten urban sites around the city of Oslo were additionally included (white).
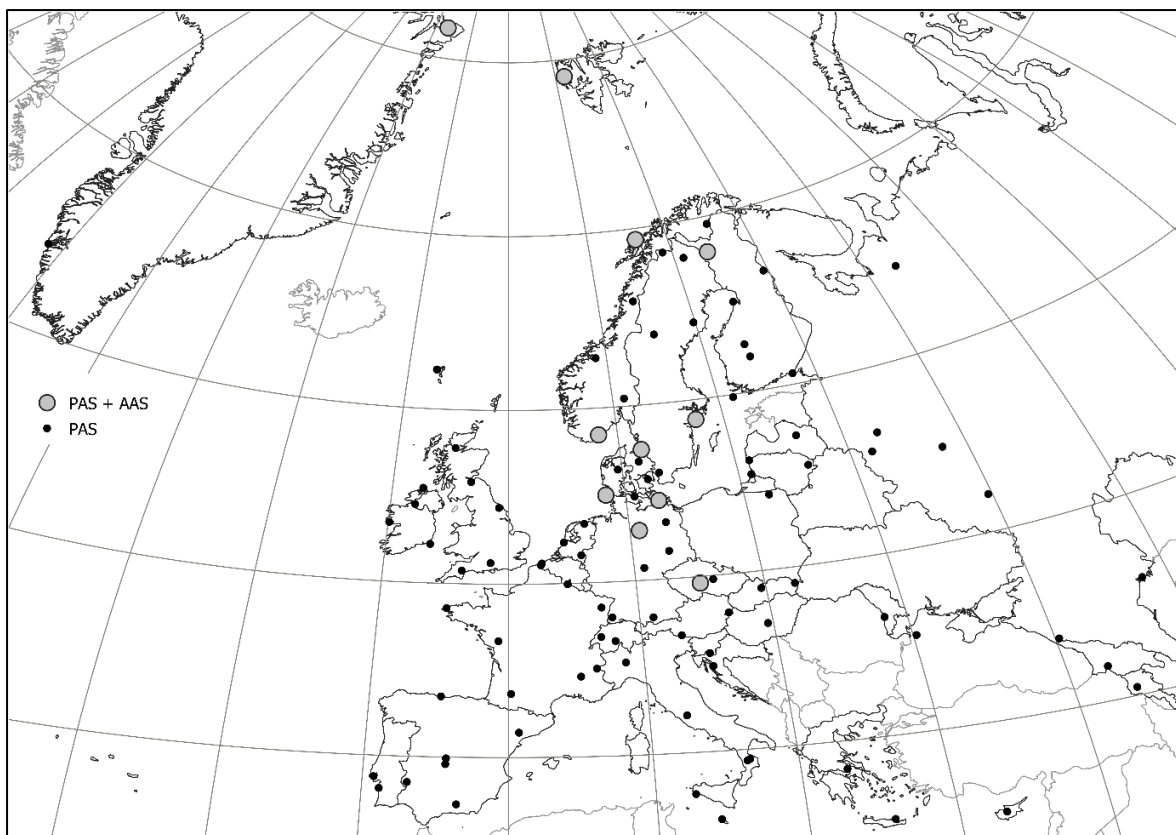
Figure 5. The spatial coverage of sampling sites using PAS (black/grey) along with the spatial coverage of sites in the European Monitoring and Evaluation Programme (EMEP) sampling POPs using AAS (grey) (Aas & Bohlin-Nizzetto, 2018).

3.3. Sample collection

The sampling in both the Norwegian and European campaigns were carried out with the PUF-based passive air sampler (Section 3.1). Passive air sampling was carried out in combination with active air sampling at selected EMEP sites (**Paper I** and **II**), to evaluate possible uncertainties associated with PUF-PAS. New PUF disks (14.1 cm diameter x 1.4 cm thick) were pre-cleaned and spiked with PRCs prior to sampling.

In the field, PUF-PAS were attached to a suitable structure (e.g. trees), at least 1.5 meters above ground. In the Norwegian campaign, they were mounted by NILU personnel, while in the European campaign they were deployed at or close-by the monitoring stations by those responsible for the sampling site. The PUF-PAS were exposed for about three months (during the period June-October, 2016).

3.4. Sample preparation

Analytical methods for POPs in air (PUF media) are widely available (Muir & Sverko, 2006; Yusa et al., 2009). Soxhlet extraction with hexane:diethylether 9:1, followed by treatment with concentrated sulfuric acid and further clean-up by solid-phase extraction (SPE) with silica, is the recommended procedure of participating laboratories in the EMEP to determine legacy POPs in PUF-based air samples (EMEP, 2001). This method was also used by Halse et al. (2011) in the European survey from 2006. However, this thesis additionally includes the analysis of selected OCECs in the dataset collected in 2016. Many of the OCECs are less hydrophobic and often less acid-labile than the legacy POPs, e.g. some of the alternative flame retardants. Also some OCPs, including dieldrin, endrin, endosulfan I + II and trans-heptachlor epoxide, can be sulfonized when treated with concentrated sulfuric acid (Chung & Chen, 2011) and are therefore excluded from monitoring programmes. To enable the analysis of a broader range of POPs and OCECs, including the acid-labile compounds, in a single PUF-PAS extract, a non-destructive sample preparation method was targeted.

Schematic descriptions of the analytical methods used for the European and Norwegian samples are given in Figure 6. All PUF disks from both the Norwegian and European campaign were initially added internal standards prior to Soxhlet extraction, to compensate for loss during the extraction and clean-up procedure. Furthermore, column based solid-phase extraction (SPE) was used as basis in the sample preparation of all samples. SPE is a common alternative method to sulfuric acid, in which co-extracted components are retained more strongly than the analytes of interest (Muir & Sverko, 2006; Yusa et al., 2009). A more thorough description of

the methods used for the Norwegian and European samples, including adjustments made during the process are given below. These mainly include: i) selection of an efficient solvent mixture for extraction of a broad range of compounds, ii) a non-destructive Florisil-based SPE method (Norwegian samples) and iii) a non-destructive dual-layer SPE method (European samples). The internal standards assure high accuracy in the determination of concentrations regardless of which analytical method that is used, and they also assure that the concentrations obtained with the different methods are comparable. However, interferences during instrumental analysis may lower the quality of the data (section 3.5). After repeated attempts on clean-up with the non-destructive methods, it was apparent that sulfuric acid was needed to sufficiently remove co-extracted PUF-related matrix for enabling instrumental analyses of some of the targeted compounds (e.g. DDTs).

Norway:

Soxhlet : acetone:*n*-hexane (1:1)

↓

SPE: florisil

↓

PCBs, PeCB/HCB, HCHs, other OCPs, dechloranes ← Back-exctraction to *n*-hexane

↓

Concentrated sulfuric acid

↓

DDTs

Europe:

Soxhlet : acetone:*n*-hexane (1:1)

↓

Dual-layer SPE: Zr-silica/C18 + florisil

↓

Back-exctraction to *n*-hexane → Other OCPs

↓

Concentrated sulfuric acid

↓

PCBs, PeCB/HCB, HCHs, DDTs, dechloranes
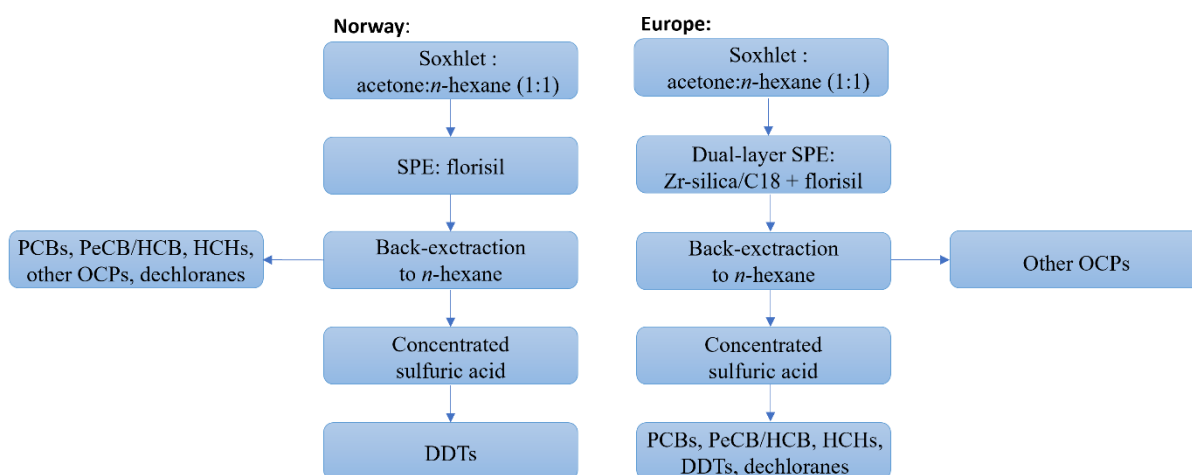
Figure 6. Summary of the analytical methods used for the European and Norwegian samples.

3.4.1. Method adjustments
i)   Extraction solvent

To extract less hydrophobic compounds more efficiently than with the conventionally used hexane:diethylether 9:1, alternative solvents were considered for Soxhlet extraction. Acetone, hexane and dichloromethane (DCM) are used in reported Soxhlet extraction methods for POPs in PUFs (Muir & Sverko, 2006; Yusa et al., 2009). Of these alternative solvents, DCM was not considered due to the increasing concern as a hazard to human health, despite its widespread use. A polar:apolar binary mixture is considered the most efficient for extracting analytes with a wide range in hydrophobicity, and acetone:*n*-hexane (1:1) was therefore chosen for testing. To assure a consistent comparison with data from 2006 (Halse et al., 2011), the extraction recovery of the legacy POPs; PCBs and PeCB/HCB, by using acetone:*n*-hexane (1:1), was also assessed. The samples from both the Norwegian and European air sampling campaign were

Soxhlet-extracted as recoveries between acetone:*n*-hexane (1:1) and the conventional hexane:diethylether 9:1 (Table 1)were comparable.

ii) *Non-destructive Florisil-based SPE method (Norwegian samples)*

To enable analysis of both acid-stabile and acid-labile POPs and OCECs, a non-destructive clean-up method was considered instead of the conventional acid-silica clean-up. Other goals were to shorten the preparation time and reduce solvent consumption to reduce blank levels of target compounds, and to improve the conditions related to the health, environment and safety of the operator by avoiding concentrated acid. Activated magnesium silicate coated silica (Florisil) is widely used as SPE-sorbent, and has been shown to successfully clean PUF-PAS extracts for analysis of acid labile OPFRs (Kurt-Karakus et al., 2018). Florisil was therefore used for clean-up in the Norwegian sampling campaign (**Paper I**).

The instrumental analysis showed negative matrix effects in the GC/MS-chromatograms for PBDEs, aBFRs and DDTs (section 3.5), and further clean-up was therefore necessary to remove co-extracted compounds. Solvent-rinsed deionized water was added to the acetonitrile extract before back-extraction into *n*-hexane to remove compounds with less hydrophobicity than the targeted compounds. Despite this, matrix-effects were evident in the GC/MS-chromatograms, and no satisfactory results were obtained for the PBDEs, aBFRs and DDTs. On the other hand, PCBs, PeCB/HCB and the other OCPs were successfully analyzed using the back-extracted extract. The remaining extract was further cleaned with sulfuric acid/silica to obtain satisfactory chromatograms also for DDT compounds. The recoveries of internal standards of PCBs and PeCB/HCB in blank samples prepared together with samples from the Norwegian campaign were comparable to the recoveries in a corresponding blank sample prepared by the conventional POP-method with acid and silica SPE (Table 1). We therefore do not expect these extra clean-ups to have affected the results of the targeted compounds.

iii) *Non-destructive dual-layer SPE method (European samples)*

For the analysis of samples from the European sampling campaign (**Paper II-IV**), the Florisil SPE-method was replaced with a dual-layer SPE method, which was hypothesized to remove PUF-matrix more efficiently than Florisil only. In this method, based on Stenerson & Brown (2015) and Röhler et al. (2021), a mixture of zirconia-coated silica and C18 polymerical bonded silica was added in the bottom sorbent bed, with Florisil in the top sorbent bed. The two layers are expected to remove co-extracted compounds by polar and non-polar interactions with

Florisil and the C18 sorbent respectively, and by Lewis acid-base interactions with zirconium (an electron pair acceptor). The method has shown to be a good substitute for sulfuric acid in the removal of fatty compounds co-extracted from sample matrices like fish and olive oil (Stenerson & Brown, 2015; Stenerson et al., 2015). PUF is a polymer with intramolecular urethane bonds (carbamate ester bond, NHR_2COOR_1) with a variety of additives (e.g. surfactants) comprising different properties. The dual-layer SPE method was therefore expected to be able to remove PUF-matrix, including possible degradation products and additives.

Acetonitrile was the preferred eluent in the original dual-layer SPE cleanup method (Stenerson et al., 2015),. Acetonitrile has intermediate polarity with the ability to dissolve a wide spectrum of different substances, including ionic and nonpolar compounds, and is also extensively used as eluent in many other rapid multi-residue analysis methods, e.g QuEChERS (Anastassiades et al., 2003). Acetonitrile was therefore chosen as eluent also in the preparation of the European samples.

The instrumental analysis showed negative matrix effects in the GC/MS-chromatograms for PBDEs, aBFRs and DDTs even after this dual-layer clean-up method. Back-extraction into *n*-hexane did not improve the chromatograms. Consequently, the hexane extract was split 20:80. In the European campaign, the larger aliquot (80%) was further cleaned with concentrated sulfuric acid and analyzed for PCBs, PeCB/HCB, HCHs, DDTs and dechloranes, while the other OCPs were determined directly on the smaller aliquot (20%), to include also the acid-labile OCPs.

Despite extensive clean-up of the samples from the European campaign, the recoveries of internal standards of PCBs and PeCB/HCB in blank samples were comparable with the conventional POP method (Table 1). This shows that the results are not affected by the extra clean-up steps.

Table 1. Comparison of recovery of internal standard in blank samples. Bold=indicator PCB.

Compound	Conventional POP method	Conventional POP method (with aceton/hexane 1:1)	Norway: Florisil SPE method (+ back-extraction)	Europe: Dual-layer SPE method (+ back-extraction), followed by acid treatment + SPE silica
	Recovery %	Recovery %	Recovery %	Recovery %
PeCB	10	9	25	25
HCB	21	19	45	32
PCB-28	**40**	**47**	**71**	**55**
PCB-52	**46**	**51**	**82**	**56**
PCB-101	**59**	**61**	**58**	**74**
PCB-105	74	78	60	79
PCB-114	72	78	58	76
PCB-123	71	79	61	82
PCB-138	**69**	**77**	**59**	**84**
PCB-153	**72**	**72**	**56**	**78**
PCB-156	76	84	59	82
PCB-157	77	81	59	81
PCB-167	73	74	58	83
PCB-180	**77**	**78**	**58**	**84**
PCB-189	78	77	51	81
PCB-209	72	74	56	85

3.5. Instrumental analysis and quantification

Samples from both the Norwegian and European campaign were analyzed for 32 polychlorinated biphenyls (PCBs), penta- and hexachlorobenzene (PeCB/HCB), 27 organochlorine pesticides (OCPs) and six dechloranes by using gas chromatography (GC) coupled to a high-resolution mass spectrometry (MS). For PCBs, PeCB/HCB, DDT related compounds and HCHs, an Agilent 7890A GC was coupled to a magnetic sector MS (VG Autospec Micromass). For the other OCPs and dechloranes, the GC was coupled to a quadrupole time-of-flight MS (Agilent 7200 Q-TOF). More information concerning the instrumentation, GC columns and operating parameters is presented in the individual studies (**Paper I-IV**).

Even if MS-detectors provide high specificity, co-extracted substances may interfere during the GC/MS-analysis. Deposition of non-volatile matrix in the front part of the GC-system not only leads to an increasing need for maintenance, but also adverse changes in performance of the chromatographic system e.g. irregular baseline, and tailing or broadening of peaks (Hajšlová & Zrostlíková, 2003). This may result in increased detection limits and low resolution of separated peaks. Concerning DDT, it can be thermally converted to DDD and DDE. This was monitored by comparing the peak area of ^{13}C-labelled *p,p'*-DDD, with the [13]C-

labelled *p,p'*-DDT in the internal standard. Furthermore, loss of intensity in EI may occur due to the binding of target ions with other ions present in the gas phase (Panuwet et al., 2016).

The quantification is based on an internal standard method using mean relative response factors of calibration standards to quantify the samples (Eq. 6-7). The integration of signals (i.e. areas), automatically obtained by the quantification tool (Targetlynx, Waters), is verified manually. The isotope ratios ($^{35}Cl/^{37}Cl$ or $^{79}Br/^{81}Br$) for two monitored masses, should be within ± 20% of the theoretical value. Larger deviations are an indication of interfering compounds.

$$Relative\ Response\ Factor\ (RRF)_{analyte} = \frac{mass_{ISTD}(pg) \times Area_{analyte}}{mass_{analyte}(pg) \times Area_{ISTD}} \qquad (Eq.\ 6)$$

$$mass\ in\ sample_{analyte} = \frac{mass_{ISTD}(pg) \times Area_{analyte}}{RRF_{analyte} \times Area_{ISTD}} \qquad (Eq.\ 7)$$

3.6. Deriving air concentrations

For all samples, loss of PRCs ($\frac{C}{C_0}$) were calculated. The average amounts of PRCs in two spiked field blanks were used as reference to account for any losses not caused by sampling. The loss differed between different PRCs.

For the Norwegian samples, the site-specific sampling rates ranged from 2.8 to 4.5 m³/day (average: 3.6 m³/day). The average sampling rate was used for sites experiencing insufficient loss of the PRCs (n<3).

For the European samples, the site-specific sampling rates were more variable, ranging from 2.0-15 m³/day (median: 3.7 m³/day), due to more variable environmental conditions, i.e. ambient air temperature (-13 to 29°C) and wind speed (2-7 m/s). For the sites with none- or only one PRC fulfilling the required loss, the sampling rates were estimated from the wind speed at the given sites (section 3.1.2).

The average/median sampling rate in both campaigns was in good agreement with the general sampling rate for PUF-PAS (3-4 m³/day) (Wania & Shunthirasingham, 2020). The resulting sampling rates and number of PRCs used at the individual sites are presented in **Paper I-II**.

The sampling rates together with the deployment periods were used to estimate the collected air volumes (V_{air}, section 3.1.2). Air concentrations were then derived from the mass of target analyte in the sample (M_{PUF});

$C_{air} = M_{PUF} / V_{air}$ *(Eq. 8)*

3.7. Quality assurance

In all papers, field blanks were included to account for possible contamination during deployment and transport of the samples. Additionally, laboratory blanks were included for blank level control of laboratory procedures. These underwent the same laboratory procedures as the exposed samples and the field blanks.

For the calculation of sum, average and median, and for the statistical analysis, concentrations below MDL were replaced by ½ MDL. Though it has been reported that the substitution of values below MDL can introduce uncertainty when the detection frequency is lower than 60% (Helsel, 2006), the replacement method was used to allow for comparison with Halse et al. (2011).

The internal standard recoveries of both exposed and blank samples were monitored by quantification relative to an instrument performance standard (Eq. 9).

$$Rec\% \ ISTD = \frac{mass \ ISTD_{measured}}{mass \ ISTD_{added}} \times 100\% \qquad \qquad (Eq. \ 9)$$

A known amount of ^{12}C target analytes was added to three clean PUF disks to assess the method bias for the targeted POPs in **Paper I-II**. These were analyzed with the Florisil method (section 3.4), and bias was calculated from the added amount (Eq. 10).

$$Bias\% = \frac{(mass \ analyte_{added} - mass \ analyte_{measured})}{mass \ analyte_{added}} \times 100\% \qquad \qquad (Eq. \ 10)$$

Furthermore, the reproducibility of the PAS method was assessed by the relative standard deviation of POP concentrations in duplicate PUF-PAS at selected sites.

3.8. Estimating population density within 50km radius

In **Paper II-IV** (Europe), estimates of the mean number of persons within 50 km of each sampling site were retrieved from the population density dataset in the collection "Gridded Population of the World, version 4" (CIESIN, 2016), by using the zonal statistics tool in QGIS ver.3.0.1. This identified nine sampling sites (Table 2) with elevated population density (690-2700 persons per km^2), compared to the other sites (<610 persons per km^2), and reflected the presence of a city within 50 km radius. The Wilcoxon signed-rank test was used to compare the concentrations of POPs for these "suburban" sites with concentrations for the remaining background sites. Also, a correlation between population density and the relative contribution of national emissions, predicted by GLEMOS, was examined.

In **Paper I**, the sites around the city of Oslo had elevated population density (510-580 persons per km^2) compared to the background sites (<250 persons per km^2).

*Table 2. Nine "suburban" sites with elevated population density due to the presence of city area within 50 km radius from the sites (**Paper II**).*

Sites	habitants per km²	City area within radius 50 km
De Zilk/Netherlands	2700	Amsterdam/the Hague/ Rotterdam
Giordan lighthouse/Malta	1800	Valletta
Nuuk/Greenland	1200	Nuuk
Alfragide/Portugal	1200	Lisbon
Montelibretti/Italy	990	Rome
Risoe/Denmark	960	Copenhagen
Vredepeel/Netherlands	820	Hertogenbosch/Eindhoven
Ispra/Italy	730	Milan
Råö/Sweden	690	Goteborg

3.9. Atmospheric transport modelling tools

While sampling and analysis are time consuming and expensive, models may be used complementary to predict concentrations, fate and behavior of POPs (Wania & Mackay, 1999). In **Papers I-II** and **IV**, multiple modelling approaches were used to explore whether the observed spatial patterns may be explained by the models and hence rationalized in mechanistical terms, and to help identify the main sources controlling atmospheric burdens of POPs across Norway (**Paper I**) and the whole of Europe (**Paper II** and **IV**).

3.9.1. GLEMOS

In **Paper I-II**, model simulations of concentration of PCB-153 in air were carried out using the Global EMEP Multi-media Modeling System (GLEMOS) (Malanichev et al., 2004). The spatial resolution was 0.4° x 0.4° within the EMEP domain, and 1° x 1° outside EMEP. The model predictions were stored for each individual site, corresponding to the actual deployment periods, by the Meteorological Synthesizing Centre - East under the European Monitoring and Evaluation Programme (EMEP). GLEMOS was used to predict the relative contributions attributed to primary- and secondary emissions, for each site. While the total primary emissions are separated into contributions from national emissions and transboundary transport (within/outside EMEP), this is not specified for the secondary emissions.

3.9.2. FLEXPART

In **Paper I-II**, model simulations of PCB-153 were also carried out using the Lagrangian particle dispersion model FLEXPART V10.4 in backward mode (Pisso et al., 2019; Stohl et al., 1998). Similar to GLEMOS, the model generated a predicted concentration for each individual site, with a spatial output resolution of 1° x 1°. Furthermore, FLEXPART predicted

so-called "footprints" that illustrate where the air mass had the potential to take up pollutants from sources near the ground. Combining the footprints with emission data (Breivik et al., 2007) enabled predictions of the primary source regions contributing to the observed concentration at each sampling site.

3.9.3. NEM

In **Paper IV**, a model simulation with the Nested Exposure Model (NEM) (Breivik et al., 2021) was carried out. NEM is a dynamic multimedia fate and transport model. Chemical transport between adjacent grid cells may occur in three mobile media (air, sea water and fresh water). As no suitable emission inventory for PCB-11 is known to exist, a unit emission rate for PCB-11 was used as model input, using global population density as a proxy for spatial distribution of the unit emission rate. The model predicted generic concentrations in air with a spatial resolution of $5° \times 5°$, averaged over the 3-month sampling period.

3.10.   Data analysis

In all papers, data processing was carried out using Microsoft Excel. The ratio between maximum and minimum concentrations in air (MMR) was used as a simple measure of spatial variability. When calculating MMR, the minimum and maximum according to a box-whisker plot (i.e. outliers excluded) were used, with MDL as the minimum value when samples below MDL were present.

In **Paper II**, Europe was divided into four regions; north, south, central-east and west (Figure 9), according to the geographical division by the European Union (EuroVoc, 2021).

The statistical analyses were performed by using R Studio with R 4.1.1. The concentrations were not normally distributed and were tested to better fit a log-normal distribution. Logarithmic concentrations were therefore used when testing linear correlations. The linear correlation between variables (e.g. POP concentrations and latitude/longitude) was tested by the null-hypothesis H_0: $b_1 = 0$ in a linear model ($y = b_0 + b_1 x$), which was rejected if its probability was less than 5% ($p < 0.05$). The Pearson correlation coefficient (r) was used as a measure of the linear relationship (between -1 and 1) between two variables. The non-parametric Wilcoxon signed-rank test was used to test if there was a significant difference between two groups (e.g. between geographical regions) (Miller, 2010). Furthermore, the matched-pair Wilcoxon signed-rank test was used to assess the temporal change in concentrations between this study and the earlier European campaign from 2006 (Halse et al., 2011), for sites that were included in both studies (n=6 **Paper I** and n=73 **Paper II**).

4. Results and discussion

4.1. I-PCBs

In the Norwegian campaign (**Paper I**), 18 of the 31 targeted PCBs were detected in 84-100% of the samples, with the median concentrations of the individual PCB congeners ranging from 0.03 to 0.8 pg/m^3. The other 13 PCBs were detected in 0-57% of the samples with median concentrations <0.02 pg/m^3. The concentrations of $\sum_6$PCBs (PCB-28, -52, -101, -138, -153 and -180) at the background sites in Norway ranged from 1 to 6 pg/m^3 (median 2.0 pg/m^3) with higher concentrations observed in southern Norway compared to northern Norway. The highest concentrations of $\sum_6$PCBs in Norway were observed within the urban area of Oslo (5-42 pg/m^3, median 20 pg/m^3, Figure 7).

In the European campaign (**Paper II**), 30 of 31 PCBs were detected in 69-100% of the samples and their individual medians ranged from 0.01 to 3.3 pg/m^3. The median of $\sum_6$PCBs in Europe was 6 times higher than the median of background sites in Norway (Figure 7). The difference between Europe and Norway increased with increasing chlorination degree, i.e. while the median for PCB-28 and PCB-52 in Europe were a factor of 5 higher than Norway, the median for PCB-180 was a factor of 10 higher. The concentrations of $\sum_6$PCBs at the nine highly populated sites within Europe (13-70 pg/m^3, median 45 pg/m^3) were even higher than the concentrations within the urban area of Oslo/Norway.

When comparing to the AAS concentrations reported to EMEP for the same sites and time periods (Aas & Bohlin-Nizzetto, 2018), the concentrations of $\sum_6$PCBs using PAS in our study were on median 1.8 times higher (PAS/AAS-ratio: 0.4-9.6), which is within the uncertainty of PAS and AAS in combination (Holt et al., 2017). A direct comparison to EMEP data is affected by differences in sampling methodologies, including sampling artifacts associated with both PAS and AAS (section 3.1), and analytical uncertainties (due to e.g. different chemical laboratories being involved in the EMEP programme).

When assessing the congeners detected at all sites and excluding outliers, generally lower spatial variability of PCBs was observed in Norway (MMR 3-6) compared to the European campaign (MMR 23-100) (Figure 7). The low concentrations and relatively low spatial variability across Norway indicate that concentrations of PCBs in the Norwegian background atmosphere are highly influenced by LRAT. Furthermore, a significant negative correlation with latitude across Europe, with higher concentrations in the southern part, suggests that sites in the historical source regions of Europe are influenced by continuing emissions (primary

and/or secondary) to a larger extent than more remote regions at northern latitudes in Europe. The higher proportion of the more chlorinated PCB-153 compared to PCB-28 observed in the southern part, further implies more influence of primary sources. As PCBs are mostly related to products it was not surprising that a positive correlation (r=0.6) between $\sum_6$PCBs and estimated population density (within a radius of 50km of the sampling sites) was observed within Europe (**Paper II**).

An overall reduction (28%) in atmospheric concentrations for $\sum_6$PCBs were observed from 2006 to 2016 when considering the 73 European sites that are common to the sites included in the study by Halse et al. (2011). This may reflect a general decline in primary emissions in the study region. The highest decrease was observed in the northern part of Europe, with approximately 50% reduction for $\sum_6$PCBs within Norway (**Paper I**, n=6). However, no significant decrease was observed in the southern part of Europe. This trend was also evident from the different latitudinal correlations in 2006 versus 2016 (Figure 8).

GLEMOS predicted that secondary emissions of PCB-153 were approximately four times more important than total primary emissions (i.e. national emissions and transboundary transport within/outside EMEP) in controlling atmospheric burdens in Norway, as well as in Europe (median 82% and 78% contribution respectively) (Figure 9). In accordance with the interpretation of observations, GLEMOS predicted the influence from national primary emissions to be highest for the European urban sites (median 25%), followed by the Norwegian urban sites (median 16%) and the European background sites (median 11%). This was in contrast to the Norwegian background sites, for which the influence from national primary emissions were far lower (median 2%). Instead, the relative contributions from primary emissions attributed to LRAT were predicted to be the highest within Norway (median 15%). Both GLEMOS and FLEXPART predicted large input from western Europe to this area. The results indicate that further reductions in atmospheric concentrations of PCBs in the southern part of Europe may be achieved through control measures targeting primary emissions in the individual countries, while international collaboration and other measures are necessary in the northern part of Europe.
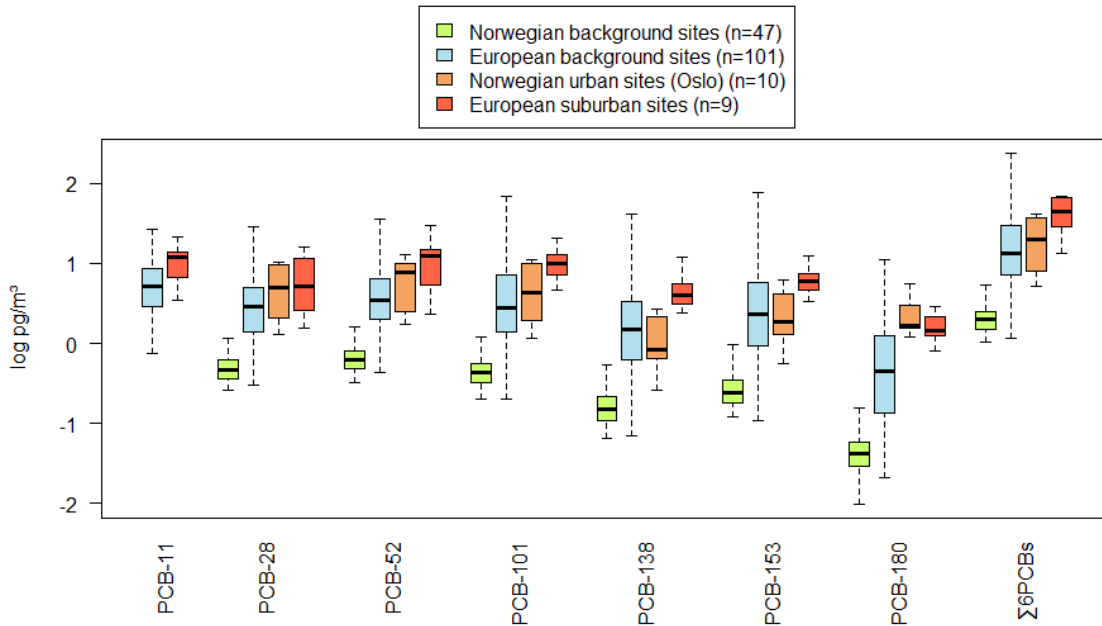
*Figure 7. The distribution of atmospheric concentrations (log pg/m³) of six PCB congeners indicators for the technical mixtures (**Paper I-II**), and the unintentionally generated PCB-11 (**Paper IV**) Outliers are excluded.*
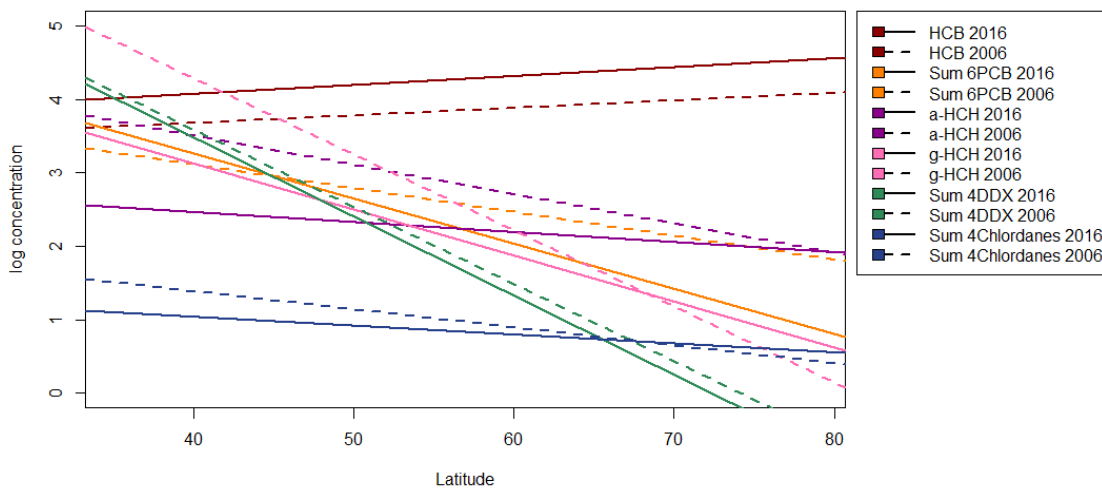
*Figure 8. Comparison of the latitudinal correlations of the POP concentrations at 73 common European sites in 2006 (Halse et al., 2011) and 2016 (**Paper II**).*
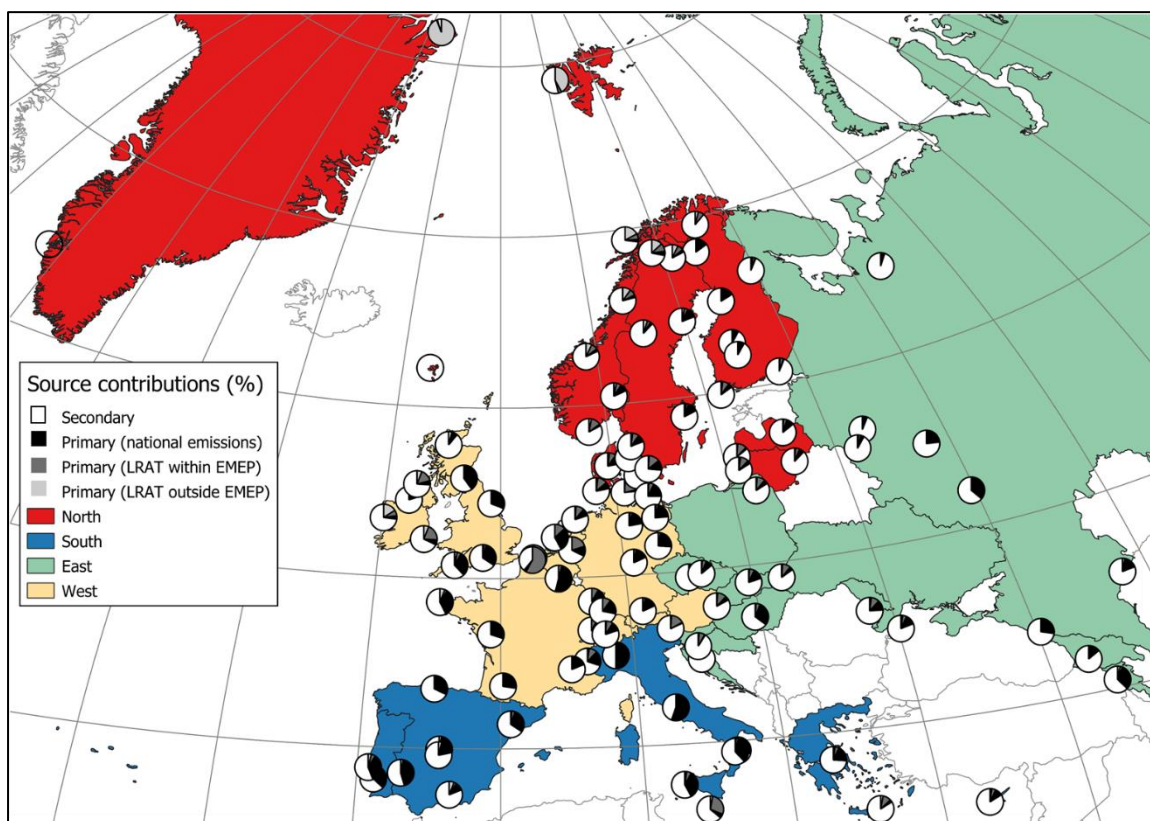
*Figure 9. Predicted relative contributions of secondary and primary emissions of PCB-153 attributed to national emissions and transboundary transport from countries within/outside EMEP, predicted by The Global EMEP Multi-media Modeling System (GLEMOS). The background colors represent the geographical regions (EuroVoc, 2021) that were compared in **Paper II**.*

4.2. PCB-11

PCB-11 was detected in background air all over Europe (median 5 pg/m^3) and exceeded the individual median concentrations of the other PCBs, including six indicator PCBs (0.4-3 pg/m^3, Figure 7). This strongly suggests significant emissions of PCB-11 in Europe. High concentrations were observed in central- and eastern parts of Europe, while low concentrations were observed in the north, suggesting population density may serve as an indicator for the spatial distribution of emissions in Europe. The detection of PCB-11 in the remote Arctic is a strong indication of LRAT, given that this region is less affected by primary sources.

The spatial variability of PCB-11 (MMR 24, excluding outliers) was comparable to the most volatile indicator PCB (PCB-28, Figure 7), and both correlated to latitude to the same extent (r=-0.4). While there are generally strong correlations between I-PCBs with similar chlorination degree, the correlation between PCB-11 (di-CB) and PCB-28 (tri-CB) (r=0.6) was considerably lower than anticipated from differences in chlorination agree alone. In comparison, the correlation between PCB-28 and PCB-52 (tetra-CB) is r=0.9. This offers

strong support for the hypothesis that the sources/source regions for PCB-11 are different to the I-PCBs.

A significant correlation between measured concentrations of PCB-11 and population density was observed, which also was illustrated by significantly higher concentrations for the nine high-populated sites (Figure 7). However, no significant correlation to population density was observed in the north region. A slightly better correlation to the generic concentrations predicted using the NEM model, indicated that concentrations of PCB-11 in the more remote regions in Europe cannot be rationalized on basis of population densities alone.

4.3. HCB and PeCB

In both the Norwegian and European campaign (**Paper I-II**), HCB and PeCB were detected at all background sites in comparable concentrations (median Norway and Europe: 74 and 67 pg/m^3 for HCB, and 21 and 25 pg/m^3 for PeCB) (Figure 11). The concentrations for sites within the urban area of Oslo/Norway (median 70 pg/m^3 and 16 pg/m^3 for HCB and PeCB, respectively) and the "suburban" sites within Europe (median 50 and 25 pg/m^3) were also similar to or lower than the concentrations in the background areas. This demonstrates that HCB and PeCB are well-distributed in air and emphasize that the concentrations are uncorrelated to population density.

Interestingly, HCB was the only POP that was significantly positively correlated to latitude, both overall within Europe (r=0.44, p<0.001), and within Norway only. The highest concentrations of HCB were observed in the Arctic (Station Nord/Greenland 247 pg/m^3, and two sites at Spitsbergen, 130-136 pg/m^3). As HCB has reached equilibrium between the PUF and air well within the sampling period at all sites, it may be questioned if the lower concentrations in warmer regions are due to a decreasing $K_{PUF-air}$ with temperature. However, the concentrations at the Zeppelin station/Spitsbergen were in agreement with AAS data measured in the Norwegian national air monitoring program (Bohlin-Nizzetto et al., 2017). A PAS/AAS ratio of 1.6 at this site is within the expected range (2-3) (Holt et al., 2017), and hence reflect that the environmental conditions have been compensated for in the estimation of sampling volumes at Zeppelin (section 3.1.2). Despite some variations in the PAS/AAS-ratios for the other co-located sites reporting to EMEP (1.6-4.8, Figure 10), the max-min ratio (i.e. spatial variability with Europe) of 9 when the outlier Rucava/Latvia is excluded, exceeds the bias expected from volume estimation. For the European dataset, it is still a significant positive correlation with latitude (r=0.37, p<0.001), when excluding Station Nord/Greenland and

Zeppelin/Spitsbergen. This suggests generally higher concentrations of HCB in northern Europe, not only in the Arctic. It should also be noted that PeCB was uncorrelated to latitude, which further emphasizes that the observed spatial trend for HCB is caused by factors other than artifacts related to sampling as PeCB has similar physical-chemical properties as HCB.
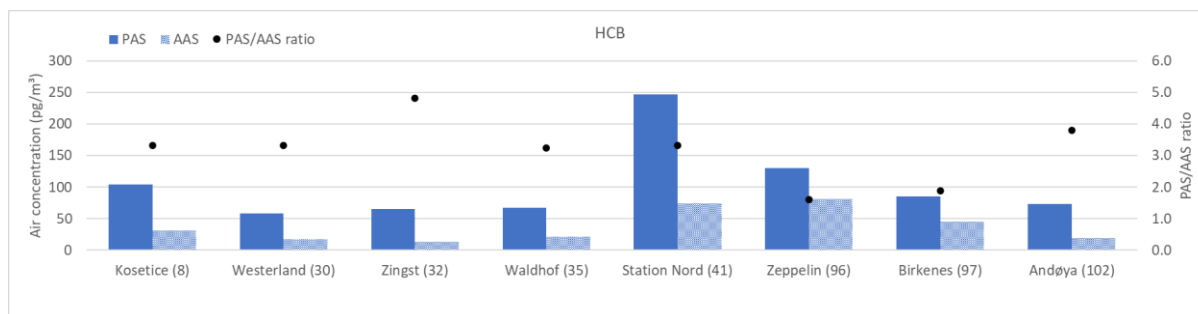
Figure 10. Comparison of PAS derived concentrations of HCB in air obtained in our study with the concentrations from routine AAS measurements reported to EMEP for the same sampling period (Aas & Bohlin-Nizzetto, 2018).

The high concentrations of HCB relative to the other POPs (Figure 7, Figure 11) may be explained by a combination of secondary emissions and unintentional primary emissions due to by-production and usage of chlorinated compounds contaminated with HCB in some parts of the world (Hung et al., 2016). HCB was the only POP with a higher median concentration in 2016 than in 2006 (Halse et al., 2011), when considering the European dataset (Figure 8). Higher concentrations in 2016 than 2006 were observed at 68% of the sites, with no clear spatial pattern observed with a median increase of 56%. In the Norwegian dataset, was similar or concentrations up to a factor of 2.5 higher than 2006 observed. Data from long-term monitoring sites based on AAS shows an inconsistent time-trend in HCB concentrations (Gusev et al., 2015; Ilyin et al., 2022; Kalina et al., 2019; Wong et al., 2021). High concentrations of HCB due to pesticide use have previously been reported in central parts of Europe (Barber et al., 2005), and enhanced influence of secondary emissions from previously contaminated soil may be a reason for increased concentrations. However, the increase in concentrations of HCB in air may also be a consequence of an increase in primary emissions. Both enhanced re-emissions and increasing primary emissions have been put forward as possible explanations for the higher concentrations of HCB in the Arctic (Hung et al., 2010; Ma et al., 2011; Platt et al., 2022). As HCB is relatively volatile and a limited spatial variability is observed, it is difficult to make any inferences about the likely source regions on the basis of the data presented.
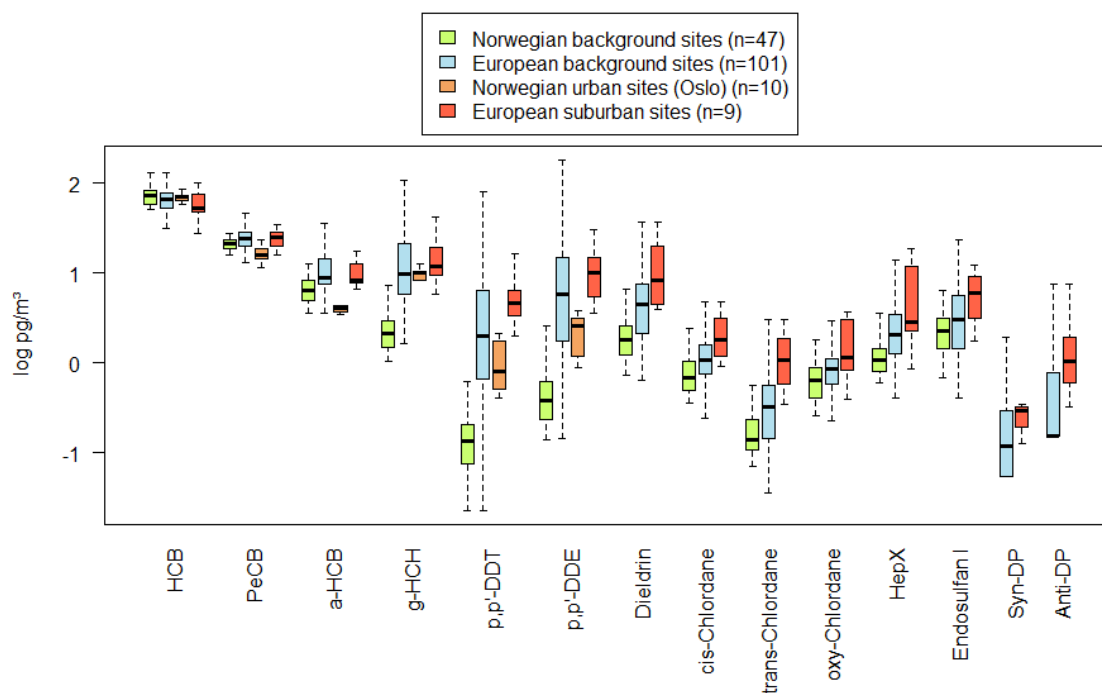
Figure 11. The distribution of atmospheric concentrations (log pg/m³) of HCB/PeCB, 10 selected OCPs and syn-/anti-DP. Outliers are excluded.

4.4. HCHs

Next after HCB and PeCB, the highest concentrations within Europe were measured for α- and γ-HCH (median: 9 pg/m³) (Figure 11). Both isomers were detected at all background sites in Europe and in Norway. β-HCH were only detected in 56% of the samples within Europe and 4% of the samples within Norway. This may be due to a lower content of β-HCH in technical HCH and the absence of β-HCH in lindane. β-HCH is also likely to have a more limited LRATP than the other two isomers due to differences in physical-chemical properties (Table A1, (Xiao et al., 2004)). The concentrations of α- and γ-HCH using PAS in our study were on median 2.2 times higher (PAS/AAS-ratio: 1.0-23) than the concentrations measured using AAS for the same sites and time periods.

The spatial variability of α- and γ-HCH across Europe were lower than most POPs and generally lower in Norway (MMR 4 and 7, outliers excluded) than in Europe (MMR 6 and 21, outliers excluded). No or small difference between the median concentration of α-HCH were observed between Europe and Norway (i.e. Europe/Norway 1.4). Contrary, a relatively large difference between Europe and Norway was observed for γ-HCH (Europe/Norway 4.3, Figure 11), with γ-HCH significantly correlating with latitude (r=-0.55). The spatial differences between the two HCHs are to a large extent explained by different LRATP with α- HCH having a longer residence time in the atmosphere compared to γ-HCH (Beyer et al., 2003). This may

help to explain why α-HCH showed a more even distribution across Europe. γ-HCH is more prone to wet deposition and is therefore likely to deposit closer to its source. The spatial distribution suggests that sites in the historical source regions of Europe are influenced by continuing emissions (primary or secondary) to a larger extent than in more remote regions at northern latitudes in Europe. Furthermore, correlations to longitude likely reflect more recent use and large stock-piles of α-HCH in central-east Europe, and the more extensive use of Lindane in the west region.

Significantly lower median atmospheric concentrations in 2016 compared to 2006 were observed in the European study (-59% and -48% for α- and γ-HCH respectively). The largest decreases were observed in historical source regions, while only a minor temporal change was observed within Norway (-17% and -4% for α- and γ-HCH respectively, not significant). This is also reflected in the different correlations with latitude in 2006 and 2016 (Figure 8).

4.5. DDTs and metabolites

In the Norwegian campaign (**Paper I**), three DDXs (p,p'-DDE, o,p'-DDT and p,p'-DDT) were detected in 98-100% of the samples, with median concentrations of 0.4, 0.2 and 0.1 pg/m^3 respectively. The other three DDXs (o,p'-DDE, o,p'-DDD and p,p'-DDD) were detected in 0-41% of the samples with median concentrations <0.06 pg/m^3.

In the European campaign (**Paper II**), all six DDXs were detected in 88-100% of the samples. The highest concentrations were measured for the metabolite p,p'-DDE, followed by p,p'-DDT and o,p'-DDT, at concentrations ten times higher than in Norway (medians 6, 2 and 1 pg/m^3 respectively) (Figure 11). When comparing concentrations of $\sum_3$DDXs (p,p'-DDD/-DDE/-DDT) using AAS within EMEP, the concentrations using PAS in our study were on median 2.4 times higher (PAS/AAS-ratio: 1.0-6.8).

Relatively large spatial variability compared to other POPs was observed for $\sum_6$DDXs within Europe (MMR>200, excluding outliers) (Figure 11), with a significant north-south gradient (r=-0.61). A significant north-south gradient was also observed for $\sum_3$DDXs within Norway (r=-0.71), but the spatial variability was significantly lower in Norway (MMR 6, excluding outliers) than within Europe (MMR>295 for $\sum_3$DDXs, excluding outliers). Lower concentrations and lower spatial variability generally in the northern part of Europe suggest that LRAT largely influences the atmospheric concentrations in this region.

Large differences between the median concentrations in the Norwegian and European study were observed for both p,p'-DDE and p,p'-DDT (Europe/Norway 15-16, Figure 11). Due to

degradation of p,p'-DDT to p,p'-DDE and p,p'-DDD, the high isomeric ratios observed for all sampling sites within Norway (p,p'-DDE/ p,p'-DDT 2-5), as well as for 92% of the sites in the European dataset ((p,p'-DDE+p,p'-DDD)/ p,p'-DDT > 1.3), indicate that most sites are influenced by secondary emissions of technical DDT. As DDXs are relatively low volatility compounds likely to deposit close to their source, the spatial trends observed suggest that high concentrations are related to the proximity to historical source regions.

The concentrations of p,p'-DDT and p,p'-DDE at the European "suburban" sites were higher (5 and 10 pg/m3 respectively) than both the background concentrations in Europe and the Norwegian urban samples (0.8 and 3 pg/m^3, respectively). Furthermore, the concentrations in the Norwegian urban samples were higher compared to the Norwegian background concentrations. The median concentration of p,p'-DDE relative to p,p'-DDT was lower in the European "suburban" samples compared to the background sites (p,p'-DDE/ p,p'-DDT ratio of 2 and 3 respectively). While the use of technical DDT was different from the I-PCBs and also may be related to applications in rural areas, these results suggest a possible continued influence from primary emissions in the more densely populated areas in Europe.

No significant temporal change from 2006 to 2016 was observed for the $\sum_3$DDXs (p,p'-DDE/o,p'-DDT/p,p'-DDT) within Norway which may in part reflect an increasing influence of secondary emissions from reservoirs contaminated in the past. In contrast, 12% lower median atmospheric concentration in 2016 compared to 2006 was observed for $\sum_4$DDXs (p,p'-DDD/-DDE/-DDT, o,p'-DDT) within Europe. The decline was only significant in the west region and not in the central-east region where the observed concentrations were the highest both years (Halse et al., 2011). For some sites that had a lower ratio of (p,p'-DDE+p,p'-DDD)/ p,p'-DDT) in 2016 than in 2006, the concentrations of p,p'-DDT were also increased. This implies that the influence from primary emissions in 2016 at some sites may be larger than in 2006.

4.6. Aldrin and metabolites

The metabolite dieldrin was detected in 98% of the samples in the European dataset and in 86% of the samples in the Norwegian dataset. Aldrin, isodrin and endrin, on the other hand, were only detected in <4% of the samples with median concentrations ≤1.7 pg/m^3. The high abundance of dieldrin may indicate re-volatilization of either dieldrin and/or aldrin, and therefore largely reflects elevated emissions from historical use.

In the correlation analysis, dieldrin was found to strongly correlate with $\sum_4$chlordanes, heptachlor-exo-epoxide and oxy-chlordane (r>0.8), reflecting their similar spatial patterns, with highest concentrations measured in western Europe (e.g. Netherlands and Belgium). Despite higher median concentration within Europe than within Norway (medians of 4 and 2 pg/m^3 respectively), the concentrations of dieldrin were not significantly correlated to latitude.

4.7. Chlordanes

In both the Norwegian and European dataset, all four chlordanes and oxy-chlordane were detected in >79% of the samples. The highest concentrations were found for oxy-chlordane, cis-chlordane and trans-nonachlor (medians 0.6-1.0), with small differences in concentrations between the European and Norwegian dataset (Figure 11). Trans-chlordane and cis-nonachlor were detected at median concentrations of 0.1 to 0.3 pg/m^3.

The occurrence of the metabolite oxy-chlordane strongly suggests influence from secondary emissions across Europe. Because of greater reactivity of trans-chlordane compared to cis-chlordane in the environment (Becker et al., 2012; Bidleman et al., 2002), a trans-/cis-chlordane ratio less than 1.6 at 99% of the sites in the European dataset similarly indicated historical usage.

The highest concentrations of $\sum_4$chlordanes and oxy-chlordane were measured in the west region (e.g. Netherlands and Belgium) and therefore suggests the influence from secondary emissions to be largest in this area. While a positive correlation between $\sum_4$chlordanes and estimated population density (within 50 km of the sampling sites) was observed, there was no significant correlation with latitude.

While no significant reduction for $\sum_4$chlordanes was observed within Norway, the median atmospheric concentrations within Europe in 2016 were 23% lower compared to 2006. The decrease was only significant in the west region.

4.8. Heptachlor and metabolites

The degradation product of heptachlor (heptachlor-exo-epoxide) was detected at all sites within Europe and at 86% of the sites within Norway. Heptachlor, on the other hand, was detected only in <7% of the European samples and not detected at all in the Norwegian samples. The detection frequency of the endo-isomer (heptachlor-endo-epoxide) was only 1 and 2% within Europe and Norway respectively. The dominance of heptachlor-exo-epoxide indicates past

usage of either heptachlor or technical chlordane, in which heptachlor also is a constituent (7%) (Dearth & Hites, 1991).

The median concentrations of heptachlor-exo-epoxide within Europe and Norway were 2 and 1 pg/m^3 respectively (Figure 11), but the positive correlation with latitude was not significant.

Similar to dieldrin and the chlordanes, the highest concentrations of heptachlor-exo-epoxide were measured in the west region, suggesting a higher contribution of secondary emissions in this area, compared to other regions.

4.9. Endosulfans

In the Norwegian campaign, endosulfan I was detected at highest concentrations (2 pg/m^3), while endosulfan II and endosulfan sulfate were detected less frequently (100% vs. 5% and 7%) and at lower concentrations (0.4 and 0.3 pg/m^3 respectively). In the European campaign, endosulfan I was also detected in highest concentrations (3 pg/m^3), while endosulfan II and endosulfan sulfate were detected less frequently (48% and 27% of the samples), and at lower concentrations (0.7 and 0.5 pg/m^3 respectively). As endosulfan II is converted to endosulfan I in the environment (Schmidt et al., 1997; Weber et al., 2010), the high endosulfan I/endosulfan II-ratio across Europe (median 8.5), may suggest previous use of endosulfan.

A relatively larger spatial variability was observed for endosulfan I within Europe (MMR 25, outliers excluded), compared to Norway (MMR 7, outliers excluded) (Figure 11). The concentrations within Europe were significantly negatively correlated with latitude (r=-0.44), and suggest a higher influence from secondary emission in the southern part of Europe. It is also noteworthy that endosulfan II is detected more frequently in the European study than in the Norwegian study, which may be a result of endosulfan II being more prone to wet deposition during LRAT in comparison to endosulfan I (Shen et al., 2005).

4.10. Dechloranes

In the European campaign (**Paper III**), syn-DP (<0.1-1.9 pg/m^3) and anti-DP (<0.3-11 pg/m^3) were present across the study area at levels in the lower range of the other POPs (Figure 11). Due to considerable blank levels (13% and 7% of the average concentrations in the samples), the concentrations were blank corrected. Still, a lower detection frequency (51% and 44% respectively of 97 analyzed samples) was observed compared to the POPs. In comparison, Mirex, one of the flame retardants the DPs have replaced, was detected in 27% at concentrations (<0.2-1.2 pg/m^3).

Concentrations of ∑DPs correlated with latitude (r=-0.21), with the highest concentrations found in central continental Europe (e.g., northern France, Austria, Netherlands, and Germany), and concentrations below MDL dominating in the northern part of the study area (e.g., Norway, Sweden, and Russia). This indicates higher emissions of DP in central Europe with LRAT to more remote areas. The presence of DPs in the Arctic (i.e. Station Nord/Greenland and Zeppelin/Spitsbergen) further supports their potential for LRAT. It has previously been suggested that DPs in the Arctic are transported directly from source areas and that secondary re-emissions to air from surface media are less likely as these are involatile chemicals (Hansen et al., 2020).

As anti-DP may be more prone to degradation in the environment than syn-DP (Olukunle et al., 2018), the fraction of anti-DP (f_{anti} = anti-DP/(syn-DP + anti-DP)) may indicate past or ongoing emissions. Within Europe, f_{anti} ranged 0.6-0.9 and were close to that of the commercial mixture of DP (Wang et al., 2010). A considerable variation in atmospheric concentrations (i.e. MMR 61, excluding outliers), give further indications that the concentrations of DP in Europe are influenced by primary emissions (Jaward et al., 2004).

The concentrations of ∑DPs for the "suburban" sites within Europe (n=7) were a factor 5.6 higher compared to remaining background sites (Figure 11). This suggests that primary emissions of DPs are related to population density, which is expected given their use in electrical coatings and building materials. The median f_{anti} was 0.85 for these high-populated sites, which is in the upper range of f_{anti} for all sites. The ratio is expected to decrease with increasing distance from source areas, due to atmospheric degradation of anti-DP. A higher ratio in source areas is therefore expected.

DP was not analyzed in the study by Halse et al. (2011), and comparison to other studies was therefore necessary to assess a possible temporal change in concentrations. When compared to results from a study by Schuster et al. (2021b) from 2005-2006, an increasing tendency was observed at four of the five common sites. However, consistent time-trends are needed to elucidate the temporal trend of dechloranes in the atmosphere.

Of the dechlorane related compounds, Dec-602 was the only detected compound (in 27% of the samples), but at relatively low levels (<0.01 to 0.33 pg/m^3) compared to the DPs and POPs. The other analyzed DRCs were <0.03 pg/m^3. Dec-602 was significantly correlated to ∑DPs, but the lower levels suggest lower primary emissions of Dec-602 compared to DPs.

5. Conclusions

This thesis presents a comprehensive assessment of the occurrence, distribution and main sources of selected legacy POPs and OCECs in background air across Norway and Europe. The thesis is based on consistent and high-spatial resolution observations in combination with mechanistic modelling approaches. This research not only offers new data on how the atmospheric concentrations of these chemicals vary across European regions, but it also discusses how the observed spatial variabilities in atmospheric burdens have changed over a decade. The thesis demonstrates that a combination of observations and mechanistic modelling may provide valuable insights into the main sources controlling atmospheric burdens of POPs and OCECs across Europe which cannot be readily inferred from measurements alone. This knowledge can be used by policy makers to assess potential opportunities for further emission reductions of legacy POPs.

The main findings by individual compounds / compound groups can be summarized as follows:

I-PCBs:

- GLEMOS predicted secondary emissions to be more important than primary emissions in controlling atmospheric burdens of PCB-153 across Europe (including Norway), albeit with a stronger influence of primary sources in the southern part.
- Concentrations of I-PCBs in more populated areas of Europe showed a less noticeable decline from 2006 to 2016 and a higher spatial variability than the more remote regions. This suggests that primary emissions sources could still be affecting the atmospheric concentrations in these areas.
- Low concentrations of I-PCBs were observed in the more remote regions of Europe (e.g. Norway and the Arctic), mainly attributed to LRAT.

PCB-11:

- PCB-11 is present all over Europe, including the Arctic, reflecting its LRTAP.
- Concentrations of PCB-11 were higher in more densely populated areas in Europe.
- The emissions of PCB-11 in Europe are significant, and the sources and/or source regions of PCB-11 are also notably different to the I-PCBs.
- The concentrations of PCB-11 that were observed at the most remote sites were higher than anticipated by the NEM model.

HCB/PeCB:

- Concentrations of HCB/PeCB were high compared to other POPs with a fairly uniform distribution across Europe.
- HCB was the only POP with concentrations significantly increasing with latitude, both within the European and Norwegian dataset.
- HCB was also the only POP with higher concentrations in 2016 than in 2006.

HCHs:

- The concentrations of HCHs were higher than most other POPs, except HCB/PeCB.
- While the distribution of α-HCH across Europe was relatively uniform, γ-HCH was significantly higher in the southern part of Europe.
- Higher concentrations of α-HCH were observed in central-east Europe while higher concentrations of γ-HCH were observed in the west region. Correlations between HCHs and longitude likely reflect differences in the historical source regions.
- Atmospheric concentrations of HCHs were significantly lower in 2016 compared to 2006 for both isomers.

DDTs and metabolites:

- The highest concentrations of $\sum_6$DDXs were observed in the central-east region with no significant change in concentrations from 2006 to 2016.
- The metabolite p,p'-DDE was the most abundant isomer across Europe. The median concentration of p,p'-DDE within Europe was 15 times higher than within Norway.
- The results for DDTs suggest that secondary emissions from historical use of technical DDT are significant. However, continuing primary emissions in more highly-populated regions in Europe were also indicated.

Aldrin and metabolites:

- Only the metabolite dieldrin was detected across Europe, suggesting an influence from secondary emissions.
- While high concentrations were measured in the west region (e.g. Netherlands and Belgium), there were no significant north-south gradient.
- Dieldrin showed a similar spatial pattern as $\sum_4$chlordanes, heptachlor-exo-epoxide and oxy-chlordane (r>0.8).

Chlordanes:

- The metabolite oxy-chlordane was detected in similar concentrations to the most dominant isomers from the technical mixture (cis-chlordane and trans-nonachlor).
- The trans-/cis-chlordane ratio suggests a large influence of secondary emissions.
- A decline in concentrations of $\sum_4$chlordanes from 2016 to 2006 were only observed in the west region, where the highest concentrations were measured in 2016.

Heptachlor and metabolites:

- The dominance of the degradation product heptachlor-exo-epoxide indicated past usage of technical chlordane and/or heptachlor in Europe.
- The spatial pattern indicated a stronger influence from secondary emissions in the west region than in the east region.

Endosulfans:

- Concentrations of endosulfan I were higher than endosulfan II across Europe and indicated past usage of technical endosulfan, with a higher influence from secondary emission in the southern part of Europe.
- A lower detection frequency of endosulfan II in the Norwegian dataset compared to the European dataset suggested that endosulfan II is more readily washed out during LRAT.

Dechloranes:

- The detection of syn/anti dechlorane plus (DPs) all over Europe, including the Arctic, strongly indicates that these chemicals have potential for LRAT.
- The concentration of DPs correlated to population density. As DPs are relatively involatile, this suggests a strong influence by primary emissions.
- Dec-602 was the only of the other dechlorane related compounds detected within Europe, but at concentrations 1-18% of the $\sum$DPs.

6. Future perspectives

Based on the findings in this thesis, recommendations for further investigation are as follows:

- The existing monitoring program within Europe measuring POPs in background air using AAS (EMEP) is based on a very limited number of monitoring sites. This network is less likely to capture the spatial variability across Europe for less volatile chemicals that have limited LRATP and/or are characterized by a high spatial variability in emissions (e.g. DDTs and PCBs). Additional monitoring sites will better capture gradients in atmospheric burdens in order to identify ongoing emissions and help to evaluate LRAT models operating with a high spatial resolution.

- It is recommended to include DP as well as PCB-11 along with other PCBs in future monitoring efforts due to their widespread occurrence in background air.

- While several atmospheric transport models may be "fit for purpose" for assessing source-receptor relationships of POPs (e.g. PCB-153), their utility is often hampered by the lack of reliable emission scenarios (e.g. PCB-11). This mitigates opportunities to realistically predict concentrations in air for many chemicals. Further efforts are recommended to develop emission inventories for a wider range of chemicals of interest and concern.

- While the methodological approach for assessing the relative importance of primary and secondary emission sources (i.e. GLEMOS) was limited to PCB-153, the strategy should be expanded towards a wider range of semi-volatile organic chemicals in the future (e.g. HCB).

- The number of organic chemicals of concern has greatly increased since the Stockholm Convention came into effect. As LRATP is among the four hazard criteria which characterizes a POP, empirical approaches to screen chemicals for LRATP are needed. Simple and cost-effective strategies like PAS-PUF may play a prominent role in the initial empirical assessment of LRATP, and also help identify further research needs and inform chemical management strategies.

- High background levels and relatively high method detection limit were observed for the DPs. This indicates a need to either try to reduce the blank contribution during sampling and analysis, or to collect larger amounts of analytes (e.g. larger sample volumes) using alternative approaches to PAS-PUF e.g. targeting the particle phase.

- Several emerging organic contaminants are acid labile. Further development of non-destructive sample preparation methods that remove matrix-related compounds with

the same efficiency as conventional methods, should be considered. This will make it feasible to target a broader range of chemicals of interest/concern, such as other alternative flame retardants.

- Despite the semi-quantitative nature related to the PAS-PUF methodology, this study shows that the method is useful for assessing the spatial distribution of a wide range of chemicals. However, complementary and/or alternative sampling strategies should be developed and/or considered in future studies for relatively volatile chemicals that overreach the linear uptake phase (e.g. PeCB, HCB and PCB-11) as well as for the less volatile and particle associated chemicals. Examples of alternative sampling strategies for the more volatile chemicals are those that rely on sorbents with a higher sorptive capacity, such as XAD. For relatively involatile chemicals that are mainly associated with particles (e.g. DPs), complementary approaches like active sampling on filters and deposition samplers should be considered to assess the concentration in air and atmospheric deposition, respectively.

References

Anastassiades, M., Lehotay, S. J., Stajnbaher, D., & Schenck, F. J. (2003). Fast and easy multiresidue method employing acetonitrile extraction/partitioning and "dispersive solid-phase extraction" for the determination of pesticide residues in produce. *Journal of Aoac International, 86*(2), 412-431. https://doi.org/10.1093/jaoac/86.2.412

Anderson, P. N., & Hites, R. A. (1996). OH Radical Reactions: The Major Removal Pathway for Polychlorinated Biphenyls from the Atmosphere. *Environmental Science & Technology, 30*(5), 1756-1763. https://doi.org/10.1021/es950765k

Aoki, Y. (2001). Polychlorinated Biphenyls, Polychloronated Dibenzo-p-dioxins, and Polychlorinated Dibenzofurans as Endocrine Disrupters—What We Have Learned from Yusho Disease. *Environmental Research, 86*(1), 2-11. https://doi.org/10.1006/enrs.2001.4244

Bailey, R. E. (2001). Global hexachlorobenzene emissions. *Chemosphere, 43*(2), 167-182. https://doi.org/10.1016/S0045-6535(00)00186-7

Bailey, R. E., van Wijk, D., & Thomas, P. C. (2009). Sources and prevalence of pentachlorobenzene in the environment. *Chemosphere, 75*(5), 555-564. https://doi.org/10.1016/j.chemosphere.2009.01.038

Barber, J. L., Sweetman, A. J., van Wijk, D., & Jones, K. C. (2005). Hexachlorobenzene in the global environment: Emissions, levels, distribution, trends and processes. *Science of The Total Environment, 349*(1), 1-44. https://doi.org/10.1016/j.scitotenv.2005.03.014

Bartkow, M. E., Booij, K., Kennedy, K. E., Muller, J. F., & Hawker, D. W. (2005). Passive air sampling theory for semivolatile organic compounds. *Chemosphere, 60*(2), 170-176. https://doi.org/10.1016/j.chemosphere.2004.12.033

Bartkow, M. E., Jones, K. C., Kennedy, K. E., Holling, N., Hawker, D. W., & Muller, J. F. (2006). Evaluation of performance reference compounds in polyethylene-based passive air samplers. *Environmental Pollution, 144*(2), 365-370. https://doi.org/10.1016/j.envpol.2005.12.043

Becker, S., Halsall, C. J., Tych, W., Kallenborn, R., Schlabach, M., & Manø, S. (2012). Changing sources and environmental factors reduce the rates of decline of organochlorine pesticides in the Arctic atmosphere. *Atmos. Chem. Phys., 12*(9), 4033-4044. http://doi.org/10.5194/acp-12-4033-2012

Beyer, A., Wania, F., Gouin, T., Mackay, D., & Matthies, M. (2003). Temperature Dependence of the Characteristic Travel Distance. *Environmental Science & Technology, 37*(4), 766-771. http://doi.org/10.1021/es025717w

Bidleman, T. F., Jantunen, L. M., Helm, P. A., Brorstrom-Lunden, E., & Juntto, S. (2002). Chlordane enantiomers and temporal trends of chlordane isomers in arctic air. *Environmental Science & Technology, 36*(4), 539-544. https://doi.org/10.1021/es011142b

Bidleman, T. F., & Olney, C. E. (1974). High-volume collection of atmospheric polychlorinated biphenyls. *Bulletin of Environmental Contamination and Toxicology, 11*(5), 442-450. https://doi.org/10.1007/BF01685302

Boethling, R., Fenner, K., Howard, P., Klečka, G., Madsen, T., Snape, J. R., & Whelan, M. J. (2009). Environmental Persistence of Organic Pollutants: Guidance for Development and Review of POP Risk Profiles. *Integrated Environmental Assessment and Management, 5*(4), 539-556. https://doi.org/10.1897/IEAM_2008-090.1

Bohlin-Nizzetto, P., Melymuk, L., White, K. B., Kalina, J., Madadi, V. O., Adu-Kumi, S., Prokeš, R., Přibylová, P., & Klánová, J. (2020). Field- and model-based calibration of polyurethane foam passive air samplers in different climate regions highlights differences in sampler uptake performance. *Atmospheric Environment, 238*, 117742. https://doi.org/10.1016/j.atmosenv.2020.117742

Bohlin-Nizzetto, P., Aas, W., & Warner, N. (2017). *Monitoring of environmental contaminants in air and precipitation, annual report 2016*. (NILU report 17/2017). Kjeller: NILU Retrieved from http://hdl.handle.net/11250/2461410.

Bohlin, P., Audy, O., Škrdlíková, L., Kukučka, P., Přibylová, P., Prokeš, R., Vojta, Š., & Klánová, J. (2014). Outdoor passive air monitoring of semi volatile organic compounds (SVOCs): a critical evaluation of performance and limitations of polyurethane foam (PUF) disks. *Environmental Science: Processes & Impacts, 16*(3), 433-444. https://doi.org/10.1039/C3EM00644A

Breivik, K., Armitage, J. M., Wania, F., Sweetman, A. J., & Jones, K. C. (2016). Tracking the Global Distribution of Persistent Organic Pollutants Accounting for E-Waste Exports to Developing Regions. *Environmental Science & Technology, 50*(2), 798-805. https://doi.org/10.1021/acs.est.5b04226

Breivik, K., Eckhardt, S., McLachlan, M. S., & Wania, F. (2021). Introducing a nested multimedia fate and transport model for organic contaminants (NEM). *Environ Sci Process Impacts, 23*(8), 1146-1157. https://doi.org/10.1039/d1em00084e

Breivik, K., Pacyna, J. M., & Münch, J. (1999). Use of α-, β- and γ-hexachlorocyclohexane in Europe, 1970–1996. *Science of The Total Environment, 239*(1-3), 151-163. https://doi.org/10.1016/s0048-9697(99)00291-0

Breivik, K., Sweetman, A., Pacyna, J. M., & Jones, K. C. (2002a). Towards a global historical emission inventory for selected PCB congeners--a mass balance approach. 1. Global production and consumption. *Sci Total Environ, 290*(1-3), 181-198. https://doi.org/10.1016/s0048-9697(01)01075-0

Breivik, K., Sweetman, A., Pacyna, J. M., & Jones, K. C. (2002b). Towards a global historical emission inventory for selected PCB congeners--a mass balance approach. 2. Emissions. *Sci Total Environ, 290*(1-3), 199-224. https://doi.org/10.1016/s0048-9697(01)01076-2

Breivik, K., Sweetman, A., Pacyna, J. M., & Jones, K. C. (2007). Towards a global historical emission inventory for selected PCB congeners - A mass balance approach-3. An update. *Science of The Total Environment, 377*(2-3), 296-307. https://doi.org/10.1016/j.scitotenv.2007.02.026

Buha Djordjevic, A., Antonijevic, E., Curcic, M., Milovanovic, V., & Antonijevic, B. (2020). Endocrine-disrupting mechanisms of polychlorinated biphenyls. *Current Opinion in Toxicology, 19*, 42-49. https://doi.org/10.1016/j.cotox.2019.10.006

Campfens, J., & Mackay, D. (1997). Fugacity-Based Model of PCB Bioaccumulation in Complex Aquatic Food Webs. *Environmental Science & Technology, 31*(2), 577-583. https://doi.org/10.1021/es960478w

Carson, R. (1962). *Silent Spring* (2002 ed.): Houghton Mifflin.

Chaemfa, C., Wild, E., Davison, B., Barber, J. L., & Jones, K. C. (2009). A study of aerosol entrapment and the influence of wind speed, chamber design and foam density on polyurethane foam passive air samplers used for persistent organic pollutants. *Journal of Environmental Monitoring, 11*(6), 1135-1139. https://doi.org/10.1039/B823016A

Chung, S. W. C., & Chen, B. L. S. (2011). Determination of organochlorine pesticide residues in fatty foods: A critical review on the analytical methods and their testing capabilities. *Journal of Chromatography A, 1218*(33), 5555-5567. https://doi.org/10.1016/j.chroma.2011.06.066

CIESIN. (2016). Documentation for the Gridded Population of the World, Version 4 (GPWv4). Retrieved from https://doi.org/10.7927/H4D50JX4. Access Nov 2018.

Clausen, J., & Berg, O. L. E. (1975). THE CONTENT OF POLYCHLORINATED HYDROCARBONS IN ARCTIC ECOSYSTEMS. In P. Varo (Ed.), *Pesticide Chemistry–3* (pp. 223-232): Butterworth-Heinemann.

Dearth, M. A., & Hites, R. A. (1991). Complete analysis of technical chlordane using negative ionization mass spectrometry. *Environmental Science & Technology, 25*(2), 245-254. https://doi.org/10.1021/es00014a005

Drage, D. S., Newton, S., de Wit, C. A., & Harrad, S. (2016). Concentrations of legacy and emerging flame retardants in air and soil on a transect in the UK West Midlands. *Chemosphere, 148*, 195-203. https://doi.org/10.1016/j.chemosphere.2016.01.034

Eckhardt, S., Breivik, K., Manø, S., & Stohl, A. (2007). Record high peaks in PCB concentrations in the Arctic atmosphere due to long-range transport of biomass burning emissions. *Atmospheric Chemistry and Physics, 7*(17), 4527-4536. https://doi.org/10.5194/acp-7-4527-2007

EMEP. (2001). EMEP Manual for sampling and analysis. Retrieved from https://projects.nilu.no/ccc/manual/index.html). Access Feb 2018.

EuroVoc. (2021). Browse by EuroVoc. Retrieved from https://eur-lex.europa.eu/browse/eurovoc.html. Access Dec 2021.

Francisco, A. P., Harner, T., & Eng, A. (2017). Measurement of polyurethane foam – air partition coefficients for semivolatile organic compounds as a function of temperature: Application to passive air sampler monitoring. *Chemosphere, 174*, 638-642. https://doi.org/10.1016/j.chemosphere.2017.01.135

Gannon, N., & Bigger, J. H. (1958). The Conversion of Aldrin and Heptachlor to Their Epoxides in Soil1. *Journal of Economic Entomology, 51*(1), 1-2. https://doi.org/10.1093/jee/51.1.1

Gioia, R., Sweetman, A. J., & Jones, K. C. (2007). Coupling Passive Air Sampling with Emission Estimates and Chemical Fate Modeling for Persistent Organic Pollutants (POPs): A Feasibility Study for Northern Europe. *Environmental Science & Technology, 41*(7), 2165-2171. https://doi.org/10.1021/es0626739

Gohlke, R. S., & McLafferty, F. W. (1993). Early gas chromatography/mass spectrometry. *Journal of the American Society for Mass Spectrometry, 4*(5), 367-371. https://doi.org/10.1016/1044-0305(93)85001-E

Gouin, T., Mackay, D., Jones, K. C., Harner, T., & Meijer, S. N. (2004). Evidence for the "grasshopper" effect and fractionation during long-range atmospheric transport of organic contaminants. *Environmental Pollution, 128*(1), 139-148. https://doi.org/10.1016/j.envpol.2003.08.025

Gusev, A., Rozovskaya, O., Shatalov, V., Aas, W., & Bohlin-Nizzetto, P. (2015). *Assessment of spatial and temporal trends of POP pollution on regional and global scale*. (EMEP Status Report 3/2015). Moscow: Meteorological Synthesizing Centre – East Retrieved from https://www.msceast.org/reports/3_2015.pdf.

Hajšlová, J., & Zrostlíková, J. (2003). Matrix effects in (ultra)trace analysis of pesticide residues in food and biotic matrices. *Journal of Chromatography A, 1000*(1), 181-197. https://doi.org/10.1016/S0021-9673(03)00539-9

Halse, A. K., Schlabach, M., Eckhardt, S., Sweetman, A., Jones, K. C., & Breivik, K. (2011). Spatial variability of POPs in European background air. *Atmospheric Chemistry and Physics, 11*(4), 1549-1564. https://doi.org/10.5194/acp-11-1549-2011

Halse, A. K., Schlabach, M., Sweetman, A., Jones, K. C., & Breivik, K. (2012). Using passive air samplers to assess local sources versus long range atmospheric transport of POPs. *J Environ Monit, 14*(10), 2580-2590. https://doi.org/10.1039/c2em30378g

Hansen, K. M., Fauser, P., Vorkamp, K., & Christensen, J. H. (2020). Global emissions of Dechlorane Plus. *Science of The Total Environment, 742*, 140677. https://doi.org/10.1016/j.scitotenv.2020.140677

Harner, T. (2017). 2017_v1_5_Template for calculating Effective Air Sample Volumes for PUF and SIP Disk Samplers_Sept_15. Retrieved from https://www.researchgate.net/publication/319764519_2017_v1_5_Template_for_calculating_Effective_Air_Sample_Volumes_for_PUF_and_SIP_Disk_Samplers_Sept_15. Access June 2019.

Harner, T., Farrar, N. J., Shoeib, M., Jones, K. C., & Gobas, F. A. P. C. (2003). Characterization of Polymer-Coated Glass as a Passive Air Sampler for Persistent Organic Pollutants. *Environmental Science & Technology, 37*(11), 2486-2493. https://doi.org/10.1021/es0209215

Harner, T., Shoeib, M., Diamond, M., Stern, G., & Rosenberg, B. (2004). Using Passive Air Samplers To Assess Urban–Rural Trends for Persistent Organic Pollutants. 1. Polychlorinated Biphenyls and Organochlorine Pesticides. *Environmental Science & Technology, 38*(17), 4474-4483. https://doi.org/10.1021/es040302r

Helsel, D. R. (2006). Fabricating data: How substituting values for nondetects can ruin results, and what can be done about it. *Chemosphere, 65*(11), 2434-2439. https://doi.org/10.1016/j.chemosphere.2006.04.051

Hermanson, M. H., Isaksson, E., Forsstrom, S., Teixeira, C., Muir, D. C. G., Pohjola, V. A., & van de Wal, R. S. V. (2010). Deposition History of Brominated Flame Retardant Compounds in an Ice Core from Holtedahlfonna, Svalbard, Norway. *Environmental Science & Technology, 44*(19), 7405-7410. https://doi.org/10.1021/es1016608

Holoubek, I., Klanova, J., Cupr, P., Kukucka, P., Boruvkova, J., Kohoutek, J., Prokes, R., & Kares, R. (2011). POPs in ambient air from MONET network - global and regional trends. *WIT Transactions on Ecology and the Environment, 147*, 173 - 184. https://doi.org/10.2495/AIR110161

Holt, E., Bohlin-Nizzetto, P., Borůvková, J., Harner, T., Kalina, J., Melymuk, L., & Klánová, J. (2017). Using long-term air monitoring of semi-volatile organic compounds to evaluate the uncertainty in polyurethane-disk passive sampler-derived air concentrations. *Environmental Pollution, 220*, 1100-1111. https://doi.org/10.1016/j.envpol.2016.11.030

Hu, D., & Hornbuckle, K. C. (2010). Inadvertent Polychlorinated Biphenyls in Commercial Paint Pigments. *Environmental Science & Technology, 44*(8), 2822-2827. https://doi.org/10.1021/es902413k

Huckins, J. N., Petty, J. D., Lebo, J. A., Almeida, F. V., Booij, K., Alvarez, D. A., Cranor, W. L., Clark, R. C., & Mogensen, B. B. (2002). Development of the permeability/performance reference compound approach for in situ calibration of semipermeable membrane devices. *Environmental Science & Technology, 36*(1), 85-91. https://doi.org/10.1021/es010991w

Hung, H., Halsall, C., Ball, H., Bidleman, T., Dachs, J., De Silva, A., Hermanson, M., Kallenborn, R., Muir, D., Sühring, R., Wang, X., & Wilson, S. (2022). Climate change influence on the levels and trends of persistent organic pollutants (POPs) and chemicals of emerging Arctic concern (CEACs) in the Arctic physical environment – a review. *Environmental Science: Processes & Impacts, 24*(10), 1577-1615. 10.1039/D1EM00485A

Hung, H., Kallenborn, R., Breivik, K., Su, Y., Brorstrom-Lunden, E., Olafsdottir, K., Thorlacius, J. M., Leppanen, S., Bossi, R., Skov, H., Mano, S., Patton, G. W., Stern, G., Sverko, E., & Fellin, P. (2010). Atmospheric monitoring of organic pollutants in the Arctic under the Arctic Monitoring and Assessment Programme (AMAP): 1993-2006. *Science of The Total Environment, 408*(15), 2854-2873. https://doi.org/10.1016/j.scitotenv.2009.10.044

Hung, H., Katsoyiannis, A. A., Brorstrom-Lunden, E., Olafsdottir, K., Aas, W., Breivik, K., Bohlin-Nizzetto, P., Sigurdsson, A., Hakola, H., Bossi, R., Skov, H., Sverko, E., Barresi, E., Fellin, P., & Wilson, S. (2016). Temporal trends of Persistent Organic Pollutants (POPs) in arctic air: 20 years of monitoring under the Arctic Monitoring and Assessment Programme (AMAP). *Environmental Pollution, 217*, 52-61. https://doi.org/10.1016/j.envpol.2016.01.079

Ilyin, I., Batrakova, N., Gusev, A., Kleimenov, M., Rozovskaya, O., Shatalov, V., Strizhkina, I., Travnikov, O., Vulykh, N., Breivik, K., Bohlin-Nizzetto, P., Pfaffhuber, K. A., Aas, W., Poupa, S., Wankmueller, R., Ullrich, B., Bank, M., Ho, Q. T., Vivanco, M. G., Theobald, M. R., Garrido, J. L., Gil, V., Couvidat, F., Collette, A., Mircea, M., Adani, M., Delia, I., Kouznetsov, R. D., & Kadancev, E. V. (2022). *Assessment of heavy metal and POP pollution on global, regional and national scales*. (Status Report 2/2022). Moscow: Meteorological Synthesizing Centre - East Retrieved from https://www.msceast.org/reports/2_2022.pdf.

Ishikawa, Y., Noma, Y., Yamamoto, T., Mori, Y., & Sakai, S.-i. (2007). PCB decomposition and formation in thermal treatment plant equipment. *Chemosphere, 67*(7), 1383-1393. https://doi.org/10.1016/j.chemosphere.2006.10.022

Jaward, F. M., Farrar, N. J., Harner, T., Sweetman, A. J., & Jones, K. C. (2004). Passive air sampling of PCBs, PBDEs, and organochlorine pesticides across Europe. *Environmental Science & Technology, 38*(1), 34-41. https://doi.org/10.1021/es034705n

Jensen, S. (1972). The PCB Story. *Ambio, 1*(4), 123-131. http://www.jstor.org/stable/4311963

Jones, K. (1994). Observations on long-term air-soil exchange of organic contaminants. *Environmental Science and Pollution Research, 1*, 172. https://doi.org/10.1007/BF02986940

Kalina, J., Scheringer, M., Boruvkova, J., Kukucka, P., Pribylova, P., Bohlin-Nizzetto, P., & Klanova, J. (2017). Passive Air Samplers As a Tool for Assessing Long-Term Trends in Atmospheric Concentrations of Semivolatile Organic Compounds. *Environmental Science & Technology, 51*(12), 7047-7054. https://doi.org/10.1021/acs.est.7b02319

Kalina, J., Scheringer, M., Boruvkova, J., Kukucka, P., Pribylova, P., Sanka, O., Melymuk, L., Vana, M., & Klanova, J. (2018). Characterizing Spatial Diversity of Passive Sampling Sites for Measuring Levels and Trends of Semivolatile Organic Chemicals. *Environmental Science & Technology, 52*(18), 10599-10608. https://doi.org/10.1021/acs.est.8b03414

Kalina, J., White, K. B., Scheringer, M., Pribylova, P., Kukucka, P., Audy, O., & Klanova, J. (2019). Comparability of long-term temporal trends of POPs from co-located active and passive air monitoring networks in Europe. *Environmental Science: Processes & Impacts, 21*(7), 1132-1142. https://doi.org/10.1039/c9em00136k

Kidd, K. A., Hesslein, R. H., Ross, B. J., Koczanski, K., Stephens, G. R., & Muir, D. C. G. (1998). Bioaccumulation of organochlorines through a remote freshwater food web in the Canadian Arctic. *Environmental Pollution, 102*(1), 91-103. https://doi.org/10.1016/S0269-7491(98)00068-2

Klanova, J., Eupr, P., Kohoutek, J., & Harner, T. (2008). Assessing the influence of meteorological parameters on the performance of polyurethane foam-based passive air samplers. *Environmental Science & Technology, 42*(2), 550-555. https://doi.org/10.1021/es072098o

Kurt-Karakus, P., Alegria, H., Birgul, A., Gungormus, E., & Jantunen, L. (2018). Organophosphate ester (OPEs) flame retardants and plasticizers in air and soil from a highly industrialized city in Turkey. *Science of The Total Environment, 625*, 555-565. https://doi.org/10.1016/j.scitotenv.2017.12.307

Letcher, R. J., Bustnes, J. O., Dietz, R., Jenssen, B. M., Jørgensen, E. H., Sonne, C., Verreault, J., Vijayan, M. M., & Gabrielsen, G. W. (2010). Exposure and effects assessment of persistent organohalogen contaminants in arctic wildlife and fish. *Science of The Total Environment, 408*(15), 2995-3043. https://doi.org/10.1016/j.scitotenv.2009.10.038

Letcher, R. J., Gebbink, W. A., Sonne, C., Born, E. W., McKinney, M. A., & Dietz, R. (2009). Bioaccumulation and biotransformation of brominated and chlorinated contaminants and their metabolites in ringed seals (Pusa hispida) and polar bears (Ursus maritimus) from East Greenland. *Environment International, 35*(8), 1118-1124. https://doi.org/10.1016/j.envint.2009.07.006

Li, L., Chen, C., Li, D., Breivik, K., Abbasi, G., & Li, Y. (2023). What do we know about the production and release of persistent organic pollutants in the global environment? *Environmental Science: Advances, 2*(1), 55-68. 10.1039/D2VA00145D

Li, L., & Wania, F. (2018). Occurrence of Single- and Double-Peaked Emission Profiles of Synthetic Chemicals. *Environmental Science & Technology, 52*(8), 4684-4693. http://doi.org/10.1021/acs.est.7b06478

Li, Y. F., & Macdonald, R. W. (2005). Sources and pathways of selected organochlorine pesticides to the Arctic and the effect of pathway divergence on HCH trends in biota: a review. *Sci Total Environ, 342*(1-3), 87-106. https://doi.org/10.1016/j.scitotenv.2004.12.027

Ma, J., Hung, H., Tian, C., & Kallenborn, R. (2011). Revolatilization of persistent organic pollutants in the Arctic induced by climate change. *Nature Climate Change, 1*, 255-260. https://doi.org/10.1038/nclimate1167

Mackay, D., McCarty, L. S., & MacLeod, M. (2001). On the validity of classifying chemicals for persistence, bioaccumulation, toxicity, and potential for long-range transport. *Environmental Toxicology and Chemistry, 20*(7), 1491-1498. https://doi.org/10.1002/etc.5620200711

Malanichev, A., Mantseva, E., Shatalov, V., Strukov, B., & Vulykh, N. (2004). Numerical evaluation of the PCBs transport over the Northern Hemisphere. *Environmental Pollution, 128*(1-2), 279-289. https://doi.org/10.1016/j.envpol.2003.08.040

Maleky, F., & Sarafpur, S. (2001). Environmental estrogens and their wildlife and human health effects: a review. *Annals of Saudi Medicine, 21*(1-2), 53-58. https://doi.org/10.5144/0256-4947.2001.53

Markovic, M. Z., Prokop, S., Staebler, R. M., Liggio, J., & Harner, T. (2015). Evaluation of the particle infiltration efficiency of three passive samplers and the PS-1 active air sampler. *Atmospheric Environment, 112*, 289-293. https://doi.org/10.1016/j.atmosenv.2015.04.051

Mastin, J., Harner, T., Schuster, J. K., & South, L. (2022). A review of PCB-11 and other unintentionally produced PCB congeners in outdoor air. *Atmospheric Pollution Research, 13*(4), 101364. https://doi.org/10.1016/j.apr.2022.101364

McLachlan, M. S., Czub, G., MacLeod, M., & Arnot, J. A. (2011). Bioaccumulation of organic contaminants in humans: a multimedia perspective and the importance of biotransformation. *Environmental Science & Technology, 45*(1), 197-202. https://doi.org/10.1021/es101000w

Megson, D., Benoit, N. B., Sandau, C. D., Chaudhuri, S. R., Long, T., Coulthard, E., & Johnson, G. W. (2019). Evaluation of the effectiveness of different indicator PCBs to estimating total PCB concentrations in environmental investigations. *Chemosphere, 237*, 124429. https://doi.org/10.1016/j.chemosphere.2019.124429

Meijer, S. N., Ockenden, W. A., Steinnes, E., Corrigan, B. P., & Jones, K. C. (2003). Spatial and temporal trends of POPs in Norwegian and UK background air: Implications for global cycling. *Environmental Science & Technology, 37*(3), 454-461. https://doi.org/10.1021/es025620+

Melymuk, L., Bohlin, P., Sanka, O., Pozo, K., & Klanova, J. (2014). Current Challenges in Air Sampling of Semivolatile Organic Contaminants: Sampling Artifacts and Their Influence on Data Comparability. *Environmental Science & Technology, 48*(24), 14077-14091. https://doi.org/10.1021/es502164r

Meyer, T., Muir, D. C., Teixeira, C., Wang, X., Young, T., & Wania, F. (2012). Deposition of brominated flame retardants to the Devon Ice Cap, Nunavut, Canada. *Environmental Science & Technology, 46*(2), 826-833. https://doi.org/10.1021/es202900u

Miller, J. N. (2010). *Statistics and chemometrics for analytical chemistry* (6th ed.). Harlow, England: Pearson Prentice Hall.

Moeckel, C., Harner, T., Nizzetto, L., Strandberg, B., Lindroth, A., & Jones, K. C. (2009). Use of depuration compounds in passive air samplers: results from active sampling-supported field deployment, potential uses, and recommendations. *Environmental Science & Technology, 43*(9), 3227-3232. https://doi.org/10.1021/es802897x

Muir, D., & Sverko, E. (2006). Analytical methods for PCBs and organochlorine pesticides in environmental monitoring and surveillance: a critical appraisal. *Analytical and Bioanalytical Chemistry, 386*(4), 769-789. https://doi.org/10.1007/s00216-006-0765-y

Munoz-Arnanz, J., Roscales, J. L., Ros, M., Vicente, A., & Jimenez, B. (2016). Towards the implementation of the Stockholm Convention in Spain: Five-year monitoring (2008-2013) of POPs in air based on passive sampling. *Environmental Pollution, 217*, 107-113. https://doi.org/10.1016/j.envpol.2016.01.052

Nizzetto, L., Macleod, M., Borga, K., Cabrerizo, A., Dachs, J., Di Guardo, A., Ghirardello, D., Hansen, K. M., Jarvis, A., Lindroth, A., Ludwig, B., Monteith, D., Perlinger, J. A., Scheringer, M., Schwendenmann, L., Semple, K. T., Wick, L. Y., Zhang, G., & Jones, K. C. (2010). Past, present, and future controls on levels of persistent organic pollutants in the global environment. *Environmental Science & Technology, 44*(17), 6526-6531. https://doi.org/10.1021/es100178f

Olukunle, O. I., Lehman, D. C., Salamova, A., Venier, M., & Hites, R. A. (2018). Temporal trends of Dechlorane Plus in air and precipitation around the North American Great Lakes. *Science of The Total Environment, 642*, 537-542. https://doi.org/10.1016/j.scitotenv.2018.05.268

Ottar, B. (1976). Organization of long range transport of air pollution monitoring in Europe. *Water, Air, and Soil Pollution, 6*(2), 219-229. https://doi.org/10.1007/BF00182866

Ottar, B. (1981). The transfer of airborne pollutants to the Arctic region. *Atmospheric Environment, 15*(8), 1439-1445. https://doi.org/10.1016/0004-6981(81)90350-4

Pacyna, J. M., Breivik, K., Münch, J., & Fudala, J. (2003). European atmospheric emissions of selected persistent organic pollutants, 1970–1995. *Atmospheric Environment, 37*, 119-131. https://doi.org/10.1016/S1352-2310(03)00240-1

Panuwet, P., Hunter, R. E., Jr., D'Souza, P. E., Chen, X., Radford, S. A., Cohen, J. R., Marder, M. E., Kartavenka, K., Ryan, P. B., & Barr, D. B. (2016). Biological Matrix Effects in Quantitative Tandem Mass Spectrometry-Based Analytical Methods: Advancing Biomonitoring. *Critical Reviews in Analytical Chemistry, 46*(2), 93-105. https://doi.org/10.1080/10408347.2014.980775

Petty, J. D., Huckins, J. N., & Zajicek, J. L. (1993). Application of semipermeable membrane devices (SPMDs) as passive air samplers. *Chemosphere, 27*(9), 1609-1624. https://doi.org/10.1016/0045-6535(93)90143-S

Pisso, I., Sollum, E., Grythe, H., Kristiansen, N. I., Cassiani, M., Eckhardt, S., Arnold, D., Morton, D., Thompson, R. L., Groot Zwaaftink, C. D., Evangeliou, N., Sodemann, H., Haimberger, L., Henne, S., Brunner, D., Burkhart, J. F., Fouilloux, A., Brioude, J., Philipp, A., Seibert, P., & Stohl, A. (2019). The Lagrangian particle dispersion model FLEXPART version 10.4. *Geoscientific Model Development, 12*(12), 4955-4997. https://doi.org/10.5194/gmd-12-4955-2019

Platt, S. M., Hov, Ø., Berg, T., Breivik, K., Eckhardt, S., Eleftheriadis, K., Evangeliou, N., Fiebig, M., Fisher, R., Hansen, G., Hansson, H. C., Heintzenberg, J., Hermansen, O., Heslin-Rees, D., Holmén, K., Hudson, S., Kallenborn, R., Krejci, R., Krognes, T., Larssen, S., Lowry, D., Lund Myhre, C., Lunder, C., Nisbet, E., Nizzetto, P. B., Park, K. T., Pedersen, C. A., Aspmo Pfaffhuber, K., Röckmann, T., Schmidbauer, N., Solberg, S., Stohl, A., Ström, J., Svendby, T., Tunved, P., Tørnkvist, K., van der Veen, C., Vratolis, S., Yoon, Y. J., Yttri, K. E., Zieger, P., Aas, W., & Tørseth, K. (2022). Atmospheric composition in the European Arctic and 30 years of the Zeppelin Observatory, Ny-Ålesund. *Atmospheric Chemistry and Physics, 22*(5), 3321-3369. http://doi.org/10.5194/acp-22-3321-2022

Pozo, K., Harner, T., Shoeib, M., Urrutia, R., Barra, R., Parra, O., & Focardi, S. (2004). Passive-sampler derived air concentrations of persistent organic pollutants on a north-south transect in Chile. *Environmental Science & Technology, 38*(24), 6529-6537. https://doi.org/10.1021/es049065i

Pozo, K., Harner, T., Wania, F., Muir, D. C. G., Jones, K. C., & Barrie, L. A. (2006). Toward a global network for persistent organic pollutants in air: Results from the GAPS study. *Environmental Science & Technology, 40*(16), 4867-4873. https://doi.org/10.1021/es060447t

Qiu, X., Zhu, T., Yao, B., Hu, J., & Hu, S. (2005). Contribution of dicofol to the current DDT pollution in China. *Environmental Science & Technology, 39*(12), 4385-4390. https://doi.org/10.1021/es050342a

Ricking, M., & Schwarzbauer, J. (2012). DDT isomers and metabolites in the environment: an overview. *Environmental Chemistry Letters, 10*(4), 317-323. https://doi.org/10.1007/s10311-012-0358-2

Ross, P. S., De Swart, R. L., Reijnders, P. J., Van Loveren, H., Vos, J. G., & Osterhaus, A. D. (1995). Contaminant-related suppression of delayed-type hypersensitivity and antibody responses in harbor seals fed herring from the Baltic Sea. *Environmental Health Perspectives, 103*(2), 162-167. https://doi.org/10.1289/ehp.95103162
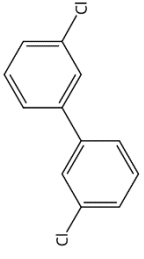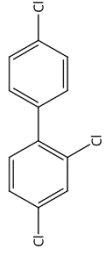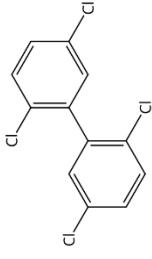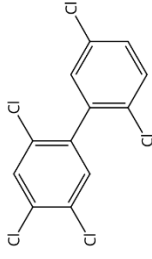
Rowe, A. A., Totten, L. A., Xie, M., Fikslin, T. J., & Eisenreich, S. J. (2007). Air-water exchange of polychlorinated biphenyls in the Delaware River. *Environmental Science & Technology, 41*(4), 1152-1158. https://doi.org/10.1021/es061797i

Röhler, L., Bohlin-Nizzetto, P., Rostkowski, P., Kallenborn, R., & Schlabach, M. (2021). Non-target and suspect characterisation of organic contaminants in ambient air – Part 1: Combining a novel sample clean-up method with comprehensive two-dimensional gas chromatography. *Atmospheric Chemistry and Physics, 21*(3), 1697-1716. https://doi.org/10.5194/acp-21-1697-2021

Schlingermann, M., Berrow, S., Craig, D., McHugh, B., Marrinan, M., O'Brien, J., O'Connor, I., Mudzatsi, E., & White, P. (2020). High concentrations of persistent organic pollutants in adult killer whales (Orcinus orca) and a foetus stranded in Ireland. *Marine Pollution Bulletin, 151*, 110699. https://doi.org/10.1016/j.marpolbul.2019.110699

Schmidt, W. F., Hapeman, C. J., Fettinger, J. C., Rice, C. P., & Bilboulian, S. (1997). Structure and Asymmetry in the Isomeric Conversion of β- to α-Endosulfan. *Journal of Agricultural and Food Chemistry, 45*(4), 1023-1026. https://doi.org/10.1021/jf970020t

Schuster, J. K., Harner, T., Eng, A., Rauert, C., Su, K., Hornbuckle, K. C., & Johnson, C. W. (2021a). Tracking POPs in Global Air from the First 10 Years of the GAPS Network (2005 to 2014). *Environmental Science & Technology, 55*(14), 9479-9488. https://doi.org/10.1021/acs.est.1c01705

Schuster, J. K., Harner, T., & Sverko, E. (2021b). Dechlorane Plus in the Global Atmosphere. *Environmental Science & Technology Letters, 8*(1), 39-45. https://doi.org/10.1021/acs.estlett.0c00758

Shang, H., Li, Y., Wang, T., Wang, P., Zhang, H., Zhang, Q., & Jiang, G. (2014). The presence of polychlorinated biphenyls in yellow pigment products in China with emphasis on 3,3'-dichlorobiphenyl (PCB 11). *Chemosphere, 98*, 44-50. https://doi.org/10.1016/j.chemosphere.2013.09.075

Shen, L., Wania, F., Lei, Y. D., Teixeira, C., Muir, D. C., & Bidleman, T. F. (2005). Atmospheric distribution and long-range transport behavior of organochlorine pesticides in North America. *Environmental Science & Technology, 39*(2), 409-420. https://doi.org/10.1021/es049489c

Shoeib, M., & Harner, T. (2002). Characterization and comparison of three passive air samplers for persistent organic pollutants. *Environmental Science & Technology, 36*(19), 4142-4151. https://doi.org/10.1021/es020635t

Shoeib, M., Harner, T., Lee, S. C., Lane, D., & Zhu, J. (2008). Sorbent-impregnated polyurethane foam disk for passive air sampling of volatile fluorinated chemicals. *Analytical Chemistry, 80*(3), 675-682. https://doi.org/10.1021/ac701830s

Sovocool, G. W., Lewis, R. G., Harless, R. L., Wilson, N. K., & Zehr, R. D. (1977). Analysis of technical chlordane by gas chromatography/mass spectrometry. *Analytical Chemistry, 49*(6), 734-740. https://doi.org/10.1021/ac50014a018

Stenerson, K. K., & Brown, C. (2015). *Analysis of PolyChlorinated Biphenyls in Fish Oil using Supelclean EZ-POP NP, Silica Gel SPE and an SLB-5ms GC Column* (Supelco US Reporter 33.4).

Stenerson, K. K., Shimelis, O., Halpenny, M. R., Espenschied, K., & Ye, M. M. (2015). Analysis of polynuclear aromatic hydrocarbons in olive oil after solid-phase extraction using a dual-layer sorbent cartridge followed by high-performance liquid chromatography with fluorescence detection. *Journal of Agricultural and Food Chemistry, 63*(20), 4933-4939. https://doi.org/10.1021/jf506299f

Stohl, A., Hittenberger, M., & Wotawa, G. (1998). Validation of the lagrangian particle dispersion model FLEXPART against large-scale tracer experiment data. *Atmospheric Environment, 32*(24), 4245-4264. https://doi.org/10.1016/S1352-2310(98)00184-8

Sverko, E., Tomy, G. T., Reiner, E. J., Li, Y. F., McCarry, B. E., Arnot, J. A., Law, R. J., & Hites, R. A. (2011). Dechlorane plus and related compounds in the environment: a review.
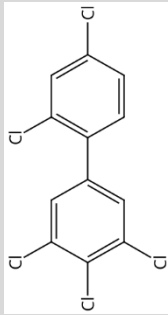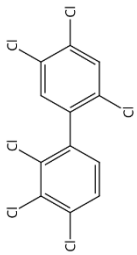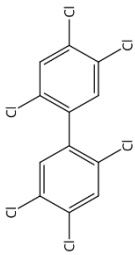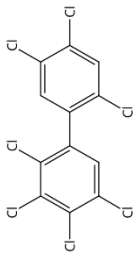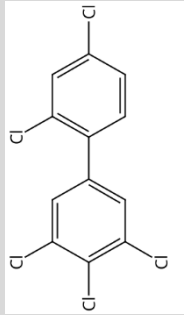
Environmental Science & Technology, 45(12), 5088-5098.
https://doi.org/10.1021/es2003028

Tuduri, L., Harner, T., & Hung, H. (2006). Polyurethane foam (PUF) disks passive air samplers: Wind effect on sampling rates. *Environmental Pollution, 144*(2), 377-383.
https://doi.org/10.1016/j.envpol.2005.12.047

Tørseth, K., Aas, W., Breivik, K., Fjaeraa, A. M., Fiebig, M., Hjellbrekke, A. G., Myhre, C. L., Solberg, S., & Yttri, K. E. (2012). Introduction to the European Monitoring and Evaluation Programme (EMEP) and observed atmospheric composition change during 1972-2009. *Atmospheric Chemistry and Physics, 12*(12), 5447-5481. https://doi.org/10.5194/acp-12-5447-2012

UNECE. (1998). *The 1998 Aarhus Protocol on Persistent organic Pollutants (POPs)*. Denmark: Executive Body for the Convention on Long-range

Transboundary Air Pollution Retrieved from https://unece.org/environment-policy/air/protocol-persistent-organic-pollutants-pops.

UNEP. (2013). *Global monitoring plan for persistent organic pollutants as amended after the fourth meeting of the Conference of the Parties to the Stockholm Convention*. Switzerland: Secretariat of the Stockholm Convention Retrieved from http://chm.pops.int/Implementation/GlobalMonitoringPlan/MonitoringReports/tabid/525/Default.aspx.

UNEP. (2019). *Proposal to list Dechlorane Plus and its syn-isomer and anti-isomer in Annexes A, B and/or C to the Stockholm Convention on Persistent Organic Pollutants*. Switzerland: Persistent Organic Pollutants Review Committee Retrieved from http://chm.pops.int/Convention/POPsReviewCommittee/Chemicals/tabid/243/Default.aspx.

UNEP. (2020). *Stockholm Convention on Persistent Organic Pollutants (POPs). Texts and annexes. Revised in 2019.* Switzerland: Secretariat of the Stockholm Convention Retrieved from http://chm.pops.int/TheConvention/Overview/TextoftheConvention/tabid/2232/Default.aspx.

UNEP. (2023). *Recommendation by the Persistent Organic Pollutants Review Committee to list Dechlorane Plus in Annex A to the Convention and draft text of the proposed amendment*. (UNEP/POPS/COP.11/13). Switzerland: Persistent Organic Pollutants Review Committee Retrieved from https://chm.pops.int/TheConvention/ConferenceoftheParties/Meetings/COP11/tabid/9310/Default.aspx.

Van den Berg, M., Birnbaum, L., Bosveld, A. T., Brunstrom, B., Cook, P., Feeley, M., Giesy, J. P., Hanberg, A., Hasegawa, R., Kennedy, S. W., Kubiak, T., Larsen, J. C., van Leeuwen, F. X., Liem, A. K., Nolt, C., Peterson, R. E., Poellinger, L., Safe, S., Schrenk, D., Tillitt, D., Tysklind, M., Younes, M., Waern, F., & Zacharewski, T. (1998). Toxic equivalency factors (TEFs) for PCBs, PCDDs, PCDFs for humans and wildlife. *Environmental Health Perspectives, 106*(12), 775-792.
https://doi.org/10.1289/ehp.98106775

Vijgen, J., de Borst, B., Weber, R., Stobiecki, T., & Forter, M. (2019). HCH and lindane contaminated sites: European and global need for a permanent solution for a long-time neglected issue. *Environmental Pollution, 248*, 696-705. https://doi.org/10.1016/j.envpol.2019.02.029

Vorkamp, K. (2016). An overlooked environmental issue? A review of the inadvertent formation of PCB-11 and other PCB congeners and their occurrence in consumer products and in the environment. *Science of The Total Environment, 541*, 1463-1476.
https://doi.org/10.1016/j.scitotenv.2015.10.019

Vorkamp, K., & Riget, F. F. (2014). A review of new and current-use contaminants in the Arctic environment: Evidence of long-range transport and indications of bioaccumulation. *Chemosphere, 111*, 379-395. https://doi.org/10.1016/j.chemosphere.2014.04.019

Wang, D. G., Yang, M., Qi, H., Sverko, E., Ma, W. L., Li, Y. F., Alaee, M., Reiner, E. J., & Shen, L. (2010). An Asia-specific source of dechlorane plus: concentration, isomer profiles, and other related
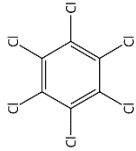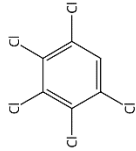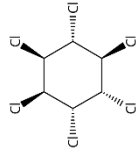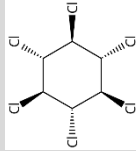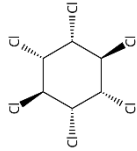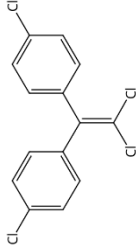
compounds. *Environmental Science & Technology, 44*(17), 6608-6613. https://doi.org/10.1021/es101224y

Wania, F. (2003). Assessing the Potential of Persistent Organic Chemicals for Long-Range Transport and Accumulation in Polar Regions. *Environmental Science & Technology, 37*(7), 1344-1351. https://doi.org/10.1021/es026019e

Wania, F., & Mackay, D. (1993). Global Fractionation and Cold Condensation of Low Volatility Organochlorine Compounds in Polar-Regions. *Ambio, 22*(1), 10-18. http://www.jstor.org/stable/4314030

Wania, F., & Mackay, D. (1996). Tracking the distribution of persistent organic pollutants. *Environmental Science & Technology, 30*(9), A390-A396.

Wania, F., & Mackay, D. (1999). The evolution of mass balance models of persistent organic pollutant fate in the environment. *Environmental Pollution, 100*(1), 223-240. https://doi.org/10.1016/S0269-7491(99)00093-7

Wania, F., Shen, L., Lei, Y. D., Teixeira, C., & Muir, D. C. G. (2003). Development and calibration of a resin-based passive sampling system for monitoring persistent organic pollutants in the atmosphere. *Environmental Science & Technology, 37*(7), 1352-1359. https://doi.org/10.1021/es026166c

Wania, F., & Shunthirasingham, C. (2020). Passive air sampling for semi-volatile organic chemicals. *Environmental Science: Processes & Impacts, 22*(10), 1925-2002. https://doi.org/10.1039/D0EM00194E

Weber, J., Halsall, C. J., Muir, D., Teixeira, C., Small, J., Solomon, K., Hermanson, M., Hung, H., & Bidleman, T. (2010). Endosulfan, a global pesticide: a review of its fate in the environment and occurrence in the Arctic. *Science of The Total Environment, 408*(15), 2966-2984. https://doi.org/10.1016/j.scitotenv.2009.10.077

Webster, E., Mackay, D., & Wania, F. (1998). Evaluating environmental persistence. *Environmental Toxicology and Chemistry, 17*(11), 2148-2158. https://doi.org/10.1002/etc.5620171104

Weihe, P., Debes, F., Halling, J., Petersen, M. S., Muckle, G., Odland, J. O., Dudarev, A., Ayotte, P., Dewailly, E., Grandjean, P., & Bonefeld-Jorgensen, E. (2016). Health effects associated with measured levels of contaminants in the Arctic. *International Journal of Circumpolar Health, 75*(1), 33805. https://doi.org/10.3402/ijch.v75.33805

Whitman, W. G. (1923). The two-film theory of gas absorption. *Chemical and Metallurgical Engineering, 29*, 146-150.

Wong, F., Hung, H., Dryfhout-Clark, H., Aas, W., Bohlin-Nizzetto, P., Breivik, K., Mastromonaco, M. N., Lunden, E. B., Olafsdottir, K., Sigurethsson, A., Vorkamp, K., Bossi, R., Skov, H., Hakola, H., Barresi, E., Sverko, E., Fellin, P., Li, H., Vlasenko, A., Zapevalov, M., Samsonov, D., & Wilson, S. (2021). Time trends of persistent organic pollutants (POPs) and Chemicals of Emerging Arctic Concern (CEAC) in Arctic air from 25 years of monitoring. *Science of The Total Environment, 775*, 145109. https://doi.org/10.1016/j.scitotenv.2021.145109

Xiao, H., Li, N., & Wania, F. (2004). Compilation, Evaluation, and Selection of Physical-Chemical Property Data for α-, β-, and γ-Hexachlorocyclohexane. *Journal of Chemical & Engineering Data, 49*(2), 173-185. https://doi.org/10.1021/je034214i

Yusa, V., Coscolla, C., Mellouki, W., Pastor, A., & de la Guardia, M. (2009). Sampling and analysis of pesticides in ambient air. *Journal of Chromatography A, 1216*(15), 2972-2983. https://doi.org/10.1016/j.chroma.2009.02.019

Zhang, X., Tsurukawa, M., Nakano, T., Lei, Y. D., & Wania, F. (2011). Sampling Medium Side Resistance to Uptake of Semivolatile Organic Compounds in Passive Air Samplers. *Environmental Science & Technology, 45*(24), 10509-10515. 10.1021/es2032373

Aas, W., & Bohlin-Nizzetto, P. (2018). *Heavy metals and POP measurements, 2016*. (EMEP/CCC-Report 3/2018). Kjeller: NILU Retrieved from http://hdl.handle.net/11250/2563390.
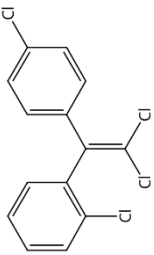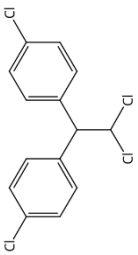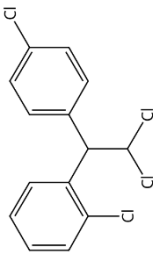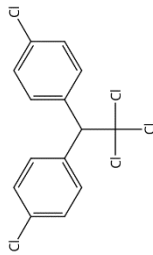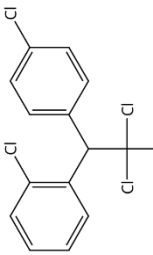
Appendix
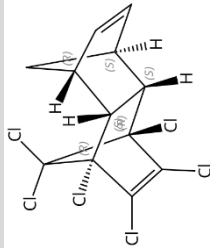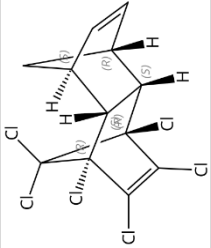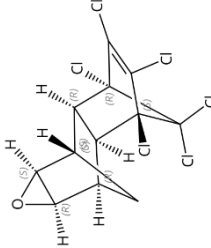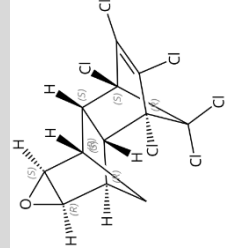
Table A1. Detailed information for the individual compounds examined in this thesis, including log K_{OA}, the main sources and the year of regulation. Grey shading=detection frequency <60% in Europe (*Paper II*).
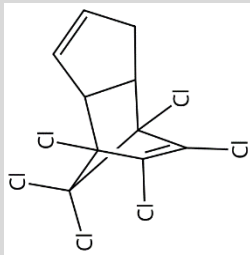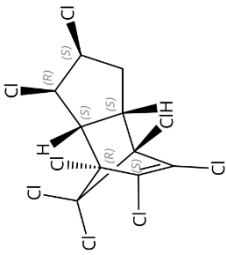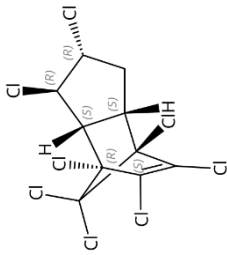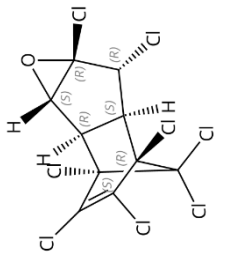
Trivial name	Full name	log K_{OA}[1]	Structural formula[2]	Main sources/uses	Aarhus Protocol[3]	Stockholm Convention[3]
PCB-11	3,3'-dichlorobiphenyl	7.72		UI-PCB i.e. byproduct in pigment and dye manufacturing (diarylide yellow) (Hu & Hornbuckle, 2010) and thermal processes involving organic matter and chlorine (Vorkamp, 2016)	E (2003, articles in use exempted) + UI (2022)	E (2004, articles in use exempted) + UI (2004)
PCB-28	2,4,4'-trichlorobiphenyl	8.25		I-PCB in technical mixtures (e.g. Aroclor, Monsanto) used as heat exchange fluids in capacitors and transformers and as additives in a variety of products. Also UI-PCB present in yellow pigments (Shang et al., 2014).	E (2003, articles in use exempted) + UI (2022)	E (2004, articles in use exempted) + UI (2004)
PCB-52	2,2',5,5'-tetrachlorobiphenyl	8.57		I-PCB in technical mixtures (e.g. Aroclor, Monsanto) used as heat exchange fluids in capacitors and transformers and as additives in a variety of products	E (2003, articles in use exempted) + UI (2022)	E (2004, articles in use exempted) + UI (2004)
PCB-101	2,2',4,5,5'-pentachlorobiphenyl	9.34		I-PCB in technical mixtures (e.g. Aroclor, Monsanto) used as heat exchange fluids in capacitors and transformers and as additives in a variety of products	E (2003, articles in use exempted) + UI (2022)	E (2004, articles in use exempted) + UI (2004)
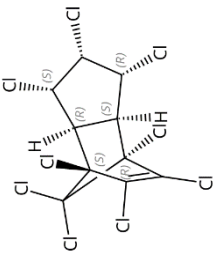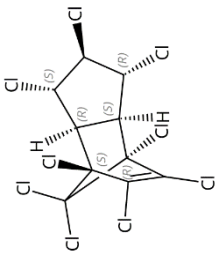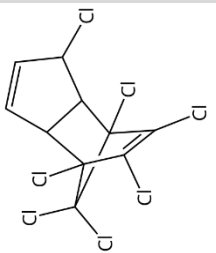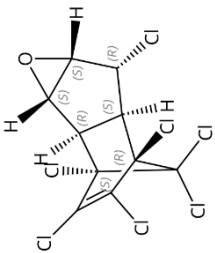
				E (2003, articles in use exempted) + UI (2022)	E (2004, articles in use exempted) + UI (2004)
PCB-123	2,3′,4,4′,5′-pentachlorobiphenyl		UI-PCB (dioxin-like) i.e. mainly thermal processes involving organic matter and chlorine (Mastin et al., 2022), also found in pigments (Hu & Hornbuckle, 2010)	E (2003, articles in use exempted) + UI (2022)	E (2004, articles in use exempted) + UI (2004)
PCB-138	2,2′,3,4,4′,5′-hexachlorobiphenyl		I-PCB in technical mixtures (e.g. Aroclor, Monsanto) used as heat exchange fluids in capacitors and transformers and as additives in a variety of products	E (2003, articles in use exempted) + UI (2022)	E (2004, articles in use exempted) + UI (2004)
PCB-153	2,2′,4,4′,5,5′-hexachlorobiphenyl		I-PCB in technical mixtures (e.g. Aroclor, Monsanto) used as heat exchange fluids in capacitors and transformers and as additives in a variety of products	E (2003, articles in use exempted) + UI (2022)	E (2004, articles in use exempted) + UI (2004)
PCB-180	2,2′,3,4,4′,5,5′-heptachlorobiphenyl		I-PCB in technical mixtures (e.g. Aroclor, Monsanto) used as heat exchange fluids in capacitors and transformers and as additives in a variety of products	E (2003, articles in use exempted) + UI (2022)	E (2004, articles in use exempted) + UI (2004)
PCB-209	2,2′,3,3′,4,4′, 5,5′,6,6′-decachlorobiphenyl		UI-PCB e.g. combustion of automobile shredder residue (Ishikawa et al., 2007), also in pigments, e.g. phthalocyanine green (Hu & Hornbuckle, 2010) and titanium dioxide white pigments (Rowe et al., 2007)	E (2003, articles in use exempted) + UI (2022)	E (2004, articles in use exempted) + UI (2004)

The values 10.1, 10.3, 10.1, 10.9, 12.1 appear in a column between the name and structure for PCB-123, PCB-138, PCB-153, PCB-180, PCB-209 respectively.

56
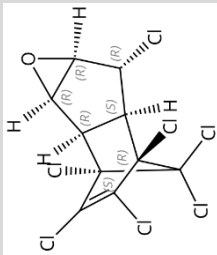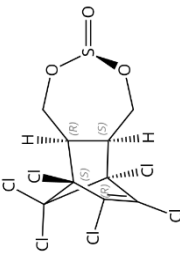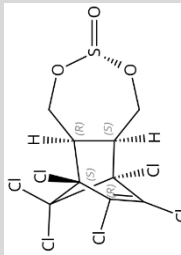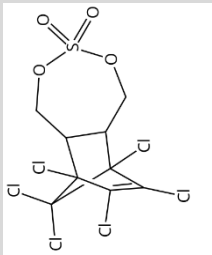
	Chemical name	log K_{ow}	Structure	Use / origin		
HCB	Hexachlorobenzene	7.56		Used as fungicide (i.e. an OCP). Also a byproduct in chlorinated chemicals and a combustion product.	E (2003) + UI (2022)	E (2004, with some excemptions) + UI (2004)
PeCB	Pentachlorobenzene	6.40		Used as e.g. fungicide (i.e. an OCP). Also a byproduct in chlorinated chemicals and a combustion product.	E (2022)	E (2010) + UI (2010)
α-HCH	(1α,2α,3β,4α,5β,6β)-1,2,3,4,5,6-hexachlorocyclohexane	7.80		In technical HCH (55-80% (Breivik et al., 1999)), used as insecticide (i.e. OCP). Also unintentional by-product of lindane.	E (2022)	E (2010)
β-HCH	(1α,2β,3α,4β,5α,6β)-1,2,3,4,5,6-hexachlorocyclohexane	9.16		In technical HCH (5-14% (Breivik et al., 1999)) used as insecticide (i.e. OCP). Also unintentional by-product of lindane.	E (2022)	E (2010)
γ-HCH	(1α,2α,3β,4α,5α,6β)-1,2,3,4,5,6-hexachlorocyclohexane	8.05		In Lindane and in technical HCH (8-15% (Breivik et al., 1999)) used as insecticide (i.e. OCP).	E (2022, exception for pubic health purposes)	E (2004, exception for pubic health purposes)
p,p'-DDE	4,4'-dichlorodiphenyldichloroethylene	9.97		Degradation product of p,p'-DDT (Ricking & Schwarzbauer, 2012).		
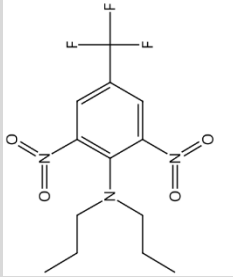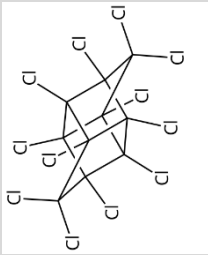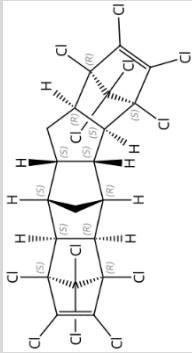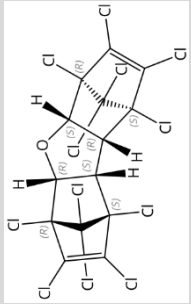
Compound	Chemical name	Value	Structure	Description	Status
o,p'-DDE	2,4'-dichlorodiphenyldichloroethylene	9.16		Degradation product of o,p'-DDT (Ricking & Schwarzbauer, 2012). Impurity of Dicofol (18%, (Qiu et al., 2005)).	
p,p'-DDD	4,4'-dichlorodiphenyldichloroethane	10.3		Degradation product of p,p'-DDT (Ricking & Schwarzbauer, 2012).	
o,p'-DDD	2,4'-dichlorodiphenyldichloroethane	9.12		Degradation product of o,p'-DDT (Ricking & Schwarzbauer, 2012).	
p,p'-DDT	4,4'-dichlorodiphenyltrichloroethane	10.1		In technical DDT (80% (Li & Macdonald, 2005)), used as insecticide e.g. in the control of malaria (i.e. OCP). Impurity of Dicofol (7%, (Qiu et al., 2005)).	E (2003) + R (2003-2022, acceptable for public health protection and Dicofol intermediate) — R (2004, acceptable for public health protection and Dicofol intermediate)
o,p'-DDT	2,4'-dichlorodiphenyltrichloroethane	9.72		In technical DDT (20% (Li & Macdonald, 2005)), used as insecticide e.g. in the control of malaria (i.e. OCP). Impurity of Dicofol (46%, (Qiu et al., 2005)).	E (Dicofol, 2020)

58
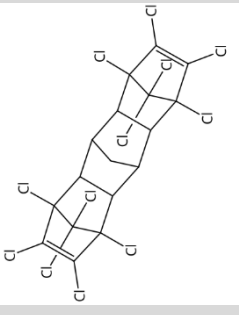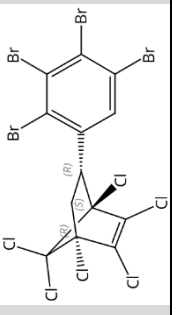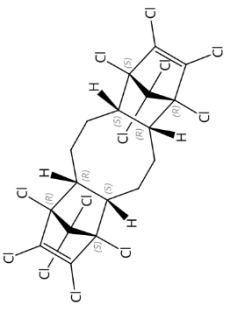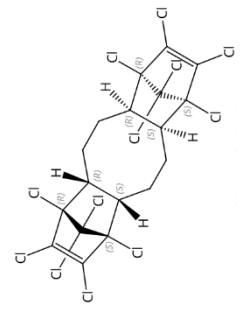
	IUPAC name	Structure		Description		
Aldrin	(1R,4S,4aS,5S,8R,8aR)-1,2,3,4,10,10-hexachloro-1,4,4a,5,8,8a-hexahydro-1,4:5,8-dimethanonaphthalene		8.29	Used as OCP e.g. as termiticide.	E (2003)	E (2004)
Isodrin	(1R,4S,4aS,5R,8S,8aR)-1,2,3,4,10,10-hexachloro-1,4,4a,5,8,8a-hexahydro-1,4:5,8-dimethanonaphthalene		-	Stereoisomer of Aldrin.		
Dieldrin	(1aR,2R,2aS,3S,6R,6aR,7S,7aS)-3,4,5,6,9,9-hexachloro-1a,2,2a,3,6,6a,7,7a-octahydro-2,7:3,6-dimethanonaphtho[2,3-b]oxirene		9.12	Used as OCP e.g. as termiticide. Degradation product of Aldrin (Gannon & Bigger, 1958).	E (2003)	E (2004, with some excemptions)
Endrin	(1aR,2R,2aR,3R,6S,6aS,7S,7aS)-3,4,5,6,9,9-hexachloro-1a,2,2a,3,6,6a,7,7a-octahydro-2,7:3,6-dimethanonaphth[2,3-b]oxirene		8.39	Used as insecticide (i.e. OCP). Stereoisomer of Dieldrin.	E (2003)	E (2004)

Name	IUPAC name		Structure	Occurrence		
Chlordene	4,5,6,7,8,8-Hexachloro-3a,4,7,7a-tetrahydro-4,7-methano-1H-indene	-		In technical Chlordane (1% (Sovocool et al., 1977)), used as insecticide (i.e. OCP).		
cis-Chlordane (α)	(1R,2S,3aS,4S,7R,7aS)-1,2,4,5,6,7,8,8-octachloro-2,3,3a,4,7,7a-hexahydro-4,7-methano-1H-indene	9.21		In technical Chlordane (11% (Bidleman et al., 2002)), used as insecticide (i.e. OCP).	E (2003)	E (2004, with some excemptions)
trans-Chlordane (γ)	(1R,2R,3aS,4S,7R,7aS)-1,2,4,5,6,7,8,8-octachloro-2,3,3a,4,7,7a-hexahydro-4,7-methano-1H-indene	9.16		In technical Chlordane (13% (Bidleman et al., 2002)), used as insecticide (i.e. OCP).	E (2003)	E (2004, with some excemptions)
Oxychlordane	(1aR,1bS,2R,5S,5aR,6S,6aS)-2,3,4,5,6,6a,7,7-octachloro-1a,1b,5,5a,6,6a-hexahydro-2,5-methano-2H-indeno[1,2-b]oxirene	8.62		Degradation product of Chlordane		

					E (2004, with some excemptions)	
					E (2003)	
cis-nonachlor	(1R,3S,3aR,4S,7R,7aS)-1,2,3,4,5,6,7,8,8-nonachloro-2,3,3a,4,7,7a-hexahydro-4,7-methano-1H-indene	9.96		In technical Chlordane (<1% (Sovocool et al., 1977)), used as insecticide (i.e. OCP).		
trans-nonachlor	(1α,2β,3α,3aα,4β,7β,7aα)-1,2,3,4,5,6,7,8,8-nonachloro-2,3,3a,4,7,7a-hexahydro-4,7-methano-1H-indene	9.60		In technical Chlordane (5% (Bidleman et al., 2002)), used as insecticide (i.e. OCP).		
Heptachlor	1,4,5,6,7,8,8-heptachloro-3a,4,7,7a-tetrahydro-4,7-methano-1H-indene	7.84		In technical heptachlor and technical Chlordane (5% (Bidleman et al., 2002)), used as insecticide (i.e. OCP).		
Heptachlor epoxide (exo)	(1aR,1bS,2R,5S,5aR,6S,6aR)-2,3,4,5,6,7,7-heptachloro-1a,1b,5,5a,6,6a-hexahydro-2,5-methano-2H-indeno[1,2-b]oxirene	8.72		Degradation product of Heptachlor.		

61

Name	IUPAC name	Value	Structure	Occurrence / Description	Classification
Heptachlor epoxide (endo)	(1aR,1bR,2S,5R,5aS,6R,6aR)-2,3,4,5,6,7,7-Heptachloro-1a,1b,5,5a,6,6a-hexahydro-2,5-methano-2H-indeno[1,2-b]oxirene	8.72		Degradation product of Heptachlor.	
Endosulfan I (α)	(3α,5aβ,6α,9α,9aβ)-6,7,8,9,10,10-hexachloro-1,5,5a,6,9,9a-hexahydro-3-oxide-6,9-methano-2,4,3-benzodioxathiepin	8.89		In technical Endosulfan (60-70% (Weber et al., 2010)), used as insecticide.	E (2012, with some excemptions)
Endosulfan II (β)	(3α,5aα,6β,9β,9aα)-6,7,8,9,10,10-hexachloro-1,5,5a,6,9,9a-hexahydro-3-oxide-6,9-methano-2,4,3-benzodioxathiepin	9.53		In technical Endosulfan (30-40% (Weber et al., 2010)), used as insecticide.	E (2012, with some excemptions)
Endosulfan sulfate	6,7,8,9,10,10-hexachloro-1,5,5a,6,9,9a-hexahydro-3,3-dioxide-6,9-Methano-2,4,3-benzodioxathiepin	9.93		Degradation product of Endosulfan.	E (2012, with some excemptions)

Trifluralin	2,6-Dinitro-N,N-dipropyl-4-(trifluoromethyl)benzenamine	7.93			E (2004, with some excemptions)
Mirex (Dechlorane)	1,1a,2,2,3,3a,4,5,5,5a,5b,6-Dodecachlorooctahydro-1,3,4-metheno-1H-cyclobuta[cd]pentalene	13.7		Industrial chemical used as flame retardant and OCP.	E (2003)
Dec-601	(1R,4S,4aS,4bS,5R,5aR,6R,9S,9aS,10S,10aS,11aR)-1,2,3,4,6,7,8,9,13,13,14,14-Dodecachloro-4,4a,4b,5,5a,6,9,9a,10,10a,11,11a-dodecahydro-1,4:5,10:6,9-trimethano-1H-benzo[b]fluorene	-		Not available (Sverko et al., 2011).	
Dec-602	1,2,3,4,6,7,8,9,10,10,11,11-Dodecachloro-1,4,4a,5a,6,9,9a,9b-octahydro-1,4:6,9-dimethanodibenzofuran	13.6		Not available (Sverko et al., 2011).	

63

Dec-603	1,2,3,4,5,6,7,8,12,12,13,13-Dodecachloro-1,4,4a,5,8,8a,9,9a,10,10a-decahydro-1,4:5,8:9,10-trimethanoanthracene	-		Not available (Sverko et al., 2011).	
Dec-604	(1R,4S,5R)-1,2,3,4,7,7-Hexachloro-5-(2,3,4,5-tetrabromophenyl)bicyclo[2.2.1]hept-2-ene	16.1		Not available (Sverko et al., 2011).	
Dechlorane plus (syn)	(1R,4S,4aS,6aR,7R,10S,10aS,12aR)-1,2,3,4,7,8,9,10,13,13,14,14-Dodecachloro-1,4,4a,5,6,6a,7,10,10a,11,12,12a-dodecahydro-1,4:7,10-dimethanodibenzo[a,e]cyclooctene	15.2		In technical DP (20-40% (Wang et al., 2010)), used as flame retardant in industrial polymers in electronics and building materials.	PFL (2018)
Dechlorane plus (anti)	(1R,4S,4aS,6aS,7S,10R,10aR,12aR)-1,2,3,4,7,8,9,10,13,13,14,14-Dodecachloro-1,4,4a,5,6,6a,7,10,10a,11,12,12a-dodecahydro-1,4:7,10-dimethanodibenzo[a,e]cyclooctene	15.2		In technical DP (60-80% (Wang et al., 2010)), used as flame retardant in industrial polymers such as electrical coatings and building materials.	PFL (2018)

[1] From Harner (2017) at 20°C. "-" = not in the template.

[2] https://scifinder-n.cas.org/ (accessed 12:18, Feb 4, 2023)

[3] E = regulations to *eliminate* production and use, R = regulation to *restrict* production and use, UI = regulations to reduce or eliminate unintentional emissions, PFL = *Proposed for listing*
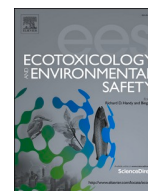
Main sources controlling atmospheric burdens of persistent organic pollutants on a national scale

Helene Lunder Halvorsen [a,b,*], Pernilla Bohlin-Nizzetto [a], Sabine Eckhardt [a], Alexey Gusev [c], Ingjerd Sunde Krogseth [a], Claudia Moeckel [a,1], Victor Shatalov [c], Lovise Pedersen Skogeng [a], Knut Breivik [a,b]

[a] *NILU - Norwegian Institute for Air Research, P.O. Box 100, 2027 Kjeller, Norway*
[b] *University of Oslo, 0351 Oslo, Norway*
[c] *Meteorological Synthesizing Centre-East, 115419 Moscow, Russian Federation*

ARTICLE INFO

ABSTRACT

National long-term monitoring programs on persistent organic pollutants (POPs) in background air have traditionally relied on active air sampling techniques. Due to limited spatial coverage of active air samplers, questions remain (i) whether active air sampler monitoring sites are representative for atmospheric burdens within the larger geographical area targeted by the monitoring programs, and thus (ii) if the main sources affecting POPs in background air across a nation are understood. The main objective of this study was to explore the utility of spatial and temporal trends in concert with multiple modelling approaches to understand the main sources affecting polychlorinated biphenyls (PCBs) and organochlorine pesticides (OCPs) in background air across a nation. For this purpose, a comprehensive campaign was carried out in summer 2016, measuring POPs in background air across Norway using passive air sampling. Results were compared to a similar campaign in 2006 to assess possible changes over one decade. We furthermore used the Global EMEP Multi-media Modeling System (GLEMOS) and the Flexible Particle dispersion model (FLEXPART) to predict and evaluate the relative importance of primary emissions, secondary emissions, long-range atmospheric transport (LRAT) and national emissions in controlling atmospheric burdens of PCB-153 on a national scale. The concentrations in air of both PCBs and most of the targeted OCPs were generally low, with the exception of hexachlorobenzene (HCB). A limited spatial variability for all POPs in this study, together with predictions by both models, suggest that LRAT dominates atmospheric burdens across Norway. Model predictions by the GLEMOS model, as well as measured isomeric ratios, further suggest that LRAT of some POPs are dictated by secondary emissions. Our results illustrate the utility of combining observations and mechanistic modelling approaches to help identify the main factors affecting atmospheric burdens of POPs across a nation, which, in turn, may be used to inform both national monitoring and control strategies.

1. Introduction

Persistent organic pollutants (POPs) are a group of organic chemicals, which mainly includes industrial chemicals and organochlorine pesticides. They are of international concern due to their slow degradation in the environment, potential to bioaccumulate through food chains, harmful effects, and ability to undergo long-range environmental transport (LRT). International agreements exist to eliminate or reduce the release of POPs into the environment (UNEP, 2018).

The atmosphere represents an important pathway of environmental transport of POPs from global source regions into background areas (Hung et al., 2010; Wania and Mackay, 1993). While temporal trends of POPs in air from remote regions are available through various international monitoring programs, e.g. in Europe (Tørseth et al., 2012) and North America (Venier and Hites, 2010), these monitoring programs are based on a limited network of conventional active air samplers (AAS). The need for trained personnel, electricity and high costs associated with AAS, may limit the use in terms of assessing the spatial variability of

---

POPs in air. A complementary strategy to expand the spatial coverage, is to use passive air samplers (PAS) (Jaward et al., 2004; Shoeib and Harner, 2002). Two examples of major PAS networks are the Global Atmospheric Passive Sampling network (GAPS) (Pozo et al., 2006) and the Monitoring Network (MONET) in Europe, Africa and Asia (Holoubek et al., 2011), which both have contributed to assess spatial and temporal trends of POPs in air across the globe and on continental scales, respectively. Further examples of studies on a regional scale include case-studies in North America (Shen et al., 2005, 2006), Africa (Klánová et al., 2009), Europe (Halse et al., 2011; Jaward et al., 2004), Asia (Hogarh et al., 2012; Jaward et al., 2005), and the UK-Norway transect (Schuster et al., 2010). However, while there are examples of national monitoring efforts in individual countries like the Czech Republic (Kalina et al., 2018) and Spain (Muñoz-Arnanz et al., 2016) most case-studies target potential contaminated areas (Kurt-Karakus et al., 2018; Mari et al., 2008; Menichini et al., 2007; Wang et al., 2007; Zhang et al., 2008). The number of studies targeting the distribution of POPs across entire nations with focus on background sites remain limited. This limits our understanding of the relative significance of long-range atmospheric transport (LRAT) versus national emissions in the control of atmospheric burdens on national scales.

A complicating aspect when seeking to identify factors controlling concentrations of POPs in air, is the potential for some POPs to undergo reversible atmospheric deposition from surface media contaminated in the past (Jones, 1994; Ma et al., 2011; Wania and Mackay, 1996). Therefore, contemporary concentrations of POPs in air may in part be controlled by secondary emissions, continuing primary emissions - or both. If secondary emissions dictate atmospheric burdens across a nation, further national primary emission reductions may have a smaller effect on the reduction of national concentrations of POPs in air. As primary emissions of regulated POPs are likely to decline, the relative influence of secondary emissions will increase (Nizzetto et al., 2010). Yet, major uncertainties remain when and where this will happen for individual POPs. What is known, however, is that many POPs, and notably industrial chemicals, have a long lifetime in the anthroposphere, leading to continuing primary emissions. An example includes PCBs which have been extensively used in long-lived building materials and electrical products. Primary emissions thus remain decades after production has been banned, particularly because significant emissions largely occur during the waste stage (Breivik et al., 2016; Li and Wania, 2018). Hence, the immediate impact of the Stockholm Convention on temporal trends of POPs in air has been questioned (Wöhrnschimmel et al., 2016).

In spite of international agreements, there is still a need to assess further measures to protect human health and the environment from POPs. To inform policy makers in individual countries, there is a need for methodologies which may both help to better (i) identify the main sources controlling atmospheric burdens and (ii) evaluate the efficacy of any national monitoring strategies.

The key objective of this study is to apply and evaluate a methodology using measurements and models in concert to assess the relative importance of primary emissions, secondary emissions, LRAT and national emissions in controlling atmospheric burdens of individual POPs across a nation. For this purpose, a passive air sampling campaign was carried out, mapping concentrations of POPs in background air across Norway (Fig. 1). The focus on data-rich legacy POPs is a deliberate restriction as this allows us to (i) address chemicals which have seen significant historical use, both within and outside the country, (ii) compare our findings with studies carried out in the past, including long-term national monitoring efforts, and (iii) parameterize, evaluate and apply two existing models to help identify the main factors controlling atmospheric burdens.

While this study was carried out in Norway, the methodology may help inform monitoring programs in other countries, and ultimately guide opportunities for further control strategies, nationally and/or internationally.
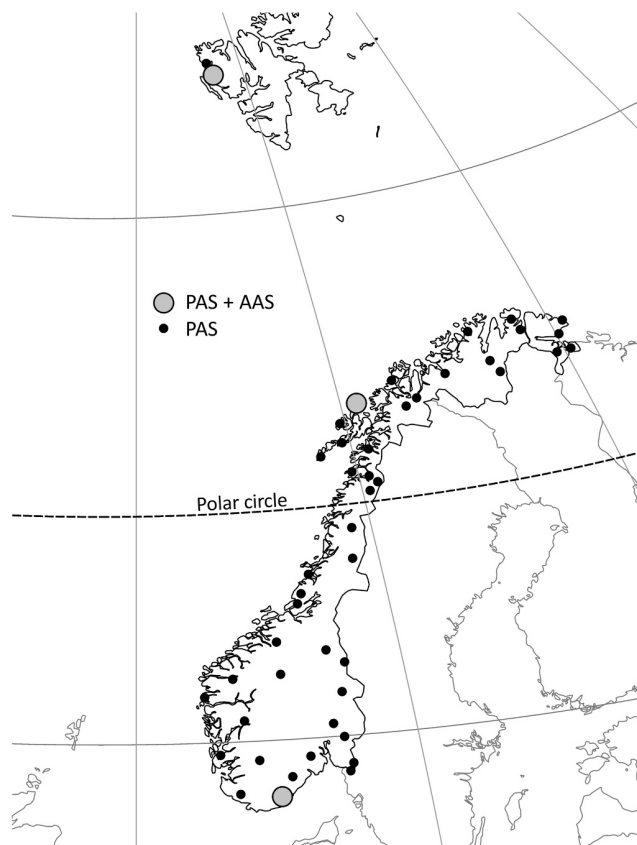
Fig. 1. The spatial coverage of sites monitoring POPs with AAS (grey) in the national monitoring program (Bohlin-Nizzetto et al., 2017) and the spatial coverage of sites measuring POPs with PAS (black) in this study.

2. Materials and methods

2.1. Sampling

In our study, air samples were collected across Norway (58°N to 79°N, 5°E to 31°E), using the same passive air samplers as within the MONET program (Kalina et al., 2017; Markovic et al., 2015), with polyurethane foam (PUF) as sampling medium, and with the same theoretical principles as described by Harner et al. (2004). The PUF disks were spiked with a performance reference compound (PRC) mixture (SI 1.1.3) for assessing sampling rate variability from site to site.

A total of 47 PUF-PAS were deployed for three months during summer 2016 (Fig. 1), at 45 remote sites (ranging from 58°N to 71°N) on mainland Norway, and two pristine sites on Svalbard (79°N). In addition, PUF-PAS were concurrently deployed at ten urban sites around the city of Oslo (60°N), to compare background concentrations with measurements from an area expected to be more influenced by local emissions. The obtained concentrations where compared to concentrations from AAS at three monitoring sites in the national monitoring program (Fig. 1) (Bohlin-Nizzetto et al., 2017). More details on the sampler preparation, deployment and exact locations of the sampling sites are given in the Supporting Information (SI).

2.2. Sample extraction and clean-up

At the end of the deployment period, the PUF-PAS were retrieved and returned to the laboratory at NILU - Norwegian Institute for Air Research. Details of sample extraction and clean-up are given in SI 1.2.

2.3. Instrumental analysis

The samples were analyzed for 31 polychlorinated biphenyls (PCBs), including six indicator PCBs (PCB-28, -52, -101, -138, -153 and -180), and 29 organochlorine pesticides (OCPs). The OCPs included penta- and hexachlorobenzene (PeCB/HCB), hexachlorocyclohexanes (HCHs), DDTs, chlordanes (CD), aldrin, endosulfans and their metabolites. Identification and quantification were carried out using a gas chromatograph (GC) coupled to a high-resolution mass spectrometer (HRMS). Details of the instrumental analysis and a list of all target compounds are given in (SI 1.3, Table SI-1.3b-c).

2.4. Quality assurance/quality control

Five method blanks and three field blanks were extracted and analyzed in the same way as the exposed samples (SI 1.4.1). All blanks had comparable levels and were used to calculate the method detection limit (MDL) (Table SI-2.1).

Of the 60 targeted analytes, only the analytes with high detection frequency ($> 60\%$ above MDL) have been evaluated in this study, i.e. 18 PCBs and 14 OCPs. The average concentrations of these selected analytes in background air exceeded the MDLs by a factor of 2–185. Concentrations below MDL were set to ½ MDL for the calculation of sum, average and median, and for the statistical analysis.

In addition to using ^{13}C-labelled internal standards (SI 1.4.2) to compensate for possible loss during sample preparation, three PUFs spiked with a ^{12}C-mixture of all target analytes were analyzed for method quality control (bias -2%–6% for PCBs and -13%–16% for OCPs, SI 1.4.3). In order to evaluate the reproducibility of the PAS method, two PUF-PAS were co-deployed at three sites (relative standard deviation 0–16% for PCBs and 0–17% for OCPs, SI 1.4.4).

2.5. Deriving concentrations in air

Concentrations of POPs in air were estimated from the amounts found in the samplers and the widely used template of Harner (2017). The uncertainties and semi-quantitative nature of PUF-PAS has been a topic of several publications (Bohlin et al., 2014; Holt et al., 2017; Kalina et al., 2017; Melymuk et al., 2014; Wania and Shunthirasingham, 2020). Studies show that PUF-PAS is a useful tool for compounds with similar volatility range, such as the PCBs and OCPs targeted in this study. In our study, the uncertainties were minimized by using PRCs and site-specific environmental conditions in estimating site-specific sampling rates, as recommended by the PAS community.

The PUF-characteristics, air temperature at each site (4–16 °C, average: 12 °C), measured loss of PRCs and their temperature-adjusted octanol-air partition coefficients (K_{OA}), were used to calculate site-specific sampling rates (2.8–4.5 m^3/day, average: 3.6 m^3/day) and to derive actual air concentrations (SI 1.5). This approach is described in detail by Moeckel et al. (2009). Compounds with low K_{OA} (e.g. HCB, PCB-18 and -28), will approach equilibrium between the PUF-PAS and the air during the deployment period in this study. This means that the uptake is not gradually increasing during the whole sampling period as predicted by the template (Harner, 2017) and that the PAS does not provide a true time-averaged concentration (Wania and Shunthirasingham, 2020). Underestimation of the concentrations in air for these compounds might therefore be possible.

2.6. Data analysis

The ratio between maximum and minimum concentrations in air (MMR) was used as a simple measure of the spatial variability, as utilized in e.g. Halse et al. (2011) and Jaward et al. (2004). Outliers outside the maximum according to a boxplot of the concentrations are excluded, as described in SI 1.6.1. When samples below MDL are present, MDL is used as the minimum value.

To further assess the variability across the study region, possible latitudinal gradients, differences in background concentration levels between southern- and northern Norway (divided by the Polar circle), and changes over the last decade were examined.

All statistical analyses (linear correlation, significance) were performed by using R Studio V1.1 as described in SI 1.6.

2.7. Atmospheric transport modelling tools

The Global EMEP Multi-media Modeling System (GLEMOS, 2020) developed by the Meteorological Synthesizing Centre - East under the European Monitoring and Evaluation Programme (EMEP), was used to evaluate whether the observed spatial patterns of PCB-153 can be reproduced by the model. Further, GLEMOS was used to predict the contributions attributed to the four source categories examined. The GLEMOS model predicts both the contributions of primary- and secondary emissions. While GLEMOS separates between contributions from primary emissions, whether attributed to national emissions or LRAT (within/outside the EMEP domain), the origin of secondary emissions is not defined. The contributions from primary emissions alone were further predicted by the Lagrangian particle dispersion model, FLEXPART V10.4 (Pisso et al., 2019). The model analysis does not include potential emissions of PCB-153 from wildfires (Eckhardt et al., 2007). The spatial resolution of GLEMOS was 0.4° x 0.4° within the EMEP domain, and 1° x 1° outside EMEP. As the model is gridded, the size of individual grid cells (0.4° x 0.4°) varies latitudinally from 1056 km^2 (58°N) to 352 km^2 (79°N). The spatial output resolution of FLEXPART was 1° x 1°. Both models generated predictions for each individual site, corresponding to the actual deployment periods. Further details of the modelling tools are given in SI 1.7.

3. Results and discussion

A summary of the calculated concentrations in air, method detection limits and MMRs of selected POPs in air at Norwegian background sites (including Svalbard) are presented in Table SI-2.1, and a more detailed discussion of the occurrence of the selected POPs is given in SI 2.1. Data for all target analytes at the individual sites are included in Table SI-2.2a-b.

For comparison, Table SI-2.3 shows literature data for background sites in other mapping studies of POPs with PUF-PAS on a regional/global level, and a more thorough comparison with the urban area is given in SI 2.2.

3.1. PCBs

18 PCB congeners were detected in more than 60% of the samples. The average concentrations of $\sum_{18}$PCBs from the background sites were 5 pg/m^3 (2–13 pg/m^3) and $\sum_6$PCBs 2 pg/m^3 (1–6 pg/m^3). The concentrations of $\sum_6$PCBs in air are in the lower range of the concentrations found in other studies using PUF-PAS from the last 20 years on a regional or global scale (2–121 pg/m^3, Table SI-2.3) (Gioia et al., 2007; Halse et al., 2011; Jaward et al., 2004; Pozo et al., 2009). The concentrations reported herein are also in the lower range of the more recent studies on a national level, e.g. $\sum_6$PCBs in air across Czech Republic that ranged 11–60 pg/m^3 (Kalina et al., 2018), Turkey that ranged 5.6–47 pg/m^3 (Kurt-Karakus et al., 2018) and Spain where $\sum_{18}$PCB ranged 0.1–386 pg/m^3 (of which 86% consists of Σ_6PCBs) (Torre et al., 2016).

However, the average concentration for $\sum_6$PCBs in air within the urban area included in this study was 23 pg/m^3 (ranging from 5 to 42 pg/m^3), which is approximately ten times higher than in Norwegian background air and more similar to the concentrations in Czech Republic and Turkey.

The concentrations of $\sum_6$PCBs in 2016 were significantly reduced (by ca. 50%) compared to the concentrations in 2006 from the same sites (Table 1). This decline is in agreement with a declining trend from 2006

Table 1
Percentage change in concentrations in air of selected PCBs, OCPs and relevant isomer-ratios since 2006. The difference in concentrations at each site was used in the calculation of p-values. P-values less than 0.05 (bold) indicate a significant increase or decrease for all sites combined.

Site	Zeppelin[a]	Birkenes[a]	Hurdal[a]	Kaarvatn[a]	Tustervatn[a]	Karasjok[a]	Oslo[b]	P-value[c]
$\sum_6$PCBs	–48%	–32%	–69%	25%	–31%	–60%	–52%	**0.016**
PCB-28	–57%	–44%	–63%	–21%	–44%	–64%	–41%	**0.008**
PCB-153	–10%	–28%	–78%	116%	33%	–53%	–42%	0.078
HCB	30%	85%	50%	146%	132%	58%	59%	**0.008**
$\sum_3$DDXs	–77%	48%	–18%	7%	–43%	–51%	–11%	0.19
α-HCH	–21%	–8%	–36%	43%	10%	–17%	–46%	0.078
γ-HCH	–3%	5%	–27%	98%	–4%	–23%	–33%	0.23
$\sum_2$HCHs	–19%	–3%	–32%	63%	7%	–18%	–39%	0.23
$\sum_4$Chlordanes	–46%	26%		100%	38%	–53%		0.41

[a] Halse et al. (2011).
[b] Halse et al. (2012), 2016-data based on the average for the urban sites.
[c] Two-sample Wilcoxon, paired, 1-sided.

to 2016 of PCBs in Norway and the Norwegian Arctic as reported within the national air monitoring program using AAS (Bohlin-Nizzetto et al., 2017; Hung et al., 2016).

The most abundant PCBs were PCB-18 (17%), PCB-52 (14%), PCB-28 (10%), PCB-31 (10%) and PCB-101 (10%), with the contribution to the average concentration of $\sum_{18}$PCBs given in parentheses. $\sum_6$PCBs contributed 44% to $\sum_{18}$PCBs, and the contribution of each of the six indicator PCB congeners to $\sum_6$PCBs is given in Figure SI 2.1. The abundances generally reflect the dominance of these specific PCB congeners in technical PCB mixtures (Breivik et al., 2007), but with a higher relative abundance of the more volatile tri- and tetra-CBs.

Spatial differences in the influence of LRAT and national emissions were anticipated as Norway is geographically located along an expected pollution gradient from south to north (58°N to 79°N). The spatial distribution of concentrations of $\sum_6$PCBs in air is shown in Fig. 2a. Large differences in concentrations within a region suggest that local atmospheric primary- and/or secondary emissions are influencing the atmospheric concentrations (Jaward et al., 2004). The MMRs of the six indicator PCBs detected at all sites varied between 3 and 4 (Table SI-2.1). The highest concentrations were generally observed in southern Norway while the lowest were observed in Northern Norway (Fig. 2a). The exception is the eastern-most part of northern Norway where elevated concentrations of $\sum_6$PCBs were observed (2.2–4.1 pg/m³), comparable to the southern-most sites. This part is close to the Kola peninsula, a highly industrialized area considered to be a source region for many different environmental pollutants (Berglen et al., 2015; Polder et al., 2008; Sandanger et al., 2013; Tørseth and Semb, 1998).

The obtained MMRs in Norway (Table SI-2.1) are small compared to the MMRs in Europe (35, 25, 84, 102, 87 and 122 for PCB-28, -52, -101, -138, -153 and -180 respectively) in the study by Halse et al. (2011). MMR of $\sum_6$PCBs from the background sites within the southern Norway region (5) does not differ significantly from MMR within the northern region (4), despite that southern Norway is more densely populated. These findings suggest a limited importance of local sources at background sites in our study. The declining trend of $\sum_6$PCBs with latitude (p-value 0.03, r −0.33) and significantly higher levels in southern Norway (one-sided p-value < 0.05), point towards an enhanced influence from source areas in this region. Source regions in Europe are identified to exist (Breivik et al., 2007). This, combined with differences in MMRs between Norway and Europe indicates that the occurrence of PCBs in Norway may be influenced by source regions in Europe.

Minor differences in the spatial patterns for the individual congeners were expected, due to differences in LRAT potential (Beyer et al., 2003). In our study, concentrations of PCB-153 significantly decreased with latitude (p-value 0.0016, r −0.46) and were significantly higher (by a factor of two) in southern Norway than in northern Norway (p-value 0.022). The concentrations of a more volatile congener, PCB-28, showed no significant correlation with latitude (p-value 0.16, r −0.21).

However, the local contribution in the eastern-most part of northern Norway was prominent for the concentrations of PCB-28 (Figure SI-2.2a). Consequently, the correlation with latitude was significant also for PCB-28 (p-value 0.020, r −0.37) when disregarding samples from this area. The LRAT potential is limited by a combination of net atmospheric deposition and reactivity of the PCB congener in air (Beyer et al., 2003). Both processes are strongly affected by temperature. While colder air temperatures favor atmospheric deposition, higher temperatures favor atmospheric reaction. Our study was carried out during summer, with average temperatures during the sampling period ranging from 4° to 16 °C (Table SI-1.6), declining with latitude (r −0.70). Taken together, this suggests that the observed reduction in concentrations of PCB-153 with latitude may be better explained by atmospheric deposition, rather than atmospheric reaction. Removal by atmospheric reactions, on the other hand, is likely to have a greater relative importance for PCB-28 (Wania and Daly, 2002).

The dominance of LRAT in Norway was also evident in the studies of Halse et al. (2012) and Schuster et al. (2010). The statistical analysis suggested that there were no significant changes in spatial patterns of PCB-28 or PCB-153 over the last decade (Figure SI-2.4). A halving of the MMR of PCB-153 from 2006 to 2016 (Table SI-2.4), indicates that the influence from primary sources may have decreased, but there was no significant decline in the concentrations of PCB-153 (Table 1) supporting this indication. Altogether, this suggests that the sources of PCB-28 and PCB-153 in 2006 and 2016 are comparable.

A comparison of the concentrations obtained by the PUF-PAS and conventional AAS (Bohlin-Nizzetto et al., 2017) are provided in Table SI-2.5 and Figure SI-2.5. The PUF-PAS resulted in higher concentrations of most PCB congeners at Birkenes and Andøya while the tri- and tetra-CBs were lower with PUF-PAS than AAS at Zeppelin. At Birkenes, the percentage deviation relative to AAS results varied from −58% up to −150% for 17 of the PCBs. A larger negative deviation was observed at Andøya (−139% up to −473%), where the concentrations from PUF-PAS most likely are overestimated as a consequence of underestimated sampling rate due to wind effects (SI 1.5.5). At Zeppelin, negative deviation values (−24% up to −122%) were observed for the penta-, hexa- and hepta-CBs, while positive deviation values were observed for tri- and tetra-CBs (+24% up to +86%). Both data sets also report high detection frequency of tri-CBs. PCB-180, the least volatile indicator PCB, contributed to the same extent to $\sum_6$PCBs in the passive air samplers as in the high-volume AAS confirming the utility of PAS for PCBs in air. The national monitoring using AAS shows that the concentration of $\sum_6$PCBs is almost a factor of three higher at Birkenes (southern Norway) than at Andøya (northern Norway) (Bohlin-Nizzetto et al., 2017). Both the observation of higher $\sum_6$PCBs concentrations in southern Norway and low spatial variability are consistent with our data using PAS. This suggests that the data from the existing monitoring stations in Norway largely explain the spatial variability of PCBs in air across Norway. However, elevated concentrations in hotspots/source
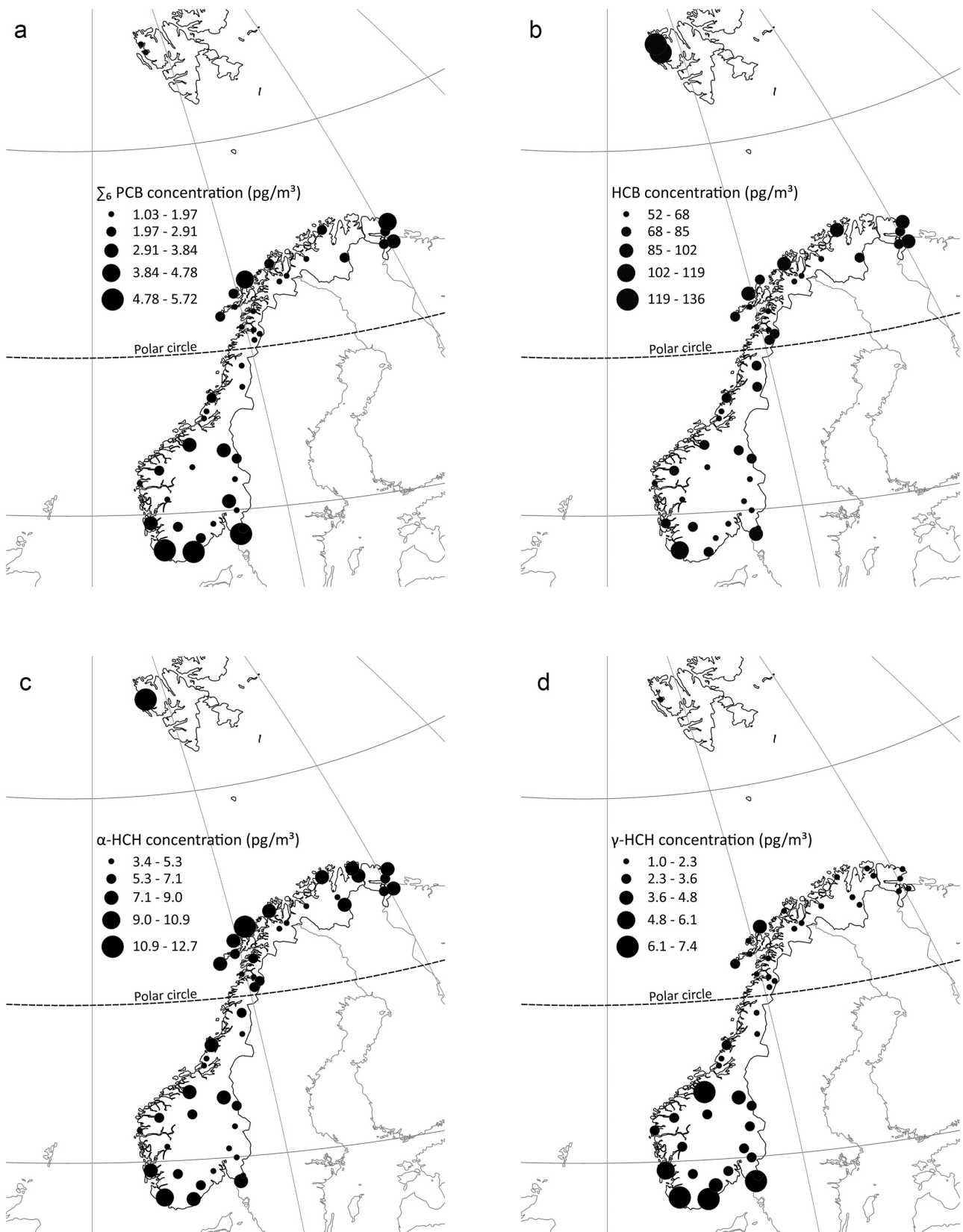
Fig. 2. (a)-(d): Concentrations of $\sum_6$PCBs(a), HCB (b), α-HCH (c) and γ-HCH (d) at 45 remote sites (ranging from 58°N to 71°N) and two pristine sites on Svalbard (79°N). Exact locations of the background sites are given in Table SI-1.1. Data for all target analytes at the individual sites, including the ten urban sites around Oslo (60°N) are included in Table SI-2.2a-b.

areas like urban areas and industrial sites are not captured by the background monitoring sites.

3.2. OCPs

Among the targeted 29 OCPs, only 14 OCPs were detected in more than 60% of the samples. These included PeCB/HCB, α-/γ-HCH ($\sum_2$HCHs), p,p′-DDE/o,p′-DDT/ p,p′-DDT ($\sum_3$DDXs), chlordanes (i.e. trans-/cis-Chlordane/-Nonachlor), Heptachlor-exo-epoxide, Dieldrin and Endosulfan I. Except for HCB, the OCP concentrations (< MDL-13 pg/m³) are generally in the lower range of concentrations found in other studies using PUF-PAS (Table SI-2.3). The highest average concentrations of OCPs in this study were observed for HCB (75 pg/m³) and PeCB (22 pg/m³), followed by α- and γ-HCH, Endosulfan I and Dieldrin (2–7 pg/m³). The concentrations of HCB, HCHs and DDXs were, like the PCBs, in agreement with active air measurements in the national air monitoring program (Bohlin-Nizzetto et al., 2017) (Table SI-2.5). The PAS resulted in higher concentrations for all OCPs at all three sites. At Birkenes and Zeppelin, the percentage deviation of PAS relative to AAS varied from −55% up to −178% for all OCPs. Similar to the PCBs, the largest negative relative deviations were observed at Andøya, which varied from −241% up to −500% for all OCPs. This is most likely caused by poor performance of the PAS under the high wind speeds at Andøya.

The concentrations of HCB in our study were in the upper range of the concentrations reported in other studies (Table SI-2.3), with the highest concentrations of HCB observed in the Norwegian Arctic (130–136 pg/m³). While the HCHs, DDXs and chlordanes did not show any significant change in concentrations between 2006 (Halse et al., 2011) and 2016 (Table 1), the concentrations of HCB were similar or higher (up to a factor of 2.5) than the concentrations measured at the same sites a decade ago. This suggests increasing HCB concentrations in this region. High concentrations of HCB as well as increasing concentrations of HCB in the Arctic during the same decade have also been reported under the Arctic Monitoring and Assessment Programme (AMAP) (Bohlin-Nizzetto et al., 2017; Hung et al., 2016). Re-emissions due to increased temperatures and e.g. reduced sea ice coverage has been put forward as one explanation (Hung et al., 2010; Ma et al., 2011). One reason for apparent lower concentrations in warmer regions (Table SI-2.3), may be that HCB, due to its low K_{OA} that decreases with temperature, has entered the curvilinear uptake phase during the deployment period. Assuming linear uptake for all the deployment time may have lead to an overestimation of the effective air sample volume and hence an underestimation of the concentrations in air is likely.

The spatial patterns of selected OCPs are presented in Fig. 2b-d. The MMRs varied between 2 and 7 for the compounds detected at all sites (Table SI-2.1). The low spatial variability indicates that LRAT is the main source for these OCPs in Norway.

Despite the low spatial variability for most OCPs, there are some differences for individual OCPs. Similar to the PCBs, these differences are likely influenced by differences in LRAT potential (Beyer et al., 2003). The OCPs with highest volatility, e.g. the chlorobenzenes and HCHs, have low MMRs (2–4). There is no significant difference between the concentrations of HCB in southern Norway (52–103 pg/m³) and northern Norway (52–136 pg/m³) (p-value 0.35), nor between the background sites (52–136 pg/m³) and the urban sites (45–85 pg/m³) (p-value 0.48). The consistent concentrations of HCBs across Norway testifies that atmospheric burdens are controlled by LRAT. This has also been shown on regional levels (Jaward et al., 2004; Koblizkova et al., 2012). As HCB is both relatively volatile and very persistent in the atmosphere, it is not possible to make any inferences about the likely source regions on the basis of data presented herein. The concentrations of α-HCH (4–13 pg/m³) were also uniformly distributed across the study region (south/north p-value 0.35, urban sites 3–8 pg/m³). However, the concentrations of the γ-isomer were significantly higher in southern Norway than in northern Norway (p-value < 0.001). Consequently, the α/γ-HCH ratio in northern Norway (4) was significantly higher

compared to southern Norway (2). Even lower ratios than 2 are observed at more southern sites in continental Europe (Halse et al., 2011; Aas and Bohlin-Nizzetto, 2018), as a consequence of higher concentrations of γ-HCH. The south-north differences of the α- and γ-isomers may reflect that the γ-isomer is more prone to wet deposition than the α-isomer during atmospheric transport (Shen and Wania, 2005), but also the proximity of southern Norway to historical source regions of γ-HCH (Breivik et al., 1999).

The concentrations of $\sum_4$Chlordanes or Heptachlor-exo-epoxide did also not differ significantly between southern and northern Norway (p-value 0.48 and 0.12, respectively). On the other hand, the concentrations of the less volatile OCPs, e.g. $\sum_3$DDXs and Endosulfan I, were significantly higher in southern Norway than northern Norway (p-value < 0.001 and 0.027, respectively), and showed the highest MMRs of the OCPs (6 and 7, respectively). The spatial patterns were similar for all the three individual DDX-isomers. Elevated concentrations of Dieldrin were also found in the south (p-value 0.019).

Concentrations of Endosulfans in background air were dominated by Endosulfan I, and Endosulfan II was only detected in 5% of the samples. This pattern could be expected as the composition of the technical mixture is 70:30 Endosulfan I: Endosulfan II. Secondly, Endosulfan II is more water-soluble than Endosulfan I (Shen and Wania, 2005) and thereby more easily washed out from the atmosphere, i.e. Endosulfan II is less prone to LRAT. Finally, it has also been reported that Endosulfan II is converted to Endosulfan I in environmental matrices (Schmidt et al., 1997; Weber et al., 2010).

The relative abundance of parent and metabolite compounds can be used to evaluate possible recent use of OCPs like DDTs (Pozo et al., 2009; Su et al., 2008). The p,p′-DDE/p,p′-DDT ratio was high (2–5) for all sampling sites, indicating influence from aged DDT. The high ratio may however also be caused by a higher volatility of p,p′-DDE than p,p′-DDT (Ricking and Schwarzbauer, 2012), resulting in higher mobilization of p,p′-DDE from source areas (e.g. contaminated soil) to air. The high ratio, together with dominance of other transformation products/metabolites indicative of past usage, i.e. oxy-chlordane, heptachlor-exo-epoxide and dieldrin, may suggest that secondary sources are important for the occurrence of other OCPs in the Norwegian atmosphere. Given that trans-Chlordane degrades more easily in the environment than cis-Chlordane, the low trans-CD/cis-CD ratio (< 1) substantiates that the levels of Chlordanes are mainly due to previous use (Bidleman et al., 2002; Harner et al., 2004).

Norway comprises both areas dominated by coastal and by inland climate. It has previously been established that oceans are major reservoirs of α-HCH (Jantunen and Bidleman, 1996; Macdonald et al., 2000). In a study by Shen et al. (2004) on HCHs in air across Northern America, elevated concentrations of α-HCH were observed in air at coastal sites, reflecting re-emissions from the sea. A similar finding has been reported in Norway (Halse et al., 2012). Figure SI-2.7 shows that the concentrations of α-HCH in air at coastal areas in our study are significantly higher (p-value 0.04) than in inland areas. This indicates a possible difference in secondary emissions from marine and terrestrial pollutant reservoirs, respectively.

3.3. Model predictions of PCB-153

3.3.1. Evaluation against observations

The map in Fig. 3 illustrates the observed spatial pattern of PCB-153 in concert with the reproduction by GLEMOS. In general, GLEMOS largely captures the observed PCB-153 concentrations; 75% of the predicted concentrations were within a factor of three of the observations (Figure SI-2.15 a). For FLEXPART, 80% were within a factor of three of the observations (Figure SI-2.15 b). Both models underestimate concentrations in air. This may in part be due to differences and large uncertainties in primary emissions used as input to the models. In FLEXPART, the European emissions were 3 kt, based on data from a global emission inventory (Breivik et al., 2007), while for GLEMOS
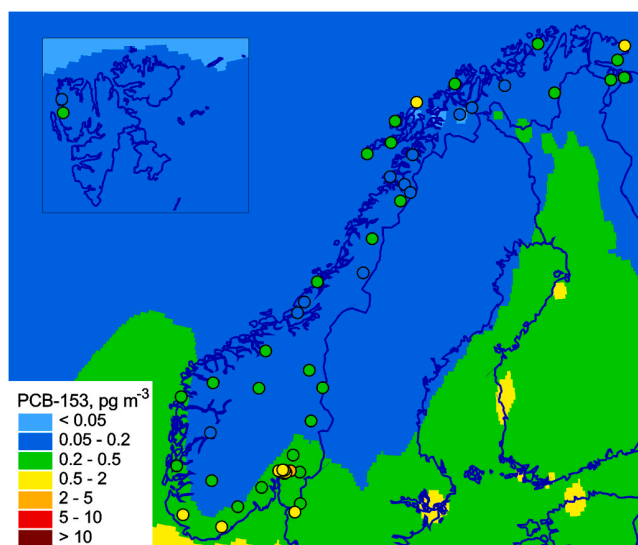
Fig. 3. The observed spatial pattern of PCB-153 across all Norwegian sites (dots) in concert with concentrations predicted by GLEMOS (colored background). (For interpretation of the references to color in this figure legend, the reader is referred to the web version of this article.)

primary emissions of 1 kt were used as input. In contrast to FLEXPART, GLEMOS relies on national emission data whenever available, complemented with data from the global emission inventory for gap filling whenever official data is lacking. Hence, differences in predicted concentrations were anticipated. This may also help to explain why FLEXPART predicted higher concentrations than GLEMOS in 61% of the cases (Figure SI 2.15c).

However, the FLEXPART predicted concentrations of PCB-153 in air at Svalbard (0.02 pg/m^3) were more than a factor of three lower than both the measured concentrations (Figure SI-2,15b) and the concentrations predicted by the GLEMOS model (Figure SI-2.15c), in spite of using higher emissions as model input. FLEXPART furthermore predicts a higher spatial variability (MMR = 27) than both observed (MMR = 4) and predicted by GLEMOS (MMR = 6). Possible explanations could be that FLEXPART overestimates atmospheric loss processes during LRAT, e.g. atmospheric reaction, and that it ignores secondary emissions.

3.3.2. Predicted sources and source regions

As climatic conditions in Norway are highly variable, e.g. between high and low latitudes, the relative significance of primary- and secondary emissions may vary spatially. GLEMOS predicted secondary emissions to be approximately four times more important (82%, median value) than primary emissions of PCB-153 at all Norwegian background sites combined (Fig. 4). Table SI-2.6 shows the predicted source
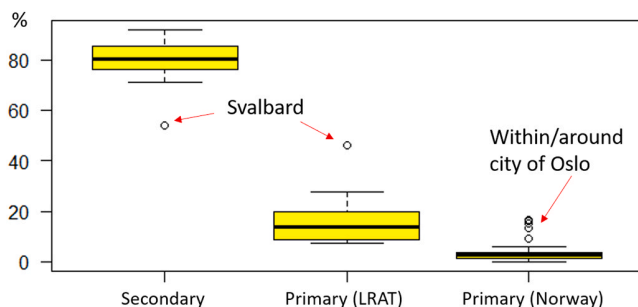
Fig. 4. Predicted contributions from primary and secondary emissions controlling atmospheric burden of PCB-153 across all Norwegian sites. Data represent the distribution of predictions by GLEMOS.

contributions to the concentrations of PCB-153 (in %) from secondary- and primary emissions for each site. Differences in source contributions to the concentrations of PCB-153 in southern- and northern Norway, are illustrated by the southern site 49 (0.78 pg/m^3) and the northern site 23 (0.13 pg/m^3), in Figure SI-2.16a and 2.17a. Contribution from secondary emissions were dominating at both sites (83% and 77%, respectively).

The median contribution from primary emissions was predicted to be 17% across all background sites, mostly attributed to LRAT (15%). Hence, the predicted median contribution from national emissions was only 2% for the background sites. As the spatial variability predicted by GLEMOS (MMR = 6) was comparable to observations (MMR = 4), this provides a strong argument for secondary emissions (whether domestic or not) and LRAT being highly influential.

GLEMOS predicted that LRAT due to primary emissions from western Europe (e.g. UK, Germany and France) were more influential in southern Norway (site 49) than in northern Norway (site 23). The predicted source regions are in accordance with model predictions from FLEXPART (Figure SI-2.16b). GLEMOS further predicted that the primary source contribution from Sweden (1%), Finland (2%) and non-EMEP countries (10%) were higher for the site in northern Norway, compared to the site in southern Norway (0%, 0% and 3% respectively). The predicted relative contributions from primary emissions at the eastern-most part of northern Norway using GLEMOS (e.g. site 12 Figure SI-2.18a-b), were dominated by non-EMEP countries (6%), followed by Russia (3%), and may explain the somewhat elevated concentrations observed in this region (Fig. 3).

GLEMOS predicted secondary emissions to be least important for PCB-153 at Svalbard in relative terms (54% for site 96, Figure SI-2.19a). While the absolute contribution from primary emissions is comparable to other Norwegian sites, this suggest secondary emissions are far less influential in absolute terms, compared to the other sites discussed. Interestingly, the relative contribution from primary emission sources outside EMEP (42%) is also predicted to be higher than at any of the other Norwegian sites (2%–16%).

3.3.3. Spatial variability in an urban area

The measured concentrations of PCB-153 in the urban area (one of the ten urban samples was excluded due to contamination during deployment) (Figure SI-2.12) ranged from 0.57 to 6.2 pg/m^3, and hence the spatial variability within the urban area was higher (MMR=11) than for the background sites (MMR = 4). The median concentration of PCB-153 in the urban area was eight times higher than all the background sites combined. However, the GLEMOS predicted concentrations within the city of Oslo were generally underestimated and did not show any variability (0.33–0.37 pg/m^3, dark blue, Figure SI-2.15a). This could be expected as GLEMOS is not designed to accurately resolve urban-rural gradients at a fine spatial resolution. Secondly, the sampling strategy in Oslo was targeting urban areas, rather than individual model grid cells. Hence, the measurements are probably biased towards areas with elevated emissions, while the predicted concentrations are based on emissions averaged over larger areas in the model.

Despite this, the model predicted the highest contribution from primary emissions in the urban area (23% on average) and at two sites in the vicinity of Oslo (sites 54 and 55). The contribution from national primary emissions was predicted to be 16%, compared to 2% for the background sites, suggesting local sources in the urban area.

4. Conclusions

The results of this multi-sited passive air sampling campaign are consistent with data reported from active air measurements from the national monitoring program. This suggests that the existing background monitoring stations largely capture the spatial variability of most of the selected POPs across Norway. A larger spatial variability was observed in some specific regions (the city of Oslo and north-eastern

Norway). Elevated concentrations in the urban area may also call for complementary monitoring efforts in source regions.

Minor temporal changes were observed for most POPs when compared to concentrations measured a decade ago. This is also in line with the national monitoring program. A less noticeable decline in air concentrations of POPs has been reported in recent years, despite a reduction in primary emissions. This may be due to an increasing influence of secondary emissions from reservoirs contaminated in the past. This aligns well with measured isomeric ratios which indicated weathered signals.

The results indicate dominance of LRAT in this region as i) the spatial variability is limited for most of the targeted POPs, ii) the concentrations of the POPs in background air are low, and iii) there is a typical south-north gradient of less volatile compounds prone to wet deposition (e.g. γ-HCH, DDXs and Endosulfan I).

Model predictions for PCB-153 by two different atmospheric transport models (GLEMOS and FLEXPART) indicated that LRAT mainly originates from western Europe. The GLEMOS model predicted further that secondary emissions of PCB-153 dominated (54%–92%) across the whole study area.

Though GLEMOS predicted the relative importance of primary emissions, secondary emissions, LRAT and national emissions, these results are restricted to PCB-153. The predicted spatial patterns need to be confronted with measurements to evaluate whether models obtain satisfactory results. Nonetheless, this example illustrates that a combination of spatial mapping using PAS and mechanistic modelling may provide valuable insights into the main sources controlling atmospheric burdens of PCB-153 on a national scale which cannot be readily inferred from measurements alone. The methodological approach explored in this study may be further developed and used to inform national monitoring efforts in countries other than Norway and for chemicals other than PCB-153.

CRediT authorship contribution statement

Lunder Halvorsen, H: Methodology, Validation, Formal analysis, Investigation, Writing - original draft, Project administration, Visualization. **Bohlin-Nizzetto, P:** Methodology, Validation, Writing - review & editing, Supervision. **Eckhardt, S:** Formal analysis, Writing - review & editing, Visualization. **Gusev, A:** Formal analysis, Visualization. **Krogseth, IS:** Investigation, Writing - review & editing. **Moeckel C:** Validation, Formal analysis, Investigation, Writing - review & editing, Visualization. **Skogeng, LP:** Investigation. **Shatalov, V:** Formal analysis, Visualization. **Breivik, K:** Conceptualization, Validation, Writing - review & editing, Supervision, Project administration, Funding acquisition.

Declaration of Competing Interest

The authors declare that they have no known competing financial interests or personal relationships that could have appeared to influence the work reported in this paper.

Acknowledgements

Appendix A. Supporting information

Supplementary data associated with this article can be found in the online version at doi:10.1016/j.ecoenv.2021.112172.

References

Aas, W., Bohlin-Nizzetto, P., 2018. Heavy metals and POP measurements, 2016. (EMEP/CCC-Report 3/2018). Kjeller, NILU. http://hdl.handle.net/11250/2563390.

Berglen, T.F., Dauge, F.R., Andresen, E., Nilsson, L.O., Tønnesen, D.A., Vadset, M., 2015. Grenseområdene Norge-Russland. Luft- og nedbørkvalitet, april 2014-mars 2015. (Norwegian Environment Agency Report, M-384/2015) (NILU report, 21/2015). Kjeller, NILU. http://hdl.handle.net/11250/2359730.

Beyer, A., Wania, F., Gouin, T., Mackay, D., Matthies, M., 2003. Temperature dependence of the characteristic travel distance. Environ. Sci. Technol. 37 (4), 766–771. https://doi.org/10.1021/es025717w.

Bidleman, T.F., Jantunen, L.M.M., Helm, P.A., Brorström-Lundén, E., Juntto, S., 2002. Chlordane enantiomers and temporal trends of chlordane isomers in arctic air. Environ. Sci. Technol. 36 (4), 539–544. https://doi.org/10.1021/es011142b.

Bohlin-Nizzetto, P., Aas, W., Warner, N., 2017. Monitoring of environmental contaminants in air and precipitation, annual report 2016. (NILU report 17/2017). Kjeller, NILU. http://hdl.handle.net/11250/2461410.

Bohlin, P., Audy, O., Škrdlíková, L., Kukučka, P., Přibylová, P., Prokeš, R., Klánová, J., 2014. Outdoor passive air monitoring of semi volatile organic compounds (SVOCs): a critical evaluation of performance and limitations of polyurethane foam (PUF) disks. Environ. Sci. Process. Impacts 16 (3), 433–444. https://doi.org/10.1039/C3EM00644A.

Breivik, K., Armitage, J.M., Wania, F., Sweetman, A.J., Jones, K.C., 2016. Tracking the global distribution of persistent organic pollutants accounting for e-waste exports to developing regions. Environ. Sci. Technol. 50 (2), 798–805. https://doi.org/10.1021/acs.est.5b04226.

Breivik, K., Pacyna, J.M., Münch, J., 1999. Use of α-, β- and γ-hexachlorocyclohexane in Europe, 1970–1996. Sci. Total Environ. 239 (1), 151–163. https://doi.org/10.1016/S0048-9697(99)00291-0.

Breivik, K., Sweetman, A., Pacyna, J.M., Jones, K.C., 2007. Towards a global historical emission inventory for selected PCB congeners - a mass balance approach-3. An update. Sci. Total Environ. 377 (2–3), 296–307. https://doi.org/10.1016/j.scitotenv.2007.02.026.

Eckhardt, S., Breivik, K., Manø, S., Stohl, A., 2007. Record high peaks in PCB concentrations in the Arctic atmosphere due to long-range transport of biomass burning emissions. Atmos. Chem. Phys. 7 (17), 4527–4536. https://doi.org/10.5194/acp-7-4527-2007.

Gioia, R., Sweetman, A.J., Jones, K.C., 2007. Coupling passive air sampling with emission estimates and chemical fate modeling for persistent organic pollutants (POPs): a feasibility study for Northern Europe. Environ. Sci. Technol. 41 (7), 2165–2171. https://doi.org/10.1021/es0626739.

GLEMOS, 2020. Global EMEP Multi-media Modeling System Retrieved from http://en.msceast.org/index.php/j-stuff/glemos. Accessed September 2020.

Halse, A.K., Schlabach, M., Eckhardt, S., Sweetman, A., Jones, K.C., Breivik, K., 2011. Spatial variability of POPs in European background air. Atmos. Chem. Phys. 11 (4), 1549–1564. https://doi.org/10.5194/acp-11-1549-2011.

Halse, A.K., Schlabach, M., Sweetman, A., Jones, K.C., Breivik, K., 2012. Using passive air samplers to assess local sources versus long range atmospheric transport of POPs. J. Environ. Monit. 14 (10), 2580–2590. https://doi.org/10.1039/c2em30378g.

Harner, T., 2017. 2017_v1_5_Template for calculating Effective Air Sample Volumes for PUF and SIP Disk Samplers_Sept_15. https://www.researchgate.net/publication/319764519_2017_v1_5_Template_for_calculating_Effective_Air_Sample_Volumes_for_PUF_and_SIP_Disk_Samplers_Sept_15. Accessed June 2019.

Harner, T., Shoeib, M., Diamond, M., Stern, G., Rosenberg, B., 2004. Using passive air samplers to assess urban–rural trends for persistent organic pollutants. 1. Polychlorinated biphenyls and organochlorine pesticides. Environ. Sci. Technol. 38 (17), 4474–4483. https://doi.org/10.1021/es040302r.

Hogarh, J.N., Seike, N., Kobara, Y., Habib, A., Nam, J.-J., Lee, J.-S., Masunaga, S., 2012. Passive air monitoring of PCBs and PCNs across East Asia: a comprehensive congener evaluation for source characterization. Chemosphere 86 (7), 718–726. https://doi.org/10.1016/j.chemosphere.2011.10.046.

Holoubek, I., Klanova, J., Cupr, P., Kukucka, P., Boruvkova, J., Kohoutek, J., Kares, R., 2011. POPs in ambient air from MONET network - global and regional trends. WIT Trans. Ecol. Environ. 147, 173–184. https://doi.org/10.2495/AIR110161.

Holt, E., Bohlin-Nizzetto, P., Borůvková, J., Harner, T., Kalina, J., Melymuk, L., Klánová, J., 2017. Using long-term air monitoring of semi-volatile organic compounds to evaluate the uncertainty in polyurethane-disk passive sampler-derived air concentrations. Environ. Pollut. 220, 1100–1111. https://doi.org/10.1016/j.envpol.2016.11.030.

Hung, H., Kallenborn, R., Breivik, K., Su, Y., Brorström-Lundén, E., Olafsdottir, K., Thorlacius, J.M., Leppänen, S., Bossi, R., Skov, H., Manø, S., Patton, G.W., Stern, G., Sverko, E., Fellin, P., 2010. Atmospheric monitoring of organic pollutants in the Arctic under the Arctic Monitoring and Assessment Programme (AMAP): 1993–2006. Sci. Total Environ. 408 (15), 2854–2873. https://doi.org/10.1016/j.scitotenv.2009.10.044.

Hung, H., Katsoyiannis, A.A., Brorström-Lundén, E., Olafsdottir, K., Aas, W., Breivik, K., Bohlin-Nizzetto, P., Sigurdsson, A., Hakola, H., Bossi, R., Skov, H., Sverko, E., Barresi, E., Fellin, P., Wilson, S., 2016. Temporal trends of persistent organic pollutants (POPs) in arctic air: 20 years of monitoring under the arctic monitoring

and assessment programme (AMAP). Environ. Pollut. 217, 52–61. https://doi.org/10.1016/j.envpol.2016.01.079.

Jantunen, L.M., Bidleman, T., 1996. Air-water gas exchange of hexachlorocyclohexanes (HCHs) and the enantiomers of α-HCH in Arctic regions. J. Geophys. Res. Atmos. 101 (D22), 28837–28846. https://doi.org/10.1029/96jd02352.

Jaward, F.M., Farrar, N.J., Harner, T., Sweetman, A.J., Jones, K.C., 2004. Passive air sampling of PCBs, PBDEs, and organochlorine pesticides across Europe. Environ. Sci. Technol. 38 (1), 34–41. https://doi.org/10.1021/es034705n.

Jaward, F.M., Zhang, G., Nam, J.J., Sweetman, A.J., Obbard, J.P., Kobara, Y., Jones, K.C., 2005. Passive air sampling of polychlorinated biphenyls, organochlorine compounds, and polybrominated diphenyl ethers across Asia. Environ. Sci. Technol. 39 (22), 8638–8645. https://doi.org/10.1021/es051382h.

Jones, K., 1994. Observations on long-term air-soil exchange of organic contaminants. Environ. Sci. Pollut. Res. 1, 172–177. https://doi.org/10.1007/BF02986940.

Kalina, J., Scheringer, M., Borůvková, J., Kukučka, P., Přibylová, P., Bohlin-Nizzetto, P., Klánová, J., 2017. Passive air samplers as a tool for assessing long-term trends in atmospheric concentrations of semivolatile organic compounds. Environ. Sci. Technol. 51 (12), 7047–7054. https://doi.org/10.1021/acs.est.7b02319.

Kalina, J., Scheringer, M., Borůvková, J., Kukučka, P., Přibylová, P., Sáňka, O., Klánová, J., 2018. Characterizing spatial diversity of passive sampling sites for measuring levels and trends of semivolatile organic chemicals. Environ. Sci. Technol. 52 (18), 10599–10608. https://doi.org/10.1021/acs.est.8b03414.

Klánová, J., Čupr, P., Holoubek, I., Borůvková, J., Přibylová, P., Kareš, R., Ocelka, T., 2009. Monitoring of persistent organic pollutants in Africa. Part 1: passive air sampling across the continent in 2008. J. Environ. Monit. 11 (11), 1952–1963. https://doi.org/10.1039/B913415H.

Koblizkova, M., Genualdi, S., Lee, S.C., Harner, T., 2012. Application of sorbent impregnated polyurethane foam (SIP) disk passive air samplers for investigating organochlorine pesticides and polybrominated diphenyl ethers at the global scale. Environ. Sci. Technol. 46 (1), 391–396. https://doi.org/10.1021/es2032289.

Kurt-Karakus, P.B., Ugranli-Cicek, T., Sofuoglu, S.C., Celik, H., Gungormus, E., Gedik, K., Jones, K.C., 2018. The first countrywide monitoring of selected POPs: polychlorinated biphenyls (PCBs), polybrominated diphenyl ethers (PBDEs) and selected organochlorine pesticides (OCPs) in the atmosphere of Turkey. Atmos. Environ. 177, 154–165. https://doi.org/10.1016/j.atmosenv.2018.01.021.

Li, L., Wania, F., 2018. Occurrence of single- and double-peaked emission profiles of synthetic chemicals. Environ. Sci. Technol. 52 (8), 4684–4693. https://doi.org/10.1021/acs.est.7b06478.

Macdonald, R.W., Barrie, L.A., Bidleman, T.F., Diamond, M.L., Gregor, D.J., Semkin, R. G., Yunker, M.B., 2000. Contaminants in the Canadian Arctic: 5 years of progress in understanding sources, occurrence and pathways. Sci. Total Environ. 254 (2), 93–234. https://doi.org/10.1016/S0048-9697(00)00434-4.

Mari, M., Schuhmacher, M., Feliubadaló, J., Domingo, J.L., 2008. Air concentrations of PCDD/Fs, PCBs and PCNs using active and passive air samplers. Chemosphere 70 (9), 1637–1643. https://doi.org/10.1016/j.chemosphere.2007.07.076.

Markovic, M.Z., Prokop, S., Staebler, R.M., Liggio, J., Harner, T., 2015. Evaluation of the particle infiltration efficiency of three passive samplers and the PS-1 active air sampler. Atmos. Environ. 112, 289–293. https://doi.org/10.1016/j.atmosenv.2015.04.051.

Ma, J., Hung, H., Tian, C., Kallenborn, R., 2011. Revolatilization of persistent organic pollutants in the Arctic induced by climate change. Nat. Clim. Change 1, 255–260. https://doi.org/10.1038/nclimate1167.

Melymuk, L., Bohlin, P., Sanka, O., Pozo, K., Klanova, J., 2014. Current challenges in air sampling of semivolatile organic contaminants: sampling artifacts and their influence on data comparability. Environ. Sci. Technol. 48 (24), 14077–14091. https://doi.org/10.1021/es502164r.

Menichini, E., Iacovella, N., Monfredini, F., Turrio-Baldassarri, L., 2007. Atmospheric pollution by PAHs, PCDD/Fs and PCBs simultaneously collected at a regional background site in central Italy and at an urban site in Rome. Chemosphere 69 (3), 422–434. https://doi.org/10.1016/j.chemosphere.2007.04.078.

Moeckel, C., Harner, T., Nizzetto, L., Strandberg, B., Lindroth, A., Jones, K.C., 2009. Use of depuration compounds in passive air samplers: results from active sampling-supported field deployment, potential uses, and recommendations. Environ. Sci. Technol. 43 (9), 3227–3232. https://doi.org/10.1021/es802897x.

Muñoz-Arnanz, J., Roscales, J.L., Ros, M., Vicente, A., Jiménez, B., 2016. Towards the implementation of the Stockholm Convention in Spain: five-year monitoring (2008–2013) of POPs in air based on passive sampling. Environ. Pollut. 217, 107–113. https://doi.org/10.1016/j.envpol.2016.01.052.

Nizzetto, L., Macleod, M., Borgå, K., Cabrerizo, A., Dachs, J., Guardo, A.D., Jones, K.C., 2010. Past, present, and future controls on levels of persistent organic pollutants in the global environment. Environ. Sci. Technol. 44 (17), 6526–6531. https://doi.org/10.1021/es100178f.

Pisso, I., Sollum, E., Grythe, H., Kristiansen, N.I., Cassiani, M., Eckhardt, S., Stohl, A., 2019. The Lagrangian particle dispersion model FLEXPART version 10.4. Geosci. Model Dev. 12 (12), 4955–4997. https://doi.org/10.5194/gmd-12-4955-2019.

Polder, A., Gabrielsen, G.W., Odland, J.Ø., Savinova, T.N., Tkachev, A., Løken, K.B., Skaare, J.U., 2008. Spatial and temporal changes of chlorinated pesticides, PCBs, dioxins (PCDDs/PCDFs) and brominated flame retardants in human breast milk from Northern Russia. Sci. Total Environ. 391 (1), 41–54. https://doi.org/10.1016/j.scitotenv.2007.10.045.

Pozo, K., Harner, T., Lee, S.C., Wania, F., Muir, D.C., Jones, K.C., 2009. Seasonally resolved concentrations of persistent organic pollutants in the global atmosphere

from the first year of the GAPS study. Environ. Sci. Technol. 43 (3), 796–803. https://doi.org/10.1021/es802106a.

Pozo, K., Harner, T., Wania, F., Muir, D.C.G., Jones, K.C., Barrie, L.A., 2006. Toward a global network for persistent organic pollutants in air: results from the GAPS study. Environ. Sci. Technol. 40 (16), 4867–4873. https://doi.org/10.1021/es060447t.

Ricking, M., Schwarzbauer, J., 2012. DDT isomers and metabolites in the environment: an overview. Environ. Chem. Lett. 10 (4), 317–323. https://doi.org/10.1007/s10311-012-0358-2.

Sandanger, T.M., Anda, E.E., Berglen, T.F., Evenset, A., Christensen, G., Heimstad, E.S., 2013. Health and environmental impacts in the Norwegian border area related to local Russian industrial emissions. Knowledge status. (NILU report, 40/2013). Kjeller, NILU. https://hdl.handle.net/10037/14219.

Schmidt, W.F., Hapeman, C.J., Fettinger, J.C., Rice, C.P., Bilboulian, S., 1997. Structure and asymmetry in the isomeric conversion of β- to α-endosulfan. J. Agric. Food Chem. 45 (4), 1023–1026. https://doi.org/10.1021/jf970020t.

Schuster, J.K., Gioia, R., Breivik, K., Steinnes, E., Scheringer, M., Jones, K.C., 2010. Trends in European background air reflect reductions in primary emissions of PCBs and PBDEs. Environ. Sci. Technol. 44 (17), 6760–6766. https://doi.org/10.1021/es101009x.

Shen, L., Wania, F., 2005. Compilation, evaluation, and selection of physical–chemical property data for organochlorine pesticides. J. Chem. Eng. Data 50 (3), 742–768. https://doi.org/10.1021/je049693f.

Shen, L., Wania, F., Lei, Y.D., Teixeira, C., Muir, D.C.G., Bidleman, T.F., 2004. Hexachlorocyclohexanes in the North American atmosphere. Environ. Sci. Technol. 38 (4), 965–975. https://doi.org/10.1021/es034998k.

Shen, L., Wania, F., Lei, Y.D., Teixeira, C., Muir, D.C.G., Bidleman, T.F., 2005. Atmospheric distribution and long-range transport behavior of organochlorine pesticides in North America. Environ. Sci. Technol. 39 (2), 409–420. https://doi.org/10.1021/es049489c.

Shen, L., Wania, F., Lei, Y.D., Teixeira, C., Muir, D.C.G., Xiao, H., 2006. Polychlorinated biphenyls and polybrominated diphenyl ethers in the North American atmosphere. Environ. Pollut. 144 (2), 434–444. https://doi.org/10.1016/j.envpol.2005.12.054.

Shoeib, M., Harner, T., 2002. Characterization and comparison of three passive air samplers for persistent organic pollutants. Environ. Sci. Technol. 36 (19), 4142–4151. https://doi.org/10.1021/es020635t.

Su, Y., Hung, H., Blanchard, P., Patton, G.W., Kallenborn, R., Konoplev, A., Barrie, L.A., 2008. A circumpolar perspective of atmospheric organochlorine pesticides (OCPs): results from six Arctic monitoring stations in 2000–2003. Atmos. Environ. 42 (19), 4682–4698. https://doi.org/10.1016/j.atmosenv.2008.01.054.

Torre, A. d l, Sanz, P., Navarro, I., Martínez, M.Á., 2016. Time trends of persistent organic pollutants in spanish air. Environ. Pollut. 217, 26–32. https://doi.org/10.1016/j.envpol.2016.01.040.

Tørseth, K., Aas, W., Breivik, K., Fjaeraa, A.M., Fiebig, M., Hjellbrekke, A.G., Yttri, K.E., 2012. Introduction to the European Monitoring and Evaluation Programme (EMEP) and observed atmospheric composition change during 1972-2009. Atmos. Chem. Phys. 12 (12), 5447–5481. https://doi.org/10.5194/acp-12-5447-2012.

Tørseth, K., Semb, A., 1998. Deposition of nitrogen and other major inorganic compounds in Norway, 1992–1996. Environ. Pollut. 102 (1), 299–304. https://doi.org/10.1016/S0269-7491(98)80047-X.

UNEP, 2018. Stockholm Convention on Persistent Organic Pollutants (POPs). Texts and annexes. Revised in 2017. Secretariat of the Stockholm Convention.

Venier, M., Hites, R.A., 2010. Time trend analysis of atmospheric POPs concentrations in the Great Lakes region since 1990. Environ. Sci. Technol. 44 (21), 8050–8055. https://doi.org/10.1021/es101656u.

Wang, J., Guo, L., Li, J., Zhang, G., Lee, C.S.L., Li, X., Zhong, L., 2007. Passive air sampling of DDT, chlordane and HCB in the Pearl River Delta, South China: implications to regional sources. J. Environ. Monit. 9 (6), 582–588. https://doi.org/10.1039/B700798A.

Wania, F., Daly, G.L., 2002. Estimating the contribution of degradation in air and deposition to the deep sea to the global loss of PCBs. Atmos. Environ. 36 (36), 5581–5593. https://doi.org/10.1016/S1352-2310(02)00693-3.

Wania, F., Mackay, D., 1993. Global fractionation and cold condensation of low volatility organochlorine compounds in polar-regions. Ambio 22 (1), 10–18.

Wania, F., Mackay, D., 1996. Tracking the distribution of persistent organic pollutants. Environ. Sci. Technol. 30 (9), A390–A396.

Wania, F., Shunthirasingham, C., 2020. Passive air sampling for semi-volatile organic chemicals. Environ. Sci. Process. Impacts 22 (10), 1925–2002. https://doi.org/10.1039/D0EM00194E.

Weber, J., Halsall, C.J., Muir, D., Teixeira, C., Small, J., Solomon, K., Bidleman, T., 2010. Endosulfan, a global pesticide: a review of its fate in the environment and occurrence in the Arctic. Sci. Total Environ. 408 (15), 2966–2984. https://doi.org/10.1016/j.scitotenv.2009.10.077.

Wöhrnschimmel, H., Scheringer, M., Bogdal, C., Hung, H., Salamova, A., Venier, M., Fiedler, H., 2016. Ten years after entry into force of the Stockholm Convention: what do air monitoring data tell about its effectiveness? Environ. Pollut. 217, 149–158. https://doi.org/10.1016/j.envpol.2016.01.090.

Zhang, G., Chakraborty, P., Li, J., Sampathkumar, P., Balasubramanian, T., Kathiresan, K., Jones, K.C., 2008. Passive atmospheric sampling of organochlorine pesticides, polychlorinated biphenyls, and polybrominated diphenyl ethers in Urban, Rural, and Wetland sites along the coastal length of India. Environ. Sci. Technol. 42 (22), 8218–8223. https://doi.org/10.1021/es8016667.

SUPPORTING INFORMATION

for

Main sources controlling atmospheric burdens of Persistent Organic Pollutants on a national scale

Helene Lunder Halvorsen, Pernilla Bohlin-Nizzetto, Sabine Eckhardt, Alexey Gusev, Ingjerd Sunde Krogseth, Claudia Moeckel, Victor Shatalov, Lovise Pedersen Skogeng, Knut Breivik

Contents

1. Materials and Methods detailed

2. Results and Discussion

Tables:

Text/Figures:

1 Materials and Methods detailed

Tables:

Table SI-1.1. Location of all sampling sites

Site no.	Sampling site:	Latitude (DMS):	Longitude (DMS):	Sampling start:	Sampling End:	Type:
1	Bærum	59°57'09.5"	10°29'16.9"	14.06.2016	13.09.2016	Urban
2	Holmenkollen	59°58'37.0"	10°40'50.8"	14.06.2016	13.09.2016	Urban
3	Maridalen	59°58'13.5"	10°46'05.4"	14.06.2016	13.09.2016	Urban
4	Skøyen	59°55'11.3"	10°41'23.3"	14.06.2016	13.09.2016	Urban
5	Sofienbergparken	59°55'23.1"	10°45'56.8"	14.06.2016	14.09.2016	Urban
6	Alnabru	59°55'17.8"	10°50'11.6"	14.06.2016	13.09.2016	Urban
7	Gamle Oslo	59°54'14.0"	10°47'35.0"	15.06.2016	14.09.2016	Urban
8	Botanisk hage	59°55'08.3"	10°46'07.8"	15.06.2016	14.09.2016	Urban
9	Dronningparken	59°54'58.4"	10°43'28.3"	17.06.2016	16.09.2016	Urban
10	Kjeller	59°58'31.8"	11°03'16.0"	18.06.2016	16.09.2016	Urban
11	Grøtfjord	69°46'30.7"	18°36'17.7"	16.06.2016	16.09.2016	Remote
12	Karpdalen	69°39'23.8"	30°25'14.3"	20.06.2016	21.09.2016	Remote
13	Neiden	69°38'46.5"	29°27'59.6"	20.06.2016	21.09.2016	Remote
14	Ekkerøy	70°06'38.8"	30°11'00.7"	20.06.2016	22.09.2016	Remote
15	Vardø	70°26'17.4"	30°51'36.9"	21.06.2016	22.09.2016	Remote
16	Vestertana	70°28'23.6"	27°56'57.0"	22.06.2016	22.09.2016	Remote
17	Hopseidet	70°47'55.3"	27°43'42.4"	22.06.2016	22.09.2016	Remote
18	Lakselv	69°49'42.1"	25°09'30.2"	23.06.2016	23.09.2016	Remote
19	Karasjok	69°28'40.8"	25°28'39.5"	23.06.2016	23.09.2016	Remote
20	Slåtten	70°43'59.8"	24°36'17.7"	24.06.2016	23.09.2016	Remote
21	Kvænangsbotn	69°43'21.4"	22°04'01.9"	20.06.2016	24.09.2016	Remote
22	Tamokdalen	69°11'15.7"	19°46'31.0"	20.06.2016	24.09.2016	Remote
23	Øverbygd	69°00'40.5"	18°59'04.9"	25.06.2016	24.09.2016	Remote
24	Innhavet	67°58'20.3"	15°58'15.9"	26.06.2016	27.09.2016	Remote
25	Bø i Vesterålen	68°46'24.8"	14°40'21.6"	26.06.2016	05.10.2016	Remote
26	Andøya	69°16'47.0"	16°00'30.5"	27.06.2016	05.10.2016	Remote
27	Svolvær	68°14'01.1"	14°30'28.6"	27.06.2016	05.10.2016	Remote
28	Moskenes	67°54'10.1"	13°03'18.1"	28.06.2016	03.10.2016	Remote
29	Bodø	67°23'17.9"	14°39'36.7"	29.06.2016	28.09.2016	Remote
30	Øvrevatn	67°13'07.0"	15°35'29.2"	29.06.2016	28.09.2016	Remote
31	Balvatn	67°01'45.2"	15°59'06.2"	29.06.2016	28.09.2016	Remote
32	Junkerdal	66°48'45.9"	15°25'33.6"	30.06.2016	29.09.2016	Remote
33	Tustervatn	65°49'50.8"	13°54'23.4"	30.06.2016	29.09.2016	Remote
34	Namsvatn	64°58'22.0"	13°35'28.5"	01.07.2016	30.09.2016	Remote
35	Aglen	64°37'56.7"	11°04'05.6"	03.07.2016	30.09.2016	Remote
36	Momyra	64°06'00.1"	10°30'34.4"	03.07.2016	01.10.2016	Remote
37	Bjørndalselva	63°49'19.0"	10°14'39.9"	03.07.2016	01.10.2016	Remote
38	Hummelfjell	62°27'33.7"	11°18'01.0"	04.07.2016	03.10.2016	Remote
39	Valdalen	62°04'41.0"	12°07'04.9"	04.07.2016	03.10.2016	Remote
40	Osen	61°14'50.9"	11°44'29.4"	04.07.2016	03.10.2016	Remote
41	Lom	61°51'28.6"	08°52'16.1"	05.07.2016	05.10.2016	Remote
42	Kårvatn	62°46'56.7"	08°52'36.1"	06.07.2016	02.10.2016	Remote
43	Utvikfjellet	61°47'09.9"	06°29'41.7"	07.07.2016	06.10.2016	Remote
44	Furuneset	61°17'46.5"	05°02'35.4"	07.07.2016	06.10.2016	Remote
45	Ulvik	60°35'37.3"	06°51'20.3"	08.07.2016	07.10.2016	Remote
46	Vatnedal	59°27'10.2"	07°23'29.9"	09.07.2016	09.10.2016	Remote
47	Utbjoa	59°38'16.1"	05°35'40.8"	10.07.2016	09.10.2016	Remote
48	Ualand	58°30'24.2"	06°21'56.4"	10.07.2016	10.10.2016	Remote
49	Birkenes	58°23'20.6"	08°15'12.2"	11.07.2016	10.10.2016	Remote
50	Solhomfjell	58°56'30.0"	08°49'38.5"	11.07.2016	11.10.2016	Remote
51	Hvittingfoss	59°29'35.1"	09°47'31.7"	13.07.2016	11.10.2016	Remote
52	Prestebakke	58°59'47.6"	11°31'36.4"	13.07.2016	12.10.2016	Remote
53	Aremark	59°13'18.4"	11°43'37.7"	13.07.2016	12.10.2016	Remote
54	Aurskog	59°58'36.6"	11°29'54.9"	13.07.2016	12.10.2016	Remote
55	Hurdal	60°22'20.1"	11°04'38.4"	14.07.2016	12.10.2016	Remote
96	Svalbard (Zeppelin)	78° 54' 24"	11° 53' 18.0"	20.06.2016	05.09.2016	Pristine
97	Svalbard (Erlingvatn)[a]	79° 15' 21"	11° 28' 2.3"	14.06.2016	24.08.2016	Pristine

[a] Sampling: Guttorm Christensen, Akvaplan-NIVA (Tromsø, Norway).

Table SI-1.2. List of standards. All standards were prepared in isooctane.

Performance Reference Compounds (PRCs)	Purity %	Supplier	Concentration (pg/uL)
D g-HCH	98 %	Dr. Ehrenstorfer GmbH	200
13C12 PCB 1	99 %	Cambridge Isotope Laboratories (CIL)	200
13C12 PCB 8	99 %	Cambridge Isotope Laboratories (CIL)	200
12C PCB 14	99.2 %	Chiron	200
12C PCB 30	99.9 %	Chiron	200
13C12 PCB 32	99 %	Cambridge Isotope Laboratories (CIL)	200
13C12 PCB 47	99 %	Cambridge Isotope Laboratories (CIL)	200
12C PCB 106	> 99.5 %	Chiron	200
12C PCB 198	99.0 %	Chiron	200
Internal Standards			
PCBs:			
13C12 PCB 4	99 %	Cambridge Isotope Laboratories (CIL)	250
13C12 PCB 28	100 %	Cambridge Isotope Laboratories (CIL)	250
13C12 PCB 52	100 %	Cambridge Isotope Laboratories (CIL)	250
13C12 PCB 101	99.7 %	Cambridge Isotope Laboratories (CIL)	250
13C12 PCB 105	99.3 %	Cambridge Isotope Laboratories (CIL)	250
13C12 PCB 114	100 %	Cambridge Isotope Laboratories (CIL)	250
13C12 PCB 118	100 %	Cambridge Isotope Laboratories (CIL)	250
13C12 PCB 123	99.6 %	Cambridge Isotope Laboratories (CIL)	250
13C12 PCB 138	> 99 %	Cambridge Isotope Laboratories (CIL)	250
13C12 PCB 153	99.9 %	Cambridge Isotope Laboratories (CIL)	250
13C12 PCB 156	100 %	Cambridge Isotope Laboratories (CIL)	250
13C12 PCB 157	100 %	Cambridge Isotope Laboratories (CIL)	250
13C12 PCB 167	99.9 %	Cambridge Isotope Laboratories (CIL)	250
13C12 PCB 180	100 %	Cambridge Isotope Laboratories (CIL)	250
13C12 PCB 189	100 %	Cambridge Isotope Laboratories (CIL)	250
13C12 PCB 209	99.9 %	Cambridge Isotope Laboratories (CIL)	250
OCPs:			
13C6 α-HCH	> 98%	Cambridge Isotope Laboratories (CIL)	1000
13C6 β-HCH	99 %	Chem Service	200
13C6 γ-HCH (Lindane)	> 98%	Cambridge Isotope Laboratories (CIL)	1000
13C12 Dieldrin	> 98%	Cambridge Isotope Laboratories (CIL)	500
13C12 Aldrin	> 98%	Cambridge Isotope Laboratories (CIL)	200
13C12 Endrin	> 98%	Cambridge Isotope Laboratories (CIL)	200
13C10 Mirex	> 98%	Cambridge Isotope Laboratories (CIL)	300
13C12 Isodrin	> 95%	Cambridge Isotope Laboratories (CIL)	900
d14 Trifluralin	> 95%	Chem Service	50
13C10 cis-Chlordane (α)	> 98%	Cambridge Isotope Laboratories (CIL)	20
13C10 trans-Chlordane (γ)	> 98%	Cambridge Isotope Laboratories (CIL)	20
13C10 Oxychlordane	> 98%	Cambridge Isotope Laboratories (CIL)	300
13C10 Trans-nonachlor	> 98%	Cambridge Isotope Laboratories (CIL)	20
13C10 Cis-nonachlor	> 98%	Cambridge Isotope Laboratories (CIL)	20
13C10 Heptachlor	> 98%	Cambridge Isotope Laboratories (CIL)	300
13C10 Heptachlor epoxide (exo)	> 98%	Cambridge Isotope Laboratories (CIL)	300
13C9 Endosulfan I (α)	> 98%	Cambridge Isotope Laboratories (CIL)	50
13C9 Endosulfan II (β)	> 98%	Cambridge Isotope Laboratories (CIL)	50
13C9 Endosulfan sulphate	> 98%	Cambridge Isotope Laboratories (CIL)	50
13C Hexachlorobenzene (HCB)	99 %	Chem Service	100
13C Pentachlorbenzene (PeCB)	> 98%	Cambridge Isotope Laboratories (CIL)	100
13C12 p.p.DDE	> 98%	Cambridge Isotope Laboratories (CIL)	300
13C12 o.p.DDD	> 98%	Cambridge Isotope Laboratories (CIL)	300
13C12 p.p.DDT	> 98%	Cambridge Isotope Laboratories (CIL)	300
Instrument performance standard			
1,2,3,4 Tetrachloronaphtalene (TCN)	unknown	ULTRA Scientific	100

Table SI-1.3 a). Instrument conditions

Components:	PCBs, HCB and PeCB			DDTs/ DDEs/DDDs, HCHs, PCB-1, -8 and -14			Other OCPs		
GC:	Agilent 7890A GC			Agilent 7890A GC			Agilent 6890 GC		
Column:	HT-8			ZB Multiresidue 1			2xHP-5MS UI		
dimension:	50m x 0.22mm x 0,25µm			30m x 0.25mm x 0.25µm			2 x 15m x 0.25mm x 0.25µm		
Injection:	Programmable-temperature vaporizer (PTV)			Programmable-temperature vaporizer (PTV)			Programmable-temperature vaporizer (PTV)		
Injection volume:	3 uL			3 uL			1 uL		
Vent flow:	30 ml/min (0.32 min)			8 ml/min (0.16 min)			15 mL/min (0.3 min)		
Split flow:	50 ml/min (2 min)			50 ml/min (1 min)			50 mL/min (2 min)		
Inj. Temp. program:	Rate:	Temp.	Hold time:	Rate:	Temp.	Hold time:	Rate:	Temp.	Hold time:
1		48 °C	0.35 min		46 °C	0.2 min		60°C	0.35 min
2	300 °C/min	285 °C	3 min	550 °C/min	220 °C	8 min	500 °C/min	320 °C	3 min
3	300 °C/min	310 °C	20 min	100 °C/min	240 °C	1 min	10 °C/min	290 °C	5 min
GC Temp. program:	Rate:	Temp.	Hold time:	Rate:	Temp.	Hold time:	Rate:	Temp.	Hold time:
1		45 °C	2.65 min		48 °C	1 min		55°C	2 min
2	70 °C/min	170 °C	0.5 min	22 °C/min	280 °C	3.74 min	70 °C/min	200 °C	1 min
3	3 °C/min	210 °C	0 min				10 °C/min	280 °C	1 min
4	4 °C/min	285 °C	0.5 min				10 °C/min	310 °C	0 min
5	20 °C/min	320 °C	4.7 min				70 °C/min	325 °C	10 min
Helium flow:	Pulse			Pulse			Pulse		
1	3 ml/min (2.1 min)			3 ml/min (1 min)			3/3.2 mL/min (2.1 min)		
2	1.2 ml/min			1 ml/min			1.2/1.4 mL/min		
MS:	VG AutoSpec Micromass			VG AutoSpec Micromass			Agilent 7200 Q-TOF		
MS mode:	Electron Impact ionization (EI)			Electron Impact ionization (EI)			Electrochemical negative ionization (ECNI)		
Interface temperature:	280 °C			260 °C			280 °C		
Ion source temperature:	285 °C			270 °C			120 °C		
MS lockmass standard:	Perfluorokerosene (PFK)			Perfluorotributylamine (PFTBA)			Perfluorokerosene (PFK)		

Table SI-1.3 b). Target analytes PCBs

Target analytes (PCBs)	Full name	1° m/z	2° m/z	ISTD
12C PCB-18[b]	2,2',5-TriCB	255.9613	257.9584	13C PCB 28
12C PCB-28[bc]	2,4,4'-TriCB	255.9613	257.9584	13C PCB 28
12C PCB-31[b]	2,4',5-TriCB	255.9613	257.9584	13C PCB 28
12C PCB-33[b]	2',3,4-TriCB	255.9613	257.9584	13C PCB 28
12C PCB-37[b]	3,4,4'-TriCB	255.9613	257.9584	13C PCB 28
12C PCB-47[b]	2,2',4,4'-TetCB	289.9224	291.9194	13C PCB 52
12C PCB-52[bc]	2,2',5,5'-TetCB	289.9224	291.9194	13C PCB 52
12C PCB-66[b]	2,3',4,4'-TetCB	289.9224	291.9194	13C PCB 52
12C PCB-74[b]	2,4,4',5-TetCB	289.9224	291.9194	13C PCB 52
12C PCB-99[b]	2,2',4,4',5-PenCB	325.8804	327.8775	13C PCB 101
12C PCB-101[bc]	2,2',4,5,5'-PenCB	325.8804	327.8775	13C PCB 101
12C PCB-105[b]	2,3,3',4,4'-PenCB	325.8804	327.8775	13C PCB 105
12C PCB-114	2,3,4,4',5-PenCB	325.8804	327.8775	13C PCB 114
12C PCB-118[a]	2,3',4,4',5-PenCB	325.8804	327.8775	13C PCB 118
12C PCB-122	2'3,3',4,5-PenCB	325.8804	327.8775	13C PCB 114
12C PCB-123	2',3,4,4',5-PenCB	325.8804	327.8775	13C PCB 123
12C PCB-128	2,2',3,3',4,4'-HexCB	359.8415	361.8385	13C PCB 167
12C PCB-138[bc]	2,2',3,4,4',5'-HexCB	359.8415	361.8385	13C PCB 138
12C PCB-141[b]	2,2',3,4,5,5'-HexCB	359.8415	361.8385	13C PCB 153
12C PCB-149[b]	2,2',3,4',5',6-HexCB	359.8415	361.8385	13C PCB 153
12C PCB-153[bc]	2,2',4,4',5,5'-HexCB	359.8415	361.8385	13C PCB 153
12C PCB-156	2,3,3',4,4',5-HexCB	359.8415	361.8385	13C PCB 156
12C PCB-157	2,3,3',4,4',5'-HexCB	359.8415	361.8385	13C PCB 157
12C PCB-167	2,3',4,4',5,5'-HexCB	359.8415	361.8385	13C PCB167
12C PCB-170	2,2',3,3',4,4',5-HepCB	393.8025	395.7995	13C PCB 180
12C PCB-180[bc]	2,2',3,4,4',5,5'-HepCB	393.8025	395.7995	13C PCB 180
12C PCB-183	2,2',3,4,4',5',6-HepCB	393.8025	395.7995	13C PCB 180
12C PCB-187[b]	2,2',3,4',5,5',6-HepCB	393.8025	395.7995	13C PCB 180
12C PCB-189	2,3,3',4,4',5,5'-HepCB	393.8025	395.7995	13C PCB 189
12C PCB-194	2,2',3,3',4,4',5,5'-OctCB	427.7635	429.7606	13C PCB 189
12C PCB-206	2,2',3,3',4,4',5,5',6-NonCB	461.7246	463.7217	13C PCB 209
12C PCB-209	Deca CB	497.6867	499.6798	13C PCB 209

Internal Standards (ISTD)	1° m/z	2° m/z
13C PCB 28	268.0016	269.9986
13C PCB 52	301.9226	303.9597
13C PCB 101	337.9207	339.9177
13C PCB 105	337.9207	339.9177
13C PCB 114	337.9207	339.9177
13C PCB 118	337.9207	339.9177
13C PCB 123	337.9207	339.9177
13C PCB 138	371.8817	373.8788
13C PCB 153	371.8817	373.8788
13C PCB 156	371.8817	373.8788
13C PCB 157	371.8817	373.8788
13C PCB 167	371.8817	373.8788
13C PCB 180	405.8428	407.8398
13C PCB 189	405.8428	407.8398
13C PCB 209	509.7229	511.7199
Instrument performance standard	**1° m/z**	**2° m/z**
1,2,3,4 Tetrachloronaphtalene (TCN)	263.9067	265.9038

[a] Coeluting with PCB-106 in the PRCs. Excluded.

[b] Included in sum 18 PCBs

[c] Included in sum 6 PCBs

Table SI-1.3 c). Target analytes OCPs

Target analytes (OCPs)	Full name	1° m/z	2° m/z	ISTD
12C α-HCHª	α-Hexachlorocyclohexane	216.9145	218.9116	13C α-HCH
12C β-HCH	β-Hexachlorocyclohexane	216.9145	218.9116	13C β-HCH
12C γ-HCHª	Lindane	216.9145	218.9116	13C γ-HCH
12C Dieldrin		379.8677	381.8647	13C Dieldrin
12C Aldrin		236.8413	238.8384	13C Aldrin
12C Endrin		379.8677	381.8647	13C Endrin
12C Mirex		403.7449	401.7479	13C Mirex
12C Isodrin		236.8413	238.8384	13C Isodrin
12C Trifluralin		335.1093	336.1122	d14 Trifluralin
12C Trans-chlordene		303.8961	305.8931	13C Oxychlordane
12C cis-Chlordane (α)		407.7948	409.7919	13C cis-Chlordane (α)
12C trans-Chlordane (γ)		407.7948	409.7919	13C trans-Chlordane (γ)
12C Oxychlordane		423.7711	421.7741	13C Oxychlordane
12C Trans-nonachlor		443.7529	441.7558	13C Trans-nonachlor
12C Cis-nonachlor		443.7529	441.7558	13C Cis-nonachlor
12C Heptachlor		299.8648	301.8618	13C Heptachlor
12C Heptachlor epoxide (exo)		387.8131	389.8101	13C Heptachlor epoxide (exo)
12C Heptachlor epoxide (endo)		387.8131	389.8101	13C Heptachlor epoxide (exo)
12C Endosulfan I (α)		407.811	405.8139	13C Endosulfan I (α)
12C Endosulfan II (β)		407.811	405.8139	13C Endosulfan II (β)
12C Endosulfan sulphate		385.8322	387.8292	13C Endosulfan sulphate
12C HCB	Hexachlorobenzene	283.8102	285.8072	13C Hexachlorobenzene (HCB)
12C PeCB	Pentachlorbenzene	249.8491	251.8462	13C Pentachlorbenzene (PeCB)
12C o.p.DDE	2,4'-Dichlorodiphenyldichloroethylene	246.0003	247.9974	13C p.p.DDE
12C p.p.DDEᵇ	4,4'-Dichlorodiphenyldichloroethylene	246.0003	247.9974	13C p.p.DDE
12C o.p.DDD	2,4'-Dichlorodiphenyldichloroethane	235.0081	237.0052	13C o.p.DDD
12C p.p.DDD	4,4'-Dichlorodiphenyldichloroethane	235.0081	237.0052	13C o.p.DDD
12C o.p.DDTᵇ	2,4'-Dichlorodiphenyltrichloroethane	235.0081	237.0052	13C p.p.DDT
12C p.p.DDTᵇ	4,4'-Dichlorodiphenyltrichloroethane	235.0081	237.0052	13C p.p.DDT

Internal Standards (ISTD)	1° m/z	2° m/z
13C α-HCH	222.9347	224.9317
13C β-HCH	222.9347	224.9317
13C γ-HCH	222.9347	224.9317
13C Dieldrin	391.9079	393.905
13C Aldrin	241.8581	243.8551
13C Endrin	391.9079	393.905
13C Mirex	413.7785	411.7814
13C Isodrin	241.8581	243.8551
d14 Trifluralin	349.1972	350.2001
13C cis-Chlordane (α)	417.8284	419.8254
13C trans-Chlordane (γ)	417.8284	419.8254
13C Oxychlordane	433.8047	431.8076
13C Trans-nonachlor	453.7864	451.7894
13C Cis-nonachlor	453.7864	451.7894
13C Heptachlor	309.8983	311.8954
13C Heptachlor epoxide (exo)	397.8466	399.8437
13C Endosulfan I (α)	416.8412	414.8441
13C Endosulfan II (β)	416.8412	414.8441
13C Endosulfan sulphate	394.8624	396.8594
13C Hexachlorobenzene (HCB)	289.8303	291.8273
13C Pentachlorbenzene (PeCB)	255.8693	257.8663
13C p.p.DDE	258.0406	260.0377
13C o.p.DDD	247.0484	249.0454
13C p.p.DDT	247.0484	249.0454
Instrument performance standard	1° m/z	2° m/z
1,2,3,4 Tetrachloronaphtalene (TCN)	263.9067	265.9038

ª Included in sum 2 HCHs
Included in sum 3 DDXs

Table SI-1.3 d). Target analytes PRCs

Performance Reference Compounds (PRCs)	Full name	1° m/z	2° m/z	ISTD
D g-HCH	Lindane	221.946	223.943	13C γ-HCH
13C PCB-1	2-CB	200.08		13C PCB 4
13C PCB-8	2,4'-DiCB	234.041	236.038	13C PCB 4
12C PCB-14	3,5-DiCB	222.0003	223.9975	13C PCB 4
12C PCB-30	2,4,6-TriCB	255.9613	257.9584	13C PCB 28
13C PCB-32	2,4',6-TriCB	268.0016	269.9986	13C PCB 28
13C PCB-47	2,2',4,4'-TetCB	301.9626	303.9597	13C PCB 52
12C PCB-106ª	2,3,3',4',5-PenCB	325.8804	327.8775	13C PCB 123
12C PCB-198	2,3,3',4,4',5,5'-HepCB	427.7635	429.7606	13C PCB 189

Internal Standards (ISTD)	1° m/z	2° m/z
13C γ-HCH	222.9347	224.9317
13C PCB 4	234.041	236.038
13C PCB 28	268.0016	269.9986
13C PCB 52	301.9226	303.9597
13C PCB 123	337.9207	339.9177
13C PCB 189	405.8428	407.8398

ª Coeluting with PCB-118. Excluded.

Table SI-1.4. Range (median in parentheses) of recoveries for the internal standards for exposed samples, field blanks and method blanks, as well as PRCs for field and method blanks, respectively (in %).

	Range (median)		
ISTD:	**Exposed samples**	**Method blanks**	**Field blanks**
13C PCB-28	45 - 123 (74)	52 - 75 (67)	57 - 67 (62)
13C PCB-52	47 - 110 (80)	73 - 99 (82)	56 - 84 (80)
13C PCB-101	30 - 108 (55)	37 - 80 (62)	44 - 68 (54)
13C PCB-138	24 - 106 (55)	33 - 81 (68)	40 - 73 (71)
13C PCB-153	24 - 123 (55)	31 - 84 (66)	39 - 77 (67)
13C PCB-180	22 - 104 (55)	32 - 86 (65)	40 - 77 (75)
13C PeCB	13 - 60 (29)	11 - 44 (24)	12 - 26 (18)
13C HCB	23 -139 (50)	19 - 58 (38)	17 - 39 (21)
13C a-HCH	23 - 60 (37)	24 - 36 (32)	22 - 39 (31)
13C g-HCH	19 - 47 (30)	22 - 33 (28)	21 - 35 (26)
13C p,p'-DDE	31 - 167 (85)	86 - 113 (96)	91 - 99 (93)
13C p,p'-DDT	60 - 210 (101)	88 - 135 (115)	109 - 141 (119)
13C Dieldrin	24 - 107 (79)	64 - 98 (67)	52 - 73 (70)
13C Heptachlor-exo-epoxide	24 - 75 (57)	45 - 64 (54)	42 - 61 (54)
13C trans-Chlordane	37 - 98 (70)	56 - 82 (67)	59 - 81 (81)
13C cis-Chlordane	33 - 87 (68)	56 - 75 (65)	57 - 74 (67)
13C Oxy-chlordane	34 - 87 (68)	54 - 75 (62)	51 - 68 (64)
13C trans-Nonachlor	38 - 98 (71)	57 - 81 (68)	59 - 80 (71)
13C cis-Nonachlor	33 - 83 (68)	56 - 76 (70)	62 - 79 (71)
13C Endosulfan-I		62 - 77 (69)	54 - 72 (70)
PRCs:			
D g-HCH		94 - 96 (95)[a]	92 - 96 (94)[d]
13C PCB-1		92 - 102 (97)[a]	80 - 83 (82)[d]
13C PCB-8		175 - 159 (167)[ab]	77 - 87 (82)[d]
12C PCB-14		164[abc]	78 - 88 (83)[d]
12C PCB-30		61 - 80 (71)[a]	107[cd]
13C PCB-32		91 - 105 (98)[a]	71 - 96[d]
12C PCB-198		96[a]	106 - 126[d]

[a] Based on two blanks. Calculated from added amount of PRC

[b] High recovery. Based on 13C PCB-4 as internal standard which could behave differently during clean-up.

[c] Only one blank due to instrument issues.

[d] Based on two blanks. Calculated from amount of PRC in method blanks.

Table SI-1.5 a. The relative deviation from the theoretical value (bias %) of 12C target analytes of three spiked PAS (SI 1.4.3)

	QC 1	QC 2	QC 3
PCB-28	0 %	-1 %	0 %
PCB-52	6 %	0 %	-2 %
PCB-101	3 %	-2 %	0 %
PCB-138	2 %	-2 %	-1 %
PCB-153	2 %	-2 %	0 %
PCB-180	2 %	-1 %	-2 %
Sum 6 PCB	2 %	-1 %	-1 %
Sum 18 PCB	5 %	-4 %	-2 %
PeCB	-10 %	-12 %	-14 %
HCB	-1 %	-7 %	-10 %
a-HCH	16 %	12 %	7 %
g-HCH	7 %	9 %	13 %
Sum 2 HCHs	12 %	11 %	9 %
p,p'-DDE	15 %	10 %	11 %
o,p'-DDT	5 %	-2 %	-2 %
p,p'-DDT	8 %	9 %	9 %
Sum 3 DDXs	9 %	6 %	6 %
Dieldrin	2 %	-4 %	0 %
Heptachlor-exo-epoxide	1 %	-4 %	2 %
trans-Chlordane	5 %	2 %	8 %
cis-Chlordane	7 %	-5 %	0 %
Oxy-chlordane	3 %	-7 %	-3 %
trans-Nonachlor	3 %	0 %	1 %
cis-Nonachlor	3 %	-13 %	-6 %
Sum 4 Chlordanes	5 %	-4 %	1 %
Endosulfan-I	n.a	n.a	n.a

n.a = Not available

Table SI-1.5b. The relative standard deviations of two parallel PAS

	Site 49 South	Site 12 North	Site 8 Oslo
PCB-28	0 %	0 %	0 %
PCB-52	1 %	5 %	4 %
PCB-101	2 %	2 %	4 %
PCB-138	2 %	2 %	7 %
PCB-153	1 %	3 %	3 %
PCB-180	9 %	[a]	16 %
Sum 6 PCB	0 %	1 %	4 %
Sum 18 PCB	1 %	4 %	4 %
PeCB	2 %	0 %	2 %
HCB	0 %	0 %	5 %
a-HCH	2 %	2 %	[a]
g-HCH	2 %	16 %	[a]
Sum 2 HCHs	0 %	5 %	
p,p'-DDE	5 %	2 %	6 %
o,p'-DDT	8 %	2 %	3 %
p,p'-DDT	5 %	13 %	[b]
Sum 3 DDXs	8 %	1 %	
Dieldrin	4 %	17 %	n.a
Heptachlor-exo-epoxide	2 %	8 %	n.a
trans-Chlordane	3 %	6 %	n.a
cis-Chlordane	2 %	2 %	n.a
Oxy-chlordane	1 %	1 %	n.a
trans-Nonachlor	0 %	4 %	n.a
cis-Nonachlor	5 %	[a]	n.a
Sum 4 Chlordanes	0 %	1 %	n.a
Endosulfan-I	1 %	2 %	n.a

[a] Below MDL. Excluded.

[b] Possible interference. Excluded.

n.a = Not available

Table SI-1.6. Modelled meteorological data and estimated sampling rates from the spiking of PUFs with PRCs.

Site no.	Deployment time (days):	Sampling rate (m3/day):	No. of PRCs[a]:	Modelled from ECMWF Average Temp. (°C):	Modelled from ECMWF Average Wind speed (m/s):	Modelled from ECMWF Oreography (m.a.s.l.)[b]:	Norgeskart.no (Kartverket) Oreography (m.a.s.l.)[b]:
1	91	3.0	2	15.0	2.5	322	138
2	91	3.9	1	15.0	2.5	322	450
3	91	3.9	1	15.5	2.6	249	161
4	91	3.5	3	15.0	2.5	322	4
5	92	3.6	3	15.5	2.6	249	23
6	91	2.8	1	15.5	2.6	249	112
7	91	3.2	1	15.5	2.6	249	129
8	91	3.0/3.0[c]	3/3[c]	15.5	2.6	249	23
9	91	2.8	2	15.1	2.5	322	44
10	90	4.5/3.9/4.5[c]	4/3/4[c]	15.5	2.6	249	130
11	92	4.2	3	10.3	5.2	54	152
12	93	2.5/2.7[c]	2/2[c]	12.3	3.3	134	55
13	93	2.8	3	12.2	2.9	179	1
14	94	3.6	4	11.9	3.1	131	30
15	93	5.3[f]	4	11.1	5.1	41	10
16	92	3.9[d]	4	11.3	3.1	189	62
17	92	3.2	3	10.5	5.5	58	5
18	92	3.6	1	10.9	3.0	328	72
19	92	3.6[de]	0	11.1	3.0	343	308
20	91	4.1	3	11.1	3.4	207	244
21	96	3.6[e]	0	10.4	2.7	473	39
22	96	3.6[e]	0	10.2	2.5	584	224
23	91	3.6[e]	0	10.7	2.5	494	79
24	93	3.6	3	11.2	3.3	389	59
25	101	3.1	3	11.3	5.8	8	29
26	100	10.1[f]	3	11.0	5.2	39	338
27	100	3.2	1	11.9	5.2	66	240
28	97	3.3	2	12.1	5.4	7	
29	91	3.6[e]	0	12.1	4.5	143	31
30	91	3.6[e]	0	10.5	2.8	605	19
31	91	4.2	3	10.1	2.8	688	540
32	91	3.5	3	10.5	2.8	605	269
33	91	2.7	2	10.8	2.7	566	475
34	91	3.6[e]	0	10.9	2.7	550	487
35	89	2.6	2	13.2	2.7	185	39
36	90	3.6[de]	0	13.5	2.6	176	235
37	90	3.6[e]	0	13.5	2.8	162	161
38	91	2.8	2	10.4	2.7	800	865
39	91	3.6	3	10.8	2.8	771	795
40	91	3.6[e]	0	12.7	2.5	525	449
41	92	3.6[e]	0	8.9	2.2	1073	568
42	88	2.0	1	12.0	2.8	503	208
43	91	3.6[e]	0	11.3	3.1	585	561
44	91	3.6[e]	0	13.7	5.1	107	
45	91	3.6[e]	0	9.7	2.5	915	353
46	92	3.6[e]	0	9.9	2.9	862	742
47	91	2.4	2	13.1	4.6	288	51
48	92	1.7	1	13.2	3.8	294	187
49	91	2.0/2.0[c]	2/2[c]	14.2	3.8	241	199
50	92	2.0	2	13.3	3.1	357	261
51	90	3.6[e]	0	14.1	2.8	245	404
52	91	1.8	2	15.0	3.6	92	162
53	91	3.6[e]	0	15.0	3.6	92	141
54	91	3.6[e]	0	14.0	2.8	214	182
55	90	3.6[e]	0	12.8	2.6	390	280
96	77	5.0	2	4.3	3.8	206	
97	71	3.6[e]	0	4.3	3.6	205	

[a] Number of PRCs with 40-80 % loss during deployment.
[b] Meters above sea level.
[c] Parallel PAS.
[d] Overexposure likely (ref. SI 1.5.5)
[e] No significant loss of PRCs, default value used.
[f] Possibly wind affected. Site 26 sampled at 5 m.

Table SI-1.7. PUF characteristics based on the average of ten individual PUF disks, used in the template for volume estimates (Harner, 2017).

Characteristics of Passive Sampling Media (PSM)	
Volume of PSM (m^3)	2.17E-04
Effective film thickness, D_{film} (m)	5.80E-03
Density (g/m^3)	2.70E+04
Surface Area (m^2)	3.74E-02
Mass of PUF (g)	5.87E+00

Table SI-1.8. Temperature adjusted octanol-air partition coefficients (K_{oa}) for the PRCs

	RRT[a]	log K_{oa} (at T=25 °C)[b]
d6-γ-HCH		7.84
13C PCB-1	0.2666	6.15
13C PCB-8	0.3403	7.20
PCB-14	0.3499	7.34
PCB-30	0.3598	7.48
13C PCB-32	0.3761	7.71
13C PCB-47	0.4258	8.42
PCB-198	0.598	10.86

[a] Relative Retention Time (for PCBs only) from Harju et al. (1998).

[b] For PCBs: log K_{oa} = 2.3687 + (14.204xRRT) from Harner & Bidleman (1996).

For d6-γ-HCH: log K_{oa} = -3.61 + 3415/T from Shoeib & Harner (2002).

Table SI-1.9. Input to predict a linear model of the logarithmic concentrations in air with interactions between year (x_1) and latitude (x_2). The POP concentrations from 2006 were retrieved from Halse et al. (2011) and Halse et al. (2012) (Oslo).

Year (x_1)	Site	Latitude (x_2)	y: PCB-28	PCB-153	HCB	a-HCH	g-HCH	Sum DDX	Sum 4 CD
2006	Zeppelin	78.91	0.17	-0.79	2.00	1.19	0.25	0.01	0.59
2006	Birkenes	58.39	0.31	0.03	1.66	0.98	0.83	0.38	0.36
2006	Hurdal	60.37	0.35	0.25	1.63	0.89	0.69	0.21	0.48
2006	Kaarvatn	62.78	-0.11	-0.79	1.53	0.76	0.52	0.01	0.06
2006	Tustervatn	65.83	-0.14	-0.79	1.55	0.81	0.32	0.01	0.25
2006	Karasjok	69.48	0.19	-0.33	1.68	0.96	0.37	0.01	0.53
2006	Oslo	59.90	0.99	0.67	1.63	1.17	1.19	0.78	
2016	Zeppelin	78.91	-0.20	-0.84	2.11	1.09	0.24	-0.62	0.32
2016	Birkenes	58.39	0.05	-0.11	1.93	0.94	0.85	0.55	0.46
2016	Hurdal	60.37	-0.08	-0.41	1.80	0.69	0.55	0.12	
2016	Kaarvatn	62.78	-0.21	-0.46	1.92	0.91	0.81	0.04	0.36
2016	Tustervatn	65.83	-0.39	-0.67	1.92	0.85	0.31	-0.24	0.39
2016	Karasjok	69.48	-0.26	-0.65	1.87	0.88	0.26	-0.30	0.21
2016	Oslo	59.90	0.76	0.43	1.83	0.90	1.02	0.73	

Text/Figures:

1.1 Sampling

1.1.1 Sampling sites details

The selection of the 47 remote/pristine sampling sites was based on locations with little impact from external sources, i.e. preferably > 50 km from major sources of pollution (e.g cities and highways), > 500 m from medium sources of pollution (e.g main roads or agricultural activity), and > 100 m from minor sources of pollution (e.g single houses and small roads), aiming to be in a representative area avoiding extreme topographic and climatic conditions.

Therefore, existing background sites used in previous studies were mainly chosen, e.g. Bohlin-Nizzetto et al. (2017); Halse et al. (2011); Halse et al. (2015); Schuster et al. (2010); Steinnes et al. (2016). The samplers were either deployed in close connection to an existing monitoring station, or within the same area of the studies mentioned above. The locations of all sampling sites are given in Table SI-1.1.

The ten sampling sites around Oslo were either located in connection to the stations that are part of the Norwegian air quality monitoring network (Hak, 2015), or at the PAS sites in the study of the urban environment by Herzke et al. (2017).

1.1.2 Pre-cleaning

All metal parts of the passive air sampler were soaked in a 1:100 alkali solution of Extran MA01 (Merck) and tap water over night and rinsed thoroughly with tap water. Then, all parts were cleaned with acetone and *n*-hexane, respectively. Small parts were sonicated in an ultrasonic bath for 10 minutes (rinsed twice with each solvent), while domes and rods were immersed in a large bath.

New polyurethane foam (PUF) disks (14.1 cm diameter x 1.4 cm thick; density 27 kg m^{-3}) of the type "Richfoam", purchased from Sunde Skumplast AS/Carpenter (Norway), were pre-cleaned in toluene (24 h), acetone (8 h) and *n*-hexane (8 h) consecutively, using Soxhlet extraction. The PUF disks were dried under vacuum, and stored in a desiccator before further preparation.

1.1.3 Spiking PUF disks with Performance Reference Compounds (PRCs)

Prior to deployment, the PUF disks were spiked with a sampling performance standard mixture, including compounds of different volatility that are found in negligible concentrations in air or are isotopically labelled (Table SI-1.2). 20 μL of the PRCs standard mixture was added to approximately 10 mL of pentane (Unisolv, Merck), which was evenly distributed dropwise to both sides of the PUF disk using a Pasteur pipette. To minimize the risk of contamination, the samples were handled with clean gloves or solvent-rinsed tweezers. The PUF disks were sealed in double aluminum foil and two zip-lock plastic bags, and stored in a freezer before and after deployment.

1.1.4   Deployment

In June 2016 the samplers were deployed by NILU personnel, driving by car during a 3-week period. The samplers at Svalbard were deployed by Guttorm Christensen, Akvaplan-NIVA (Tromsø, Norway).

The samplers have a UFO design, consisting of two stainless steel bowls (diameter 30 and 24 cm) held together by a metal rod, and were purchased from the Research Centre for Toxic Compounds in the Environment (RECETOX, Czech Republic). The samplers were assembled with the pre-cleaned and spiked PUF disk in the middle (Figure SI-1.1) at the deployment site.
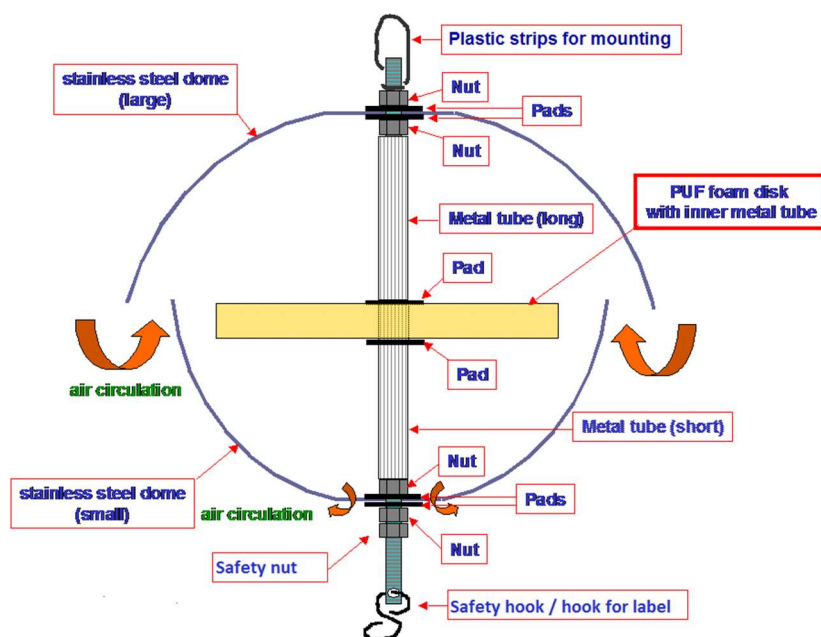
Figure SI-1.1: Schematic representation of the PUF disk sampling device

When mounting the PUF disk (Figure SI-1.2), the aluminium foil was used to hold the PUF and minimise direct contact with the single-use nitrile gloves.

Figure SI-1.2: Mounting the PUF disk

In the field, the passive air samplers were attached to a suitable structure (e.g. trees), at least 1.5 meters above ground at the sampling locations, and left for three months. Figure SI-1.3 illustrates one of the passive air samplers deployed in the field. At the end of the deployment period, the exposed PUF disks were collected, sealed in double aluminum foil and two zip-lock plastic bags, and

stored in a cool box under transportation. When arriving NILU, the disks were stored in a freezer until extraction.

Figure SI-1.3. A passive air sampler deployed in field (site 20).

1.2 Sample extraction and clean-up

Prior to extraction and clean-up, all glass equipment was soaked at least 12 h in soap solution (Extran:water), rinsed with water and baked for a minimum of 6 h at 450 °C to reduce blank contamination. In addition, all glass equipment as well as metal tweezers etc. were rinsed with a 1:1 mixture of acetone (PESTINORM, VWR) and *n*-hexane (PESTINORM, VWR) immediately before use, to reduce sample contamination.

The aluminum foil was unwrapped and the PUF-disk transferred to a Soxhlet extractor. The internal standard mixtures (Table SI-1.2) were added to 1 mL of acetone in a small vial, using a micropipette (20 μL of the PCB, HCB, DDX and HCH internal standard and 50 μL of the internal standard for the other OCPs). Then the internal standard-solvent mixture was quantitatively transferred to the PUF with several solvent rinses.

Approximately 250 mL of acetone:hexane 1:1 were added to a round-bottom flask. The PUF was then extracted under reflux for 8 hours. The extracts were then transferred to an evaporation unit, reduced to 0.5 mL on a TurboVap 500 System (Zymark) at 35-37 °C, and solvent-exchanged to acetonitrile (LiChrosolv, VWR). Small amounts of ethyl acetate (Suprasolv, VWR) were added to assure solubility between the different solvents.

The extracts were cleaned by using solid phase extraction (SPE). SPE cartridges were prepared by weighing 5 g of magnesium silicate coated silica (Supelclean LC-Florisil, SigmaAldrich) into empty SPE glass columns (105 mm long, 17 mm diameter), with glass fiber filters (frits) in the bottom of the cartridge and on top. The cartridges were topped with approximately 0.5 g anhydrous sodium

sulphate (Emsure, VWR). The SPE cartridges were first conditioned by allowing 10 mL of acetone to flow through under gravity and then dried by applying vacuum at 15 inHg for minimum 10 min. The extract was added to the cartridge and was allowed to penetrate the top frit. 16 mL of acetonitrile were used as eluent, and the collection rate was adjusted to approximately 1 drop/s.

The resulting acetonitrile extract was then back-extracted to *n*-hexane by transferring the extract to a 50 mL separation funnel, adding 2 mL MilliQ water (precleaned with *n*-hexane), and mixing twice with 10 mL of *n*-hexane (for approximately 1 minute). The hexane-phases were collected directly in an evaporation unit, concentrated and solvent exchanged to isooctane (Emsure, VWR) with the TurboVap. The sample was transferred to a small glass vial with a screw-cap.

Prior to analysis, all extracts were further reduced to approximately 250 μL by a gentle stream of nitrogen gas. The vials were kept at 4 °C until instrumental analysis.

1.2.1 Clean-up for analysis of DDXs

The analysis of DDXs showed interferences and degradation of DDT in the injector (ref. SI 1.3), and further clean-up was necessary to remove co-extracted sample matrix. The sample extract was transferred to a centrifuge glass and the volume was adjusted to approximately 2 mL with *n*-hexane. The same amount of concentrated sulfuric acid (Emsure, VWR) was added, and the sample was vortexed for approximately 20 seconds before standing until phase separation. The procedure was repeated by removing the acid from the bottom of the glass before adding more acid. After removing the acid again, approximately 2 mL MilliQ water (precleaned with *n*-hexane) were added to remove acid residues. After mixing and phase separation, the hexane phase was transferred to an evaporation unit, concentrated and prepared for instrument analysis as described under SI 1.3.

1.3 Instrumental analysis

Prior to instrumental analysis, 20 µL of the instrument performance standard (Table SI-1.2) was added to the samples with a micropipette and mixed well. Analysis of all target analytes was performed with GC/HRMS with Helium as carrier gas. See Table SI-1.3a for more details regarding instrumentation, GC columns, operating parameters, temperature programs etc.

The quantification is based on an internal standard method with isotope labelled internal standards. For identification and quantification, calibration standards containing known concentrations of both target analytes and internal standards (ISTD) were injected for every fifth sample, and mean relative response factors (Eq. I) were used to quantify the samples, by using the Masslynx V4.2 quantification tool, Targetlynx (Waters). The software automatically integrates the signal based on the processing method, but the integration is verified manually. The ^{35}Cl/^{37}Cl-isotope ratio for the two monitored masses, should be within ± 20 % of the theoretical value. Larger deviations are an indication of interfering compounds. The sum of areas of the primary (1°) and secondary (2°) ions, given in Table SI-1.3b-d, are calculated. Because the amounts of internal standards added to the samples are known, the amount of analyte can be quantified from Equation II. The quantification is controlled with a quality control standard and solvent blanks are run every tenth sample, to assess possible carry-over.

$$Relative\ Response\ Factor\ (RRF)_{analyte} = \frac{mass_{ISTD}(pg) \times Area_{analyte}}{mass_{analyte}(pg) \times Area_{ISTD}} \qquad \text{(Eq. I)}$$

$$mass\ in\ sample_{analyte} = \frac{mass_{ISTD}(pg) \times Area_{analyte}}{RRF_{analyte} \times Area_{ISTD}} \qquad \text{(Eq. II)}$$

During the GC analysis, DDT can be thermally converted to DDD and DDE. The 13C-labelled *p,p'*-DDT is used to monitor this, i.e. if the peak area of 13C *p,p'*-DDD, which is not included in the internal standard, is more than 5 % of the peak area of 13C *p,p'*-DDT, the result is rejected and more clean-up and/or replacing of PTV liner might be necessary.

1.4 Quality assurance/Quality control (QA/QC)

1.4.1 Blank level control

For blank level control, pre-cleaned PUF disks were extracted and analyzed in the same way as the exposed samples. While method blanks (n = 5) were stored in the freezer during sampling, field blanks (n = 3) were transported together with the deployed samples and exposed during mounting of the PAS. Because concentrations of target analytes were comparable in method blanks and field blanks, both types of blanks were used to calculate the method detection limit (MDL), given as the average plus 3 times the standard deviation of the concentrations of target analytes in the blank

samples (Table SI-2.1). When no target compound was detected in the blank samples, the instrumental detection limit (IDL), defined as 3 times the noise level, was used as MDL.

1.4.2 Internal standard recoveries

In order to monitor recovery rates for the extraction and clean-up procedure, internal standards were added to the PUF disks prior to extraction and clean-up, as described under SI 1.2. The internal standards were quantified relative to the instrument performance standard (Eq. I-II). The recoveries (rec %) of the internal standards are calculated from the added amount of internal standard (Eq. III), and are given in Table SI-1.4. The internal standard recoveries of deployed samples, field- and method blanks are comparable, indicating minimal matrix interference due to exposure. However, some sites had high recoveries (>100 %) for some of the internal standards, e.g. 13C *p,p'*-DDT. High recoveries were also found for the method and field blank for this internal standard.

$$Rec \ \% \ ISTD = \frac{mass \ ISTD_{measured}}{mass \ ISTD_{added}} \times 100 \ \%$$ (Eq. III)

1.4.3 Method bias

In order to assess the method bias, a known amount of 12C target analytes was added to three clean PUF disks, prior to extraction and clean-up, with the same procedure as described for the internal standards under SI 1.2. The amounts were quantified as for other samples (SI 1.3), and bias was calculated from the added amount (Eq. IV).

$$Bias \ \% = \frac{(mass \ analyte_{added} - mass \ analyte_{measured})}{mass \ analyte_{added}} \times 100 \ \%$$ (Eq. IV)

1.4.4 Duplicate PAS at selected sites

In order to assess the reproducibility of the method, duplicate PAS were co-deployed at three selected sites. All parallel samples were analyzed in the same way as described under SI 1.2 - 1.3. The relative standard deviation (RSD %) given in Table SI-1.5b is calculated from the average and the standard deviation of the samples (Eq. V), and are used as a measure of the dispersion of the samples.

$$RSD \ \% = \frac{st.dev}{avg.} \times 100 \ \%$$ (Eq. V)

1.5 Deriving air concentrations

The widely used template of Harner and colleagues (Harner, 2017) was applied to estimate sample air volumes for target compounds. Inputs to the template are given in Table SI-1.6, and are explained in more detail below. Air concentrations are derived by dividing the mass of target analytes in the sampler by the estimated air volumes.

1.5.1 PUF characteristics

The PUF characteristics (Table SI-1.7) used in the volume estimates are based on the average of ten individual PUF disks.

1.5.2 Air temperatures

The average air temperatures at each site during the exposure period are based on the ERA Interim database from European Centre for Medium-Range Weather Forecasts (ECMWF). Temperature data with 0.5° resolution were retrieved at 2 m height above ground level, and averaged every 6 h during the deployment period for each individual sampler. Altitude was retrieved additionally at each site from Norgeskart.no, in order to assess the accuracy of the model. When comparing the ECMWF derived altitudes with the altitudes at the site (Table SI-1.6), the difference in altitudes was within 600 m for all sites, implying a ± 4 °C uncertainty in the temperature determination.

1.5.3 Sampling rates (R)

PRCs were added to the PUF disks prior to deployment (described under SI 1.1.3) and were used to derive the R-values, which is the basis in the estimation of effective air sample volumes. The PRCs and the derived R-value define the rate of sampling in the linear uptake phase. The benefit of PRCs lies in capturing the influence of environmental variables such as temperature and wind speed on the sampling rates at a given site. However, they do not capture and compensate for analytes reaching the curvilinear- or equilibrium uptake phase during deployment (e.g. HCB). The result is that the PAS does not provide a true time-averaged concentration for analytes that have overtaken the linear uptake phase.

The PRCs will volatilize into the atmosphere during the deployment period, and the amounts lost are the basis in the estimation of sample air volumes. The average amounts of PRCs in the field blanks (n = 2) were used as reference, to account for any losses not caused by sampling. Loss of PRCs from individual samples was calculated from Equation VI. The amounts lost differ between different PRCs, and the loss is corrected based on the stable PCB-198, that is expected to not volatilize from the PAS. Only the compounds that experienced (corrected) losses between 40 % and 80 % were used in the calculation of an average site-specific sampling rate. In practice, the sampling rates were mainly determined by 13C PCB-8, PCB-14 and PCB-30.

$$Rec \% PRC = \frac{mass\ PRC_{measured}}{Avg.mass\ PRC_{field\ blank}} \times 100\ \% \qquad \text{(Eq. VI)}$$

In the template, the sampling rates are then used to estimate air volumes, as detailed by Moeckel et al. (2009). The resulting sampling rates and number of PRCs used in these calculations are presented in Table SI-1.6. For the sites experiencing insufficient loss of the PRCs, the average sampling rate (3.6 m^3/day) was used instead. The average sampling rate included all sites which had three or more PRCs that experienced suitable losses (40 % - 80 %), and are in good agreement with the general sampling rate (4 m^3/day) suggested by Harner et al. (2014).

1.5.4 Octanol-air partition coefficients (K_{OA})

On the basis of the template, temperature adjusted K_{OA}-values for the PCBs were derived from the correlation between log K_{OA} data reported by Harner & Bidleman (1996) and relative retention times from Harju et al. (1998), as given in Table SI-1.8. Temperature adjusted K_{OA}-values for γ-HCH were derived from the correlation between log K_{OA} and temperature, reported by Shoeib & Harner (2002b). As temperature increases, the analytes become more volatile (reduced K_{OA}). This means that the potential to proceed beyond the linear uptake phase increases at elevated temperatures, enhancing the potential for underestimating concentrations in air of the more volatile substances (low K_{OA} substances).

1.5.5 Wind effects

At three of the sites, the PAS had opened during deployment (Figure SI-1.4). Without the sheltering effect of the chamber it is therefore likely that the PUF disks have been exposed to higher wind speeds, and overexposure is likely (Tuduri et al., 2006). Though no increment in the sampling rates was found, a higher uncertainty in the air concentrations is expected. The PAS at site 26 was deployed on the roof top of a monitoring station on top of a mountain, and even if the average wind speed during the sampling period was not elevated (Table SI-1.6), the samplers are expected to have been exposed to higher wind speeds than in locations closer to the ground. This is reflected by the highest sampling rate estimated (10.1 m^3/day), and indicates that there might have been episodes with heavy wind. Apart from site 26, site 15 had the highest estimated sampling rate (5.3 m^3/day), likely due to an average wind speed at this site that was in the upper end of the range estimated for all the samples taken across Norway.

Figure SI-1.4. The PAS at site 16, 19 and 36.

1.6   Data analysis

1.6.1   Boxplots and outliers

Boxplots were produced in R Studio to visualize the data (Figure SI-1.5). The box contains the middle 50 % of the data. The horizontal line within the box is the median, while the extensions (or "whiskers") indicate the minimum and maximum. Outliers are defined as data points higher than Q3 + 1.5 x IQR, and are located outside the "whiskers". These might be due to contamination or overestimated concentrations because of the uncertainty associated with the determination of sampling air volumes (e.g. site 26, Table SI-1.6). Outliers outside the maximum are excluded from the calculation of MMRs.
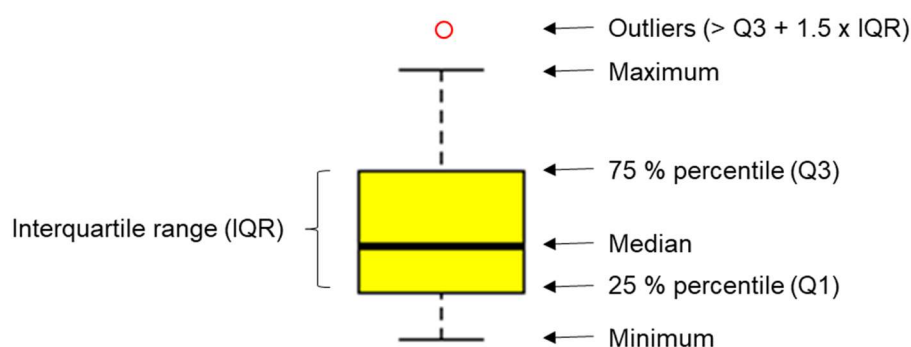
Figure SI-1.5. Illustration and explanation of boxplot.

1.6.2   Linear correlation

In order to assess if the concentrations in air were increasing or decreasing with latitude, a linear model ($y = b_0 + b_1 x$) with the concentration as the outcome (y), and latitude as the predictor (x), was predicted with R Studio. Only the background sites (Table SI-1.1) were considered and the concentrations were converted to log concentrations, to meet the criteria of normal distribution. The linear correlation between the variables is tested by the null-hypothesis H_0: $b_1 = 0$. The null-hypothesis was rejected if its probability was less than 5 % ($p < 0.05$), i.e. the correlation was significant at the 5 % level.

The Pearson correlation coefficient (r) is a measure of the linear relationship (between -1 and 1) between two variables. For the simple linear regression model, R^2 corresponds to the square of the Pearson correlation coefficient (r^2). $R^2 = 1$ means that all the values are on a straight line.

1.6.3   Wilcoxon signed rank test

To test if there was a significant difference between the concentration levels in the south (58.4°-65.8°) and north (66.8°-78.9°) of Norway, the averages in the two groups were compared by a two-sample Wilcoxon test with R Studio. The null-hypothesis tested was H_0: $\mu_{south} = \mu_{north}$, i.e. a two-sided test. A Wilcoxon test was chosen because the data are symmetrical (median ≈ average), but not normally distributed (Miller, 2010). The null-hypothesis was rejected when $p < 0.05$, i.e. that there is

a significant difference between south and north. When testing whether the concentration levels in southern Norway were higher (or lower) than the concentration levels in northern Norway, a one-sided test is performed instead, i.e. testing H_0: $\mu_{south} > \mu_{north}$ (or H_0: $\mu_{south} < \mu_{north}$). The probability of this is half the probability of the two-sided test.

1.6.4 Matched pair Wilcoxon signed rank test

The POP concentrations in air at six of the background sites were compared with the Norwegian data from a similar PUF-PAS campaign conducted all over Europe by Halse et al. (2011) in 2006. Additional data from Oslo (Halse et al., 2012) was also included in the comparison (total n = 7). A Wilcoxon test was run in R Studio by comparing the air concentrations at the seven selected sites pairwise. It should be noted that the air samples from 2006 were analyzed at the same laboratory with the same methodology and same type of instrumentation (Halse et al., 2011), and the concentrations are therefore comparable.

The null-hypothesis tests if the 2016-data are lower or higher than the 2006-data, i.e H_0: Difference < 0 or Difference > 0 (one-sided). Similar to the two-sampled test in (SI 1.6.4), the null-hypothesis was rejected when $p < 0.05$.

1.6.5 Comparing latitudinal gradient 2006 vs. 2016

To assess the temporal difference in spatial patterns from 2006 to 2016, the linear correlations between concentration in air and latitude (SI 1.6.3) were compared. To achieve this, a linear model with interactions was predicted with R Studio (Table SI-1.9); $y = b_0 + b_1x_1 + b_2x_2 + b_3x_1x_2$, where the outcome (y) is the concentration in air, and the predictors x_1 and x_2 are year and latitude respectively. x_1 is a categorical variable, which will be 0 in 2006 and 1 in 2016. The null-hypothesis tested was H_0: $b_3 = 0$, which was not rejected when $p > 0.05$, i.e. there is no difference in the linear correlation from 2006 to 2016.

1.7 Atmospheric transport modelling tools

1.7.1 GLEMOS

Model simulations of concentration of PCB-153 in air were carried out using the GLEMOS model (Malanichev et al., 2004). A description of the GLEMOS model can be found at http://en.msceast.org/index.php/j-stuff/glemos, along with numerous EMEP technical reports where the model has been described and/or used.

Emission data is one of the most important types of model input information. The GLEMOS model was based on the global PCB-153 emission inventory (Breivik et al., 2007) and officially reported PCB-153 emissions. The selected level of emissions was defined between the average and maximum emission scenarios of the inventory. The spatial distribution of emissions for the part of EMEP countries was derived from the officially reported gridded emission data. For the countries that did not report gridded data, spatial distribution of emissions was based on population density.

Meteorological data is another key input parameter when modelling long-range transport and deposition of atmospheric pollutants. More detailed information about meteorological data processing is available in technical reports found on the website.

To evaluate PCB-153 content in surface media and re-emission fluxes, long-term spin-up global modelling was performed.

1.7.2 FLEXPART

For comparison, model simulations of PCB-153 were also carried out using the Lagrangian particle dispersion model FLEXPART version 10.4 (Pisso et al., 2019; Stohl et al., 1998). FLEXPART was driven with meteorological input data from the European Centre for Medium-Range Weather Forecast (ECMWF) with 1° resolution and 3 hourly temporal resolution. It was run in backward mode, considering e.g. removal by dry and wet deposition, in order to identify the source regions of air pollutants at a particular site. These source regions are expressed as emission sensitivities (ES) in the footprint layer (0-100 m above ground) during the whole deployment period. The ES maps illustrate where the air mass had the potential to take up pollutants from sources near the ground. Multiplying ES with emission fluxes from the emission inventory (Breivik et al., 2007) yields the maps of footprint emission contribution, showing the geographical distribution of sources contributing to the predicted concentration at a given measurement site. Emission contributions (EC) give the predicted air concentrations at the measurement sites, when integrated over the whole area.

2　Results and Discussion

Tables:

Table SI-2.1. Concentrations in air (pg/m^3) of selected PCBs and OCPs at Norwegian background sites

Compounds	Background concentrations in air in Norway[a]			Blanks			
	Average ± SD pg/m^3	Median pg/m^3	Measured range pg/m^3	Measured range pg/m^3	MDL pg/m^3	Samples above MDL %	Max/min ratio[d] (MMR)
PCB-28	0.5 ± 0.2	0.5	0.3-1.1	0.008[b]-0.03[b]	0.04	100 %	3
PCB-52	0.7 ± 0.4	0.6	0.3-1.6	0.005[b]-0.03	0.03	100 %	3
PCB-101	0.5 ± 0.3	0.4	0.2-1.3	0.005[b]-0.02	0.03	100 %	4
PCB-138	0.2 ± 0.1	0.1	< MDL-0.6	0.003[b]-0.01	0.02	98 %	18[c]
PCB-153	0.3 ± 0.2	0.2	0.1-1.0	0.004[b]-0.02	0.02	100 %	4
PCB-180	0.05 ± 0.03	0.04	< MDL-0.16	0.003[b]-0.02[b]	0.02	86 %	5[c]
Sum 6 PCB	2 ± 1	2	1-6				> 4
Sum 18 PCB	5 ± 3	5	2-13				> 4
PeCB	22 ± 4	21	16-38	0.2-0.6	0.8	100 %	2
HCB	75 ± 19	74	52-136	0.08-0.4	0.4	100 %	2
a-HCH	7 ± 2	6	4-13	0.07[b]-0.2[b]	0.2	100 %	3
g-HCH	3 ± 2	2	1-7	0.06[b]-0.2	0.3	100 %	4
Sum 2 HCHs	9 ± 3	9	5-17				> 3
p,p'-DDE	0.5 ± 0.5	0.4	0.1-2.6	0.006-0.04	0.05	100 %	6
o,p'-DDT	0.2 ± 0.2	0.2	0.1-1.1	0.004[b]-0.02	0.03	100 %	6
p,p'-DDT	0.2 ± 0.2	0.1	< MDL-1.2	0.008[b]-0.02[b]	0.02	98 %	15[c]
Sum 3 DDXs	0.9 ± 0.9	0.7	0.2-4.8				> 8
Dieldrin	2 ± 1	2	< MDL-6	0.08[b]-0.3[b]	0.4	86 %	10[c]
Heptachlor-exo-epoxide	1.2 ± 0.7	1.1	< MDL-4	0.09[b]-0.3[b]	0.4	86 %	6[c]
trans-Chlordane	0.2 ± 0.1	0.1	< MDL-2.4	0.006[b]-0.03	0.04	95 %	10[c]
cis-Chlordane	0.8 ± 0.4	0.7	0.4-2.4	0.01[b]-0.04[b]	0.04	100 %	4
Oxy-chlordane	0.7 ± 0.3	0.6	< MDL-1.8	0.04[b]-0.2[b]	0.2	95 %	6[c]
trans-Nonachlor	0.7 ± 0.3	0.6	0.3-1.9	0.008[b]-0.02[b]	0.03	100 %	4
cis-Nonachlor	0.10 ± 0.07	0.10	< MDL-0.35	0.004[b]-0.04[b]	0.05	79 %	5[c]
Sum 4 Chlordanes	1.7 ± 0.8	1.5	0.7-5.1				> 4
Endosulfan-I	2 ± 1	2	0.7-6	0.009[b]-0.1[b]	0.2	100 %	7

[a] Number of samples:
PCBs and PeCB/HCB: n = 44. Three samples excluded due to low instrument sensitivity and unexpectedly low detection of many of the congeners (e.g. PCB-153).
HCHs and DDXs: n = 46. One sample not analyzed.
Other OCPs: n = 43. Two samples not analyzed and two samples excluded due to unknown amount of internal standard, high recovery % and unexpectedly low concentrations.
[b] Instrument detection limit
[c] Minimum value = method detection limit
[d] Excluding outliers

Table SI-2.2a. Concentrations in air (pg/m^3) for all target PCBs at the individual sites. Concentrations below MDL set to ½ MDL (grey).

Site No.	Type:	PCB 18[b]	PCB 28[bc]	PCB 31[b]	PCB 33[b]	PCB 37[b]	PCB 47[b]	PCB 52[bc]	PCB 66[b]	PCB 74[b]	PCB 99[b]	PCB 101[bc]
1	Urban	2.5	1.5	1.5	0.83	0.22	0.63	2.4	0.44	0.30	0.45	1.9
2	Urban	2.6	1.3	1.2	0.64	0.13	0.44	1.8	0.34	0.24	0.29	1.2
3	Urban	3.9	2.1	2.0	1.1	0.23	0.55	2.5	0.40	0.28	0.37	1.7
4	Urban	15	9.5	9.6	6.1	1.3	3.1	13	2.7	1.8	2.3	11
5	Urban	17	10	10	6.4	1.2	4.0	13	0.01	1.9	1.9	9.9
6	Urban	23	9.6	9.1	5.2	0.81	2.0	9.0	1.2	0.89	0.82	4.4
7	Urban	10	4.8	4.4	2.3	0.47	2.1	7.6	0.91	0.69	1.00	4.4
8	Urban	13	7.4	7.5	4.4	1.1	2.5	9.8	1.8	1.3	1.6	11
9	Urban[d]											
10	Urban	7.7	5.1	4.8	3.1	0.73	1.5	5.3	1.1	0.74	0.79	3.9
11	Remote	0.65	0.47	0.47	0.23	0.04	0.21	0.66	0.16	0.13	0.15	0.44
12	Remote	1.6	1.0	0.85	0.43	0.08	0.32	1.1	0.19	0.15	0.33	0.77
13	Remote	0.91	0.70	0.56	0.25	0.08	0.22	0.69	0.12	0.07	0.15	0.37
14	Remote	0.62	0.62	0.44	0.22	0.02	0.18	0.81	0.12	0.14	0.22	0.49
15	Remote	1.1	0.83	0.87	0.76	0.38	0.31	1.3	0.25	0.21	0.38	0.88
16	Remote	n.d.	n.d.	n.d.	n.d.	n.d.	n.d.	n.d.	n.d.	n.d.	n.d.	n.d.
17	Remote	n.d.	n.d.	n.d.	n.d.	n.d.	n.d.	n.d.	n.d.	n.d.	n.d.	n.d.
18	Remote	n.d.	n.d.	n.d.	n.d.	n.d.	n.d.	n.d.	n.d.	n.d.	n.d.	n.d.
19	Remote	1.0	0.55	0.53	0.24	0.04	0.19	0.62	0.12	0.09	0.15	0.44
20	Remote	0.76	0.50	0.49	0.24	0.06	0.16	0.67	0.12	0.11	0.17	0.45
21	Remote	0.46	0.28	0.27	0.14	0.03	0.10	0.33	0.04	0.04	0.07	0.20
22	Remote	0.50	0.30	0.28	0.11	0.02	0.12	0.35	0.06	0.05	0.08	0.24
23	Remote	0.40	0.26	0.25	0.10	0.02	0.09	0.36	0.05	0.05	0.06	0.22
24	Remote	0.44	0.35	0.30	0.16	0.04	0.15	0.45	0.08	0.07	0.10	0.31
25	Remote	0.63	0.54	0.58	0.29	0.06	0.22	0.80	0.13	0.13	0.18	0.53
26	Remote	1.3	0.75	0.83	0.35	0.03	0.35	1.4	0.17	0.17	0.28	0.83
27	Remote	0.55	0.40	0.37	0.17	0.03	0.17	0.50	0.06	0.07	0.11	0.36
28	Remote	1.2	0.46	0.45	0.20	0.03	0.22	0.68	0.11	0.10	0.17	0.47
29	Remote	0.48	0.30	0.26	0.12	0.02	0.12	0.37	0.06	0.05	0.08	0.24
30	Remote	0.91	0.29	0.29	0.12	0.01	0.11	0.34	0.05	0.04	0.07	0.24
31	Remote	0.64	0.36	0.33	0.14	0.02	0.14	0.47	0.08	0.08	0.10	0.32
32	Remote	0.71	0.41	0.37	0.17	0.03	0.18	0.52	0.09	0.09	0.13	0.38
33	Remote	0.98	0.41	0.38	0.18	0.02	0.17	0.56	0.09	0.09	0.11	0.37
34	Remote	0.71	0.37	0.33	0.14	0.02	0.15	0.46	0.08	0.08	0.10	0.32
35	Remote	1.0	0.55	0.59	0.26	0.04	0.23	0.79	0.11	0.09	0.17	0.54
36	Remote	0.52	0.30	0.28	0.13	0.01	0.11	0.37	0.05	0.04	0.08	0.25
37	Remote	0.52	0.29	0.27	0.12	0.01	0.10	0.35	0.04	0.04	0.07	0.23
38	Remote	1.7	0.74	0.71	0.31	0.04	0.32	1.0	0.16	0.14	0.22	0.77
39	Remote	0.73	0.51	0.49	0.24	0.04	0.23	0.74	0.13	0.11	0.15	0.56
40	Remote	0.74	0.44	0.42	0.18	0.03	0.17	0.58	0.09	0.07	0.11	0.41
41	Remote	0.88	0.41	0.41	0.19	0.03	0.16	0.54	0.08	0.07	0.11	0.37
42	Remote	1.5	0.61	0.58	0.24	0.02	0.34	1.4	0.13	0.12	0.21	0.70
43	Remote	0.80	0.38	0.35	0.16	0.02	0.17	0.53	0.09	0.08	0.11	0.47
44	Remote	0.69	0.42	0.38	0.18	0.03	0.19	0.62	0.12	0.09	0.13	0.44
45	Remote	0.54	0.31	0.29	0.12	0.02	0.14	0.43	0.07	0.07	0.09	0.30
46	Remote	1.1	0.46	0.46	0.20	0.03	0.22	0.66	0.12	0.11	0.14	0.49
47	Remote	1.2	0.69	0.67	0.34	0.07	0.34	1.1	0.25	0.20	0.23	0.76
48	Remote	1.7	1.1	0.99	0.49	0.10	0.53	1.5	0.37	0.32	0.33	1.1
49	Remote	1.7	1.1	1.1	0.54	0.11	0.56	1.6	0.42	0.33	0.34	1.2
50	Remote	0.88	0.56	0.56	0.26	0.05	0.27	0.78	0.19	0.15	0.16	0.57
51	Remote	0.68	0.45	0.42	0.20	0.04	0.19	0.60	0.14	0.11	0.11	0.37
52	Remote	1.6	1.1	1.1	0.52	0.11	0.54	1.6	0.40	0.32	0.37	1.3
53	Remote	0.73	0.51	0.46	0.21	0.05	0.23	0.66	0.17	0.13	0.15	0.49
54	Remote	0.79	0.48	0.45	0.20	0.04	0.20	0.59	0.14	0.11	0.11	0.39
55	Remote	1.3	0.84	0.81	0.38	0.08	0.35	1.0	0.24	0.19	0.21	0.72
96	Pristine	0.93	0.63	0.61	0.35	0.07	0.20	0.63	0.15	0.12	0.13	0.33
97	Pristine	0.54	0.34	0.31	0.15	0.02	0.16	0.53	0.11	0.10	0.14	0.34

[a] Coeluting with PCB-106 in the PRCs. Excluded.
[b] Included in sum 18 PCBs
[c] Included in sum 6 PCBs
[d] Contaminated. Excluded.
n.d. = Not detected

Table SI-2.2a. Concentrations in air (pg/m^3) for all target PCBs at the individual sites (continued). Concentrations below MDL set to ½ MDL (grey).

Site No.	Type:	PCB 105[b]	PCB 114	PCB 118[a]	PCB 122	PCB 123	PCB 128	PCB 138[bc]	PCB 141[b]	PCB 149[b]	PCB 153[bc]	PCB 156
1	Urban	0.13	0.01		0.01	0.01	0.08	0.64	0.22	1.6	1.29	0.03
2	Urban	0.08	0.02		0.02	0.01	0.04	0.26	0.10	0.68	0.57	0.01
3	Urban	0.10	0.02		0.01	0.01	0.05	0.42	0.13	0.91	0.77	0.02
4	Urban	0.81	0.07		0.01	0.03	0.32	2.7	0.80	5.9	5.3	0.11
5	Urban	0.75	0.06		0.01	0.03	0.28	2.1	0.58	4.2	4.2	0.09
6	Urban	0.19	0.04		0.05	0.01	0.10	0.85	0.29	2.3	1.8	0.04
7	Urban	0.22	0.01		0.01	0.01	0.11	0.83	0.29	2.6	1.9	0.03
8	Urban	0.50	0.05		0.01	0.02	0.26	2.7	1.0	9.5	6.2	0.10
9	Urban[d]											
10	Urban	0.30	0.03		0.01	0.01	0.16	1.3	0.38	2.7	2.5	0.06
11	Remote	0.04	0.01		0.00	0.01	0.03	0.14	0.04	0.26	0.25	0.01
12	Remote	0.11	0.02		0.01	0.01	0.04	0.28	0.06	0.39	0.36	0.01
13	Remote	0.03	0.03		0.03	0.03	0.02	0.15	0.03	0.26	0.22	0.01
14	Remote	0.06	0.02		0.02	0.02	0.02	0.02	0.06	0.29	0.27	0.01
15	Remote	0.15	0.02		0.02	0.02	0.05	0.42	0.10	0.58	0.54	0.01
16	Remote	n.d.	n.d.		n.d.	n.d.	n.d.	n.d.	n.d.	n.d.	n.d.	n.d.
17	Remote	n.d.	n.d.		n.d.	n.d.	n.d.	n.d.	n.d.	n.d.	n.d.	n.d.
18	Remote	n.d.	n.d.		n.d.	n.d.	n.d.	n.d.	n.d.	n.d.	n.d.	n.d.
19	Remote	0.04	0.01		0.01	0.01	0.01	0.16	0.03	0.30	0.22	0.01
20	Remote	0.04	0.01		0.01	0.01	0.02	0.17	0.04	0.41	0.24	0.01
21	Remote	0.01	0.01		0.01	0.01	0.01	0.07	0.03	0.16	0.13	0.01
22	Remote	0.02	0.01		0.01	0.01	0.01	0.08	0.03	0.20	0.14	0.01
23	Remote	0.01	0.01		0.01	0.01	0.01	0.07	0.02	0.17	0.13	0.01
24	Remote	0.03	0.01		0.01	0.01	0.01	0.11	0.04	0.30	0.18	0.01
25	Remote	0.04	0.02		0.01	0.01	0.03	0.20	0.06	0.48	0.31	0.01
26	Remote	0.06	0.02		0.02	0.03	0.01	0.32	0.06	0.63	0.51	0.01
27	Remote	0.02	0.02		0.01	0.01	0.01	0.14	0.04	0.34	0.23	0.01
28	Remote	0.04	0.02		0.01	0.01	0.01	0.17	0.05	0.43	0.31	0.01
29	Remote	0.02	0.01		0.01	0.01	0.01	0.09	0.03	0.23	0.15	0.01
30	Remote	0.01	0.01		0.01	0.01	0.01	0.07	0.03	0.18	0.12	0.01
31	Remote	0.02	0.01		0.00	0.01	0.01	0.11	0.04	0.29	0.18	0.01
32	Remote	0.03	0.02		0.01	0.01	0.01	0.13	0.04	0.35	0.23	0.01
33	Remote	0.02	0.02		0.01	0.01	0.01	0.13	0.04	0.34	0.22	0.01
34	Remote	0.02	0.01		0.01	0.01	0.01	0.11	0.03	0.27	0.18	0.01
35	Remote	0.04	0.02		0.01	0.02	0.01	0.22	0.07	0.54	0.37	0.01
36	Remote	0.01	0.02		0.01	0.01	0.01	0.09	0.02	0.22	0.14	0.01
37	Remote	0.02	0.02		0.01	0.01	0.01	0.09	0.03	0.22	0.15	0.01
38	Remote	0.05	0.02		0.01	0.01	0.03	0.27	0.09	0.72	0.45	0.01
39	Remote	0.03	0.02		0.01	0.01	0.02	0.20	0.06	0.47	0.32	0.01
40	Remote	0.02	0.01		0.01	0.01	0.01	0.13	0.04	0.32	0.23	0.01
41	Remote	0.03	0.01		0.01	0.01	0.01	0.13	0.04	0.34	0.23	0.01
42	Remote	0.04	0.03		0.01	0.01	0.02	0.18	0.07	0.51	0.35	0.01
43	Remote	0.02	0.01		0.01	0.01	0.02	0.26	0.09	0.52	0.37	0.02
44	Remote	0.03	0.02		0.01	0.01	0.01	0.16	0.05	0.37	0.27	0.01
45	Remote	0.02	0.01		0.01	0.01	0.01	0.11	0.03	0.26	0.18	0.01
46	Remote	0.03	0.01		0.01	0.01	0.02	0.17	0.05	0.43	0.29	0.01
47	Remote	0.05	0.02		0.01	0.01	0.03	0.31	0.07	0.60	0.50	0.01
48	Remote	0.07	0.03		0.01	0.03	0.02	0.43	0.14	1.0	0.73	0.01
49	Remote	0.08	0.03		0.01	0.02	0.05	0.48	0.12	0.98	0.78	0.02
50	Remote	0.03	0.01		0.01	0.01	0.02	0.22	0.06	0.44	0.35	0.01
51	Remote	0.02	0.02		0.01	0.01	0.01	0.13	0.04	0.34	0.22	0.01
52	Remote	0.09	0.03		0.01	0.01	0.05	0.55	0.15	1.3	0.95	0.03
53	Remote	0.03	0.02		0.01	0.01	0.02	0.20	0.06	0.45	0.34	0.01
54	Remote	0.02	0.02		0.01	0.01	0.01	0.14	0.04	0.32	0.25	0.01
55	Remote	0.04	0.02		0.01	0.01	0.02	0.23	0.07	0.55	0.39	0.01
96	Pristine	0.03	0.01		0.01	0.01	0.02	0.10	0.01	0.19	0.15	0.01
97	Pristine	0.03	0.02		0.01	0.01	0.01	0.13	0.01	0.19	0.18	0.01

[a] Coeluting with PCB-106 in the PRCs. Excluded.

[b] Included in sum 18 PCBs

[c] Included in sum 6 PCBs

[d] Contaminated. Excluded.

n.d. = Not detected

Table SI-2.2a. Concentrations in air (pg/m^3) for all target PCBs at the individual sites (continued). Concentrations below MDL set to ½ MDL (grey).

Site No.	Type:	PCB 157	PCB 167	PCB 170	PCB 180[b][c]	PCB 183	PCB 187[b]	PCB 189	PCB 194	PCB 206	PCB 209	Sum 18 PCBs	Sum 6 PCBs
1	Urban	0.01	0.01	0.05	0.23	0.08	0.23	0.01	0.02	0.02	0.01	17	8
2	Urban	0.01	0.01	0.01	0.07	0.04	0.08	0.01	0.02	0.02	0.01	12	5
3	Urban	0.01	0.01	0.01	0.10	0.04	0.08	0.01	0.02	0.02	0.01	17	7.5
4	Urban	0.02	0.05	0.15	0.62	0.24	0.60	0.01	0.02	0.02	0.01	92	42
5	Urban	0.01	0.05	0.12	0.47	0.20	0.51	0.01	0.02	0.02	0.01	89	40
6	Urban	0.01	0.01	0.05	0.21	0.10	0.26	0.01	0.02	0.02	0.01	72	26
7	Urban	0.01	0.01	0.05	0.20	0.09	0.23	0.01	0.02	0.02	0.01	45	20
8	Urban	0.01	0.04	0.14	0.74	0.34	0.76	0.01	0.02	0.02	0.01	83	38
9	Urban[d]												
10	Urban	0.01	0.03	0.10	0.39	0.16	0.40	0.01	0.02	0.01	0.01	43	18
11	Remote	0.01	0.01	0.03	0.06	0.02	0.06	0.01	0.02	0.01	0.01	4.5	2.0
12	Remote	0.01	0.01	0.01	0.06	0.02	0.06	0.01	0.02	0.01	0.01	8.2	3.6
13	Remote	0.01	0.01	0.03	0.03	0.02	0.03	0.02	0.02	0.02	0.01	4.9	2.2
14	Remote	0.01	0.01	0.03	0.02	0.02	0.02	0.01	0.01	0.02	0.01	4.6	2.2
15	Remote	0.01	0.01	0.03	0.10	0.05	0.11	0.02	0.01	0.02	0.01	9.2	4.1
16	Remote	n.d.	n.d.	n.d.	n.d.	n.d.	n.d.	n.d.	n.d.	n.d.	n.d.	n.d.	n.d.
17	Remote	n.d.	n.d.	n.d.	n.d.	n.d.	n.d.	n.d.	n.d.	n.d.	n.d.	n.d.	n.d.
18	Remote	n.d.	n.d.	n.d.	n.d.	n.d.	n.d.	n.d.	n.d.	n.d.	n.d.	n.d.	n.d.
19	Remote	0.01	0.01	0.01	0.04	0.02	0.05	0.01	0.01	0.01	0.01	4.8	2.0
20	Remote	0.01	0.01	0.01	0.03	0.03	0.05	0.01	0.01	0.01	0.01	4.7	2.1
21	Remote	0.01	0.01	0.01	0.01	0.01	0.02	0.01	0.01	0.01	0.01	2.4	1.0
22	Remote	0.01	0.01	0.01	0.03	0.01	0.03	0.01	0.01	0.01	0.01	2.6	1.1
23	Remote	0.01	0.01	0.01	0.01	0.01	0.03	0.01	0.01	0.01	0.01	2.3	1.0
24	Remote	0.01	0.01	0.01	0.04	0.01	0.05	0.01	0.01	0.01	0.01	3.2	1.4
25	Remote	0.01	0.01	0.01	0.06	0.03	0.09	0.01	0.01	0.01	0.01	5.3	2.4
26	Remote	0.01	0.01	0.02	0.10	0.02	0.13	0.01	0.01	0.01	0.01	8.2	3.9
27	Remote	0.01	0.01	0.01	0.04	0.02	0.06	0.01	0.01	0.01	0.01	3.7	1.7
28	Remote	0.01	0.01	0.01	0.05	0.02	0.08	0.01	0.01	0.01	0.01	5.2	2.1
29	Remote	0.01	0.01	0.01	0.03	0.01	0.04	0.01	0.01	0.01	0.01	2.7	1.2
30	Remote	0.01	0.01	0.01	0.01	0.01	0.03	0.01	0.01	0.01	0.01	2.9	1.1
31	Remote	0.01	0.00	0.01	0.03	0.02	0.05	0.01	0.01	0.01	0.01	3.4	1.5
32	Remote	0.01	0.01	0.01	0.04	0.02	0.06	0.01	0.01	0.01	0.01	4.0	1.7
33	Remote	0.01	0.01	0.01	0.04	0.01	0.06	0.01	0.02	0.01	0.01	4.2	1.7
34	Remote	0.01	0.01	0.01	0.03	0.01	0.04	0.01	0.01	0.01	0.01	3.4	1.5
35	Remote	0.01	0.01	0.03	0.06	0.04	0.09	0.01	0.02	0.01	0.01	5.8	2.5
36	Remote	0.01	0.01	0.01	0.02	0.01	0.04	0.01	0.01	0.01	0.01	2.7	1.2
37	Remote	0.01	0.01	0.01	0.02	0.01	0.04	0.01	0.01	0.01	0.01	2.6	1.1
38	Remote	0.01	0.01	0.01	0.08	0.04	0.12	0.01	0.02	0.01	0.01	7.9	3.3
39	Remote	0.01	0.01	0.01	0.06	0.03	0.09	0.01	0.01	0.01	0.01	5.2	2.4
40	Remote	0.01	0.01	0.01	0.04	0.01	0.06	0.01	0.01	0.01	0.01	4.1	1.8
41	Remote	0.01	0.01	0.01	0.04	0.02	0.06	0.01	0.01	0.01	0.01	4.1	1.7
42	Remote	0.01	0.01	0.02	0.05	0.02	0.08	0.01	0.02	0.02	0.01	7.2	3.3
43	Remote	0.01	0.01	0.04	0.11	0.04	0.10	0.01	0.01	0.01	0.01	4.7	2.1
44	Remote	0.01	0.01	0.01	0.05	0.02	0.07	0.01	0.01	0.01	0.01	4.3	2.0
45	Remote	0.01	0.01	0.01	0.03	0.01	0.05	0.01	0.01	0.01	0.01	3.1	1.4
46	Remote	0.01	0.01	0.01	0.05	0.03	0.08	0.01	0.01	0.01	0.01	5.0	2.1
47	Remote	0.01	0.01	0.01	0.08	0.04	0.13	0.01	0.02	0.01	0.01	7.6	3.4
48	Remote	0.01	0.01	0.05	0.13	0.07	0.21	0.01	0.03	0.02	0.01	11	5.0
49	Remote	0.01	0.01	0.04	0.14	0.06	0.21	0.01	0.02	0.02	0.01	12	5.3
50	Remote	0.01	0.01	0.01	0.06	0.03	0.10	0.01	0.01	0.01	0.01	5.7	2.5
51	Remote	0.01	0.01	0.01	0.03	0.01	0.05	0.01	0.01	0.01	0.01	4.2	1.8
52	Remote	0.01	0.01	0.05	0.16	0.08	0.24	0.01	0.03	0.02	0.01	13	5.7
53	Remote	0.01	0.01	0.01	0.06	0.03	0.08	0.01	0.01	0.01	0.01	5.0	2.3
54	Remote	0.01	0.01	0.01	0.04	0.02	0.05	0.01	0.01	0.01	0.01	4.4	1.9
55	Remote	0.01	0.01	0.01	0.06	0.03	0.09	0.01	0.01	0.01	0.01	7.6	3.3
96	Pristine	0.01	0.01	0.01	0.02	0.01	0.03	0.01	0.02	0.01	0.01	4.7	1.9
97	Pristine	0.01	0.01	0.01	0.03	0.01	0.05	0.01	0.02	0.01	0.01	3.4	1.6

[a] Coeluting with PCB-106 in the PRCs. Excluded.
[b] Included in sum 18 PCBs
[c] Included in sum 6 PCBs
[d] Contaminated. Excluded.
n.d. = Not detected

Table SI-2.2b. Concentrations in air (pg/m^3) for all target OCPs at the individual sites. Concentrations below MDL set to ½ MDL (grey).

Site No.	Type:	Dieldrin	Aldrin	Isodrin	Endrin	Heptachlor-exo-epoxide	Heptachlor-endo-epoxide	trans-Chlordane	cis-Chlordane	Oxy-chlordane
1	Urban	134	14	44	45	93	76	2.7	5.2	30
2	Urban	106	11	36	36	74	61	2.2	4.1	24
3	Urban	105	11	35	36	74	60	2.1	4.1	24
4	Urban	116	12	39	39	81	66	2.4	4.5	26
5	Urban	114	12	38	39	80	65	2.3	4.4	26
6	Urban	144	15	47	48	100	81	2.9	5.6	32
7	Urban	129	13	42	43	90	73	2.6	5.0	29
8	Urban	135	14	44	45	94	77	2.8	5.3	30
9	Urban	145	15	47	48	101	82	3.0	5.7	32
10	Urban	98	11	33	34	69	56	2.0	3.8	22
11	Remote	2.2	0.36	1.4	1.4	0.98	2.1	0.15	0.83	0.82
12	Remote	1.8	0.48	1.1	0.20	1.3	0.23	0.13	0.81	0.74
13	Remote	0.34	0.44	1.05	0.18	0.27	0.21	0.02	0.59	0.68
14	Remote	1.8	0.34	0.82	0.14	0.21	0.16	0.13	0.69	0.63
15	Remote	2.9	0.25	0.59	0.10	1.5	0.11	0.24	1.3	0.89
16	Remote	0.41	0.33	0.77	0.21	1.3	0.20	0.02	0.77	0.80
17	Remote	0.24	0.39	0.93	0.16	0.89	0.71	0.56	1.1	0.88
18	Remote	0.25	0.35	0.84	0.14	0.21	0.17	0.07	0.41	0.26
19	Remote	1.6	0.35	0.84	0.14	1.3	0.17	0.12	0.74	0.71
20	Remote	2.7	0.32	0.76	0.13	1.5	0.15	0.20	1.0	0.88
21	Remote	0.73	0.34	0.80	0.14	0.20	0.16	0.08	0.36	0.09
22	Remote	1.0	0.34	0.80	0.14	0.76	0.16	0.09	0.46	0.38
23	Remote	0.78	0.35	0.84	0.15	0.21	0.17	0.08	0.40	0.10
24	Remote	1.7	0.35	0.84	0.15	1.1	0.17	0.13	0.68	0.56
25	Remote	3.7	0.37	0.89	0.15	2.1	0.18	0.24	1.3	0.99
26	Remote	6.6	0.15	0.34	0.45	3.6	0.06	0.44	2.4	1.8
27	Remote	1.7	0.37	0.87	0.15	1.1	0.17	0.12	0.60	0.44
28	Remote	n.a.	n.a.	n.a.	n.a.	n.a.	n.a.	n.a.	n.a.	n.a.
29	Remote	1.3	0.36	0.85	0.15	0.76	0.17	0.10	0.50	0.39
30	Remote	1.1	0.35	0.84	0.15	0.68	0.17	0.10	0.44	0.36
31	Remote	1.4	0.31	0.74	0.13	0.92	0.15	0.11	0.57	0.47
32	Remote	2.0	0.36	0.86	0.15	1.2	0.17	0.15	0.74	0.68
33	Remote	1.9	0.46	1.1	0.19	1.4	0.22	0.33	1.2	1.0
34	Remote	1.5	0.35	0.84	0.15	0.96	0.17	0.12	0.69	0.54
35	Remote	3.4	0.49	1.2	0.20	2.0	0.23	0.28	1.1	0.95
36	Remote	1.1	0.36	0.87	0.15	0.61	0.17	0.11	0.44	0.34
37	Remote	0.88	0.36	0.87	0.15	0.77	0.17	0.09	0.42	0.33
38	Remote	3.2	0.44	1.1	0.18	2.0	0.21	0.25	1.1	0.95
39	Remote	2.2	0.36	0.85	0.15	1.4	0.17	0.17	0.86	0.69
40	Remote	1.1	0.36	0.85	0.15	0.81	0.17	0.12	0.44	0.35
41	Remote	1.5	0.34	0.82	0.14	0.89	0.16	0.15	0.60	0.50
42	Remote	2.8	0.64	1.5	0.27	2.0	0.31	0.23	1.02	0.86
43	Remote	2.0	0.35	0.85	0.15	1.1	0.17	0.15	0.66	0.53
44	Remote	2.3	0.36	0.86	0.15	1.1	0.17	0.14	0.59	0.49
45	Remote	1.5	0.35	0.83	0.14	0.83	0.17	0.10	0.43	0.38
46	Remote	2.5	0.35	0.83	0.14	1.3	0.16	0.14	0.75	0.65
47	Remote	4.3	0.51	1.2	0.21	1.9	0.24	0.25	1.1	0.82
48	Remote	5.0	0.69	1.7	0.29	2.4	0.34	0.25	1.1	1.1
49	Remote	5.0	0.61	1.5	0.26	2.4	0.30	0.38	1.3	1.0
50	Remote	2.2	0.36	0.85	0.15	1.2	0.17	0.15	0.59	0.53
51	Remote	1.4	0.37	0.87	0.15	0.78	0.17	0.12	0.42	0.40
52	Remote	5.1	0.68	1.6	0.28	2.2	0.33	0.31	1.2	1.0
53	Remote	1.8	0.37	0.87	0.15	0.90	0.17	0.14	0.49	0.41
54	Remote	b	b	b	b	b	b	b	b	b
55	Remote	b	b	b	b	b	b	b	b	b
96	Pristine	1.3	0.29	1.0	1.2	1.4	1.4	0.17	1.0	0.94
97	Pristine	n.a.	n.a.	n.a.	n.a.	n.a.	n.a.	n.a.	n.a.	n.a.

[a] Analytical error. Excluded.

[b] Excluded due to unknown amount of internal standard, high recovery % and unexepectedly low concentrations.

n.a. = Not analyzed

Table SI-2.2b. Concentrations in air (pg/m^3) for all target OCPs at the individual sites (continued). Concentrations below MDL set to ½ MDL (grey).

Site No.	Type:	Chlordene	Heptachlor	trans-Nonachlor	cis-Nonachlor	Endosulfan-I	Endosulfan-II	Endosulfan-sulphate	Trifluralin	Mirex
1	Urban	19	33	2.6	11	7.8	16	18	5.7	4.6
2	Urban	15	28	2.1	8.6	6.2	13	14	4.7	3.6
3	Urban	15	28	2.1	8.6	6.2	13	14	4.7	3.6
4	Urban	16	30	2.3	9.5	6.8	14	16	5.1	4.0
5	Urban	16	30	2.2	9.3	6.7	14	15	5.0	3.9
6	Urban	20	35	2.8	12	8.4	18	20	6.1	5.0
7	Urban	18	32	2.5	11	7.5	16	17	5.5	4.4
8	Urban	19	34	2.7	11	7.9	16	18	5.8	4.6
9	Urban	20	36	2.9	12	8.5	18	20	6.1	5.0
10	Urban	14	27	1.9	8.0	5.8	12	13	4.5	3.3
11	Remote	0.17	0.35	0.64	0.12	2.65	0.22	0.17	0.07	0.11
12	Remote	0.28	0.39	0.63	0.03	1.2	0.20	0.15	0.10	0.16
13	Remote	0.26	0.36	0.42	0.03	0.90	0.19	0.14	0.10	0.15
14	Remote	0.20	0.29	0.52	0.02	1.0	0.14	0.10	0.08	0.11
15	Remote	0.14	0.22	1.0	0.12	1.5	0.10	0.08	0.06	0.08
16	Remote	0.19	0.27	0.65	0.02	1.2	0.13	0.17	0.07	0.11
17	Remote	0.23	0.32	0.80	0.13	1.4	0.16	0.12	0.08	0.13
18	Remote	0.20	0.29	0.30	0.02	0.69	0.15	0.45	0.08	0.11
19	Remote	0.20	0.29	0.63	0.13	2.8	0.14	0.30	0.08	0.11
20	Remote	0.18	0.27	0.86	0.18	3.2	0.13	0.10	0.07	0.10
21	Remote	0.20	0.28	0.27	0.02	1.2	0.14	0.10	0.07	0.11
22	Remote	0.20	0.28	0.37	0.02	1.6	0.14	0.10	0.07	0.11
23	Remote	0.21	0.29	0.32	0.02	1.2	0.15	0.11	0.08	0.11
24	Remote	0.21	0.29	0.56	0.02	2.4	0.15	0.11	0.08	0.11
25	Remote	0.22	0.31	1.0	0.24	3.8	0.15	0.11	0.08	0.12
26	Remote	0.07	0.15	1.9	0.35	6.4	0.16	0.04	0.04	0.27
27	Remote	0.21	0.31	0.52	0.12	1.7	0.15	0.27	0.08	0.12
28	Remote	n.a.	n.a.	n.a.	n.a.	n.a.	n.a.	n.a.	n.a.	n.a.
29	Remote	0.21	0.30	0.42	0.09	1.3	0.15	0.11	0.08	0.11
30	Remote	0.21	0.29	0.35	0.07	1.4	0.15	0.11	0.08	0.11
31	Remote	0.18	0.26	0.49	0.11	2.3	0.13	0.09	0.07	0.10
32	Remote	0.21	0.30	0.60	0.13	2.6	0.15	0.11	0.08	0.12
33	Remote	0.27	0.37	0.80	0.13	2.8	0.19	0.14	0.10	0.15
34	Remote	0.21	0.29	0.56	0.10	2.2	0.15	0.11	0.08	0.11
35	Remote	0.29	0.40	0.97	0.17	3.3	0.21	0.15	0.11	0.16
36	Remote	0.21	0.31	0.39	0.06	1.5	0.15	0.11	0.08	0.12
37	Remote	0.21	0.31	0.37	0.06	1.3	0.15	0.11	0.08	0.12
38	Remote	0.26	0.36	0.92	0.13	4.3	0.19	0.14	0.10	0.15
39	Remote	0.21	0.30	0.67	0.14	3.4	0.15	0.11	0.08	0.12
40	Remote	0.21	0.30	0.38	0.06	1.8	0.15	0.11	0.08	0.11
41	Remote	0.20	0.28	0.51	0.08	2.3	0.14	0.11	0.08	0.11
42	Remote	0.39	0.51	0.92	0.13	4.6	0.66	0.20	0.14	0.22
43	Remote	0.21	0.30	0.59	0.09	2.6	0.15	0.11	0.08	0.11
44	Remote	0.21	0.31	0.49	0.08	1.6	0.15	0.11	0.08	0.11
45	Remote	0.21	0.29	0.39	0.05	1.6	0.15	0.24	0.08	0.11
46	Remote	0.20	0.29	0.65	0.11	2.9	0.14	0.11	0.08	0.11
47	Remote	0.30	0.41	0.93	0.11	3.0	0.22	0.16	0.25	0.17
48	Remote	0.42	0.55	1.1	0.14	3.7	0.30	0.22	0.15	0.24
49	Remote	0.37	0.49	1.1	0.14	3.7	0.26	0.19	0.13	0.21
50	Remote	0.21	0.30	0.55	0.08	2.2	0.15	0.11	0.08	0.11
51	Remote	0.21	0.31	0.39	0.05	1.4	0.15	0.11	0.08	0.12
52	Remote	0.41	0.54	1.0	0.14	3.5	0.29	0.21	0.14	0.23
53	Remote	0.21	0.31	0.42	0.05	1.4	0.15	0.11	0.08	0.11
54	Remote	b	b	b	b	b	b	b	b	b
55	Remote	b	b	b	b	b	b	b	b	b
96	Pristine	0.18	0.24	0.75	0.16	3.5	0.17	0.13	0.06	0.10
97	Pristine	n.a.	n.a.	n.a.	n.a.	n.a.	n.a.	n.a.	n.a.	n.a.

[a] Analytical error. Excluded.

[b] Excluded due to unknown amount of internal standard, high recovery % and unexepectedly low concentrations.

n.a. = Not analyzed

Table SI-2.2b. Concentrations in air (pg/m^3) for all target OCPs at the individual sites (continued). Concentrations below MDL set to ½ MDL (grey).

Site No.	Type:	PeCB	HCB	a-HCH	β-HCH	g-HCH	o.p'-DDE	p,p'-DDE	o,p'-DDD	p,p'-DDD	o,p'-DDT
1	Urban	17	73	4.1	6.1	12	0.38	3.1	0.43	0.44	0.50
2	Urban	14	68	3.4	4.8	3.4	0.30	1.2	0.34	0.35	0.39
3	Urban	11	45	3.4	4.8	3.4	0.29	0.89	0.34	0.34	0.39
4	Urban	15	58	3.7	5.3	12	0.33	3.5	0.38	0.38	1.4
5	Urban	29	85	3.6	5.2	a	0.32	3.9	0.37	0.37	1.8
6	Urban	23	70	4.3	6.6	11	0.40	1.4	0.46	0.47	0.53
7	Urban	19	76	4.0	5.9	8.2	0.36	2.7	0.42	0.42	0.47
8	Urban	16	73	4.1	6.2	10	0.38	2.5	0.44	0.44	1.1
9	Urban	17	71	4.3	6.6	9.7	0.41	1.2	0.47	0.48	0.54
10	Urban	14	65	8.0	4.5	10	0.27	2.9	0.32	0.32	1.3
11	Remote	28	88	8.5	0.14	1.7	0.06	0.34	0.02	0.05	0.11
12	Remote	25	99	8.1	0.27	1.7	0.04	0.35	0.02	0.08	0.20
13	Remote	24	81	5.8	0.21	1.4	0.04	0.20	0.02	0.07	0.13
14	Remote	25	78	6.5	0.16	1.4	0.03	0.24	0.03	0.06	0.14
15	Remote	25	85	8.2	0.25	2.0	0.07	0.50	0.06	0.04	0.26
16	Remote	n.a.	n.a.	7.4	0.15	1.5	0.03	0.25	0.03	0.05	0.17
17	Remote	n.a.	n.a.	8.4	0.19	1.6	0.03	0.33	0.04	0.07	0.19
18	Remote	n.a.	n.a.	4.9	0.16	1.1	0.03	0.14	0.01	0.06	0.08
19	Remote	22	75	7.5	0.16	1.8	0.03	0.26	0.01	0.06	0.15
20	Remote	22	90	8.1	0.15	1.7	0.03	0.31	0.03	0.05	0.18
21	Remote	17	54	3.8	0.16	1.1	0.03	0.14	0.01	0.06	0.07
22	Remote	20	60	4.9	0.16	1.1	0.03	0.16	0.01	0.06	0.10
23	Remote	18	54	4.3	0.17	1.2	0.03	0.15	0.01	0.06	0.08
24	Remote	19	64	5.5	0.16	1.5	0.03	0.22	0.01	0.06	0.12
25	Remote	22	92	8.2	0.18	2.2	0.03	0.45	0.04	0.06	0.18
26	Remote	23	73	13	0.19	4.3	0.08	0.74	0.06	0.02	0.30
27	Remote	20	67	5.8	0.17	1.6	0.03	0.24	0.03	0.06	0.09
28	Remote	21	71	7.4	0.17	2.3	0.03	0.44	0.04	0.06	0.19
29	Remote	17	52	4.3	0.17	1.4	0.03	0.25	0.01	0.06	0.10
30	Remote	16	55	5.1	0.17	1.3	0.03	0.16	0.01	0.06	0.07
31	Remote	18	70	6.0	0.14	1.7	0.02	0.20	0.03	0.05	0.13
32	Remote	18	77	6.6	0.17	2.2	0.03	0.28	0.01	0.06	0.15
33	Remote	19	83	7.1	0.22	2.0	0.04	0.29	0.02	0.08	0.16
34	Remote	23	76	3.7	0.17	1.0	0.03	0.14	0.01	0.06	0.06
35	Remote	19	81	8.4	0.23	2.8	0.04	0.53	0.08	0.08	0.25
36	Remote	20	57	4.7	0.17	1.4	0.03	0.23	0.01	0.06	0.11
37	Remote	19	53	4.4	0.17	1.4	0.03	0.22	0.01	0.06	0.10
38	Remote	21	85	8.4	0.21	4.3	0.04	0.76	0.02	0.07	0.37
39	Remote	20	69	7.1	0.17	3.4	0.03	0.55	0.03	0.06	0.26
40	Remote	18	52	4.4	0.17	2.7	0.03	0.48	0.01	0.06	0.18
41	Remote	17	57	5.4	0.16	2.6	0.03	0.40	0.01	0.06	0.21
42	Remote	18	83	8.2	0.31	6.5	0.05	0.54	0.02	0.11	0.31
43	Remote	23	77	6.3	0.17	2.7	0.03	0.72	0.01	0.06	0.33
44	Remote	21	66	5.1	0.17	3.0	0.03	0.62	0.03	0.06	0.16
45	Remote	16	55	4.3	0.17	2.4	0.03	1.2	0.01	0.06	0.21
46	Remote	22	75	6.4	0.16	3.3	0.03	0.59	0.03	0.06	0.18
47	Remote	20	78	8.3	0.24	5.8	0.14	1.3	0.04	0.09	0.33
48	Remote	25	103	9.7	0.34	7.4	0.06	1.9	0.06	0.12	0.57
49	Remote	22	85	8.8	0.30	7.1	0.08	1.9	0.07	0.11	0.73
50	Remote	22	61	5.5	0.17	3.7	0.03	0.67	0.01	0.06	0.28
51	Remote	24	61	4.7	0.17	2.7	0.03	0.55	0.01	0.06	0.18
52	Remote	26	101	8.4	0.33	6.4	0.06	2.6	0.07	0.12	1.1
53	Remote	23	57	4.2	0.17	2.7	0.03	0.72	0.03	0.06	0.23
54	Remote	23	52	3.6	0.33	2.7	0.03	0.55	0.01	0.06	0.12
55	Remote	24	64	4.9	0.17	3.6	0.03	0.81	0.01	0.06	0.24
96	Pristine	38	130	12	0.14	1.7	0.02	0.14	0.01	0.05	0.07
97	Pristine	31	136	n.a.	n.a.	n.a.	n.a.	n.a.	n.a.	n.a.	n.a.

a Analytical error. Excluded.

b Excluded due to unknown amount of internal standard, high recovery % and unexepectedly low concentrations.

n.a. = Not analyzed

Table SI-2.3. Literature data of background concentrations in air with PAS

	Kalina et al. 2018	Kurt-Karakus et al. 2018	Gioia et al. 2007	Halse et al. 2011	Jaward et al. 2004	Pozo et al. 2009
Study area	Czech Republic. n = 13	Turkey. n = 16 (rural only)	Northern Europe (Ireland, UK, Norway, Denmark, Sweden, Finland, Russia) n=23	Europe, 35 countries. n=96	Europe, 22 countries. n=40 (rural/remote only)	Globally, 17 countries. n=23 (background only)
Study period	2015 (July-Sep.)	2014 (Aug.-Oct.)	2004 (Aug.-Oct.)	2006 (July-Oct.)	2002 (June/July)	2005 (June-Sep.)
Sum 6 PCB	11 - 60 ng/m³	5.6 - 47 pg/m³ [f]	13 - 32 pg/m³ [ab]	2 - 121 pg/m³ [c]	1.0 - 33 pg/m³ [d]	< MDL - 702 pg/m³ [e]
HCB	43 - 76 pg/m³	19 - 1261 pg/m³	39 - 61 pg/m³ [b]	23 - 115 pg/m³	1.4 - 8.9 pg/m³	
a-HCH	6 - 16 pg/m³	< MDL - 482 [g]		5 - 156 pg/m³	1.7 - 10 pg/m³	< MDL - 55 pg/m³
g-HCH	8 - 20 pg/m³			1.8 - 170 pg/m³	1.1 - 65 pg/m³	< MDL - 56 pg/m³
p,p'-DDE	9 - 129 pg/m³	18 - 1666 pg/m³ [g]		< MDL - 281 pg/m³	0.05 - 1.5 pg/m³	< MDL - 137 pg/m³
o,p'-DDT				< MDL - 39 pg/m³		
p,p'-DDT				< MDL - 46 pg/m³	0.08 - 11 pg/m³	
cis-Chlordane				< MDL - 4.6 pg/m³	0.05 - 1.4 pg/m³	< MDL - 39 pg/m³
trans-Chlordane				< MDL - 7.3 pg/m³	0.05 - 1.3 pg/m³	< MDL - 41 pg/m³
trans-Nonachlor				< MDL - 7.0 pg/m³		< MDL - 47 pg/m³
cis-Nonachlor				< MDL - 0.5 pg/m³		
Heptachlor		7 - 389 pg/m³ [g]				< MDL
Heptachlor-epoxide						< MDL - 46 pg/m³
Endosulfan-I		12 - 303 pg/m³ [g]				2 - 491 pg/m³
Endosulfan-II						< MDL - 103 pg/m³
Endosulfan-sulphate						< MDL - 8 pg/m³
Comments:		[f] PCB118 additionally. [g]Sum of OCPs, i.e. sum of a-, b-, g,- d-HCH, sum of (o,p'-DDT, -DDD, -DDE) and (p,p'-DDT, -DDD, -DDE), sum of heptachlor and heptachlor-epoxide, sum of endosulfan-I, -II and - sulphate respectively.	[a] PCB118 instead of PCB138. Coelution PCB90/101. [b] Limited to Denmark, Finland, Norway, UK.	[c] PCB118 additionally.	[d] Coelution PCB90/101 and PCB153/132.	[e] Sum 48 PCB only available.

Table SI-2.4 Comparison of MMRs at six selected sites (Oslo excluded) between 2006 and 2016.

Site	MMR 2006	MMR 2016
Sum 6 PCB	4	3
PCB28	3	3
PCB153	11	5
HCB	3	2
Sum 3 DDX	2	15
op/pp-DDT	2	2
pp-DDT/-DDE	10	1
a-HCH	3	2
g-HCH	4	4
Sum 2 HCH	2	2
a/g-HCH	6	6
Sum CD	3	2
trans/cis-CD	5	2

Table SI-2.5. Comparison of concentrations in air obtained from PAS with concentrations in air obtained from AAS (Bohlin-Nizzetto et al., 2017), at the Norwegian monitoring sites during the same time period (Table SI-1.1). Except PCB-47 and the tri-tetra-CB at Zeppelin, PAS generally overestimates the concentrations in air (i.e. negative deviation values).

PCB congener:	Birkenes (site 49)			Andøya (site 26)			Zeppelin (site 96)			MMR Birkenes/Andøya	
	PAS	AAS	Deviation	PAS	AAS	Deviation	PAS	AAS	Deviation	PAS	AAS
	pg/m³	pg/m³	%	pg/m³	pg/m³	%	pg/m³	pg/m³	%	pg/m³	pg/m³
18	1.74ᵃ	0.019		1.28	0.313	-308 %	0.935	3.89	76 %		
28	1.13	0.716	-58 %	0.745	0.276	-170 %	0.633	3.48	82 %	1.5	2.6
31	1.10	0.644	-71 %	0.827	0.250	-231 %	0.611	3.32	82 %		
33	0.539	0.340	-58 %	0.347	0.126	-176 %	0.353	2.58	86 %		
37	0.109	0.065	-68 %	< MDL	0.019		0.070	0.328	79 %		
47	0.559	1.23	55 %	0.347	0.753	54 %	0.204	0.566	64 %		
52	1.63	0.928	-76 %	1.36	0.346	-292 %	0.632	1.08	42 %		
66	0.407	0.231	-76 %	0.170	0.071	-139 %	0.147	0.217	32 %		
74	0.316	0.162	-95 %	0.171	0.053	-223 %	0.119	0.157	24 %		
99	0.340	0.178	-92 %	0.281	0.070	-304 %	0.126	0.087	-46 %		
101	1.20	0.598	-101 %	0.834	0.209	-299 %	0.333	0.269	-24 %		
105	0.080	0.038	-113 %	0.057	0.013	-352 %	0.030	0.015	-95 %		
138	0.468	0.208	-125 %	0.322	0.067	-378 %	0.102	0.048	-112 %		
141	0.117	0.065	-80 %	0.059	0.017	-241 %	< MDL	0.012			
149	0.963	0.430	-124 %	0.626	0.140	-348 %	0.189	0.107	-76 %		
153	0.773	0.381	-103 %	0.515	0.117	-340 %	0.145	0.077	-90 %	1.5	3.3
180	0.127	0.065	-95 %	0.101	0.018	-473 %	0.021	0.010	-103 %		
187	0.201	0.081	-150 %	0.126	0.028	-350 %	0.033	0.015	-122 %		
Sum 6 PCB	5.33	2.90	-84 %	3.87	1.03	-275 %	1.87	4.97	62 %	1.4	2.8
Sum 18 PCB	10.1	6.38	-58 %	8.16	2.88	-183 %	4.68	16.3	71 %	1.2	2.2
HCB	85.0	45.3	-88 %	72.8	19.2	-279 %	130	81.2	-60 %	1.2	2.4
α-HCH	8.90	5.74	-55 %	12.7	3.40	-274 %	12.3	5.45	-125 %	0.7	1.7
γ-HCH	7.01	3.96	-77 %	4.32	1.11	-290 %	1.73	0.773	-124 %	1.6	3.6
o,p'-DDD	0.072	0.028	-156 %	0.060	0.010	-500 %	< MDL	0.007		1.2	2.8
o,p'-DDE	0.104	0.053	-96 %	0.084	0.024	-252 %	< MDL	0.011		1.2	2.2
o,p'-DDT	0.776	0.303	-156 %	0.299	0.074	-302 %	0.073	0.033	-121 %	2.6	4.1
p,p'-DDD	< MDL	0.018		< MDL	0.006		< MDL	0.007			3.1
p,p'-DDE	1.97	0.854	-131 %	0.736	0.155	-373 %	0.142	0.051	-178 %	2.7	5.5
p,p'-DDT	0.955	0.343	-178 %	0.185	0.054	-241 %	< MDL	0.019		5.2	6.3
Sum 3 DDX	3.70	1.50	-147 %	1.22	0.284	-329 %	0.215	0.103	-108 %	3.0	5.3

ᵃ Analytical error

32

Table SI-2.6. Contributions (in %) from secondary emissions (re-emission from surface compartments) and primary anthropogenic emissions nationally and of selected EMEP countries, as well as other sources within/outside the EMEP domain, predicted by GLEMOS for all sampling sites.

Site No.	Site	Secondary	Start	Norway	Belgium	Germany	Denmark	Finland	France	UK	Netherlands	Russia	Sweden	Other EMEP	Non-EMEP
1	Bærum	77 %	0 %	15 %	0 %	1 %	0 %	0 %	1 %	2 %	0 %	0 %	0 %	0 %	3 %
2	Holmenkollen	77 %	0 %	15 %	0 %	1 %	0 %	0 %	1 %	2 %	0 %	0 %	0 %	0 %	3 %
3	Maridalen	77 %	0 %	15 %	0 %	1 %	0 %	0 %	1 %	2 %	0 %	0 %	0 %	0 %	3 %
4	Skøyen	76 %	0 %	17 %	0 %	1 %	0 %	0 %	1 %	2 %	0 %	0 %	0 %	0 %	3 %
5	Sofienbergparken	76 %	0 %	16 %	0 %	1 %	0 %	0 %	1 %	2 %	0 %	0 %	0 %	0 %	2 %
6	Alnabru	76 %	0 %	16 %	0 %	1 %	0 %	0 %	1 %	2 %	0 %	0 %	0 %	0 %	2 %
7	Gamle Oslo	76 %	0 %	16 %	0 %	1 %	0 %	0 %	1 %	2 %	0 %	0 %	0 %	0 %	2 %
8	Botanisk hage	76 %	0 %	16 %	0 %	1 %	0 %	0 %	1 %	2 %	0 %	0 %	0 %	0 %	2 %
9	Dronningparken	76 %	0 %	17 %	0 %	1 %	0 %	0 %	1 %	1 %	0 %	0 %	0 %	0 %	2 %
10	Kjeller	79 %	0 %	13 %	0 %	1 %	0 %	0 %	1 %	2 %	0 %	0 %	1 %	0 %	3 %
11	Grøtfjord	76 %	0 %	4 %	0 %	1 %	0 %	1 %	1 %	2 %	0 %	0 %	0 %	0 %	15 %
12	Karpdalen	88 %	0 %	1 %	0 %	0 %	0 %	1 %	0 %	1 %	0 %	3 %	0 %	0 %	6 %
13	Neiden	90 %	0 %	1 %	0 %	0 %	0 %	2 %	0 %	0 %	0 %	2 %	0 %	0 %	4 %
14	Ekkerøy	89 %	0 %	1 %	0 %	0 %	0 %	1 %	0 %	1 %	0 %	1 %	0 %	0 %	6 %
15	Vardø	85 %	0 %	0 %	0 %	0 %	0 %	1 %	1 %	1 %	0 %	1 %	0 %	0 %	9 %
16	Vestertana	88 %	0 %	1 %	0 %	0 %	0 %	3 %	0 %	1 %	0 %	0 %	0 %	0 %	6 %
17	Hopseidet	86 %	0 %	0 %	0 %	1 %	0 %	2 %	1 %	1 %	0 %	0 %	0 %	0 %	8 %
18	Lakselv	86 %	0 %	1 %	0 %	1 %	0 %	5 %	1 %	1 %	0 %	0 %	0 %	0 %	6 %
19	Karasjok	89 %	0 %	0 %	0 %	0 %	0 %	5 %	0 %	0 %	0 %	0 %	0 %	0 %	4 %
20	Slåtten	85 %	0 %	1 %	0 %	1 %	0 %	1 %	1 %	1 %	0 %	0 %	0 %	0 %	9 %
21	Kvænangsbotn	79 %	0 %	1 %	0 %	1 %	0 %	8 %	1 %	1 %	0 %	0 %	0 %	1 %	7 %
22	Tamokdalen	76 %	0 %	3 %	0 %	1 %	0 %	4 %	1 %	1 %	0 %	0 %	1 %	1 %	11 %
23	Øverbygd	77 %	0 %	4 %	0 %	1 %	0 %	2 %	1 %	1 %	0 %	0 %	1 %	1 %	10 %
24	Innhavet	77 %	0 %	3 %	0 %	1 %	0 %	0 %	1 %	1 %	0 %	0 %	1 %	1 %	12 %
25	Bø i Vesterålen	75 %	0 %	3 %	0 %	1 %	0 %	0 %	1 %	2 %	0 %	0 %	0 %	1 %	15 %
26	Andøya	73 %	0 %	3 %	0 %	1 %	0 %	0 %	1 %	2 %	0 %	0 %	1 %	1 %	17 %
27	Svolvær	79 %	0 %	3 %	0 %	1 %	0 %	0 %	1 %	2 %	0 %	0 %	0 %	1 %	11 %
28	Moskenes	74 %	0 %	1 %	1 %	1 %	0 %	0 %	2 %	3 %	0 %	0 %	0 %	1 %	16 %
29	Bodø	76 %	0 %	6 %	0 %	1 %	0 %	0 %	1 %	2 %	0 %	0 %	1 %	1 %	12 %
30	Øvrevatn	75 %	0 %	4 %	1 %	1 %	0 %	0 %	1 %	1 %	0 %	0 %	4 %	1 %	11 %
31	Balvatn	71 %	0 %	1 %	1 %	2 %	0 %	0 %	2 %	1 %	0 %	0 %	8 %	1 %	12 %
32	Junkerdal	76 %	0 %	3 %	0 %	1 %	0 %	0 %	1 %	1 %	0 %	0 %	4 %	1 %	11 %
33	Tustervatn	80 %	0 %	3 %	0 %	1 %	0 %	0 %	1 %	1 %	0 %	0 %	1 %	1 %	10 %
34	Namsvatn	82 %	0 %	1 %	0 %	1 %	0 %	0 %	1 %	1 %	0 %	0 %	2 %	1 %	9 %
35	Aglen	85 %	0 %	2 %	0 %	1 %	0 %	0 %	1 %	2 %	0 %	0 %	0 %	1 %	7 %
36	Momyra	83 %	0 %	2 %	1 %	2 %	0 %	0 %	2 %	2 %	0 %	0 %	0 %	1 %	8 %
37	Bjørndalselva	82 %	0 %	4 %	1 %	2 %	0 %	0 %	2 %	2 %	0 %	0 %	0 %	1 %	7 %
38	Hummelfjell	89 %	0 %	2 %	0 %	1 %	0 %	0 %	1 %	1 %	0 %	0 %	0 %	1 %	4 %
39	Valdalen	88 %	0 %	1 %	0 %	1 %	0 %	0 %	1 %	1 %	0 %	1 %	1 %	1 %	4 %
40	Osen	90 %	0 %	2 %	0 %	1 %	0 %	0 %	1 %	1 %	0 %	0 %	1 %	0 %	3 %
41	Lom	77 %	0 %	3 %	1 %	3 %	0 %	0 %	2 %	2 %	0 %	0 %	0 %	2 %	9 %
42	Kårvatn	82 %	0 %	3 %	0 %	2 %	0 %	0 %	2 %	1 %	0 %	0 %	1 %	1 %	7 %
43	Utvikfjellet	81 %	0 %	4 %	1 %	2 %	0 %	0 %	2 %	2 %	0 %	0 %	0 %	1 %	7 %
44	Furuneset	92 %	0 %	1 %	0 %	1 %	0 %	0 %	1 %	2 %	0 %	0 %	0 %	0 %	2 %
45	Ulvik	75 %	0 %	2 %	1 %	3 %	0 %	0 %	3 %	3 %	1 %	0 %	0 %	1 %	9 %
46	Vatnedal	76 %	0 %	1 %	1 %	4 %	0 %	0 %	3 %	4 %	1 %	0 %	0 %	1 %	8 %
47	Utbjoa	88 %	0 %	2 %	1 %	1 %	0 %	0 %	2 %	3 %	0 %	0 %	0 %	0 %	3 %
48	Ualand	85 %	0 %	1 %	1 %	2 %	0 %	0 %	3 %	4 %	1 %	0 %	0 %	0 %	3 %
49	Birkenes	83 %	0 %	2 %	1 %	2 %	1 %	0 %	2 %	3 %	1 %	0 %	0 %	0 %	3 %
50	Solhomfjell	84 %	0 %	2 %	1 %	2 %	1 %	0 %	2 %	3 %	1 %	0 %	0 %	1 %	4 %
51	Hvittingfoss	86 %	0 %	4 %	1 %	2 %	1 %	0 %	2 %	1 %	0 %	0 %	0 %	0 %	3 %
52	Prestebakke	85 %	0 %	2 %	0 %	1 %	1 %	0 %	1 %	2 %	0 %	0 %	6 %	0 %	2 %
53	Aremark	87 %	0 %	1 %	0 %	1 %	1 %	0 %	1 %	2 %	0 %	0 %	4 %	0 %	2 %
54	Aurskog	86 %	0 %	5 %	0 %	1 %	0 %	0 %	1 %	1 %	0 %	0 %	1 %	0 %	3 %
55	Hurdal	82 %	0 %	9 %	0 %	1 %	0 %	0 %	1 %	1 %	0 %	0 %	1 %	0 %	3 %
96	Svalbard (Zeppelin)	54 %	0 %	0 %	0 %	0 %	0 %	0 %	0 %	1 %	0 %	1 %	0 %	1 %	42 %
97	Svalbard (Erlingvatn)	54 %	0 %	0 %	0 %	0 %	0 %	0 %	0 %	2 %	0 %	1 %	0 %	1 %	42 %

Text/Figures:

2.1   The occurrence of POPs in Norway

2.1.1   PCB

Boxplot concentrations of the six indicator PCB congeners is given in Figure SI-2.1. Figures SI-2.2a-b show the spatial distribution of the volatile PCB-28 and PCB153 respectively in background air across Norway.
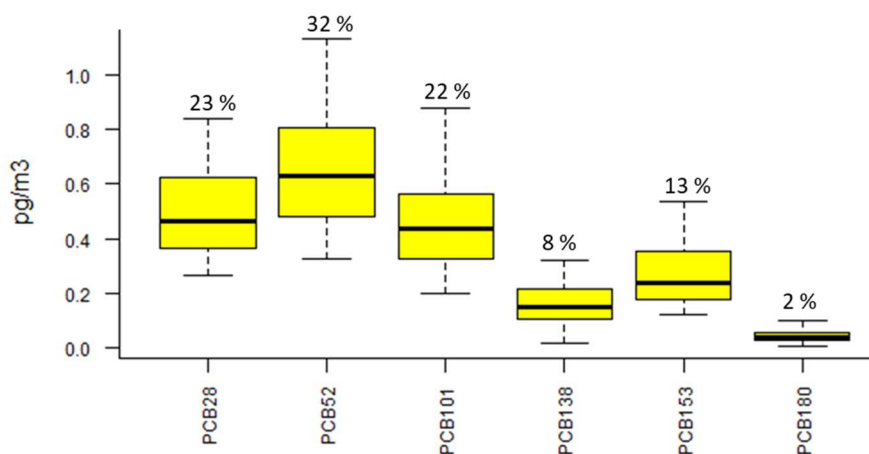
Figure SI-2.1 Boxplot concentrations of six selected PCB congeners in air (pg/m³) at Norwegian background sites (n = 44). Outliers are excluded. The average abundance of each congener given relative to ∑₆PCBs is indicated.
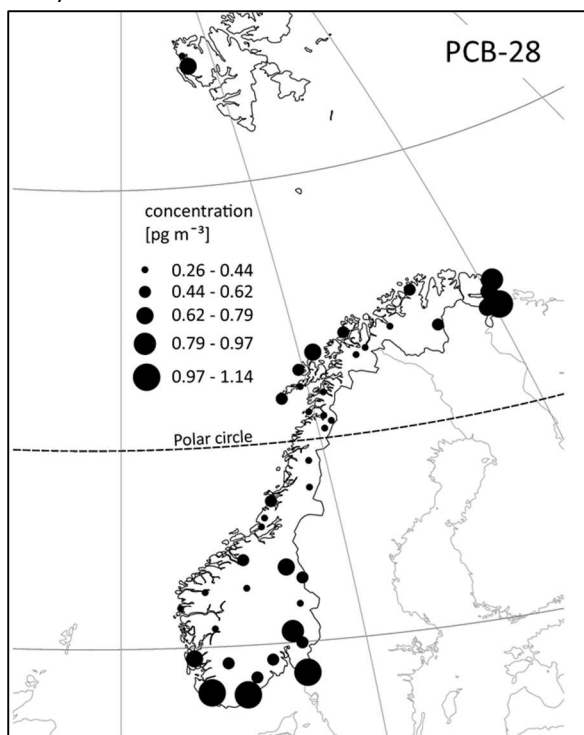
2.2a)   2.2b)
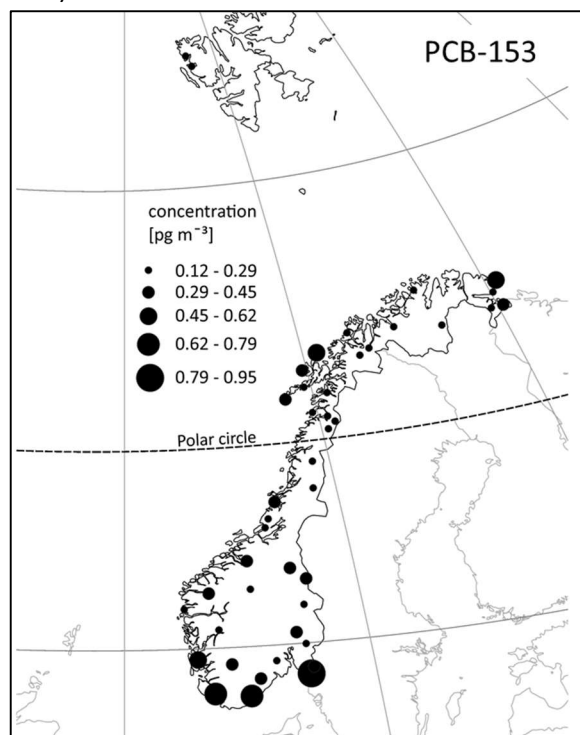
Figure SI-2.2a-b. The spatial distribution of concentrations of PCB28 and PCB153 in background air across Norway.

2.1.2 Latitudinal correlations

Figure SI-2.3 shows the trend of the selected POPs with latitude, as described in SI 1.6.3. In Figure SI-2.4 the correlation with latitude between 2006 and 2016 is compared, according to SI 1.6.6.

	Sum 18 PCB	PCB28	PCB153	HCB	a-HCH	g-HCH	Sum HCH	Sum DDX	Sum 4 CD	Dieldrin	HepX	Endo I
Correlation ρ	-0.33	-0.21	-0.46	0.41	0.27	-0.68	-0.12	-0.71	-0.02	-0.43	-0.29	-0.24
p-value	0.030	0.16	0.0016	0.0058	0.0700	< 0.001	0.43	< 0.001	0.92	0.004	0.06	0.12
Lin.reg R^2	0.11		0.21	0.17		0.47		0.51		0.18		
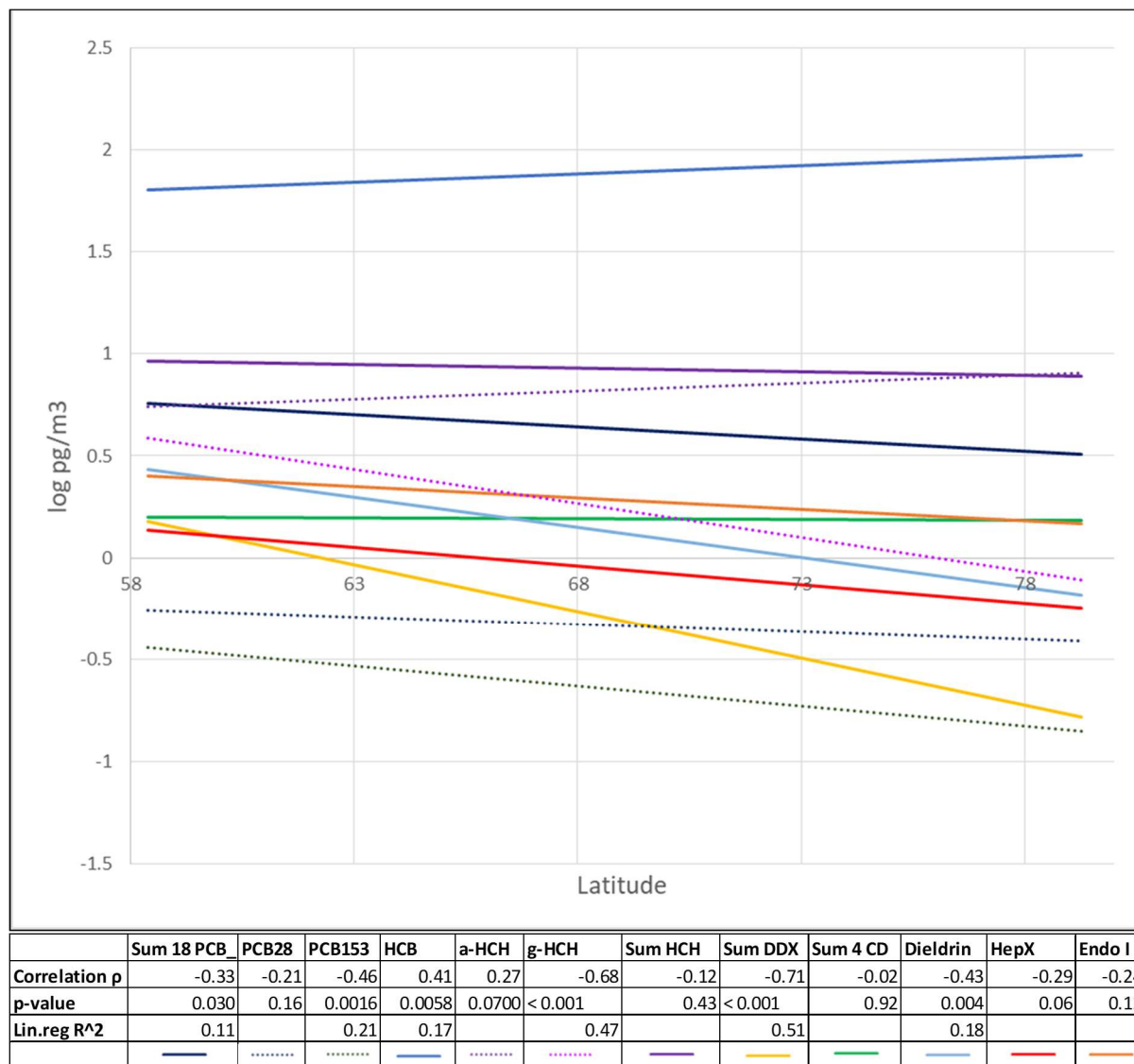
Figure SI-2.3. Linear correlation of log concentrations with latitude of selected compounds. CD = Chlordanes, Hepx = Heptachlor-exo-epoxide, Endo I = Endosulfan-I.
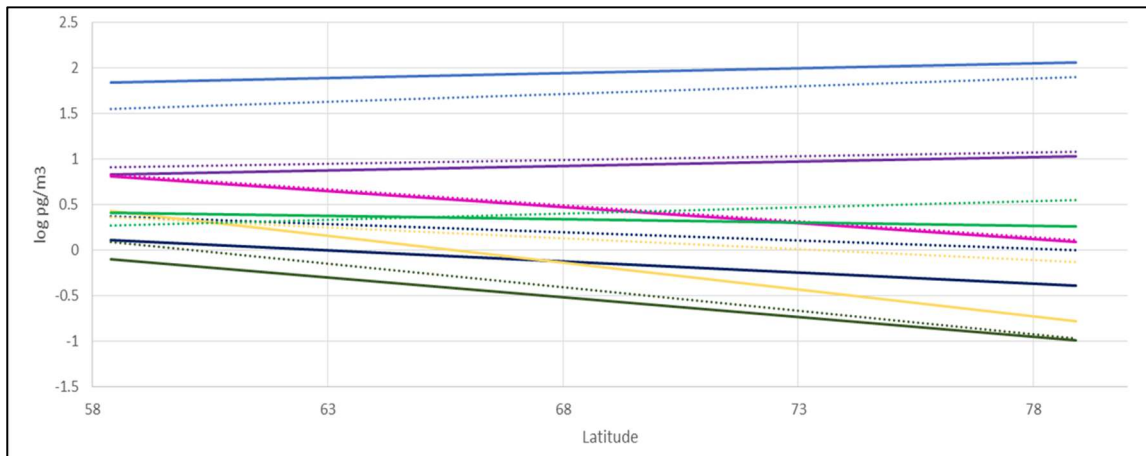
	PCB28	PCB153	HCB	a-HCH	g-HCH	Sum DDX	Sum 4 CD
p-value	0.84	0.81	0.42	0.89	1.00	0.11	0.17
2016:							
2006:							

Figure SI-2.4 Comparison of correlation of the logarithmic concentration with latitude between 2006 and 2016. P-values below 0.05 indicate there is a significant difference in the latitudinal gradient between 2006 and 2016.

2.1.3 Comparison with active air sampling (AAS)

Figures SI-2.5a–e show a simple comparison of concentrations of selected POPs in air obtained from PAS with concentrations in air obtained from AAS (Bohlin-Nizzetto et al., 2017). A more thorough comparison is given in Table SI-2.5.

2.5a)
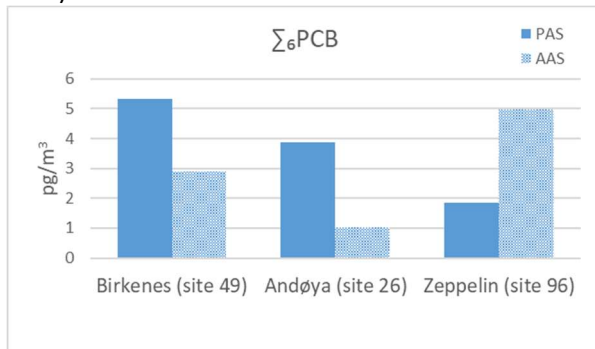
2.5b)
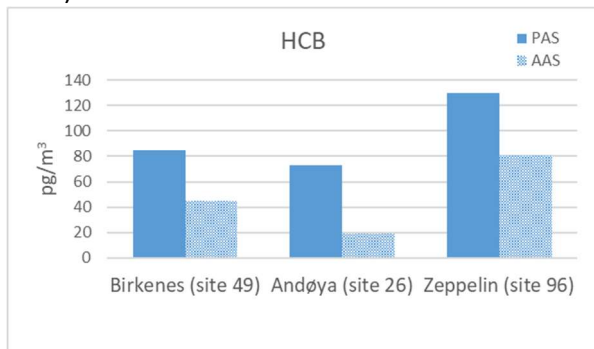
2.5c)
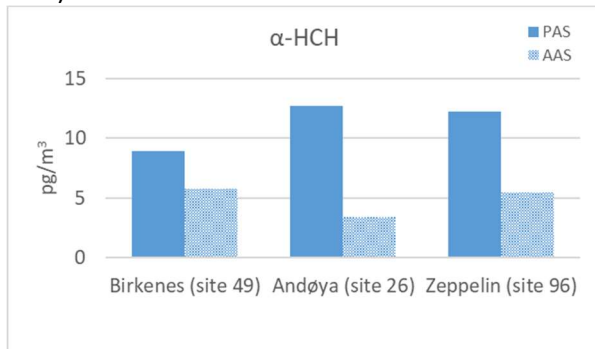
2.5d)
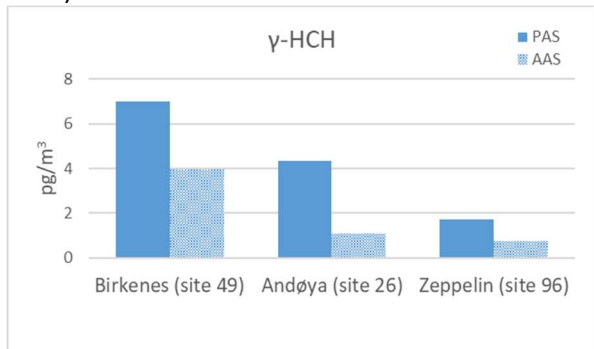
2.5e)
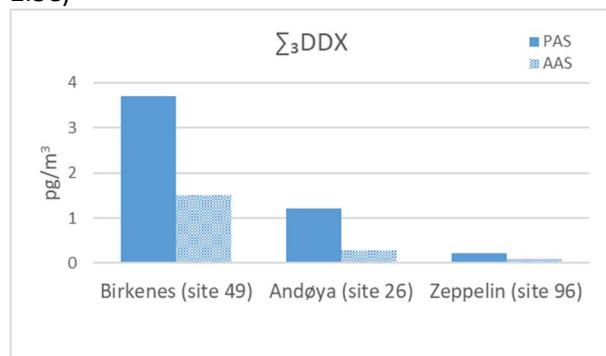
Figure SI-2.5 a-e. Comparison of concentrations in air of (a)PCBs, (b)HCB, (c)α-HCH, (d)γ-HCH and (e)DDXs obtained from PAS (blue), with concentrations in air obtained from AAS (blue dotted) (Bohlin-Nizzetto et al., 2017).

2.1.4   HCB and PeCB

Release of HCB has been suggested to continue due to by-production and usage of chlorinated compounds contaminated with HCB in some parts of the world (Hung et al., 2016). The highest concentrations of HCB and PeCB were found on Svalbard, almost two times the median, and indicated as outliers in the boxplot in Figure SI-2.6. The HCB concentration is two to three times higher than the average concentrations found in Europe (Halse et al., 2011; Aas & Bohlin-Nizzetto, 2018). Also PeCB is mostly associated with unintentional emissions, but less information is available on atmospheric concentrations. The concentrations found in the present study are in the same range as those measured in North America using XAD-based PAS (Shen et al., 2005).

In Figure SI-2.3, HCB is the only OCP that shows a significant positive correlation with latitude (p-value 0.0058, corr 0.41). By excluding the two elevated concentrations at Svalbard, the increasing trend is no longer significant (p-value 0.47, corr 0.11).
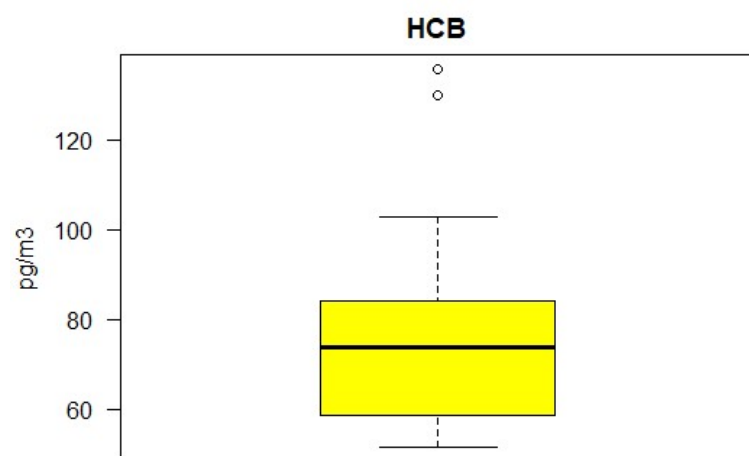
Figure SI-2.6. Boxplot concentrations of HCB at 44 sites. The two outliers from Svalbard are indicated with circles (> 120 pg/m^3).

2.1.5 HCHs

HCHs were used as insecticides, originally in a technical mixture of several isomers, containing 60-70 % α-HCH and 10-12 % γ-HCH, and later in lindane, consisting almost entirely of the γ-isomer (Li & Macdonald, 2005). As expected, α- and γ-HCH were the most abundant HCH-isomers, contributing 71 % and 29 % respectively to the average concentration. The average concentration of the sum of α- and γ-HCHs ($\sum_2$ HCHs) was 9 pg/m^3 (SD ± 3 pg/m^3), and in the same range as observed for other background areas (Hung et al., 2016; Pozo et al., 2009).
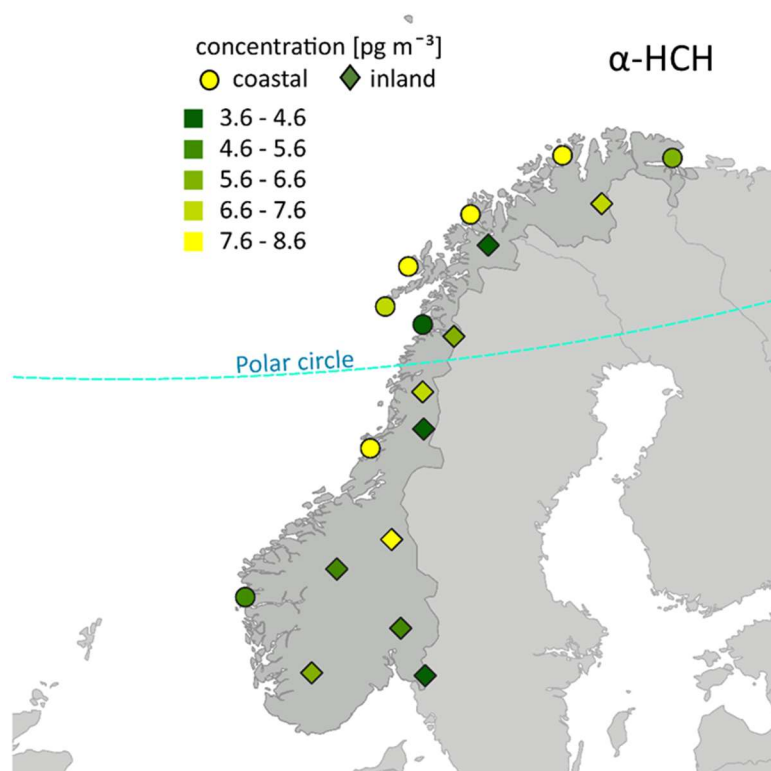
Figure SI-2.7. Concentrations of α-HCH in air at 8 coastal- (circles) and 10 inland (diamond) sites in Norway.

2.1.6 DDXs

DDT has been widely used as an insecticide in the past, but is now limited to use in control of malaria disease and as an intermediate in the production of Dicofol (UNECE, 1998). In the environment, DDT is converted to DDE and DDD, and DDX is a term to include both DDT and its metabolites. Technical DDT is composed of a mixture of isomers, with 75 % p,p'-DDT, 15 % o,p'-DDT and 5 % p,p'-DDE, and a dominance of these compounds are expected. The average concentration of sum p,p'-DDE, o,p'-DDT and p,p'-DDT ($\sum_3$ DDXs) in air at Norwegian background sites (0.9 ± 0.9 pg/m^3) was in agreement with levels found in the other studies (Table SI-2.3). The metabolite p,p'-DDE was the dominating compound (57 %), followed by its parent p,p'-DDT (20 %) and o,p'-DDT (23 %). The spatial distribution of $\sum_3$ DDXs across Norway is given in Figure SI-2.8.

While the high p,p'-DDE/p,p'-DDT ratio for all sampling sites indicates old sources of DDT, the ratio of the o,p'-DDT isomer compared to p,p'-DDT (0.8-1.8) may indicate influence of usage of the miticide Dicofol, which is on the proposal list under the Stockholm Convention. Dicofol is synthesized from DDT (Qiu et al., 2005) and has shown to have a higher content of the o,p'-DDT isomer compared to technical DDT (Qiu et al., 2005). It is worth noting that o,p'-DDT/p,p'-DDT ratio was correlated to latitude with significantly lower values observed in southern Norway (p-value < 0.001). This may indicate that the influence of Dicofol is stronger in northern Norway, or that there are differences in the LRAT potential of the two isomers.
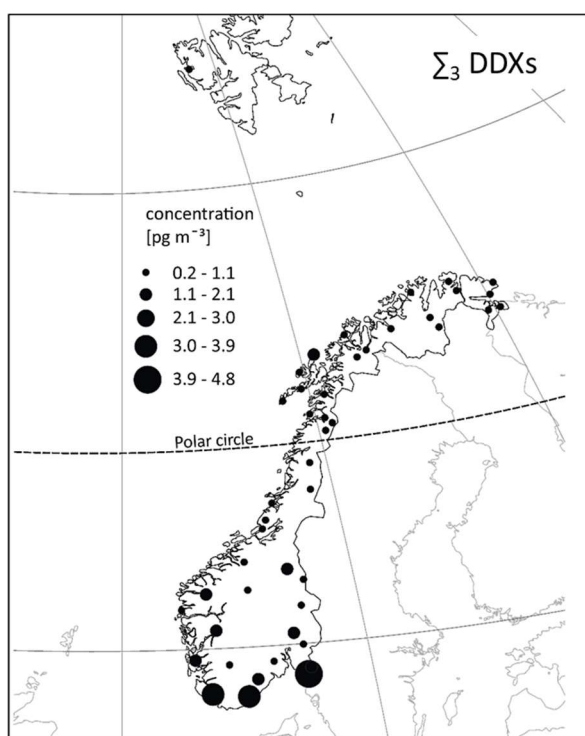
Figure SI-2.8 The spatial distribution of concentrations of sum 3 DDXs in background air across Norway.

2.1.7 Chlordanes

Technical Chlordane was widely used in agriculture and in control of termites, ants and others. The insecticide consists mainly of cis- and trans-Chlordane (19 % and 24 % respectively), but contains also Heptachlor and trans-Nonachlor in reasonable amounts (both 7 %) (Dearth & Hites, 1991; Sovocool et al., 1977). Heptachlor has additionally been used in an independent technical mixture. In our study, five Chlordane-related compounds were detected in more than 60 % of the samples, i.e. trans-/cis-Chlordane (trans-/cis-CD), Oxy-Chlordane, trans-/cis-Nonachlor (trans-/cis-NO) and Heptachlor-exo-epoxide (HepX). The spatial distribution of $\sum_4$ Chlordanes across Norway is given in Figure SI-2.9a. Despite being banned for many years, Chlordanes were found in air at the Norwegian

background sites, with an average concentration of $\sum_4$ Chlordanes ($\sum$ trans/cis-Chlordane and trans/cis-Nonachlor) of 1.7 ± 0.8 pg/m^3. Cis-Chlordane and trans-Nonachlor were the most dominant compounds, accounting for 46 % and 38 % respectively of $\sum_4$ Chlordanes. These values are consistent with the other studies (Table SI-2.3) and remarkably similar to the concentrations found under AMAP (Bohlin-Nizzetto et al., 2017). While Heptachlor-exo-epoxide were among the OCPs with highest measured levels (1.2 ± 0.7 pg/m^3), Oxy-Chlordane was detected in comparable levels to cis-Chlordane and trans-Nonachlor (0.7 ± 0.3 pg/m^3). Despite relatively high concentrations, both compounds were only 2-3 times higher than the MDL and are in the same range as found in background areas (Hung et al., 2016; Pozo et al., 2009). Heptachlor, Heptachlor-endo-epoxide and Chlordene were not detected.

While the Chlordanes showed no latitudinal gradient (Figure SI-2.3), the metabolite Heptachlor-exo-epoxide showed a slightly declining trend with latitude (corr -0.29). However, there was no significant difference between the southern- and northern levels (p-value 0.12). The spatial distribution of Heptachlor-exo-epoxide across Norway is given in Figure SI-2.9b.
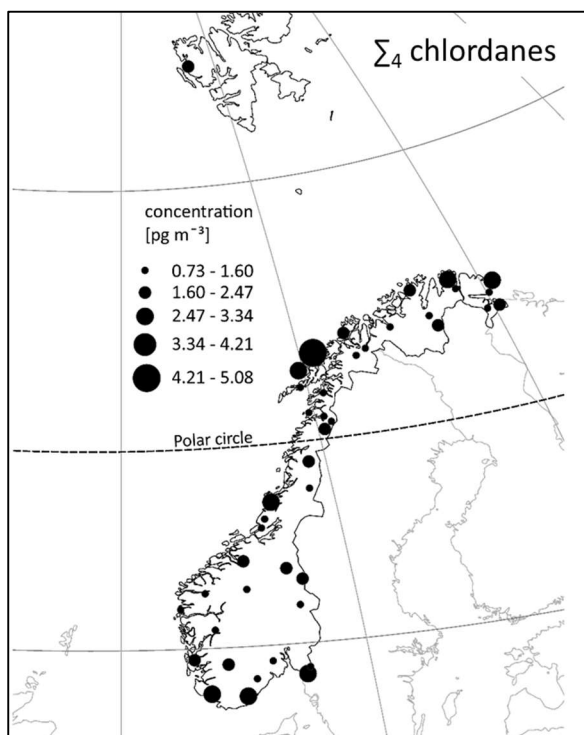
2.9 a)   2.9 b)
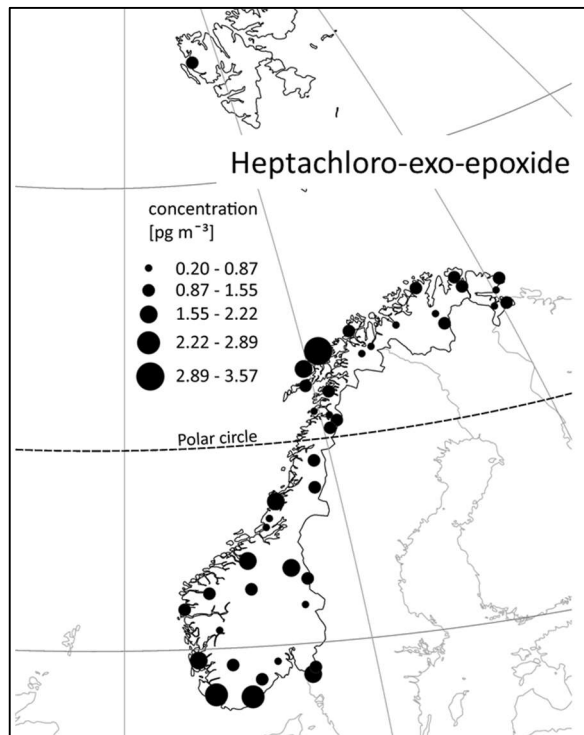
Figure SI-2.9 a-b. The spatial distribution of concentrations of sum 4 Chlordanes and the metabolite Heptachlor-exo-epoxide in background air across Norway

2.1.8 Endosulfans

Endosulfan was widely used throughout the world (Li & Macdonald, 2005; Weber et al., 2010) until its regulation in 2011, and elevated concentrations in air in areas with agricultural activity have been reported by Pozo et al. (2006) and Harner et al. (2004). In our study, Endosulfan I was also detected (Figure SI-2.10), but in much lower concentrations (2 ± 1 pg/m^3) compared to the previous studies (Table SI-2.3). The degradation product Endosulfan sulphate was detected only in a limited number of samples (7 %).
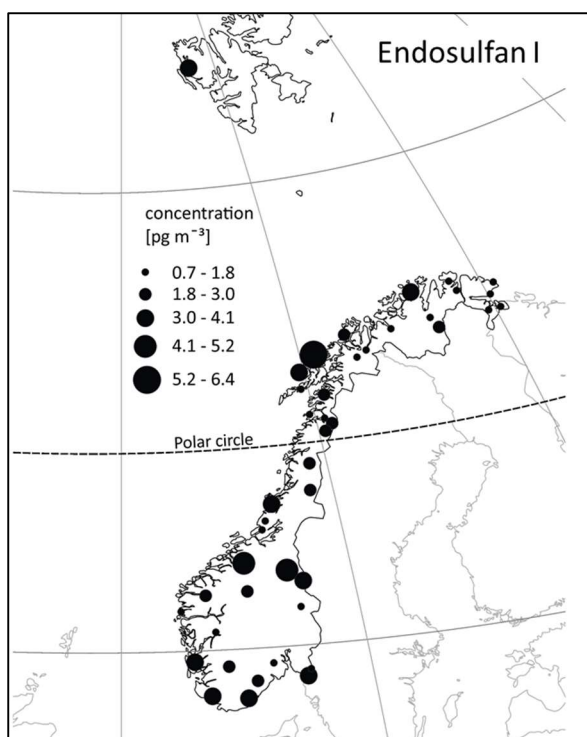
Figure SI-2.10 The spatial distribution of concentrations of Endosulfan I in background air across Norway.

2.1.9 Dieldrin

The spatial distribution of the insecticide Dieldrin across Norway is given in Figure SI-2.11, and was measured at comparable levels to Endosulfan I (2 ± 1 pg/m^3). Dieldrin is also a degradation product of Aldrin. The concentrations found were in the lower range of what Pozo et al. (2009) reported globally and in the same range as found in the Arctic (Hung et al., 2016). Aldrin, on the other hand, was not detected in any of the samples, nor were the two corresponding stereoisomers, Endrin and Isodrin.
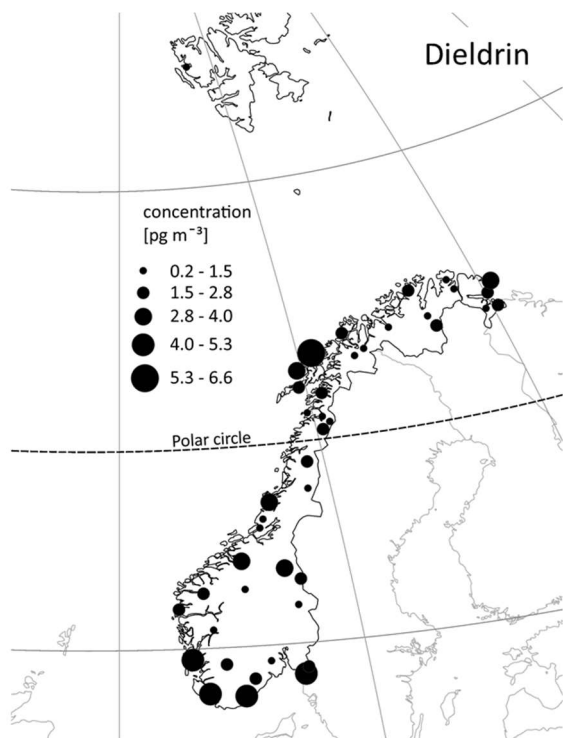
Figure SI-2.11 The spatial distribution of concentrations of Dieldrin in background air across Norway.

2.2   Comparison with an urban environment

The concentrations in urban air were generally approximately 10 times higher than the concentrations in background air for $\sum_6$PCBs and 4.5 times higher for $\sum_3$DDXs. The concentrations of HCB and $\sum_2$HCHs were roughly the same in urban and background air.

In addition to the PCB congeners found in the background samples, PCB114, PCB156 and PCB170 were also detected in > 80 % of the urban samples. Tri-CBs were the dominating congener group, with the proportion of Tri-CBs in the urban samples (50 %) being somewhat larger than in the background samples (43 %). However, comparing the proportion of each of the PCB-congeners with matched pair Wilcoxon signed rank test (SI 1.6.5), there was no significant difference found between the composition of urban and background air (p-value 0.13). Similar to the rest of southern Norway, PCB-28 is more dominating (two times higher fraction) than PCB-153 in the urban samples.

Due to challenges with matrix and dilution of the extracts for the urban samples, a high MDL (0.3 - 115 pg/m^3) was retrieved for the OCPs, resulting in a low detection frequency of the compounds (Table SI-2.2 b). PeCB/HCB and the most abundant HCHs and DDXs were detected, though all (except PeCB/HCB and p,p'DDE) to a smaller extent than in the background samples. While α-HCH, for instance, was detected in all of the background samples, it was only detected in one of the ten urban samples due to the elevated detection limit. The same compounds were included in the sums even though they were detected in less than 60 % of the samples.

While the map in Figure SI-2.12 shows the distribution of the measured concentrations of PCB-153 around Oslo, Figures SI-2.13 - 2.14 show the predicted source contributors to the overall concentration of PCB-153 in Oslo (given by site 8), simulated by GLEMOS and FLEXPART, respectively. Both models show influence from western Europe, but GLEMOS also suggests considerable national contribution from primary sources.
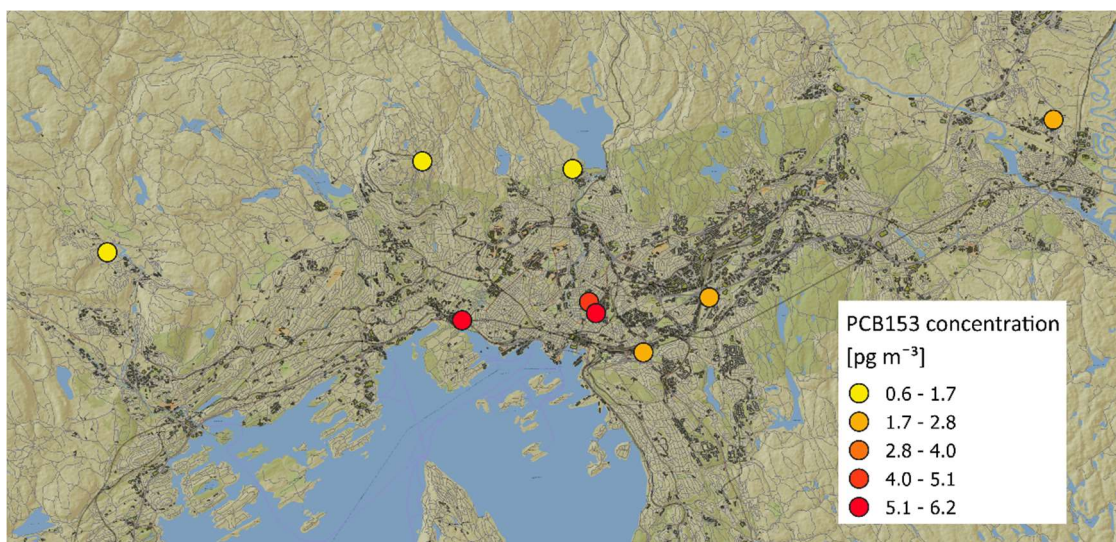
Figure SI-2.12. Map of concentrations of PCB-153 in air across the urban area showing approximately ten times higher concentrations compared to the Norwegian background levels (average: 0.3 pg/m^3).
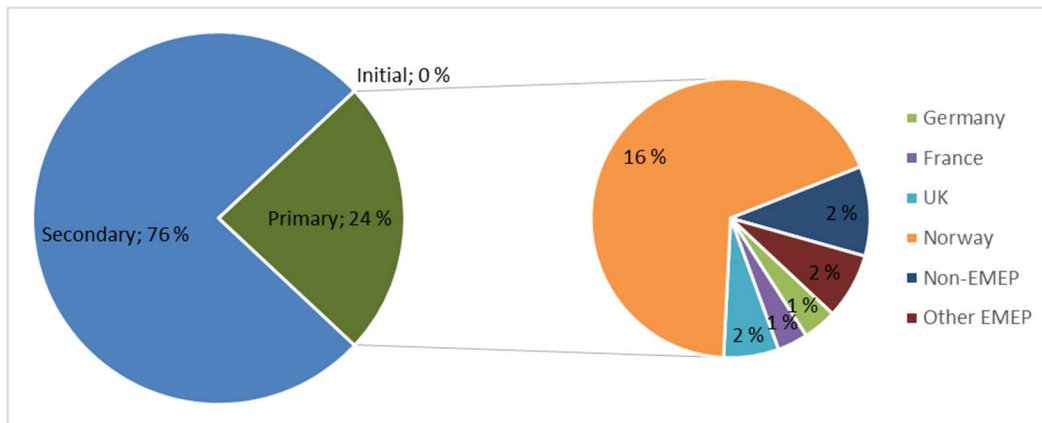
Figure SI-2.13. The relative contributions to the overall concentration of PCB-153 at site 8 (Oslo), simulated with GLEMOS, showing considerable national contribution from primary sources, but also strong influence from secondary sources.
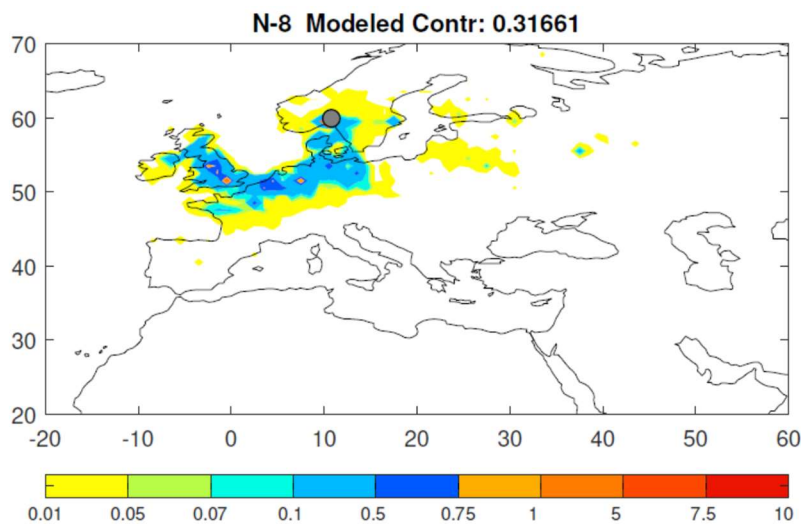
Figure SI-2.14. Maps of footprint emission contribution at site 8 (Oslo), simulated with FLEXPART, showing strong influence from western Europe, similar to the rest of southern Norway.

2.3   Model predictions of PCB-153
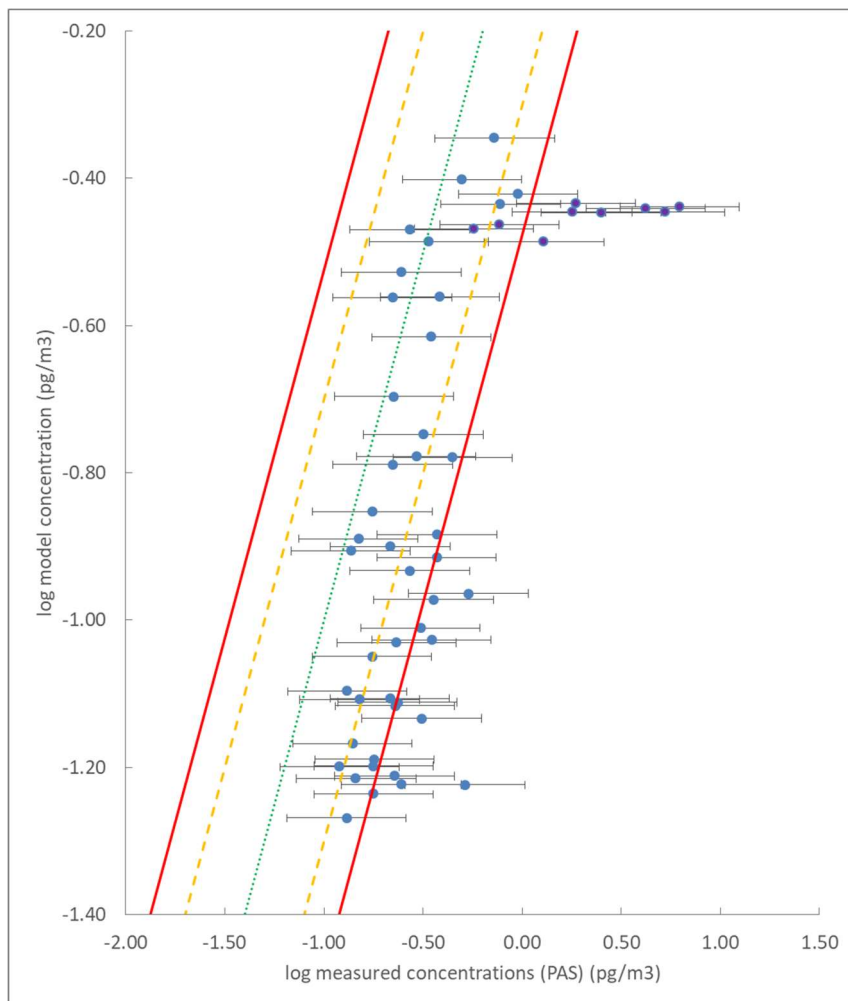
Figure SI-2.15a. The modelled versus observed concentrations of PCB-153 in Norway for GLEMOS expressed on a logarithmic basis. The brackets represent the accuracy (factor two) of the PAS-derived concentrations (Shoeib & Harner, 2002a). The dashed yellow lines represent deviations of a factor of two from the observed concentrations, while the solid red lines represent deviations of a factor of three. Largest deviations are found for the urban samples (dark blue).
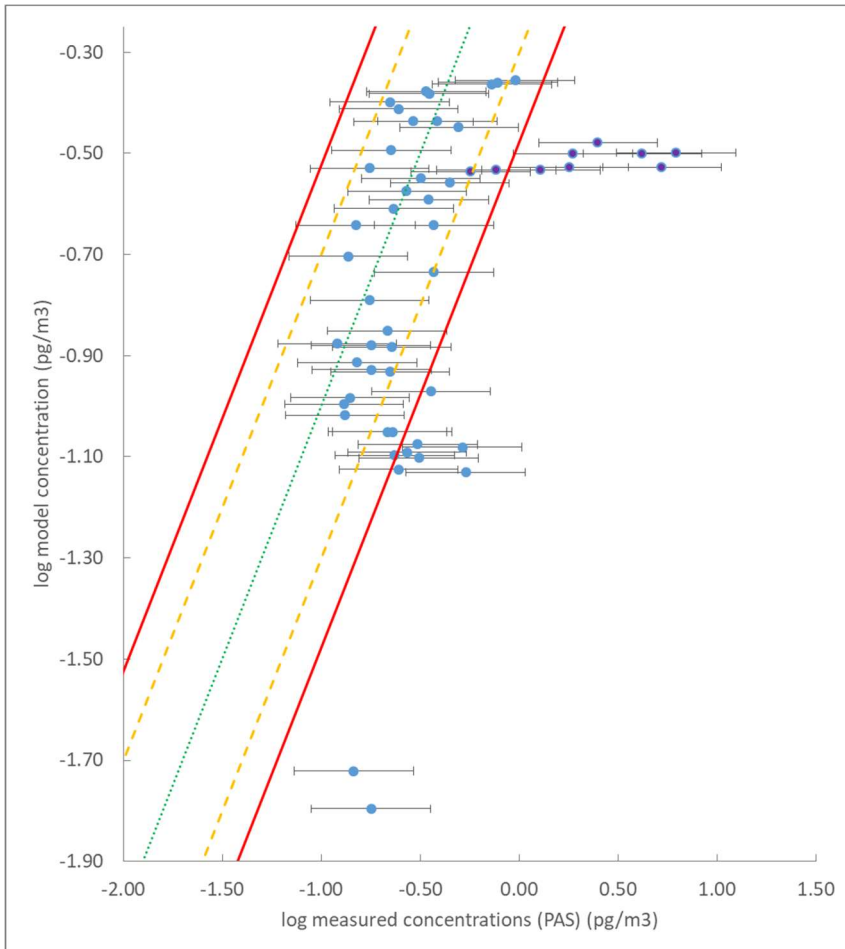
Figure SI-2.15b. The modelled versus observed concentrations of PCB-153 in Norway for FLEXPART expressed on a logarithmic basis. The brackets represent the accuracy (factor two) of the PAS-derived concentrations (Shoeib & Harner, 2002a). The dashed yellow lines represent deviations of a factor of two from the observed concentrations, while the solid red lines represent deviations of a factor of three. Largest deviations are found for the urban samples (dark blue) and for the sites at Svalbard (lower end of the figure).
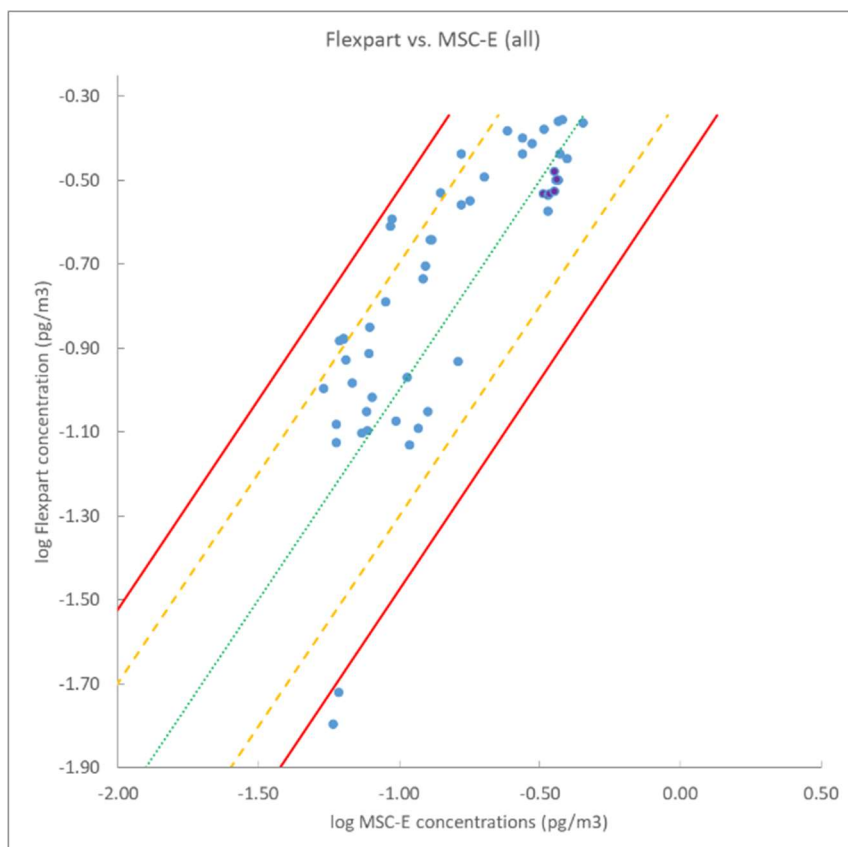
Figure SI-2.15c. The modelled concentrations of PCB-153 simulated with FLEXPART, compared with the modelled concentrations of PCB-153 simulated with GLEMOS. Both expressed on a logarithmic basis. The dashed yellow lines represent deviations of a factor of two between FLEXPART and GLEMOS concentrations, while the solid red lines represent deviations of a factor of three. 61% of the FLEXPART concentrations were higher than those predicted by the GLEMOS model. The concentrations at Svalbard simulated with FLEXPART were more than a factor of three lower than the GLEMOS model.
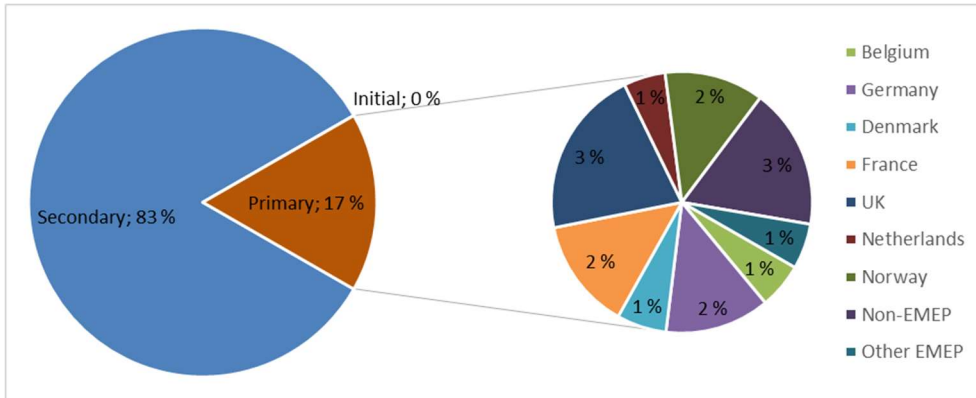
Figure SI-2.16a. The relative contributions to the overall concentration of PCB-153 at site 49 (southern Norway), simulated with GLEMOS, showing strong influence from western Europe (e.g. UK and Germany).
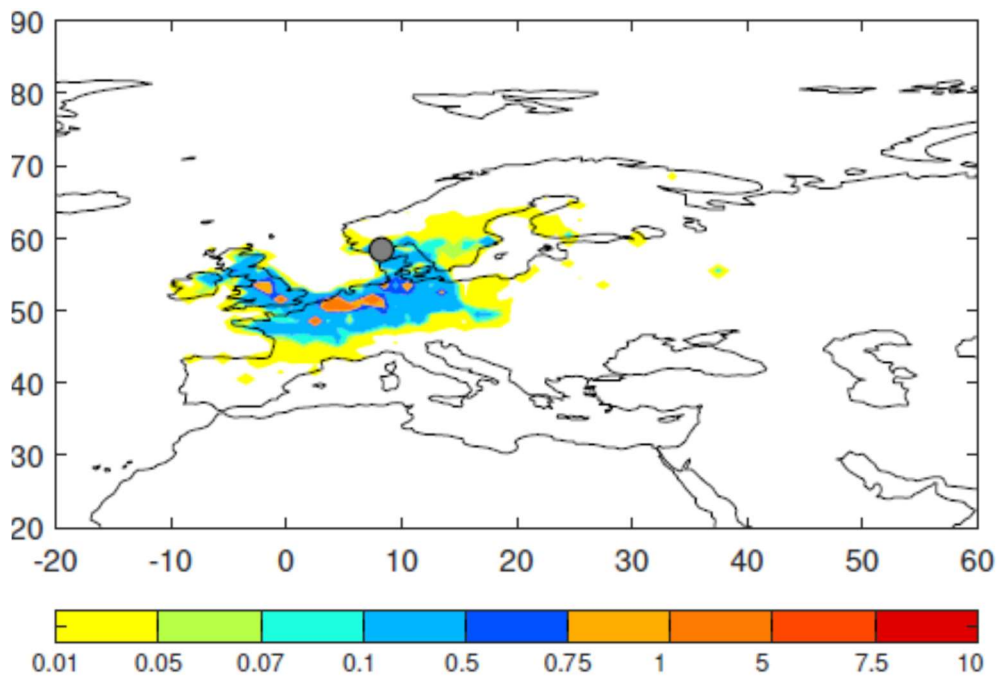
Figure SI-2.16b. Maps of footprint emission contribution at site 49 (southern Norway), simulated with FLEXPART, showing strong influence from western Europe.
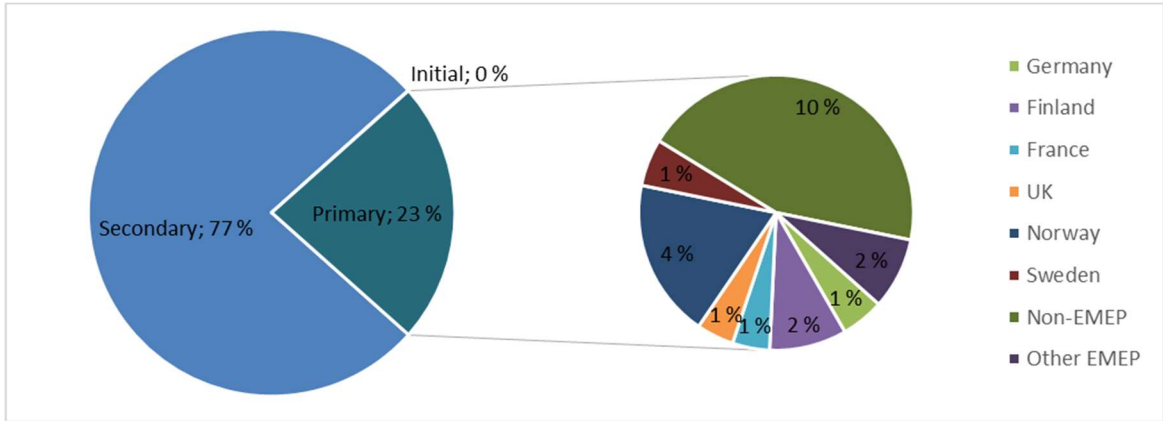
Figure SI-2.17a. The relative contributions to the overall concentration of PCB-153 at site 23 (northern Norway), simulated with GLEMOS, showing influence from western Europe (e.g. Germany) and minor contributions from other countries (e.g. Norway and Finland).
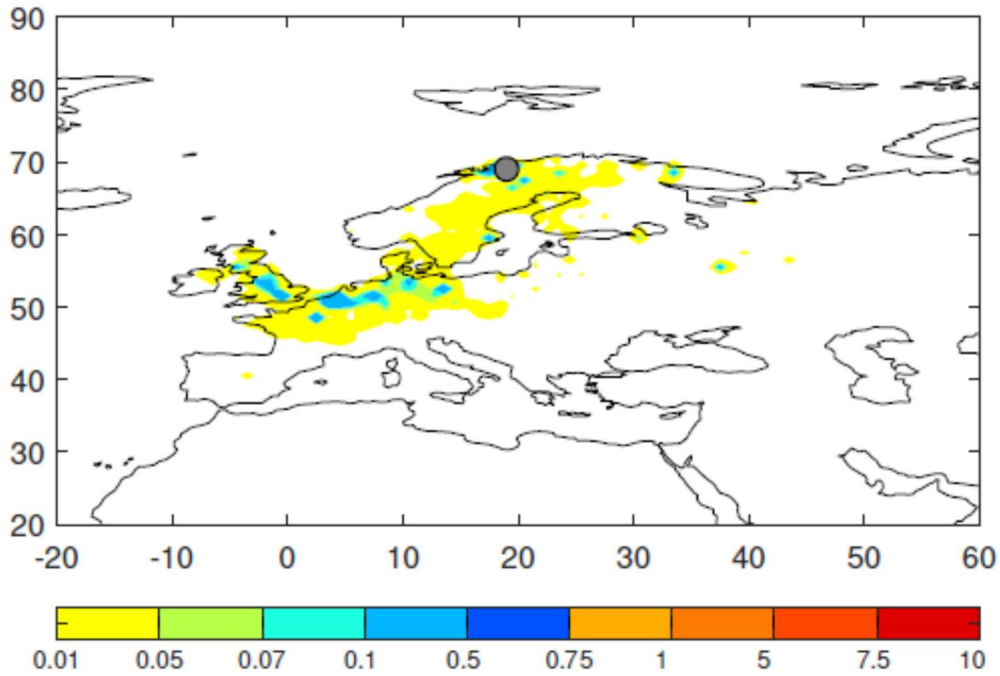
Figure SI-2.17b. Maps of footprint emission contribution at site 23 (northern Norway), simulated with FLEXPART, showing influence from western Europe, and minor influence from east.
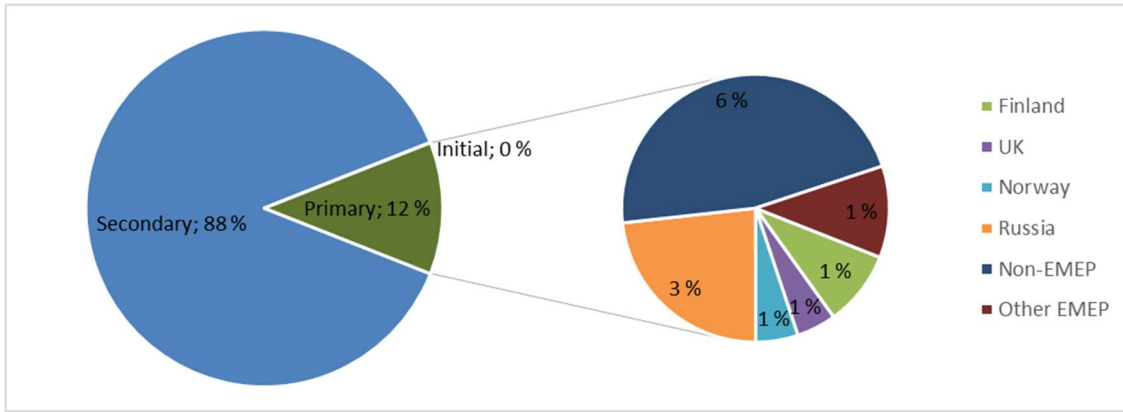
Figure SI-2.18a. The relative contributions to the overall concentration of PCB-153 at site 12 (eastern-most part of northern Norway), simulated with GLEMOS, showing influence from non-EMEP countries and e.g. Russia.
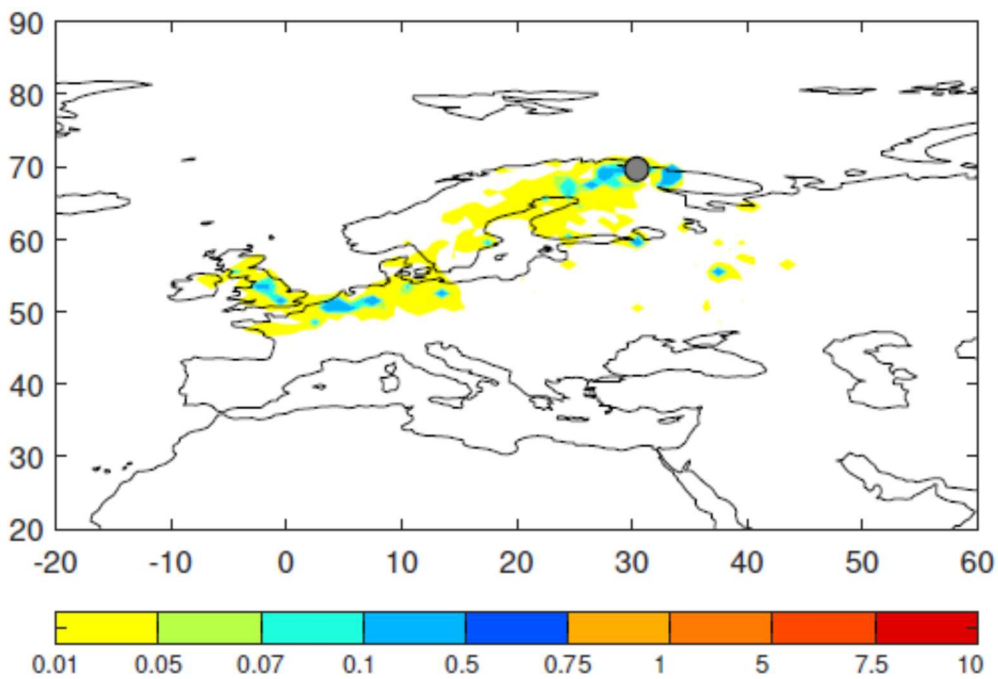
Figure SI-2.18b. Maps of footprint emission contribution at site 12 (eastern-most part of northern Norway), simulated with FLEXPART, showing influence from western Europe and e.g. Kola peninsula.
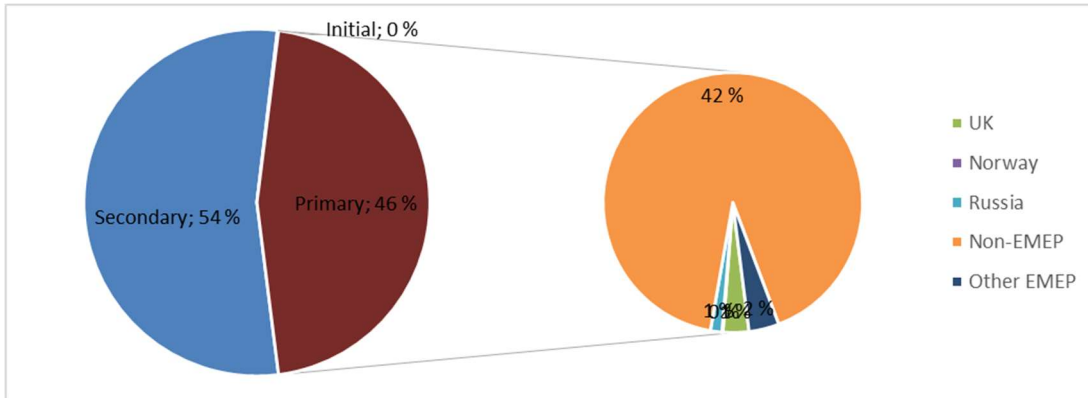
Figure SI-2.19a. The relative contributions to the overall concentration of PCB-153 at site 96 (Svalbard), simulated with GLEMOS, showing less contribution from secondary emissions compared to the other sites and strong influence from primary sources outside EMEP.
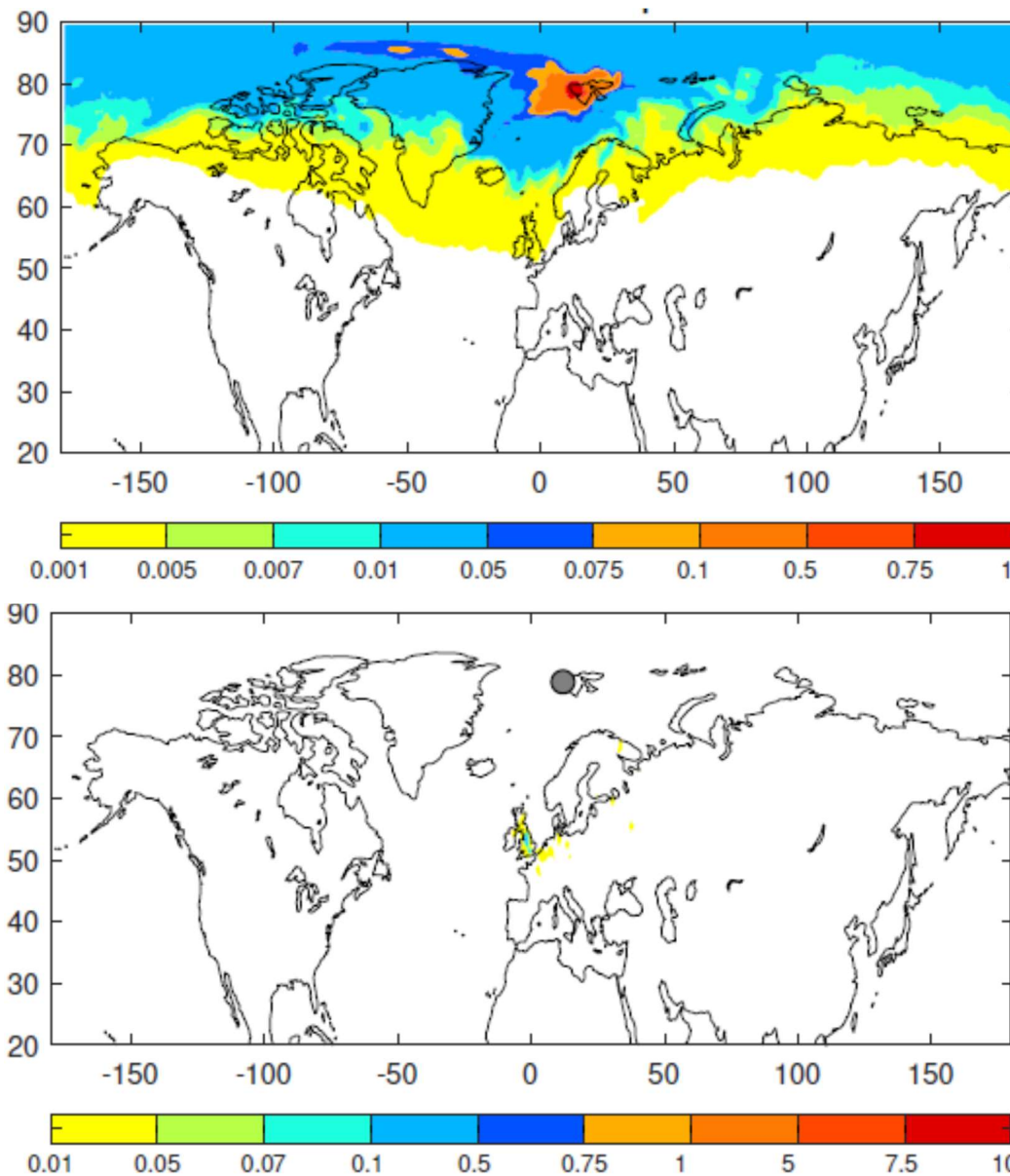
Figure SI-2.19b. Maps of footprint emission sensitivities (ES) and emission contribution (EC) at site 96 (Svalbard), simulated with FLEXPART, showing air masses generally from west (top).

Bohlin-Nizzetto, P., Aas, W., & Warner, N. (2017). *Monitoring of environmental contaminants in air and precipitation, annual report 2016*. (NILU report 17/2017). Kjeller: NILU Retrieved from http://hdl.handle.net/11250/2461410.

Breivik, K., Sweetman, A., Pacyna, J. M., & Jones, K. C. (2007). Towards a global historical emission inventory for selected PCB congeners - A mass balance approach-3. An update. *Science of The Total Environment, 377*(2-3), 296-307. https://doi.org/10.1016/j.scitotenv.2007.02.026

Dearth, M. A., & Hites, R. A. (1991). Complete analysis of technical chlordane using negative ionization mass spectrometry. *Environmental Science & Technology, 25*(2), 245-254. https://doi.org/10.1021/es00014a005

Hak, C. (2015). *Norway's air quality monitoring network. Assessment of station siting according to regulations in EU's air quality directives*. (NILU report 15/2015). Kjeller: NILU.

Halse, A. K., Schlabach, M., Eckhardt, S., Sweetman, A., Jones, K. C., & Breivik, K. (2011). Spatial variability of POPs in European background air. *Atmospheric Chemistry and Physics, 11*(4), 1549-1564. https://doi.org/10.5194/acp-11-1549-2011

Halse, A. K., Schlabach, M., Schuster, J. K., Jones, K. C., Steinnes, E., & Breivik, K. (2015). Endosulfan, pentachlorobenzene and short-chain chlorinated paraffins in background soils from Western Europe. *Environ Pollut, 196*, 21-28. https://doi.org/10.1016/j.envpol.2014.09.009

Halse, A. K., Schlabach, M., Sweetman, A., Jones, K. C., & Breivik, K. (2012). Using passive air samplers to assess local sources versus long range atmospheric transport of POPs. *J Environ Monit, 14*(10), 2580-2590. https://doi.org/10.1039/c2em30378g

Harju, M., Haglund, P., & Naikwadi, K. (1998). Gas-chromatographic properties of the 209 PCB congeners on non-polar, chiral and liquid-crystal columns. *Organohalogen compounds, 35*, 111-114.

Harner, T. (2017). 2017_v1_5_Template for calculating Effective Air Sample Volumes for PUF and SIP Disk Samplers_Sept_15. Retrieved from https://www.researchgate.net/publication/319764519_2017_v1_5_Template_for_calculating_Effective_Air_Sample_Volumes_for_PUF_and_SIP_Disk_Samplers_Sept_15. Access June 2019.

Harner, T., & Bidleman, T. F. (1996). Measurements of Octanol−Air Partition Coefficients for Polychlorinated Biphenyls. *Journal of Chemical & Engineering Data, 41*(4), 895-899. https://doi.org/10.1021/je960097y

Harner, T., Mitrovic, M., Ahrens, L., & Schuster, J. (2014). Characterization of PUF disk passive air samplers for new priority chemicals: a review. *Organohalogen compounds, 76*, 442-445.

Harner, T., Shoeib, M., Diamond, M., Stern, G., & Rosenberg, B. (2004). Using Passive Air Samplers To Assess Urban−Rural Trends for Persistent Organic Pollutants. 1. Polychlorinated Biphenyls and Organochlorine Pesticides. *Environmental Science & Technology, 38*(17), 4474-4483. https://doi.org/10.1021/es040302r

Herzke, D., Nygård, T., & Heimstad, E. S. (2017). *Environmental pollutants in the terrestial and urban environment 2016*. (NILU report 33/2017). Kjeller: NILU.

Hung, H., Katsoyiannis, A. A., Brorstrom-Lunden, E., Olafsdottir, K., Aas, W., Breivik, K., . . . Wilson, S. (2016). Temporal trends of Persistent Organic Pollutants (POPs) in arctic air: 20 years of monitoring under the Arctic Monitoring and Assessment Programme (AMAP). *Environ. Pollut. (Oxford, U. K.), 217*, 52-61. https://doi.org/10.1016/j.envpol.2016.01.079

Kartverket. Norgeskart. Retrieved from https://norgeskart.no/#!?project=norgeskart&layers=1002&zoom=4&lat=7197864.00&lon=396722.00. Access Oct 22 2018.

Li, Y. F., & Macdonald, R. W. (2005). Sources and pathways of selected organochlorine pesticides to the Arctic and the effect of pathway divergence on HCH trends in biota: a review. *Sci Total Environ, 342*(1-3), 87-106. https://doi.org/10.1016/j.scitotenv.2004.12.027

Malanichev, A., Mantseva, E., Shatalov, V., Strukov, B., & Vulykh, N. (2004). Numerical evaluation of the PCBs transport over the Northern Hemisphere. *Environmental Pollution, 128*(1), 279-289. https://doi.org/10.1016/j.envpol.2003.08.040

Miller, J. N. (2010). *Statistics and chemometrics for analytical chemistry* (6th ed.). Harlow, England: Pearson Prentice Hall.

Moeckel, C., Harner, T., Nizzetto, L., Strandberg, B., Lindroth, A., & Jones, K. C. (2009). Use of Depuration Compounds in Passive Air Samplers: Results from Active Sampling-Supported Field Deployment, Potential Uses, and Recommendations. *Environmental Science & Technology, 43*(9), 3227-3232. https://doi.org/10.1021/es802897x

Pisso, I., Sollum, E., Grythe, H., Kristiansen, N. I., Cassiani, M., Eckhardt, S., . . . Stohl, A. (2019). The Lagrangian particle dispersion model FLEXPART version 10.4. *Geosci. Model Dev., 12*(12), 4955-4997. https://doi.org/10.5194/gmd-12-4955-2019

Pozo, K., Harner, T., Lee, S. C., Wania, F., Muir, D. C., & Jones, K. C. (2009). Seasonally resolved concentrations of persistent organic pollutants in the global atmosphere from the first year of the GAPS study. *Environ Sci Technol, 43*(3), 796-803. https://doi.org/10.1021/es802106a

Pozo, K., Harner, T., Wania, F., Muir, D. C. G., Jones, K. C., & Barrie, L. A. (2006). Toward a global network for persistent organic pollutants in air: Results from the GAPS study. *Environmental Science & Technology, 40*(16), 4867-4873. https://doi.org/10.1021/es060447t

Qiu, X., Zhu, T., Yao, B., Hu, J., & Hu, S. (2005). Contribution of Dicofol to the Current DDT Pollution in China. *Environmental Science & Technology, 39*(12), 4385-4390. https://doi.org/10.1021/es050342a

Schuster, J. K., Gioia, R., Breivik, K., Steinnes, E., Scheringer, M., & Jones, K. C. (2010). Trends in European Background Air Reflect Reductions in Primary Emissions of PCBs and PBDEs. *Environmental Science & Technology, 44*(17), 6760-6766. https://doi.org/10.1021/es101009x

Shen, L., Wania, F., Lei, Y. D., Teixeira, C., Muir, D. C. G., & Bidleman, T. F. (2005). Atmospheric Distribution and Long-Range Transport Behavior of Organochlorine Pesticides in North America. *Environmental Science & Technology, 39*(2), 409-420. https://doi.org/10.1021/es049489c

Shoeib, M., & Harner, T. (2002a). Characterization and comparison of three passive air samplers for persistent organic pollutants. *Environmental Science & Technology, 36*(19), 4142-4151. https://doi.org/10.1021/es020635t

Shoeib, M., & Harner, T. (2002b). Using measured octanol-air partition coefficients to explain environmental partitioning of organochlorine pesticides. *Environmental Toxicology and Chemistry, 21*(5), 984-990. https://doi.org/10.1002/etc.5620210513

Sovocool, G. W., Lewis, R. G., Harless, R. L., Wilson, N. K., & Zehr, R. D. (1977). Analysis of technical chlordane by gas chromatography/mass spectrometry. *Analytical Chemistry, 49*(6), 734-740. https://doi.org/10.1021/ac50014a018

Steinnes, E., Uggerud, H. T., Pfaffhuber, K. A., & Berg, T. (2016). *Atmospheric deposition of heavy metals in Norway, national moss survey 2015*. (NILU report 28/2016). Kjeller: NILU.

Stohl, A., Hittenberger, M., & Wotawa, G. (1998). Validation of the lagrangian particle dispersion model FLEXPART against large-scale tracer experiment data. *Atmospheric Environment, 32*(24), 4245-4264. https://doi.org/10.1016/S1352-2310(98)00184-8

Tuduri, L., Harner, T., & Hung, H. (2006). Polyurethane foam (PUF) disks passive air samplers: Wind effect on sampling rates. *Environmental Pollution, 144*(2), 377-383. https://doi.org/10.1016/j.envpol.2005.12.047

UNECE. (1998). Protocol on Persistent Organic Pollutants (POPs).   Retrieved from http://www.unece.org/env/lrtap/pops_h1.html. Access Feb 23.

Weber, J., Halsall, C. J., Muir, D., Teixeira, C., Small, J., Solomon, K., . . . Bidleman, T. (2010). Endosulfan, a global pesticide: A review of its fate in the environment and occurrence in the Arctic. *Science of The Total Environment, 408*(15), 2966-2984. https://doi.org/10.1016/j.scitotenv.2009.10.077

Aas, W., & Bohlin-Nizzetto, P. (2018). *Heavy metals and POP measurements, 2016*. (EMEP/CCC-Report 3/2018). Kjeller: NILU Retrieved from http://hdl.handle.net/11250/2563390.

Paper II

Spatial variability and temporal changes of POPs in European background air

Helene Lunder Halvorsen [a,b,*], Pernilla Bohlin-Nizzetto [a], Sabine Eckhardt [a], Alexey Gusev [c], Claudia Moeckel [a,d], Victor Shatalov [c], Lovise Pedersen Skogeng [a], Knut Breivik [a,b]

[a] NILU - Norwegian Institute for Air Research, P.O. Box 100, 2027, Kjeller, Norway
[b] Centre for Biogeochemistry in the Anthropocene, Department of Chemistry, University of Oslo, 0351, Oslo, Norway
[c] Meteorological Synthesizing Centre-East, 115419, Moscow, Russian Federation
[d] Department of Materials and Environmental Chemistry, Stockholm University, 11418, Stockholm, Sweden

HIGHLIGHTS

- Selected POPs were measured in background air across 101 sites in Europe.
- The spatial and temporal variability of POPs across Europe was assessed.
- Mechanistic modelling provided complementary information on source contributions.

GRAPHICAL ABSTRACT
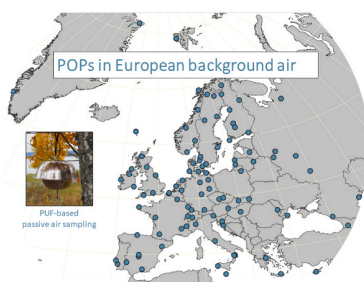
ARTICLE INFO

ABSTRACT

Concentration data on POPs in air is necessary to assess the effectiveness of international regulations aiming to reduce the emissions of persistent organic pollutants (POPs) into the environment. POPs in European background air are continuously monitored using active- and passive air sampling techniques at a limited number of atmospheric monitoring stations. As a result of the low spatial resolution of such continuous monitoring, there is limited understanding of the main sources controlling the atmospheric burdens of POPs across Europe. The key objectives of this study were to measure the spatial and temporal variability of concentrations of POPs in background air with a high spatial resolution (n = 101) across 33 countries within Europe, and to use observations and models in concert to assess if the measured concentrations are mainly governed by secondary emissions or continuing primary emissions. Hexachlorobenzene (HCB) was not only the POP detected in highest concentrations (median: 67 pg/m^3), but also the only POP that had significantly increased over the last decade. HCB was also the only POP that was positively correlated to latitude. For the other targeted POPs, the highest concentrations were observed in the southern part of Europe, and a declining temporal trend was observed. Spatial differences in temporal changes were observed. For example, γ-HCH (hexachlorocyclohexane) had the largest decrease in the south of Europe, while α-HCH had declined the most in central-east Europe. High occurrence of degradation products of the organochlorine pesticides and isomeric ratios indicated past usage. Model predictions of PCB-153 (2,2',4,4',5,5'-hexachlorobiphenyl) by the Global EMEP Multi-media Modelling

* Corresponding author. NILU - Norwegian Institute for Air Research, P.O. Box 100, 2027, Kjeller, Norway.
E-mail address: hlu@nilu.no (H. Lunder Halvorsen).

System suggest that secondary emissions are more important than primary emissions in controlling atmospheric burdens, and that the relative importance of primary emissions are more influential in southern Europe compared to northern Europe. Our study highlights the major advantages of combining high spatial resolution observations with mechanistic modelling approaches to provide insights on the relative importance of primary- and secondary emission sources in Europe. Such knowledge is considered vital for policy makers aiming to assess the potential for further emission reduction strategies of legacy POPs.

1. Introduction

Persistent organic pollutants (POPs) are regulated organic chemicals that may cause harmful health- and environmental effects, due to their toxicity and bioaccumulating properties. They are persistent and can be transported over long distances, far away from their sources. The atmosphere represents an important pathway of environmental transport across national boundaries and into remote areas (Wania and Mackay, 1993).

Though international regulations have reduced the primary emissions of POPs into the environment, POPs are still present both in source regions and remote regions like the Arctic (Wong et al., 2021). The occurrence of POPs in the atmosphere and other environmental compartments may in part be due to continuing primary emissions (Breivik et al., 2004; UNEP, 2020). However, the relative importance of secondary sources from historically contaminated surface media (Jones, 1994; Li and Wania, 2018) is excpected to increase, due to the decrease in primary emissions (Nizzetto et al., 2010) and/or increased global temperatures (Ma et al., 2011). Monitoring of POPs in air is therefore important to identify the main sources controlling the atmospheric burdens, and to assess the effectiveness of control measures for legacy POPs (Wöhrnschimmel et al., 2016).

POPs have been included in the air monitoring programme of EMEP (the European Monitoring and Evaluation Programme) since 1999 (Tørseth et al., 2012). In 2016, 12 atmospheric monitoring stations in Europe, utilizing active air sampling (AAS) techniques, reported concentrations of POPs in background air to EMEP (Aas and Bohlin-Nizzetto, 2018). These samplers, driven by pumps, provide data with high temporal resolution, but are costly and thereby result in low spatial coverage. The continous monitoring under EMEP is crucial for time-trend analysis at individual sites, but the analysis of spatial variability in Europe is hampered by a low number of EMEP sites and chemical analysis performed by different laboratories. Passive air samplers (PAS) based on diffusive uptake, are independent of electricity and represent a simple and low-cost alternative. PAS may complement AAS by expanding the spatial coverage of air measurement assessments (Jaward et al., 2004; Shoeib and Harner, 2002), such as the EMEP programme. Within Europe, two PAS monitoring networks (Kalina et al., 2019; Schuster et al., 2021) and a few case-studies (Gioia et al., 2007; Halse et al., 2011; Jaward et al., 2004) have contributed to assess the spatial trends, but except Halse et al. (2011) (n = 86), the number of sampling sites in background areas within Europe has been limited (n < 46). Therefore, a need exists for studies aiming to improve the understanding of the spatial patterns of POPs in European air, as the source contributions are known to be variable across Europe, e.g. due to differences in production and use from country to country. In more central parts of Europe, the production and use of POPs have been widespread (Barber et al., 2005; Breivik et al., 1999, 2002), and we therefore expect the influence of primary emissions to be higher in this region, compared to remote areas in Europe (Jaward et al., 2004; Lunder Halvorsen et al., 2021; Meijer et al., 2003). Furthermore, it is also known that there are major spatial differences in the historical use of legacy POPs within Europe. A notable example is the insecticide lindane (>99% g-HCH) which was used more extensively in western parts of Europe, whereas the historical use of technical HCH (predominantly a-HCH) mainly occurred in eastern parts of Europe (Breivik et al., 1999). We therefore hypothesize that the concentrations of POPs in air within Europe may be

a) variable across regions, b) variable for different POPs (both on a group level and for individual compounds), c) likely to have decreased over time in response to primary emission reductions, and d) increasingly influenced by secondary emissions.

The main objective of this study was to assess the spatial and temporal variability of legacy POPs in air across Europe, using a combination of measurements and modelling, both with high resolution. In this study, a comprehensive passive air sampling campaign with 101 sites across Europe was conducted in 2016, mapping background concentrations of POPs in air. The analysis of all PAS was performed by one laboratory, providing a consistent dataset. The study focuses on legacy POPs, that have seen significant historical use in the study region, and enables us to assess the spatial distribution of POPs in European air and their temporal change in concentrations by comparing with studies carried out in the past, including data from a similar PAS campaign conducted in 2006 (Halse et al., 2011). Lunder Halvorsen et al. (2021) recently proposed a strategy on how to combine high spatial resolution measurements with modelling approaches to better understand the main sources controlling atmospheric burdens of POPs across a nation. In our study, the approach was expanded to the whole of Europe.

2. Materials and methods

2.1. Sampling

Passive air samples were collected at 101 background sites across 33 countries within Europe (35°N to 82°N, 52°W to 48°E, Figure SI-1.1) in a coordinated and comprehensive sampling campaign during summer 2016. Most of the sites (n = 96) were monitoring stations reporting various inorganic and organic compounds in air to EMEP (see e.g. Tørseth et al. (2012)). Among these, 11 sites (Figure SI-1.1) reported some of the targeted POPs based on AAS to EMEP in 2016 (Aas and Bohlin-Nizzetto, 2018). Passive air samplers were deployed and collected by trained personnel already involved in the EMEP program (Table SI-3.1), following standard operating procedures for passive air sampling of POPs.

Polyurethane foam based passive air samplers (PUF-PAS) with the MONET design of the sampler housing (diameter upper and lower bowl 30 and 24 cm respectively) were used for sampling (Kalina et al., 2017; Markovic et al., 2015). The PUF disks (14 cm diameter x 1.4 cm thickness, 0.027 g/cm^3) were purchased from Sunde Skumplast AS/Carpenter (Norway). Prior to deployment, the PUF disks were pre-cleaned, spiked with sampling performance reference compounds (PRCs, Table 1.2a) and distributed to the sampling sites by NILU. The PUF-PAS were deployed at or close-by the monitoring stations and exposed from July to October (77–125 days). Details of sampler preparation and deployment are described in Lunder Halvorsen et al. (2021) while an overview of the sampling sites is presented in the Supporting Information (Table SI-1.1).

2.2. Sample extraction and clean-up

The exposed PUF disks were returned to the laboratory at NILU for analysis. A description of sample extraction and clean-up is given in SI 1.2.

2.3. Instrumental analysis

Prior to instrumental analysis, an instrument performance standard was added to the samples. The samples were analyzed for 31 polychlorinated biphenyls (PCBs), penta- and hexachlorobenzene (PeCB/HCB) and 27 organochlorine pesticides (OCPs). This included the six indicator PCBs (PCB-28, -52, −101, −138, −153 and −180), hexachlorocyclohexanes (HCHs), dichlorodiphenyldichloroethylenes (DDTs), chlordanes (CDs), aldrin, endosulfans, and their metabolites. A list of all target compounds is given in Table SI-1.2b-c. Analysis was performed with a gas chromatograph (GC) coupled to a high-resolution mass spectrometer (HRMS) following the method described in Lunder Halvorsen et al. (2021).

2.4. QA/QC

Blank level control was performed by extracting and analyzing 14 method blank samples and 11 field blank samples in the same way as the exposed samples. The method detection limits (MDLs) were calculated as the average plus three times the standard deviation of target analytes in blank samples, normalized by the average sample volume (Table SI-2.1b). While the levels in field- and method blanks for the OCPs were comparable and were all used to calculate the MDL, only the method blanks were used to calculate the MDL for PCB and PeCB/HCB. Of the 60 targeted analytes, only analytes with more than 60% detection frequency, i.e. 30 PCBs, PeCB/HCB and 16 OCPs, were evaluated in this study. The median concentrations of these analytes exceeded the MDLs by a factor of 6–111. For the calculation of sum, average and median, and for the statistical analysis, concentrations below MDL were replaced by ½ MDL, for consistency with Halse et al. (2011). There are uncertainties related to the statistical interpretation of data when substituting values below MDL, especially for analytes with less than 85% detection frequency (Helsel, 2006).

The internal standard recoveries of deployed samples, field- and method blanks are given in Table SI-1.3. For further method quality control, a known amount of ^{12}C target analytes was added to three clean PUF disks to assess the method bias (−2%-6% for PCBs and −13%-27% for OCPs, Table SI-1.4a). PUF-PAS were co-deployed at 11 selected sites to assess the reproducibility of the PAS method (0–33 RSD%, Table SI-1.4b).

2.5. Deriving air concentrations

Air concentrations were derived from the amounts found in the samplers and air volumes estimated from the template of Harner (2017), with the same approach described in Lunder Halvorsen et al. (2021). A detailed description of the required parameters is included in SI section 1.3. In short, site-specific sampling rates (2.0–15 m^3/day, median: 3.7 m^3/day, Table SI-1.5) were estimated accounting for i) the measured loss of PRCs from the PUF-PAS, and ii) site-specific environmental conditions, i.e. ambient air temperature (−13-29 °C) and wind speed (2–7 m/s). The median sampling rate in our study is within the range often reported for PUF-PAS (3–4 m^3/day) (Wania and Shunthirasingham, 2020).

The PCBs and OCPs targeted in our study are predominantly in gas-phase (Bohlin et al., 2014), and the lower uptake efficiency for particles with the MONET sampler (Bohlin et al., 2014; Markovic et al., 2015) is therefore not taken into consideration when estimating air volumes. For more volatile compounds with $K_{OA} < 10^8$ (e.g. HCB and PCB-18), equilibrium is reached during the 3-month deployment period (Francisco et al., 2017). The Harner-template accounts for this and the estimated air volumes of HCB are consequently lower than e.g. PCB-153 (Table SI-1.5). However, the PAS does not provide a true time-averaged concentration as the rate of uptake is decreasing during the sampling period. The amount of HCB in the PUF that is in equilibrium with the atmosphere may also change. (Wania and Shunthirasingham, 2020).

2.6. Data analysis

The ratio between maximum and minimum concentrations in air (MMR) was used as a simple measure of the spatial variability. For comparison with the Norwegian study (Lunder Halvorsen et al., 2021), MMR was calculated excluding outliers (SI 1.4.1).

Regional differences in the measured concentrations of POPs between north, south, central-east and west (Figure SI-1.1), according to the geographical division of Europe by the European Union (EuroVoc, 2021), were assessed using significance tests. The spatial variability was further assessed by examining possible correlations between the target compounds, with latitude/longitude as well as with population density estimated within 50 km of each sampling site (SI 1.4.2). All data, except latitude/longitude were log-transformed prior to the correlation tests.

Significance tests were also performed to assess the temporal change in concentrations between this study and an earlier European campaign from 2006 (Halse et al., 2011), for 73 sites that were included in both studies. A consistent comparison to the earlier campaign was assured by using similar sampling and analytical methods, and the same approach for deriving air concentrations accounting for the temperature dependence of $K_{PUF-air}$.

All statistical analyses were performed by using R Studio with R 4.1.1 (details in SI 1.4).

2.7. Source-receptor modelling tools

Model simulations of concentration of PCB-153 in air were carried out for each individual site, corresponding to the actual deployment periods, using the GLEMOS model (Malanichev et al., 2004). The results were initially used to evaluate if the observed spatial pattern is explained by the model. For each site, the relative contributions attributed to primary- and secondary emissions were predicted by GLEMOS. While the total primary emissions are separated into contributions from national emissions and transboundary transport (within/outside EMEP), this is not specified for the secondary emissions. A correlation between the predicted contribution from national emissions and population density (within 50 km of each site, SI 1.4.2) was examined. Furthermore, regional differences in the relative contribution of the main sources were examined, by using significance tests.

To further examine the source regions and contributions from primary emissions alone, simulations of PCB-153 were also carried out using the Lagrangian particle dispersion model FLEXPART V10.4 in backward mode (Pisso et al., 2019; Stohl et al., 1998). FLEXPART predicts so-called "footprints" that illustrate where the air mass had the potential to take up pollutants from sources near the ground. Combining the footprints with emission data (Breivik et al., 2007) enables us to identify the primary source regions contributing to the predicted concentration at each sampling site.

We refer to Lunder Halvorsen et al. (2021) for further details on the model simulations that were carried out.

3. Results and discussion

3.1. Overall results

An overview of concentrations in air, detection frequencies (i.e. percentage of samples above MDL) and MMRs of selected POPs in air is provided in Table SI-2.1a, while concentrations for all target analytes at the individual sites are presented in Tables SI-2.2a-b. The median concentration of $\sum_{30}$PCBs was 29 pg/m^3 (range: 3–405 pg/m^3), and 30 of the 31 targeted PCB congeners were detected in more than 60% of the samples. The six indicator PCBs (45% of $\sum_{30}$PCBs), PCB-18 (11%), PCB-31 (8%), and PCB-149 (8%) were most abundant. The concentrations of $\sum_6$PCBs (median: 13 pg/m^3, range: 1–241 pg/m^3) were comparable to

previously reported passive air data from European background sites in the Global Atmospheric Passive Sampling (GAPS) network (n = 11, 5 coinciding with our study) between 2011 and 2014 (median $\sum_7$PCBs: 12 pg/m^3) (Schuster et al., 2021). The median ratio between PAS concentrations of $\sum_6$PCB in our study and AAS concentrations reported to EMEP (Aas and Bohlin-Nizzetto, 2018) for the same sites (n = 10) and sampling period, was 1.8 (PAS/AAS-ratio: 0.4–9.6, Figure SI-1.3a), which is within the uncertainty of PAS and AAS in combination (Holt et al., 2017).

The highest concentrations were measured for HCB (median: 67 pg/m^3) and PeCB (median: 25 pg/m^3). Of the 27 targeted OCPs, 16 were detected in more than 88% of the samples (Table SI-2.1a). The other 11 OCPs were only detected in <60% of the samples with median concentrations ≤0.7 pg/m^3. α- and γ-HCHs were detected in highest amounts (median: 9 pg/m^3), followed by *p,p'*-DDE, dieldrin and endosulfan I (medians: 6, 4 and 3 pg/m^3, respectively). On average, *p,p'*-DDE accounted for 58% of the sum of all six targeted DDTs (median $\sum_6$DDXs: 10 pg/m^3), while *p,p'*-DDT and *o,p'*-DDT accounted for 18% and 14% respectively. Heptachlor-exo-epoxide, a degradation product of Heptachlor, was detected in all samples, with concentrations (median: 2 pg/m^3) similar to the concentrations of the sum of four chlordanes (Table SI-2.1a, median $\sum_4$chlordanes: 2 pg/m^3). Of the chlordanes, cis-chlordane and trans-nonachlor were dominating (41% and 38% of median $\sum_4$chlordanes respectively). The oxygenated metabolite of chlordanes, oxy-chlordane, was found in similar concentrations to trans-nonachlor and cis-chlordane (median: 1 pg/m^3).

The median concentrations of HCHs, Dieldrin, cis-chlordane and trans-nonachlor in this study were within a factor of two of the concentrations from PAS deployed at European background sites in the study of Schuster et al. (2021). However, the median concentration of endosulfan I in our study was a factor of five lower than in the study by Schuster et al. (2021) (16 pg/m^3). This may be explained by the steeper declining rate of endosulfan I compared to other compounds, as a consequence of later phase-out (i.e. 2011) and higher environmental degradation rate (Schuster et al., 2021). The concentrations of HCB, HCHs, $\sum_3$DDXs (*p,p'*-DDD/-DDE/-DDT) and Dieldrin using PAS in our study were on average 2.4 times higher (PAS/AAS-ratio: 1.0–23) than the concentrations from AAS reported to EMEP (n = 11) for the same sites and time period (Figures SI-1.3 b-f) (Aas and Bohlin-Nizzetto, 2018). Differences between studies may be caused by analytical uncertainties (due to e.g. different chemical laboratories) and uncertainty in the estimated sampling volumes (due to sampling artifacts or environmental conditions not being fully accounted for in the calculations, SI-1.3.1). A direct comparison to EMEP is further affected by differences in sampling methodology, including differences in AAS strategies within the EMEP program.

3.2. Spatial variability

The spatial variability of $\sum_6$PCBs in Europe, when excluding outliers (MMR in this study = 60) (SI 1.4.1), is considerably larger than in Norway (MMR~4) (Lunder Halvorsen et al., 2021). The lowest concentrations of $\sum_6$PCBs (<5 pg/m^3) were generally found in northern Europe (e.g. Norway, Sweden, Finland) and on the British Isles (west region) (Figure SI-2.2a). The correlation analysis (Table SI-2.4) further showed a significant north-south gradient for PCBs (r = −0.46, p < 0.001), whereby the median concentration within the south region (13 pg/m^3, Table SI-2.3) was twice as high as in the north (6.5 pg/m^3, p = 0.008). The larger spatial variability within Europe compared to Norway, together with the observed north-south gradient, implies that the atmospheric concentrations of PCBs at southern latitudes in Europe may be influenced by primary emissions of PCBs to a larger extent than at northern latitudes (Breivik et al., 2007; Jaward et al., 2004). The low levels of PCBs on the British Isles may be explained by the prevailing wind regimes with transport of air masses arriving from the Atlantic Ocean, as shown by the map of footprint emission sensitivities for

PCB-153 (e.g. Yarner Wood, site 92, UK, Figure SI-2.3).

Hotspots (outliers >60 pg/m^3) for PCBs were Abastumani (site 29, Georgia) and Zmeiny Island (site 88, Ukraine) in the central-east region (241 and 100 pg/m^3), Ayia Marina (site 7, Cyprus) in the south region (90 pg/m^3), Keldsnor (site 11, Denmark), Risoe (site 13, Denmark) and Nuuk (site 40, Greenland) in the north region (73, 70 and 66 pg/m^3), and De Zilk (site 60, the Netherlands, 70 pg/m^3) in the west region. Significantly elevated concentrations of PCBs at a specific site may indicate influence from local sources and imply that the site may not be representative for background concentrations in that area. Examples of sources resulting in possible local influence may be populated areas (e.g. Nuuk, Greenland), forest fires (e.g Ayia Marina, Cyprus) (San-Miguel-Ayanz et al., 2017) and PCB contaminated building materials, equipment etc. in the vicinity of the sampler (e.g. Keldsnor, Denmark) (Halse et al., 2011). However, such possible local influences are less likely when several sites in the same area are consistently high (e.g. the Netherlands, 52–70 pg/m^3, n = 3).

The lowest spatial variabilities were found for HCB (and PeCB) (MMR = 15 and 6). HCB has previously been shown to be evenly distributed across Europe (Jaward et al., 2004) and the globe (Shunthirasingham et al., 2010) explained by the long residence time of HCB in the atmosphere (Beyer et al., 2003). Elevated concentrations at e.g. Rucava (site 52, Latvia, 413 pg/m^3) may however implicate that emissions of HCB are still ongoing in the vicinity of some sites (Fig. 1a). This has also been suggested by Hung et al. (2016).

Interestingly, HCB was the only POP in our study that was significantly positively correlated to latitude (r = 0.44, p < 0.001, Table SI-2.4). After Rucava (Latvia), the highest concentrations were observed at the Arctic sites; Station Nord (site 41, Greenland, 247 pg/m^3) and Zeppelin (site 96, Spitsbergen, 130 pg/m^3). As HCB has reached equilibrium between the PUF and air well within the sampling period at all sites, the sample volumes for this compound are largely depended on $K_{PUF-air}$ (Francisco et al., 2017). Consequently, the low temperatures at Zeppelin (Spitsbergen) and Station Nord (Greenland) (4 °C and −13 °C respectively, Table SI-1.5) resulted in sample air volumes (355 m^3 and 297 m^3) in the upper range of the other sites (average 217 m^3, Table SI-1.5). When comparing the concentrations at these sites with concentrations from the co-located AAS reported to EMEP (Figures SI-1.3b) (Aas and Bohlin-Nizzetto, 2018), the PAS/AAS-ratio was 1.6 and 3.3 respectively. These ratios are within the expected range (2–3) (Holt et al., 2017) and hence reflect that the environmental conditions have been compensated for in the estimation of sampling volumes. Enhanced re-emissions from previously contaminated surface reservoirs (Ma et al., 2011) and increasing primary emissions have been put forward as possible explanations (Platt et al., 2022) for the higher concentrations of HCB in the Arctic compared to central Europe. Model predictions in the latter study suggested that Arctic haze periods with high concentrations of HCB in air in the Norwegian Arctic were associated with transport of contaminated air masses from Asia. When excluding the three above-mentioned sites, there is still a significant positive correlation with latitude (r = 0.37, p < 0.001), suggesting generally higher concentrations of HCB in northern Europe, not only in the Arctic.

Similar to PCBs, a north-south gradient (r < 0, Table SI-2.4) was also observed for the OCPs, though not statistically significant for all. One example is the HCHs, for which only γ-HCH was significantly negatively correlated to latitude (r = −0.55, p < 0.001), while a minor correlation was found for α-HCH (r = −0.14, p = 0.15). The spatial variability for γ-HCH (2–109 pg/m^3, MMR = 55) was also larger compared to α-HCH (4–47 pg/m^3, MMR = 12). These differences may reflect the higher LRAT potential of α-HCH compared to γ-HCH (Beyer et al., 2003), but also that Lindane (>99% γ-HCH) was exempted from the SC for use in the control of head lice and scabies (UNEP, 2020), and hence used more recently than technical HCH (55–80% α-HCH, 8–15% γ-HCH (Breivik et al., 1999)). The HCHs were furthermore correlated to longitude; the highest concentrations of α-HCH (Figure SI-2.4a) were observed in the
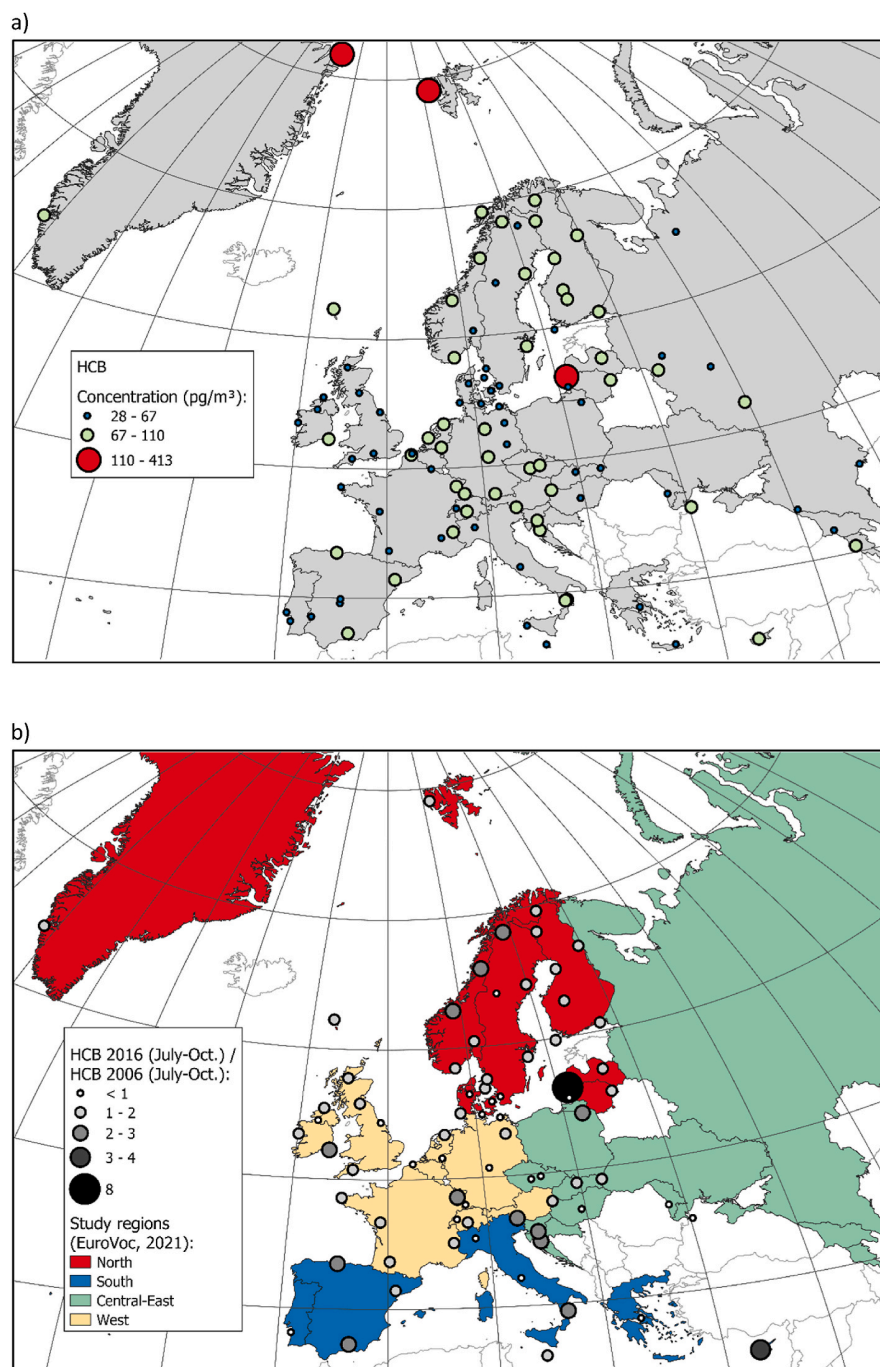
Fig. 1. (a) Concentrations of HCB in air across Europe (n = 101, this study), and (b) measured concentrations of HCB in 2016 (this study) divided by measured concentrations of HCB in 2006 (Halse et al., 2011) at European sites for which data for both years are available (n = 73).

central-east region (median: 18 pg/m^3), while the highest concentrations of γ-HCH (Figure SI-2.4b) were observed in the west region (median: 27 pg/m^3). This may reflect the later phase-out and large stockpiles of pesticides in the central-east region (e.g. Moldova and Ukraine) (Pribylova et al., 2012), and that Lindane was extensively used in e.g. France in the west region (Breivik et al., 1999; Vijgen et al., 2019).

The $\sum_6$DDXs (Figure SI-2.5) showed the largest variability in Europe (0.3–286 pg/m^3, MMR $\sum_6$DDX >953) of the targeted compounds. The variability of e.g. *p,p'*-DDT (MMR~433) was substantially larger in Europe, compared to Norway (MMR~15) (Lunder Halvorsen et al.,

2021). This suggests that some European sites may be influenced by continuing primary sources. The most significant difference (p < 0.001) between the south- and the north region were also found for $\sum_6$DDXs (south/north-ratio 6.5, Table SI-2.3), reflecting that the LRAT potential is less than for the more volatile HCB and HCHs (Shen et al., 2005), but also the continued use of DDT (UNEP, 2020). Like α-HCH, a west-east gradient was observed for $\sum_6$DDXs, with highest median concentration of $\sum_6$DDXs in the central-east region (35 pg/m^3), approximately four times higher than the west region (9.2 pg/m^3). High concentrations of $\sum_6$DDX were measured at sites in e.g. Ukraine, Moldova and the Czech Republic (146–286 pg/m^3), in line with previous findings (Halse

et al., 2011; Pribylova et al., 2012).

Similar to $\sum_6$DDXs, significantly (p < 0.001) higher concentrations were observed for endosulfan I in the south region than in the north region (south/north-ratio 4.6, Table SI-2.3), with the proximity to primary sources in the south region as a possible explanation. Though elevated concentrations of endosulfan I (16–21 pg/m^3, Figure SI-2.6) were measured in Armenia (site 1, Amberd) and Georgia (site 29, Abastumani) in the central-east region, endosulfan I was not significantly correlated to longitude. The very high concentrations of endosulfan I at Iskrba (site 72, Slovenia, 82 pg/m^3) may be an indication of local contribution.

The correlation analysis between the target POPs (Table SI-2.4) appears to reflect some similarities in the spatial patterns of emission sources. The positive correlation between all targeted POPs (except HCB) is likely to be a result of consistently higher concentrations in southern Europe compared to northern Europe. Furthermore, the positive correlation with estimated population density (within 50 km of the sampling sites) observed for all POPs (except HCB and α-HCH), suggests that high concentrations of most POPs can largely be attributed to elevated emissions occurring in the most populated areas in Europe.

The strongest correlation (0.84 < r < 0.95) was found between dieldrin (<MDL-37 pg/m^3), $\sum_4$chlordanes (0.5–35 pg/m^3), heptachlor-exo-epoxide (0.4–63 pg/m^3) and oxy-chlordane (<MDL-9 pg/m^3). These OCPs also have similar spatial patterns, with highest concentrations measured in the west region (e.g. Netherlands and Belgium, Figures SI-2.7-2.10). The median concentrations of these OCPs in the west region were up to three times higher than the median concentrations in the central-east region (Table SI-2.3). This finding aligns with the results by Halse et al. (2011), who also reported elevated levels of $\sum_4$chlordanes in the Netherlands and Belgium.

3.3. Temporal change

When comparing our results on the basis of median concentrations of all POPs with the 73 common European sites in the study of Halse et al. (2011), only HCB had higher median concentration in 2016 than in 2006 (56% increase, Table SI-2.5). The increase for HCB (i.e. 2016/2006-ratio >1.2) was evident at 68% of the sampling sites (Fig. 1b), while no obvious change (i.e. 2016/2006-ratio: 0.8.-1.2) was observed for the remaining sites. Data from long-term monitoring sites based on AAS shows an inconsistent time-trend in HCB concentrations (Gusev et al., 2015; Ilyin et al., 2022; Kalina et al., 2019; Wong et al., 2021). Of three sites with available AAS-data for both 2006 and 2016 (i. e. Zeppelin, Birkenes and Kosetice), only Zeppelin showed an increase in the HCB concentration with a 2016/2006 ratio of 1.1 (Table SI-2.6), while the ratio was below 1 at the other two sites. In comparison, our PAS results showed an increase at two of the three sites, i.e Birkenes and Zeppelin, with a 2016/2006 ratio of 1.8 and 1.3 respectively. This difference may be explained by that the PAS and AAS have been exposed to different air masses (i.e. time-average of 3 months-vs. daily/weekly-samples).

No clear spatial pattern was observed, but the increase was larger at some specific sites. For example, at Rucava (site 52, Latvia), the concentration of HCB in 2016 was almost eight times higher than in 2006, substantiating possible local contribution at this site in 2016. The increase observed in the Arctic (e.g. site 96, Zeppelin, 2016/2006-ratio: 1.3), is in accordance with the stable or increasing concentrations reported in the Arctic from 1992 to 2018 by Wong et al. (2021).

The concentrations of the other POPs (i.e. PCBs, HCHs, DDXs and chlordanes) have decreased significantly (p < 0.05) between 2006 and 2016 (Table SI-2.5), i.e. −28% decrease in the median concentrations for $\sum_6$PCBs, −59% for α-HCHs, −48% for γ-HCHs, −12% for $\sum_4$DDXs (*p,p'*-DDD/-DDE/-DDT, *o,p'*-DDT) and −23% for $\sum_4$chlordanes. For both $\sum_4$DDXs and $\sum_4$chlordanes, a significant decrease was only observed in the west region (−45% and −27% respectively). This is consistent with the overall decreasing trend reported for these POPs at

AAS sites within EMEP (Gusev et al., 2015; Hung et al., 2016; Kalina et al., 2019). While there were small differences in the median concentrations of $\sum_4$chlordanes between the four regions, in both 2006 (2.2–3.7 pg/m^3) and 2016 (2.0–3.1 pg/m^3), $\sum_4$DDXs were substantially higher for the central-east region (77 pg/m^3 in 2006 and 61 pg/m^3 in 2016), compared to the other regions (Figure SI-2.11 c).

It should be noted that the detection frequencies of the DDXs were higher in 2016 than in 2006. This may be explained by a lower method detection limit in 2016. For example, the MDL for *p,p'*-DDE was 0.18 pg/m^3 in 2016 while 1.6 pg/m^3 in 2006, and consequently *p,p'*-DDE was detected in all samples in 2016, while only in 74% of the samples in 2006. When disregarding the 20 sites where the concentration of *p,p'*-DDE in 2006 was below MDL, a decrease in the median concentration of *p,p'*-DDE for the remaining 53 sites was still observed (Figure SI-2.12), but it was not statistically significant (p = 0.084). As a consequence of lower MDL and the ability to detect lower concentrations in 2016, the variability of *p,p'*-DDE was substantially larger in our study (MMR 1017) when considering all sites, than reported by both Halse et al. (2011) (MMR>177) and Jaward et al. (2004) (MMR>29).

For PCBs, the largest decrease in median concentrations was observed in the north- and central-east regions (−48% and −35%), followed by the west region (−22%). On the other hand, the median concentration of $\sum_6$PCBs in the south region in 2016 were comparable to 2006. The MMR of $\sum_6$PCBs in 2016 is 211 when including all sites, which is higher than previously reported for the background sites in the European studies of Schuster et al. (2021) (MMR $\sum_7$PCBs = 58, n = 11) and Jaward et al. (2004) (MMR $\sum_6$PCBs >24, n = 46). A smaller difference in MMRs is observed when comparing only with the common sites (n = 73) in the study of Halse et al. (2011) (MMR 45 in 2006 and MMR 88 in 2016). The high MMR when including all sites in 2016 may therefore likely reflect the larger spatial coverage across Europe in our study compared to previous studies, which illustrates the benefits of high spatial resolution.

α-HCH was found at highest concentrations in the central-east region in both 2016 (median 17 pg/m^3) and in 2006 (median 55 pg/m^3), but the median concentration has decreased substantially (−69%). In the north region, the decrease of α-HCH was smaller than in the other regions (−22%) (Figure SI-2.11 a-d). This may be explained by the northern sites being more influenced by climate change and thereby from increased re-volatilization from sea and ice melting (Halse et al., 2012; Ma et al., 2011; Shen et al., 2004), compared to the other regions in Europe. For γ-HCH, the decrease was substantially higher for the south- (−76%), central-east- (−56%) and west region (−45%), compared to the north region (−21%). Consequently, the south/north-ratio (of medians) was reduced from 6.7 in 2006 to 2.0 in 2016. The largest decrease for α-HCH and γ-HCH is observed in the historical primary source regions were technical HCH and Lindane have been more extensively used, respectively (Breivik et al., 1999), and reflect that the immediate effect on air concentrations from emissions reductions is larger in source areas, compared to more remote areas.

3.4. Source indications

A higher proportion of the more chlorinated PCBs is expected closer to source regions, as heavier PCBs tend to be less prone to LRAT (Beyer et al., 2003). Accordingly, high relative abundance of PCB-153, compared to PCB-28 (Figure SI-2.13), in combination with elevated measured concentrations, may reveal potential source areas and/or locally affected sites. Consequently, higher PCB-153/PCB-28 ratios were observed in southern Europe than in northern Europe. The highest ratio was observed for Abastumani (site 29, Georgia, PCB-153/PCB-28-ratio: 14, Figure SI-2.13), followed by Keldsnor (site 11, Denmark), Porspoder (site 26, France) and Risoe (site 13, Denmark) (PCB-153/PCB-28-ratios: 3–4). For all these sites (except Porspoder), the high ratios are accompanied with elevated $\sum_6$PCB concentrations (i.e. outliers >70 pg/m^3, Figure SI-2.2a), substantiating that sources may exist in the vicinity.

The α-/γ–HCH–ratios in this study (range: 0.1–7.7, Figure SI-2.14) and within EMEP (range: 0.2–41 (Aas and Bohlin-Nizzetto, 2018),) were highest in northern Europe (correlation with latitude in this study; r = 0.53, p < 0.001), suggesting that LRAT and/or re-volatilization of α-HCH are important in this region (Halse et al., 2012; Shen and Wania, 2005). The lower α-/γ–HCH–ratios in southern Europe may further reflect the vicinity to countries which have experienced significant historical use and emissions of γ-HCH (Breivik et al., 1999). For example, the α-/γ–HCH–ratio at Waldhof (site 35, Germany) were 0.3 in this study and 0.2 within EMEP respectively.

Isomeric ratios can be used to assess whether more "weathered" isomers are dominating, and hence indicate possible shifts from primary-to secondary sources (Becker et al., 2012; Pozo et al., 2006). One example is the DDXs, for which a weathered signal with the ratio (*p, p'*-DDE + *p,p'*-DDD)/*p,p'*-DDT larger than 1.3 was found at 92% of the sites (Figure SI-2.15a), indicating past usage of technical DDT in Europe. (Li and Macdonald, 2005; Ricking and Schwarzbauer, 2012). A weathered signal of *p,p'*-DDT in European air was also shown in 2006 (Halse et al., 2011). When comparing the ratio for the 53 sites above MDL in 2006 with the ratio in 2016, 17 sites had a lower ratio in 2016 (Figure SI-2.15b). For Montelibretti (site 47) and Ispra (site 46) in Italy, the ratios decreased from 2.8 to 1.5 and 2.6 to 1.5 respectively. As the *p, p'*-DDT concentration at the site had increased, while there was no reduction in the *p,p'*-DDE concentration, the observed decrease may be a result of possible influence from primary emissions of *p,p'*-DDT.

Several countries in Europe (e.g. Spain, Italy and Turkey) have utilized dicofol in agriculture (Denier van der Gon et al., 2007). Dicofol is synthesized from DDT (Qiu et al., 2005) and has shown to have a higher content of the *o,p'*-DDT isomer compared to technical DDT. In our study, 29% of the sites had *o,p'*-DDT/*p,p'*-DDT ratios between 1.0 and 3.2 (Figure SI-2.15c), and influence from dicofol may therefore be expected. However, elevated ratios up to 14 have previously been reported in areas where dicofol is suspected to be the dominant source (Ricking and Schwarzbauer, 2012). The highest ratios in our study were found in northern Europe (including Svalbard with ratio 3.2), which instead may be explained by differences in the LRAT potential of the two isomers due to a greater vapour pressure of the *o,p'*-DDT isomer (Spencer and Cliath, 1972). Preferential mobilization of the *o,p'*-DDT isomer from soil to air (Ricking and Schwarzbauer, 2012) may also explain the elevated ratios at some of the sites in our study.

The expected proportion of trans- and cis-chlordane from technical chlordane in ambient air is 1.6 (Jantunen et al., 2000). Due to greater reactivity of trans-chlordane compared to cis-chlordane in the environment (Becker et al., 2012; Bidleman et al., 2002), the low trans-/-cis-chlordane ratio observed in our study (median 0.27, less than 1.6 at 99% of the sites) may indicate that the occurrence of chlordanes in European atmosphere is mostly influenced by historical use. This is further supported by the high detection frequency of oxy-chlordane (99%), which is a metabolite of the chlordanes. Houtem (site 4) in Belgium, with the highest concentration of $\sum_4$chlordanes (35 pg/m^3), also shows a high ratio of trans-/cis-chlordane (2.2, Figure SI-2.16), which implicates possible influence from more recent use of technical chlordane in the vicinity of the site.

Technical chlordane also contains 7% of heptachlor (Dearth and Hites, 1991). The dominance of the degradation product heptachlor-exo-epoxide (detected at all sites) in our study, compared to heptachlor (7% detected frequency), could therefore indicate past usage of technical chlordane in Europe, but could also be due to past usage of technical heptachlor (Bidleman et al., 2002). It should be noted that heptachlor was detected with highest concentration in the sample from Houtem (21 pg/m^3, 32 times the MDL). This substantiates possible fresh usage of one of these pesticides at the site (Hung et al., 2002).

While aldrin was not detected in any of the samples, dieldrin was detected in 98% of the samples. Aldrin is degraded to dieldrin in the environment (Gannon and Bigger, 1958), and the high abundance of dieldrin may therefore implicate re-volatilization of either dieldrin and/or aldrin.

The technical mixture of endosulfan consists of >95% of the endosulfan I and –II, in ratios between 2:1 and 7:3 (Weber et al., 2010). While endosulfan I was detected at all sites, the detection frequency of endosulfan II was only 45%. This may be explained by the higher content of endosulfan I in the technical mixture and that endosulfan II may be converted to endosulfan I in the environment (Schmidt et al., 1997; Weber et al., 2010). The high median endosulfan I/endosulfan II-ratio (8.5) across Europe may further suggest high degree of conversion of endosulfan II, and hence implicates previous use of endosulfan. In contrast, the low ratios at Iskrba (site 72, Slovenia, ratio: 1.4) and Capo Granitola (site 50, Spain, ratio: 2.4) (Figure SI-2.17), accompanied with the highest measured concentrations of both endosulfan I (82 and 24 pg/m^3) and endosulfan-II (58 and 9.9 pg/m^3), suggest more recent use at these sites. It is also noteworthy that the detection frequency of endosulfan II is higher compared to the detection frequency in the Norwegian study (5% only) (Lunder Halvorsen et al., 2021), which may be a result of endosulfan II being washed out more easily during atmospheric transport (Shen et al., 2005).

3.5. Model predictions of PCB-153

Concentrations of PCB-153 in air predicted by GLEMOS and FLEXPART were within a factor of three of the observed concentrations for 62% and 65% of the sampling sites respectively. Both models generally underestimated the measured concentrations, i.e. the ratio of measured/predicted concentrations was larger than one for 81% of the sites with GLEMOS and 84% of the sites with FLEXPART. The highest deviations were found in the north and east regions (Figure SI-2.18). The underestimation observed for both FLEXPART and GLEMOS may in part be due to uncertainties in the emission data used as input to the models (Lunder Halvorsen et al., 2021). Secondly, FLEXPART ignores secondary emissions, hence lower predicted concentrations with FLEXPART are expected. However, FLEXPART predicted lower concentrations only at 45% of the sites and the FLEXPART/GLEMOS ratio ranged from 0.3 to 3.0. Thirdly, there are also uncertainties related to the estimated atmospheric loss during transport with the two models. A comparison of predicted and observed concentrations (Figure SI-2.18), may help identifying sites or areas where emissions are either under- or overestimated. The most noticeable example is Abastumani (site 29, Georgia) where the highest measured concentration of PCB-153 (78 pg/m^3) was found in this study. The measured concentration at this site far exceeds what both GLEMOS (0.45 pg/m^3) and FLEXPART (0.31 pg/m^3) predict. When excluding the concentration measured at Abastumani, the spatial variabilities of PCB-153 obtained from the two models (MMR = 566 for GLEMOS, MMR = 229 for FLEXPART), are larger than the observed spatial variability (MMR = 161) in the study region. The underestimation with GLEMOS is largest when low concentrations are predicted (e.g. in the north region, Figure SI-2.18), resulting in a possible overestimated MMR.

GLEMOS (Table SI-2.7) predicts that secondary emissions are, on average, four times more important (median 78%) than total primary emissions (i.e. national emissions and transboundary transport within/outside EMEP) in controlling atmospheric burdens. The contributions from secondary emissions (Fig. 2) are predicted to be largest at sites in Russia and Finland (92–95%, e.g. Pinega, site 64, Figure SI-2.19a). The footprint map of Pinega, obtained from FLEXPART (Figure SI-2.19b), shows low input of primary emissions from other areas.

According to GLEMOS, the contributions from total primary emissions (Fig. 2) to the measured concentrations on the sites varied from 5% to 61% (median 22%), with the exception of Station Nord at Greenland (site 41, 94%). Significantly larger (p-value<0.001) contribution from primary emissions in the south and west region (median 35% and 28% respectively), compared to the north and central-east region (median 18% and 16% respectively) were observed. National primary emissions (Fig. 2) were predicted to contribute 0–53% (median 11%) to the
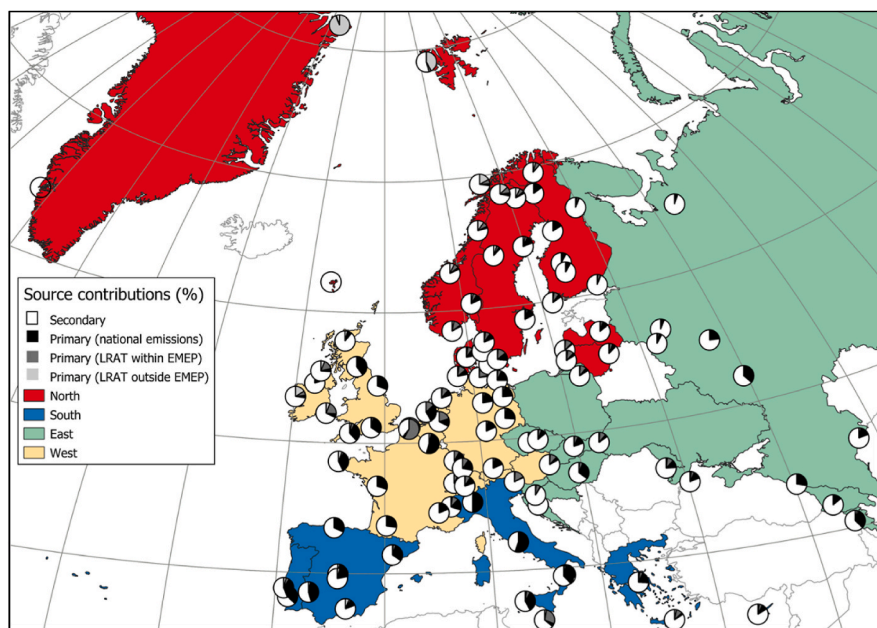
Fig. 2. Predicted relative contribution of secondary and primary emissions of PCB-153 attributed to national emissions and transboundary transport from countries within/outside EMEP, predicted by The Global EMEP Multi-media Modeling System (GLEMOS). The different study regions are indicated in the background map.

concentrations of PCB-153 and followed a similar spatial pattern as the total primary emissions. Barcarotta in Spain (site 78, south region, Figure SI-2.20a) is an example of a site that is predicted to be highly influenced by national emissions (41%). The footprint map (Figure SI-2.20b), showing largest input in the vicinity to the sampling site, also reflects this.

It should be noted that many of the selected background sites are not necessarily designated sites for the measurement of PCBs, but rather background sites for other air quality indicators. Both the observed concentrations of PCB-153 and the predicted total primary emissions correlated significantly (p-values <0.001) with the estimated population density within 50 km radius of the sampling site (r = 0.63 and r = 0.51). The highest densities (690–2700 persons per km^2) were found for nine sampling sites which had a city within this region (red circles in Figure SI-1.8), and it may therefore be questioned if these are representative background sites in the measurement of PCBs. For example, Alfragide (site 63, Portugal) was located in the immediate vicinity of Lisbon city. Not surprisingly, the observed concentrations of PCB-153 for these "suburban" sites (3.3–17 pg/m^3) were found to be significantly higher (p < 0.001) than all other sites (median 1.8 pg/m^3, <610 habitants/km^2). This "suburban effect" was largely captured by GLE-MOS, which predicted the influence from national emissions to be significantly higher (p-value = 0.01) for the "suburban" sites (5–53%), compared to the other sites (median 11%).

On the other hand, the influence from transboundary transport within/outside EMEP (Fig. 2) were 5% and 2% (medians) respectively, and were predicted to be largest in the north region (median 9%). This is in line with the findings in our Norwegian study (Lunder Halvorsen et al., 2021), in which 15% was attributed to LRAT. Both Station Nord (site 41, Greenland) and Zeppelin (site 96, Spitsbergen) in the north region were predicted to be highly influenced by primary sources outside EMEP (93% and 42% respectively), compared to the other sites (<17%). This was also demonstrated in the footprint map for Zeppelin (Lunder Halvorsen et al., 2021). Malanichev et al. (2004) has further shown that American emission sources are one of the main contributors to the atmospheric concentrations of PCB-153 in the Arctic in summer. In contrast, e.g. Houtem (site 4, Belgium) had the largest predicted influence from transboundary transport within EMEP (58%),

predominantly from France (56%) (Figure SI-2.21a). The footprint map (Figure SI-2.21b) further showed high emission contributions beyond the nation's boundaries, within the EMEP region. The EMEP countries that contributed most frequently to the atmospheric burdens of PCB-153 at sites in other countries, were France (67%), Germany (48%), UK (38%), Belgium (18%), Italy (18%), Russia (17%), Spain (16%), Sweden (16%), Finland (11%), Netherlands (10%), Denmark (10%) and Ukraine (9%). However, these numerical values are affected by the geographical location and density of sites, as well as the predominant air flow across Europe (west to east). For example, as the number of sites is relatively large east of the French border, a relatively large number of sites are likely to have been influenced by emissions in France.

4. Conclusions

In this extensive spatial mapping study, HCB and HCHs were found to dominate the atmospheric background concentrations of POPs across Europe. The highest spatial variability, on the other hand, was found for $\sum_6$DDXs (MMR>953) and $\sum_6$PCB (MMR = 240). For most POPs, higher concentrations were observed in southern Europe than in northern Europe, reflecting the proximity to historical source regions. In contrast, the concentrations of HCB increased with latitude. The elevated concentrations of HCB observed in the Arctic may be explained by enhanced influence of re-volatilization, but primary emissions of HCB have also been suggested to be influential (Platt et al., 2022).

HCB was the only POP with higher concentrations in 2016 than in 2006. An increase was observed at 68% of the sites, distributed across Europe, with an increase of 56% in the median concentration of HCB from 2006 to 2016. High concentrations of HCB due to pesticide use have previously been reported in central parts of Europe (Barber et al., 2005), and enhanced influence of secondary emissions from previously contaminated soil may be possible. However, the increase in concentrations of HCB in air could also be a consequence of an increase in primary emissions. This highlights the need for further studies separating the contributions from primary and secondary sources of HCB, and future source-receptor modelling studies should therefore target HCB. The increased concentrations also imply that further monitoring of HCB is needed.

On the other hand, the observed decline in the median atmospheric concentrations from 2006 to 2016 for α-HCH (−59%), γ-HCH (−48%), $\sum_6$PCBs (−28%), $\sum_4$chlordanes (−23%) and $\sum_4$DDXs (−12%) reflects that the primary emissions in the study region have declined. The largest decreases are observed in historical primary source regions while the smallest decreases are observed in remote regions which are more influenced by secondary emissions and/or long-range atmospheric transport from outside Europe. For the PCBs, no significant decrease and a higher proportion of the more chlorinated PCB-153 than PCB-28 was observed in the south region, implying more influence of primary sources in this region. This was supported by model predictions of PCB-153 using GLEMOS that showed that the contribution from secondary emissions is, on average, four times higher than primary emissions in most of the study area while primary emissions of PCB-153 are more influential at southern latitudes.

For $\sum_6$DDXs and $\sum_4$chlordanes, the decrease was only significant in the west region. Isomeric ratios for OCPs showed that most sites are influenced by secondary sources from historical usage of pesticides. For DDXs, however, the isomeric ratio indicates that some sites may be influenced by primary emissions of technical DDT. Furthermore, the spatial patterns of the dominating isomers suggest that the influence of secondary sources was largest at southern latitudes in Europe. Secondary emissions from applications of technical aldrin, -chlordane and -heptachlor were more dominating in the west region than the east region.

Implications of continued influence of primary emissions of PCBs and DDXs in some regions, suggest that these compounds should be prioritized in future monitoring of POPs. Within EMEP, the MMRs based on active air sampling concentrations were 11 for $\sum_6$PCB (n = 10) and 328 for sum of p,p'-DDD/DDE/DDT (n = 11). This is substantially lower than the spatial variability (240 and 1135 respectively) based on all sites in our study (n = 101) and suggests that the spatial variability of PCBs and DDXs in Europe is not fully captured by the ongoing monitoring activities within EMEP.

Our study highlights the advantages of combining high spatial resolution observations with mechanistic modelling approaches as an important supplement to ongoing long-term monitoring efforts at EMEP sites. As this study offers results which provide new insights on the relative importance of primary and secondary emission sources on a European scale, it thereby also offers knowledge which can be used by policy makers to assess potential opportunities for further emission reductions of legacy POPs. While this study has focused on selected legacy POPs only, the strategy of combining high resolution monitoring and modelling can be expanded towards a wider range of semi-volatile organic chemicals in the future. However, due to the lower uptake efficiency for particles with our MONET-sampler (Markovic et al., 2015), alternative sampling strategies will ideally be required if targeting trace-levels of particle-associated chemicals.

CRediT authorship contribution statement

Helene Lunder Halvorsen: Methodology, Validation, Formal analysis, Investigation, Writing – original draft, Project administration, Visualization. **Pernilla Bohlin-Nizzetto:** Methodology, Investigation, Validation, Writing – review & editing, Supervision. **Sabine Eckhardt:** Formal analysis, Writing – review & editing, Visualization. **Alexey Gusev:** Formal analysis, Visualization. **Claudia Moeckel:** Validation, Formal analysis, Investigation, Writing – review & editing, Visualization. **Victor Shatalov:** Formal analysis, Visualization. **Lovise Pedersen Skogeng:** Investigation. **Knut Breivik:** Conceptualization, Validation, Writing – review & editing, Supervision, Project administration, Funding acquisition.

Declaration of competing interest

The authors declare that they have no known competing financial interests or personal relationships that could have appeared to influence the work reported in this paper.

Data availability

Data will be made available on request.

Appendix A. Supplementary data

Supplementary data to this article can be found online at https://doi.org/10.1016/j.atmosenv.2023.119658.

References

Aas, W., Bohlin-Nizzetto, P., 2018. Heavy Metals and POP Measurements, 2016. EMEP/CCC-Report 3/2018). Kjeller: NILU Retrieved from. http://hdl.handle.net/11250/2563390.

Barber, J.L., Sweetman, A.J., van Wijk, D., Jones, K.C., 2005. Hexachlorobenzene in the global environment: emissions, levels, distribution, trends and processes. Sci. Total Environ. 349 (1), 1–44. https://doi.org/10.1016/j.scitotenv.2005.03.014.

Becker, S., Halsall, C.J., Tych, W., Kallenborn, R., Schlabach, M., Manø, S., 2012. Changing sources and environmental factors reduce the rates of decline of organochlorine pesticides in the Arctic atmosphere. Atmos. Chem. Phys. 12 (9), 4033–4044. https://doi.org/10.5194/acp-12-4033-2012.

Beyer, A., Wania, F., Gouin, T., Mackay, D., Matthies, M., 2003. Temperature dependence of the characteristic travel distance. Environ. Sci.Technol. 37 (4), 766–771. https://doi.org/10.1021/es025717w.

Bidleman, T.F., Jantunen, L.M.M., Helm, P.A., Brorström-Lundén, E., Juntto, S., 2002. Chlordane enantiomers and temporal trends of chlordane isomers in arctic air. Environ. Sci.Technol. 36 (4), 539–544. https://doi.org/10.1021/es011142b.

Bohlin, P., Audy, O., Škrdlíková, L., Kukučka, P., Přibylová, P., Prokeš, R., Vojta, Š., Klánová, J., 2014. Outdoor passive air monitoring of semi volatile organic compounds (SVOCs): a critical evaluation of performance and limitations of polyurethane foam (PUF) disks. Environ. Sci. J. Integr. Environ. Res.: Process. Impacts 16 (3), 433–444. https://doi.org/10.1039/C3EM00644A.

Breivik, K., Pacyna, J.M., Münch, J., 1999. Use of α-, β- and γ-hexachlorocyclohexane in Europe, 1970–1996. Sci. Total Environ. 239 (1–3), 151–163. https://doi.org/10.1016/s0048-9697(99)00291-0.

Breivik, K., Sweetman, A., Pacyna, J.M., Jones, K.C., 2002. Towards a global historical emission inventory for selected PCB congeners–a mass balance approach. 2. Emissions. Sci. Total Environ. 290 (1–3), 199–224. https://doi.org/10.1016/s0048-9697(01)01076-2.

Breivik, K., Alcock, R., Li, Y.F., Bailey, R.E., Fiedler, H., Pacyna, J.M., 2004. Primary sources of selected POPs: regional and global scale emission inventories. Environ. Pollut. 128 (1–2), 3–16. https://doi.org/10.1016/j.envpol.2003.08.031.

Breivik, K., Sweetman, A., Pacyna, J.M., Jones, K.C., 2007. Towards a global historical emission inventory for selected PCB congeners - a mass balance approach-3. An update. Sci. Total Environ. 377 (2–3), 296–307. https://doi.org/10.1016/j.scitotenv.2007.02.026.

Dearth, M.A., Hites, R.A., 1991. Complete analysis of technical chlordane using negative ionization mass spectrometry. Environ. Sci.Technol. 25 (2), 245–254. https://doi.org/10.1021/es00014a005.

Denier van der Gon, H., van het Bolscher, M., Visschedijk, A., Zandveld, P., 2007. Emissions of persistent organic pollutants and eight candidate POPs from UNECE–Europe in 2000, 2010 and 2020 and the emission reduction resulting from the implementation of the UNECE POP protocol. Atmos. Environ. 41 (40), 9245–9261. https://doi.org/10.1016/j.atmosenv.2007.06.055.

EuroVoc, 2021. Browse by EuroVoc. Retrieved from. https://eur-lex.europa.eu/browse/eurovoc.html. Access Dec 2021.

Francisco, A.P., Harner, T., Eng, A., 2017. Measurement of polyurethane foam – air partition coefficients for semivolatile organic compounds as a function of temperature: application to passive air sampler monitoring. Chemosphere 174, 638–642. https://doi.org/10.1016/j.chemosphere.2017.01.135.

Gannon, N., Bigger, J.H., 1958. The conversion of aldrin and heptachlor to their epoxides in Soil1. J. Econ. Entomol. 51 (1), 1–2. https://doi.org/10.1093/jee/51.1.1.

Gioia, R., Sweetman, A.J., Jones, K.C., 2007. Coupling passive air sampling with emission estimates and chemical fate modeling for persistent organic pollutants (POPs): a feasibility study for northern Europe. Environ. Sci.Technol. 41 (7), 2165–2171. https://doi.org/10.1021/es0626739.

Gusev, A., Rozovskaya, O., Shatalov, V., Aas, W., Bohlin-Nizzetto, P., 2015. EMEP Status Report 3/2015. Assessment of Spatial and Temporal Trends of POP Pollution on Regional and Global Scale. Moscow: Meteorological Synthesizing Centre – East Retrieved from. https://www.msceast.org/reports/3_2015.pdf.

Halse, A.K., Schlabach, M., Eckhardt, S., Sweetman, A., Jones, K.C., Breivik, K., 2011. Spatial variability of POPs in European background air. Atmos. Chem. Phys. 11 (4), 1549–1564. https://doi.org/10.5194/acp-11-1549-2011.

Halse, A.K., Schlabach, M., Sweetman, A., Jones, K.C., Breivik, K., 2012. Using passive air samplers to assess local sources versus long range atmospheric transport of POPs. J. Environ. Monit. 14 (10), 2580–2590. https://doi.org/10.1039/c2em30378g.

Harner, T., 2017. 2017_v1_5_Template for Calculating Effective Air Sample Volumes for PUF and SIP Disk Samplers_Sept_15. Retrieved from. https://www.researchgate.net/publication/319764519_2017_v1_5_Template_for_calculating_Effective_Air_Sample_Volumes_for_PUF_and_SIP_Disk_Samplers_Sept_15. Access June 2019.

Helsel, D.R., 2006. Fabricating data: how substituting values for nondetects can ruin results, and what can be done about it. Chemosphere 65 (11), 2434–2439. https://doi.org/10.1016/j.chemosphere.2006.04.051.

Holt, E., Bohlin-Nizzetto, P., Borůvková, J., Harner, T., Kalina, J., Melymuk, L., Klánová, J., 2017. Using long-term air monitoring of semi-volatile organic compounds to evaluate the uncertainty in polyurethane-disk passive sampler-derived air concentrations. Environ. Pollut. 220, 1100–1111. https://doi.org/10.1016/j.envpol.2016.11.030.

Hung, H., Halsall, C.J., Blanchard, P., Li, H.H., Fellin, P., Stern, G., Rosenberg, B., 2002. Temporal trends of organochlorine pesticides in the Canadian arctic atmosphere. Environ. Sci.Technol. 36 (5), 862–868. https://doi.org/10.1021/es011204y.

Hung, H., Katsoyiannis, A.A., Brorstrom-Lunden, E., Olafsdottir, K., Aas, W., Breivik, K., Bohlin-Nizzetto, P., Sigurdsson, A., Hakola, H., Bossi, R., Skov, H., Sverko, E., Barresi, E., Fellin, P., Wilson, S., 2016. Temporal trends of persistent organic pollutants (POPs) in arctic air: 20 years of monitoring under the arctic monitoring and assessment programme (AMAP). Environ. Pollut. 217, 52–61. https://doi.org/10.1016/j.envpol.2016.01.079.

Ilyin, I., Batrakova, N., Gusev, A., Kleimenov, M., Rozovskaya, O., Shatalov, V., Strizhkina, I., Travnikov, O., Vulykh, N., Breivik, K., Bohlin-Nizzetto, P., Pfaffhuber, K.A., Aas, W., Poupa, S., Wankmueller, R., Ullrich, B., Bank, M., Ho, Q.T., Vivanco, M.G., Theobald, M.R., Garrido, J.L., Gil, V., Couvidat, F., Collette, A., Mircea, M., Adani, M., Delia, I., Kouznetsov, R.D., Kadancev, E.V., 2022 (Status Report 2/2022). Assessment of Heavy Metal and POP Pollution on Global, Regional and National Scales. Moscow: Meteorological Synthesizing Centre - East Retrieved from. https://www.msceast.org/reports/2_2022.pdf.

Jantunen, L.M.M., Bidleman, T.F., Harner, T., Parkhurst, W.J., 2000. Toxaphene, chlordane, and other organochlorine pesticides in Alabama air. Environ. Sci. Technol. 34 (24), 5097–5105. https://doi.org/10.1021/es001197y.

Jaward, F.M., Farrar, N.J., Harner, T., Sweetman, A.J., Jones, K.C., 2004. Passive air sampling of PCBs, PBDEs, and organochlorine pesticides across Europe. Environ. Sci. Technol. 38 (1), 34–41. https://doi.org/10.1021/es034705n.

Jones, K., 1994. Observations on long-term air-soil exchange of organic contaminants. Environ. Sci. Pollut. Control Ser. 1, 172. https://doi.org/10.1007/BF02986940.

Kalina, J., Scheringer, M., Borůvková, J., Kukučka, P., Přibylová, P., Bohlin-Nizzetto, P., Klánová, J., 2017. Passive air samplers as a tool for assessing long-term trends in atmospheric concentrations of semivolatile organic compounds. Environ. Sci. Technol. 51 (12), 7047–7054. https://doi.org/10.1021/acs.est.7b02319.

Kalina, J., White, K.B., Scheringer, M., Přibylová, P., Kukučka, P., Audy, O., Klánová, J., 2019. Comparability of long-term temporal trends of POPs from co-located active and passive air monitoring networks in Europe. Environ. Sci. J. Integr. Environ. Res.: Process. Impacts 21 (7), 1132–1142. https://doi.org/10.1039/C9EM00136K.

Li, Y.F., Macdonald, R.W., 2005. Sources and pathways of selected organochlorine pesticides to the Arctic and the effect of pathway divergence on HCH trends in biota: a review. Sci. Total Environ. 342 (1–3), 87–106. https://doi.org/10.1016/j.scitotenv.2004.12.027.

Li, L., Wania, F., 2018. Occurrence of single- and double-peaked emission profiles of synthetic chemicals. Environ. Sci. Technol. 52 (8), 4684–4693. https://doi.org/10.1021/acs.est.7b06478.

Lunder Halvorsen, H., Bohlin-Nizzetto, P., Eckhardt, S., Gusev, A., Krogseth, I.S., Moeckel, C., Shatalov, V., Skogeng, L.P., Breivik, K., 2021. Main sources controlling atmospheric burdens of persistent organic pollutants on a national scale. Ecotoxicol. Environ. Saf. 217, 112172 https://doi.org/10.1016/j.ecoenv.2021.112172.

Ma, J., Hung, H., Tian, C., Kallenborn, R., 2011. Revolatilization of persistent organic pollutants in the Arctic induced by climate change. Nat. Clim. Change 1, 255–260. https://doi.org/10.1038/nclimate1167.

Malanichev, A., Mantseva, E., Shatalov, V., Strukov, B., Vulykh, N., 2004. Numerical evaluation of the PCBs transport over the northern hemisphere. Environ. Pollut. 128 (1), 279–289. https://doi.org/10.1016/j.envpol.2003.08.040.

Markovic, M.Z., Prokop, S., Staebler, R.M., Liggio, J., Harner, T., 2015. Evaluation of the particle infiltration efficiency of three passive samplers and the PS-1 active air sampler. Atmos. Environ. 112, 289–293. https://doi.org/10.1016/j.atmosenv.2015.04.051.

Meijer, S.N., Ockenden, W.A., Steinnes, E., Corrigan, B.P., Jones, K.C., 2003. Spatial and temporal trends of POPs in Norwegian and UK background air: implications for global cycling. Environ. Sci.Technol. 37 (3), 454–461. https://doi.org/10.1021/es025620+.

Nizzetto, L., Macleod, M., Borgå, K., Cabrerizo, A., Dachs, J., Guardo, A.D., Ghirardello, D., Hansen, K.M., Jarvis, A., Lindroth, A., Ludwig, B., Monteith, D., Perlinger, J.A., Scheringer, M., Schwendenmann, L., Semple, K.T., Wick, L.Y., Zhang, G., Jones, K.C., 2010. Past, present, and future controls on levels of persistent organic pollutants in the global environment. Environ. Sci.Technol. 44 (17), 6526–6531. https://doi.org/10.1021/es100178f.

Pisso, I., Sollum, E., Grythe, H., Kristiansen, N.I., Cassiani, M., Eckhardt, S., Arnold, D., Morton, D., Thompson, R.L., Groot Zwaaftink, C.D., Evangeliou, N., Sodemann, H., Haimberger, L., Henne, S., Brunner, D., Burkhart, J.F., Fouilloux, A., Brioude, J., Philipp, A., Seibert, P., Stohl, A., 2019. The Lagrangian particle dispersion model FLEXPART version 10.4. Geosci. Model Dev. (GMD) 12 (12), 4955–4997. https://doi.org/10.5194/gmd-12-4955-2019.

Platt, S.M., Hov, Ø., Berg, T., Breivik, K., Eckhardt, S., Eleftheriadis, K., Evangeliou, N., Fiebig, M., Fisher, R., Hansen, G., Hansson, H.C., Heintzenberg, J., Hermansen, O., Heslin-Rees, D., Holmén, K., Hudson, S., Kallenborn, R., Krejci, R., Krognes, T., Larssen, S., Lowry, D., Lund Myhre, C., Lunder, C., Nisbet, E., Nizzetto, P.B., Park, K.T., Pedersen, C.A., Aspmo Pfaffhuber, K., Röckmann, T., Schmidbauer, N., Solberg, S., Stohl, A., Ström, J., Svendby, T., Tunved, P., Tørnkvist, K., van der Veen, C., Vratolis, S., Yoon, Y.J., Yttri, K.E., Zieger, P., Aas, W., Tørseth, K., 2022. Atmospheric composition in the European arctic and 30 years of the Zeppelin observatory, ny-ålesund. Atmos. Chem. Phys. 22 (5), 3321–3369. https://doi.org/10.5194/acp-22-3321-2022.

Pozo, K., Harner, T., Wania, F., Muir, D.C.G., Jones, K.C., Barrie, L.A., 2006. Toward a global network for persistent organic pollutants in air: results from the GAPS study. Environ. Sci.Technol. 40 (16), 4867–4873. https://doi.org/10.1021/es060447t.

Pribylova, P., Kares, R., Boruvkova, J., Cupr, P., Prokes, R., Kohoutek, J., Holoubek, I., Klanova, J., 2012. Levels of persistent organic pollutants and polycyclic aromatic hydrocarbons in ambient air of Central and Eastern Europe. Atmos. Pollut. Res. 3 (4), 494–505. https://doi.org/10.5094/APR.2012.057.

Qiu, X., Zhu, T., Yao, B., Hu, J., Hu, S., 2005. Contribution of dicofol to the current DDT pollution in China. Environ. Sci.Technol. 39 (12), 4385–4390. https://doi.org/10.1021/es050342a.

Ricking, M., Schwarzbauer, J., 2012. DDT isomers and metabolites in the environment: an overview. Environ. Chem. Lett. 10 (4), 317–323. https://doi.org/10.1007/s10311-012-0358-2.

San-Miguel-Ayanz, J., Durrant, T., Boca, R., Libertà, G., Branco, A., De Rigo, D., Ferrari, D., Maianti, P., Vivancos, T., Schulte, E., Loffler, P., 2017. Forest Fires in Europe, Middle East and North Africa 2016. (EUR 28707 EN). Publications Office of the European Union, Luxembourg. Retrieved from. https://data.europa.eu/doi/10.2760/17690.

Schmidt, W.F., Hapeman, C.J., Fettinger, J.C., Rice, C.P., Bilboulian, S., 1997. Structure and asymmetry in the isomeric conversion of β- to α-endosulfan. J. Agric. Food Chem. 45 (4), 1023–1026. https://doi.org/10.1021/jf970020t.

Schuster, J.K., Harner, T., Eng, A., Rauert, C., Su, K., Hornbuckle, K.C., Johnson, C.W., 2021. Tracking POPs in global air from the first 10 Years of the GAPS network (2005 to 2014). Environ. Sci.Technol. 55 (14), 9479–9488. https://doi.org/10.1021/acs.est.1c01705.

Shen, L., Wania, F., 2005. Compilation, evaluation, and selection of Physical–Chemical property data for organochlorine pesticides. J. Chem. Eng. Data 50 (3), 742–768. https://doi.org/10.1021/je049693f.

Shen, L., Wania, F., Lei, Y.D., Teixeira, C., Muir, D.C.G., Bidleman, T.F., 2004. Hexachlorocyclohexanes in the north American atmosphere. Environ. Sci.Technol. 38 (4), 965–975. https://doi.org/10.1021/es034998k.

Shen, L., Wania, F., Lei, Y.D., Teixeira, C., Muir, D.C.G., Bidleman, T.F., 2005. Atmospheric distribution and long-range transport behavior of organochlorine pesticides in north America. Environ. Sci.Technol. 39 (2), 409–420. https://doi.org/10.1021/es049489c.

Shoeib, M., Harner, T., 2002. Characterization and comparison of three passive air samplers for persistent organic pollutants. Environ. Sci.Technol. 36 (19), 4142–4151. https://doi.org/10.1021/es020635t.

Shunthirasingham, C., Oyiliagu, C.E., Cao, X., Gouin, T., Wania, F., Lee, S.-C., Pozo, K., Harner, T., Muir, D.C.G., 2010. Spatial and temporal pattern of pesticides in the global atmosphere. J. Environ. Monit. 12 (9), 1650–1657. https://doi.org/10.1039/C0EM00134A.

Spencer, W.F., Cliath, M.M., 1972. Volatility of DDT and related compounds. J. Agric. Food Chem. 20 (3), 645–649. https://doi.org/10.1021/jf60181a057.

Stohl, A., Hittenberger, M., Wotawa, G., 1998. Validation of the Lagrangian particle dispersion model FLEXPART against large-scale tracer experiment data. Atmos. Environ. 32 (24), 4245–4264. https://doi.org/10.1016/S1352-2310(98)00184-8.

Tørseth, K., Aas, W., Breivik, K., Fjaeraa, A.M., Fiebig, M., Hjellbrekke, A.G., Myhre, C.L., Solberg, S., Yttri, K.E., 2012. Introduction to the European Monitoring and Evaluation Programme (EMEP) and observed atmospheric composition change during 1972-2009. Atmos. Chem. Phys. 12 (12), 5447–5481. https://doi.org/10.5194/acp-12-5447-2012.

UNEP, 2020. Stockholm Convention on Persistent Organic Pollutants (POPs). *Texts and annexes. Revised in 2019.* Switzerland: Secretariat of the Stockholm Convention Retrieved from. http://chm.pops.int/TheConvention/Overview/TextoftheConvention/tabid/2232/Default.aspx.

Vijgen, J., de Borst, B., Weber, R., Stobiecki, T., Forter, M., 2019. HCH and lindane contaminated sites: European and global need for a permanent solution for a long-time neglected issue. Environ. Pollut. 248, 696–705. https://doi.org/10.1016/j.envpol.2019.02.029.

Wania, F., Mackay, D., 1993. Global fractionation and cold condensation of low volatility organochlorine compounds in polar-regions. Ambio 22 (1), 10–18.

Wania, F., Shunthirasingham, C., 2020. Passive air sampling for semi-volatile organic chemicals. Environ. Sci. J. Integr. Environ. Res.: Process. Impacts 22 (10), 1925–2002. https://doi.org/10.1039/D0EM00194E.

Weber, J., Halsall, C.J., Muir, D., Teixeira, C., Small, J., Solomon, K., Hermanson, M., Hung, H., Bidleman, T., 2010. Endosulfan, a global pesticide: a review of its fate in the environment and occurrence in the Arctic. Sci. Total Environ. 408 (15), 2966–2984. https://doi.org/10.1016/j.scitotenv.2009.10.077.

Wöhrnschimmel, H., Scheringer, M., Bogdal, C., Hung, H., Salamova, A., Venier, M., Katsoyiannis, A., Hites, R.A., Hungerbuhler, K., Fiedler, H., 2016. Ten years after entry into force of the Stockholm Convention: what do air monitoring data tell about its effectiveness? Environ. Pollut. 217, 149–158. https://doi.org/10.1016/j.envpol.2016.01.090.

Wong, F., Hung, H., Dryfhout-Clark, H., Aas, W., Bohlin-Nizzetto, P., Breivik, K., Mastromonaco, M.N., Lundén, E.B., Ólafsdóttir, K., Sigurðsson, Á., Vorkamp, K., Bossi, R., Skov, H., Hakola, H., Barresi, E., Sverko, E., Fellin, P., Li, H., Vlasenko, A., Zapevalov, M., Samsonov, D., Wilson, S., 2021. Time trends of persistent organic pollutants (POPs) and Chemicals of Emerging Arctic Concern (CEAC) in Arctic air from 25 years of monitoring. Sci. Total Environ. 775, 145109 https://doi.org/10.1016/j.scitotenv.2021.145109.

SUPPORTING INFORMATION

for

Spatial variability and temporal changes of POPs in European background air

Helene Lunder Halvorsen, Pernilla Bohlin-Nizzetto, Sabine Eckhardt, Alexey Gusev, Claudia Moeckel, Victor Shatalov, Lovise Pedersen Skogeng, Knut Breivik

Contents

1. Materials and Methods detailed

Tables:

Text/Figures:

2. Results and Discussion

Tables:

Text/Figures:

1 Materials and Methods detailed

Tables:

Table SI-1.1. Location of all sampling sites

Site no.	Country	Sampling site	Region (EuroVoc, 2021)	EMEP code	Latitude (DD)	Longitude (DD)	Sampling start	Sampling End
1	Armenia	Amberd	Central-east	AM0001R	40.38	44.26	24.06.2016	23.09.2016
2	Austria	Illmitz	West	AT0002R	47.77	16.77	22.06.2016	27.09.2016
3	Austria	Vorhegg	West	AT0005R	46.68	12.97	13.07.2016	05.10.2016
4	Belgium	Houtem	West	BE0013R	51.02	2.58	01.07.2016	30.09.2016
5	Belgium	Koksijde	West	BE0014R	51.12	2.66	01.07.2016	30.09.2016
6	Croatia	Zavizan	Central-east	HR0004R	44.81	14.98	30.06.2016	29.09.2016
7	Cyprus	Ayia Marina	South	CY0002R	35.04	33.06	23.06.2016	15.09.2016
8	Czech Rep	Kosetice [a]	Central-east	CZ0003R	49.57	14.98	24.06.2016	26.09.2016
9	Czech Rep	Svratouch	Central-east	CZ0001R	49.73	16.03	22.06.2016	23.09.2016
10	Denmark	Tange	North	DK0003R	56.35	9.60	30.06.2016	29.09.2016
11	Denmark	Keldsnor	North	DK0005R	54.75	10.74	27.06.2016	16.09.2016
12	Denmark	Anholt	North	DK0008R	56.72	11.52	01.07.2016	01.10.2016
13	Denmark	Risoe (Lille Valby)	North	DK0041R	55.69	12.09	24.06.2016	04.10.2016
14	Faroe Islands	Norðuri á Fossum	North		62.18	-7.19	01.07.2016	01.10.2016
15	Finland	Pallas [a]	North	FI0036R	67.97	24.12	30.06.2016	04.10.2016
16	Finland	Ähtäri I	North	FI0004R	62.58	24.18	30.06.2016	30.09.2016
17	Finland	Utö	North	FI0009R	59.78	21.38	01.07.2016	02.10.2016
18	Finland	Virolahti II	North	FI0017R	60.53	27.69	01.07.2016	30.09.2016
19	Finland	Oulanka	North	FI0022R	66.32	29.40	01.07.2016	30.09.2016
20	Finland	Hailuoto II	North	FI0053R	65.00	24.69	04.07.2016	04.10.2016
21	Finland	Hyytiälä	North	FI0050R	61.86	24.29	04.07.2016	03.10.2016
22	France	Donon	West	FR0008R	48.50	7.13	05.07.2016	04.10.2016
23	France	Peyrusse Vieille	West	FR0013R	43.62	0.18	28.06.2016	27.09.2016
24	France	La Tardière	West	FR0015R	46.66	-0.75	28.06.2016	27.09.2016
25	France	Le Casset	West	FR0016R	45.00	6.47	28.06.2016	27.09.2016
26	France	Porspoder	West	FR0090R	48.52	-4.75	02.07.2016	05.10.2016
27	France	Revin	West	FR0009R	49.90	4.63	28.06.2016	27.09.2016
28	France	Saint-Nazaire-Le-Désert	West	FR0023R	47.31	-2.15	05.07.2016	11.10.2016
29	Georgia	Abastumani	Central-east	GE0001R	41.76	42.83	21.06.2016	14.09.2016
30	Germany	Westerland [a]	West	DE0001R	54.93	8.31	01.07.2016	05.10.2016
31	Germany	Schmücke	West	DE0008R	50.65	10.77	01.07.2016	30.09.2016
32	Germany	Zingst [a]	West	DE0009R	54.44	12.73	01.07.2016	30.09.2016
33	Germany	Schauinsland	West	DE0003R	47.91	7.91	01.07.2016	30.09.2016
34	Germany	Neuglobsow	West	DE0007R	53.17	13.03	01.07.2016	04.10.2016
35	Germany	Waldhof [a]	West	DE0002R	52.80	10.76	01.07.2016	30.09.2016
36	Germany	Melpitz	West	DE0044R	51.53	12.93	20.06.2016	19.09.2016
37	Germany	Hohenpeissenberg	West	DE0043G	47.80	11.02	28.06.2016	28.09.2016
38	Greece	Aliartos	South	GR0001R	38.38	23.11	07.07.2016	07.10.2016
39	Greece	Finokalia (Crete)	South	GR0002R	35.34	25.67	28.06.2016	04.10.2016
40	Greenland	Nuuk	North	DK0011G	64.17	-51.73	10.06.2016	12.09.2016
41	Greenland	Station Nord [a]	North	DK0010G	81.60	-16.67	01.09.2016	04.12.2016
42	Hungary	K-puszta	Central-east	HU0002R	46.97	19.55	30.06.2016	30.09.2016
43	Ireland	Mace Head	West	IE0031R	53.33	-9.90	13.07.2016	11.10.2016
44	Ireland	Malin Head	West	IE0006R	55.38	-7.34	01.06.2016	29.09.2016
45	Ireland	Carnsore Point	West	IE0008R	52.18	-6.37	13.07.2016	12.10.2016
46	Italy	Ispra	South	IT0004R	45.30	8.63	01.07.2016	30.09.2016
47	Italy	Montelibretti	South	IT0001R	42.10	12.63	30.06.2016	29.09.2016
48	Italy	Longobucco	South	IT0011R	39.39	16.61	04.07.2016	17.10.2016
50	Italy	Capo Granitola (Sicily) [b]	South	IT0014R	37.58	12.66	17.06.2016	21.09.2016
51	Italy	Monte Curcio [b]	South		39.32	16.42	04.07.2016	17.10.2016

[a] POP-EMEP AAS site

[b] Part of the framework I-AMICA

Table SI-1.1. Location of all sampling sites continued

Site no.	Country	Sampling site	Region (EuroVoc, 2021)	EMEP code	Latitude (DD)	Longitude (DD)	Sampling start	Sampling End
52	Latvia	Rucava	North	LV0010R	56.16	21.17	01.07.2016	21.10.2016
53	Latvia	Zoseni	North	LV0016R	57.14	25.91	05.07.2016	24.10.2016
54	Lithuania	Preila	North	LT0015R	55.38	21.03	01.07.2016	01.10.2016
55	Lithuania	Rugsteliskis	North		55.43	26.07	19.07.2016	19.10.2016
56	Malta	Giordan lighthouse	South	MT0001R	36.07	14.22	30.09.2016	07.10.2016
57	Moldova	Leova	Central-east	MD0013R	46.50	28.27	04.07.2016	04.10.2016
58	Netherlands	Kollumerwaard	West	NL0009R	53.33	6.28	13.07.2016	19.10.2016
59	Netherlands	Vredepeel	West	NL0010R	51.54	5.85	12.07.2016	18.10.2016
60	Netherlands	De Zilk	West	NL0091R	52.30	4.50	14.07.2016	19.10.2016
97	Norway	Birkenes [a]	North	NO0002R	58.39	8.25	11.07.2016	10.10.2016
98	Norway	Tustervatn	North	NO0015R	65.83	13.91	30.06.2016	29.09.2016
99	Norway	Kårvatn	North	NO0039R	62.78	8.88	06.07.2016	02.10.2016
100	Norway	Hurdal	North	NO0056R	60.37	11.08	14.07.2016	12.10.2016
101	Norway	Karasjok	North	NO0055R	69.48	25.48	23.06.2016	23.09.2016
102	Norway	Andøya [a]	North	NO0090R	69.28	16.01	27.06.2016	05.10.2016
96	Spitsbergen	Zeppelin [a]	North	NO0042G	78.91	11.89	07.07.2016	28.09.2016
61	Poland	Diabla Gora	Central-east	PL0005R	54.12	22.04	01.07.2016	01.10.2016
62	Portugal	Monte Velho	South	PT0004R	38.08	-8.80	07.07.2016	07.10.2016
63	Portugal	Alfragide	South	PT0006R	38.74	-9.21	08.07.2016	10.10.2016
64	Russia	Pinega	Central-east	RU0013R	64.56	43.22	01.07.2016	30.09.2016
65	Russia	Lesnoy	Central-east	RU0020R	56.45	32.95	12.07.2016	10.10.2016
66	Russia	Astrakhan [c]	Central-east		45.75	47.92	13.07.2016	10.10.2016
67	Russia	Caucasus [c]	Central-east		43.70	40.22	09.07.2016	12.10.2016
68	Russia	Voronezh [c]	Central-east		51.90	39.60	12.07.2016	12.10.2016
69	Russia	Danki	Central-east	RU0018R	54.90	37.80	01.07.2016	01.10.2016
95	Russia	Smolenskoe Poozerie	Central-east		55.50	31.85	21.07.2016	21.10.2016
70	Slovakia	Chopok	Central-east	SK0002R	48.97	19.60	01.07.2016	04.10.2016
71	Slovakia	Starina	Central-east	SK0006R	49.04	22.26	01.07.2016	03.10.2016
72	Slovenia	Iskrba	Central-east	SI0008R	45.56	14.86	01.07.2016	30.09.2016
73	Spain	Víznar	South	ES0007R	37.24	-3.53	27.07.2016	04.11.2016
74	Spain	Niembro	South	ES0008R	43.44	-4.85	09.08.2016	09.11.2016
75	Spain	Els Torms	South	ES0014R	41.39	0.73	05.08.2016	07.11.2016
76	Spain	San Pablo de los Montes	South	ES0001R	39.55	-4.35	02.08.2016	02.11.2016
77	Spain	Mahon	South	ES0006R	39.88	-4.32	02.08.2016	02.11.2016
78	Spain	Barcarrota	South	ES0011R	38.47	-6.92	28.07.2016	28.10.2016
79	Sweden	Råö [a]	North	SE0014R	57.40	11.92	27.06.2016	03.10.2016
80	Sweden	Aspvreten [a]	North	SE0012R	58.81	17.39	07.07.2016	03.10.2016
81	Sweden	Vavihill	North	SE0011R	56.02	13.15	13.06.2016	30.09.2016
82	Sweden	Bredkälen	North	SE0005R	63.84	15.32	05.07.2016	11.10.2016
83	Sweden	Esrange	North	SE0013R	67.88	21.07	21.06.2016	24.10.2016
84	Sweden	Abisko	North	SE0093R	68.35	18.82	23.06.2016	26.09.2016
85	Sweden	Vindeln	North	SE0035R	64.23	19.77	30.06.2016	10.10.2016
86	Switzerland	Jungfraujoch	West	CH0001G	46.55	7.99	13.07.2016	06.10.2016
87	Switzerland	Payerne	West	CH0002R	46.81	6.94	06.07.2016	12.10.2016
88	Ukraine	Zmeiny Island	Central-east	UA0008R	45.26	30.20	01.07.2016	30.09.2016
89	United Kingdom	Chilbolton	West	GB1055R	51.15	-1.44	29.06.2016	27.09.2016
90	United Kingdom	Aucencorth Moss	West	GB0048R	55.79	-3.24	01.07.2016	28.09.2016
91	United Kingdom	Lough Navar	West	GB0006R	54.43	-7.90	01.07.2016	03.10.2016
92	United Kingdom	Yarner Wood	West	GB0013R	50.70	-3.72	05.07.2016	11.10.2016
93	United Kingdom	High Muffles	West	GB0014R	54.33	-0.80	29.06.2016	28.09.2016
94	United Kingdom	Strath Vaich Dam	West	GB0015R	57.73	-4.78	01.07.2016	03.10.2016

[a] POP-EMEP AAS site

[c] Part of the Integrated Background Monitoring Network (IBMoN)

Table SI-1.2a. Target analytes PRCs

Performance Reference Compounds (PRCs)	Full name
D g-HCH	Lindane
13C PCB-1	2-CB
13C PCB-8	2,4'-DiCB
12C PCB-14	3,5-DiCB
12C PCB-30	2,4,6-TriCB
13C PCB-32	2,4',6-TriCB
12C PCB-106[a]	2,3,3',4',5-PenCB
12C PCB-198	2,3,3',4,4',5,5'-HepCB

[a] Coeluting with PCB-118. Excluded.

Table SI-1.2b. Target analytes PCBs

Target analytes (PCBs)	Full name
12C PCB-18	2,2',5-TriCB
12C PCB-28[c]	2,4,4'-TriCB
12C PCB-31	2,4',5-TriCB
12C PCB-33	2',3,4-TriCB
12C PCB-37	3,4,4'-TriCB
12C PCB-47	2,2',4,4'-TetCB
12C PCB-52[c]	2,2',5,5'-TetCB
12C PCB-66	2,3',4,4'-TetCB
12C PCB-74	2,4,4',5-TetCB
12C PCB-99	2,2',4,4',5-PenCB
12C PCB-101[c]	2,2',4,5,5'-PenCB
12C PCB-105	2,3,3',4,4'-PenCB
12C PCB-114	2,3,4,4',5-PenCB
12C PCB-118[a]	2,3',4,4',5-PenCB
12C PCB-122	2'3,3',4,5-PenCB
12C PCB-123	2',3,4,4',5-PenCB
12C PCB-128	2,2',3,3',4,4'-HexCB
12C PCB-138[c]	2,2',3,4,4',5'-HexCB
12C PCB-141	2,2',3,4,5,5'-HexCB
12C PCB-149	2,2',3,4',5,6-HexCB
12C PCB-153[c]	2,2',4,4',5,5'-HexCB
12C PCB-156	2,3,3',4,4',5-HexCB
12C PCB-157	2,3,3',4,4',5'-HexCB
12C PCB-167	2,3',4,4',5,5'-HexCB
12C PCB-170	2,2',3,3',4,4',5-HepCB
12C PCB-180[c]	2,2',3,4,4',5,5'-HepCB
12C PCB-183	2,2',3,4,4',5',6-HepCB
12C PCB-187	2,2',3,4',5,5',6-HepCB
12C PCB-189[b]	2,3,3',4,4',5,5'-HepCB
12C PCB-194	2,2',3,3',4,4',5,5'-OctCB
12C PCB-206	2,2',3,3',4,4',5,5',6-NonCB
12C PCB-209	Deca CB

[a] Coeluting with PCB-106 in the PRCs. Excluded.

[b] Not included in sum 30 PCBs

[c] Included in sum 6 PCBs

Table SI-1.2c. Target analytes OCPs

Target analytes (OCPs)	Full name
12C α-HCH[a]	α-Hexachlorocyclohexane
12C β-HCH	β-Hexachlorocyclohexane
12C γ-HCH[a]	Lindane
12C Dieldrin	
12C Aldrin	
12C Endrin	
12C Mirex	
12C Isodrin	
12C Trifluralin	
12C Trans-chlordene	
12C cis-Chlordane (α)	
12C trans-Chlordane (γ)	
12C Oxychlordane	
12C Trans-nonachlor	
12C Cis-nonachlor	
12C Heptachlor	
12C Heptachlor epoxide (exo)	
12C Heptachlor epoxide (endo)	
12C Endosulfan I (α)	
12C Endosulfan II (β)	
12C Endosulfan sulphate	
12C HCB	Hexachlorobenzene
12C PeCB	Pentachlorbenzene
12C o.p.DDE[b]	2,4'-Dichlorodiphenyldichloroethylene
12C p.p.DDE[b]	4,4'-Dichlorodiphenyldichloroethylene
12C o.p.DDD[b]	2,4'-Dichlorodiphenyldichloroethane
12C p.p.DDD[b]	4,4'-Dichlorodiphenyldichloroethane
12C o.p.DDT[b]	2,4'-Dichlorodiphenyltrichloroethane
12C p.p.DDT[b]	4,4'-Dichlorodiphenyltrichloroethane

[a] Included in sum 2 HCHs

[b] Included in sum 6 DDXs

Table SI-1.3. Recoveries (%) - ranges (median) for the internal standards for exposed samples, field blanks and method blanks, as well as PRCs for field- and method blanks.

	Range (median)		
ISTD:	**Exposed samples**	**Method blanks**	**Field blanks**
13C PCB-28	39 - 94 (55)	41 - 67 (53)	34 - 68 (50)
13C PCB-52	44 - 102 (60)	50 - 93 (60)	50 - 84 (58)
13C PCB-101	51 - 115 (75)	64 - 126 (74)	44 - 87 (69)
13C PCB-138	42 - 118 (73)	71 - 120 (84)	40 - 93 (78)
13C PCB-153	38 - 123 (70)	68 - 131 (79)	39 - 87 (75)
13C PCB-180	40 - 140 (74)	76 - 133 (88)	40 - 104 (80)
13C PeCB	7 - 82 (23)	15 - 94 (25)	12 - 33 (24)
13C HCB	17 -139 (34)	23 - 108 (34)	17 - 46 (34)
13C a-HCH	13 - 85 (27)	13 - 40 (19)	5 - 39 (19)
13C g-HCH	11 - 66 (22)	11 - 38 (19)	12 - 35 (19)
13C p,p'-DDE	57 - 122 (76)	70 - 126 (88)	76 - 99 (88)
13C o,p'-DDD	30 - 97 (62)	38 - 113 (63)	43 - 97 (69)
13C p,p'-DDT	53 - 160 (89)	59 - 156 (81)	69 - 141 (85)
13C Dieldrin	46 - 148 (78)	52 - 92 (69)	58 - 113 (73)
13C Heptachlor-exo-epoxide	29 - 93 (49)	45 - 76 (57)	43 - 85 (59)
13C Oxy-Chlordane	43 - 100 (62)	52 - 81 (69)	61 - 101 (68)
13C trans-Chlordane	43 - 109 (63)	61 - 94 (76)	66 - 106 (79)
13C cis-Chlordane	34 - 94 (56)	57 - 84 (69)	59 - 97 (71)
13C trans-Nonachlor	34 - 96 (60)	63 - 91 (77)	71 - 107 (80)
13C cis-Nonachlor	28 - 94 (51)	53 - 92 (69)	55 - 95 (74)
13C Endosulfan-I	44 - 116 (67)	45 - 84 (69)	59 - 108 (72)
PRCs:			
D g-HCH		88 - 89 (89)[a]	97 - 114 (105)[c]
13C PCB-1		95 - 109 (102)[a]	83[cd]
13C PCB-8		149 - 153 (151)[ab]	82[cd]
12C PCB-14		169 - 171 (170)[ab]	79[cd]
12C PCB-30		114 - 124 (119)[a]	72[cd]
13C PCB-32		100 - 101 (100)[a]	61 - 93 (77)[c]
12C PCB-198		100 - 103 (101)[a]	98 - 103 (100)[c]

[a] Based on two blanks. Calculated from added amount of PRC

[b] High recovery. Based on 13C PCB-4 as internal standard which could behave differently during clean-up.

[c] Based on two blanks. Calculated from amount of PRC in method blanks.

[d] Only one blank due to instrumental issues.

Table SI-1.4a. The relative deviation from the theoretical value (bias %) of ^{12}C target analytes of three spiked PAS

	QC 1	QC 2	QC 3
PCB-28	0 %	-1 %	0 %
PCB-52	6 %	0 %	-2 %
PCB-101	3 %	-2 %	0 %
PCB-138	2 %	-2 %	-1 %
PCB-153	2 %	-2 %	0 %
PCB-180	2 %	-1 %	-2 %
Sum 6 PCB	2 %	-1 %	-1 %
Sum 30 PCB	-1 %	-3 %	-2 %
PeCB	-10 %	-12 %	-14 %
HCB	-1 %	-7 %	-10 %
a-HCH	16 %	12 %	7 %
g-HCH	7 %	9 %	13 %
Sum 2 HCHs	12 %	11 %	9 %
o.p'-DDE	20 %	17 %	20 %
p,p'-DDE	15 %	10 %	11 %
o,p'-DDD	16 %	8 %	10 %
p,p'-DDD	26 %	12 %	27 %
o,p'-DDT	5 %	-2 %	-2 %
p,p'-DDT	8 %	9 %	9 %
Sum 6 DDXs	15 %	9 %	12 %
Dieldrin	2 %	-4 %	0 %
Heptachlor-exo-epoxide	1 %	-4 %	2 %
oxy-Chlordane	3 %	-7 %	-3 %
trans-Chlordane	5 %	2 %	8 %
cis-Chlordane	7 %	-5 %	0 %
trans-Nonachlor	3 %	0 %	1 %
cis-Nonachlor	3 %	-13 %	-6 %
Sum 4 Chlordanes	5 %	-4 %	1 %
Endosulfan-I	n.a	n.a	n.a

n.a = Not available

Table SI-1.4b. The relative standard deviations of two parallel PAS

Site no:	1	8	15	30	35	53	73	79	88	92	97
Country:	Armenia	Czech Rep.	Finland	Germany	Germany	Latvia	Spain	Sweden	Ukraine	UK	Norway
PCB-28	b	9 %	0 %	10 %	1 %	3 %	c	c	6 %	4 %	0 %
PCB-52	b	9 %	1 %	9 %	1 %	2 %	c	c	12 %	3 %	1 %
PCB-101	b	14 %	1 %	6 %	1 %	3 %	c	c	10 %	5 %	2 %
PCB-138	b	15 %	1 %	8 %	1 %	2 %	c	c	6 %	3 %	2 %
PCB-153	b	14 %	2 %	9 %	2 %	2 %	c	c	8 %	3 %	1 %
PCB-180	b	17 %	1 %	14 %	6 %	2 %	c	c	5 %	4 %	9 %
Sum 6 PCB	b	12 %	1 %	9 %	1 %	3 %	c	c	9 %	4 %	0 %
Sum 30 PCB	b	12 %	6 %	9 %	2 %	1 %	c	c	8 %	3 %	0 %
PeCB	b	4 %	1 %	3 %	3 %	1 %	c	c	8 %	0 %	2 %
HCB	b	5 %	1 %	1 %	1 %	0 %	c	c	2 %	8 %	0 %
a-HCH	5 %	c	0 %	3 %	4 %	3 %	6 %	4 %	3 %	8 %	2 %
g-HCH	2 %	c	1 %	10 %	7 %	4 %	4 %	11 %	3 %	4 %	2 %
Sum 2 HCHs	4 %	c	0 %	8 %	4 %	3 %	5 %	8 %	1 %	5 %	0 %
o,p'-DDE	9 %	c	0 %	15 %	8 %	15 %	11 %	1 %	18 %	10 %	a
p,p'-DDE	11 %	c	3 %	12 %	4 %	7 %	8 %	4 %	2 %	14 %	5 %
o,p'-DDD	15 %	c	11 %	13 %	8 %	1 %	8 %	3 %	16 %	1 %	15 %
p,p'-DDD	10 %	c	a	10 %	7 %	7 %	10 %	3 %	20 %	8 %	a
o,p'-DDT	17 %	c	1 %	6 %	2 %	6 %	1 %	3 %	13 %	7 %	8 %
p,p'-DDT	13 %	c	4 %	12 %	33 %	4 %	20 %	4 %	16 %	12 %	5 %
Sum 6 DDXs	12 %	c	0 %	11 %	8 %	6 %	4 %	4 %	4 %	12 %	6 %
Dieldrin	4 %	10 %	0 %	10 %	3 %	9 %	1 %	12 %	12 %	14 %	4 %
Heptachlor-exo-epoxide	3 %	7 %	5 %	7 %	1 %	10 %	2 %	12 %	18 %	5 %	2 %
oxy-Chlordane	8 %	7 %	6 %	14 %	5 %	4 %	6 %	14 %	15 %	13 %	1 %
trans-Chlordane	6 %	10 %	2 %	10 %	2 %	1 %	3 %	10 %	13 %	10 %	3 %
cis-Chlordane	2 %	d	1 %	8 %	2 %	1 %	1 %	3 %	12 %	13 %	2 %
trans-Nonachlor	2 %	13 %	1 %	11 %	2 %	4 %	1 %	5 %	14 %	12 %	0 %
cis-Nonachlor	7 %	16 %	3 %	8 %	1 %	1 %	1 %	6 %	10 %	7 %	5 %
Sum 4 Chlordanes	0 %	15 %	1 %	9 %	1 %	2 %	1 %	5 %	13 %	12 %	0 %
Endosulfan-I	8 %	10 %	0 %	7 %	0 %	2 %	4 %	9 %	14 %	9 %	1 %

a Below MDL. Excluded.

b Possible contamination of one parallel. Excluded.

c High RSD% due to not prepared/analyzed in parallel. Excluded.

d Possible interference. Excluded.

Table SI-1.5. Modelled meteorological data and estimated sampling rates (R) from the spiking of PUFs with PRCs.

Site no.	Deployment time (days):	Sampling rate (m³/day):	No. of PRCs[a]:	Sampling volume HCB (m³):	Sampling volume PCB-153 (m³):	Average Temp. (°C):	Average Wind speed (m/s):	Altitude (m.a.s.l.)[b]:	Reference Altitude (m.a.s.l.)[b]:	Correction Average Temp. (°C):
						Modelled from ECMWF			**Reference**	**Correction**
1	91	4.4/3.9[c]	4/5[c]	212/202	389/351	18.0	2.4	1707	2080	
2	97	3.5[d]	1	185	337	20.5	2.9	213	117	
3	84	3.2	3	185	270	14.9	2.0	1135	1020	
4	91	3.9	4	201	352	18.3	4.2	27	10	
5	91	4.0	5	202	357	18.3	4.2	27	4	
6	91	4.9[m]	5	260	441	20.4	3.4	376	1594	12.5
7	84	3.0	3	129	247	29.0	3.2	122	520	
8	94	3.0/2.8[c]	4/4[c]	176/171	277/262	18.3	2.9	482	535	
9	93	3.5	5	190	324	18.7	3.0	447	737	
10	91	3.6	4	204	328	16.0	4.5	20	13	
11	81	3.4	3	176	270	17.5	5.4	15	10	
12	92	3.7	5	203	335	16.8	6.6	13	40	
13	102	4.2[d]	1	228	422	16.7	5.3	12	10	
14[e]	92	6.3[m]	4	307	567	10.9	7.3	0	300	
15	96	3.0/3.0[c]	3/3[c]	206/205	289/287	11.4	2.9	303	340	
16	92	2.8	2	183	257	13.7	3.1	141	162	
17	93	4.4	5	229	406	15.9	6.4	3	7	
18	91	3.8	4	211	345	15.7	5.2	21	4	
19[f]	91	2.8	2	186	255	12.4	2.8	242	310	
20	92	3.8	4	221	350	13.9	5.1	5	4	
21	91	2.5	3	170	230	13.6	3.1	141	181	
22	91	2.6	3	157	231	18.6	2.4	359	775	
23	91	3.7	4	187	333	20.0	2.0	457	200	
24	91	3.0	4	168	267	19.6	3.2	107	133	
25	91	4.2	4	225	379	15.1	1.6	1571	1750	
26	95	5.3	2	244	496	16.8	5.9	144	50	
27	91	2.7	3	163	241	17.9	3.2	196	390	
28	98	3.7	4	205	359	17.8	2.8	906	605	
29	85	3.4	5	175	283	19.2	2.0	1393	1650	
30	96	6.5/6.5[c]	2/2[c]	260/260	606/605	16.9	5.9	7	12	
31	91	3.4	5	188	304	17.6	2.9	388	937	
32	91	3.8	5	200	339	17.6	6.2	8	1	
33	91	4.7[m]	5	245	425	18.7	2.1	499	1205	14.1
34	95	3.4	4	191	317	18.1	3.4	44	62	
35	91	3.6/3.5[c]	5/5[c]	193/189	327/313	18.2	3.5	48	74	
36	91	6.1	2	229	545	19.6	3.1	147	86	
37	92	5.8	2	249	522	16.7	2.2	766	985	
38	92	6.0	2	193	533	24.1	2.9	280	110	
39	98	4.8[d]	0	179	456	25.2	7.1	97	250	
40[g]	94	8.2[m]	2	385	763	7.7	2.4	-1	320	
41	94	4.3[d]	1	355	401	-12.8[h]	5.5	-1	20	
42	92	3.3	4	175	301	20.6	2.6	116	125	
43	90	5.0[d]	0	246	439	14.6	7.5	12	5	
44	120	5.8	2	296	683	14.3	6.8	-6	20	
45	91	4.7[d]	0	235	417	15.4	6.7	54	9	
46	91	3.2	4	174	286	19.8	2.0	671	209	
47	91	3.4	2	163	305	23.6	2.0	339	48	
48	105	2.3	4	147	242	23.2	2.6	268	1379	
50	96	3.9[d]	0	171	368	24.7	4.4	58	5	
51	105	4.5[m]	4	262	467	23.2	2.6	268	1796	13.3

[a] Number of PRCs with 40-80 % loss during deployment

[b] Meters above sea level

[c] Parallel PAS

[d] No significant loss of PRCs. Found from correlation with wind speed (v): R = 2.8456 x e^(0.074 x v).

[e] Had fallen down on the ground when collected

[f] PAS opened during sampling

[g] Deployed on a roof top

[h] Sampled during winter (01.09 - 04.12)

[i] Lunder Halvorsen et al. 2021

[j] One PRC excluded. Agrees with sampling rate from wind correlation.

[k] High sampling rate. Sampled at high altitude.

[l] Sampling rate from first parallel used for both.

[m] Higher uncertainty, not included when deriving the R(v)-expression.

Table SI-1.5 continued. Modelled meteorological data and estimated sampling rates (R) from the spiking of PUFs with PRCs.

Site no.	Deployment time (days):	Sampling rate (m³/day):	No. of PRCsᵃ:	Sampling volume HCB (m³):	Sampling volume PCB-153 (m³):	Average Temp. (°C):	Average Wind speed (m/s):	Altitude (m.a.s.l.)ᵇ:	Reference Altitude (m.a.s.l.)ᵇ:	Correction Average Temp. (°C):
						Modelled from ECMWF			Reference	Correction
52	112	4.2	5	247	463	15.3	5.8	19	18	
53	111	3.4/3.5ᶜ	5/4ᶜ	276/279	376/383	13.2	3.8	113	188	
54	92	4.1ᵈ	1	213	374	17.1	5.0	17	5	
55	92	3.0	2	192	275	13.6	3.6	142	120	
56	91	3.9ᵈ	0	169	350	25.5	4.4	-8	167	
57	92	4.3	2	192	387	21.4	3.1	126	156	
58	98	4.5ᵈ	1	229	432	16.9	6.1	1	1	
59	98	5.6	2	247	534	17.2	3.4	47	28	
60	97	4.3ᵈ	1	223	413	17.2	5.7	-3	4	
97ⁱ	91	2.0/2.0ᶜ	2/2ᶜ	141/141	181/181	14.2	3.8	241	199	
98ⁱ	91	2.7	2	185	246	10.8	2.7	566	475	
99ⁱ	88	2.0ᵐ	1	139	171	12.0	2.8	503	208	
100ⁱ	90	3.6ᵐ	0	215	322	12.8	2.6	390	280	
101ⁱ	92	3.6ᵐ	0	226	329	11.1	3.0	343	308	
102ⁱ	100	10.1ᵐ	3	370	985	11.0	5.2	39	338	
96	77	5.0	2	297	409	4.3	3.8	206	474	
61	92	4.5	4	225	410	16.6	3.3	126	157	
62	92	4.2	2	192	380	21.3	5.4	33	43	
63	94	4.9	2	203	452	21.5	5.2	89	109	
64	91	3.9ʲᵐ	1	218	354	14.9	3.1	74	28	
65	90	3.8ᵈᵐ	1	213	337	14.6	3.9	229	340	
66	89	2.9	5	151	251	23.1	4.2	-20	-25	
67	95	2.3	3	145	219	21.1	2.8	446	400	
68	92	3.7ᵈ	0	198	336	17.8	3.6	160	145	
69	92	3.7ᵈ	0	203	338	17.0	3.7	175	150	
95	92	3.7ᵈ	0	219	336	13.2	3.5	198		
70	95	15.3ᵏᵐ	2	465	1415	16.4	2.4	621	2008	7.3
71	94	3.8	4	203	351	17.7	2.6	424	345	
72	91	2.4	3	147	215	19.7	2.5	431	520	
73	100	4.2/4.9ᶜᵐ	4/2ᶜ	236/252	417/479	23.5	2.7	-22	1265	15.1
74	92	3.2	3	187	295	17.2	4.2	457	134	
75	94	3.0	3	172	281	19.8	2.0	479	470	
76	92	4.2	4	210	382	22.7	2.5	199	917	18.1
77	92	3.7	2	178	330	21.6	2.4	438	78	
78	92	3.7	2	170	333	23.5	2.4	89	393	
79	98	5.9/5.9ᶜ	2/1ᶜ	264/264	566/566	15.8	4.5	65	5	
80	88	3.3	2	187	283	16.0	3.8	15	20	
81	109	3.5	4	217	374	16.4	4.3	46	175	
82	98	4.7	2	275	456	10.9	2.9	438	404	
83	125	3.9	4	295	477	9.1	2.8	514	475	
84	95	3.0	3	205	279	10.2	2.5	646	385	
85	102	3.4	4	226	345	12.6	3.2	155	225	
86	85	9.8ᵏᵐ	3	323	813	13.2	1.5	1440	3578	-0.7
87	98	5.1	2	250	487	15.7	2.1	850	489	
88	91	4.0/4.0ᶜᵈ	0	178/178	354/354	22.8	4.5	7		
89	90	6.1	2	248	539	17.2	4.3	35	78	
90	89	6.5	2	276	571	14.5	4.6	-6	260	
91	94	4.1ᵈ	0	232	383	14.1	5.0	8	126	
92	98	4.1/3.1ᶜ	5/4ᶜ	226/194	399/302	16.1	6.0	10	119	
93	91	3.9	5	214	350	15.4	5.6	8	267	
94	94	4.8	5	260	446	12.8	5.1	-6	270	

ᵃ Number of PRCs with 40-80 % loss during deployment
ᵇ Meters above sea level
ᶜ Parallel PAS
ᵈ No significant loss of PRCs. Found from correlation with wind speed (v): R = 2.8456 x e^(0.074 x v).
ᵉ Had fallen down on the ground when collected
ᶠ PAS opened during sampling

ᵍ Deployed on a roof top
ʰ Sampled during winter (01.09 - 04.12)
ⁱ Lunder Halvorsen et al. 2021
ʲ One PRC excluded. Agrees with sampling rate from wind correlation.
ᵏ High sampling rate. Sampled at high altitude.
ˡ Sampling rate from first parallel used for both.
ᵐ Higher uncertainty, not included when deriving the R(v)-expression.

Text/Figures:

1.1 Sampling sites details

Figure SI-1.1 shows the spatial coverage of passive air samplers in our study, EMEP sites also monitoring POPs using AAS (n=11), and the four study regions. The passive air samplers were deployed in close connection to existing monitoring stations (Figure SI-1.2). The locations of all sampling sites are given in Table SI-1.1.
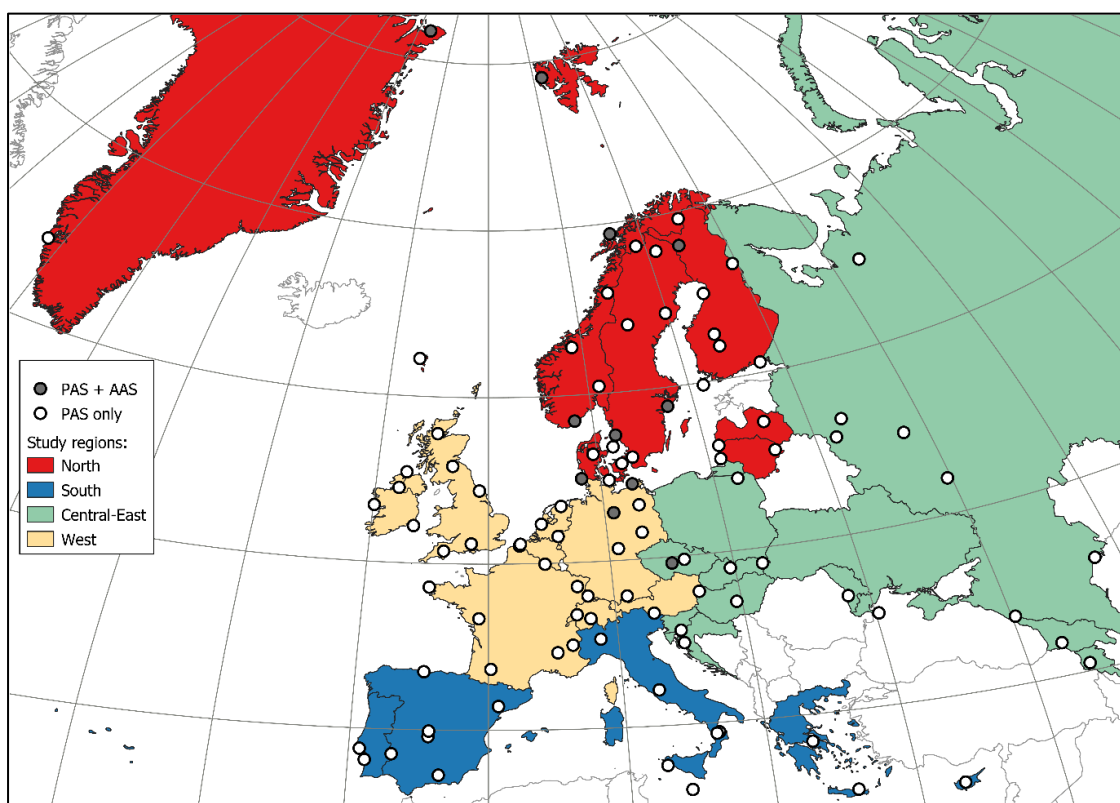
Figure SI-1.1. The spatial coverage of sampling sites using PAS (white/grey) in this study along with the spatial coverage of EMEP sites monitoring POPs using AAS (grey). The background colors represents the regions included in the study area (EuroVoc, 2021).

Figure SI-1.2. Passive air samplers deployed in close connection to existing monitoring stations, illustrated by site 4 (Houtem) in Belgium (photo: E. Adriaenssens) and site 13 (Risoe) in Denmark (photo: T. Ellermann).

1.2 Sample extraction and clean-up

The samples were spiked with ^{13}C-labelled internal standards, prior to Soxhlet extraction for 8 hours in acetone:hexane (1:1), as described in Lunder Halvorsen et al. (2021). The extracts were concentrated and solvent-exchanged to acetonitrile before clean-up. Unlike the extracts within Lunder Halvorsen et al. (2021), the clean-up was done with a dual layer SPE method. SPE cartridges were prepared by weighing 2 g of a mixture of zirconia-coated silica (Supel QuE Z-sep, SigmaAldrich) and C18 polymerical bonded silica (Discovery DSC-18, SigmaAldrich) in the bottom sorbent bed, and 2 g activated magnesium silicate coated silica (Supelclean LC-Florisil, SigmaAldrich) in the top sorbent bed, separated with a frit. Acetonitrile was used as eluent, and the resulting acetonitrile extract was back-extracted to *n*-hexane, in the same way as the extracts within Lunder Halvorsen et al. (2021).

Zirconium-based SPE has shown to be well suited for removing fatty compounds co-extracted from sample matrices (K. Stenerson & Brown, 2015; K. K. Stenerson et al., 2015). Zirconia-coated silica, in combination with C18 and Florisil sorbents, is able to remove interfering compounds through Lewis acid-base interactions, additionally to polar and non-polar interactions. Polyurethane (PUR) is a polymer with intramolecular urethane bonds (carbamate ester bond, i.e. NHR_2COOR_1) with a variety of additives (e.g surfactants), and it was expected that clean-up with the described SPE-method also was suitable for the retention of co-extracted substances in air samples.

Similarly to SPE clean-up with Florisil only (Lunder Halvorsen et al., 2021), the analysis of DDXs showed interferences and degradation of DDT in the injector also with the dual layer SPE method. Consequently, the hexane extract was splitted 20:80. The larger aliquot (80%) was further cleaned with concentrated sulfuric acid (Lunder Halvorsen et al., 2021) in order to remove co-extracted sample matrix prior to preparation for instrumental analysis of PCBs, PeCB/HCB, HCHs and DDXs. Some OCPs, including Dieldrin, Endrin, Endosulfan I + II and trans-Heptachlor epoxide, could be sulfonized when treated with concentrated sulfuric acid (Chung & Chen, 2011), and the smaller aliquot (20%) was only concentrated and solvent exchanged to isooctane prior to instrumental analysis of the rest of the OCPs.

1.3 Deriving air concentrations

Air concentrations are derived using the same approach described in Lunder Halvorsen et al. (2021). The PUF characteristics and temperature adjusted K_{OA}-values are similar to the data given in the above-mentioned study. Other input to the template of Harner are given in Table SI-1.5. Similar to Lunder Halvorsen et al. (2020), the average air temperatures and wind speeds at each site during the exposure period were retrieved from the ERA Interim database from European Centre for Medium-Range Weather Forecasts (ECMWF). For seven high altitude sites, large differences (> 700 m)

between the model altitude and the altitude at the sites were noted. In these cases, the ECMWF data were adjusted by assuming a temperature decrease by altitude of -0.65 °C per 100 m.

The amount loss of PRCs is the basis in the estimation of sample air volumes. The average amounts of PRCs in two spiked field blanks were used as reference to account for any losses not caused by sampling. The loss differs between different PRCs and is next corrected based on the stable PCB-198, that is expected to not volatilize from the PAS. Only the compounds that experienced (corrected) losses between 40 % and 80 % were used in the calculation of an average site-specific sampling rate. Hence in practice, 13C PCB-1 was not used in the determination of the sampling rates.

For the sites with none- or only one PRC fulfilling the required loss, the sampling rates were estimated from the modelled wind speed (v) at the given sites (Moeckel et al., 2009; Tuduri et al., 2006). The correlation between sampling rate and wind speed (r=0.14, p<0.001) was found from the other sites (n=78), where the sampling rates were confirmed by two or more PRCs, and by excluding high-altitude sites and other sites with possible sampling artifacts (Table SI-1.5); R (m³/day) = $2.8456e^{0.074v}$.

For verification, the PAS derived concentrations of ∑₆PCB, HCB, HCHs, ∑₃DDXs (*p,p'*-DDD/-DDE/-DDT) and Dieldrin in our study were compared with the concentrations from routine active air measurements reported to EMEP for the same sampling period (Aas & Bohlin-Nizzetto, 2018) (Figures SI 1.3 a-f).

a)

b)

15
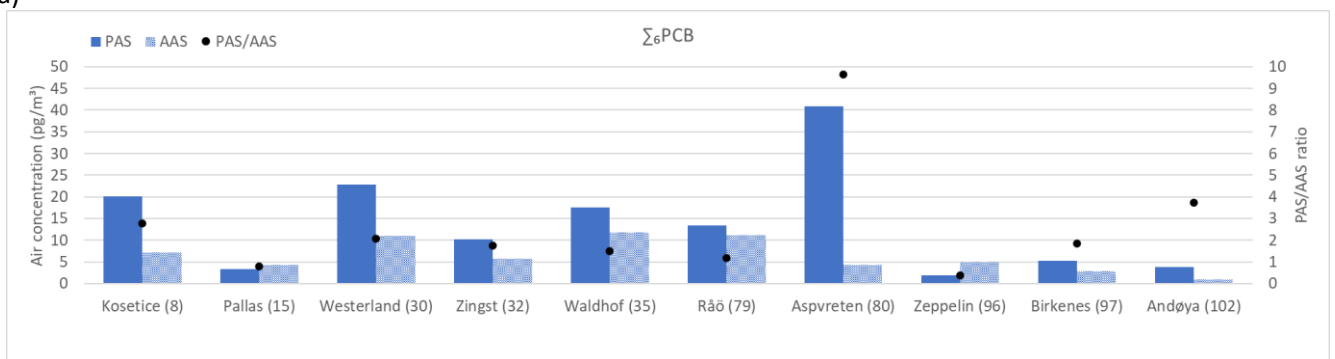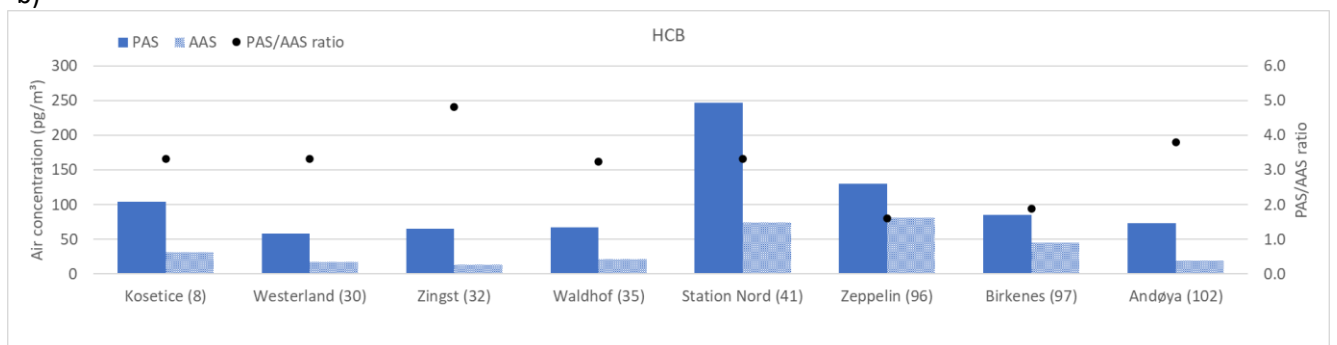
c)
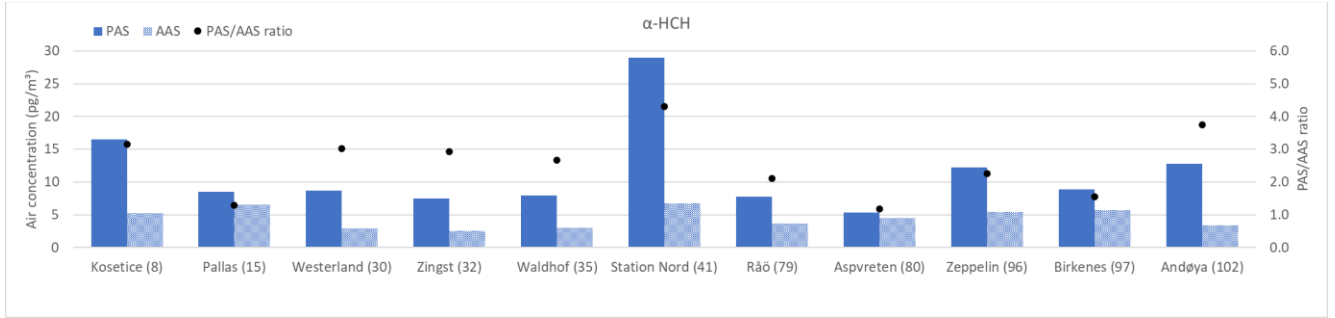
d)
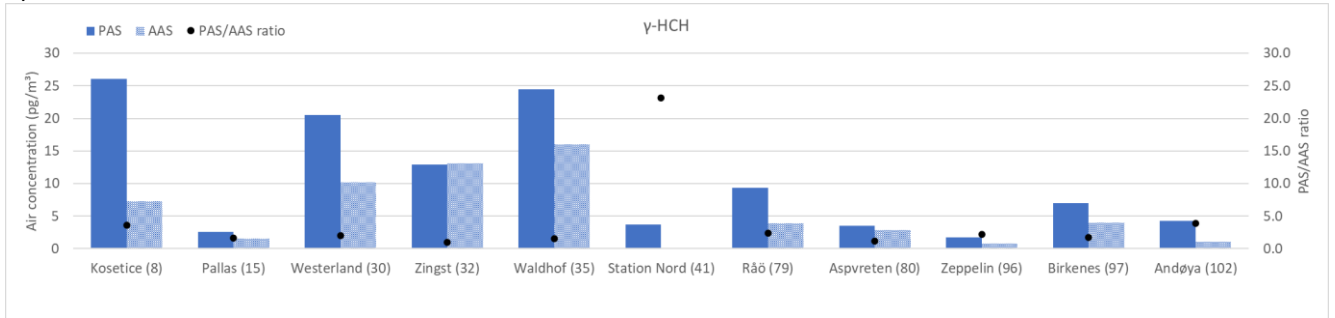
e)
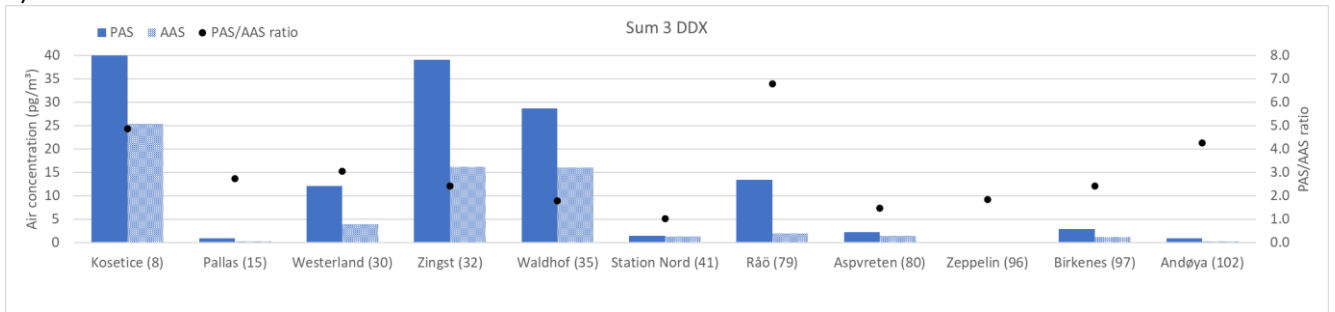
*PAS Kosetice: 123 pg/m3

f)
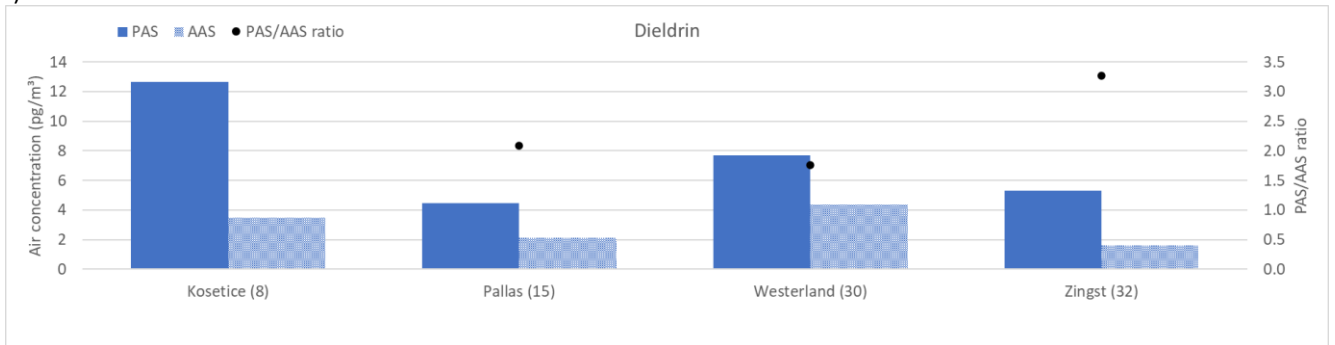
Figure SI-1.3a-f. Comparison of PAS derived concentrations in air obtained in our study with the concentrations from routine AAS measurements reported to EMEP for the same sampling period (Aas & Bohlin-Nizzetto, 2018).

1.3.1 Sampling artifacts

The range of all derived sampling rates are presented in Figure SI-1.4a. Elevated sampling rates (outliers) are found for PAS exposed to high wind (e.g. high-altitude/coastal sites). The sites with highest sampling rates (outliers) are illustrated in Figure 1.4b-c.
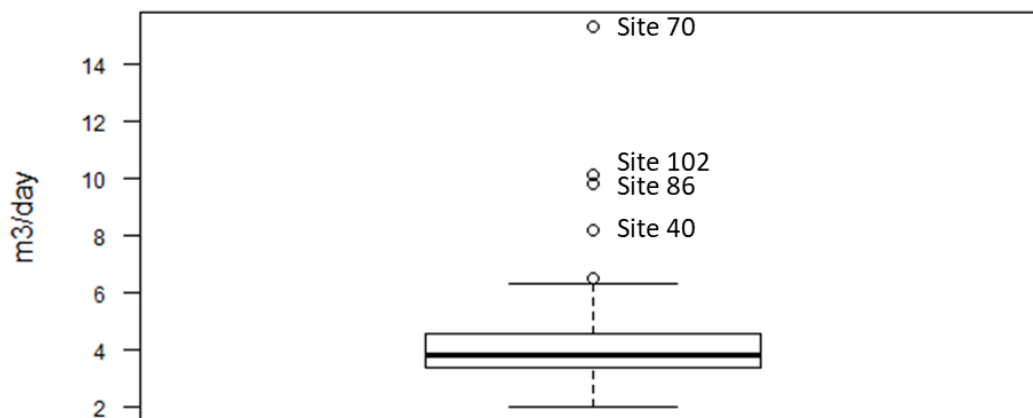
Figure SI-1.4a. Boxplot of derived sampling rates (m3/day) for 101 European sites (Table SI-1.5).

Figure SI-1.4b. Site 70 (Chopok, Slovakia) and site 86 (Jungfraujoch, Switzerland), situated at high altitudes (2008 and 3578 m.a.s.l. respectively), resulting in both low temperatures and high exposure to wind (and hence elevated sampling rates).

Figure SI-1.4c. Site 40 (Nuuk, Greenland) and site 102 (Andøya, Norway), situated on top of a roof top and on top of a hill (by the coast) respectively, resulting in elevated sampling rates due to high exposure to wind.

The uptake with PUF-PAS is generally influenced by both windspeed and temperature at a given site. Though the PUF is sheltered with two surrounding steel bowls, it has been shown that wind generally has the strongest influence on the uptake rate (Klánová et al., 2008; Tuduri et al., 2006). In our study, the sampling locations ranged from sea level (majority of sites) and up to almost 4000 m (Table SI-1.5), resulting in high variations in both temperature and wind speed (Table SI-1.5). Other irregularities during sampling (e.g. opening of PAS) may also cause potential overexposure of the PUF-PAS. In our study, the PRCs compensate for different sampling conditions in the estimation of site-specific sampling rates. However, contamination from precipitation may still influence the measured concentration of POPs in the PUF.

1.4 Data analysis

1.4.1 Outliers

When calculating MMR, outliers outside the maximum according to a box-whisker plot (Figure SI-1.7) may be excluded. These are defined as datapoints higher than Q3 + 1.5 x IQR, where Q3 is the 75 % percentile and IQR is the interquartile range.
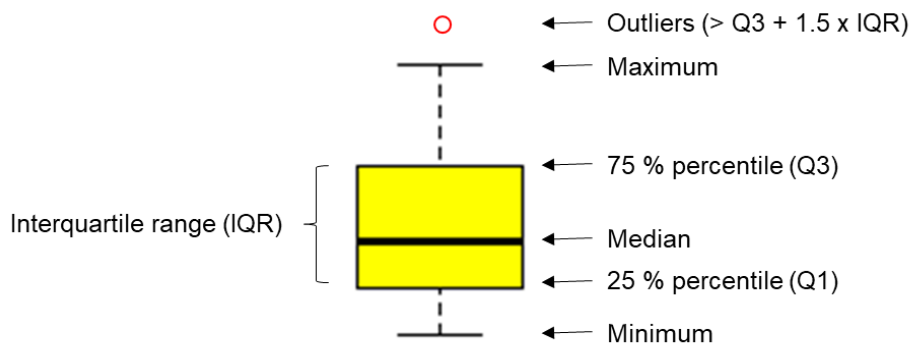
Figure SI-1.5. Illustration and explanation of boxplots (Lunder Halvorsen et al., 2021).

1.4.2 Estimating population density within 50km radius

From the population density dataset in the collection "Gridded Population of the World, version 4" (CIESIN, 2016), estimates of the mean number of persons within 50 km of each sampling site were retrieved, by using the zonal statistics tool in QGIS ver.3.0.1 (Figure SI-1.8). The population density used was consistent with national censuses and population registers, for the year 2015. Further the grid cell area (in km^2) at each site was calculated from the following equation;

$$Grid\ cell\ area\ (km^2) = \left(\frac{\cos(latitude)\times 6371km\ \times 2\pi}{360\times 60\times 2}\right) \times \left(\frac{6371km\ \times 2\pi}{360\times 60\times 2}\right)$$

The population density within 50 km of each sampling site was then estimated;

$$Population\ density\ (persons\ per\ km^2) = \frac{mean\ number\ of\ persons}{grid\ cell\ area\ (km^2)}$$

18

The results revealed nine sampling sites (red circles) with elevated population density due to the presence of a city within 50 km radius from the sites, indicating that these are not designated background sites for the measurement of POPs.
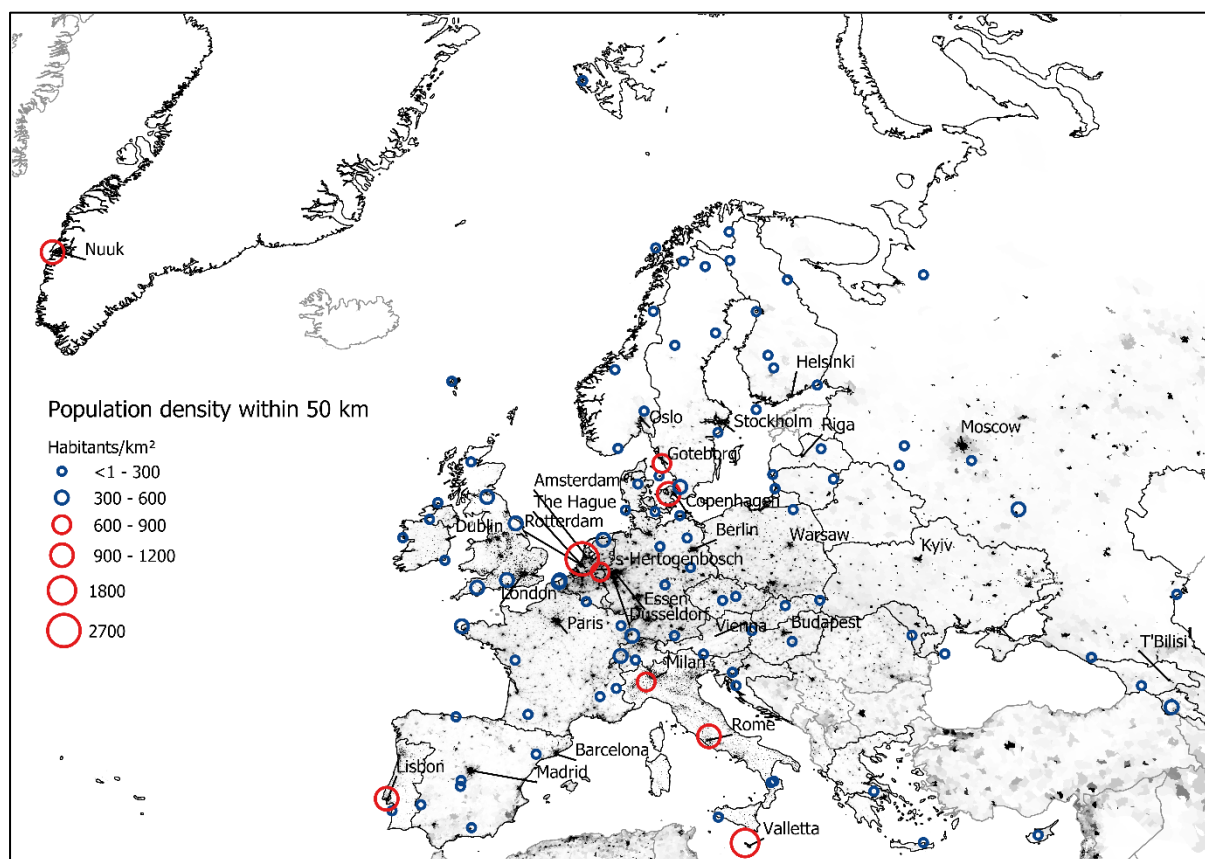
Figure SI-1.8. The spatial distribution of the estimated population density within 50 km of each site, with the gridded population across Europe in the background (CIESIN, 2016).

1.4.3   Correlation tests

1.4.3.1   Linear correlation

The Pearson correlation coefficient (r) gives a measure of the linear relationship between two variables (Y and X). The correlation can be either negative or positive (between -1 and 1).

In order to decide how two variables (e.g. POP concentrations, latitude/longitude or population density within 50 km) correlates, a linear regression model of how y is depending on x were fitted by using R Studio (method of least squares, Eq. 1). All POP concentrations were log-transformed in order to fulfill the assumption of normality.

Eq. 1 $\hat{y}_i = b_0 + b_1\, x_i$

The null hypothesis that $b_1 = 0$ were tested, versus the alternative hypothesis that $b_1 \neq 0$.

p-values less than 0.05, mean that we can reject the H_0 with more than 95 % significance, and that there is a linear relationship (given by r) between the two variables.

1.4.4   Significant tests

1.4.4.1   Wilcoxon signed rank test

A Wilcoxon test was used to compare two-and-two regions, without log-transforming the concentrations, by using R Studio. In this case, the null-hypothesis tests if one region is lower or higher than another, i.e H_0: Difference < 0 or Difference > 0 (one-sided). The null-hypothesis was rejected when $p < 0.05$.

1.4.4.2   Matched pair Wilcoxon signed rank test

To compare the POP concentrations in air with data from a similar PUF-PAS campaign conducted all over Europe by Halse et al. (2011) in 2006, a Wilcoxon test was run in R Studio by comparing the concentrations at the 73 common sites pairwise. It should be noted that the air samples from 2006 were analyzed at the same laboratory with the same methodology and same type of instrumentation (Halse et al., 2011), and the concentrations are therefore comparable.

The null-hypothesis tests if the 2016-data are lower or higher than the 2006-data, i.e H_0: Difference < 0 or Difference > 0 (one-sided). The null-hypothesis was rejected when $p < 0.05$.

2   Results and Discussion

Tables:

Table SI-2.1a. Summary of measured concentrations in air (pg/m^3) of selected PCBs and OCPs at European background sites, including detection frequencies and max-min ratios

Compounds	Background concentrations in air in Europe[a]					
	Average ± SD pg/m³	Median pg/m³	Measured range pg/m³	Detection frequency %	MMR	MMR[c]
PCB-28	4 ± 6	2	0.3-28	100 %	93	27
PCB-52	5 ± 6	3	0.4-36	100 %	90	25
PCB-101	5 ± 8	3	0.2-69	100 %	345	60
PCB-138	3 ± 5	1	0.07-42	100 %	600	86
PCB-153	4 ± 8	2	0.1-78	100 %	780	80
PCB-180	0.8 ± 1.3	0.4	0.02-11	100 %	550	100
Sum 6 PCB	22 ± 30	13	1-241		240	60
Sum 30 PCB	49 ± 59	29	3-405		135	31
PeCB	26 ± 10	25	13-74	100 %	6	3
HCB	72 ± 43	67	28-413	100 %	15	4
a-HCH	12 ± 8	9	4-47	100 %	12	6
g-HCH	16 ± 17	9	2-109	100 %	55	21
Sum 2 HCHs	28 ± 20	22	7-116		17	11
o.p'-DDE	0.7 ± 1.4	0.2	<MDL-10	95 %	1000[b]	150[b]
p,p'-DDE	17 ± 31	6	<MDL-183	100 %	1017	194
o,p'-DDD	0.4 ± 1.2	0.1	<MDL-12	94 %	1200[b]	60[b]
p,p'-DDD	0.3 ± 1.2	0.1	<MDL-12	88 %	1200[b]	50[b]
o,p'-DDT	4 ± 6	1	0.07-37	100 %	529	333
p,p'-DDT	5 ± 10	2	<MDL-81	99 %	2700[b]	433[b]
Sum 6 DDXs	28 ± 47	10	0.3-286		> 953	> 200
dieldrin	6 ± 7	4	<MDL-37	98 %	93[b]	35[b]
heptachlor-exo-epoxide	3 ± 7	2	0.4-63	100 %	158	15
oxy-chlordane	1 ± 1	1	<MDL-9	99 %	45[b]	10[b]
trans-chlordane	0.6 ± 1.7	0.3	<MDL-16	99 %	800[b]	45[b]
cis-chlordane	1 ± 1	1	0.2-7	100 %	35	100
trans-nonachlor	1 ± 1	1	0.2-10	100 %	50	10
cis-nonachlor	0.2 ± 0.2	0.1	<MDL-0.8	95 %	40[b]	20[b]
Sum 4 chlordanes	3 ± 4	2	0.5-35		> 70	> 14
endosulfan-I	5 ± 9	3	0.4-82	100 %	205[b]	25[b]

[a] Number of samples:

PCBs and PeCB/HCB: n = 101.

HCHs and DDXs: n = 101.

Other OCPs: n = 99. Two samples not analyzed.

[b] Minimum value = method detection limit

[c] Excluding outliers (SI 1.4.1)

Table SI-2.1b. Summary of concentrations in field blanks and method blanks, including method detection limit (MDL), for selected PCBs and OCPs

Compounds	Field blanks (n=11)[a]		Method blanks (n=14)[a]		
	Median pg/m³	Measured range pg/m³	Median pg/m³	Measured range pg/m³	MDL[b] pg/m³
PCB-28	0.03	0.02-0.06	0.02[c]	0.01[c]-0.04	0.04
PCB-52	0.03	0.02-0.05	0.02	0.01-0.03	0.03
PCB-101	0.02	0.01-0.04	0.01	0.006-0.04	0.04
PCB-138	0.009	0.005-0.04	0.006	0.001[c]-0.02	0.03
PCB-153	0.01	0.007-0.06	0.01	0.001[c]-0.03	0.03
PCB-180	0.005	0.003-0.03	0.004	0.001[c]-0.008	0.01
Sum 6 PCB					
Sum 30 PCB					
PeCB	0.8	0.6-13	0.4	0.2-0.7	0.9
HCB	0.4	0.2-0.6	0.2	0.1-0.7	0.8
a-HCH	0.1[c]	0.04[b]-0.8	0.1[c]	0.05[c]-0.2[c]	0.3
g-HCH	0.2[c]	0.04[b]-0.3	0.1[c]	0.04[c]-0.2[c]	0.3
Sum 2 HCHs					
o.p'-DDE	0.002[c]	0.001[c]-0.005[c]	0.004[c]	0.001[c]-0.01[c]	0.01
p,p'-DDE	0.03	0.01-0.1	0.04	0.006-0.1	0.18
o,p'-DDD	0.006[c]	0.003[c]-0.01[c]	0.006[c]	0.003[c]-0.01[c]	0.01
p,p'-DDD	0.006[c]	0.003[c]-0.01[c]	0.007[c]	0.003[c]-0.01[c]	0.01
o,p'-DDT	0.01[c]	0.004[c]-0.02	0.01[c]	0.004[c]-0.02[c]	0.03
p,p'-DDT	0.01[c]	0.006[c]-0.02	0.02[c]	0.004[c]-0.02[c]	0.03
Sum 6 DDXs					
dieldrin	0.3[c]	0.2[c]-0.5[c]	0.3[c]	0.1[c]-0.4[c]	0.4
heptachlor-exo-epoxide	0.2[c]	0.2[c]-0.4[c]	0.2[c]	0.1[c]-0.3[c]	0.3
oxy-chlordane	0.1[c]	0.08[c]-0.14[c]	0.08[c]	0.06[c]-0.11[c]	0.2
trans-chlordane	0.01[c]	0.01[c]-0.02[c]	0.01[c]	0.008[c]-0.02[c]	0.02
cis-chlordane	0.03[c]	0.02[c]-0.04[c]	0.02[c]	0.01[c]-0.03[c]	0.03
trans-nonachlor	0.02[c]	0.01[c]-0.02[c]	0.01[c]	0.009[c]-0.02[c]	0.02
cis-nonachlor	0.01[c]	0.009[c]-0.02[c]	0.009[c]	0.006[c]-0.01[c]	0.02
Sum 4 chlordanes					
endosulfan-I	0.02[c]	0.02[c]-0.06[c]	0.02[c]	0.01[c]-0.03[c]	0.1

[a] Based on averaged sample volume of all sites (excluding sites 40, 41, 44, 70, 86 and 102)

[b] For PCBs and PeCB/HCB: MDL based on method blanks only.

[c] Instrument detection limit

Table SI-2.2a. Concentrations in air (pg/m^3) for all target PCBs at the individual sites. Concentrations below MDL set to ½ MDL (grey).

Country no.	Site no.	PCB 18	PCB 28[c]	PCB 31	PCB 33	PCB 37	PCB 47	PCB 52[c]	PCB 66	PCB 74	PCB 99	PCB 101[c]
1	1[e]	13.7	13.7	12.3	7.09	2.34	5.06	14.8	8.54	6.01	6.55	12.9
2	2	12.7	12.4	11.2	6.57	1.91	4.93	12.9	4.74	3.36	2.43	11.8
2	3	3.40	2.87	2.62	1.34	0.29	1.11	3.33	0.92	0.71	0.70	3.09
3	4	3.11	3.56	3.23	2.09	0.75	1.95	6.82	2.61	1.69	2.30	7.32
3	5	3.49	3.93	3.60	2.37	0.82	2.18	8.19	3.02	1.97	2.78	8.80
4	6	5.84	5.01	4.46	2.59	0.67	1.58	4.61	1.65	1.19	1.03	3.74
5	7	27.2	26.0	22.9	13.7	4.52	7.82	26.5	19.4	13.5	16.7	20.9
6	8[e]	4.41	4.88	3.91	2.23	0.65	2.04	4.05	1.73	1.18	0.77	3.91
6	9	6.39	7.04	5.52	3.20	1.05	3.80	5.55	2.40	1.61	1.01	5.33
7	10	2.42	2.23	2.08	1.24	0.34	3.54	3.44	1.04	0.66	0.77	2.94
7	11	4.39	4.26	4.09	2.63	0.76	2.09	12.5	2.52	1.71	2.57	25.7
7	12	1.87	1.99	1.81	1.06	0.31	1.17	2.98	1.04	0.62	0.79	3.15
7	13	3.62	5.15	5.32	3.05	1.09	2.42	12.4	2.51	1.77	2.10	20.5
8	14	0.88	0.53	0.50	0.26	0.05	0.25	0.86	0.20	0.16	0.20	0.59
9	15[e]	0.95	0.84	0.70	0.36	0.09	2.79	0.98	0.30	0.26	0.27	0.77
9	16	1.23	1.11	0.98	0.52	0.14	0.61	1.17	0.35	0.30	0.26	0.89
9	17	2.15	1.89	1.71	0.90	0.28	0.83	2.25	0.78	0.60	0.68	2.14
9	18	2.55	2.40	2.00	1.13	0.40	0.83	2.19	0.89	0.68	0.69	1.84
9	19	1.33	1.13	0.94	0.51	0.14	0.51	1.01	0.34	0.28	0.28	0.69
9	20	1.42	1.11	1.02	0.52	0.14	0.55	1.31	0.39	0.33	0.36	1.13
9	21	1.68	1.42	1.23	0.64	0.17	0.60	1.60	0.45	0.39	0.37	1.31
10	22	2.97	2.75	2.66	1.49	0.34	1.48	5.13	1.51	1.15	1.16	4.64
10	23	0.95	0.96	0.92	0.54	0.16	0.54	1.96	0.67	0.45	0.56	1.92
10	24	1.04	1.06	1.00	0.61	0.16	0.53	2.05	0.69	0.48	0.59	1.91
10	25	2.01	2.06	1.83	1.02	0.28	0.95	3.53	1.04	0.76	0.91	3.63
10	26	0.82	0.82	0.78	0.43	0.15	0.50	2.04	0.75	0.51	0.86	2.66
10	27	3.53	3.28	2.94	1.73	0.46	1.45	5.40	1.60	1.09	1.25	4.48
10	28	1.69	1.74	1.62	0.95	0.27	1.21	3.53	1.10	0.81	1.06	3.99
11	29	4.76	5.60	4.94	2.42	2.46	3.11	35.9	6.06	7.17	12.2	68.5
12	30[e]	2.81[d]	3.12[d]	2.78[d]	1.60	0.57	1.82	5.13	2.00	1.11[d]	1.65	6.20
12	31	5.21	4.76	4.39	2.42	0.62	2.70	6.49	2.10	1.55	1.30	6.28
12	32	2.22	2.09	1.85	1.06	0.26	1.18	2.56	0.83	0.50	0.60	2.33
12	33	4.25	3.78	3.94	2.20	0.57	2.01	7.35	2.38	1.75	1.55	7.49
12	34	2.87	2.65	2.36	1.37	0.34	1.44	4.65	1.16	0.76	1.07	4.92
12	35[e]	2.80	2.89	2.76	1.56	0.39	2.11	4.08	1.43	1.01	0.79	4.03
12	36	5.15	4.48	3.98	2.20	0.57	1.91	4.58	1.55	1.10	1.01	4.46
12	37	5.32	4.65	4.85	2.60	0.70	3.51	9.15	2.71	2.09	2.08	9.46
13	38	4.67	4.29	3.91	2.42	0.67	1.09	3.01	1.33	0.84	0.60	1.51
13	39	5.46	5.60	5.11	2.85	0.66	1.90	5.83	2.75	1.87	1.94	4.80
14	40	21.7	15.9	19.4	9.59	2.63	8.64	29.61	10.2	6.90	3.70	12.9
14	41	4.16	3.05	3.18	1.68	0.39	1.49	4.89	1.57	1.09	0.75	2.29
15	42	13.2	6.55	5.31	3.11	1.13	2.01	4.13	2.15	1.33	0.62	2.21
16	43	1.74	1.44	1.36	0.78	0.22	0.77	2.10	0.59	0.44	0.50	1.40
16	44	0.82	0.63	0.61	0.36	0.14	0.30	0.85	0.29	0.20	0.21	0.61
16	45	4.07	3.96	3.33	1.86	0.87	1.76	4.39	2.30	1.20	1.47	3.67
17	46	9.62	7.68	7.03	4.43	1.26	2.97	15.0	3.79	2.90	3.94	11.5
17	47	4.12	3.72	3.39	2.19	0.70	1.46	5.99	2.08	1.49	1.78	7.32
17	48	2.73	2.16	1.94	1.13	0.23	0.79	2.63	0.77	0.64	0.66	2.42
17	50	3.39	5.09	4.55	3.40	2.52	2.25	6.76	4.68	2.60	2.29	7.61
17	51	2.34	2.04	1.85	1.06	0.25	0.87	2.90	0.90	0.68	0.81	3.04

[a] Coeluting with PCB-106 in the PRCs. Excluded.

[b] Not included in sum 30 PCBs.

[c] Included in sum 6 PCBs.

[d] Blank contribution possible.

[e] Average of two parallel PAS.

[f] Lunder Halvorsen et al., 2021

23

Table SI-2.2a. (continued) Concentrations in air (pg/m^3) for all target PCBs at the individual sites. Concentrations below MDL set to ½ MDL (grey).

Country no.	Site no.	PCB 18	PCB 28[c]	PCB 31	PCB 33	PCB 37	PCB 47	PCB 52[c]	PCB 66	PCB 74	PCB 99	PCB 101[c]
18	52	4.17	3.13	2.63	1.55	0.41	1.01	2.64	0.99	0.67	0.68	1.78
18	53[e]	4.53	3.96	3.26	1.94	0.43	1.16	2.74	1.00	0.71	0.63	1.49
19	54	3.79	5.83	4.93	3.13	1.03	2.21	6.02	2.59	1.70	2.34	6.06
19	55	2.65	2.59	2.01	1.10	0.30	0.91	1.98	0.90	0.59	0.65	1.24
20	56	2.90	2.59	2.43	1.43	0.36	1.51	5.36	1.94	1.45	2.01	7.40
21	57	22.9	12.5	10.2	6.02	2.89	2.52	7.65	4.29	2.88	2.31	4.52
22	58	9.77	10.5	9.83	6.03	1.95	5.27	13.5	5.90	3.63	3.60	12.4
22	59	15.5	13.5	13.3	9.02	2.62	5.54	14.7	5.99	3.83	2.57	10.0
22	60	10.2	11.6	11.0	6.74	2.42	6.48	18.2	7.12	4.25	5.11	14.9
23	97[e,f]	1.72	1.13	1.11	0.54	0.11	0.56	1.62	0.42	0.33	0.34	1.18
23	98[f]	0.98	0.41	0.38	0.18	0.02	0.17	0.56	0.09	0.09	0.11	0.37
23	99[f]	1.54	0.61	0.58	0.24	0.02	0.34	1.39	0.13	0.12	0.21	0.70
23	100[f]	1.29	0.84	0.81	0.38	0.08	0.35	1.05	0.24	0.19	0.21	0.72
23	101[f]	1.02	0.55	0.53	0.24	0.04	0.19	0.62	0.12	0.09	0.15	0.44
23	102[f]	1.28	0.75	0.83	0.35	0.03	0.35	1.36	0.17	0.17	0.28	0.83
23	96	0.93	0.63	0.61	0.35	0.07	0.20	0.63	0.15	0.12	0.13	0.33
24	61	1.76	2.77	2.14	1.22	0.32	1.09	2.57	0.97	0.67	0.64	1.85
25	62	1.61	1.28	1.19	0.90	0.23	0.46	1.35	0.49	0.32	0.35	1.27
25	63	2.73	2.58	2.38	1.60	0.64	1.22	3.27	1.16	0.82	0.84	4.59
26	64	0.67	0.98	0.72	0.40	0.11	0.27	0.68	0.28	0.19	0.19	0.37
26	65	2.16	2.88	2.10	1.16	0.35	0.75	2.04	0.89	0.63	0.67	1.21
26	66	4.90	4.44	3.55	2.05	0.53	1.04	3.47	1.41	0.98	1.27	2.45
26	67	3.43	3.67	2.89	1.42	0.41	1.23	3.49	1.47	1.06	1.50	2.69
26	68	19.3	7.71	6.15	3.44	1.02	1.60	5.05	2.25	1.55	1.51	2.56
26	69	63.4	28.3	21.3	11.4	4.28	5.35	13.8	6.46	4.36	3.36	5.55
26	95	19.1	6.42	5.57	3.02	0.63	1.50	4.47	1.31	1.02	1.16	2.25
27	70	6.73	7.77	6.34	3.64	1.03	2.38	5.50	2.46	1.63	0.92	4.02
27	71	13.0	22.8	15.8	10.8	6.79	6.22	9.90	15.0	7.28	1.76	4.37
28	72	9.54	5.88	5.84	3.69	0.57	5.12	4.29	0.79	0.62	0.32	2.07
29	73[e]	1.47	1.04	0.97	0.64	0.18	0.46	1.34	0.39	0.29	0.36	1.33
29	74	3.99	3.02	2.87	1.84	0.48	1.30	3.17	1.18	0.77	0.68	2.67
29	75	2.43	2.09	1.94	1.22	0.30	0.78	2.20	0.67	0.47	0.45	1.75
29	76	7.27	4.73	4.29	2.70	0.74	0.81	1.98	0.82	0.50	0.20	1.01
29	77	1.49	1.32	1.20	0.72	0.16	0.68	2.39	0.66	0.41	0.76	2.67
29	78	0.93	0.67	0.63	0.40	0.10	0.25	0.72	0.20	0.16	0.17	0.62
30	79[e]	1.80	1.56	1.47	0.91	0.25	0.96	2.33	0.78	0.55	0.56	2.71
30	80	3.86	3.77	3.62	2.14	0.66	2.59	6.43	2.50	1.75	1.99	9.12
30	81	4.11	3.66	3.58	2.02	0.55	2.34	5.91	2.13	1.49	1.66	6.98
30	82	0.83	0.65	0.58	0.30	0.07	0.32	0.79	0.23	0.17	0.17	0.70
30	83	1.54	1.44	1.39	0.76	0.20	0.97	2.09	0.74	0.52	0.44	2.07
30	84	0.81	0.59	0.53	0.26	0.05	0.26	0.80	0.19	0.17	0.20	0.67
30	85	0.91	0.66	0.59	0.30	0.06	0.37	0.85	0.20	0.18	0.20	0.75
31	86	2.83	2.04	2.00	1.08	0.21	1.05	4.15	0.97	0.78	0.83	3.04
31	87	4.49	2.98	2.94	1.69	0.45	1.58	8.05	1.71	1.41	1.94	7.72
32	88[e]	21.7	28.2	23.6	12.8	5.16	7.79	25.9	13.1	8.17	10.3	19.9
33	89	2.46	2.16	2.04	1.27	0.40	1.11	2.63	0.86	0.62	0.66	2.01
33	90	1.04	0.98	0.88	0.49	0.16	0.48	1.16	0.38	0.27	0.26	0.79
33	91	0.37	0.30	0.30	0.16	0.03	0.15	0.44	0.08	0.07	0.07	0.20
33	92[e]	1.87	1.60	1.47	0.85	0.24	0.86	2.07	0.62	0.46	0.56	1.59
33	93	1.97	1.84	1.68	1.11	0.34	1.34	2.08	0.70	0.57	0.47	1.49
33	94	0.59	0.45	0.41	0.21	0.05	0.25	0.71	0.16	0.14	0.15	0.46

[a] Coeluting with PCB-106 in the PRCs. Excluded.

[b] Not included in sum 30 PCBs.

[c] Included in sum 6 PCBs.

[d] Blank contribution possible (< 10%)

[e] Average of two parallel PAS.

[f] Lunder Halvorsen et al., 2021

Table SI-2.2a. (continued) Concentrations in air (pg/m^3) for all target PCBs at the individual sites. Concentrations below MDL set to ½ MDL (grey).

Country no.	Site no.	PCB 105	PCB 114	PCB 118[a]	PCB 122	PCB 123	PCB 128	PCB 138[c]	PCB 141	PCB 149	PCB 153[c]	PCB 156
1	1[e]	5.09	0.42		0.24	0.18	1.33	5.64	1.40	7.32	7.35	0.33
2	2	1.36	0.12		0.22	0.04	1.11	7.11	2.39	12.53	12.5	0.29
2	3	0.32	0.06		0.05	0.01	0.23	1.50	0.48	2.75	2.72	0.06
3	4	0.90	0.09		0.08	0.01	0.59	5.15	1.03	5.86	6.51	0.19
3	5	1.06	0.10		0.09	0.01	0.65	5.55	1.08	6.45	6.80	0.19
4	6	0.32	0.05		0.06	0.02	0.21	1.58	0.54	3.35	2.79	0.07
5	7	14.4	1.15		0.41	0.53	2.73	8.29	1.00	5.67	8.18	0.65
6	8[e]	0.37	0.07		0.07	0.04	0.30	2.24	0.79	4.23	4.18	0.09
6	9	0.53	0.06		0.09	0.02	0.45	3.29	1.15	6.01	6.17	0.13
7	10	0.22	0.05		0.04	0.01	0.15	1.23	0.33	2.04	1.77	0.06
7	11	1.03	0.17		0.34	0.08	0.92	11.0	3.96	21.0	17.1	0.41
7	12	0.26	0.04		0.05	0.01	0.16	1.50	0.39	2.55	2.19	0.06
7	13	0.96	0.14		0.27	0.04	1.01	11.9	4.13	20.0	17.4	0.44
8	14	0.04	0.01		0.01	0.002	0.03	0.20	0.05	0.43	0.37	0.01
9	15[e]	0.06	0.02		0.01	0.01	0.02	0.27	0.09	0.56	0.43	0.01
9	16	0.07	0.03		0.01	0.02	0.04	0.32	0.11	0.65	0.53	0.02
9	17	0.18	0.03		0.02	0.01	0.14	1.15	0.32	1.85	1.82	0.06
9	18	0.20	0.03		0.02	0.01	0.10	0.75	0.22	1.28	1.17	0.04
9	19	0.07	0.03		0.01	0.004	0.03	0.23	0.07	0.44	0.36	0.01
9	20	0.09	0.03		0.01	0.003	0.06	0.47	0.16	0.85	0.76	0.03
9	21	0.09	0.04		0.01	0.004	0.05	0.46	0.16	0.89	0.76	0.02
10	22	0.39	0.06		0.05	0.01	0.23	2.33	0.56	3.44	3.37	0.08
10	23	0.21	0.03		0.02	0.01	0.13	1.10	0.24	1.58	1.51	0.04
10	24	0.20	0.04		0.02	0.01	0.12	1.07	0.22	1.36	1.42	0.04
10	25	0.28	0.04		0.04	0.005	0.18	1.74	0.44	2.94	2.69	0.05
10	26	0.33	0.04		0.03	0.002	0.25	2.19	0.43	2.38	2.80	0.08
10	27	0.38	0.05		0.04	0.01	0.21	2.07	0.47	3.05	2.83	0.06
10	28	0.56	0.05		0.05	0.09	0.27	2.33	0.50	3.00	2.93	0.08
11	29	4.86	0.23		1.18	0.11	5.86	41.9	15.0	71.0	77.7	1.16
12	30[e]	0.46	0.08		0.11	0.03	0.49	4.21	1.07	6.23	5.97	0.15
12	31	0.68	0.07		0.10	0.02	0.45	3.03	1.01	5.49	4.91	0.13
12	32	0.14	0.03		0.03	0.01	0.11	1.11	0.30	1.92	1.77	0.04
12	33	0.60	0.07		0.08	0.02	0.43	4.29	1.04	5.88	5.22	0.14
12	34	0.31	0.05		0.06	0.02	0.23	2.05	0.59	3.30	2.94	0.08
12	35[e]	0.24	0.05		0.05	0.004	0.22	2.66	0.67	3.61	3.27	0.08
12	36	0.49	0.05		0.07	0.01	0.37	2.37	0.76	4.25	3.82	0.10
12	37	1.15	0.10		0.17	0.03	0.77	4.66	1.63	8.30	7.34	0.21
13	38	0.38	0.04		0.03	0.01	0.19	0.79	0.20	1.17	1.10	0.04
13	39	1.51	0.13		0.13	0.04	0.89	3.32	0.73	4.48	4.12	0.17
14	40	1.25	0.11		0.12	0.07	0.44	2.97	0.94	5.08	4.04	0.18
14	41	0.20	0.03		0.02	0.01	0.08	0.53	0.16	1.03	0.80	0.03
15	42	0.20	0.02		0.01	0.01	0.09	1.15	0.34	2.10	1.81	0.05
16	43	0.11	0.02		0.01	0.01	0.07	0.51	0.12	1.01	0.92	0.02
16	44	0.05	0.01		0.01	0.004	0.03	0.23	0.06	0.48	0.38	0.01
16	45	0.46	0.05		0.05	0.03	0.34	2.13	0.36	2.99	3.43	0.07
17	46	1.19	0.10		0.10	0.05	0.47	3.36	1.06	6.32	5.87	0.15
17	47	0.86	0.07		0.09	0.04	0.49	3.95	1.15	6.08	6.04	0.18
17	48	0.20	0.05		0.03	0.004	0.14	1.09	0.35	2.21	1.82	0.04
17	50	1.27	0.10		0.14	0.05	0.81	5.29	1.26	7.05	8.05	0.26
17	51	0.30	0.03		0.04	0.01	0.19	1.47	0.45	2.89	2.51	0.06

[a] Coeluting with PCB-106 in the PRCs. Excluded.
[b] Not included in sum 30 PCBs.
[c] Included in sum 6 PCBs.
[d] Blank contribution possible.
[e] Average of two parallel PAS.
[f] Lunder Halvorsen et al., 2021

Table SI-2.2a. (continued) Concentrations in air (pg/m³) for all target PCBs at the individual sites. Concentrations below MDL set to ½ MDL (grey).

Country no.	Site no.	PCB 105	PCB 114	PCB 118[a]	PCB 122	PCB 123	PCB 128	PCB 138[c]	PCB 141	PCB 149	PCB 153[c]	PCB 156
18	52	0.29	0.04		0.01	0.004	0.12	0.95	0.18	1.13	1.12	0.04
18	53[e]	0.18	0.03		0.005	0.01	0.07	0.59	0.12	0.91	0.76	0.02
19	54	0.93	0.09		0.09	0.03	0.65	4.80	0.98	6.35	6.24	0.21
19	55	0.39	0.04		0.004	0.005	0.11	0.72	0.11	0.65	0.71	0.05
20	56	0.82	0.07		0.12	0.02	0.70	4.99	1.30	8.00	7.42	0.19
21	57	1.03	0.09		0.05	0.06	0.40	2.53	0.44	2.49	2.79	0.15
22	58	1.08	0.15		0.17	0.07	1.08	10.0	1.90	13.0	11.8	0.28
22	59	1.04	0.11		0.12	0.05	0.64	5.53	1.40	7.27	6.52	0.22
22	60	1.36	0.17		0.18	0.01	1.19	10.1	1.77	13.5	12.5	0.32
23	97[e,f]	0.08	0.03		0.01	0.02	0.05	0.48	0.12	0.98	0.78	0.02
23	98[f]	0.02	0.02		0.01	0.01	0.01	0.13	0.04	0.34	0.22	0.01
23	99[f]	0.04	0.03		0.01	0.01	0.02	0.18	0.07	0.51	0.35	0.01
23	100[f]	0.04	0.02		0.01	0.01	0.02	0.23	0.07	0.55	0.39	0.01
23	101[f]	0.04	0.01		0.01	0.01	0.01	0.16	0.03	0.30	0.22	0.01
23	102[f]	0.06	0.02		0.02	0.03	0.01	0.32	0.06	0.63	0.51	0.01
23	96	0.03	0.01		0.00	0.01	0.02	0.10	0.01	0.19	0.15	0.005
24	61	0.17	0.01		0.01	0.01	0.08	0.98	0.25	1.62	1.33	0.03
25	62	0.12	0.03		0.02	0.01	0.08	0.69	0.20	1.13	1.10	0.04
25	63	0.46	0.04		0.07	0.02	0.40	3.16	1.06	4.17	4.58	0.20
26	64	0.05	0.01		0.003	0.004	0.01	0.11	0.03	0.19	0.18	0.01
26	65	0.30	0.01		0.003	0.004	0.10	0.64	0.10	0.57	0.67	0.07
26	66	0.81	0.09		0.05	0.03	0.30	1.00	0.17	1.10	1.17	0.06
26	67	1.12	0.12		0.05	0.04	0.35	1.26	0.20	1.13	1.43	0.09
26	68	0.44	0.02		0.01	0.02	0.13	0.85	0.14	0.95	0.95	0.04
26	69	1.09	0.10		0.04	0.06	0.28	1.86	0.29	1.97	2.09	0.10
26	95	0.32	0.02		0.00	0.02	0.11	0.80	0.14	0.91	0.93	0.04
27	70	0.50	0.04		0.07	0.01	0.37	2.31	0.74	4.07	4.16	0.10
27	71	1.32	0.13		0.09	0.05	0.33	1.76	0.52	3.04	2.91	0.08
28	72	0.07	0.04		0.01	0.004	0.05	0.55	0.20	1.26	0.96	0.03
29	73[e]	0.13	0.02		0.02	0.01	0.08	0.62	0.21	1.18	1.02	0.03
29	74	0.25	0.05		0.03	0.01	0.14	1.20	0.38	2.32	2.13	0.06
29	75	0.17	0.03		0.02	0.01	0.12	1.02	0.24	1.65	1.38	0.03
29	76	0.08	0.02		0.02	0.02	0.07	0.88	0.38	1.64	1.69	0.04
29	77	0.27	0.01		0.01	0.01	0.21	1.94	0.49	2.93	2.99	0.06
29	78	0.07	0.02		0.01	0.00	0.05	0.33	0.10	0.59	0.51	0.02
30	79[e]	0.23	0.04		0.04	0.01	0.28	2.41	0.72	3.23	3.35	0.12
30	80	0.83	0.06		0.17	0.03	0.98	7.60	2.38	10.2	10.9	0.48
30	81	0.62	0.06		0.10	0.02	0.64	5.03	1.56	7.36	7.59	0.29
30	82	0.05	0.02		0.01	0.02	0.04	0.35	0.12	0.60	0.55	0.02
30	83	0.13	0.02		0.02	0.00	0.12	1.12	0.38	1.87	1.72	0.06
30	84	0.05	0.03		0.01	0.01	0.03	0.26	0.08	0.52	0.41	0.01
30	85	0.05	0.02		0.01	0.02	0.04	0.33	0.10	0.63	0.51	0.02
31	86	0.29	0.03		0.04	0.01	0.14	1.13	0.36	2.06	1.73	0.05
31	87	0.74	0.06		0.07	0.03	0.36	2.56	0.73	4.26	3.62	0.13
32	88[e]	7.81	0.54		0.40	0.26	3.16	11.2	1.76	10.4	13.1	0.70
33	89	0.21	0.03		0.02	0.01	0.12	0.86	0.22	1.43	1.29	0.04
33	90	0.07	0.02		0.01	0.004	0.04	0.28	0.07	0.55	0.43	0.02
33	91	0.01	0.002		0.002	0.01	0.01	0.07	0.02	0.13	0.11	0.01
33	92[e]	0.15	0.03		0.02	0.01	0.09	0.64[d]	0.16	1.12	1.06[d]	0.03
33	93	0.14	0.03		0.02	0.01	0.07	0.51	0.14	1.00	0.79	0.04
33	94	0.04	0.02		0.002	0.01	0.02	0.18	0.05	0.36	0.29	0.01

[a] Coeluting with PCB-106 in the PRCs. Excluded.

[b] Not included in sum 30 PCBs.

[c] Included in sum 6 PCBs.

[d] Blank contribution possible.

[e] Average of two parallel PAS.

[f] Lunder Halvorsen et al., 2021

Table SI-2.2a. (continued) Concentrations in air (pg/m^3) for all target PCBs at the individual sites. Concentrations below MDL set to ½ MDL (grey).

Country no.	Site no.	PCB 157	PCB 167	PCB 170	PCB 180[c]	PCB 183	PCB 187	PCB 189[b]	PCB 194	PCB 206	PCB 209	Sum 30 PCBs	Sum 6 PCBs
1	1[e]	0.05	0.24	0.39	1.14	0.47	1.09	0.01	0.05	0.02	0.01	136	55.6
2	2	0.03	0.27	0.77	2.57	1.04	2.52	0.02	0.12	0.05	0.03	130	59.2
2	3	0.01	0.06	0.13	0.48	0.21	0.51	0.003	0.02	0.01	0.01	30.0	14.0
3	4	0.03	0.12	0.48	1.54	0.44	1.61	0.02	0.08	0.04	0.03	60.2	30.9
3	5	0.03	0.14	0.43	1.41	0.46	1.50	0.02	0.08	0.03	0.02	67.2	34.7
4	6	0.01	0.04	0.16	0.57	0.27	0.73	0.01	0.04	0.02	0.02	43.2	18.3
5	7	0.13	0.40	0.18	0.42	0.17	0.29	0.01	0.02	0.02	0.01	244	90.3
6	8[e]	0.01	0.08	0.25	0.87	0.37	0.87	0.01	0.04	0.01	0.01	44.7	20.1
6	9	0.01	0.12	0.40	1.43	0.57	1.34	0.01	0.09	0.02	0.01	64.8	28.8
7	10	0.01	0.03	0.12	0.38	0.15	0.42	0.003	0.03	0.01	0.01	27.7	12.0
7	11	0.04	0.23	0.86	2.86	1.30	3.05	0.02	0.07	0.01	0.01	128	73.3
7	12	0.01	0.04	0.13	0.41	0.17	0.51	0.003	0.02	0.01	0.01	25.3	12.2
7	13	0.05	0.24	0.95	2.93	1.20	2.96	0.01	0.07	0.01	0.02	125	70.3
8	14	0.00	0.01	0.02	0.06	0.03	0.11	0.002	0.01	0.01	0.01	5.89	2.62
9	15[e]	0.001	0.00	0.02	0.07	0.04	0.10	0.003	0.01	0.004	0.003	10.0	3.37
9	16	0.002	0.01	0.02	0.09	0.04	0.12	0.003	0.01	0.005	0.003	9.65	4.10
9	17	0.01	0.03	0.12	0.34	0.16	0.41	0.002	0.02	0.01	0.01	20.9	9.60
9	18	0.01	0.02	0.06	0.20	0.09	0.24	0.002	0.01	0.004	0.01	20.1	8.54
9	19	0.002	0.01	0.01	0.05	0.03	0.07	0.003	0.01	0.005	0.003	8.61	3.47
9	20	0.01	0.01	0.02	0.05	0.14	0.07	0.16	0.01	0.01	0.01	0.01	11.2	4.92
9	21	0.004	0.01	0.04	0.13	0.06	0.16	0.004	0.01	0.01	0.003	12.8	5.68
10	22	0.01	0.05	0.18	0.63	0.23	0.63	0.004	0.03	0.02	0.01	37.6	18.9
10	23	0.01	0.02	0.09	0.28	0.11	0.31	0.003	0.02	0.01	0.01	15.4	7.73
10	24	0.01	0.02	0.09	0.30	0.10	0.30	0.003	0.02	0.01	0.01	15.4	7.80
10	25	0.01	0.04	0.12	0.48	0.21	0.61	0.002	0.02	0.01	0.01	27.9	14.1
10	26	0.01	0.06	0.25	0.73	0.21	0.70	0.01	0.04	0.01	0.01	20.8	11.2
10	27	0.01	0.04	0.14	0.48	0.20	0.58	0.004	0.02	0.02	0.003	37.9	18.5
10	28	0.01	0.05	0.14	0.51	0.20	0.58	0.002	0.03	0.01	0.01	29.4	15.0
11	29	0.25	2.76	3.25	11.13	5.30	10.3	0.07	0.22	0.01	0.01	405	241
12	30[e]	0.02	0.11	0.41	1.34	0.48	1.50[d]	0.01	0.06	0.02	0.02	51.6	26.0
12	31	0.02	0.11	0.27	0.88	0.38	0.91	0.01	0.04	0.01	0.01	56.3	26.3
12	32	0.01	0.02	0.09	0.31	0.13	0.36	0.003	0.01	0.01	0.01	21.9	10.2
12	33	0.01	0.10	0.31	1.02	0.42	1.11	0.01	0.05	0.04	0.01	58.1	29.2
12	34	0.01	0.05	0.14	0.44	0.21	0.49	0.003	0.02	0.01	0.01	34.6	17.6
12	35[e]	0.01	0.06	0.21	0.71	0.28	0.72	0.005	0.03	0.01	0.01	36.7	17.6
12	36	0.01	0.08	0.22	0.69	0.30	0.74	0.01	0.03	0.02	0.01	45.4	20.4
12	37	0.02	0.19	0.49	1.47	0.62	1.47	0.01	0.06	0.02	0.02	75.9	36.7
13	38	0.01	0.03	0.07	0.24	0.09	0.25	0.003	0.02	0.01	0.01	29.0	10.9
13	39	0.03	0.11	0.31	0.91	0.35	0.97	0.01	0.06	0.05	0.07	57.1	24.6
14	40	0.03	0.09	0.29	0.81	0.33	0.74	0.02	0.06	0.03	0.02	159	66.2
14	41	0.004	0.01	0.04	0.13	0.06	0.16	0.002	0.01	0.01	0.01	27.9	11.7
15	42	0.01	0.02	0.19	0.36	0.15	0.40	0.004	0.01	0.01	0.01	48.7	16.2
16	43	0.004	0.01	0.03	0.12	0.07	0.28	0.002	0.01	0.01	0.02	14.7	6.50
16	44	0.003	0.01	0.02	0.07	0.04	0.13	0.001	0.01	0.01	0.01	6.59	2.78
16	45	0.02	0.06	0.15	0.51	0.23	1.10	0.01	0.04	0.03	0.02	40.9	18.1
17	46	0.02	0.09	0.27	1.23	0.50	1.70	0.003	0.07	0.04	0.01	92.7	44.6
17	47	0.03	0.10	0.40	1.52	0.56	1.47	0.01	0.09	0.04	0.03	57.5	28.5
17	48	0.002	0.03	0.11	0.40	0.18	0.54	0.004	0.03	0.02	0.02	23.4	10.5
17	50	0.05	0.16	0.59	2.18	0.77	2.35	0.02	0.15	0.12	0.10	75.9	35.0
17	51	0.01	0.03	0.15	0.57	0.26	0.76	0.004	0.03	0.04	0.06	26.6	12.5

[a] Coeluting with PCB-106 in the PRCs. Excluded.

[b] Not included in sum 30 PCBs.

[c] Included in sum 6 PCBs.

[d] Blank contribution possible.

[e] Average of two parallel PAS.

[f] Lunder Halvorsen et al., 2021

Table SI-2.2a. (continued) Concentrations in air (pg/m³) for all target PCBs at the individual sites. Concentrations below MDL set to ½ MDL (grey).

Country no.	Site no.	PCB 157	PCB 167	PCB 170	PCB 180^c	PCB 183	PCB 187	PCB 189	PCB 194	PCB 206	PCB 209	Sum 30 PCBs	Sum 6 PCBs
18	52	0.01	0.02	0.07	0.16	0.07	0.21	0.002	0.01	0.01	0.39	24.5	9.78
18	53^e	0.004	0.01	0.06	0.10	0.05	0.13	0.002	0.004	0.003	0.01	24.9	9.65
19	54	0.03	0.11	0.43	1.24	0.41	1.28	0.01	0.06	0.03	0.03	63.6	30.2
19	55	0.01	0.02	0.04	0.09	0.04	0.10	0.003	0.01	0.005	0.003	18.0	7.32
20	56	0.04	0.11	0.61	2.13	0.79	2.46	0.02	0.18	0.08	0.08	59.5	29.9
21	57	0.02	0.07	0.24	0.47	0.17	0.41	0.002	0.02	0.01	0.01	90.1	30.4
22	58	0.04	0.23	0.59	2.17	0.77	2.74	0.02	0.09	0.05	0.10	129	60.4
22	59	0.03	0.13	0.39	1.44	0.46	1.17	0.02	0.06	0.02	0.03	123	51.8
22	60	0.05	0.24	0.62	2.21	0.75	2.72	0.02	0.10	0.05	0.05	146	69.6
23	97^{e,f}	0.01	0.01	0.04	0.14	0.06	0.21	0.01	0.02	0.02	0.01	12.2	5.33
23	98^f	0.005	0.01	0.01	0.04	0.01	0.06	0.01	0.02	0.01	0.01	4.33	1.72
23	99^f	0.01	0.01	0.02	0.05	0.02	0.08	0.01	0.02	0.02	0.01	7.36	3.29
23	100^f	0.004	0.01	0.01	0.06	0.03	0.09	0.01	0.01	0.01	0.01	7.73	3.28
23	101^f	0.004	0.01	0.01	0.04	0.02	0.05	0.01	0.01	0.01	0.01	4.96	2.03
23	102^f	0.01	0.01	0.02	0.10	0.02	0.13	0.01	0.01	0.01	0.01	8.36	3.87
23	96	0.003	0.00	0.01	0.02	0.01	0.03	0.01	0.02	0.01	0.01	4.79	1.87
24	61	0.003	0.01	0.08	0.23	0.11	0.29	0.01	0.01	0.004	0.01	21.2	9.72
25	62	0.01	0.02	0.08	0.25	0.10	0.29	0.002	0.02	0.01	0.01	13.7	5.94
25	63	0.03	0.12	0.41	1.25	0.45	0.97	0.02	0.07	0.02	0.01	39.3	19.4
26	64	0.001	0.00	0.003	0.02	0.01	0.03	0.002	0.005	0.004	0.002	5.51	2.34
26	65	0.01	0.02	0.05	0.08	0.03	0.07	0.003	0.005	0.004	0.005	17.6	7.53
26	66	0.01	0.04	0.05	0.12	0.05	0.11	0.003	0.01	0.01	0.02	31.3	12.6
26	67	0.02	0.07	0.04	0.13	0.05	0.11	0.004	0.01	0.01	0.01	29.5	12.7
26	68	0.01	0.02	0.09	0.08	0.03	0.07	0.003	0.005	0.004	0.01	56.0	17.2
26	69	0.02	0.04	0.12	0.17	0.07	0.16	0.003	0.005	0.01	0.02	176	51.8
26	95	0.01	0.01	0.003	0.11	0.04	0.11	0.003	0.01	0.004	0.01	50.0	15.0
27	70	0.01	0.08	0.26	0.91	0.38	0.92	0.01	0.05	0.03	0.01	57.4	24.7
27	71	0.01	0.07	0.19	0.63	0.25	0.63	0.01	0.05	0.02	0.01	126	42.3
28	72	0.002	0.01	0.04	0.15	0.07	0.16	0.004	0.01	0.01	0.004	42.3	13.9
29	73^e	0.004	0.02	0.08	0.29	0.11	0.32	0.002	0.02	0.01	0.005	12.6	5.64
29	74	0.01	0.03	0.16	0.52	0.21	0.64	0.01	0.03	0.02	0.01	30.2	12.7
29	75	0.01	0.02	0.09	0.34	0.12	0.43	0.003	0.03	0.01	0.01	20.0	8.78
29	76	0.03	0.03	0.27	0.99	0.27	0.76	0.01	0.06	0.02	0.01	32.3	11.3
29	77	0.01	0.04	0.23	0.78	0.25	0.78	0.003	0.04	0.03	0.02	23.6	12.1
29	78	0.004	0.01	0.04	0.14	0.05	0.16	0.003	0.01	0.004	0.00	6.98	2.99
30	79^e	0.02	0.07	0.34	0.97	0.30	0.79	0.01	0.04	0.01	0.01	26.9	13.3
30	80	0.06	0.28	1.09	3.10	1.10	2.63	0.03	0.13	0.03	0.02	80.5	40.9
30	81	0.03	0.17	0.64	1.90	0.73	1.83	0.02	0.08	0.03	0.02	63.1	31.1
30	82	0.00	0.01	0.05	0.13	0.05	0.13	0.002	0.01	0.003	0.002	6.97	3.17
30	83	0.01	0.03	0.13	0.43	0.18	0.42	0.005	0.02	0.01	0.01	18.8	8.86
30	84	0.001	0.01	0.02	0.08	0.04	0.10	0.003	0.01	0.005	0.003	6.22	2.81
30	85	0.003	0.01	0.03	0.09	0.04	0.12	0.002	0.005	0.004	0.002	7.10	3.20
31	86	0.01	0.03	0.11	0.41	0.15	0.42	0.004	0.03	0.01	0.01	26.0	12.5
31	87	0.02	0.07	0.20	0.64	0.27	0.69	0.01	0.04	0.01	0.01	49.5	25.6
32	88^e	0.14	0.49	0.65	1.96	0.74	1.68	0.03	0.12	0.06	0.06	232	100
33	89	0.01	0.02	0.07	0.25	0.11	0.35	0.004	0.02	0.02	0.01	21.3	9.20
33	90	0.001	0.01	0.02	0.09	0.04	0.14	0.003	0.01	0.01	0.01	8.70	3.73
33	91	0.001	0.002	0.01	0.03	0.01	0.03	0.002	0.004	0.003	0.002	2.62	1.14
33	92^e	0.01	0.02	0.05	0.19^d	0.09	0.28	0.003	0.01	0.01	0.01	16.2	7.16
33	93	0.01	0.01	0.05	0.16	0.08	0.23	0.01	0.02	0.01	0.01	17.0	6.88
33	94	0.001	0.005	0.02	0.08	0.03	0.09	0.002	0.01	0.01	0.01	4.82	2.17

^{a} Coeluting with PCB-106 in the PRCs. Excluded.
^{b} Not included in sum 30 PCBs.
^{c} Included in sum 6 PCBs.
^{d} Blank contribution possible.
^{e} Average of two parallel PAS.
^{f} Lunder Halvorsen et al., 2021

Table SI-2.2b. Concentrations in air (pg/m^3) for all target OCPs at the individual sites. Concentrations below MDL set to ½ MDL (grey).

Country no.	Site no.	PeCB	HCB	a-HCH	β-HCH	g-HCH	o,p'-DDE	p,p'-DDE	o,p'-DDD	p,p'-DDD	o,p'-DDT	p,p'-DDT
1	1[a]	26.5	69.4	33.5[c]	3.04	7.27[c]	3.51	50.5[c]	0.77	0.33	8.68	6.94
2	2	46.0	82.0	19.9	1.40	54.2	1.90	139	0.63	0.55	12.1	20.0
2	3	22.1	70.1	9.08	0.36	13.3	0.19	3.12	0.04	0.03	1.28	1.31
3	4	22.2	71.3	11.3	3.41	58.6	0.27	11.9	0.26	0.23	2.78	5.76
3	5	20.9	57.9	10.3	1.75	40.1	0.29	11.5	0.26	0.16	1.98	3.22
4	6	31.1	81.6	17.3	0.39	19.9	0.77	23.8	0.18	0.10	5.12	5.41
5	7	50.4	82.8	10.6	1.65	5.99	1.36	12.2	0.22	0.15	4.49	4.82
6	8	28.8[a]	105[a]	16.5	1.58	26.1[b]	2.21	95.5	0.78	0.61	19.4	26.9
6	9	32.5	93.0	17.7	1.22	21.0	1.09	50.1	0.40	0.33	8.31	13.3
7	10	20.4	64.7	6.38	0.30	7.44	0.14	4.12	0.12	0.08	1.05	1.38
7	11	17.8	66.9	6.64	1.18	12.8	0.43	15.2	0.26	0.23	3.84	5.37
7	12	20.6	65.7	7.49	0.71	8.70	0.19	5.44	0.15	0.10	1.29	1.74
7	13	23.6	64.1	8.40	0.77	11.8	0.41	17.5	0.31	0.20	3.11	4.59
8	14	23.7	74.3	10.42	0.17	3.79	0.06	0.72	0.05	0.03	0.20	0.15
9	15[a]	27.1	92.2	8.50	0.33	2.61	0.05	0.64	0.03	0.01	0.30	0.21
9	16	22.3	73.2	6.58	0.37	3.13	0.05	0.88	0.04	0.02	0.41	0.40
9	17	21.9	65.9	7.66	1.45	4.10	0.12	3.03	0.11	0.10	0.81	0.85
9	18	21.9	67.8	7.89	0.28	3.71	0.13	2.05	0.12	0.10	0.53	0.70
9	19	25.2	80.2	7.97	0.38	2.29	0.06	0.57	0.03	0.01	0.24	0.24
9	20	26.9	79.9	7.76	0.28	4.01	0.07	2.81	0.10	0.17	2.36	6.83
9	21	40.0	87.7	8.07	0.42	4.93	0.07	1.44	0.05	0.03	0.59	0.59
10	22	27.0	78.5	14.2	1.78	38.4	0.15	3.71	0.05	0.02	1.03	1.23
10	23	13.9	38.1	8.18	1.44	33.0	0.12	4.75	0.06	0.04	0.89	1.48
10	24	17.2	47.5	14.1	3.43	49.1	0.10	3.39	0.05	0.03	0.81	1.18
10	25	26.6	74.6	14.1	1.02	26.3	0.20	2.14	0.05	0.02	1.14	1.03
10	26	21.3	55.0	14.6	2.12	33.4	0.16	2.36	0.19	0.15	2.06	2.58
10	27	19.1	60.4	11.1	2.78	35.3	0.11	3.18	0.06	0.04	0.64	1.07
10	28	33.9	58.5	16.0	2.28	37.1	0.19	3.35	0.06	0.04	1.37	1.66
11	29	22.2	51.9	37.9	7.55	21.6	4.80	32.5	0.81	0.41	10.9	10.1
12	30[a]	24.5	57.9	8.70	0.70	20.5	0.36	9.11	0.61	0.38	1.95	2.67
12	31	26.6	87.6	17.3	0.99	29.3	0.57	23.3	0.27	0.22	6.41	8.49
12	32	21.7	64.9	7.44	0.88	12.9	0.72	23.0	0.63	0.55	9.52	15.5
12	33	22.9	67.4	15.5	1.91	62.8	0.18	5.44	0.07	0.05	1.38	2.11
12	34	22.4	61.9	7.82	0.31	18.0	0.89	37.6	0.73	0.70	15.2	26.0
12	35[a]	20.2	67.2	7.93	0.33	24.5	0.38	17.8[c]	0.21	0.16	5.76	10.7
12	36	26.0	55.0	11.4	1.59	27.3	1.81	84.4	0.84	0.55	20.4	27.4
12	37	25.8	71.0	16.4	1.39	51.6	0.27	5.72	0.11	0.08	2.95	4.73
13	38	23.7	35.6	11.7	2.94	8.78	3.59	53.5	0.75	0.48	13.3	21.4
13	39	15.2	40.1	13.5	10.37	7.09	1.82	29.6	0.86	0.44	17.0	12.2
14	40	31.0	100	17.5	0.13	5.77	0.06	0.54	0.06	0.06	0.24	0.34
14	41	69.1	247	28.9	0.24	3.75	0.12	1.16	0.04	0.02	0.33	0.20
15	42	39.8	49.8	12.2	1.74	16.7	1.48	66.3	0.30	0.16	7.62	7.08
16	43	22.6	60.9	19.3	1.12	7.59	0.13	1.61	0.14	0.10	0.37	0.27
16	44	14.9	45.6	8.70	0.15	7.85	0.04	0.65	0.07	0.04	0.20	0.21
16	45	28.5	71.2	12.1	5.18	11.0	0.27	6.81	0.31	0.22	1.01	0.99
17	46	25.1	48.2	7.78	0.50	9.72	0.99	5.50	0.31	0.12	2.89	3.77
17	47	24.9	52.3	6.69	0.43	7.59	0.80	9.53	0.20	0.13	4.56	6.44
17	48	30.7	92.7	10.9	0.41	7.91	0.63	7.93	0.13	0.08	2.97	3.38
17	50	17.5	37.2	6.89	1.56	8.37	4.47	102	2.23	1.90	23.1	81.0
17	51	16.0	69.4	12.2	0.36	8.58	0.56	7.49	0.12	0.07	3.42	4.30

[a] Average of two parallel PAS.

[b] Matrix effects, possible interferring compounds

[c] Blank contribution possible (< 10%)

[d] Blank contribution possible (< 40%)

[e] Lunder Halvorsen et al., 2021

[f] Excluded due to unknown amount of internal standard, high recovery % and unexepectedly low concentrations.

n.a. = Not analyzed

Table SI-2.2b. (continued) Concentrations in air (pg/m^3) for all target OCPs at the individual sites. Concentrations below MDL set to ½ MDL (grey).

Country no.	Site no.	PeCB	HCB	a-HCH	β-HCH	g-HCH	o,p'-DDE	p,p'-DDE	o,p'-DDD	p,p'-DDD	o,p'-DDT	p,p'-DDT
18	52	38.8	413	10.3	1.05	5.28	0.29	6.79	0.34	0.16	4.30	3.15
18	53[a]	42.8	97.8	11.7	0.65	4.98	0.21	3.80[c]	0.09	0.06	1.44	1.29
19	54	17.1	58.3	13.2	4.26	12.5	0.88	29.0	1.67	1.23	8.06	9.87
19	55	26.5	74.1	8.44	0.77	4.17	0.16	3.23	0.08	0.05	1.22	1.14
20	56	19.7	44.0	10.9	4.26	13.2[b]	1.38	15.0	1.14	0.80	8.83	16.3
21	57	24.6	50.8	47.4	8.74	23.0	5.19	126	1.48	0.67	25.1	21.5
22	58	50.6	110	17.0	1.19	39.0	0.93	36.2	0.59	0.59	5.20	9.81
22	59	35.1	77.3	12.7	1.30	42.3	0.41	13.6	0.34	0.20	4.60	9.12
22	60	28.0	76.3	15.2	0.63	34.5	0.85	30.5	0.94	0.68	3.96	6.39
23	97[a,e]	21.8	85.0	0.30	7.13	15.9	1.91	0.07	0.11	0.73	0.92	3.81
23	98[e]	18.6	82.6	7.13	0.22	2.03	0.04	0.29	0.02	0.08	0.16	0.13
23	99[e]	17.8	83.0	8.22	0.31	6.49	0.05	0.54	0.02	0.11	0.31	0.24
23	100[e]	23.8	63.6	4.95	0.17	3.56	0.03	0.81	0.01	0.06	0.24	0.27
23	101[e]	21.8	74.9	7.53	0.16	1.82	0.03	0.26	0.01	0.06	0.15	0.10
23	102[e]	22.7	72.8	12.7	0.19	4.32	0.08	0.74	0.06	0.02	0.30	0.18
23	96	37.5	130	12.3	0.14	1.73	0.02	0.14	0.01	0.05	0.07	0.02
24	61	19.8	62.6	11.3	1.18	10.1	0.51	19.1	0.45	0.31	6.23	7.19
25	62	14.2	31.8	3.62	0.26	6.89	0.09	1.67	0.05	0.04	0.38	0.57
25	63	16.0	27.8	3.55	0.22	19.5	0.19	3.62	0.09	0.07	1.20	2.00
26	64	26.1	54.6	5.58	0.41	1.65	0.04	0.41	0.03	0.02	0.33	0.34
26	65	27.3	64.2	9.40	0.43	3.47	0.11	1.91	0.05	0.02	0.90	0.69
26	66	24.9	60.7	35.2	4.70	7.04	0.64	10.3	0.54	0.39	3.15	5.17
26	67	27.3	62.2	22.7	4.21	4.64	0.72	7.32	0.21	0.10	3.36	1.84
26	68	32.9	73.7	23.6	2.11	6.11	0.82	13.8	0.23	0.09	4.42	3.13
26	69	32.2	66.6	15.9	1.48	5.54	0.49	8.91	0.25	0.16	3.49	3.31
26	95	50.8	99.3	19.3	1.17	7.63	0.27	3.57	0.12	0.08	1.83	1.75
27	70	25.0	56.8	20.1	1.20	20.0	0.88	28.3	0.26	0.12	7.54	7.06
27	71	29.4	66.0	17.6	1.07	12.2	1.04	34.9	0.59	0.66	6.88	6.93
28	72	74.2	100	8.91	0.46	14.5	0.27	8.21	0.06	0.04	1.38	1.83
29	73[a]	34.7[d]	73.8	5.71[c]	0.66	6.84	0.57	8.03	0.06	0.03	1.06	1.48
29	74	30.2	73.3	8.50	4.83	18.9	0.09	1.06	0.07	0.02	0.67	0.65
29	75	36.2	71.4	8.73	0.73	14.4	0.47	5.92	0.21	0.15	1.29	1.27
29	76	23.4	47.2	7.02	0.89	109	0.40	7.92	0.04	0.02	0.69	0.71
29	77	19.1	46.3	6.16	1.45	18.5	0.46	8.21	0.32	0.24	2.16	3.09
29	78	20.7	42.5	5.81	0.30	3.80	0.36	9.17	0.09	0.06	0.82	1.70
30	79[a]	18.4	48.1	7.75	1.05	9.31	0.30	9.96	0.23	0.15	2.55	3.30
30	80	20.9	74.8	5.33	0.34	3.48	0.06	1.69	0.04	0.03	0.44	0.49
30	81	18.8	61.3	6.00	0.26	8.51	0.23	9.12	0.15	0.10	2.55	3.39
30	82	16.3	45.0	4.08	0.21	6.62	0.03	0.41	0.03	0.02	0.43	0.45
30	83	12.9	45.1	8.03	0.20	2.49	0.05	0.56	0.02	0.01	0.28	0.19
30	84	21.7	87.8	7.89	0.34	2.17	0.03	0.33	0.01	0.01	0.19	0.12
30	85	25.9	70.3	6.00	0.28	2.26	0.05	0.53	0.02	0.01	0.30	0.27
31	86	26.4	99	12.5	0.23	8.7	0.18	1.50	0.03	0.02	0.94	0.98
31	87	26.1	50.1	8.68	0.62	17.1	0.23	5.56	0.10	0.12	2.41	5.34
32	88[a]	26.0	68.0	46.0	60.8	23.9	10.0	183[b,c]	12.1	12.4	37.2	32.1
33	89	16.4	41.1	6.65	0.18	31.3	0.12	6.63	0.10	0.66	0.84	1.14
33	90	19.4	53.5	7.14	0.17	12.7	0.07	1.72	0.12	0.06	0.44	0.44
33	91	20.0	47.9	3.88	0.25	10.8	0.01	0.17	0.03	0.01	0.08	0.07
33	92[a]	25.1	60.8	7.14	0.28	15.8	0.11	2.24	0.07	0.04	0.62	0.65
33	93	38.1	59.3	6.60	0.28	25.9	0.17	4.95	0.17	0.10	0.84	0.95
33	94	19.5	63.5	7.69	0.62	4.98	0.04	0.50	0.04	0.02	0.17	0.14

[a] Average of two parallel PAS.

[b] Matrix effects, possible interferring compounds

[c] Blank contribution possible (< 10%)

[d] Blank contribution possible (< 40%)

[e] Lunder Halvorsen et al., 2021

[f] Excluded due to unknown amount of internal standard, high recovery % and unexepectedly low concentrations.

n.a. = Not analyzed

Table SI-2.2b. (continued) Concentrations in air (pg/m^3) for all target OCPs at the individual sites. Concentrations below MDL set to ½ MDL (grey).

Country no.	Site no.	Dieldrin	Aldrin	Isodrin	Endrin	Heptachlor-exo-epoxide	Heptachlor-endo-epoxide	trans-Chlordane	cis-Chlordane	Oxy-chlordane
1	1[a]	0.96	0.09	0.59	0.16	0.94	0.13	0.07	0.67	0.44
2	2	15.3	0.10	0.66	0.18	8.02	0.14	0.70	2.55	2.26
2	3	3.44	0.11	0.75	0.21	2.57	0.17	0.29	1.07	0.81
3	4	30.1	0.09	0.62	0.17	62.6	0.13	16.2	7.38	8.83
3	5	18.3	0.09	0.61	0.17	13.9	0.13	2.19	2.34	3.02
4	6	6.80	0.07	0.48	0.13	3.47	0.11	0.38	1.47	1.10
5	7	2.71	0.14	0.95	0.27	1.87	0.20	0.57	1.29	0.69
6	8	4.35	0.11	0.76	0.21	3.03	0.17	0.25	1.08	0.93
6	9	5.61	0.10	0.67	0.19	3.65	0.15	0.32	1.32	1.11
7	10	6.72	0.09	0.64	0.18	2.07	0.14	0.30	1.11	0.95
7	11	6.98	0.11	0.77	0.21	2.13	0.17	0.29	0.90	0.76
7	12	8.56	0.09	0.64	0.18	2.34	0.14	0.29	1.28	0.95
7	13	n.a.	n.a.	n.a.	n.a.	n.a.	n.a.	n.a.	n.a.	n.a.
8	14	4.77	0.06	0.38	0.11	2.12	0.08	0.30	1.65	1.10
9	15[a]	2.11	0.10	0.69	0.19	1.40	0.16	0.15	0.88	0.76
9	16	1.69	0.11	0.78	0.22	1.03	0.18	0.13	0.62	0.57
9	17	4.41	0.08	0.53	0.15	1.68	0.12	0.23	1.15	0.89
9	18	2.94	0.09	0.61	0.17	1.42	0.14	0.17	0.86	0.71
9	19	1.36	0.11	0.78	0.22	1.01	0.18	0.14	0.63	0.63
9	20	2.57	0.09	0.60	0.17	1.41	0.13	0.18	0.92	0.74
9	21	4.33	0.13	0.86	0.24	1.23	0.20	0.14	0.74	0.61
10	22	1.22	0.13	0.89	0.25	1.00	0.20	0.09	0.24	0.29
10	23	2.18	0.10	0.66	0.19	1.12	0.15	0.14	0.21	0.26
10	24	1.49	0.12	0.79	0.22	0.76	0.17	0.10	0.21	0.20
10	25	4.62	0.25	0.84	0.16	2.63	0.20	0.33	1.41	0.94
10	26	1.79	0.07	0.46	0.15	1.29	0.11	0.17	0.41	0.37
10	27	7.18	0.13	0.85	0.24	9.94	0.19	0.82	1.35	2.23
10	28	1.01	0.09	0.61	0.17	0.62	0.13	0.07	0.19	0.16
11	29	0.97	0.11	0.75	0.21	1.14	0.17	0.14	0.69	0.51
12	30[a]	12.7	0.06	0.40	0.11	3.30	0.08	0.46	1.63	1.23
12	31	5.72	0.10	0.70	0.19	5.14	0.15	0.49	1.44	1.44
12	32	4.47	0.09	0.63	0.18	1.90	0.14	0.22	0.82	0.75
12	33	1.13	0.12	0.61	0.22	0.79	0.17	0.08	0.26	0.23
12	34	3.82	0.10	0.68	0.19	2.42	0.15	0.24	0.77	0.79
12	35[a]	7.70	0.10	0.67	0.19	3.52	0.15	0.38	0.87	0.90
12	36	4.66	0.07	0.45	0.12	3.63	0.09	0.32	1.02	1.04
12	37	7.09	0.07	0.44	0.12	4.64	0.09	0.55	1.86	1.43
13	38	5.16	0.07	0.50	0.14	2.89	0.10	1.56	1.24	0.65
13	39	9.33	0.08	0.57	0.16	5.34	0.11	0.83	2.62	1.55
14	40	8.19	0.04	0.29	0.08	1.98	0.06	1.06	1.71	1.23
14	41	5.32	0.07	0.47	0.13	2.65	0.11	0.63	2.35	1.60
15	42	6.13	0.11	0.73	0.20	1.83	0.16	0.20	0.74	0.65
16	43	13.5	0.07	0.49	0.14	5.31	0.11	1.24	4.54	2.43
16	44	6.43	0.05	0.35	0.09	1.91	0.07	0.29	1.55	0.93
16	45	19.0	0.08	0.52	0.14	6.46	0.11	0.92	4.41	2.83
17	46	3.90	0.11	0.75	0.21	2.87	0.16	0.62	0.91	0.87
17	47	4.28	0.11	0.75	0.21	2.66	0.16	1.45	1.90	0.81
17	48	4.63	0.13	0.90	0.25	3.58	0.19	0.41	1.70	0.93
17	50	10.5	0.10	0.66	0.18	6.13	0.14	1.35	3.09	1.81
17	51	5.68	0.07	0.46	0.13	3.90	0.10	0.53	2.19	1.37

[a] Average of two parallel PAS.
[b] Matrix effects, possible interferring compounds
[c] Blank contribution possible (< 10%)
[d] Blank contribution possible (< 40%)
[e] Lunder Halvorsen et al., 2021
[f] Excluded due to unknown amount of internal standard, high recovery % and unexepectedly low concentrations.
n.a. = Not analyzed

Table SI-2.2b. (continued) Concentrations in air (pg/m^3) for all target OCPs at the individual sites. Concentrations below MDL set to ½ MDL (grey).

Country no.	Site no.	Dieldrin	Aldrin	Isodrin	Endrin	Heptachlor-exo-epoxide	Heptachlor-endo-epoxide	trans-Chlordane	cis-Chlordane	Oxy-chlordane
18	52	2.71	0.07	0.48	0.13	1.28	0.10	0.14	0.72	0.62
18	53[a]	2.31	0.08	0.55	0.15	1.35	0.13	0.14	0.78	0.71
19	54	12.5	0.09	0.58	0.16	4.30	0.13	0.52	2.69	1.99
19	55	1.32	0.11	0.74	0.20	0.87	0.17	0.08	0.43	0.47
20	56	20.2	0.10	0.68	2.04	11.8	0.14	1.06	4.75	2.91
21	57	2.98	0.09	0.60	0.17	1.90	0.13	0.42	0.74	0.60
22	58	26.1	0.08	0.52	0.14	11.2	0.11	1.56	3.01	2.78
22	59	19.2	0.07	0.44	0.12	18.4	0.09	3.08	2.35	3.70
22	60	37.2	0.08	0.54	1.67	11.6	0.12	2.46	4.31	3.14
23	97[a,e]	5.05	0.61	1.47	0.26	2.39	0.30	0.38	1.26	1.00
23	98[e]	1.91	0.46	1.09	0.19	1.38	0.22	0.33	1.18	1.00
23	99[e]	2.82	0.64	1.54	0.27	1.98	0.31	0.23	1.02	0.86
23	100[e]	f	f	f	f	f	f	f	f	f
23	101[e]	1.63	0.35	0.84	0.14	1.30	0.17	0.12	0.74	0.71
23	102[e]	6.57	0.15	0.34	0.45	3.57	0.06	0.44	2.40	1.79
23	96	1.34	0.29	1.01	1.15	1.43	1.44	0.17	1.03	0.94
24	61	4.00	0.08	0.54	0.15	1.95	0.12	0.17	1.00	0.95
25	62	2.97	0.09	0.61	0.17	1.15	0.13	0.36	1.00	0.47
25	63	4.62	0.08	0.53	0.65	0.87	0.11	0.55	1.00	0.40
26	64	0.22	0.09	0.60	0.16	0.40	0.13	0.03	0.25	0.20
26	65	0.81	0.09	0.62	0.17	0.84	0.68	0.05	0.38	0.38
26	66	1.02	0.13	0.87	0.24	1.04	0.19	0.01	0.74	0.47
26	67	0.92	0.14	0.95	0.27	1.11	0.21	0.10	0.55	0.55
26	68	0.83	0.09	0.64	0.18	0.64	0.14	0.04	0.32	0.28
26	69	0.83	0.09	0.63	0.18	0.76	0.14	0.07	0.42	0.40
26	95	1.27	0.09	0.61	0.17	1.08	0.14	0.11	0.63	0.53
27	70	7.10	0.03	0.18	0.05	3.58	0.04	0.33	1.56	1.27
27	71	4.33	0.09	0.62	0.17	2.37	0.13	0.21	1.08	0.92
28	72	2.42	0.14	0.96	0.27	1.58	0.21	0.14	0.62	0.55
29	73[a]	2.86	0.08	0.49	0.14	2.92	0.11	0.42	0.95	0.60
29	74	6.06	0.10	0.71	0.20	2.71	0.16	0.45	1.41	1.01
29	75	0.71	0.11	0.76	0.21	0.50	0.17	0.08	0.20	0.09
29	76	2.28	0.09	0.58	0.16	1.60	0.12	0.32	0.84	0.44
29	77	7.40	0.10	0.68	0.19	3.73	0.15	0.60	1.55	1.01
29	78	1.66	0.10	0.70	0.19	1.04	0.15	0.18	0.70	0.40
30	79[a]	8.24	0.06	0.41	0.11	2.78	0.09	0.34	1.40	1.06
30	80	1.99	0.11	0.73	0.20	0.83	0.16	0.11	0.54	0.43
30	81	4.16	0.09	0.58	0.16	1.52	0.13	0.18	0.73	0.66
30	82	0.63	0.07	0.46	0.13	0.55	0.10	0.10	0.34	0.30
30	83	2.13	0.06	0.43	0.12	1.40	0.10	0.16	0.96	0.74
30	84	2.21	0.10	0.71	0.20	1.41	0.16	0.14	0.98	0.78
30	85	1.70	0.09	0.60	0.17	1.02	0.13	0.11	0.62	0.58
31	86	2.65	0.07	0.49	0.14	2.06	0.11	0.32	1.58	0.88
31	87	5.74	0.07	0.46	0.13	2.04	0.10	0.42	0.87	0.68
32	88[a]	7.71	0.10	0.66	0.18	4.45	0.14	1.04	1.92	1.59
33	89	19.7	0.06	0.43	0.12	2.66	0.09	0.41	1.17	0.92
33	90	8.71	0.06	0.40	0.11	1.81	0.09	0.39	1.24	0.85
33	91	1.96	0.08	0.55	0.15	0.57	0.12	0.08	0.39	0.32
33	92[a]	11.1	0.09	0.62	0.17	2.79	0.14	0.34	1.16	0.91
33	93	18.7	0.09	0.60	0.17	2.13	0.13	0.33	1.13	0.91
33	94	7.00	0.07	0.48	0.13	1.48	0.11	0.29	1.26	0.75

[a] Average of two parallel PAS.

[b] Matrix effects, possible interferring compounds

[c] Blank contribution possible (< 10%)

[d] Blank contribution possible (< 40%)

[e] Lunder Halvorsen et al., 2021

[f] Excluded due to unknown amount of internal standard, high recovery % and unexepectedly low concentrations.

n.a. = Not analyzed

Table SI-2.2b. (continued) Concentrations in air (pg/m^3) for all target OCPs at the individual sites. Concentrations below MDL set to ½ MDL (grey).

Country no.	Site no.	Chlordene	Heptachlor	trans-Nonachlor	cis-Nonachlor	Endosulfan-I	Endosulfan-II	Endosulfan-sulphate	Trifluralin	Mirex
1	1[a]	0.16	0.32	0.46	0.05	21.0	3.74	0.72	0.06	0.08
2	2	0.17	0.36	2.89	0.42	12.0	2.73	1.02	1.71	0.42
2	3	0.21	0.38	1.07	0.13	3.82	0.49	0.71	0.07	0.11
3	4	0.17	20.7	10.4	0.84	12.4	2.49	0.87	4.90	0.20
3	5	0.16	1.36	3.64	0.36	8.15	1.51	0.44	1.82	0.08
4	6	0.13	0.25	1.39	0.21	5.64	0.55	0.42	0.05	0.24
5	7	0.24	0.52	0.94	0.18	8.70	1.92	0.47	1.09	0.12
6	8	0.21	0.39	1.07	0.15	3.21	0.31	0.17	0.89	0.25
6	9	0.18	0.35	1.26	0.18	3.99	0.37	0.52	4.04	0.09
7	10	0.18	0.33	1.09	0.17	1.63	0.11	0.15	3.16	0.09
7	11	0.21	0.39	0.97	0.11	1.46	0.13	0.18	0.63	0.11
7	12	0.17	0.33	1.14	0.17	1.65	0.11	0.14	0.29	0.09
7	13	n.a.	n.a.	n.a.	n.a.	n.a.	n.a.	n.a.	n.a.	n.a.
8	14	0.10	0.21	1.24	0.21	1.61	0.06	0.08	0.04	0.15
9	15[a]	0.20	0.34	0.71	0.13	1.44	0.12	0.17	0.06	0.10
9	16	0.22	0.39	0.51	0.08	1.08	0.14	0.19	0.15	0.11
9	17	0.14	0.29	0.94	0.16	1.20	0.09	0.12	0.05	0.14
9	18	0.17	0.32	0.69	0.11	1.25	0.10	0.14	0.65	0.08
9	19	0.22	0.38	0.51	0.08	1.01	0.14	0.19	0.07	0.11
9	20	0.16	0.31	0.74	0.14	1.17	0.10	0.14	0.06	0.08
9	21	0.25	0.42	0.58	0.10	1.13	0.15	0.21	0.27	0.13
10	22	0.25	0.45	0.33	0.03	0.84	0.15	0.21	0.08	0.12
10	23	0.18	0.36	0.29	0.03	0.76	0.11	0.14	0.49	0.09
10	24	0.22	0.41	0.23	0.03	0.80	0.13	0.18	1.00	0.11
10	25	0.32	0.79	1.22	0.17	5.52	0.65	0.43	0.06	0.20
10	26	0.12	0.26	0.40	0.05	0.43	0.07	0.10	0.52	0.06
10	27	0.24	0.43	2.88	0.24	3.87	0.63	0.20	0.77	0.12
10	28	0.16	0.33	0.22	0.03	1.05	0.21	0.13	0.06	0.08
11	29[a]	0.20	0.39	0.52	0.06	16.1	2.56	1.43	0.07	0.10
12	30[a]	0.10	0.24	1.51	0.24	2.50	0.27	0.08	0.92	0.18
12	31	0.19	0.36	1.68	0.20	4.15	0.44	0.53	0.46	0.09
12	32	0.17	0.34	0.74	0.11	1.57	0.10	0.14	0.21	0.08
12	33	0.14	0.31	0.30	0.04	0.98	0.08	0.11	0.05	0.10
12	34	0.18	0.36	0.80	0.10	2.05	0.11	0.15	0.07	0.09
12	35[a]	0.18	0.35	0.94	0.12	2.43	0.28	0.15	0.27	0.09
12	36	0.11	0.27	1.17	0.17	3.11	0.37	0.10	0.77	0.21
12	37	0.11	0.25	1.99	0.29	7.11	1.18	0.70	0.12	0.26
13	38	0.12	0.32	0.93	0.12	8.02	1.76	0.37	11.0	0.11
13	39	0.14	0.35	2.02	0.44	6.67	1.13	0.12	0.06	0.56
14	40	0.08	2.53	1.32	0.20	1.74	0.05	0.06	0.03	0.11
14	41	0.14	0.21	1.81	0.32	3.19	0.09	0.12	0.04	0.20
15	42	0.19	0.39	0.65	0.10	3.64	0.58	0.41	4.01	0.10
16	43	0.13	1.40	3.34	0.57	3.85	0.08	0.11	0.31	0.40
16	44	0.09	0.20	1.15	0.21	1.61	0.05	0.07	0.28	0.16
16	45	0.14	0.28	3.76	0.56	3.69	0.09	0.12	0.83	0.50
17	46	0.20	0.39	1.06	0.12	5.07	0.71	0.17	0.47	0.10
17	47	0.19	0.41	1.47	0.22	6.36	1.26	0.16	5.31	0.09
17	48	0.24	0.47	1.41	0.22	8.61	1.23	0.60	0.09	0.12
17	50	0.16	0.38	2.94	0.60	23.82	9.93	1.51	0.40	0.36
17	51	0.12	0.25	1.76	0.29	10.81	1.52	0.45	0.05	0.34

[a] Average of two parallel PAS.
[b] Matrix effects, possible interferring compounds
[c] Blank contribution possible (< 10%)
[d] Blank contribution possible (< 40%)
[e] Lunder Halvorsen et al., 2021
[f] Excluded due to unknown amount of internal standard, high recovery % and unexepectedly low concentrations.
n.a. = Not analyzed

Table SI-2.2b. (continued) Concentrations in air (pg/m^3) for all target OCPs at the individual sites. Concentrations below MDL set to ½ MDL (grey).

Country no.	Site no.	Chlordene	Heptachlor	trans-Nonachlor	cis-Nonachlor	Endosulfan-I	Endosulfan-II	Endosulfan-sulphate	Trifluralin	Mirex
18	52	0.13	0.26	0.60	0.09	1.23	0.08	0.12	0.33	0.06
18	53[a]	0.15	0.29	0.64	0.10	1.41	0.09	0.16	0.34	0.08
19	54	0.16	0.31	2.38	0.47	3.87	0.37	0.16	0.22	0.50
19	55	0.21	0.37	0.39	0.05	0.87	0.13	0.18	0.27	0.11
20	56	0.17	0.38	4.43	0.77	12.2	1.95	0.75	0.44	0.69
21	57	0.15	0.34	0.71	0.11	1.97	0.09	0.13	48.0	0.07
22	58	0.14	0.28	3.64	0.43	7.84	1.04	n.a	1.76	1.23
22	59	0.11	1.45	3.95	0.33	9.58	2.19	1.55	0.89	0.05
22	60	0.14	1.09	4.57	0.63	8.44	1.44	0.40	1.86	0.41
23	97[a,e]	0.37	0.49	1.10	0.14	3.72	0.26	0.19	0.13	0.21
23	98[e]	0.27	0.37	0.80	0.13	2.80	0.19	0.14	0.10	0.15
23	99[e]	0.39	0.51	0.92	0.13	4.57	0.66	0.20	0.14	0.22
23	100[e]	f	f	f	f	f	f	f	f	f
23	101[e]	0.20	0.29	0.63	0.13	2.75	0.14	0.30	0.08	0.11
23	102[e]	0.07	0.15	1.89	0.35	6.36	0.16	0.04	0.04	0.27
23	96	0.18	0.24	0.75	0.16	3.51	0.17	0.13	0.06	0.10
24	61	0.14	0.29	0.89	0.15	3.99	0.94	0.97	0.52	0.07
25	62	0.16	0.34	0.80	0.12	4.34	1.55	0.13	0.06	0.07
25	63	0.13	0.31	0.77	0.13	5.73	1.01	0.11	0.06	0.06
26	64	0.16	0.31	0.22	0.01	0.41	0.10	0.14	0.06	0.08
26	65	0.17	0.32	0.31	0.01	0.67	0.10	0.15	0.06	0.09
26	66	0.23	0.46	0.51	0.09	1.25	0.14	0.19	0.69	0.11
26	67	0.26	0.49	0.45	0.01	3.06	0.45	0.22	0.20	0.13
26	68	0.17	0.34	0.27	0.01	0.66	0.11	0.14	4.66	0.09
26	69	0.17	0.33	0.36	0.05	1.18	0.10	0.14	0.24	0.08
26	95	0.17	0.31	0.48	0.07	1.02	0.11	0.14	0.06	0.09
27	70	0.04	0.12	1.38	0.21	6.86	0.68	0.61	0.12	0.22
27	71	0.17	0.33	0.90	0.14	3.54	0.51	0.14	0.21	0.08
28	72	0.27	0.48	0.54	0.08	82.1	57.5	3.38	0.09	0.13
29	73[a]	0.13	0.27	0.98	0.12	8.60	1.59	0.42	0.26	0.07
29	74	0.20	0.37	1.18	0.16	2.01	0.12	0.16	0.07	0.10
29	75	0.21	0.40	0.19	0.02	0.83	0.13	0.17	0.07	0.10
29	76	0.15	0.31	0.66	0.10	3.05	0.39	0.13	0.06	0.07
29	77	0.18	0.37	1.45	0.23	3.24	0.39	0.15	0.07	0.09
29	78	0.18	0.39	0.51	0.09	3.00	0.44	0.14	0.07	0.09
30	79[a]	0.10	0.24	1.27	0.20	1.88	0.15	0.09	0.24	0.05
30	80	0.20	0.37	0.43	0.06	0.70	0.12	0.17	0.07	0.10
30	81	0.16	0.31	0.68	0.10	1.34	0.09	0.13	0.12	0.08
30	82	0.13	0.54	0.26	0.04	0.59	0.08	0.11	0.11	0.06
30	83	0.12	0.23	0.72	0.13	1.44	0.07	0.10	0.04	0.06
30	84	0.20	0.35	0.76	0.14	1.43	0.13	0.17	0.07	0.10
30	85	0.17	0.30	0.51	0.08	0.98	0.10	0.14	0.06	0.08
31	86	0.14	0.25	1.22	0.19	4.48	0.23	0.24	0.05	0.23
31	87	0.12	0.26	1.07	0.12	4.01	0.91	0.28	0.44	0.06
32	88[a]	0.17	0.37	1.78	0.29	3.97	0.17	0.14	4.84	0.36
33	89	0.11	0.25	1.24	0.16	1.75	0.07	0.09	1.58	0.05
33	90	0.10	0.23	0.94	0.15	1.42	0.06	0.13	0.47	0.05
33	91	0.15	0.29	0.31	0.01	0.57	0.09	0.13	0.15	0.08
33	92[a]	0.17	0.32	1.11	0.16	1.81	0.10	0.17	1.30	0.08
33	93	0.16	0.32	1.04	0.15	1.66	0.10	0.17	7.33	0.08
33	94	0.13	0.25	0.94	0.17	1.59	0.08	0.11	0.05	0.06

[a] Average of two parallel PAS.

[b] Matrix effects, possible interferring compounds

[c] Blank contribution possible (< 10%)

[d] Blank contribution possible (< 40%)

[e] Lunder Halvorsen et al., 2021

[f] Excluded due to unknown amount of internal standard, high recovery % and unexepectedly low concentrations.

n.a. = Not analyzed

Table SI-2.3. Median concentrations (pg/m^3) for the four European regions (Figure SI-1.1)

	North	South	Central-East	West	All
∑$_6$PCBs	6.5	13	18	18	13
HCB	74	47	66	62	67
α-HCH	7.9	7.8	18	11	9.0
γ-HCH	4.1	8.6	12	27	10
∑$_6$DDXs	2.3	15	35	9.2	10
∑$_4$CDs	2.0	3.2	1.4	2.8	2.5
Dieldrin	2.8	4.6	2.4	7.0	4.3
HepX	1.4	2.9	1.6	2.6	2.0
OxyCD	0.8	0.8	0.5	0.9	0.8
Endo I	1.4	6.4	3.5	2.5	2.8

Table SI-2.4. Correlation analysis of log-transformed concentrations of the detected PCBs and OCPs, Latitude, Longitude and log-transformed estimations of population density within 50 km of the sampling site (ref. SI 1.4.2). The Pearson correlation coefficient (r) is stated when the correlation is significant (p-value < 0.05).

	Latitude	Longitude	∑$_6$PCBs	HCB	α-HCH	γ-HCH	∑$_6$DDXs	∑$_4$CDs	Dieldrin	HepX	OxyCD	Endo I
Longitude												
∑$_6$PCBs	-0.46[a]											
HCB	0.44[a]											
α-HCH		0.30	0.51[a]	0.29								
γ-HCH	-0.55[a]	-0.30	0.54[a]	-0.20	0.28							
∑$_6$DDXs	-0.61[a]	0.27	0.75[a]		0.46[a]	0.56[a]						
∑$_4$CDs		-0.30	0.33[a]			0.25	0.29					
Dieldrin	-0.45[a]	0.33[a]				0.43[a]	0.33[a]	0.88[a]				
HepX		-0.24	0.42[a]		0.20	0.45[a]	0.43[a]	0.93[a]	0.86[a]			
OxyCD		0.29					0.25	0.95[a]	0.84[a]	0.93[a]		
Endo I	-0.44[a]	0.44[a]			0.25	0.27	0.46[a]	0.65[a]	0.48[a]	0.64[a]	0.58[a]	
Pop.dens	-0.51[a]	-0.30	0.60[a]			0.57[a]	0.54[a]	0.36[a]	0.52[a]	0.42[a]	0.27	0.32

[a] Significance level of more than 99.9% (p<0.001)

Table SI-2.5: Comparison of median concentrations at 73 common European sites in 2006 (Halse et al., 2011) and 2016 (this study).

	Sum 6 PCB	HCB	a-HCH	g-HCH	Sum 4 DDX	Sum 4 CD
p-value[1]	0.003	< 0.001	< 0.001	< 0.001	0.047	0.014
Difference (median)	-28 %	56 %	-59 %	-48 %	-12 %	-23 %
Min. Difference (region)	0 % (south/west)	44 % (west)	-22 % (north)	-47 % (north)	43 % (north)	-8 % (east)
Max. Difference (region)	-48 % (north)	77 % (south)	-69 % (east)	-76 % (south)	-45 % (west)	-27 % (west)

[1]Two-sample Wilcoxon, paired, 1-sided. P-value < 0.05 implies that the difference is significant.

Table SI-2.6: Measured concentrations of HCB in 2016 (this study) divided by measured concentrations of HCB in 2006 (Halse et al., 2011) at European sites for which also AAS-data for both years are available (n=3), and a comparison to the same ratio obtained from the AAS-data.

	PAS 2016/2006	AAS 2016/2006
Kosetice (site 8, Czech Rep.)	1.0	0.4
Zeppelin (site 96, Spitsbergen)	1.3	1.1
Birkenes (site 97, Norway)	1.8	0.7

Table SI-2.7. The estimated population density within radius 50 km (SI 1.4.2) and results from predictions by GLEMOS (GLEMOS, 2020) and FLEXPART (FLEXPART, 2022), at the individual sites.

Site no.	Country:	Sampling site:	Population density (per km²)	PCB153 GLEMOS (pg/m³)	Primary national (%)	Primary EMEP (%)	Primary outside EMEP (%)	Secondary (%)	PCB153 FLEXPART (pg/m³)
1	Armenia	Amberd	502	0.63	31	3	3	63	0.45
2	Austria	Illmitz	223	1.5	5	11	1	83	1.8
3	Austria	Vorhegg	60	1.0	1	16	1	82	1.7
4	Belgium	Houtem	526	8.7	3	58	0	39	2.7
5	Belgium	Koksijde	565	7.3	4	53	0	43	2.7
6	Croatia	Zavizan	32	0.80	1	8	2	90	1.1
7	Cyprus	Ayia Marina	195	0.39	9	5	2	84	0.24
8	Czech Rep	Kosetice	121	1.7	7	6	1	87	1.8
9	Czech Rep	Svratouch	187	1.7	8	5	1	86	2.3
10	Denmark	Tange	226	0.72	12	8	2	78	0.69
11	Denmark	Keldsnor	168	1.2	2	20	1	76	1.16
12	Denmark	Anholt	19	0.79	7	12	2	79	0.54
13	Denmark	Risoe (Lille Valby)	958[a]	1.2	20	8	1	71	0.75
14	Faroe Islands	Norðuri á Fossum	17	[b]	[b]	[b]	[b]	[b]	0.04
15	Finland	Pallas	3	0.20	11	2	2	86	0.20
16	Finland	Ähtäri I	18	0.37	4	2	2	93	0.30
17	Finland	Utö	38	0.46	5	8	2	85	0.28
18	Finland	Virolahti II	77	0.53	1	4	1	95	0.36
19	Finland	Oulanka	6	0.15	1	3	2	93	0.21
20	Finland	Hailuoto II	84	0.41	14	1	1	84	0.24
21	Finland	Hyytiälä	131	0.38	5	2	1	92	0.29
22	France	Donon	199	4.9	22	8	0	70	3.8
23	France	Peyrusse Vieille	70	1.8	24	2	1	72	2.0
24	France	La Tardière	142	1.8	26	2	2	70	2.2
25	France	Le Casset	32	0.98	18	10	2	70	2.0
26	France	Porspoder	429	0.56	34	3	6	58	0.73
27	France	Revin	126	12	50	4	0	46	4.0
28	France	Saint-Nazaire-Le-Dése	64	2.4	16	2	1	82	3.1
29	Georgia	Abastumani	48	0.45	11	2	1	86	0.31
30	Germany	Westerland	117	1.4	8	12	2	79	1.0
31	Germany	Schmücke	259	3.0	15	3	0	81	3.2
32	Germany	Zingst	176	1.1	18	6	1	75	1.2
33	Germany	Schauinsland	469	4.2	18	10	0	72	3.9
34	Germany	Neuglobsow	94	1.7	20	3	1	77	2.3
35	Germany	Waldhof	150	2.3	18	3	1	78	3.3
36	Germany	Melpitz	252	3.1	23	3	0	74	3.4
37	Germany	Hohenpeissenberg	288	2.9	15	3	0	81	3.2
38	Greece	Aliartos	77	0.51	19	5	2	74	0.49
39	Greece	Finokalia (Crete)	104	0.41	3	10	3	84	0.39
40	Greenland	Nuuk	1194[a]	[b]	[b]	[b]	[b]	[b]	
41	Greenland	Station Nord	[b]	0.02	0	1	93	5	0.02
42	Hungary	K-puszta	130	1.6	29	5	1	65	1.4
43	Ireland	Mace Head	31	0.15	4	7	16	73	0.24
44	Ireland	Malin Head	218	0.28	5	15	6	74	0.14
45	Ireland	Carnsore Point	128	0.41	6	20	6	68	0.41
46	Italy	Ispra	731[a]	8.5	48	2	0	50	3.8
47	Italy	Montelibretti	988[a]	4.0	53	2	1	45	3.3
48	Italy	Longobucco	219	1.2	25	3	1	71	1.8
50	Italy	Capo Granitola (Sicily)	278	1.4	34	6	2	58	1.7
51	Italy	Monte Curcio	243	1.5	34	3	1	62	1.8

[a] Suburban sites with a city within 50 km (Figure SI-1.8)

[b] no data

Table SI-2.7. (continued) The estimated population density within radius 50 km (SI 1.4.2) and results from predictions by GLEMOS (GLEMOS, 2020) and FLEXPART (FLEXPART, 2022), at the individual sites.

Site no.	Country:	Sampling site:	Population density (per km²)	PCB153 GLEMOS (pg/m³)	Primary national (%)	Primary EMEP (%)	Primary outside EMEP (%)	Secondary (%)	PCB153 FLEXPART (pg/m³)
52	Latvia	Rucava	106	0.59	2	11	1	85	0.55
53	Latvia	Zoseni	35	0.30	9	4	1	85	0.52
54	Lithuania	Preila	203	0.85	4	10	2	84	0.75
55	Lithuania	Rugsteliskis	44	0.54	6	5	1	87	0.75
56	Malta	Giordan lighthouse	1803ª	0.95	5	28	3	64	1.6
57	Moldova	Leova	113	0.67	12	10	2	76	0.78
58	Netherlands	Kollumerwaard	470	2.5	9	10	1	80	1.7
59	Netherlands	Vredepeel	815ª	5.0	12	20	0	67	4.4
60	Netherlands	De Zilk	2695ª	4.6	29	13	0	58	2.6
97	Norway	Birkenes	109	0.37	2	12	3	83	0.44
98	Norway	Tustervatn	9	0.08	3	8	10	80	0.14
99	Norway	Kårvatn	11	0.09	3	8	7	82	0.26
100	Norway	Hurdal	253	0.27	9	6	3	82	0.37
101	Norway	Karasjok	2	0.16	0	7	4	89	0.12
102	Norway	Andøya	32	0.06	3	7	17	73	0.08
96	Spitsbergen	Zeppelin	1	0.06	0	4	42	54	0.02
61	Poland	Diabla Gora	97	0.94	5	10	1	84	0.83
62	Portugal	Monte Velho	46	0.62	28	5	4	63	0.54
63	Portugal	Alfragide	1153ª	0.57	35	5	4	56	0.50
64	Russia	Pinega	3	0.14	2	1	2	95	0.20
65	Russia	Lesnoy	14	0.42	3	2	1	95	0.45
66	Russia	Astrakhan	31	0.29	14	2	3	81	0.28
67	Russia	Caucasus	100	0.32	23	2	2	73	0.40
68	Russia	Voronezh	332	0.95	34	1	1	64	0.90
69	Russia	Danki	190	1.3	23	0	0	77	1.8
95	Russia	Smolenskoe Poozerie	13	0.39	4	3	1	92	0.53
70	Slovakia	Chopok	129	1.3	13	6	1	80	1.4
71	Slovakia	Starina	119	0.81	4	10	1	85	1.0
72	Slovenia	Iskrba	118	1.1	1	7	1	91	1.3
73	Spain	Víznar	152	0.54	10	3	6	81	1.6
74	Spain	Niembro	35	2.7	30	1	1	68	1.4
75	Spain	Els Torms	153	1.4	29	4	1	65	1.8
76	Spain	San Pablo de los Montes	41	0.62	16	2	4	79	1.5
77	Spain	Mahon	99	0.76	25	2	3	71	1.9
78	Spain	Barcarrota	50	0.87	41	2	3	55	1.1
79	Sweden	Råö	690ª	0.81	9	8	2	81	0.65
80	Sweden	Aspvreten	153	0.34	12	3	2	82	0.39
81	Sweden	Vavihill	390	1.2	12	13	1	73	0.65
82	Sweden	Bredkälen	4	0.10	3	4	5	88	0.23
83	Sweden	Esrange	3	0.07	3	7	7	82	0.16
84	Sweden	Abisko	9	0.06	5	10	13	72	0.11
85	Sweden	Vindeln	18	0.14	12	4	3	81	0.22
86	Switzerland	Jungfraujoch	109	1.8	11	8	1	80	2.1
87	Switzerland	Payerne	440	3.6	31	8	0	61	3.1
88	Ukraine	Zmeiny Island	56	0.68	12	5	2	81	0.55
89	United Kingdom	Chilbolton	612	2.0	30	3	1	65	1.6
90	United Kingdom	Aucencorth Moss	511	0.81	37	1	2	60	0.68
91	United Kingdom	Lough Navar	64	0.18	7	6	7	80	0.24
92	United Kingdom	Yarner Wood	329	0.84	30	5	3	62	0.65
93	United Kingdom	High Muffles	386	1.8	28	2	1	69	1.0
94	United Kingdom	Strath Vaich Dam	40	0.28	5	2	4	89	0.23

ª Suburban sites with a city within 50 km (Figure SI-1.8)
b no data

Text/Figures:

2.1   Overall results

The boxplot in Figure SI-2.1 illustrates that the HCB concentrations are dominating across Europe.

The results further show that the DDXs have the largest variability across Europe.
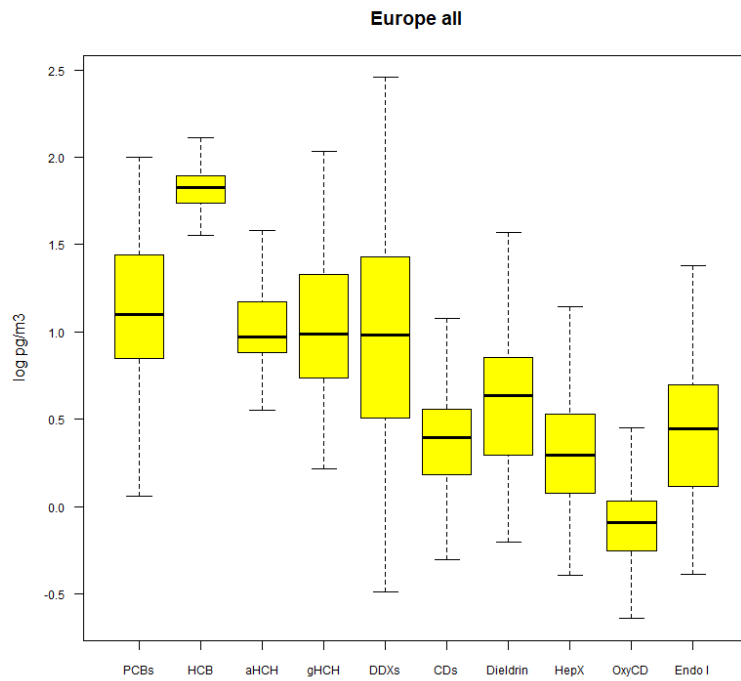
Figure SI-2.1. Comparison of the logarithmic concentrations of $\sum_6$PCBs and selected OCPs in air at European background sites.

2.2   Spatial variability

In the following section maps of selected POPs are given.

a)
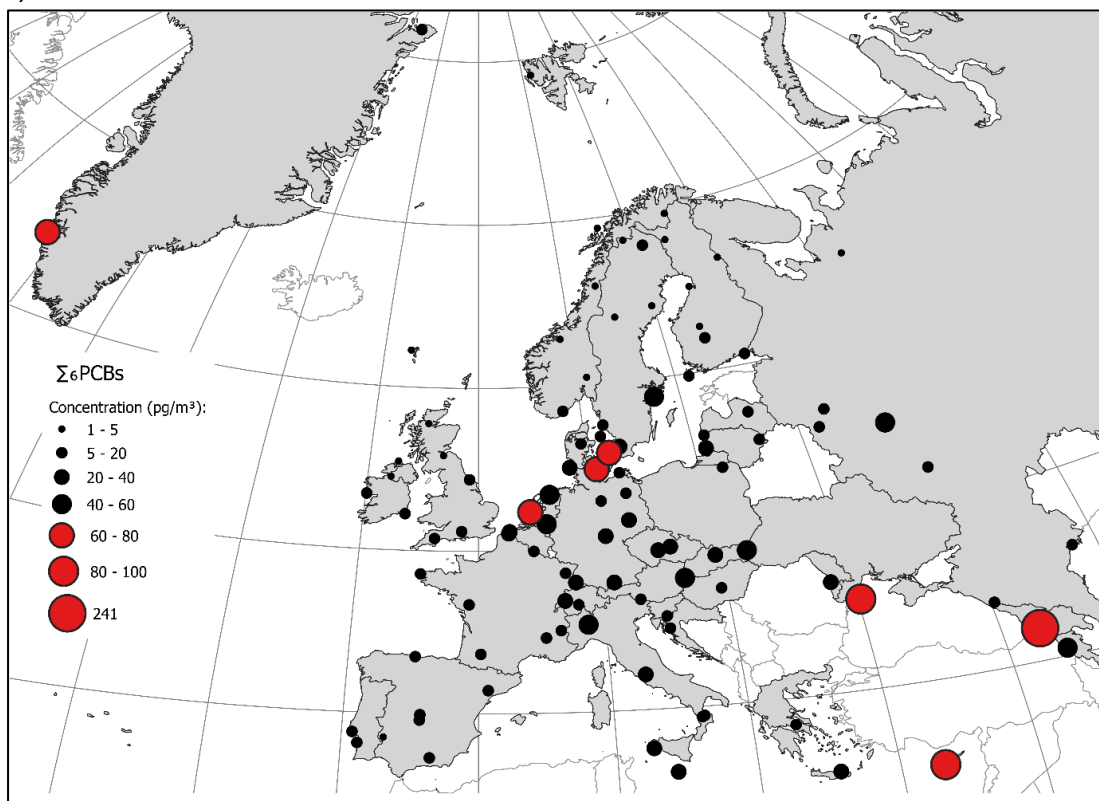
b)

Figure SI-2.2a-c. The spatial distribution of concentrations of $\sum_6 PCBs$ (a), and the individual PCB-28 (b) and PCB-153 (c) in background air across Europe.

c)
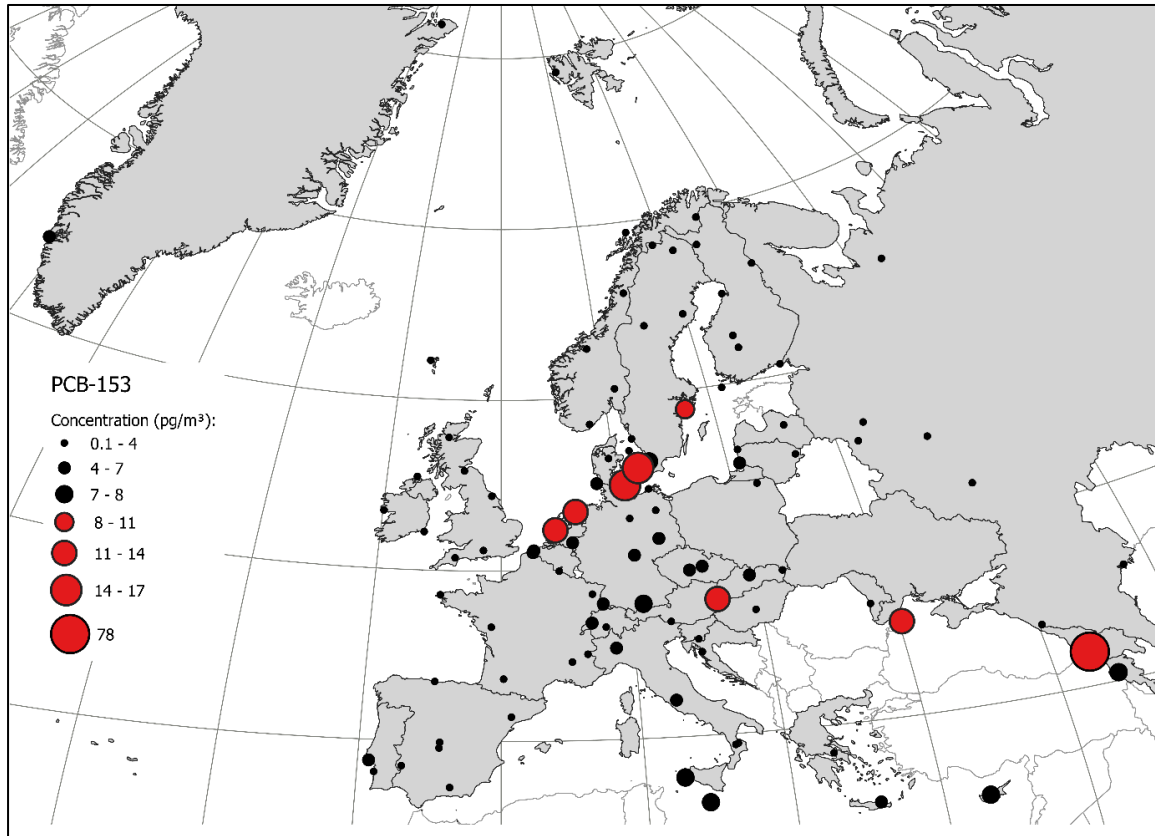
Figure SI-2.2a-c. (continued) The spatial distribution of concentrations of ∑$_6$PCBs (a), and the individual PCB-28 (b) and PCB-153 (c) in background air across Europe.
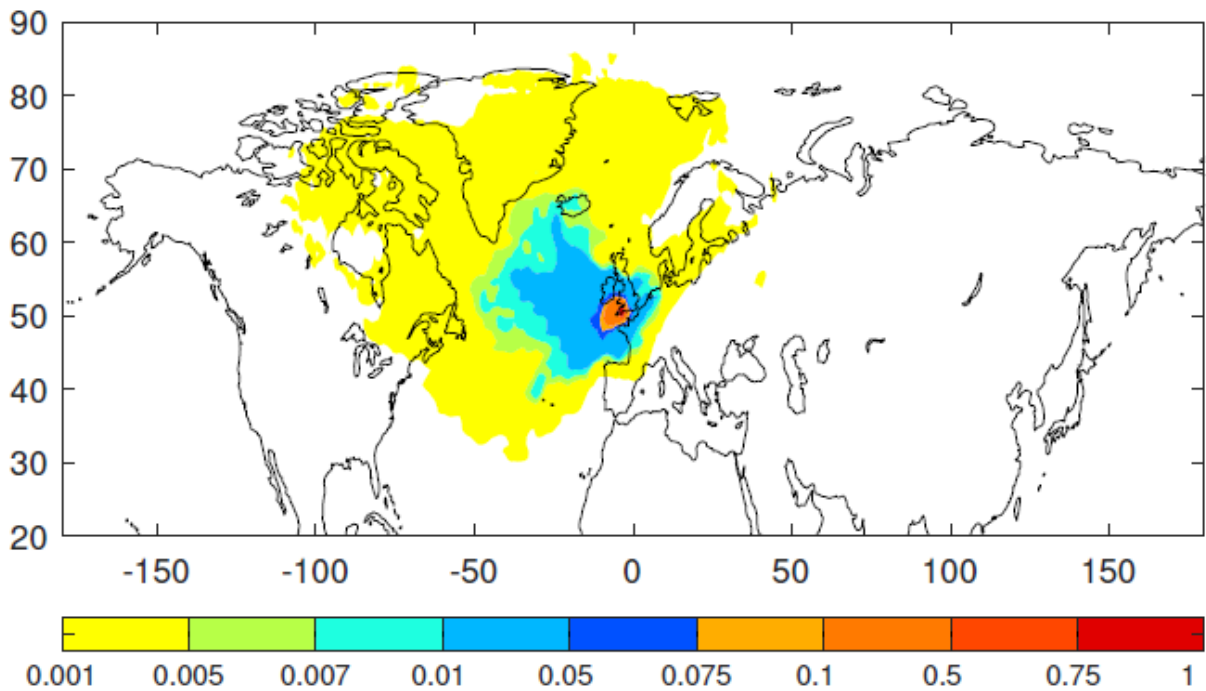
Figure SI-2.3 Map of footprint emission sensitivities (ES) for PCB-153 of Yarner Wood (site 92, UK), predicted to be influenced by air masses from west.

a)
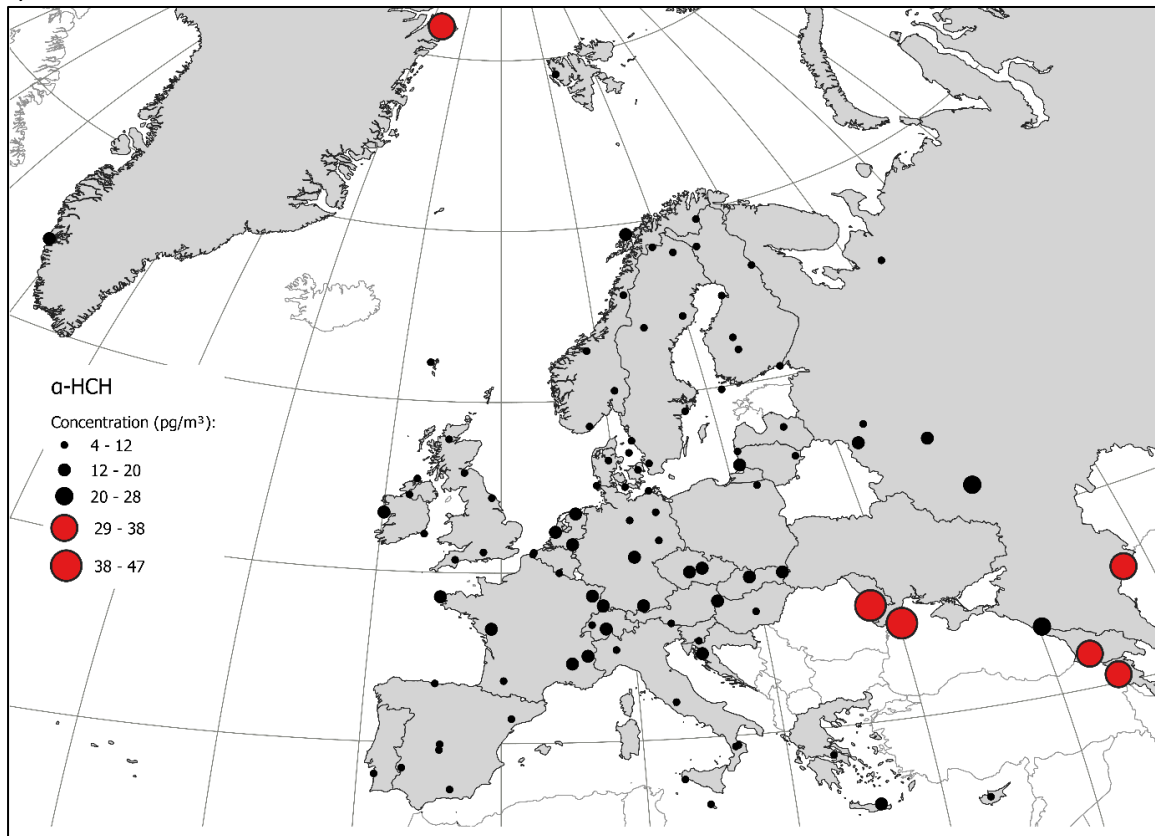
b)
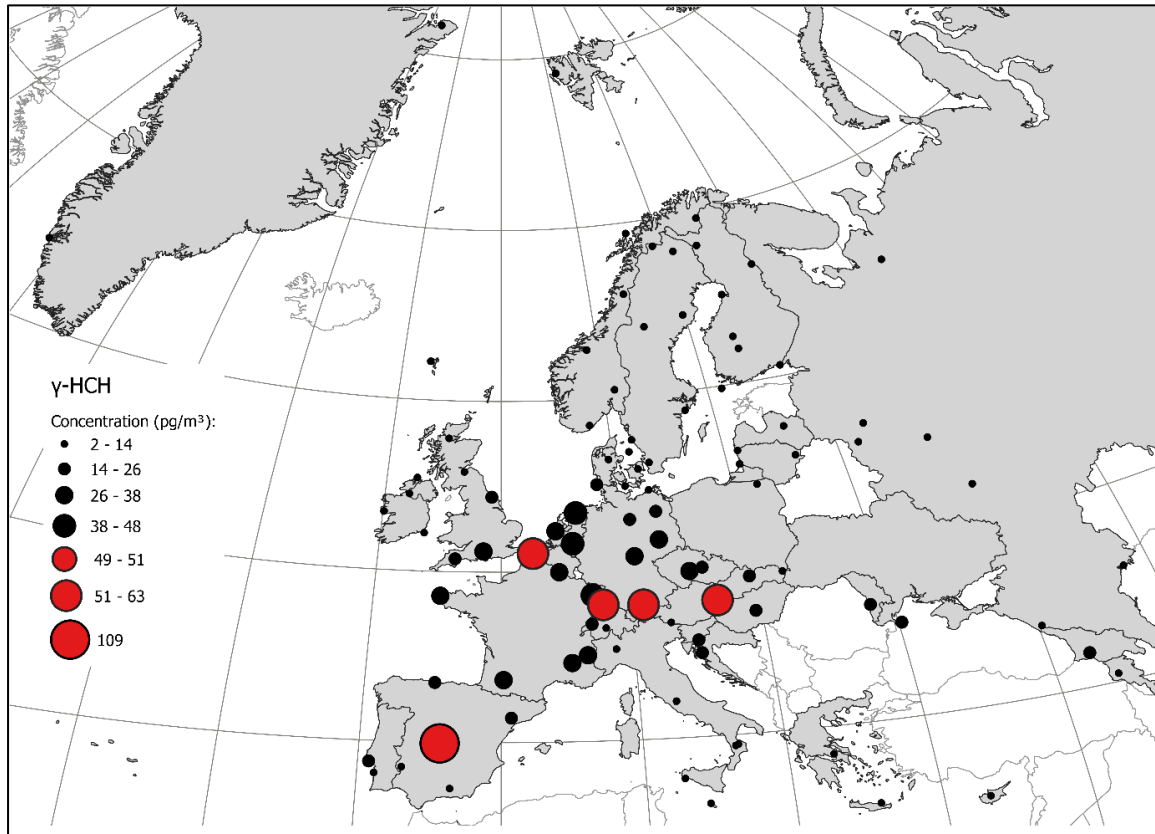
Figure SI-2.4a-b. The spatial distribution of concentrations of α-HCH (a) and γ-HCH (b) in background air across Europe.
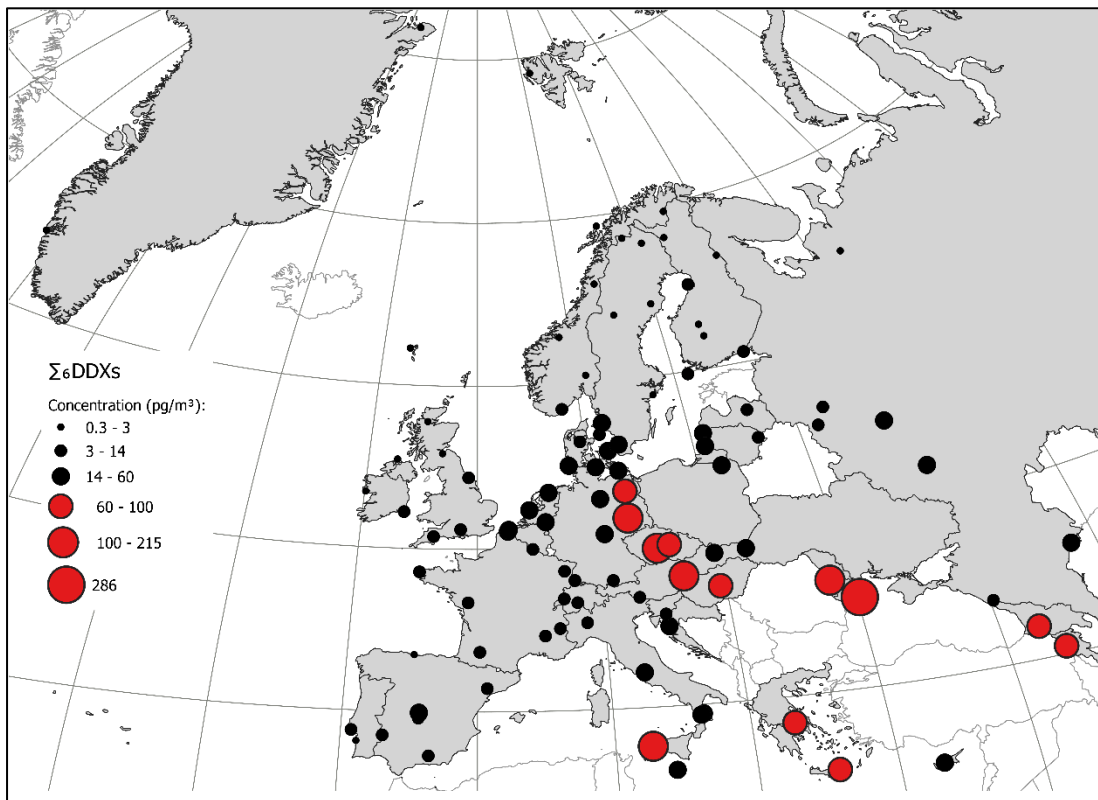
Figure SI-2.5. The spatial distribution of concentrations of ∑₆DDXs in background air across Europe.
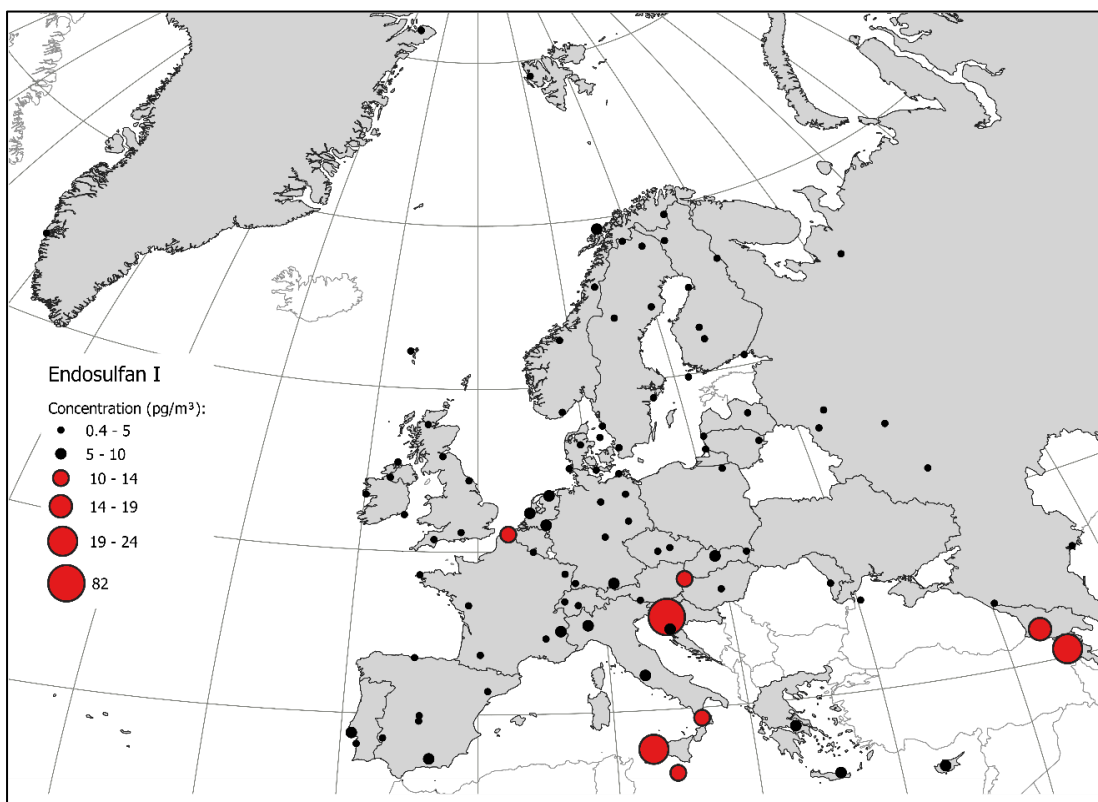
Figure SI-2.6. The spatial distribution of concentrations of Endosulfan I in background air across Europe.
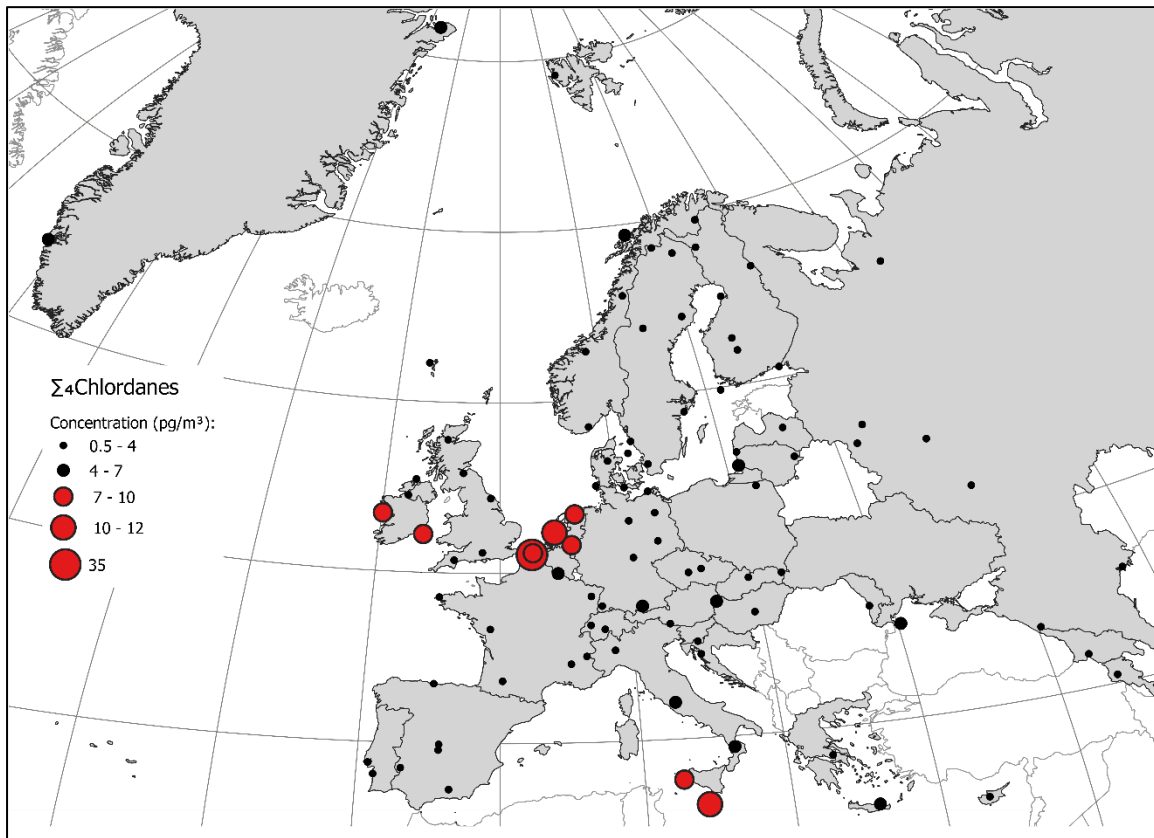
Figure SI-2.7. The spatial distribution of concentrations of ∑₄Chlordanes in background air across Europe.
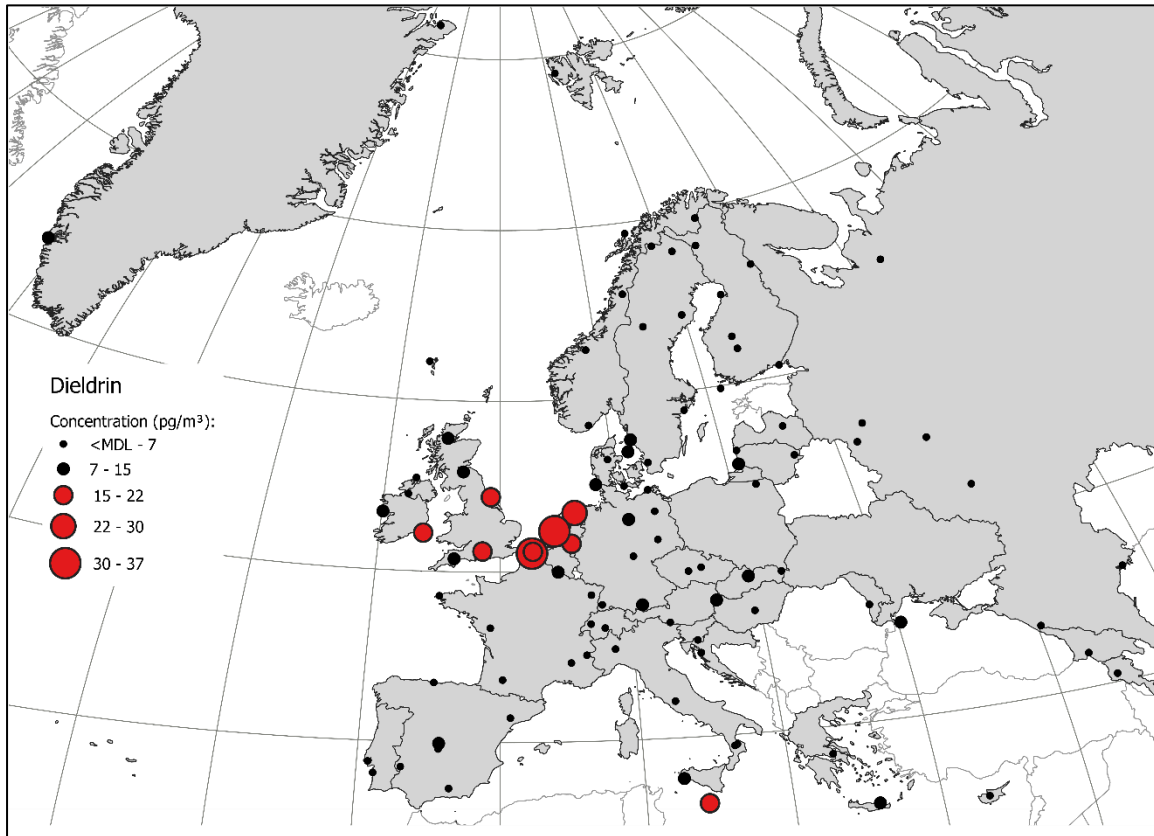
Figure SI-2.8. The spatial distribution of concentrations of Dieldrin in background air across Europe.
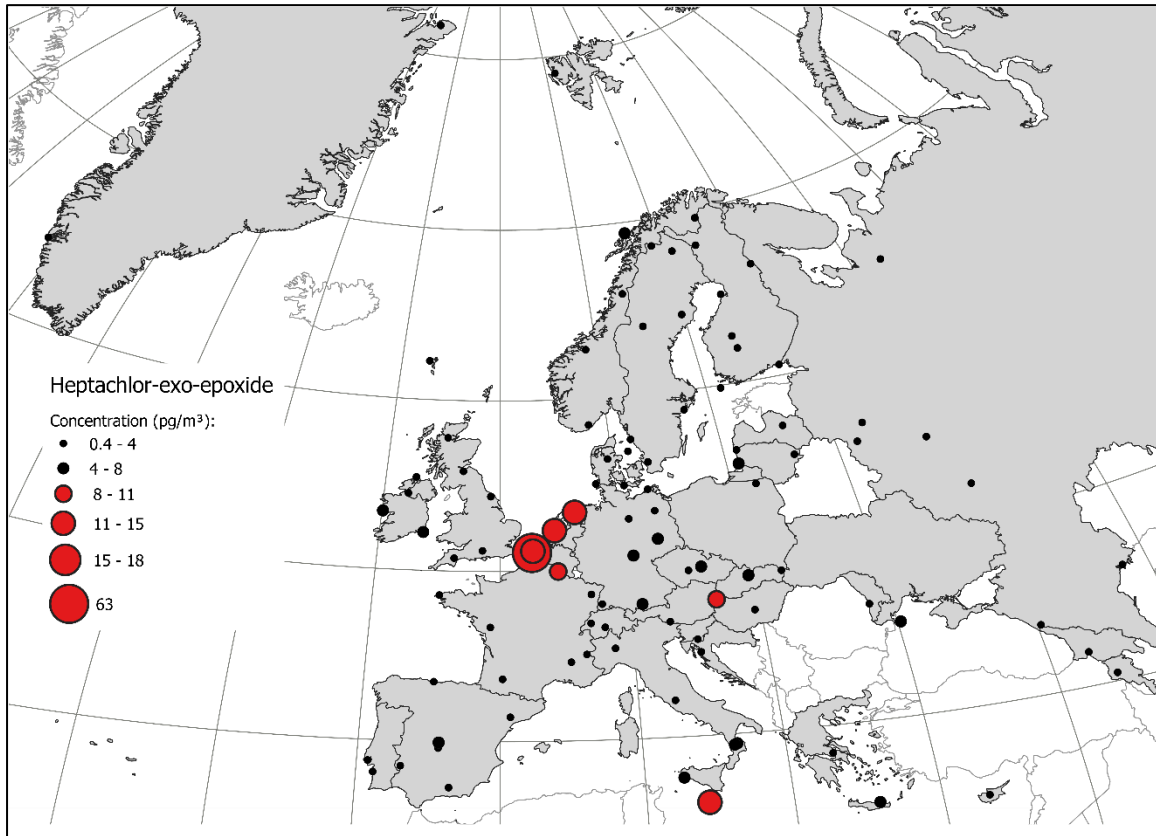
Figure SI-2.9. The spatial distribution of concentrations of Heptachlor-exo-epoxide in background air across Europe.
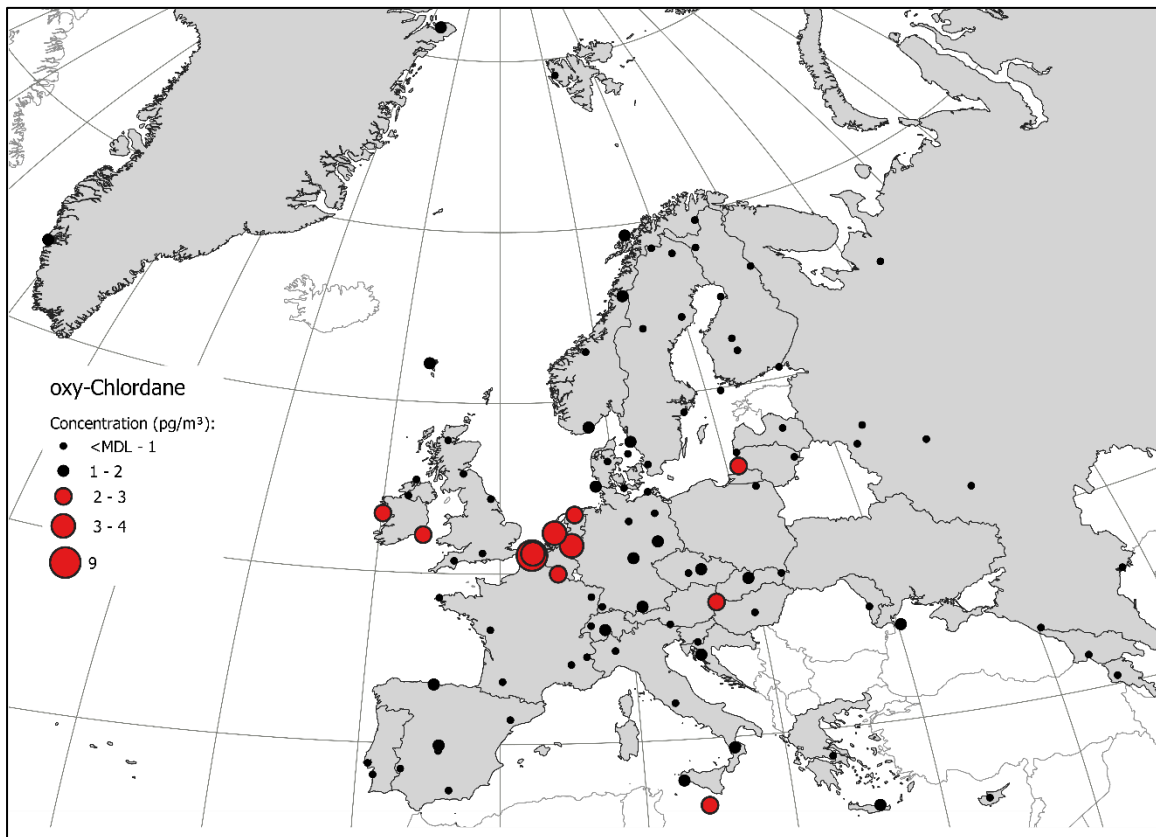
Figure SI-2.10. The spatial distribution of concentrations of oxy-Chlordane in background air across Europe.

2.3 Temporal change

a)

b)

c)

d)
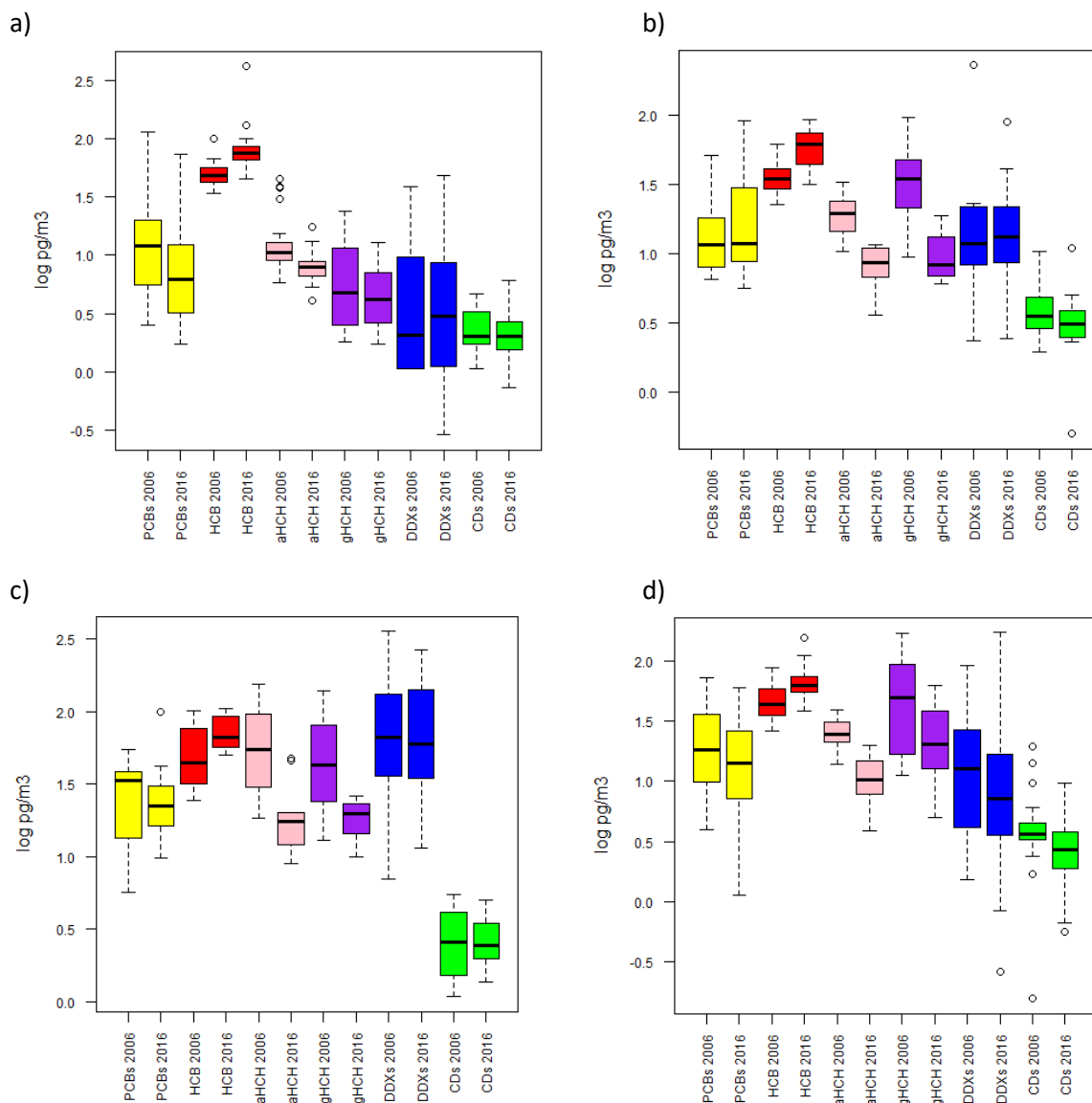
Figure SI-2.11 a-d. Comparison of the logarithmic concentrations of ∑₆PCBs and selected OCPs between the north region (a), south region (b), central-east region (c) and west region (d) in Europe (Figure SI-1.1), from 2006 (Halse et al., 2011) to 2016 (this study).
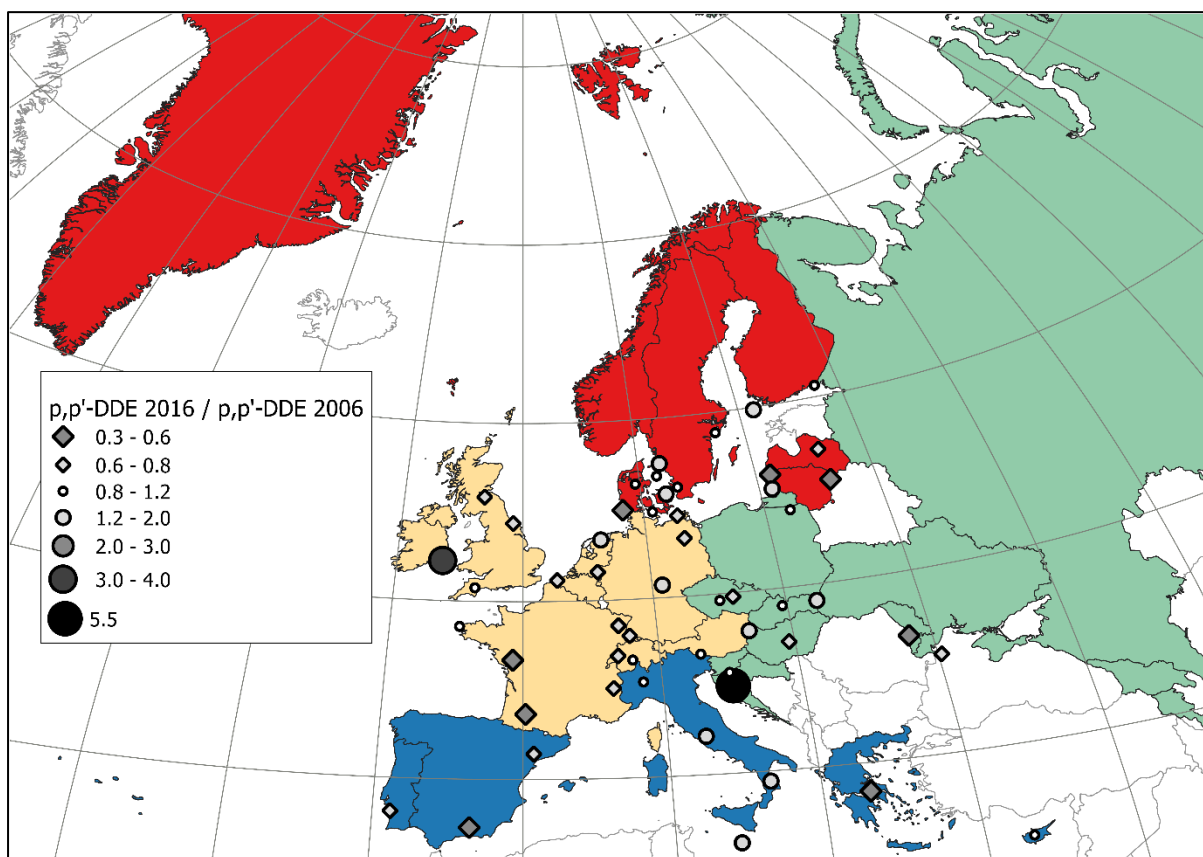
Figure SI-2.12. Measured concentrations of p,p'-DDE in 2016 (this study) divided by measured concentrations of p,p'-DDE in 2006 (Halse et al., 2011) at European sites for which data above MDL for both years are available (n=53).

2.4   Source indications

2.4.1   Observations
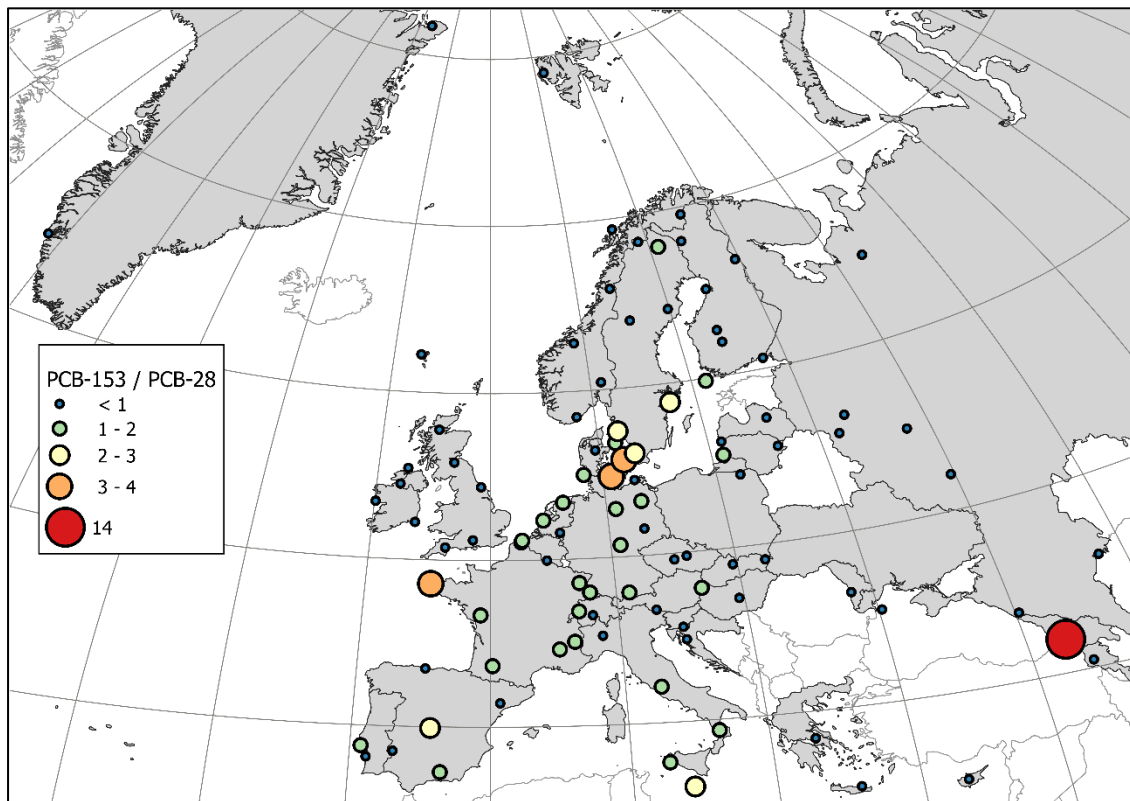
Figure SI-2.13: Relative abundance of PCB-153/PCB-28 across Europe.
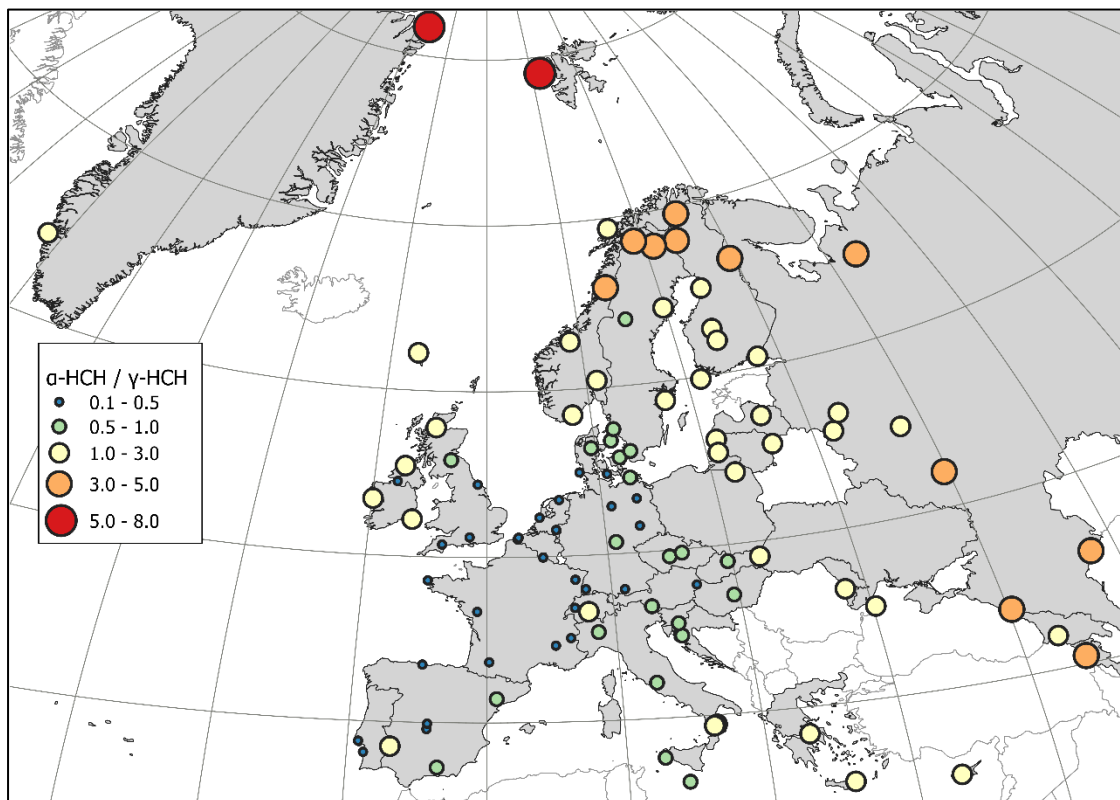
Figure SI-2.14. The relative abundance of α-HCH/γ-HCH across Europe.
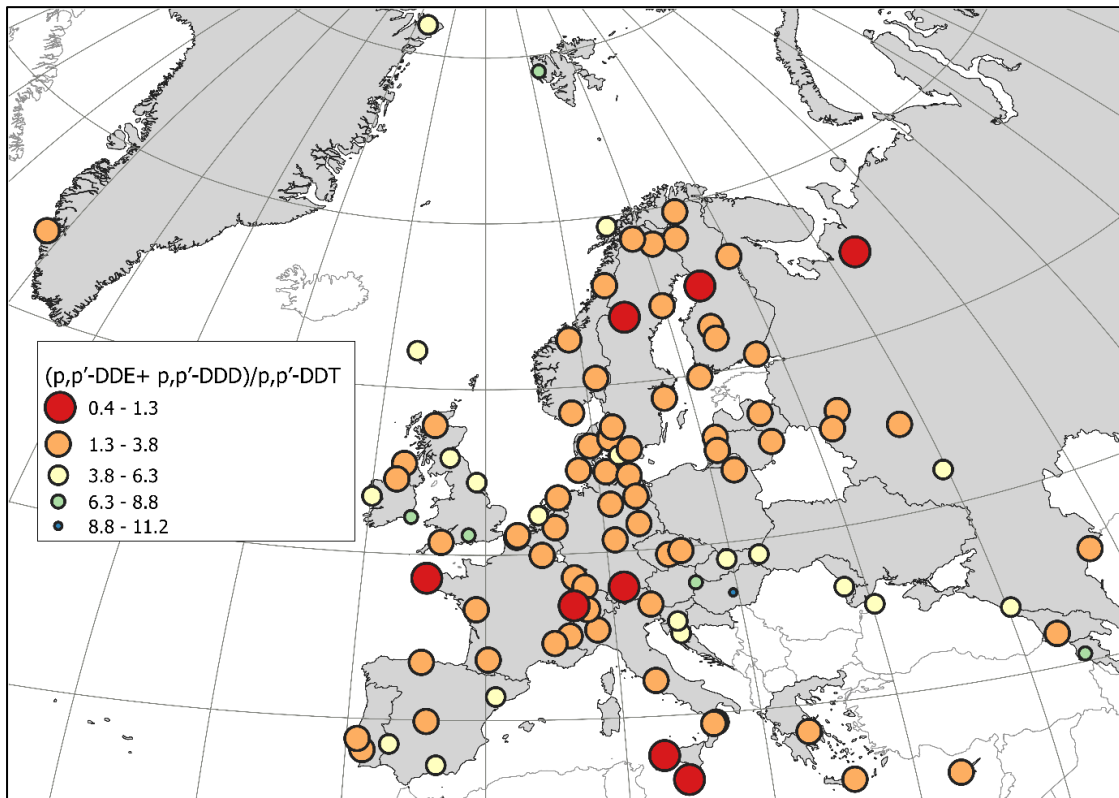
Figure SI-2.15a. The relative abundance of (p,p'-DDE+ p,p'-DDD)/p,p'-DDT across Europe.
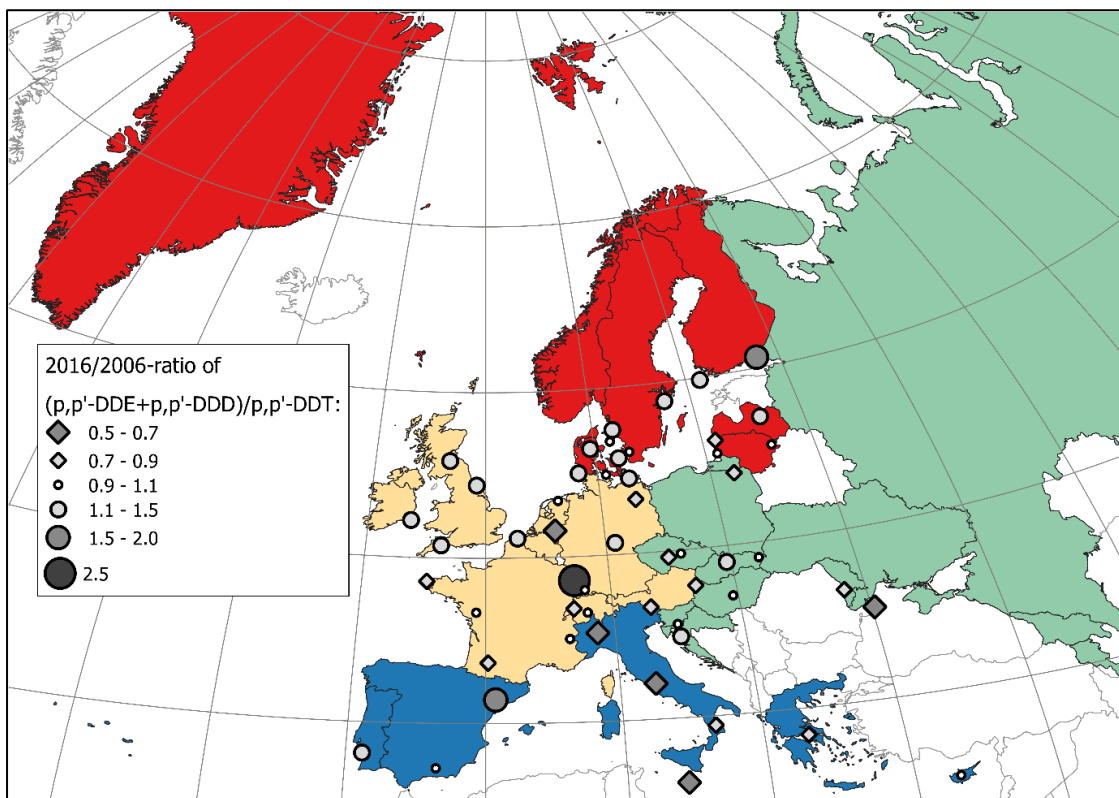
Figure SI-2.15b. The relative abundance of (p,p'-DDE+ p,p'-DDD)/p,p'-DDT in 2016 (this study) divided by the relative abundance of (p,p'-DDE+ p,p'-DDD)/p,p'-DDT in 2006 (Halse et al., 2011) at European sites for which data above MDL for both years are available (n=53).
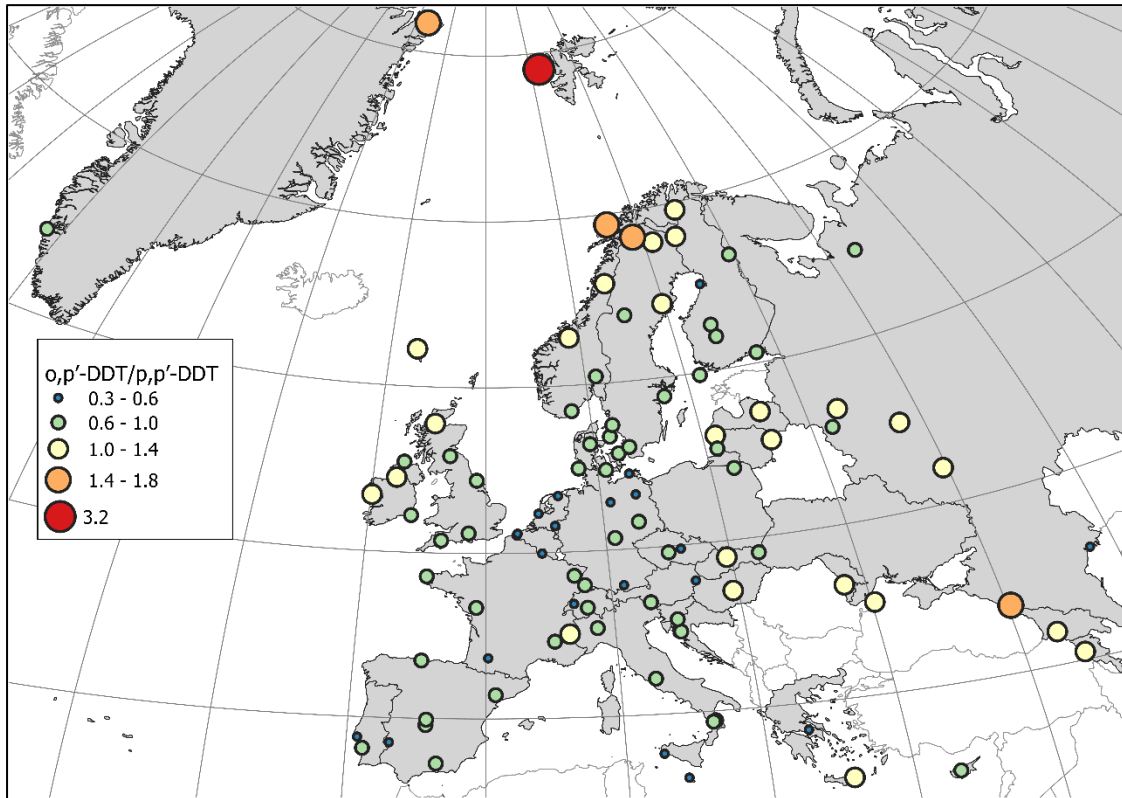
Figure SI-2.15c. The relative abundance of o,p'-DDT/p,p'-DDT across Europe.
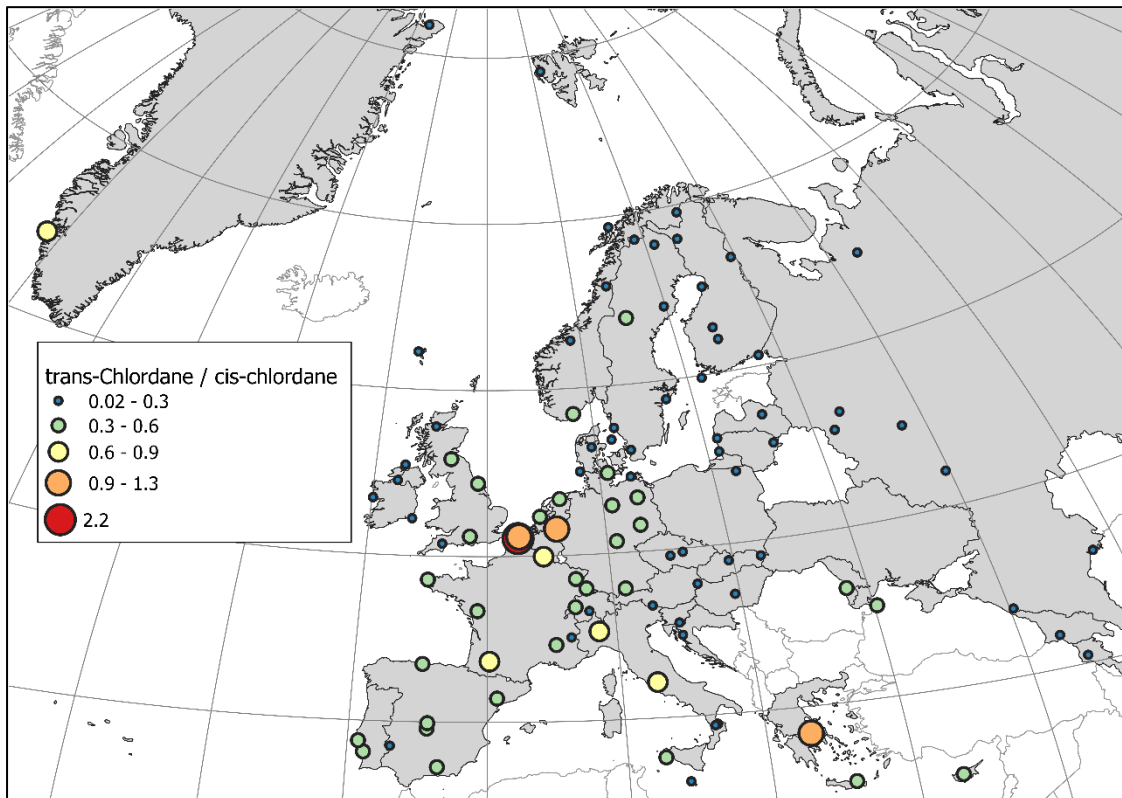
Figure SI-2.16. The relative abundance of trans-Chlordane/cis-Chlordane across Europe.
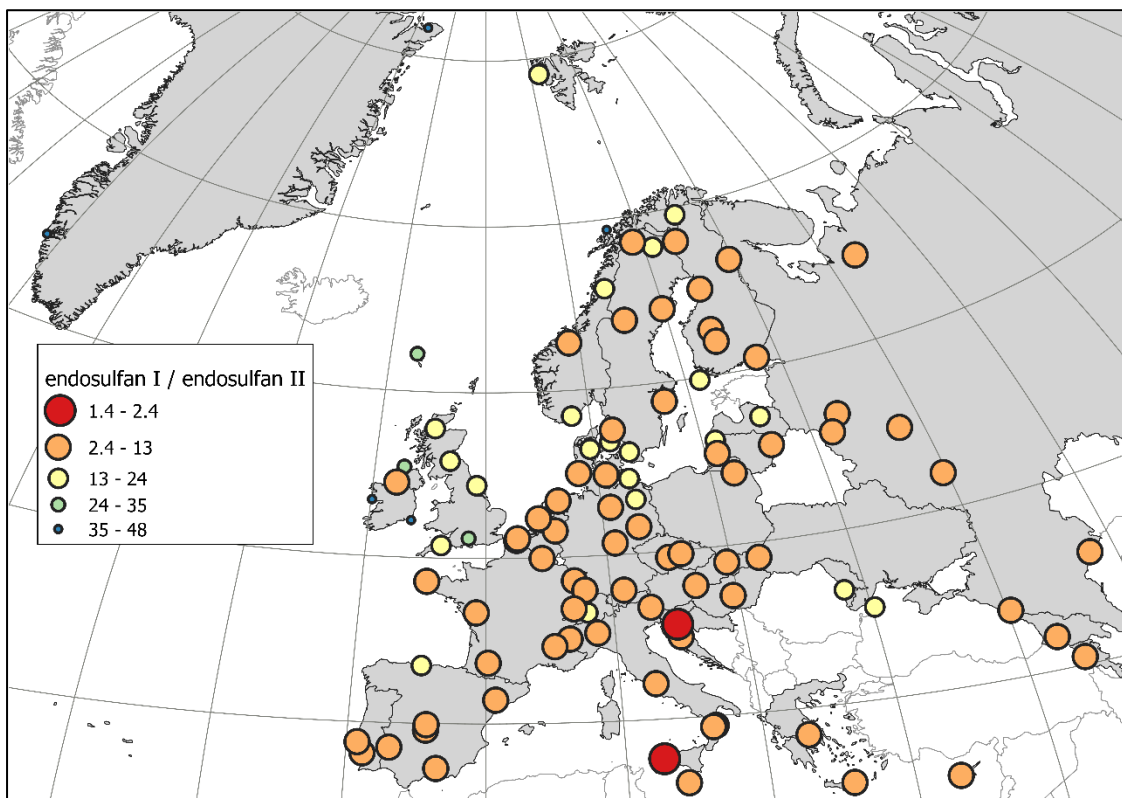
Figure SI-2.17. The relative abundance of endosulfan I/endosulfan II across Europe.

2.4.2   Model predictions
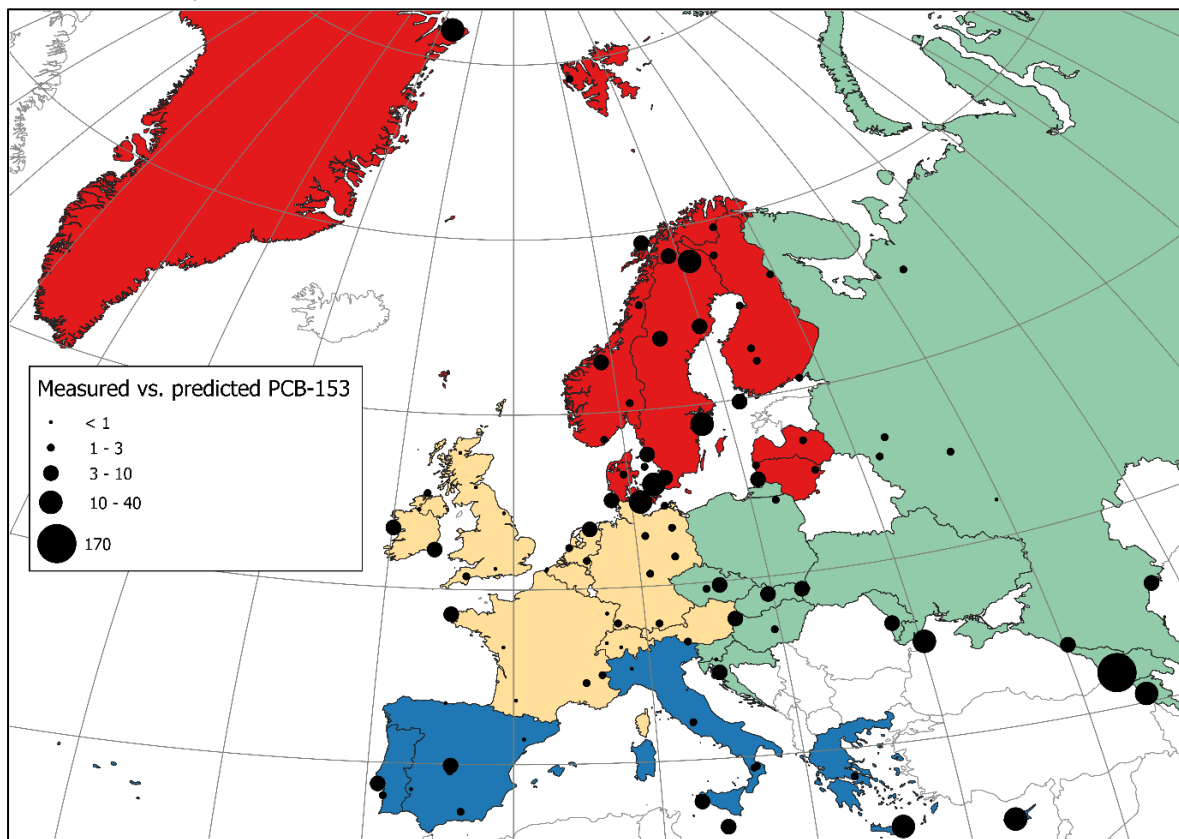
Figure SI-2.18. The ratio of the observed concentrations of PCB-153 in Europe relative to the modelled concentration with GLEMOS.
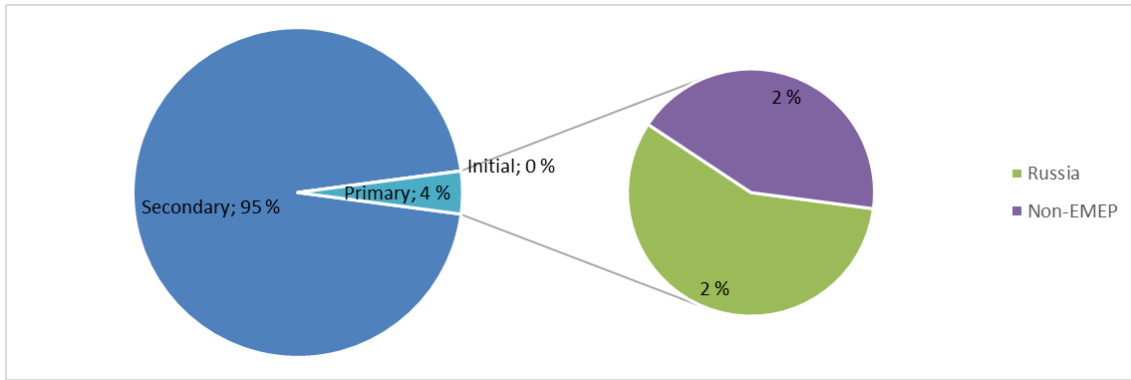
Figure SI-2.19a. The relative contributions to the overall concentration of PCB-153 at Pinega (site 64, Russia), simulated with GLEMOS.
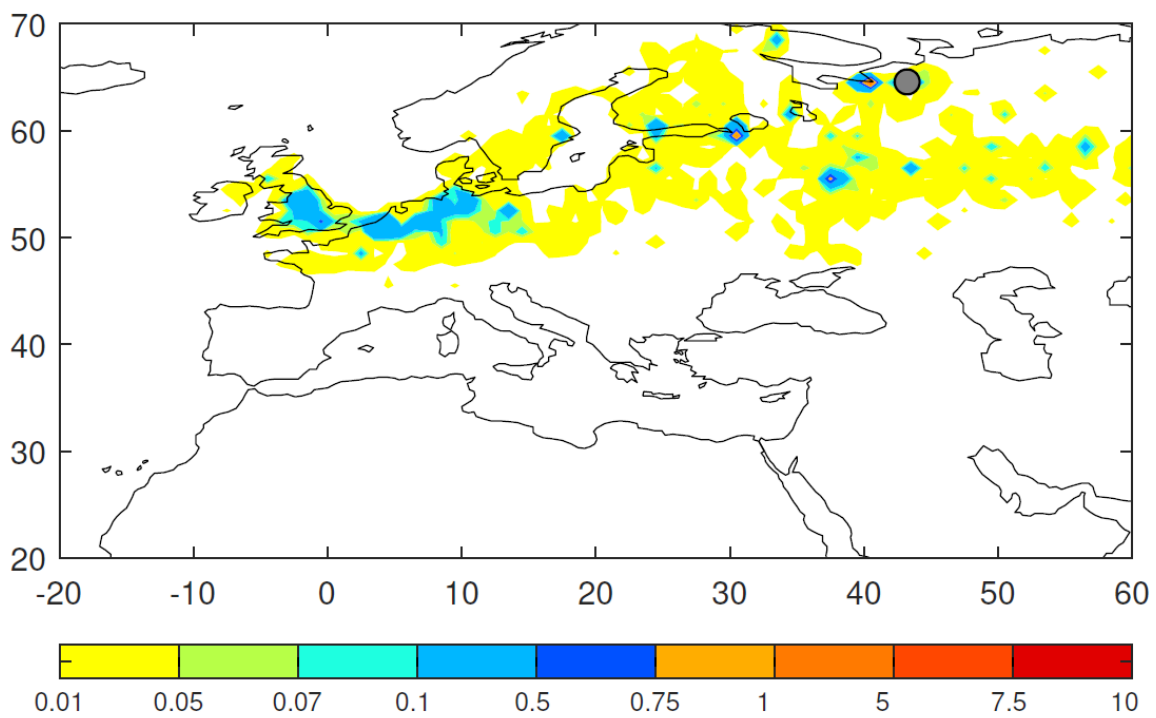

Figure SI-2.19b. Map of footprint emission contribution (EC) of Pinega (site 64, Russia), simulated with FLEXPART.
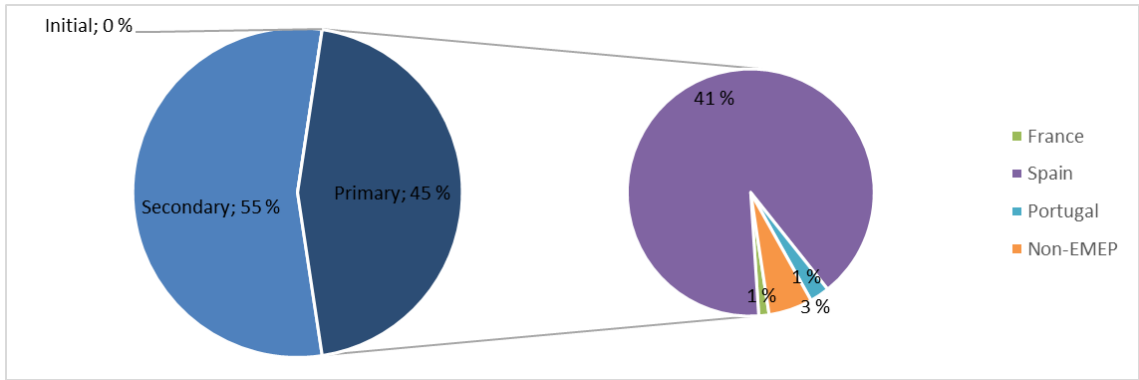
Figure SI-2.20a. The relative contributions to the overall concentration of PCB-153 at Barcarotta (site 78, Spain), simulated with GLEMOS.
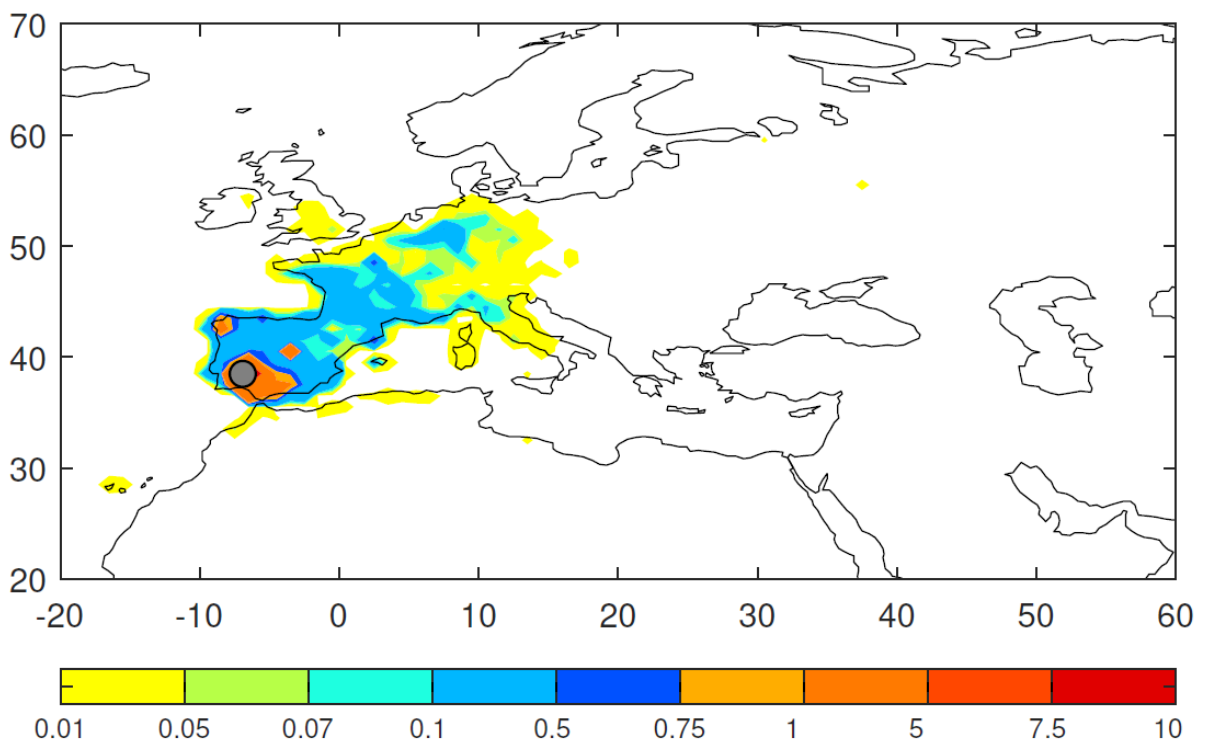

Figure SI-2.20b. Map of footprint EC of Barcarotta (site 78, Spain), simulated with FLEXPART.
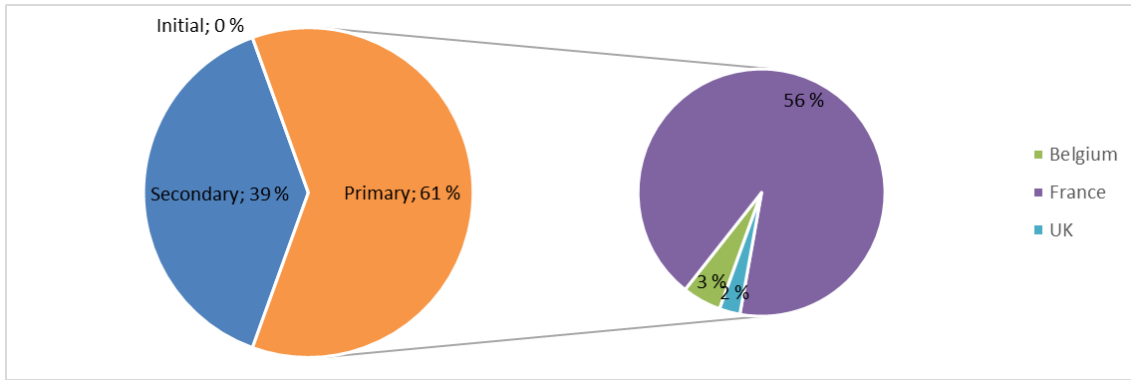
Figure SI-2.21a. The relative contributions to the overall concentration of PCB-153 at Houtem (site 4, Belgium), simulated with GLEMOS.
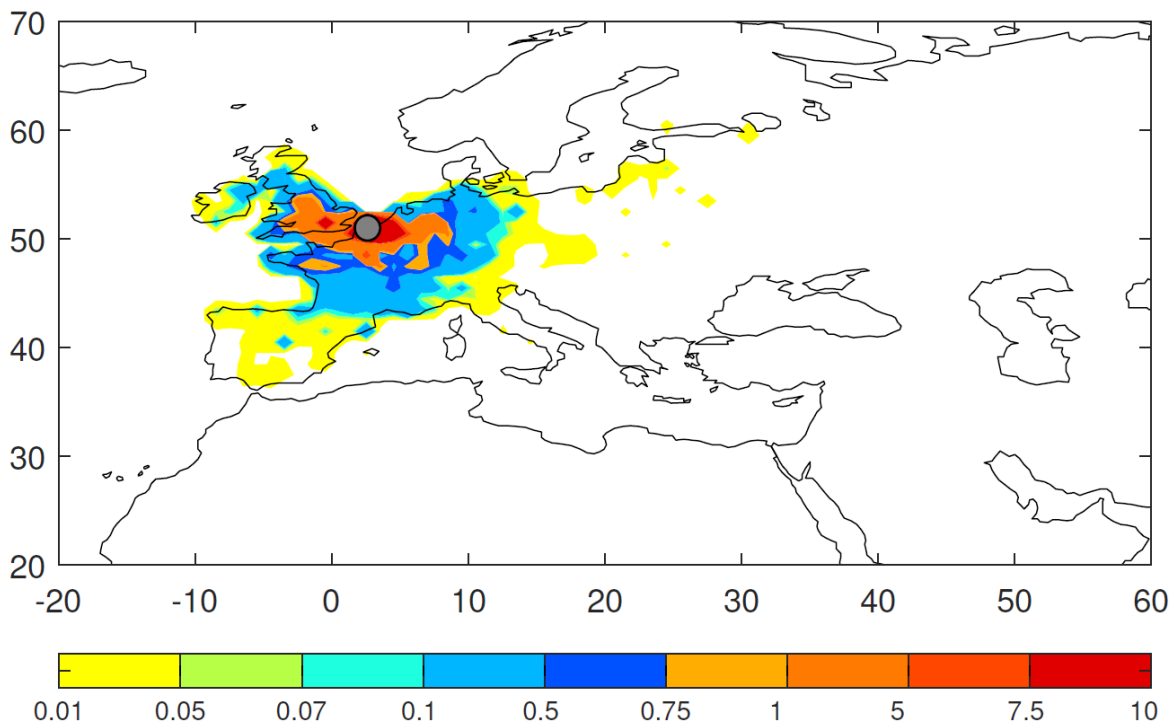

Figure SI-2.21b. Map of footprint EC of Houtem (site 4, Belgium), simulated with FLEXPART.
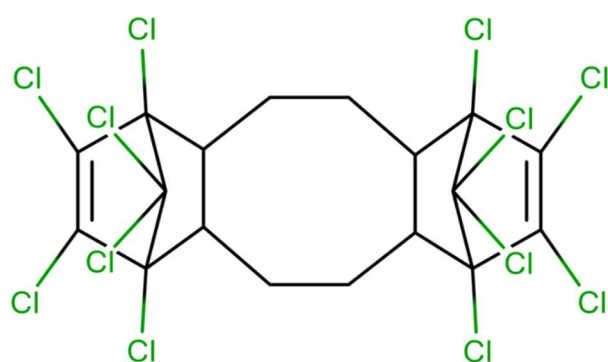
3 Acknowledgments

Table SI-3.1. Contributors within the EMEP programme

Country:	Contributor:	Institute:
Armenia	Arpine Gabrielyan	Environmental Impact Monitoring Center (EIMC)
Austria	Iris Buxbaum	Umweltbundesamt GmbH
Belgium	Elke Adriaenssens	Flemish Environment Agency (VMM)
Croatia	Jadranka Skevin Sovic	Meteorological and Hydrological Service of Croatia
Cyprus	Adamos Adamides	Ministry of Labour, Welfare and Social Insurance
Czech Rep	Adela Holubova	Chech Hydrometeorological Institute (CHMI)
Denmark	Thomas Ellermann	Insitut for Miljøvidenskab, Aarhus universitet
Faroe Islands	Rakul Mortensen	Environment Agency of Faroe Islands
Finland	Mika Vestenius	Finnish Meteorological Institute
France	Aude Pascaud	Mines-Douai
Georgia	Marine Arabidze	National Environment Agency
Germany	Elke Bieber	Umweltbundesamt (UBA)
Germany	Gerald Spindler	Leibniz-Institut für Troposphärenforschung (TROPOS)
Germany	Anja Claude	Deutscher Wetterdienst
Greece	A. Adamopoulos	Departement of Air Quality, Hellenic Ministry of the Environment & Energy
Greece	Kouvarakis Giorgos	Department of Chemistry, University of Crete
Greenland	Dorthe Petersen	Asiaq - Greenland Survey
Greenland	Rossana Bossi	Department of Environmental Science, Aarhus University
Hungary	Krisztina Labancz	Országos Meteorológiai Szolgálat
Ireland	Darius Ceburnis	School of Physics, National University of Ireland Galway (NUI Galway)
Ireland	Martin Haran	Met Èireann
Ireland	John McEntagart	Environment Protection Agency (EPA)
Italy	Jean-Philippe Putaud	Joint Researrch Centre (JRC)
Italy	Catia Balducci/Angelo Cecinato	CNR - Institute of Atmospheric Pollution Research
Italy	Francesca Sprovieri	CNR - Institute of Atmospheric Pollution Research
Italy	Angela Marinoni	CNR - Institute of Atmospheric Sciences and Climate
Italy	Francesca Sprovieri	CNR - Institute of Atmospheric Pollution Research
Latvia	Marina Frolova	Latvian Environment, Geology and Meteorology Centre
Lithuania	Dalia Jasineviciene	Centre for Physical Sciences and Technology
Malta	Raymond Ellul	Atmospheric Research, University of Malta
Moldova	Violeta Balan	Air Quality and Environmental Radioactivity Monitoring Center
Netherlands	Ronald Spoor	National Institute of Public Health and the Environment (RIVM)
Norway	Ingjerd S. Krogseth / Helene Lunder Halvorsen	Norwegian Institute of Air Research (NILU)
Norway	Guttorm Christensen	Akvaplan-NIVA
Poland	Anna Degorska	Institute of Environmental Protection - NRI
Portugal	João Matos	Portugese Environment Agency, Environmental Reference Laboratory (LRA)
Russia	Sergey Gromov	Institute of Global Climate and Ecology
Slovakia	Marta Mitosinkova	Slovak Hydrometeorlogical Institute, Department of Air Quality
Slovenia	Marijana Murovec	Slovenian Environment Agency, Air Quality Division
Spain	Juan Ramón Moreta González / Alberto Orio Hernandez	Agencia Estatal de Meteorología (AEMET) / Ministry of Agriculture, Food and Environment - Air Quality and Atmosphere Protection
Sweden	Malin Fredricsson	IVL Svenska Miljöinstitutet
Switzerland	Christoph Hüglin	Swiss Federal Laboratories for Materials Science and Technology
Ukraine	Vladimir Medinets, Olga Konareva	Odessa National I.Imechnikov University
United Kingdom	Sim Yuk tang / Braban, Christine F.	Centre for Ecology and Hydrology

Chung, S. W. C., & Chen, B. L. S. (2011). Determination of organochlorine pesticide residues in fatty foods: A critical review on the analytical methods and their testing capabilities. *Journal of Chromatography A, 1218*(33), 5555-5567. 10.1016/j.chroma.2011.06.066

CIESIN. (2016). Documentation for the Gridded Population of the World, Version 4 (GPWv4). Retrieved from http://dx.doi.org/10.7927/H4D50JX4. Access Nov 2018.

EuroVoc. (2021). Browse by EuroVoc. Retrieved from https://eur-lex.europa.eu/browse/eurovoc.html. Access Dec 2021.

FLEXPART. (2022). FLEXible PARTicle dispersion mode. Retrieved from https://www.flexpart.eu/. Access Aug 2022.

GLEMOS. (2020). Global EMEP Multi-media Modeling System Retrieved from http://en.msceast.org/index.php/j-stuff/glemos. Access Sep 2020.

Halse, A. K., Schlabach, M., Eckhardt, S., Sweetman, A., Jones, K. C., & Breivik, K. (2011). Spatial variability of POPs in European background air. *Atmospheric Chemistry and Physics, 11*(4), 1549-1564. https://doi.org/10.5194/acp-11-1549-2011

Klánová, J., Èupr, P., Kohoutek, J., & Harner, T. (2008). Assessing the Influence of Meteorological Parameters on the Performance of Polyurethane Foam-Based Passive Air Samplers. *Environmental Science & Technology, 42*(2), 550-555. 10.1021/es072098o

Lunder Halvorsen, H., Bohlin-Nizzetto, P., Eckhardt, S., Gusev, A., Krogseth, I. S., Moeckel, C., Shatalov, V., Skogeng, L. P., & Breivik, K. (2021). Main sources controlling atmospheric burdens of persistent organic pollutants on a national scale. *Ecotoxicology and Environmental Safety, 217*, 112172. https://doi.org/10.1016/j.ecoenv.2021.112172

Moeckel, C., Harner, T., Nizzetto, L., Strandberg, B., Lindroth, A., & Jones, K. C. (2009). Use of Depuration Compounds in Passive Air Samplers: Results from Active Sampling-Supported Field Deployment, Potential Uses, and Recommendations. *Environmental Science & Technology, 43*(9), 3227-3232. https://doi.org/10.1021/es802897x

Stenerson, K., & Brown, C. (2015). *Analysis of PolyChlorinated Biphenyls in Fish Oil using Supelclean EZ-POP NP, Silica Gel SPE and an SLB-5ms GC Column* (Supelco US Reporter 33.4).

Stenerson, K. K., Shimelis, O., Halpenny, M. R., Espenschied, K., & Ye, M. M. (2015). Analysis of polynuclear aromatic hydrocarbons in olive oil after solid-phase extraction using a dual-layer sorbent cartridge followed by high-performance liquid chromatography with fluorescence detection. *J Agric Food Chem, 63*(20), 4933-4939. 10.1021/jf506299f

Tuduri, L., Harner, T., & Hung, H. (2006). Polyurethane foam (PUF) disks passive air samplers: Wind effect on sampling rates. *Environmental Pollution, 144*(2), 377-383. https://doi.org/10.1016/j.envpol.2005.12.047

Aas, W., & Bohlin-Nizzetto, P. (2018). *Heavy metals and POP measurements, 2016*. (EMEP/CCC-Report 3/2018). Kjeller: NILU Retrieved from http://hdl.handle.net/11250/2563390.

Check for updates

Spatial distribution of Dechlorane Plus and dechlorane related compounds in European background air

Lovise P. Skogeng[1,2]*, Helene Lunder Halvorsen[1,3], Knut Breivik[1,3], Sabine Eckhardt[1], Dorte Herzke[1,2], Claudia Moeckel[1,4] and Ingjerd S. Krogseth[1,2]

[1]Department of Environmental Chemistry, NILU—Norwegian Institute for Air Research, Tromsø, Norway, [2]Department for Arctic and Marine Biology, UiT—The Arctic University of Norway, Tromsø, Norway, [3]Department of Chemistry, University of Oslo, Oslo, Norway, [4]Department of Materials and Environmental Chemistry, Stockholm University, Stockholm, Sweden

The highly chlorinated chemical Dechlorane Plus (DP) was introduced as a replacement flame retardant for Mirex, which is banned through the Stockholm Convention (SC) for its toxicity (T), environmental persistence (P), potential for bioaccumulation (B) and long-range environmental transport potential (LRETP). Currently, Dechlorane Plus is under consideration for listing under the Stockholm Convention and by the European Chemical Agency as it is suspected to also have potential for P, B, T and LRET. Knowledge of atmospheric concentrations of chemicals in background regions is vital to understand their persistence and long-range atmospheric transport but such knowledge is still limited for Dechlorane Plus. Also, knowledge on environmental occurrence of the less described Dechlorane Related Compounds (DRCs), with similar properties and uses as Dechlorane Plus, is limited. Hence, the main objective of this study was to carry out a spatial mapping of atmospheric concentrations of Dechlorane Plus and Dechlorane Related Compounds at background sites in Europe. Polyurethane foam passive air samplers were deployed at 99 sites across 33 European countries for 3 months in summer 2016 and analyzed for dechloranes. The study showed that syn- and anti-DP are present across the European continent (<MDL-2.6 pg/m^3 and <MDL-12.3 pg/m^3, respectively), including parts of the Arctic. This supports that these compounds have potential for long-range atmospheric transport to remote regions. The highest concentrations of Dechlorane Plus were observed in central continental Europe, with anti-DP fractions close to the commercial mixture of Dechlorane Plus. The only detected Dechlorane Related Compounds was Dechlorane-602, which was found in 27% of the samples (<MDL-0.33 pg/m^3). The measured concentrations and spatial patterns of Dechlorane Plus and Dechlorane-602 in air across Europe indicate the influence of primary sources of these compounds on background concentrations in European air. Future air monitoring efforts targeting dechloranes is needed in both background and source areas, including consistent temporal trends.

KEYWORDS

passive air sampling (PAS), spatial distribution, flame retardant, background air, emerging contaminant

1 Introduction

Dechlorane Plus (bis(hexachlorocyclopentadieno) cyclooctane, $C_{18}H_{12}Cl_{12}$) (DP, sometimes referred to as DDC-CO (Bergman et al., 2012), Supporting Information (SI) Supplementary Table S1, S2) is a highly chlorinated flame retardant used in industrial polymers such as electrical coatings and building materials. It was first introduced in the mid-1960 s by OxyChem (United States) as a replacement product for the flame retardant and pesticide Mirex (Dechlorane, Supplementary Table S1, S2) (Hoh et al., 2006) and later for the flame retardant Decabromodiphenyl ether (Deca-BDE) (Sverko et al., 2011), which are both listed for elimination of production and use through the international Stockholm Convention (SC) under annex A (UNEP, 2020).

The production volume of DP is highly uncertain, with estimated global production volumes varying between 750 and 6000 tonnes annually in 2020, and Europe is predicted to be accountable for 24% of the global emissions of DP to the atmosphere (Hansen et al., 2020). ECHA (2021) reports that there is no production of DP in Europe, but between 90 and 230 tons of DP are estimated to be imported annually. The commercial mixture of DP consists of the stereoisomers syn- and anti-DP, with an approximate ratio of 1:3, i.e., anti-DP fraction (f_{anti} = anti-DP/(syn-DP + anti-DP)) of 0.75, but usually between 0.59 and 0.80 (Wang et al., 2010). Some Dechlorane Related Compounds (DRCs, Supplementary Table S1, S2), i.e. Dechlorane-601 (Dec-601 or DDC-ID), Dechlorane-602 (Dec-602 or DDC-DBF), Dechlorane-603 (Dec-603 or DDC-Ant), and Dechlorane-604 (Dec-604 or HCTBPH), have also been used as replacements for Mirex and were introduced as flame retardants in polymers in the late 1960s (Shen et al., 2010). Production volumes for the DRCs are even less known than for DP.

DP remains unregulated at international level but has been proposed for listing under the SC since 2018 (UNEP, 2022). In January 2022, the Persistent Organic Pollutant Review Committee moved DP to the next review stage, which includes evaluating risk management and control measures. Parallel to this, DP is under review by the European Chemicals Agency (ECHA) for restrictions under the EU regulation Registration, Evaluation, Authorisation and restriction of Chemicals (REACH) (ECHA, 2021). The DRCs are expected to behave similarly to DP and Mirex in the environment (Shen et al., 2010), but to our knowledge, the DRCs are currently not under review for international restrictions.

DP was first detected in the environment in 2004, in air and sediments from the Great Lakes region (US/Canada), close to the local DP manufacturing plant (Hoh et al., 2006). DRCs are often detected together with DP in environmental samples (Wang et al., 2010; Moller et al., 2011; Moller et al., 2012). Dec-602, Dec-603 and Dec-604 were first detected in 2009 in biota, and also in sediment core samples dated back to the 1960s–70s (Shen et al., 2010), coinciding with the introduction of DP in the mid-1960s (Hoh et al., 2006). According to literature, Dec-602 is more ubiquitously detected than Dec-601, Dec-603 and Dec-604 (Wang et al., 2010; Moller et al., 2011; Moller et al., 2012; Yu et al., 2015; Bohlin-Nizzetto, 2020a; Nipen et al., 2021).

DP has also been measured in air close to point-sources of DP (e.g., landfills or urban regions), in e.g., China (Ren et al., 2008; Wang et al., 2010; Chen et al., 2011; Zhang et al., 2015), Tanzania (Nipen et al., 2021), and Norway (Morin et al., 2017). Many studies of DP in the atmosphere also report detectable concentrations of Dec-602 (Wang et al., 2010; Moller et al., 2011; Moller et al., 2012; Yu et al., 2015; Bohlin-Nizzetto et al., 2020b; Nipen et al., 2021). Though studies of both DP and DRCs in background regions exist (Moller et al., 2012; Bohlin-Nizzetto et al., 2020c; Schuster et al., 2021a), the knowledge of the spatial distribution of DP and DRCs in background regions in Europe is limited.

The main objective of this study was to carry out a spatial mapping of atmospheric concentrations of DP and DRCs at background sites in Europe to provide insight into 1) the spatial distribution of the dechlorane compounds across the European continent, 2) possible primary source regions and influence of local sources of dechlorane compounds on measured concentrations, 3) the long-range atmospheric transport potential (LRATP) of dechlorane compounds, and 4) knowledge of the background concentrations of these compounds prior to possible international restrictions. To achieve this, a passive air sampling (PAS) campaign at 99 sites across Europe was carried out in 2016. PAS was chosen as it allows for coordinated deployment of a high number of samples, without the need of electricity, and provides estimates of time-averaged concentrations suitable for evaluation of spatial trends (Shoeib and Harner, 2002; Jaward et al., 2004).

2 Materials and methods

2.1 Air sampling

Between 95% (Zhang et al., 2015) and 99% (Sverko et al., 2011) of DP may be particle-bound in the atmosphere due to its high octanol-air partition coefficient (Supplementary Table S1). In this study, passive air samplers (PAS) of the MONET design (Shoeib and Harner, 2002; Kalina et al., 2017) were used for air sampling. This sampler tends to accumulate particles, but the sampling efficiency of particle-associated compounds has shown to be lower compared to gas-phase compounds (Bohlin et al., 2014; Markovic et al., 2015). The samplers consisted of a PUF disk (14 cm diameter × 1.4 cm thickness, 0.027 g/m³, Sunde Skumplast AS/Carpenter, Norway) as sampling medium, protected by a housing made from two stainless steel bowls (diameter 30 and 24 cm) and a metal rod and PUF disks (14 cm diameter × 1.4 cm thickness, 0.027 g/m³ Sunde Skumplast AS/Carpenter, Norway) as sampling media. All metal parts of the sampler were pre-cleaned with alkali soap and water, followed by rinsing with acetone and n-hexane. PUF disks were pre-cleaned with toluene, acetone, and n-hexane consecutively, dried under vacuum, wrapped in aluminium foil and stored cool in zip-lock bags until shipment. More details on the preparation of samplers are described elsewhere (Lunder Halvorsen et al., 2021).

The PAS were deployed by site keepers at 99 sampling locations across Europe (from 35°N to 82°N, and 52°W to 48°E) for approximately 3 months during summer 2016 (Lunder Halvorsen et al., in review). The locations were chosen based on the European Monitoring and Evaluation Programme (EMEP) sampling network (Tørseth et al., 2012). Details on sample locations and deployment periods can be found in Supplementary Table S3. After sampling, the PUF disks were wrapped in aluminium foil and zip-lock bags, and sent to the NILU laboratory in Kjeller, Norway, where they were stored at -20°C awaiting further processing.

2.2 Chemical analysis

The sample PUF disks were spiked with isotopic-labelled syn-DP (Cambridge Isotope Laboratories, Inc.) as internal standard, followed by 8 h Soxhlet extraction with 1:1 acetone/n-hexane. A multi-analyte clean-up method based on Röhler et al. (2021) was initially chosen in order to include acid-labile organic contaminants simultaneously with dechloranes. Therefore, 2 g of a mixture of Supel QuE Z-zep (SigmaAldrich) and Discovery DSC-18 (SigmaAldrich) in the bottom sorbent bed, and 2 g Supelclean LC-Florisil (Sigma Aldrich) in the top sorbent bed was used for solid phase extraction. Acetonitrile was used for elution, and the samples were further back-extracted to n-hexane and cleaned with concentrated sulfuric acid in order to sufficiently remove co-extracted sample matrix (Lunder Halvorsen et al., in review). Prior to instrumental analysis, the volume was reduced and 1,2,3,4-tetrachloronaphthalene (ULTRA scientific, now a part of Agilent) was added as an instrument performance standard.

The samples were analyzed for syn- and anti-DP, Dec-601, Dec-602, Dec-603 and Dec-604 using an Agilent 7890 gas chromatograph (GC) coupled to an Agilent 7200 high-resolution quadruple time-of-flight mass spectrometer (HRqToFMS) (details in SI section 1). The chromatograms were processed using MassHunter Quant version B.09.00, and integrated areas of target analytes and isotopic labelled syn-DP were used to quantify the concentration of dechloranes from the relative response factors of calibration standards (i.e., internal standard method).

2.3 Quality assurance and quality control

Selected sampling locations (Finland/Pallas, Ukraine/Zmeiny Island, and United Kingdom/Yarner Wood, Supplementary Table S3) were supplied with field blanks (FB) (n = 3). These were pre-cleaned PUF-disks, transported together with the samples and exposed during mounting and dismantling of the samplers. This was done to account for possible contamination during deployment, handling in the field and transport of the samples. Additionally, laboratory blanks (LB) were included (n = 14) to account for potential contamination during the laboratory procedures. These blanks underwent the same laboratory procedures as the exposed samples. The DP concentrations in FB and LB were comparable (average syn-DP concentrations were 16 ± 7.8 pg/sample and 13 ± 5.2 pg/sample in LB and FB, respectively; and average anti-DP concentrations were 36 ± 22 pg/sample and 25 ± 12 pg/sample in LB and FB, respectively), indicating that the blank contribution from sampling and transport was minimal. The average syn- and anti-DP concentrations in blank samples (FB and LB) were 13% and 7.1% of the average concentrations in the samples, respectively. All samples were blank corrected for using all blanks (average of FB and LB). Similarly, all blanks were used to calculate the method detection limit (MDL, in pg), given as three times the standard deviation of DP concentration in blanks (normalized by the average sample volume 212 m³ to give the MDL in pg/m³). The MDLs of syn-DP and anti-DP were 22 pg/sample (0.11 pg/m³) and 64 pg/sample (0.30 pg/m³), respectively. In calculations of sum, median, average concentrations, standard deviations, and for the statistical analysis, samples below MDL were set to 1/2 of the respective MDL. None of the DRCs were detected in the blank samples. Thus, the

instrumental detection limits were used for these compounds. The MDLs for Dec-601, Dec-602, Dec-603 and Dec-604 were 3.0 pg/sample (0.01 pg/m³), 2.2 pg/sample (0.01 pg/m³), 2.6 pg/sample (0.01 pg/m³) and 6.7 pg/sample (0.03 pg/m³), respectively.

The internal standard compensates for possible loss during sample preparation, and was quantified relative to the instrument performance standard to monitor recovery rates for the extraction and clean-up procedure. Recovery >130% may indicate possible matrix effects. The internal standard recoveries of both exposed and blank samples are listed in Supplementary Table S4.

To investigate the reproducibility of the PAS, 11 sampling locations were supplied with two parallel samples. These were treated and analysed in the same way, and the relative standard deviation (RSD) of the two samples for each location was calculated. The RSDs were 9–85% (n = 5), 3–52% (n = 5) and 3% (n = 1) for syn-DP, anti-DP and Dec-602, respectively, for samples where the compounds were detected in both parallels (Supplementary Table S5). Dec-601, Dec-603 and Dec-604 were not detected in any parallel samples. The RSDs of syn- and anti-DP at some sites (i.e. Czech Republic/Kosetice, Germany/Waldhof and Sweden/0052åö) are larger compared to the RSDs found for e.g. PCB-180 and p,p'-DDE at the same sites (<17%) in (Lunder Halvorsen et al., in review). The log Koa of DP is even higher than for these two POPs, and the larger RSDs found in our study may therefore imply that the uptake of particles are more variable than for more gaseous compounds. For further data analysis, the dechlorane concentrations from the sites supplied with parallel PAS were averaged.

2.4 Deriving concentrations in air

Due to variability in the sampling period (81–125 days) (Supplementary Table S3), all measured concentrations (in pg/sample) were normalized to a sample period of 90 days. The concentrations per sample (pg/sample) were used when assessing the spatial patterns in our study.

To enable comparison with other studies, a conversion to volumetric air concentrations was done by using a generic sampling rate from the literature. The sampling rates for are typically in the range 4 ± 2 m³/day (Harner et al., 2014). However, the uptake efficiency for particles with the MONET sampler (54%) (Markovic et al., 2015) suggest a lower sampling rate for particle-bound compounds (Bohlin et al., 2014). Drage et al. (2016) collected both gaseous and particulate phases and derived a sampling rate of 2.3 m³/day for BDE-209 and DP. This sampling rate reflects the lower uptake efficiency of particles reported by Markovic et al. (2015). Even lower uptake efficiency (10%) and uptake rates (0.7 m³/day) of particle-bound PAHs with the MONET sampler have been reported by Klánová et al. (2008).

However, as both DP and Dec-602 are likely to predominantly sorb to atmospheric particles (similar to BDE-209), a sampling rate of 2.3 m³/day was chosen to derive concentrations in air (in pg/m³) for both DP and Dec-602 in our study, consistent with Drage et al. (2016). The selection of 2.3 m³/day contrary to 0.7 m³/day (Klanova et al., 2008), may be considered to pose the potential risk of underestimation rather than overestimation of air concentrations. This is a semiquantitative approach (Wania and Shunthirasingham, 2020).

TABLE 1 Detection frequency (%), method detection limit (MDL), range, average ± standard deviations (St.dev.) and median for the atmospheric concentrations of Dechlorane Plus syn- and anti-isomers, ΣDP (the sum of syn-DP and anti-DP), and Dec-602, at 97 sites across Europe. The results are given in mass per sample (pg/sample) and in mass per volume (pg/m³) in brackets (derived from a sampling rate of 2.3 m³/day).

Dechlorane	Detection frequency %	MDL pg/sample (pg/m³)	Range pg/sample (pg/m³)	Average ± St.dev. pg/sample (pg/m³)	Median pg/sample (pg/m³)
syn-DP	48	23 (0.1)	<MDL—390 (<MDL—1.9)	49 ± 70 (0.2 ± 0.3)	<MDL (<MDL)
anti-DP	42	64 (0.3)	<MDL—2300 (<MDL—11)	210 ± 410 (1.0 ± 2.0)	<MDL (<MDL)
ΣDP	54	43	<MDL—2700 (<MDL—13)	250 ± 470 (1.2 ± 2.3)	63 (0.3)
Dec-602	27	2.2 (0.01)	<MDL—74 (<MDL—0.33)	4.7 ± 9.3 (0.02 ± 0.04)	<MDL (<MDL)

[a]Calculated with 0.5·MDL.
[b]Fraction of samples with one or two of the DP-isomers above MDL.

2.5 Statistical analysis

Possible linear relationships between the concentration of ΣDP and latitude, longitude, wind speed, temperature, f_{anti}, and Dec-602 concentrations were investigated by using the Pearson's correlation coefficient (r). The concentrations of ΣDP and Dec-602, wind speed and temperature were log-transformed prior to the correlation test. The Wilcoxon signed-rank test was used for group comparison to investigate possible influence of elevated population density. All statistical analyses were performed by using R Studio with R 4.1.1 and a significance level of $p < 0.05$.

3 Results and discussion

Detection frequency, MDL, range, median, average and standard deviation of the measured concentrations for the dechlorane compounds are listed in Table 1. Concentrations of the dechloranes in individual samples are listed in Supplementary Table S6.

3.1 Concentrations of dechlorane plus in European background air

When evaluating all samples together, syn-DP and anti-DP were detected in 51% and 44% of the samples, respectively. The concentrations of ΣDP (syn-DP + anti-DP) ranged from <MDL to 31,000 pg/sample (median: 63 pg/sample) (n = 99). Generally, the highest number of sites with concentrations below MDL were found in northern Europe (e.g., Norway, Sweden, and Russia), and the highest concentrations were found in central continental Europe (e.g., northern France, Austria, Netherlands, and Germany). The highest concentration of ΣDP (31,000 pg/sample), measured in the sample from Hungary/Puszta, was 490 times higher than the median, and indicates possible local contribution at this site. The second highest concentration was measured in the sample from Greenland/Nuuk (3200 pg/sample), but this sampler was installed on a rooftop in the city of Nuuk and may thus be influenced by local sources. Hence, these outliers were excluded from the dataset. This provided a concentration range of ΣDP in the remaining samples of <MDL to 2700 pg/sample (n = 97) (Figure 1A, Table 1).

Applying a sampling rate of 2.3 m³/day provided ΣDP concentrations ranging from <MDL to 13 pg/m³ (n = 97). Air concentrations of dechloranes from other studies are compiled in Supplementary Table

S8 for comparison. The lowest concentrations of ΣDP above MDL in our study (0.12–0.13 pg/m³), found in Great Britain and Ireland, are 2–4 times lower than concentrations reported for two remote locations in North America using active air sampling (AAS) in the period 2005–2013 (0.26–0.43 pg/m³) (Liu et al., 2016). Low concentrations of ΣDPs (0.01–1.8 pg/m³) were also obtained with a flow-through sampler in a sub-Arctic region in Canada from 2011–2014 (Yu et al., 2015). The upper concentration range in our study (12–13 pg/m³), found in France and Austria, is within the range reported at a rural site in China in 2007–2008 using AAS (0.47–36 pg/m³) (Chen et al., 2011).

The concentration range in our study is also in line with Schuster et al. (2021b), reporting concentrations of ΣDP sampled with PAS in the Global Atmospheric Passive Sampling (GAPS) network in 2005–2006; <MDL to 9.9 pg/m³ and <MDL to 8.7 pg/m³ for 35 background and five polar sites, respectively. Five sampling sites were identical in our study and in Schuster et al., 2021a: Czech Republic/Kosetice, Finland/Pallas, Ireland/Malin Head, Spitsbergen/Zeppelin Mountain and Russia/Danki. The concentrations in 2005–2006 were lower compared to 2016 (our study) for four of the sites (ratio Schuster/Skogeng: 0.2–0.6) (Supplementary Table S7), indicating possible increased emission of DP. Increasing trends have also previously been suggested at three of five Great Lake sites from 2005 to 2013 (Liu et al., 2016), and in an urban area in China from 2008 to 2013 (Li et al., 2016). On the other hand, the sample from Spitsbergen/Zeppelin station had a ratio of 2.1. In Schuster et al., 2021a, elevated and varied concentrations of DP were observed at this site, which may explain the higher ratio. No conclusions of temporal trends in atmospheric concentrations of ΣDP can be made based on only two time-points. Furthermore, comparison between the two datasets may be hampered by differences in sampling methodology and analytical procedures; While the MONET sampler used in our study is placed in freely hanging position, the PAS used within GAPS (diameter 24.5 and 19.5 cm) is placed in a fixed position and has a PUF-disk with lower density (0.021 g/cm³) (Hoh et al., 2006). The GAPS sampler has been shown to have higher efficiency of particle collection than the MONET sampler (Chaemfa et al., 2009; Markovic et al., 2015). Such differences should though have been adjusted for by using a lower sampling rate for the MONET sampler. A generic sampling rate was used in our study, while Schuster et al., 2021a used site-specific sampling rates in the estimation of the sampling volumes. Additionally, Schuster et al. (2021b), sampled through all seasons in 2005–2006 (Schuster et al., 2021a), while our study was performed during summer only and seasonal variations in atmospheric concentrations of ΣDP may occur.
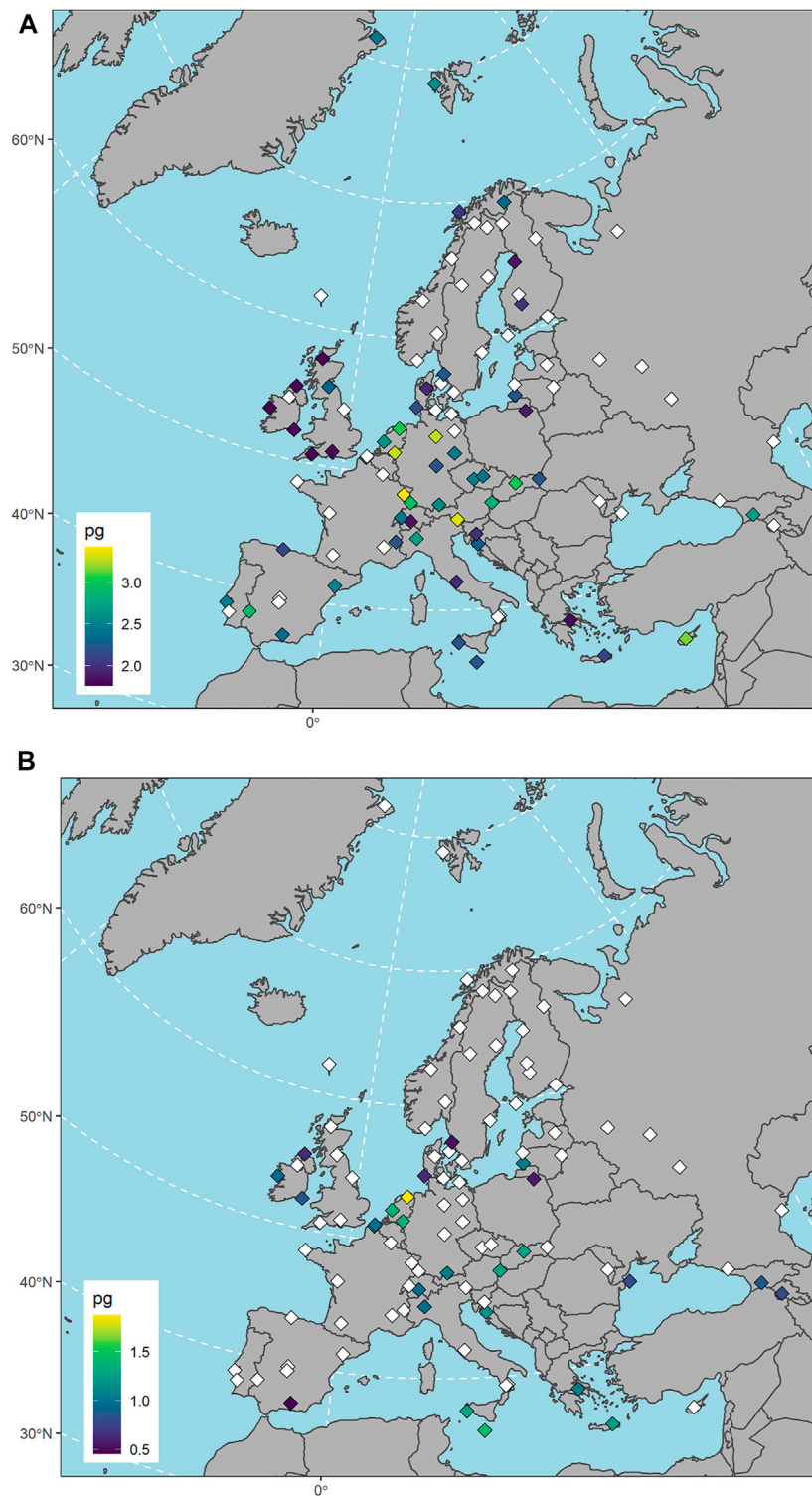
FIGURE 1
Spatial distribution of ΣDP (syn-DP + anti-DP) **(A)** and Dechlorane-602 **(B)**. Concentrations are displayed as log pg/sample to allow for visual comparison between the sample locations. Note the different scales between the two maps. Locations with concentrations of both DPs/Dec-602 below MDL are shown as white points. Equivalent maps for syn- and anti-DP separately are given in Supplementary Figure S1.

Spitsbergen/Zeppelin station is included in the Norwegian monitoring program for environmental contaminants in air and precipitation. The first AAS of dechloranes at Zeppelin were done in 2017. The syn-DP and anti-DP were detected in 35% and 30% of the

active air samples collected on weekly basis in 2017 with concentrations of <0.02–0.16 pg/m³ and <0.05–0.21 pg/m³, respectively (Bohlin-Nizzetto et al., 2018). The measured concentrations at Zeppelin in our study (0.6 pg/m³ for syn-DP and

1.4 pg/m^3 for anti-DP) were 30 times higher than the MDLs (i.e. medians) with AAS in 2017. This deviation is higher than observed for POPs at Zeppelin in the study of Lunder Halvorsen (SUBMITTED) and more than expected when considering the uncertainty of PAS and AAS in combination (Holt et al., 2017). Differences between the studies may be caused by different sampling techniques (AAS vs. PAS), different sampling periods (2016 vs. 2017) and different seasons (summer vs. annual). The uncertainty in the estimated sampling volumes is also higher when using a constant sampling rate of 2.3 m^3/day as in this study, compared to using site-specific sampling rates as in Lunder Halvorsen (SUBMITTED). A constant sampling rate does not account for sampling conditions such as temperature and wind speed at the sampling sites. Hence, it is possible that the elevated concentrations at Zeppelin measured in this study are caused by an underestimated sampling rate. However, the predominantly particle-bound dechloranes (Hansen et al., 2020) are less affected by changes in temperature than more volatile compounds, as the uptake is still in the linear phase regardless of the temperature (Shoeib and Harner, 2002; Bohlin-Nizzetto et al., 2020b). Neither was an elevated average wind speed observed at the site (Supplementary Table S3).

Figure 1A illustrates that while DP was detected across the whole study area, the abundance of samples above MDL was highest in central continental Europe. This indicates higher emissions in this region. Furthermore, a significant ($p = 0.04$) linear correlation was observed when plotting the logarithmic concentrations of ∑DP against latitude ($r = -0.21$), which may reflect LRAT from areas of high use to more remote areas. A similar pattern was also predicted by Hansen et al. (2020), which further suggested that DP in the Arctic is transported directly from source areas and that secondary re-emissions to air from surface media is less likely. In our study, no significant correlation with longitude was found ($r = -0.13$, $p = 0.22$).

Corresponding to Lunder Halvorsen (SUBMITTED), the sample locations were categorized into the regions northern Europe (NE), central-eastern Europe (CEE), southern Europe (SE) and western Europe (WE), based on the EuroVoc system (Supplementary Figure S2, Retrieved from https://eur-lex.europa.eu/browse/eurovoc.html). The highest detection frequencies of ∑DP were observed in SE and WE (71% and 70%, respectively), compared to CEE and NE (47% and 30%, respectively). In SE, the concentrations of ∑DP ranged from <MDL to 1400 pg/sample (median 140 pg/sample), with the highest concentration measured in Cyprus/Ayia Marina. In WE, the concentrations of ∑DP ranged from <MDL to 2700 pg/sample (France/Donon) and a median of 72 pg/sample. The median values in CEE and NE were both < MDL. The higher atmospheric concentrations of ∑DP observed in SE and WE may be linked to higher population density in these areas, compared to CEE and NE (Supplementary Figure S3). In our study, seven "suburban" sites were identified to have elevated population within an area of 50 km radius, due to a nearby city (Supplementary Figure S3) (Lunder Halvorsen et al., in review). This questions whether these seven sites are representative background sites in the measurement of dechloranes. The observed median concentration of ∑DP for these sites were significantly ($p = 0.002$) higher (280 pg/sample) than the median concentration of ∑DP in the 90 remaining samples (50 pg/sample), substantiating that there is a correlation between population density and atmospheric concentrations of ∑DP.

Large variations in atmospheric contaminant concentrations across a region may be interpreted as a continuing influence of primary emissions on atmospheric levels (Jaward et al., 2004; Halse et al., 2011). The spatial

variability of ∑DP, represented by the ratio between the maximum measured concentration (excluding outliers) and the minimum value (from MDLs), is 61. This is in the lower range of the variability found for POPs in European background air (max-min ratio <700) (Jaward et al., 2004; Halse et al., 2011). The max-min ratio is also lower than for the low-volatile POPs (e.g., >200 for sum of dichlorodiphenyldichloroethylenes (DDTs), outliers excluded) in the study of Lunder Halvorsen (SUBMITTED). This may be explained by higher and more variable contribution from blanks for ∑DP than for the legacy POPs, consequently resulting in higher MDLs and lower detection frequency. Still, compared to the even distribution of HCB (max-min ratio = 4) in Lunder Halvorsen (SUBMITTED), the spatial variability for ∑DP is higher. This may reflect the lower LRATP of less volatile compounds.

There is some uncertainty in the sampling methodology which may have affected the observed differences in measured concentrations between sites (Wania and Shunthirasingham, 2020). The uptake of contaminants to the PUF is influenced by the meteorological conditions at a given site. Though the PUF is sheltered with two surrounding steel bowls, it has been shown that wind generally has the strongest influence on the uptake rate (Schuster et al. (2021b).; Herkert et al., 2018). In our study, the sampling locations represented a broad range of elevations, ranging from sea level up to almost 4000 m (Supplementary Table S3), with variations in both temperature and wind speed. The average wind speeds (from European Centre for Medium-Range Weather Forecasts) for the sampling sites in the sampling period ranged from 2 to 7 m/s across the study region (Supplementary Table S3) (Lunder Halvorsen et al., in review). Similar to the study of Bohlin-Nizzetto et al. (2020a), no correlation with temperature was found. The concentrations of ∑DP (in pg/sample) were negatively correlated to wind speed ($r = -0.24$, $p = 0.02$), indicating that high concentrations are related to sites with low wind.

The detected syn-DP in our study ranged from <MDL to 390 pg/sample (1.9 pg/m^3) with a median concentration <MDL, as more than half of samples were below MDL (Table 1). Anti-DP ranged from <MDL to 2300 pg/sample (11 pg/m^3) with a median concentration <MDL (Table 1). Both syn- and anti-DP followed the same spatial pattern as for ∑DP, with the highest detection frequencies in SE and WE, compared to CEE and NE. Excluding the previously discussed outliers, the highest and second highest syn- and anti-DP concentrations were found in WE: 390 pg/sample syn-DP in Germany/Waldhof followed by 350 pg/sample syn-DP in France/Donon, and 2300 pg/sample anti-DP in France/Donon followed by 2000 pg/sample anti-DP in Austria/Vorhegg.

3.2 DP isomer fractional abundances

Anti-DP may be more prone to degradation in the environment than syn-DP, due to syn-DP being more sterically hampered (Olukunle et al., 2018). Hence, the isomer fraction f_{anti} can indicate whether DP has been affected by degradation and suggest if the measured DP originate from on-going emissions or not. For the sites that had concentrations >MDL of both DP isomers (37%), f_{anti} was calculated (range: 0.40–0.91, Supplementary Table S6). The spatial distribution of f_{anti} is shown in Figure 2. The lowest f_{anti}, found in Kosetice/Czech Republic, is well below the commercial mixture f_{anti} range (Figure 3). This site was supplied with two parallel samples and had a high RSD for syn-DP measured in the two parallels (85% for syn-DP, but 5% for anti-DP) (Supplementary Table S5). One of the parallels had ten times higher concentration of syn-DP than the other (360 pg/sample vs. 31 pg/sample), providing f_{anti} for each
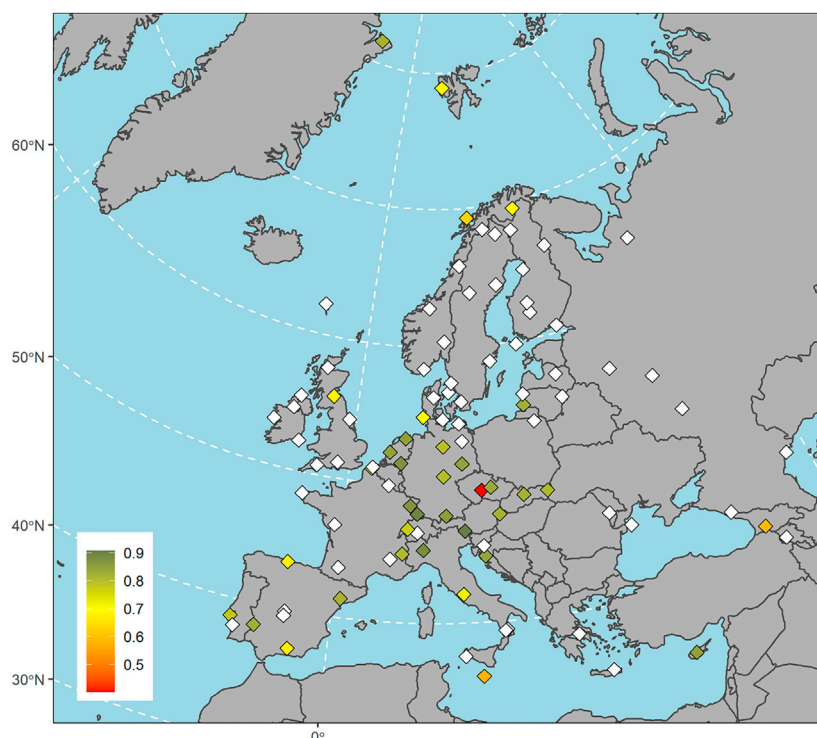
FIGURE 2
The fraction of the anti-DP isomer (f_{anti} = anti-DP/(ΣDP)) in samples where both the anti- and the syn-DP isomers are present. Sample locations where one or both DP isomers were below MDL are shown as white points. The commercial mixtures of DP have a f_{anti} between 0.59 and 0.80 (Wang et al., 2010).
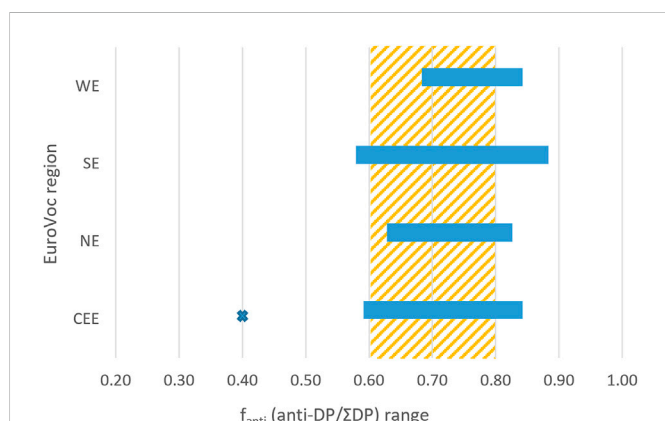

FIGURE 3
The range of the anti-DP fraction, f_{anti}, for the four different regions Western Europe (WE) (n = 16), Southern Europe (SE) (n = 9), Northern Europe (NE) (n = 5) and Central-Eastern Europe (CEE) (n = 6). The range of f_{anti} in commercial mixtures of DP is indicated as the orange shaded area. An outlier in the CEE region (Czech Republic/Kosetice) is seen as a blue cross at f_{anti} 0.4 and is discussed in the text.

for the EuroVoc regions SE, NE, WE, and CEE (Figure 3) show that there are no considerable differences in f_{anti} between the four regions. The f_{anti} was positively correlated with the measured concentration of ΣDP concentrations (r = 0.30, p = 0.004), indicating that f_{anti} decreases with distance from source areas. This makes sense as it reflects a higher atmospheric degradation of anti-DP further from source areas where ΣDP concentrations are lower. Hence, there are many indications in this study of existing sources of ΣDP to the European atmosphere, which is expected considering that DP is an unregulated compound.

3.3 Dechlorane related compounds

Of the DRCs, only Dec-602 was detected above MDL (<0.01–0.33 pg/m³). This indicates that the three other DRCs (Dec-601, -603, and -604) are not present or only present at low concentrations (MDLs: 2.6–6.7 pg/sample or 0.01–0.03 pg/m³) in the European background atmosphere. Higher detection frequency of Dec-602, compared to the other DRCs has also been reported in other studies (Supplementary Table S8). In the study of Yu et al. (2015) from Canada's Western Sub-Arctic, Dec-602 was in the range <MDL-0.06 pg/m³ (n = 42) during 2011–2014, whereas Dec-604 was detected in 2014. In the marine atmosphere from East China Sea to the Arctic, Dec-602 (<MDL - 0.2 pg/m³), Dec-603 (<MDL—0.4 pg/m³) and Dec-604 (<MDL - 0.05 pg/m³) were all detected using AAS (Moller et al., 2011; Moller et al., 2012). Higher concentrations of Dec-602, than in our study, were observed in the vicinity of a Chinese manufacturing facility (4.1–5.1 pg/m³) (Wang et al., 2010), while Dec-603 and Dec-604 were not detected. Atmospheric concentrations of Dec-602 and

parallel separately of 0.28 and 0.81, respectively. Hence, large uncertainty is associated with the f_{anti} for this site.

Disregarding f_{anti} from Czech Republic/Kosetice, the observed range of f_{anti} for the other sites (0.58–0.91) was close to the range for the commercial mixture of DP (0.59–0.80) (Wang et al., 2010). It is also in the same range as found for the background (0.63 ± 0.16) and polar (0.74 ± 0.15) sites in Schuster et al., 2021a. The overlapping f_{anti} ranges

Dec-603 using PAS were detected (<MDL—0.2 pg/m³) close to an urban region in Tanzania (Nipen et al., 2021).

The detection frequency of Dec-602 was 27% with concentrations ranging from <MDL to 74 pg/sample (Table 1), considerably lower than the concentrations of syn-DP and anti-DP. In samples where both Dec-602 and DP were detected (n = 23), Dec-602 was 1–18% of the concentration of ∑DP. This likely reflects lower primary emissions of Dec-602 than of DP in Europe.

The spatial distribution of Dec-602 is shown in Figure 1B. The highest concentration was measured in the Netherlands/Kollumerwaard (74 pg/sample, 0.33 pg/m³), followed by Malta/Giordan Lighthouse (27 pg/sample, 0.13 pg/m³) and the Netherlands/De Zilk (24 pg/sample, 0.11 pg/m³). Dec-602 has previously been measured in background atmospheric samples from Canada (0.004 pg/m³—0.06 pg/m³) (Yu et al., 2015); and in an Asian-Arctic marine transect (<0.003 pg/m³—0.02 pg/m³) (Moller et al., 2012). These concentrations are in the lower range of our measured Dec-602 concentrations. Since 2017, Dec-602 has been continuously screened for at the Zeppelin station, but not detected above MDLs (<0.025 pg/m³) (Bohlin-Nizzetto et al., 2020b). Dec-602 was not detected at Zeppelin in our study either (Supplementary Table S6).

A significant linear correlation was found between Dec-602 and ∑DP concentrations (r = 0.35, p < 0.001, n = 97) (Supplementary Figure S2A–C). This suggests that the sources and/or source regions of Dec-602 and DP are likely to be similar. For example, it cannot be excluded that Dec-602 may be an impurity in DP. As both Dec-602 and DP are likely to be predominantly sorbed to particles in the atmosphere, and have similar atmospheric half-lives (Zhang et al., 2016), their LRATP behaviour is also likely to be similar.

4 Conclusion

This study shows that syn- and anti-DP are present across the European continent, including parts of the Arctic. This supports that these compounds have potential for LRAT to remote regions. Concentrations of ∑DP correlated with latitude, with low detection of DP in northern Europe, and the highest concentrations observed in central continental Europe.

The individual isomers follow a similar spatial pattern. With f_{anti} fractions close to that of the commercial mixture of DP, the concentrations of DP in Europe are expected to be influenced by primary emissions. The max-min ratio of ∑DP concentrations (61), when excluding outliers, give further indications of continuing influence of primary emissions in the study area. Elevated concentrations of ∑DP for seven "suburban" sites, may suggest that primary emissions of DP are related to population density. More atmospheric monitoring, including consistent time-trends, is needed to elucidate the temporal trend of dechloranes in the atmosphere.

Dec-602 was the only DRC detected in our study, but was detected at lower concentrations compared to syn-/anti-DP (i.e., 1-18% of ∑DP). The other analysed DRCs were not detected above MDL at any of the sites across Europe (<0.03 pg/m³). This suggests generally lower primary emissions of DRCs than of DPs, and a significant correlation between Dec-602 and DP concentrations indicates similar sources and environmental behaviour of these compounds.

Our study shows that despite uncertainty related to the PAS methodology, it is suitable for assessing the spatial distribution of the dechloranes and estimate the background concentrations of the unregulated DP. However, the dominance of concentrations close to or below MDL indicates a need to reduce blank contamination or to consider measures increasing the sampling volume of DP and DRCs. This can be explored in future studies by deploying the PAS samplers for prolonged time periods, or by using sampling strategies targeting particle phase (e.g. AAS).

While ongoing air monitoring projects in Europe mainly focuses on POPs (Aas and Pernilla, 2018; Kalina et al., 2019; Schuster et al. (2021b)), our study shows that there is a need for future air monitoring efforts targeting dechloranes.

Data availability statement

The original contributions presented in the study are included in the article/Supplementary Material, further inquiries can be directed to the corresponding author.

Author contributions

KB contributed with the conceptualization and funding acquisition for the study. ISK supplied the resources and supervision of the study. The investigation, methodology, validation and project administration was carried out by HLH and LPS. LPS, HLH, CM, DH and SE contributed with the data curation and formal analysis. LPS wrote the original draft of the manuscript and carried out the visualization. All authors contributed to the manuscript revision, editing and approval of the submitted version.

Funding

Acknowledgments

Conflict of interest

The authors declare that the research was conducted in the absence of any commercial or financial relationships that could be construed as a potential conflict of interest.

Publisher's note

All claims expressed in this article are solely those of the authors and do not necessarily represent those of their affiliated

organizations, or those of the publisher, the editors and the reviewers. Any product that may be evaluated in this article, or claim that may be made by its manufacturer, is not guaranteed or endorsed by the publisher.

Supplementary material

The Supplementary Material for this article can be found online at: https://www.frontiersin.org/articles/10.3389/fenvs.2022.1083011/full#supplementary-material

References

Aas, W., and Pernilla, B-P., (2018). Heavy metals and POP measurements. EMEP/CCC-Report;3/2018.

Bergman, A., Ryden, A., Law, R. J., De Boer, J., Covaci, A., Alaee, M., et al. (2012). A novel abbreviation standard for organobromine, organochlorine and organophosphorus flame retardants and some characteristics of the chemicals. *Environ. Int.* 49, 57–82. doi:10.1016/j.envint.2012.08.003

Bohlin, P., Audy, O., Skrdlikova, L., Kukucka, P., Pribylova, P., Prokes, R., et al. (2014). Outdoor passive air monitoring of semi volatile organic compounds (SVOCs): A critical evaluation of performance and limitations of polyurethane foam (PUF) disks. *Environ. Sci. Process Impacts* 16, 433–444. doi:10.1039/c3em00644a

Bohlin-Nizzetto, P., Aas, W., Lunder Halvorsen, H., Nikiforov, V., and Pfaffhuber, K. A., (2020a). Monitoring of environmental contaminants in air and precipitation - annual report 2020. NILU report 12/2021.

Bohlin-nizzetto, P., Aas, W., and Nikiforov, V. (2020b). Monitoring of environmental contaminants in air and precipitation - annual report 2019. NILU report 06/2020.

Bohlin-nizzetto, P., Aas, W., and Warner, N. (2018). Monitoring of environmental contaminants in air and precipitation - annual report 2017. Report number: M-1062.

Bohlin-nizzetto, P., Melymuk, L., White, K. B., Kalina, J., Madadi, V. O., Adu-Kumi, S., et al. (2020c). Field- and model-based calibration of polyurethane foam passive air samplers in different climate regions highlights differences in sampler uptake performance. *Atmos. Environ.* 238, 117742. doi:10.1016/j.atmosenv.2020.117742

Chaemfa, C., Barber, J. L., Kim, K. S., Harner, T., and Jones, K. C. (2009). Further studies on the uptake of persistent organic pollutants (POPs) by polyurethane foam disk passive air samplers. *Atmos. Environ.* 43, 3843–3849. doi:10.1016/j.atmosenv.2009.05.020

Chen, S. J., Tian, M., Wang, J., Shi, T., Luo, Y., Luo, X. J., et al. (2011). Dechlorane Plus (DP) in air and plants at an electronic waste (e-waste) site in South China. *Environ. Pollut.* 159, 1290–1296. doi:10.1016/j.envpol.2011.01.026

Drage, D. S., Newton, S., De Wit, C. A., and Harrad, S. (2016). Concentrations of legacy and emerging flame retardants in air and soil on a transect in the UK West Midlands. *Chemosphere* 148, 195–203. doi:10.1016/j.chemosphere.2016.01.034

ECHA (2021). *ANNEX XV restriction report: Proposal for a restriction.* Helsinki, Finland: ECHA.

Halse, A. K., Schlabach, M., Eckhardt, S., Sweetman, A., Jones, K. C., and Breivik, K. (2011). Spatial variability of POPs in European background air. *Atmos. Chem. Phys.* 11, 1549–1564. doi:10.5194/acp-11-1549-2011

Hansen, K. M., Fauser, P., Vorkamp, K., and Christensen, J. H. (2020). Global emissions of dechlorane plus. *Sci. Total Environ.* 742, 140677. doi:10.1016/j.scitotenv.2020.140677

Herkert, J. K., Spak, S. N., Smith, A., Schuster, J. K., Harner, T., Martinez, A., et al. (2018). Calibration and evaluation of PUF-PAS sampling rates across the global atmospheric passive sampling (GAPS) network. *Environ. Sci. Process. Impacts* 20, 210–219. doi:10.1039/c7em00360a

Hoh, E., Zhu, L., and Hites, R. A. (2006). Dechlorane plus, a chlorinated flame retardant, in the Great Lakes. *Environ. Sci. Technol.* 40, 1184–1189. doi:10.1021/es051911h

Holt, E., Bohlin-Nizzetto, P., Boruvkova, J., Harner, T., Kalina, J., Melymuk, L., et al. (2017). Using long-term air monitoring of semi-volatile organic compounds to evaluate the uncertainty in polyurethane-disk passive sampler-derived air concentrations. *Environ. Pollut.* 220, 1100–1111. doi:10.1016/j.envpol.2016.11.030

Jaward, F. M., Farrar, N. J., Harner, T., Sweetman, A. J., and Jones, K. C. (2004). Passive air sampling of PCBs, PBDEs, and organochlorine pesticides across Europe. *Environ. Sci. Technol.* 38, 34–41. doi:10.1021/es034705n

Kalina, J., Scheringer, M., Boruvkova, J., Kukucka, P., Pribylova, P., Bohlin-Nizzetto, P., et al. (2017). Passive air samplers as a tool for assessing long-term trends in atmospheric concentrations of semivolatile organic compounds. *Environ. Sci. Technol.* 51, 7047–7054. doi:10.1021/acs.est.7b02319

Kalina, J., White, K. B., Scheringer, M., Pribylova, P., Kukucka, P., Audy, O., et al. (2019). Comparability of long-term temporal trends of POPs from co-located active and passive

air monitoring networks in Europe. *Environ. Sci. Process Impacts* 21, 1132–1142. doi:10.1039/c9em00136k

Klanova, J., Eupr, P., Kohoutek, J., and Harner, T. (2008). Assessing the influence of meteorological parameters on the performance of polyurethane foam-based passive air samplers. *Environ. Sci. Technol.* 42, 550–555. doi:10.1021/es072098o

Li, W. L., Liu, L. Y., Song, W. W., Zhang, Z. F., Qiao, L. N., Ma, W. L., et al. (2016). Five-year trends of selected halogenated flame retardants in the atmosphere of Northeast China. *Sci. Total Environ.* 539, 286–293. doi:10.1016/j.scitotenv.2015.09.001

Liu, L. Y., Salamova, A., Venier, M., and Hites, R. A. (2016). Trends in the levels of halogenated flame retardants in the Great Lakes atmosphere over the period 2005-2013. *Environ. Int.* 92-93, 442–449. doi:10.1016/j.envint.2016.04.025

Lunder Halvorsen, H., Bohlin-Nizzetto, P., Eckhardt, S., Gusev, A., Krogseth, I. S., Moeckel, C., et al. (2021). Main sources controlling atmospheric burdens of persistent organic pollutants on a national scale. *Ecotoxicol. Environ. Saf.* 217, 112172. doi:10.1016/j.ecoenv.2021.112172

Lunder Halvorsen, H., Bohlin-Nizzetto, P., Eckhardt, S., Gusey, A., Möckel, C., Shatalov, V., et al. ((in review)). Spatial variability of POPs in background air across Europe - changes over a decade and source contributions.

Markovic, M. Z., Prokop, S., Staebler, R. M., Liggio, J., and Harner, T. (2015). Evaluation of the particle infiltration efficiency of three passive samplers and the PS-1 active air sampler. *Atmos. Environ.* 112, 289–293. doi:10.1016/j.atmosenv.2015.04.051

Möller, A., Xie, Z., Cai, M., Sturm, R., and Ebinghaus, R. (2012). Brominated flame retardants and dechlorane plus in the marine atmosphere from Southeast Asia toward Antarctica. *Environ. Sci. Technol.* 46, 3141–3148. doi:10.1021/es300138q

Moller, A., Xie, Z., Cai, M., Zhong, G., Huang, P., Cai, M., et al. (2011). Polybrominated diphenyl ethers vs alternate brominated flame retardants and Dechloranes from East Asia to the Arctic. *Environ. Sci. Technol.* 45, 6793–6799. doi:10.1021/es201850n

Morin, N. A. O., Andersson, P. L., Hale, S. E., and Arp, H. P. H. (2017). The presence and partitioning behavior of flame retardants in waste, leachate, and air particles from Norwegian waste-handling facilities. *J. Environ. Sci. (China)* 62, 115–132. doi:10.1016/j.jes.2017.09.005

Nipen, M., Vogt, R. D., Bohlin-Nizzetto, P., Borga, K., Mwakalapa, E. B., Borgen, A. R., et al. (2021). Spatial trends of chlorinated paraffins and dechloranes in air and soil in a tropical urban, suburban, and rural environment. *Environ. Pollut.* 292, 118298. doi:10.1016/j.envpol.2021.118298

Olukunle, O. I., Lehman, D. C., Salamova, A., Venier, M., and Hites, R. A. (2018). Temporal trends of dechlorane plus in air and precipitation around the North American Great Lakes. *Sci. Total Environ.* 642, 537–542. doi:10.1016/j.scitotenv.2018.05.268

Ren, N., Sverko, E., Li, Y. F., Zhang, Z., Harner, T., Wang, D., et al. (2008). Levels and isomer profiles of dechlorane plus in Chinese air. *Environ. Sci. Technol.* 42, 6476–6480. doi:10.1021/es800479c

Röhler, L., Bohlin-Nizzetto, P., Rostkowski, P., Kallenborn, R., and Schlabach, M. (2021). Non-target and suspect characterisation of organic contaminants in ambient air – Part 1: Combining a novel sample clean-up method with comprehensive two-dimensional gas chromatography. *Atmos. Chem. Phys.* 21, 1697–1716. doi:10.5194/acp-21-1697-2021

Schuster, J. K., Harner, T., Eng, A., Rauert, C., Su, K., Hornbuckle, K. C., et al. (2021b). Tracking POPs in global air from the first 10 Years of the GAPS network (2005 to 2014). *Environ. Sci. Technol.* 55, 9479–9488. doi:10.1021/acs.est.1c01705

Schuster, J. K., Harner, T., and Sverko, E. (2021a). Dechlorane plus in the global atmosphere. *Environ. Sci. Technol. Lett.* 8, 39–45. doi:10.1021/acs.estlett.0c00758

Shen, L., Reiner, E. J., Macpherson, K. A., Kolic, T. M., Sverko, E., Helm, P. A., et al. (2010). Identification and screening analysis of halogenated norbornene flame retardants in the Laurentian Great Lakes: Dechloranes 602, 603, and 604. *Environ. Sci. Technol.* 44, 760–766. doi:10.1021/es902482b

Shoeib, M., and Harner, T. (2002). Characterization and comparison of three passive air samplers for persistent organic pollutants. *Environ. Sci. Technol.* 36, 4142–4151. doi:10.1021/es020635t

Sverko, E., Tomy, G. T., Reiner, E. J., Li, Y. F., Mccarry, B. E., Arnot, J. A., et al. (2011). Dechlorane plus and related compounds in the environment: A review. *Environ. Sci. Technol.* 45, 5088–5098. doi:10.1021/es2003028

Tørseth, K., Aas, W., Breivik, K., Fjæraa, A. M., Fiebig, M., Hjellbrekke, A. G., et al. (2012). Introduction to the European Monitoring and Evaluation Programme (EMEP) and observed atmospheric composition change during 1972–2009. *Atmos. Chem. Phys.* 12, 5447–5481. doi:10.5194/acp-12-5447-2012

UNEP (2022). Report of the persistent organic pollutants review committee on the work of its seventeenth meeting: Risk profile for dechlorane plus.

UNEP (2020). Stockholm convention on persistent organic pollutants (POPs), in *Texts and annexes. Revised in 2019.* Châtelaine, Switzerland: Secretariat of the Stockholm Convention.

Wang, D. G., Yang, M., Qi, H., Sverko, E., Ma, W. L., Li, Y. F., et al. (2010). An Asia-specific source of dechlorane plus: Concentration, isomer profiles, and other related compounds. *Environ. Sci. Technol.* 44, 6608–6613. doi:10.1021/es101224y

Wania, F., and Shunthirasingham, C. (2020). Passive air sampling for semi-volatile organic chemicals. *Environ. Sci. Process Impacts* 22, 1925–2002. doi:10.1039/d0em00194e

Yu, Y., Hung, H., Alexandrou, N., Roach, P., and Nordin, K. (2015). Multiyear measurements of flame retardants and organochlorine pesticides in air in Canada's western sub-arctic. *Environ. Sci. Technol.* 49, 8623–8630. doi:10.1021/acs.est.5b01996

Zhang, Q. H., Zhu, C. F., Zhang, H. D., Wang, P., Li, Y. M., Ren, D. W., et al. (2015). Concentrations and distributions of Dechlorane Plus in environmental samples around a Dechlorane Plus manufacturing plant in East China. *Science Bulletin* 60, 792–797. doi:10.1007/s11434-015-0768-1

Zhang, X., Suhring, R., Serodio, D., Bonnell, M., Sundin, N., and Diamond, M. L. (2016). Novel flame retardants: Estimating the physical-chemical properties and environmental fate of 94 halogenated and organophosphate PBDE replacements. *Chemosphere* 144, 2401–7. doi:10.1016/j.chemosphere.2015.11.017

Supplementary Material

1. **Supplementary text**

Instrumental analysis and quantification

The samples were analyzed for syn- and anti-DP, Dec-601, Dec-602, Dece-603 and Dec-604 using an Agilent 7890 gas chromatograph (GC) coupled to an Agilent 7200 high resolution quadruple time-of-flight mass spectrometer (HRqToFMS). 1 µL of the concentrated extract was injected into a Gerstel programmed temperature vaporization (PTV) injector operated in solvent vent mode. Two 15 m 0.25mmx0.25µm Agilent HP5 UI columns connected in series were used for separation, with Helium at 1.4 mL/min constant flow as carrier gas. The temperature program was 55°C, 2 min, 70°C/min to 200°C, 1 min, 10°C/min to 310°C, 0 min, 70 min°C/min to 325 min, 10 min. The MS was operated in electron capture negative ionization (ECNI) mode using methane as moderating gas and with an ion source at 120°C. The quantification was performed using MassHunter Quant version B.09.00, and integrated areas of targeted analytes and internal standards were used to quantify the concentration of Dechloranes (i.e. internal standard method).

2. Supplementary Figures and Tables

2.1. Tables

Table S1: Information on Mirex, Dechlorane Plus (Syn- and Anti-isomers) and Dechlorane Related Compounds Dechlorane-601, -602, -603, and -604. Information is collected from PubChem (Kim, 2021). *Where several abbreviations are available, the one used in this study is outlined in **bold**.

CAS#	Common name(s)*	Abbr.(s)*	Chemical formula	IUPAC	MW (g/mol)	Log K_{OA}
2385-85-5	**Mirex,** Dechlorane	MIREX	$C_{10}Cl12$	1,2,3,4,5,5,6,7,8,9,10,10-dodecachloropentacyclo[5.3.0.0^{2,6}.0^{3,9}.0^{4,8}]decane	545.5	11.3*
13560-89-9	**Dechlorane Plus,** Dechlorane-605	**DP**, Dec-605, DDC-CO	$C_{18}H_{12}Cl_{12}$	1,6,7,8,9,14,15,16,17,17,18,18-dodecachloropentacyclo[12.2.1.1^{6,9}.0^{2,13}.0^{5,10}]octadeca-7,15-diene	653.7	14.8*
135821-03-3	*Syn-*Dechlorane Plus	**Syn-DP**, Syn-DDC-CO	DP isomer	-	-	-
135821-74-8	*Anti-*Dechlorane Plus	**Anti-DP**, Anti-DDC-CO	DP isomer	-	-	-
13560-90-2	Dechlorane-601	**Dec-601**, DDC-ID	$C_{20}H_{12}Cl_{12}$	4,5,6,7,13,14,15,16,19,19,20,20-dodecachloroheptacyclo[9.6.1.14,7.113,16.02,10.03,8.012,17]icosa-5,14-diene	677.7	16.7**
31107-44-5	Dechlorane-602	**Dec-602**, DDC-DBF	$C_{14}H_4Cl_{12}O$	1,4,5,6,7,11,12,13,14,14,15,15-dodecachloro-9-oxapentacyclo[9.2.1.1^{4,7}.0^{2,10}.0^{3,8}]pentadeca-5,12-diene	613.6	15.0*
13560-92-4	Dechlorane-603	**Dec-603**, DDC-Ant	$C_{17}H_8Cl_{12}$	3,4,5,6,10,11,12,13,16,16,17,17-dodecachlorohexacyclo[6.6.1.1^{3,6}.1^{10,13}.0^{2,7}.0^{9,14}]heptadeca-4,11-diene	637.7	15.2*
34571-16-9	Dechlorane-604	**Dec-604**, HCTBPH	$C_{13}H_4Br_4Cl_6$	1,2,3,4,7,7-hexachloro-5-(2,3,5,6-tetrabromophenyl)bicyclo[2.2.1]hept-2-ene	692.5	14.9*

*EPI Suite estimations collected from Zhang et al. (2016).

**EAS-E Suite (Ver.0.96 - BETA, release Nov., 2022). www.eas-e-suite.com. Accessed 28.11.2022. Developed by ARC Arnot Research and Consulting Inc., Toronto, ON, Canada

Table S2: Chemical structures of Mirex, Dechlorane Plus and Dechlorane Related Compounds Dechlorane-601, -602, -603, and -604. Collected from https://pubchem.ncbi.nlm.nih.gov/ (Kim, 2021).
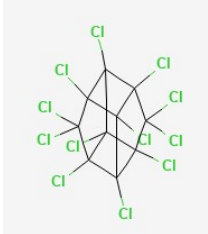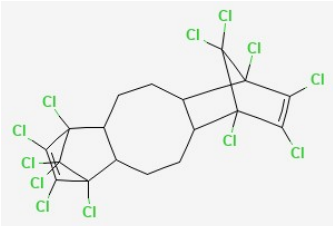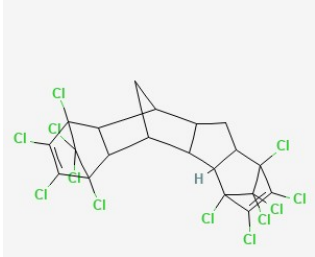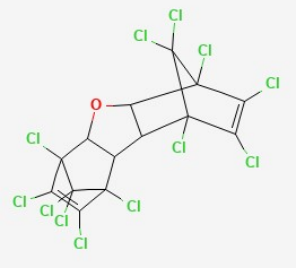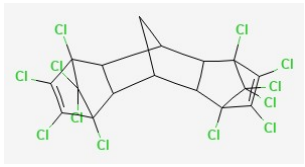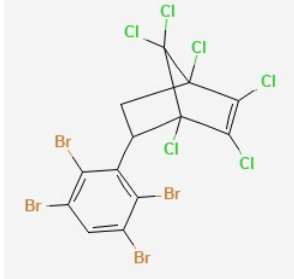
Mirex	Dechlorane Plus	Dechlorane-601
Dechlorane-602	**Dechlorane-603**	**Dechlorane-604**

Table S3: Station name, country, geographic coordinates, sampling periods, temperature, wind speed, orography, exposure time, applied sample volume (estimated from a sampling rate of 2.26 m³/day and the exposure time).

Station	Country	Lat. (°N)	Long. (°E)	T[1] (°C)	Wind speed[1] (m/s)	Altitude[1] (m.a.s.l.)	Sampling start	Sampling end	Exp. time (days)	Vol. (m³)
ARM/Amberd*	Armenia	40.4	44.3	18	2.39	2080	24.06.2016	23.09.2016	91	206
AUT/Illmitz	Austria	47.8	16.8	20.5	2.94	117	22.06.2016	27.09.2016	97	219
AUT/Vorhegg	Austria	46.7	13.0	14.9	2.02	1020	13.07.2016	05.10.2016	84	190
BEL/Houtem	Belgium	51.0	2.6	18.3	4.2	10	01.07.2016	30.09.2016	91	206
BEL/Koksijde	Belgium	51.1	2.7	18.3	4.2	4	01.07.2016	30.09.2016	91	206
CHE/Jungfraujoch	Switzerland	46.5	8.0	-0.7	1.54	3578	13.07.2016	06.10.2016	85	192
CHE/Payerne	Switzerland	46.8	6.9	15.7	2.09	489	06.07.2016	12.10.2016	98	221
CYP/Ayia Marina	Cyprus	35.0	33.1	29	3.18	520	23.06.2016	15.09.2016	84	190
CZE/Kosetice*	Czech Republic	49.6	15.0	18.3	2.87	535	24.06.2016	26.09.2016	94	212
CZE/Svratouch	Czech Republic	49.7	16.0	18.7	3.04	737	22.06.2016	23.09.2016	93	210
DEU/Hohenpeissenberg	Germany	47.8	11.0	16.7	2.17	985	28.06.2016	28.09.2016	92	208
DEU/Melpitz	Germany	51.5	12.9	19.6	3.06	86	20.06.2016	19.09.2016	91	206
DEU/Neuglobsow	Germany	53.2	13.0	18.1	3.39	62	01.07.2016	04.10.2016	95	215
DEU/Schaulnsland	Germany	47.9	7.9	14.1	2.1	1205	01.07.2016	30.09.2016	91	206
DEU/Schmücke	Germany	50.7	10.8	17.6	2.86	937	01.07.2016	30.09.2016	91	206
DEU/Waldhof*	Germany	52.8	10.8	18.2	3.5	74	01.07.2016	30.09.2016	91	206
DEU/Westerland*	Germany	54.9	8.3	16.9	5.9	12	01.07.2016	05.10.2016	96	217
DEU/Zingst	Germany	54.4	12.7	17.6	6.16	1	01.07.2016	30.09.2016	91	206
DNK/Anholdt	Denmark	56.7	11.5	16.8	6.61	40	01.07.2016	01.10.2016	92	208
DNK/Keldsnor	Denmark	54.7	10.7	17.5	5.36	10	27.06.2016	16.09.2016	81	183
DNK/Tange	Denmark	56.4	9.6	16	4.48	13	30.06.2016	29.09.2016	91	206
ESP/Barcarrota	Spain	38.5	-6.9	23.5	2.37	393	28.07.2016	28.10.2016	92	208
ESP/Els Torms	Spain	41.4	0.7	19.8	2.03	470	05.08.2016	07.11.2016	94	212
ESP/Mahon	Spain	39.9	-4.3	21.6	2.36	78	02.08.2016	02.11.2016	92	208
ESP/Niembro	Spain	43.4	-4.9	17.2	4.23	134	09.08.2016	09.11.2016	92	208
ESP/San Pablo de los Montes	Spain	39.5	-4.4	18.1	2.47	917	02.08.2016	02.11.2016	92	208

Station	Country									
ESP/Viznar*	Spain	37.2	-3.5	15.1	2.66	1265	27.07.2016	04.11.2016	100	226
FIN/Hailuoto	Finland	65.0	24.7	13.9	5.08	4	04.07.2016	04.10.2016	92	208
FIN/Hyytiälä	Finland	61.9	24.3	13.6	3.1	181	04.07.2016	03.10.2016	91	206
FIN/Oulanka	Finland	66.3	29.4	12.4	2.78	310	01.07.2016	30.09.2016	91	206
FIN/Pallas*	Finland	68.0	24.1	11.4	2.9	340	30.06.2016	04.10.2016	96	217
FIN/Utö	Finland	59.8	21.4	15.9	6.37	7	01.07.2016	02.10.2016	93	210
FIN/Virolahti	Finland	60.5	27.7	15.7	5.24	4	01.07.2016	30.09.2016	91	206
FIN/Ähtäri	Finland	62.6	24.2	13.7	3.05	162	30.06.2016	30.09.2016	92	208
FRA/Donon	France	48.5	7.1	18.6	2.36	775	05.07.2016	04.10.2016	91	206
FRA/La Tardiére	France	46.7	-0.8	19.6	3.16	133	28.06.2016	27.09.2016	91	206
FRA/Le Casset	France	45.0	6.5	15.1	1.58	1750	28.06.2016	27.09.2016	91	206
FRA/Peyrusse V	France	43.6	0.2	20	2.03	200	28.06.2016	27.09.2016	91	206
FRA/Porspoder	France	48.5	-4.8	16.8	5.89	50	02.07.2016	05.10.2016	95	215
FRA/Revin	France	49.9	4.6	17.9	3.24	390	28.06.2016	27.09.2016	91	206
FRA/St.Nazaire	France	44.6	5.3	17.8	2.82	605	05.07.2016	11.10.2016	98	221
GBR/Auchencorth Moss	United Kingdom	55.8	-3.2	14.5	4.61	260	01.07.2016	28.09.2016	89	201
GBR/Chilbolton	United Kingdom	51.1	-1.4	17.2	4.28	78	29.06.2016	27.09.2016	90	203
GBR/High Muffles	United Kingdom	54.3	-0.8	15.4	5.62	267	29.06.2016	28.09.2016	91	206
GBR/Lough Navar	United Kingdom	54.4	-7.9	14.1	5.01	126	01.07.2016	03.10.2016	94	212
GBR/Strathvaich Dam	United Kingdom	57.7	-4.8	12.8	5.08	270	01.07.2016	03.10.2016	94	212
GBR/Yarner Wood*	United Kingdom	50.7	-3.7	16.1	5.98	119	05.07.2016	11.10.2016	98	221
GEO/Abastumani	Georgia	41.8	42.8	19.2	1.99	1650	21.06.2016	14.09.2016	85	192
GLN/Nord	Greenland	81.6	-16.7	-12.8	5.48	20	01.09.2016	04.12.2016	94	212
GRC/Aliartos	Greece	38.4	23.1	24.1	2.88	110	07.07.2016	07.10.2016	92	208
GRC/Finokalia	Greece	35.3	25.7	25.2	7.1	250	28.06.2016	04.10.2016	98	221
GRL/Norðuri á Fossum	Faroe Islands	62.2	-7.2	10.9	7.26	300	01.07.2016	01.10.2016	92	208

HRV/Zavizan	Croatia	44.8	15.0	12.5	3.37	1594	30.06.2016	29.09.2016	91	206
IRL/Carnsore Park	Ireland	52.2	-6.4	15.4	6.65	9	13.07.2016	12.10.2016	91	206
IRL/Mace Head	Ireland	53.3	-9.9	14.6	7.49	5	13.07.2016	11.10.2016	90	203
IRL/Malin Head	Ireland	55.4	-7.3	14.3	6.75	20	01.06.2016	29.09.2016	120	271
ITA/Capo Granitola	Italy	37.6	12.7	24.7	4.37	5	17.06.2016	21.09.2016	96	217
ITA/Ispra**	Italy	45.3	8.6	19.8	1.95	209	01.07.2016	30.09.2016	91	206
ITA/Longobucco	Italy	39.4	16.6	23.2	2.56	1379	04.07.2016	17.10.2016	105	237
ITA/Monte Curcio	Italy	39.3	16.4	13.3	2.56	1796	04.07.2016	17.10.2016	105	237
ITA/Montelibretti**	Italy	42.1	12.6	23.6	2.04	48	30.06.2016	29.09.2016	91	206
LTU/Preila	Lithuania	55.4	21.0	17.1	5.01	5	01.07.2016	01.10.2016	92	208
LTU/Rugsteliskis	Lithuania	55.4	26.1	13.6	3.62	120	19.07.2016	19.10.2016	92	208
LVA/Rucava	Latvia	56.2	21.2	15.3	5.75	18	01.07.2016	21.10.2016	112	253
LVA/Zoseni*	Latvia	57.1	25.9	13.2	3.8	188	05.07.2016	24.10.2016	111	251
MDA/Leova	Moldova	46.5	28.3	21.4	3.13	156	04.07.2016	04.10.2016	92	208
MLT/Giordan Lighthouse**	Malta	36.1	14.2	25.5	4.41	167	01.07.2016	30.09.2016	91	206
NLD/De Zilk**	Netherlands	52.3	4.5	17.2	5.68	4	14.07.2016	19.10.2016	97	219
NLD/Kollumerwaard	Netherlands	53.3	6.3	16.9	6.14	1	13.07.2016	19.10.2016	98	221
NLD/Vredepeel**	Netherlands	51.5	5.9	17.2	3.38	28	12.07.2016	18.10.2016	98	221
NOR/Andøya	Norway	69.3	16.0	11	5.23	338	27.06.2016	05.10.2016	100	226
NOR/Birkenes*	Norway	58.4	8.3	14.2	3.76	199	11.07.2016	10.10.2016	91	206
NOR/Hurdal	Norway	60.4	11.1	12.8	2.55	280	14.07.2016	12.10.2016	90	203
NOR/Karasjok	Norway	69.5	25.5	11.1	3.04	308	23.06.2016	23.09.2016	92	208
NOR/Kårvatn	Norway	62.8	8.9	12	2.79	208	06.07.2016	02.10.2016	88	199
NOR/Tustervatn	Norway	65.8	13.9	10.8	2.71	475	30.06.2016	29.09.2016	91	206
NOR/Zeppelin	Norway	78.9	11.9	4.3	3.76	474	07.07.2016	28.09.2016	83	188
POL/Diabla Gora	Poland	54.1	22.0	16.6	3.27	157	01.07.2016	01.10.2016	92	208
PRT/Alfragide**	Portugal	38.7	-9.2	21.5	5.22	109	08.07.2016	10.10.2016	94	212
PRT/Monte Velho	Portugal	38.1	-8.8	21.3	5.44	43	07.07.2016	07.10.2016	92	208
RUS/Astrakhan	Russia	45.8	47.9	23.1	4.16	-25	13.07.2016	10.10.2016	89	201
RUS/Caucasus	Russia	43.7	40.2	21.1	2.77	400	09.07.2016	12.10.2016	95	215

RUS/Danki	Russia	54.9	37.8	17	3.65	150	01.07.2016	01.10.2016	92	208
RUS/Lesnoy	Russia	56.4	32.9	14.6	3.88	340	12.07.2016	10.10.2016	90	203
RUS/Pinega	Russia	64.6	43.2	14.9	3.1	28	01.07.2016	30.09.2016	91	206
RUS/Voronezh	Russia	51.9	39.6	17.8	3.55	145	12.07.2016	12.10.2016	92	208
SVK/Chopok	Slovakia	49.0	19.6	7.3	2.36	2008	01.07.2016	04.10.2016	95	215
SVK/Starina	Slovakia	49.0	22.3	17.7	2.55	345	01.07.2016	03.10.2016	94	212
SVN/Iskrba	Slovenia	45.6	14.9	19.7	2.48	520	01.07.2016	30.09.2016	91	206
SWE/Abisko	Sweden	68.4	18.8	10.2	2.53	385	23.06.2016	26.09.2016	95	215
SWE/Aspvreten	Sweden	58.8	17.4	16	3.77	20	07.07.2016	03.10.2016	88	199
SWE/Bredkälen	Sweden	63.8	15.3	10.9	2.85	404	05.07.2016	11.10.2016	98	221
SWE/Esrange	Sweden	67.9	21.1	9.1	2.81	475	21.06.2016	24.10.2016	125	283
SWE/Råö*/**	Sweden	57.4	11.9	15.8	4.5	5	27.06.2016	03.10.2016	98	221
SWE/Vavihill	Sweden	56.0	13.1	16.4	4.31	175	13.06.2016	30.09.2016	109	246
SWE/Vindeln	Sweden	64.2	19.8	12.6	3.16	225	30.06.2016	10.10.2016	102	231
UKR/Zmeiny Island*	Ukraine	45.3	30.2	22.8	4.51	-	01.07.2016	30.09.2016	91	206

*PAS locations supplied with two parallel PAS for evaluation of method reproducibility

**Identified as "suburban" sites

[1]Lunder Halvorsen (SUBMITTED)

Table S4: Recoveries of the isotope-labelled internal standard in laboratory blanks, field blanks and exposed samples, given as the range, average ± standard deviation, and median of recoveries in %.

	Range (%)	Average ± St.Dev (%)	Median (%)
Laboratory blanks (n=14)	81.2 – 173.8	108.2 ± 23.8	105.6
Field blanks (n=3)	84.9 – 145.5	110.9 ± 25.5	102.4
Exposed samples (n=115)	22.8 – 187.5	80.0 ± 26.3	80.5

Table S5: Relative standard deviation (RSD) (%) calculated from the concentration (pg/sample) of syn-DP, anti-DP and Dec-602 in two parallel PAS deployed at each station (n=11). Stations where the compounds were below MDL in one or both samples, thus prohibiting the calculation of the RSD, are indicated with "-".

Station	Country	Syn-DP RSD (%)	Anti-DP RSD (%)	Dec-602 RSD (%)
ARM/Amberd	Armenia	-	-	-
CZE/Kosetice	Czech Republic.	85	5	-
DEU/Waldhof	Germany	33	40	-
DEU/Westerland	Germany	15	3	-
ESP/Viznar	Spain	9	17	-
FIN/Pallas	Finland	-	-	-
GBR/Yarner Wood	Great Britain	13	8	-
LVA/Zoseni	Latvia	8	7	-
NOR/Birkenes	Norway	-	-	-
SWE/Råö	Sweden	37	52	-
UKR/Zmeiny Island	Ukraine	-	-	4

Table S6: Concentrations of Syn-DP, Anti-DP, ΣDP (Syn-DP + Anti-DP), and Dec-602 given in pg/sample and pg/m³ (in brackets), in addition to the region of the sample location (based on the EuroVoc system), and the Anti-DP fraction f_{anti} where both DP isomers were detected above MDL.

Station	EuroVoc	Syn-DP pg/sample (pg/m³)	Anti-DP pg/sample (pg/m³)	ΣDP pg/sample (pg/m³)	Dec-602 pg/sample (pg/m³)	f_{anti}
ARM/Amberd I	CEE	<MDL (<MDL)	<MDL (<MDL)	<MDL (<MDL)	6.1 (0.03)	-
AUT/Illmitz	WE	115.9 (0.53)	530.6 (2.42)	646.5 (2.95)	18.7 (<MDL)	0.82
AUT/Vorhegg	WE	207.6 (1.09)	2043.8 (10.77)	2251.4 (11.86)	<MDL (0.09)	0.91
BEL/Houtem	WE	53.4 (0.26)	144.8 (0.7)	198.2 (0.96)	20.9 (<MDL)	0.73
BEL/Koksijde	WE	<MDL (<MDL)	<MDL (<MDL)	<MDL (<MDL)	9.2 (0.1)	-
CHE/Jungfraujoch	WE	39.5 (0.21)	<MDL (<MDL)	39.5 (0.21)	9.3 (0.04)	-
CHE/Payerne	WE	62 (0.28)	209.4 (0.95)	271.5 (1.23)	<MDL (0.05)	0.77
CYP/Ayia Marina	SE	216.9 (1.14)	1218.7 (6.42)	1435.6 (7.56)	<MDL (<MDL)	0.85
CZE/Kosetice I	CEE	188.3 (0.89)	126.9 (0.6)	315.1 (1.48)	<MDL (<MDL)	0.4
CZE/Svratouch	CEE	42.7 (0.2)	217.5 (1.04)	260.2 (1.24)	<MDL (<MDL)	0.84
DEU/Hohenpeissenberg	WE	53.1 (0.26)	317.3 (1.53)	370.5 (1.78)	11.2 (<MDL)	0.86
DEU/Melpitz	WE	42.3 (0.21)	235.7 (1.15)	278 (1.35)	<MDL (<MDL)	0.85
DEU/Schaulnsland	WE	95.8 (0.47)	832.1 (4.05)	928 (4.51)	<MDL (<MDL)	0.9
DEU/Schmücke	WE	31.4 (0.15)	125.7 (0.61)	157 (0.76)	<MDL (<MDL)	0.8
DEU/Waldhof I	WE	391.5 (1.9)	1534.1 (7.46)	1925.6 (9.36)	<MDL (<MDL)	0.8
DEU/Westerland I	WE	44.5 (0.21)	102.5 (0.47)	147.1 (0.68)	4.3 (<MDL)	0.7
DNK/Tange	NE	<MDL (<MDL)	80 (0.39)	80 (0.39)	<MDL (<MDL)	-
ESP/Barcarrota	SE	137.5 (0.66)	648.1 (3.12)	785.6 (3.78)	<MDL (<MDL)	0.82
ESP/Els Torms	SE	59.1 (0.28)	269.5 (1.27)	328.6 (1.55)	<MDL (<MDL)	0.82
ESP/Niembro	SE	43.9 (0.21)	95 (0.46)	139 (0.67)	<MDL (<MDL)	0.68
ESP/Viznar I	SE	73.7 (0.33)	153.4 (0.68)	227.1 (1)	2.8 (<MDL)	0.68
FIN/Hailuoto	NE	42.1 (0.2)	<MDL (<MDL)	42.1 (0.2)	<MDL (<MDL)	-
FIN/Hyytiälä	NE	80.2 (0.39)	<MDL (<MDL)	80.2 (0.39)	<MDL (<MDL)	-
FRA/Donon	WE	346.1 (1.68)	2309.6 (11.23)	2655.7 (12.91)	<MDL (<MDL)	0.87
FRA/Le Casset	WE	31 (0.15)	130.1 (0.63)	161 (0.78)	<MDL (<MDL)	0.81

Site	Region					
GBR/Auchencorth Moss	WE	68.3 (0.34)	147.2 (0.73)	215.5 (1.07)	<MDL (<MDL)	0.68
GBR/Chilbolton	WE	34.9 (0.17)	<MDL (<MDL)	34.9 (0.17)	<MDL (<MDL)	-
GBR/Strathvaich Dam	WE	25.4 (0.12)	<MDL (<MDL)	25.4 (0.12)	<MDL (<MDL)	-
GBR/Yarner Wood I	WE	26.4 (0.12)	<MDL (<MDL)	26.4 (0.12)	<MDL (<MDL)	-
GEO/Abastumani	CEE	202.4 (1.05)	292.6 (1.52)	495 (2.58)	7.5 (<MDL)	0.59
GRL/Nord	NE	49.1 (0.23)	222.6 (1.05)	271.7 (1.28)	<MDL (<MDL)	0.82
GRC/Aliartos	SE	34 (0.16)	<MDL (0.3)	34 (0.47)	11.6 (<MDL)	-
GRC/Finokalia	SE	100.3 (0.45)	<MDL (<MDL)	100.3 (0.45)	17.4 (<MDL)	-
HRV/Zavizan	CEE	30.2 (0.15)	161.1 (0.78)	191.3 (0.93)	15.3 (<MDL)	0.84
IRL/Carnsore Park	WE	31.2 (0.15)	<MDL (<MDL)	31.2 (0.15)	7.2 (<MDL)	-
IRL/Mace Head	WE	27.1 (0.13)	<MDL (<MDL)	27.1 (0.13)	8.9 (0.04)	-
IRL/Malin Head	WE	31.2 (0.11)	<MDL (<MDL)	31.2 (0.11)	4.4 (<MDL)	-
ITA/Capo Granitola	SE	<MDL (<MDL)	148.4 (0.68)	148.4 (0.68)	19.4 (0.02)	-
ITA/Ispra	SE	59.6 (0.29)	452.9 (2.2)	512.5 (2.49)	9.1 (0.06)	0.88
ITA/Montelibretti	SE	26.2 (0.13)	67 (0.33)	93.3 (0.45)	<MDL (0.07)	0.72
LTU/Preila	NE	28.7 (0.14)	136.5 (0.66)	165.2 (0.79)	11.4 (0.01)	0.83
MLT/Giordan Lighthouse	SE	70.5 (0.34)	97 (0.47)	167.5 (0.81)	27.2 (0.04)	0.58
NLD/De Zilk	WE	65.9 (0.3)	363.8 (1.66)	429.7 (1.96)	24.3 (<MDL)	0.85
NLD/Kollumerwaard	WE	164.3 (0.74)	946.5 (4.27)	1110.8 (5.02)	74 (<MDL)	0.85
NLD/Vredepeel	WE	247 (1.12)	1681.8 (7.59)	1928.9 (8.71)	23 (<MDL)	0.87
NOR/Andøya	NE	41.2 (0.18)	69.7 (0.31)	110.9 (0.49)	<MDL (0.06)	0.63
NOR/Karasjok	NE	66.3 (0.32)	152.5 (0.73)	218.8 (1.05)	<MDL (<MDL)	0.7
NOR/Zeppelin	NE	115.5 (0.62)	269.1 (1.43)	384.6 (2.05)	<MDL (0.13)	0.7
POL/Diabla Gora	CEE	<MDL (<MDL)	66.9 (0.32)	66.9 (0.32)	3.7 (0.11)	-
PRT/Alfragide	SE	61.1 (0.29)	222.7 (1.05)	283.8 (1.34)	<MDL (0.33)	0.78
SVK/Chopok	CEE	185.8 (0.87)	861.6 (4.01)	1047.4 (4.88)	18.8 (<MDL)	0.82
SVK/Starina	CEE	33.1 (0.16)	139.8 (0.66)	172.9 (0.81)	<MDL (<MDL)	0.81
SVN/Iskrba	CEE	<MDL (0.11)	89.1 (0.43)	89.1 (0.54)	<MDL (0.02)	-
SWE/Råö I	NE	<MDL (<MDL)	166.3 (0.75)	166.3 (0.75)	3.4 (<MDL)	-
UKR/Zmeiny Island I	CEE	<MDL (<MDL)	<MDL (<MDL)	<MDL (<MDL)	6.3 (<MDL)	-

Table S7: Concentrations of Syn- and Anti-DP measured at stations identical between this study (Skogeng, sampled in 2016) and Schuster et al. (2021) (sampled in 2005/6).

| Station	Country	Schuster et al. (2021)			Diff. Schuster-Skogeng			Ratio (pg/m³) (Schuster/Skogeng)
		Syn-DP (pg/m³)	Anti-DP (pg/m³)	ΣDP (pg/m³)	Syn-DP (pg/m³)	Anti-DP (pg/m³)	ΣDP (pg/m³)	
CZE/Kosetice	Czech Republic	0.11	0.13	0.24	-0.77	-0.47	-1.24	0.16
FIN/Pallas	Finland	0.09	0.14	0.23	-0.01	-0.17	-0.18	0.56
IRL/Malin Head	Ireland	0.03	0.07	0.1	-0.08	-0.24	-0.32	0.23
NOR/Zeppelin	Norway	1.25	3.08	4.32	0.63	1.64	2.27	2.11
RUS/Danki	Russia	0.01	0.07	0.1	-0.09	-0.24	-0.31	0.24

Table S8: Studies reporting atmospheric concentrations of Dechlorane Plus and Dechlorane Related Compounds, given in pg/m³ and pg/sample (in brackets). BG: Background

Country/ region	Type	Sampling	Anti-DP pg/m³ (pg)	Syn-DP pg/m³ (pg)	ΣDP pg/m³ (pg)	Dec-601 pg/m³ (pg)	Dec-602 pg/m³ (pg)	Dec-603 pg/m³ (pg)	Dec-604 pg/m³ (pg)	Ref.
Europe	BG	PAS	<MDL – 11.2 (<MDL - 2310)	<MDL – 1.9 (<MDL – 392)	0.1 – 12.9 (25 - 2655)	<MDL (<MDL)	<MDL – 0.3 (<MDL - 74)	<MDL (<MDL)	<MDL (<MDL)	This study
Great Lakes	(not found)	AAS			<MDL - 490					(Hoh et al., 2006)
Great Lakes	(not found)	AAS			0.26 – 0.43					(Liu et al., 2016)
Greenland	BG	AAS	<MDL - 33.14	<MDL - 8.99						(Vorkamp et al., 2015)
Arctic-Antarctica	Marine	AAS	0.01 - 1.22	0.01 - 1.34						(Moller et al., 2010)

Location	Site	Method							Reference
Asia-Arctic	Marine	AAS	0.01 - 0.88	0.01 - 2.39	0.01 - 1.4	<MDL - 0.2	<MDL - 0.44	<MDL - 0.05	(Moller et al., 2011)
Asia-Antarctica	Marine	AAS	<MDL - 5.6	<MDL - 5.8			<MDL - 0.39		(Moller et al., 2012)
China	Industry	AAS			13.1 - 1794				(Chen et al., 2011)
China	Background	AAS			0.47 - 35.7				(Chen et al., 2011)
China	Urban	AAS	<MDL - 190	<MDL - 52	<MDL - 240				(Li et al., 2016)
China	Urban	PAS			(<MDL - 13296.6)				
China	Rural	PAS	5.8	1.9	(<MDL - 3854.3)				(Ren et al., 2008)
Norway	Industry	AAS	4.2 - 14.7	2.5 - 14.9	6.8 - 29				
Norway	Industry	AAS	648.9 - 1243.5	555.9 - 742.8	1204.9 - 1986.3				
Norway	Industry	AAS	9.1 - 24.6	5.6 - 19	14.7 - 43.6				
Norway	Industry	PAS	<MDL - 3.2	<MDL - 3.7	<MDL - 6.9				
Norway	Industry	PAS	1.8 - 39.2	1 - 28.5	2.8 - 67.6				
Norway	Industry	PAS	0.5 - 4.2	0.6 - 2.1	1 - 6.3				(Morin et al., 2017)
Norway	BG	PAS							
Canada	BG	AAS	0 - 2.8	<MDL - 0.67					(Vorkamp et al., 2019)
Canada	(not found)	PAS	0.01 - 1.04	0 - 0.72		0 - 0.06		0.02 - 0.12	(Yu et al., 2015)
Great Lakes	Urban, rural, BG	AAS			<MDL - 4.42				(Olukunle et al., 2018)
Svalbard	Urban	AAS	0.15 - 4.2	0.05 - 0.91	0.05 - 5.03				(Salamova et al., 2014)

Country	Site	Method						Reference
Tanzania	Rural	PAS	<MDL - 1 (90 - 100)					(Nipen et al., 2021)
Tanzania	Suburban	PAS	<MDL - 2 (90 - 300)	<MDL - 0.8 (60 - 100)				
Tanzania	Urban	PAS	<MDL - 16 (90 - 2000)	<MDL - 4 (60 - 500)		<MDL - 0.2 (1 - 30)	<MDL - 0.2 (1 - 30)	
Tanzania	Industry	PAS	<MDL - 7 (90 - 1000)	<MDL - 2 (60 - 300)		<MDL - 0.2 (1 - 30)	<MDL - 0.04 (1 - 6)	
China	Industry	AAS			7723 - 26734	4.1 - 5.14	<MDL	(Wang et al., 2010)
Europe	Urban	PAS	<MDL - 1.79	<MDL - 0.92	0.15 - 2.23			
Europe	Rural	PAS	<MDL - 0.68	<MDL - 0.22	0.04 - 0.9			(Schuster et al., 2021)
Europe	BG	PAS	<MDL - 6.42	<MDL - 2.49	0.03 - 8.54			
Svalbard	BG	AAS	<MDL - 1.04	<MDL - 0.32				(Bohlin-Nizzetto, 2020)
Norway	BG	AAS	<MDL - 0.27	<MDL - 0.18				
Canada	BG	AAS	0.12 - 1.9	0.07 - 0.28				(Xiao et al., 2012)

2.2. Figures

Figure S1: Maps of the spatial distribution of the Dechlorane Plus (DP) isomers Syn-DP (A), Anti-DP (B). The amounts in pg/sample are log transformed to allow for a better visual comparison between the sample locations. Note the differences in scales between the maps.
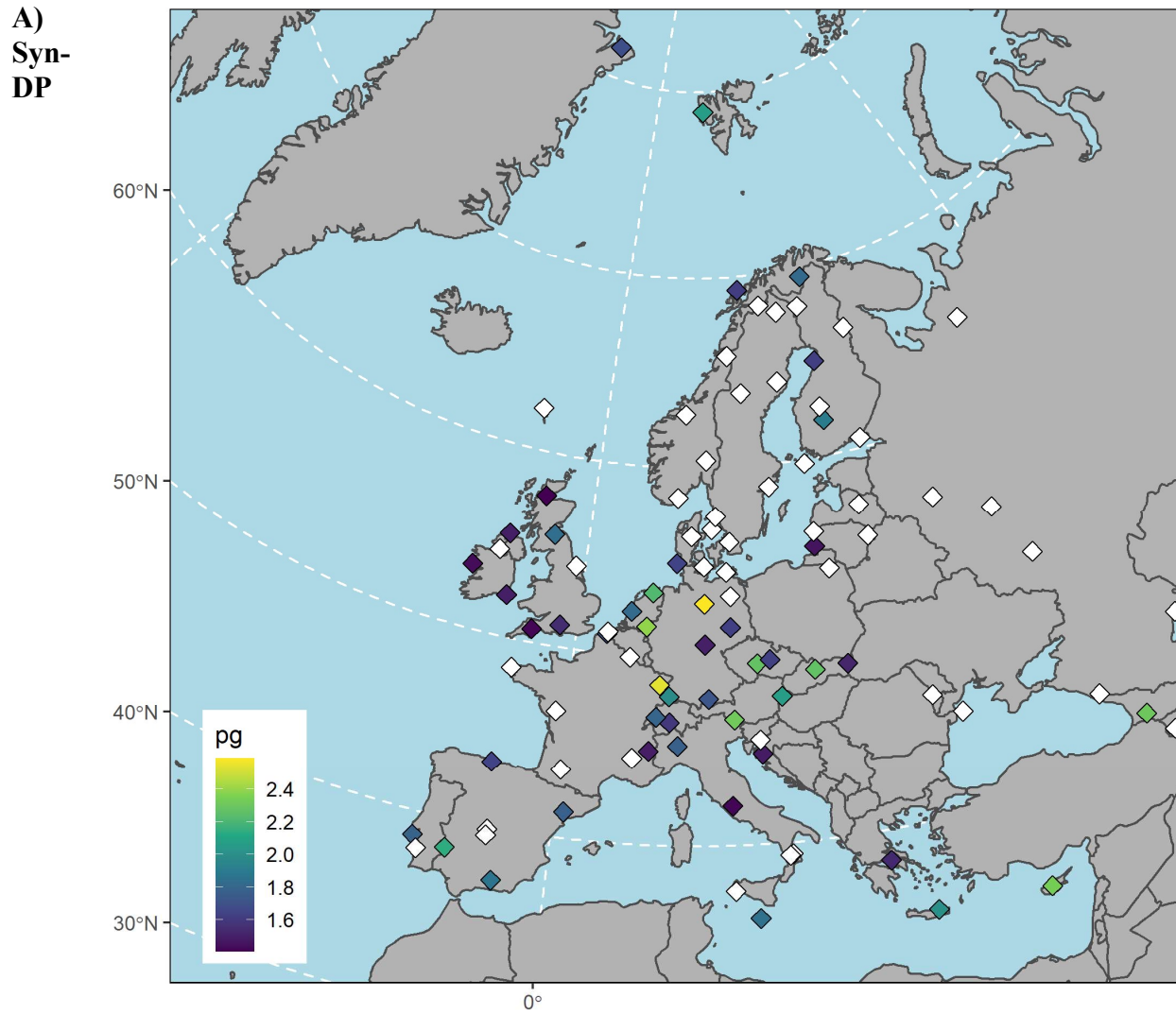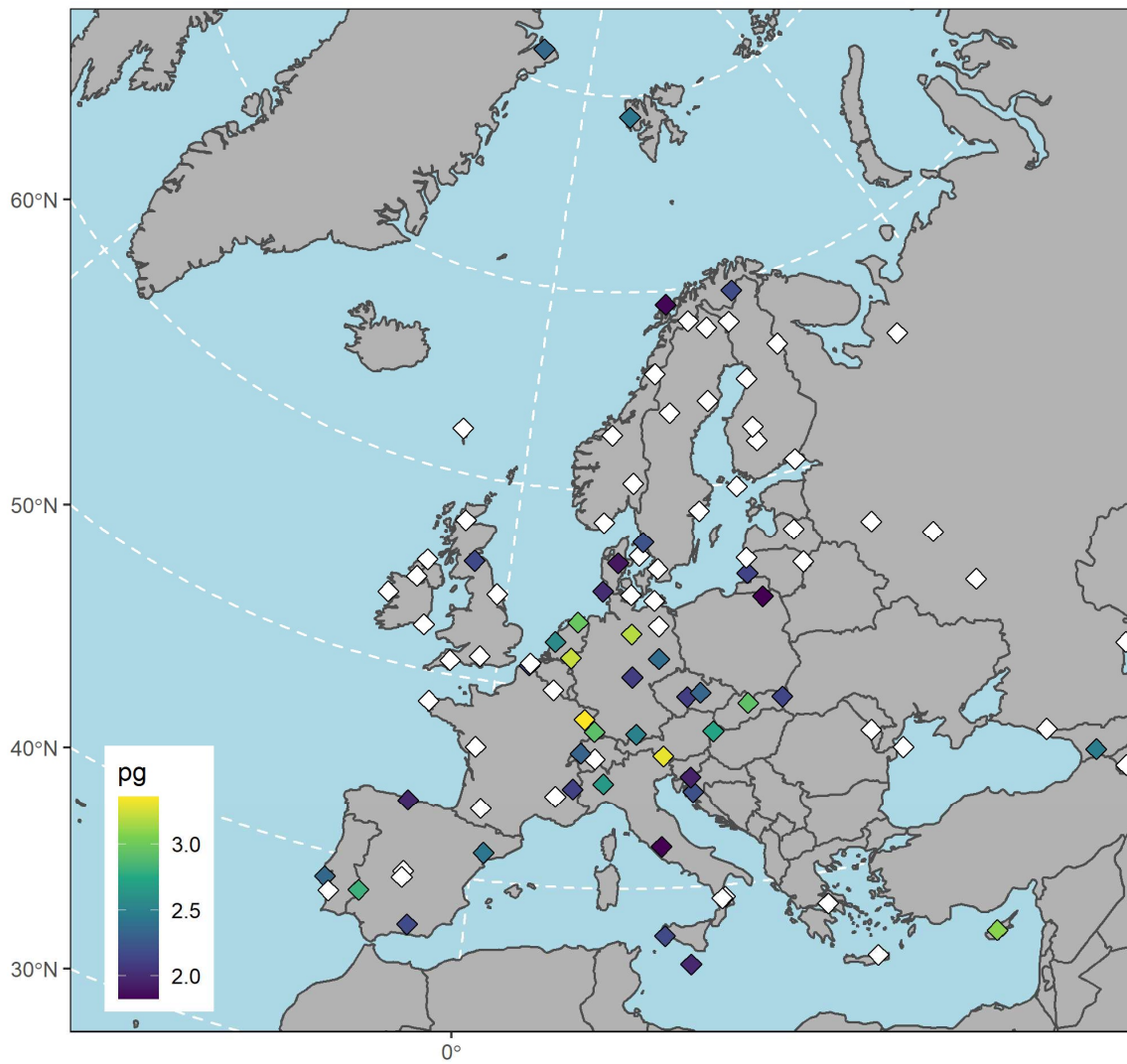
B)
Anti
-DP

Figure S2: The spatial coverage of sampling sites using PAS in this study. The background colors represent the regions included in the study area (EuroVoc, 2021).
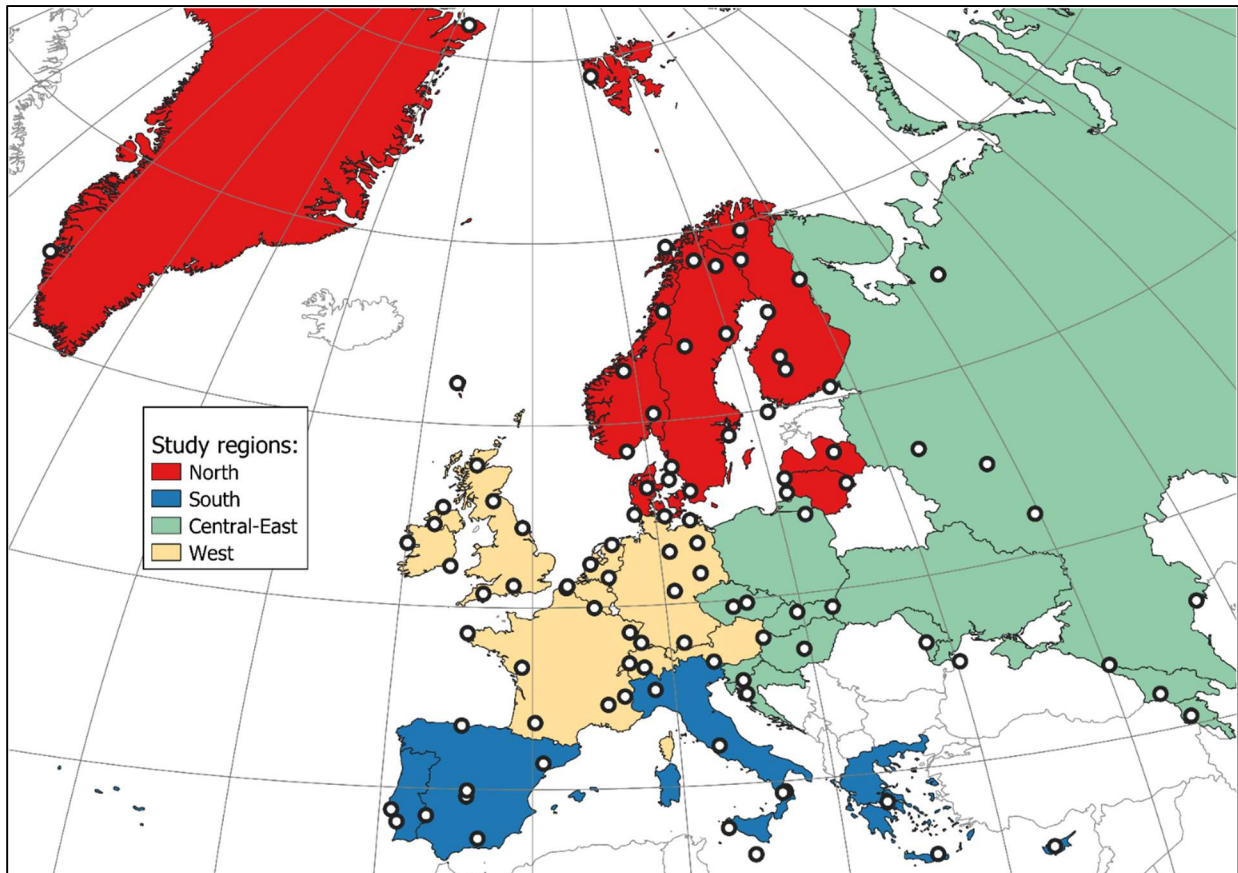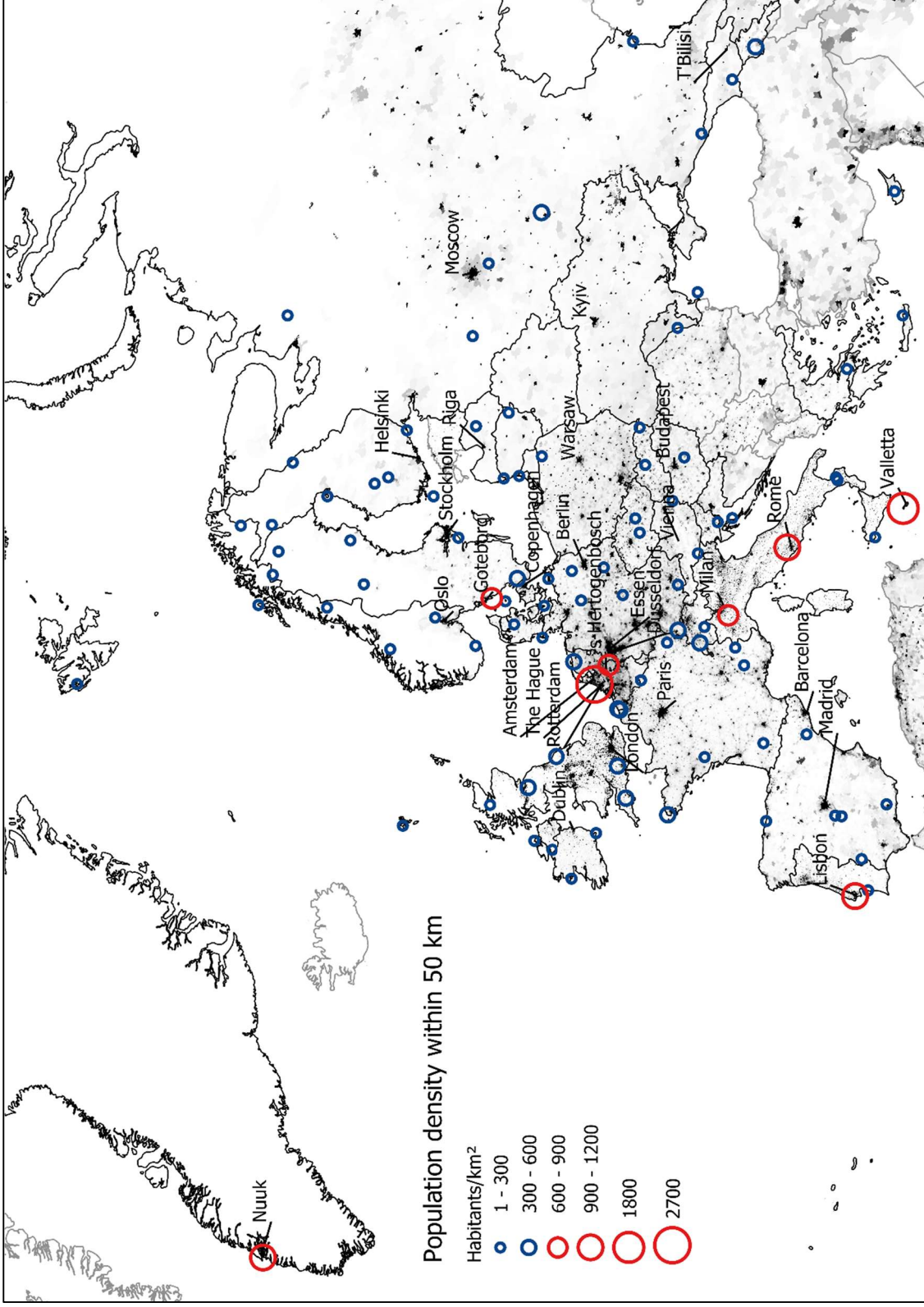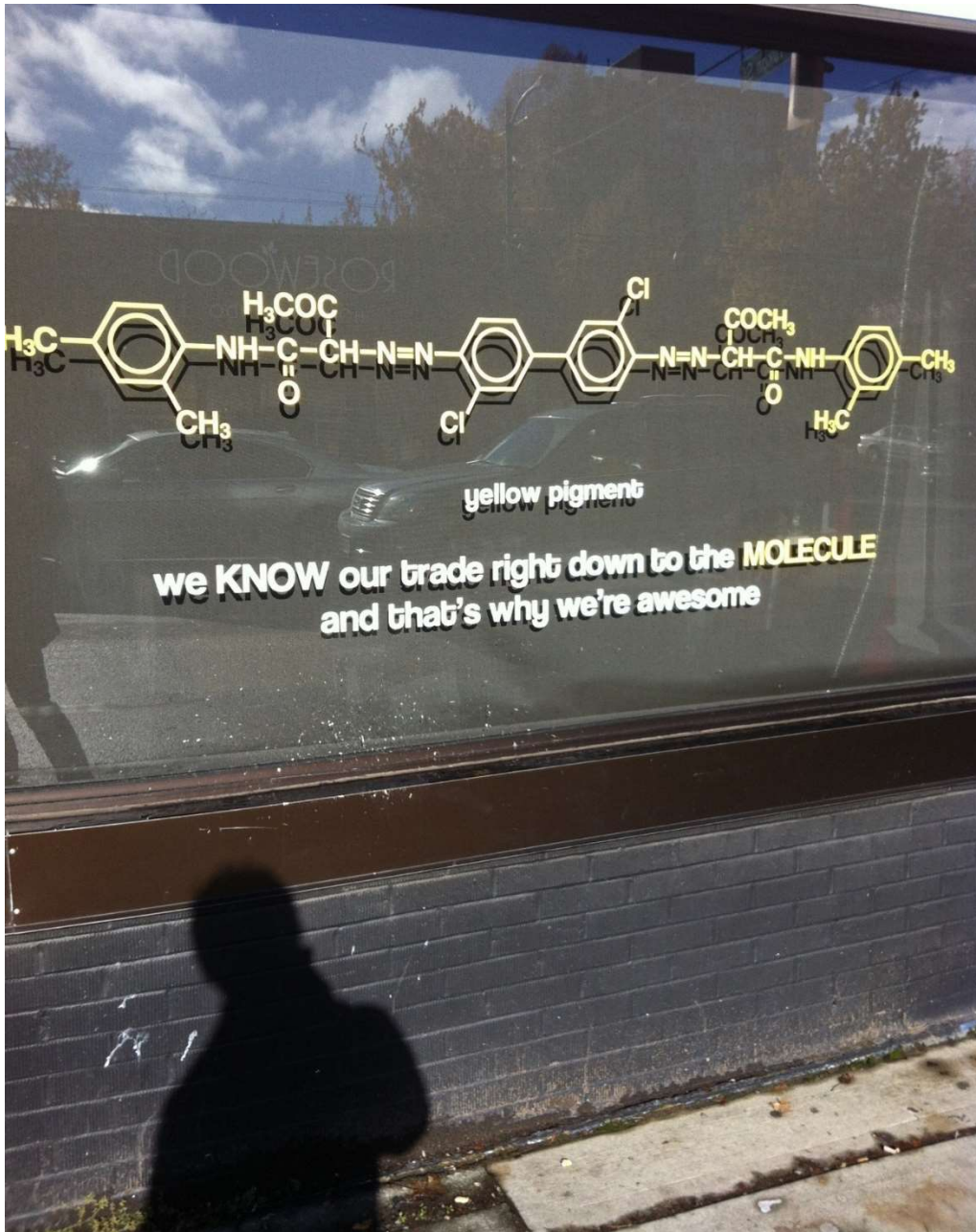
Figure S3: The spatial distribution of the estimated population density within 50 km of each site, with the gridded population density across Europe in the background (CIESIN, 2016, Lunder Halvorsen et al. (SUBMITTED)).

3. References

BOHLIN-NIZZETTO, P., AAS, W., NIKIFOROV, V. 2020. Monitoring of environmental contaminants in air and precipitation - Annual report 2019. *NILU report 06/2020*.

CHEN, S. J., TIAN, M., WANG, J., SHI, T., LUO, Y., LUO, X. J. & MAI, B. X. 2011. Dechlorane Plus (DP) in air and plants at an electronic waste (e-waste) site in South China. *Environ Pollut,* 159**,** 1290-6.

CIESIN 2016. Documentation for the Gridded Population of the World, Version 4 (GPWv4).

EUROVOC 2021. Browse by EuroVoc.

HOH, E., ZHU, L. & HITES, R. A. 2006. Dechlorane plus, a chlorinated flame retardant, in the Great Lakes. *Environ Sci Technol,* 40**,** 1184-9.

KIM, S., CHEN, J., CHENG, T., GINDULYTE, A., HE, J., HE, S., LI, Q., SHOEMAKER, B.A., THIESSEN, P.A., YU, B., ZASLAVSKY, L., ZHANG, J., BOLTON, E.E. 2021. PubChem in 2021: new data content and improved web interfaces. *Nucleic Acids Research,* 49.

LI, W. L., LIU, L. Y., SONG, W. W., ZHANG, Z. F., QIAO, L. N., MA, W. L. & LI, Y. F. 2016. Five-year trends of selected halogenated flame retardants in the atmosphere of Northeast China. *Sci Total Environ,* 539**,** 286-293.

LIU, L. Y., SALAMOVA, A., VENIER, M. & HITES, R. A. 2016. Trends in the levels of halogenated flame retardants in the Great Lakes atmosphere over the period 2005-2013. *Environ Int,* 92-93**,** 442-9.

LUNDER HALVORSEN, H., BOHLIN-NIZZETTO, P., ECKHARDT, S., GUSEY, A., MÖCKEL, C., SHATALOV, V., SKOGENG, L.S., BREIVIK, K. Submitted. Spatial Variability of POPs in Background Air across Europe - Changes over a Decade and Source Contributions.

MOLLER, A., XIE, Z., CAI, M., STURM, R. & EBINGHAUS, R. 2012. Brominated flame retardants and dechlorane plus in the marine atmosphere from Southeast Asia toward Antarctica. *Environ Sci Technol,* 46**,** 3141-8.

MOLLER, A., XIE, Z., CAI, M., ZHONG, G., HUANG, P., CAI, M., STURM, R., HE, J. & EBINGHAUS, R. 2011. Polybrominated diphenyl ethers vs alternate brominated flame retardants and Dechloranes from East Asia to the Arctic. *Environ Sci Technol,* 45**,** 6793-9.

MOLLER, A., XIE, Z., STURM, R. & EBINGHAUS, R. 2010. Large-scale distribution of dechlorane plus in air and seawater from the Arctic to Antarctica. *Environ Sci Technol,* 44**,** 8977-82.

MORIN, N. A. O., ANDERSSON, P. L., HALE, S. E. & ARP, H. P. H. 2017. The presence and partitioning behavior of flame retardants in waste, leachate, and air particles from Norwegian waste-handling facilities. *J Environ Sci (China),* 62**,** 115-132.

NIPEN, M., VOGT, R. D., BOHLIN-NIZZETTO, P., BORGA, K., MWAKALAPA, E. B., BORGEN, A. R., JORGENSEN, S. J., NTAPANTA, S. M., MMOCHI, A. J., SCHLABACH, M. & BREIVIK, K. 2021. Spatial trends of chlorinated paraffins and dechloranes in air and soil in a tropical urban, suburban, and rural environment. *Environ Pollut,* 292**,** 118298.

OLUKUNLE, O. I., LEHMAN, D. C., SALAMOVA, A., VENIER, M. & HITES, R. A. 2018. Temporal trends of Dechlorane Plus in air and precipitation around the North American Great Lakes. *Sci Total Environ,* 642**,** 537-542.

REN, N., SVERKO, E., LI, Y. F., ZHANG, Z., HARNER, T., WANG, D., WAN, X. & MCCARRY, B. E. 2008. Levels and isomer profiles of dechlorane plus in Chinese air. *Environ Sci Technol,* 42**,** 6476-80.

SALAMOVA, A., HERMANSON, M. H. & HITES, R. A. 2014. Organophosphate and halogenated flame retardants in atmospheric particles from a European Arctic site. *Environ Sci Technol,* 48**,** 6133-40.

SCHUSTER, J. K., HARNER, T. & SVERKO, E. 2021. Dechlorane Plus in the Global Atmosphere. *Environmental Science & Technology Letters,* 8**,** 39-45.

VORKAMP, K., BALMER, J., HUNG, H., LETCHER, R. J., RIGÉT, F. F. & DE WIT, C. A. 2019. Current-use halogenated and organophosphorous flame retardants: A review of their presence in Arctic ecosystems. *Emerging Contaminants,* 5**,** 179-200.

VORKAMP, K., BOSSI, R., RIGET, F. F., SKOV, H., SONNE, C. & DIETZ, R. 2015. Novel brominated flame retardants and dechlorane plus in Greenland air and biota. *Environ Pollut,* 196**,** 284-91.

WANG, D. G., YANG, M., QI, H., SVERKO, E., MA, W. L., LI, Y. F., ALAEE, M., REINER, E. J. & SHEN, L. 2010. An Asia-specific source of dechlorane plus: concentration, isomer profiles, and other related compounds. *Environ Sci Technol,* 44**,** 6608-13.

XIAO, H., SHEN, L., SU, Y., BARRESI, E., DEJONG, M., HUNG, H., LEI, Y. D., WANIA, F., REINER, E. J., SVERKO, E. & KANG, S. C. 2012. Atmospheric concentrations of halogenated flame retardants at two remote locations: the Canadian High Arctic and the Tibetan Plateau. *Environ Pollut,* 161**,** 154-61.

YU, Y., HUNG, H., ALEXANDROU, N., ROACH, P. & NORDIN, K. 2015. Multiyear Measurements of Flame Retardants and Organochlorine Pesticides in Air in Canada's Western Sub-Arctic. *Environ Sci Technol,* 49**,** 8623-30.

ZHANG, X., SUHRING, R., SERODIO, D., BONNELL, M., SUNDIN, N. & DIAMOND, M. L. 2016. Novel flame retardants: Estimating the physical-chemical properties and environmental fate of 94 halogenated and organophosphate PBDE replacements. *Chemosphere,* 144**,** 2401-7.

yellow pigment

we KNOW our trade right down to the MOLECULE
and that's why we're awesome

Paper IV